

Publikationen zum Projekt:

SOLAR-INDUZIERTER REDOXREAKTIONEN IN MIKROHETEROGENEN UND  
HOMOGENEN SYSTEMEN ZUR WASSERSTOFFERZEUGUNG

Das diesem Bericht zugrundeliegende Vorhaben wurde mit Mitteln des Bundesministers für Forschung und Technologie unter dem Förderkennzeichen 03 E 8686 A gefördert. Die Verantwortung für den Inhalt dieser Veröffentlichung liegt beim Autor.

Berichtszeitraum: 01.04.85 bis 31.03.89

Prof. Dr. H. Dürr  
Fb. 11.2, Organische Chemie  
Universität des Saarlandes

UB/TIB Hannover 89  
101 458 266



FR 6205

16771/2

UNIVERSITÄTSBIBLIOTHEK  
HANNOVER  
TECHNISCHE  
INFORMATIONSBIBLIOTHEK

## A. Verzeichnis der Publikationen:

### H. Dürr et al:

1. H. Dürr, G. Dörr, K. Zengerle, J. M. Curchod, A. Braun, *Helv. Chim. Act.*, 66, 2652 ( 1983 ).
2. H. Dürr, G. Dörr, K. Zengerle, E. Meyer, J.M. Curchod, A. Braun, *Nouv. J. Chim.*, 9, 717 ( 1985 ).
3. H. Dürr, U. Thiery, *EPA Newsletter*, p.39, July 1986.
4. I. Willner, R. Maidan, D. Mandler, G. Dörr, K. Zengerle, *J. Am. Chem. Soc.*, 109, 6080 ( 1987 ).
5. H. Dürr, K. Zengerle, H.-P. Trierweiler, *Z. Naturforsch.*, 43b, 361 ( 1988 ).
6. H. Dürr, U. Thiery, P.P. Infelta, A. Braun, *New. J. Chem.*, 13, 575 ( 1989 ).
7. H. Dürr, *Artifizielle Photosynthese*, *Magazin Forschung* 1/89, Univ. d. Saarlandes.
8. H. Dürr, H.-J. Schneider, *Nachr. Chem. Tech. Lab.*, 37 Nr.11, 1157 (1989 ).
9. H. Dürr, H.-P. Trierweiler, I. Willner, R. Maidan, *New J. Chem.*, 14, 317 ( 1990 ).
10. H. Dürr, H. Kilburg, S. Boßmann, *Synthesis*, 9, 773 ( 1990 ).
11. H. Dürr, S. Boßmann, H. Kilburg, H.-P. Trierweiler, R. Schwarz, in "Frontiers in Supramolecular Organic Chemistry and Photochemistry", H.-J. Schneider, H. Dürr Eds.; VCH Weinheim (1991).
12. H. Dürr, *Erneuerbare Energiequellen, Aktivitäten Deutscher Hochschulen*, Zentralstelle f. Solartechnik ( 1987 ).

### I. Willner et al:

1. I. Willner, D. Mandler, A. Riklin, *J. Chem. Soc., Chem Comm.*, 1022 ( 1986 ).
2. I. Willner, Z. Goren, *J. Chem. Soc., Chem. Comm.*, 172 (1986).
3. I. Willner, E. Adar, Y. Degani, Z. Goren, *J. Am. Chem. Soc.*, 108, 4696 ( 1986 ).
4. R. Maidan, I. Willner, *J. Am. Chem. Soc.*, 108, 8100 ( 1986 ).
5. A.J. Frank, I. Willner, Z. Goren, Y. Degani, *J. Am. Chem. Soc.*, 109, 3568 ( 1987 ).

6. I. Willner, D. Mandler, R. Maidan, *Nouv. J. Chim.*, 11, 110 (1987).
7. I. Willner, Y. Eichen, *J. Am. Chem. Soc.*, 109, 6882 (1987).
8. I. Willner, R. Maidan, D. Mandler, G. Dörr, K. Zengerle, *J. Am. Chem. Soc.*, 109, 6080 (1987).
9. D. Mandler, I. Eichen, *J. Am. Chem. Soc.*, 109, 7884 (1987).
10. I. Willner, E. Adar, Z. Goren, B. Steinberger, *Nouv. J. Chim.*, 11, 769 (1987).
11. I. Willner, D. Mandler, *J. Am. Chem. Soc.*, 111, 1330 (1989).
12. D. Mandler, I. Willner, *J. Chem. Soc., Perkin Trans. II*, 997 (1988).
13. I. Willner, R. Maidan, *J. Chem. Soc., Chem. Comm.*, 876 (1988).
14. I. Willner, R. Maidan, B. Willner, *Isr. J. Chem.*, 29, 289 (1989).
15. I. Willner, N. Lapidot, A. Riklin, *J. Am. Chem. Soc.*, 111, 1883 (1989).
16. I. Willner, B. Willner, in "Frontiers in Supramolecular Organic Chemistry and Photochemistry", H.-J. Schneider, H. Dürr Eds.; VCH Weinheim (1991).

B. BMFT-Berichte: '86, '87, '89.

C. Vorträge:

1. Euroforum New Energies ( Congress and Exhibition ), 24.-28.10.88 in Saarbrücken ( Germany ).
2. BMFT-Vortrag in Hannover 1988/89.

D. Tagungen:

1. Workshop on Supramolecular Organic Chemistry and Photochemistry, 27.08.-01.09.89 in Saarbrücken ( Germany ).

New sensitizer for the photocatalytic cleavage of H<sub>2</sub> / von Heinz Dürr, Klaus Zengerle, Gisela Dörr und Andre Braun in IUPAC Symposium on photochemistry; 11, Abstr. (1986); S. 390-91.

Rhodium- and cobalt-complexes as electron relays in photochemical water cleavage / von Heinz Dürr, U.Thiery, G.Dörr und Klaus Zengerle in International Conference of Photochemical Conv. a. storage of solar energy; 6, Suppl. (1986).

Erneuerbare Energiequellen, Fixierung von Kohlendioxid: photochem. Wasserspaltung in Erneuerbare Energiequellen: ZFS; (1987). S. 218-224.

Maßgeschneiderte heterolytische Rutheniumkomplexe: photophysikalische Eigenschaften / von Heinz Dürr, Andre Braun, Andreas Guldner und Eduard Mayer in Gesellschaft Deutscher Chemiker / Fachgruppe Photochemie: Abstracts.- 1987.- S. 133-135.

Tailormade mixed ligand RuL<sub>2</sub>L' complexes and their efficiency in electron transfer reactions / von Heinz Dürr und Eduard Mayer in European Society of Organic Chemistry; 5 (1987), abstracts.- S. 166-169.

Elektronentransferprozesse bei neuen Sensibilisatoren und Relais / von Heinz Dürr, Andreas Guldner, Holger Kraus und Eduard Mayer in 11. Vortragstagung Duisburg GDCH Fachgruppe Photochemie. - 1989. - S. 101-102.

Studies of electron transfer-reactions in water-reducing systems / von Heinz Dürr, Stefan Bossmann und Armin Beuerlein in Photochemistry and catalysis. - Ferrara, 1989. - S. 106-108.

Supramolecular effects in photochromic assemblies / von Heinz Dürr, Alfred Thome, Heike Kilburg und Claudia Schulz in 11. Vortragstagung Duisburg GDCH Fachgruppe Photochemie 1989. -S. 109.

## 267. Zum Mechanismus der Photoreduktion von Wasser mit Ruthenium-trisbipyrazil als Sensibilisator

von Heinz Dürr, Gisela Dörr und Klaus Zengerle

Fachbereich 14, Organische Chemie, Universität des Saarlandes, D-6600 Saarbrücken

und Jean-Marc Curchod und André M. Braun\*

Institut de chimie physique, Ecole Polytechnique Fédérale de Lausanne, Ecublens, CH-1015 Lausanne

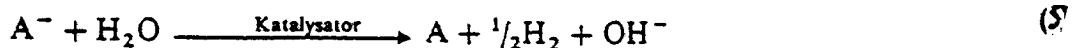
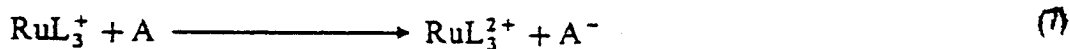
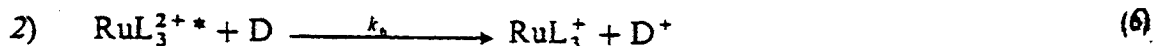
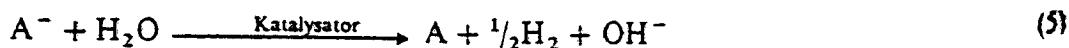
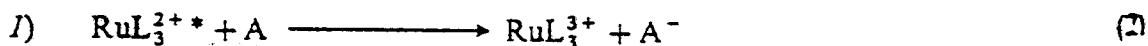
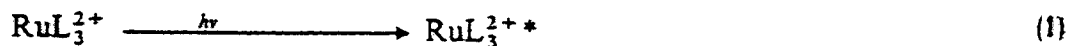
(9.XI.83)

On the Mechanism of the Photoreduction of Water with Ruthenium-trisbipyrazil as Sensitizer

### Summary

Oxidative and reductive primary steps can be differentiated in using  $\text{Ru}(\text{bipy})_3^{2+}$  and  $\text{Ru}(\text{bipz})_3^{2+}$ , respectively, as sensitizers in a photochemically induced, Pt-catalyzed sacrificial water reduction. Experimental evidence for the reductive primary step and kinetic data are given for the electron transfer to methylviologen as relay compound.

Die photochemisch induzierte Wasserspaltung hat in den letzten Jahren zunehmend Interesse geweckt, besonders im Hinblick auf eine potentielle Anwendung zur Sonnenenergiekonversion [1]. Ein wichtiges Teilproblem ist die Auswahl und die Optimierung geeigneter Sensibilisator-Systeme für die Reduktion des Wassers [2]. Diese Reduktion kann im Prinzip nach zwei verschiedenen Mechanismen erfolgen: 1) der Primärschritt ist eine Photo-oxidation; 2) der Primärschritt ist eine Photoreduktion des elektronisch angeregten Sensibilisators  $\text{RuL}_3^{2+*}$ . Für die als Sensibilisatoren weit verbreiteten Ru(II)-Komplexe sind beide Wege 1) oxidativer Zyklus [3] und 2) reduktiver Zyklus [4] bekannt.



Welche Reaktionsfolge abläuft, hängt ab von den Redoxpotentialen des Rutheniumkomplexes, sowie von den Redoxeigenschaften und Konzentrationen der Redoxpaare  $A/A^-$  und  $D/D^-$ .

Das Redoxpotential von  $RuL_3^{2+}$  kann man weitgehend durch die Wahl entsprechender Liganden beeinflussen. Bei heterocyclischen Liganden (z.B. 2,2'-Bipyridin (bipy), 2,2'-Bipyrazin (bipz)) ist der Reduktionsschritt  $RuL_3^{2+}/RuL_2^+$  ligandenzentriert und das Potential des Komplexes  $E_{1/2C}^{red}$  korreliert fast linear mit dem Reduktionspotential des Liganden  $E_{1/2L}^{red}$ :  $E_{1/2C}^{red} = E_{1/2L}^{red} + \text{const.}$  [5]. Bei Verwendung von Bipyrazin [6] an Stelle von Bipyridin als Ligand werden damit die Redoxpotentiale des Sensibilisators derart verändert (Tab.), dass in dem meist verwendeten System, mit A = Methylviologen (N,N'-Dimethyl-4,4'-bipyridinium-dikation,  $MV^{2+}$ ) als Elektronenrelais und D = EDTA (Äthylendiamin-tetraessigsäure) als Reduktionsmittel, der oxidative Zyklus I (L = bipy) in den reduktiven Zyklus 2 (L = bipz) umschlägt. Mittels LASER-Photolyse können die entsprechenden kinetischen Daten gemessen werden.

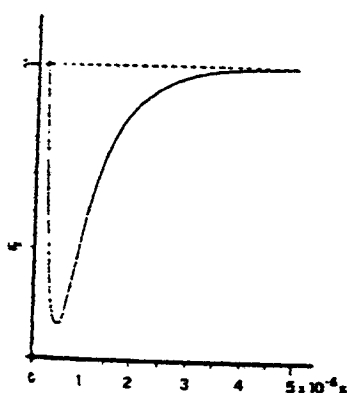


Fig. 1.  
Abklingkurve der  $Ru(bipz)_3^{2+*}$ -Emission.  $[Ru(bipz)_3^{2+}] = 6 \times 10^{-5} M$ , pH 5.  
Ar-gesättigt. Analyse: 603 nm.

Die Lebensdauer des angeregten Zustands  $Ru(bipz)_3^{2+*}$  wurde aus der Abklingkurve der Luminiszenz von  $Ru(bipz)_3^{2+*}$  bei 603 nm ermittelt (Fig. 1). Dazu wurde eine mit Ar gesättigte wässrige Lösung von  $Ru(bipz)_3Cl_2$  ( $6 \times 10^{-5} M$ ) [7], mit KH-Phthalat-Puffer (0.1 M), bei 532 nm angeregt (Nd-Laser, JK 2000, Pulsweite  $2 \times 10^{-8} s$  [8]).

Tabelle. Redoxpotential ( $E_r$ , [V]) der in den Reaktionen 1, 2, 3, 6 und 7 beschriebenen Sensibilisatormoleküle<sup>a)</sup>

	$E_r$			
	$RuL_3^{2+/+}$	$RuL_3^{2+*/+}$	$RuL_3^{3+/2+}$	$RuL_3^{3+/2+*}$
L = bipy	-1,31	0,8	1,27	-0,8
L = bipz	-0,68	1,4	1,98	-0,1

<sup>a)</sup> Gemessen gegen die gesättigte Kalomel-Elektrode [5a].

Mit  $7.5 \times 10^{-7} s$  ist die Lebensdauer von  $Ru(bipz)_3^{2+*}$  etwas niedriger als der von *Leier & Crutchley* [6] publizierte Wert. Nach *Amouyal & Zidler* [9] ist die Differenz auf die höhere Ionenstärke der von uns verwendeten Lösung ( $\mu \approx 2$ ) zurückzuführen. Bei Zusatz von EDTA-Dinatriumsalz wird ein noch schnellerer Zerfall des Luminiszenzsignals beobachtet. Der elektronisch angeregte Komplex oxidiert das Reduktionsmittel,

seine Emission wird entsprechend *Reaktion 6* gelöscht. Die gemessene Reaktionsgeschwindigkeit ist proportional  $[EDTA]$  ( $k_{obs} = f([EDTA])$ , Fig. 2). Die berechnete Reaktionsgeschwindigkeitskonstante  $k_6$  beträgt  $3,9 \times 10^7 \text{ M}^{-1} \text{ s}^{-1}$ . Konventionelle Fluoreszenzmessungen ergaben nach *Stern-Volmer* und unter Berücksichtigung der gemessenen Lebensdauer von  $7,5 \times 10^{-7} \text{ s}$  ein  $k_6$  von  $9,4 \times 10^7 \text{ M}^{-1} \text{ s}^{-1}$ . Bei Zugabe von  $MV^{2+}$  zu einer wässrigen Lösung des Sensibilisators kann keine Emissionslöschung nachgewiesen werden; dieses Resultat bestätigt den reduktiven Reaktionszyklus. Erst bei Zugabe beider Komponenten, EDTA und  $MV^{2+}$ , wird nach Laseranregung die Bildung des Methylviologenradikals  $MV^+$  beobachtet (Absorption bei 602 nm).

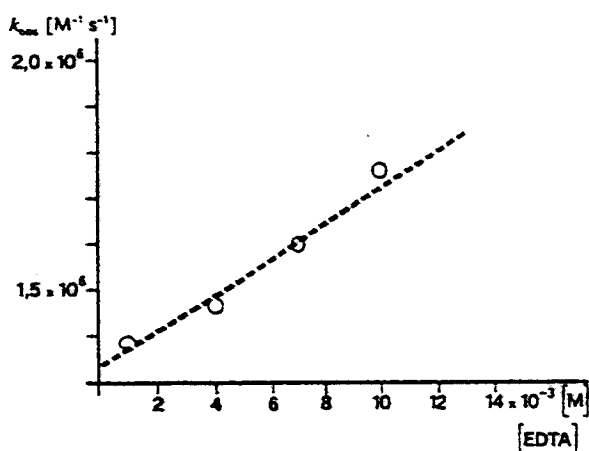
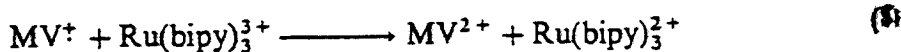


Fig. 2.

Geschwindigkeit des Elektronentransfers (6) in Abhängigkeit von  $[EDTA]$ , gemessen an der Emissionslöschung von  $Ru(bipz)_3^{2+}$  ( $[Ru(bipz)_3Cl_2] = 6 \times 10^{-5} \text{ M}$ , pH = 5, Ar gesättigt,  $k_6 = 3,9 \times 10^7 \text{ M}^{-1} \text{ s}^{-1}$ )

In einer mit Ar gesättigten wässrigen Lösung von Sensibilisator  $Ru(bipz)_3^{2+}$  ( $3 \times 10^{-4} \text{ M}$ ), EDTA-Dinatriumsalz (0,1 M), bei pH 5 (KH-Phthalatpuffer 0,1 M), und unterschiedlichen Konzentrationen von  $MV^{2+}$  ( $5 \times 10^{-3}$ ,  $7,5 \times 10^{-3}$ ,  $1 \times 10^{-2} \text{ M}$ ) entsteht das Methylviologenradikal, unabhängig von  $[MV^{2+}]$ , jeweils mit der gleichen Geschwindigkeit.  $[MV^+]$  wächst dabei praktisch so schnell an ( $k_{obs} = 5,4 \times 10^6 \text{ s}^{-1}$ ), wie  $Ru(bipz)_3^{2+}$  von EDTA deaktiviert wird ( $k_{des} = k_F + k_6[EDTA] = 5,2 \times 10^{-6} \text{ s}^{-1}$ ). Daraus schliessen wir, dass *Reaktion 7* zumindest gleich schnell verläuft wie *Reaktion 6*.

In einem Reaktionssystem, das Pt als Katalysator zur  $H_2$ -Produktion enthält, vermittelt das Viologen die Reduktion von  $H^+$  durch  $Ru(bipz)_3^+$ . Ohne Viologen entwickelt das System zwar auch  $H_2$  jedoch mit einer viel kleineren Effizienz und unter Zersetzung des  $Ru(bipz)_3^{2+}$ -Komplexes. Bezüglich der  $H_2$ -Entwicklung ist der reduktive Zyklus mit  $L = bipz$  und  $\Phi_{1/2H_2} = 0,243$  viermal effizienter als der oxidative Zyklus mit  $L = bipy$  und  $\Phi_{1/2H_2} = 0,085$  [7]. Im Fall von  $L = bipy$  wird ein grosser Teil der Anregungsenergie des Komplexes in der thermischen *Rückreaktion 8* vernichtet, bevor es zu einer Trennung der Photoredoxprodukte kommt, während sich bei



$L = bipz$  EDTA nach der Elektronenabgabe irreversibel zersetzt [9]. Für die photochemische  $H_2O$ -Reduktion, unter irreversibler Oxidation eines geeigneten Elektronendonators, verspricht damit der reduktive Zyklus eine grössere Effizienz, ohne eine Ladungstrennung durch Einführung mikroheterogener [10] oder heterogener Systeme [11] beeinflussen zu müssen.

Deutschen Forschungsgemeinschaft, dem Fonds der Chemischen Industrie, dem Schweizerischen Fonds zur Förderung der wissenschaftlichen Forschung (Projekt 4.397-0.80.4) und dem Stipendienfonds der Chemischen Industrie sei für finanzielle Unterstützung gedankt. G.D. dankt der European Photochemistry Association für die Ermöglichung eines Studienaufenthalts in Lausanne. Herrn Prof. M. Grätzel danken wir für die freundliche Überlassung der Laserphotolyse-Apparatur.

## LITERATURVERZEICHNIS

- [1] a) M. Grätzel & P. Cuendet, *Experientia* 38, 223 (1982); b) A.M. Braun, ed., 'Photochemical Conversion', Presses Polytechniques Romandes, Lausanne, 1983.
- [2] a) J.R. Durwent, P. Douglas, A. Harriman, G. Porter & M.C. Richoux, *Coord. Chem. Rev.* 44, 83 (1982); b) A. Jura, V. Balzani, F. Barigelli, P. Belscr & A. v. Zelewsky, *Israel J. Chem.* 22, 87 (1982).
- [3] a) A. Moradpour, E. Amouyal, P. Keller & H. Kagan, *Nouv. J. Chem.* 2, 547 (1978); b) K. Kalyanasundaram, J. Kwei & M. Grätzel, *Helv. Chim. Acta* 61, 2720 (1978); c) J.M. Lehn, J.P. Sauvage & M. Kirch, *Helv. Chim. Acta* 62, 1345 (1979); d) P.A. Brugger, P. Cuendet & M. Grätzel, *J. Am. Chem. Soc.* 103, 2923 (1981).
- [4] a) K. Monserrat, T.K. Foreman, M. Grätzel & D.G. Whitten, *J. Am. Chem. Soc.* 103, 6667 (1981); b) P.J. Delaire, B.P. Sullivan, T.J. Meyer & D.G. Whitten, *J. Am. Chem. Soc.* 101, 4007 (1979); c) C.V. Krishan & M. Swain, *J. Am. Chem. Soc.* 103, 2141 (1981).
- [5] a) D.P. Rillema, G. Allen, T.J. Meyer & D. Conrad, *Inorg. Chem.* 22, 1617 (1983); b) J. Watanabe, T. Saji & S. Toru, *Bull. Chem. Soc. Jpn.* 55, 327 (1982).
- [6] a) A.B.P. Lever & R.J. Crutchley, *J. Am. Chem. Soc.* 102, 7128 (1980); b) A.B.P. Lever & R.J. Crutchley, *Inorg. Chem.* 21, 2276 (1982).
- [7] H. Dürr, G. Dörr, K. Zengerle, B. Reis & A.M. Braun, *Chimia* 37, 245 (1983).
- [8] R. Humphry-Baker, A.M. Braun & M. Grätzel, *Helv. Chim. Acta* 64, 2036 (1981).
- [9] E. Amouyal & B. Zidler, *Israel J. Chem.* 22, 117 (1982).
- [10] Y. J. Turro, M. Grätzel & A.M. Braun, *Angew. Chem.* 92, 712 (1980), *Angew. Chem., Int. Ed. Engl.* 19, 675 (1980).
- [11] D. Duonghong, E. Borgarello & M. Grätzel, *J. Am. Chem. Soc.* 103, 4685 (1981).



# POSSIBILITÉS ET LIMITES DES DIAZACOMPLEXES DE Ru<sup>2+</sup> EN TANT QUE SENSIBILISATEURS INDUISANT LA PHOTOLYSE DE L'EAU \*

Heinz Dürr, Gisela Dörr, Klaus Zengerle et Eduard Mayer

Fachbereich 14, Organische Chemie,  
Universität des Saarlandes,  
D-6600 Saarbrücken.

Jean-Marc Curchod et André M. Braun \*

Institut de chimie physique,  
École Polytechnique Fédérale de Lausanne,  
Ecublens, CH-1015 Lausanne.

Reçu le 21 mai 1985.

RESUME. — Les caractéristiques physico-chimiques (durée de vie de luminescence, longueur d'onde d'émission maximale, rendement quantique de luminescence, potentiels rédox et constantes de vitesse de transferts d'électron) de sensibilisateurs RuL<sub>3</sub><sup>2+</sup> dont L est bipyridine-2,2' (1), bipyrazine-2,2' (2), bipyrimidine-2,2' (3), bipyrimidine-4,4' (4), bipyridazine-3,3' (5) et méthyl-4' (pyridyl-2')-2 pyrimidine (6) sont comparées dans les mêmes conditions expérimentales. Ces caractéristiques sont discutées en liaison avec les rendements quantiques obtenus de l'amorçage de la production d'hydrogène.

ABSTRACT. — RuL<sub>3</sub><sup>2+</sup> complexes, where L is 2,2'-bipyridine (1), 2,2'-bipyrazine (2), 2,2'-bipyrimidine (3), 4,4'-bipyrimidine (4), 3,3'-bipyridazine (5) and (4'-methyl-2' pyridyl)-2-pyrimidine (6), were used for the photocatalysed hydrogen production. The corresponding quantum yields are discussed in terms of physico-chemical parameters (luminescence lifetime, wavelength of maximal emission, luminescence quantum yield, redox potentials and rate constants of electron transfer) obtained under similar experimental conditions.

## Introduction

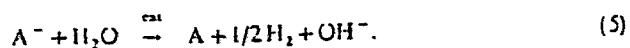
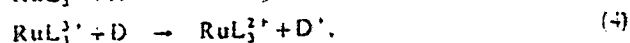
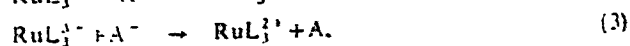
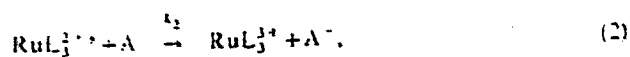
De nombreux travaux ont démontré que les complexes de Ru<sup>2+</sup> peuvent être utilisés en tant que sensibilisateurs pour l'induction de la photodissociation de la molécule d'eau<sup>1</sup>. Il est clair que les ligands L, rattachés au Ru<sup>2+</sup> sont d'une importance fondamentale vis-à-vis des caractéristiques physico-chimiques du complexe RuL<sub>3</sub><sup>2+</sup> formé, telles que : durée de vie de luminescence, τ<sub>lum</sub>; longueur d'onde d'émission maximale, λ<sub>lum, max</sub>; rendement quantique de luminescence, φ<sub>lum</sub>; potentiel rédox, E<sup>0</sup>, des couples Ru<sup>3+/2+</sup>, Ru<sup>2+/2.5+</sup>, Ru<sup>2+/1.5+</sup>, Ru<sup>2+/0.5+</sup> et constantes de transferts d'électron, k<sub>1</sub> et k<sub>2</sub>.

Dans une première phase, nous avons déterminé les valeurs caractéristiques des principaux paramètres physico-chimiques pour une gamme de sensibilisateurs dont les ligands sont des di-, tri- ou tétraazabiphényles : L = bipyrimidine-2,2' (bipm-2,2') 3; L = bipyrimidine-4,4' (bipm-4,4') 4; L = bipyridazine-3,3' (bipd) 5 et L = méthyl-4' (pyridyl-2')-2 pyrimidine (Mepym) 6. Dans une seconde phase, ces complexes sont utilisés dans un système photochimique adéquat, sensibilisateur/

relais d'électron/catalyseur/agent réducteur, permettant la production d'hydrogène et mettant ainsi en valeur la caractéristique fondamentale pour laquelle ils ont été synthétisés.

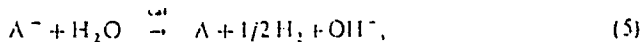
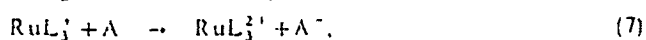
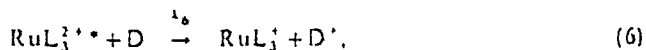
Les résultats correspondants sont comparés à ceux obtenus avec deux complexes de Ru<sup>2+</sup> utilisés comme référence : L = bipyridine-2,2' (bipy) 1<sup>2</sup> et L = bipyrazine-2,2' (bipz) 2. Ces complexes ont été choisis non seulement pour leurs caractéristiques bien connues dans ce domaine d'études, mais également parce qu'ils engendrent deux mécanismes de réaction fondamentalement différents : respectivement un cycle dit oxydant et un cycle dit réducteur<sup>3,4</sup>. Les nouveaux complexes que nous avons synthétisés peuvent alors être classés dans l'une ou l'autre de ces deux catégories

### Cycle oxydant :

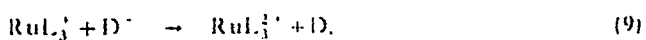
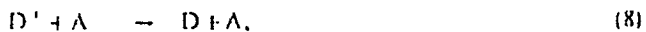


\* Publication dédiée au Prof. Tino Gäumann, Lausanne, à l'occasion de son 60<sup>e</sup> anniversaire.

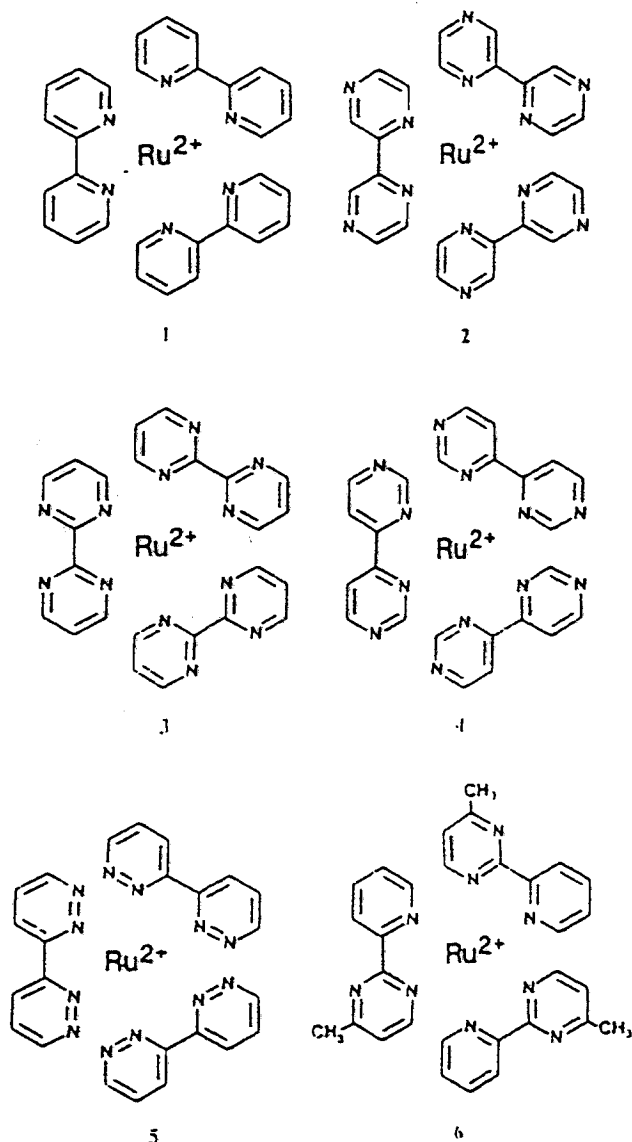
## Cycle réducteur.



où *A* est un accepteur d'électrons (méthylviologène)<sup>3</sup> et *D* un réducteur qui est oxydé irréversiblement. Par conséquent, les rétroactions telles que :



soit pour le cycle oxydant (8), soit pour le cycle réducteur [(8) et (9)], peuvent être négligées, ce qui donne au cycle réducteur l'avantage de ne pas contenir une réaction diminuant l'efficacité de la séparation de charge photoinduite [voir rétroaction (3) du cycle oxydant].



Schéma

## Partie expérimentale

Les spectres de luminescence des sensibilisateurs ont été enregistrés avec un spectrofluorimètre Perkin-Elmer MPF-44A; les rendements quantiques de luminescence  $\Phi_{Lw}$  sont déterminés par comparaison un standard de  $\text{Ru}(\text{bipy})_3^{2+}$  dont le rendement quantique est connu ( $\Phi_{Lw} = 0,042$ ), toutes les solutions étant ajustées au préalable à une densité optique de 0,3 pour une longueur d'onde d'excitation  $\lambda_e$  460 nm.

Les durées de vie de luminescence,  $\tau_{Lw}$ , les constantes d'inhibition  $k_2$  et  $k_a$ , ainsi que les rendements quantiques de production de  $\text{A}^{\cdot-}$   $\Phi_{MV^{\cdot-}}$ , sont déterminés par photolyse laser. Nous utilisons un laser au Néodyme-YAG (JK Lasers System 2000) d'une largeur d'impulsion de  $2 \cdot 10^{-8}$  s et d'une longueur d'onde d'excitation de 532 nm ce laser étant couplé à un spectrophotomètre d'analyse. Les constantes d'inhibition,  $k_2$  et  $k_a$ , sont obtenues par un traitement cinétique du type Stern-Volmer<sup>4</sup>, basé sur la mesure de la constante apparente de décroissance de la luminescence en présence d'inhibiteur à des concentrations différentes. Selon que le cycle est oxydant ou réducteur, l'inhibiteur sera *A* ( $k_2$ ) ou *D* ( $k_a$ ). Dans ce travail, *A* est du méthylviologène (dichlorure de diméthyl-N,N' bipyridine-4,4', MV<sup>2+</sup>) et *D* de l'EDTA (sel de sodium de l'acide éthylènediaminé-tetraacétique). Les échantillons sont tamponnés à pH 5 par de l'hydrogénophthalate de potassium (0,05 M) et contiennent  $6,5 \cdot 10^{-3}$  M de complexes de  $\text{Ru}^{2+}$ ; la concentration d'inhibiteur varie de  $2 \cdot 10^{-2}$  M à  $2 \cdot 10^{-3}$  M pour le MV<sup>2+</sup> et de  $5 \cdot 10^{-2}$  M à  $2 \cdot 10^{-3}$  M pour l'EDTA; chaque échantillon est désaéré par barbotage de gaz inerte (Ar).

Les rendements quantiques de production de radicaux MV<sup>•-</sup>,  $\Phi_{MV^{\cdot-}}$ , sont déterminés après étalonnage de l'énergie du faisceau laser à l'aide d'un joulemètre (Joulemeter Model 172, Laser Instrumentation Ltd., fig. 1), et après estimation expérimentale du volume de solution irradiée. Ce volume est facilement déterminé et reste pratiquement constant pour des densités optiques faibles ( $D_{\lambda, 532} < 0,1$ ). Ces rendements quantiques sont calculés selon les équations (10) à (14).

$$D_{\lambda, 602} = \log \frac{I_0}{I_0 - \Delta I_{\text{max}}} = \epsilon_{MV^{\cdot-}, 602} \cdot l \cdot [MV^{\cdot-}] \quad (\text{cf. fig. 2}) \quad (10)$$

$$N_i = \frac{R \cdot E_i}{h\nu} \quad (11)$$

$$N_{\text{abs}} = N_i \cdot (1 - 10^{-D_{\lambda, 532}}) \quad (12)$$

$$\Phi_{MV^{\cdot-}} = \frac{[MV^{\cdot-}] \cdot V \cdot l}{N_{\text{abs}}} \quad (13)$$

$$\Phi_{MV^{\cdot-}} = \frac{[MV^{\cdot-}] \cdot V \cdot l \cdot \nu \cdot D_{\lambda, 602}}{R \cdot \epsilon_{MV^{\cdot-}, 602} \cdot l \cdot E_i \cdot (1 - 10^{-D_{\lambda, 532}})} \quad (14)$$

$N_A$	nombre d'Avogadro;
$N_{\text{abs}}$	nombre de photons absorbés;
$N_i$	nombre de photons incidents;
$D_{\lambda, 532}$	densité optique de l'échantillon à 532 nm;
$D_{\lambda, 602}$	densité optique des radicaux de MV <sup>•-</sup> à 602 nm;
$\epsilon_{MV^{\cdot-}, 602}$	coefficient d'extinction des radicaux de MV <sup>•-</sup> à 602 nm; $11\,000 \text{ M}^{-1} \text{ cm}^{-1}$ .
<i>l</i>	trajet optique, [cm];
<i>R</i>	coefficient corrigeant les réflexions sur les parois (estimé expérimentalement à 1,05);
$E_i$	énergie de l'impulsion laser, [J] (cf. fig. 1);
<i>V</i>	volume de la solution irradiée, [l].

Les mesures ont été complétées par une étude à pH 8 (solution tamponnée par du dihydrogénophosphate de potassium à  $5 \cdot 10^{-2}$  M) dans laquelle l'EDTA a été remplacé par de la triéthanolamine (TEOA,  $5 \cdot 10^{-2}$  M).

Les valeurs du rendement quantique de production d'hydrogène  $\Phi_{1/2 \text{H}_2}$ , sont mesurées sur un banc optique en utilisant une électrode à hydrogène et un actinomètre intégrant<sup>4</sup>. La concentration en platine colloïdal est de 9 mg/l ( $4,6 \cdot 10^{-5}$  M).

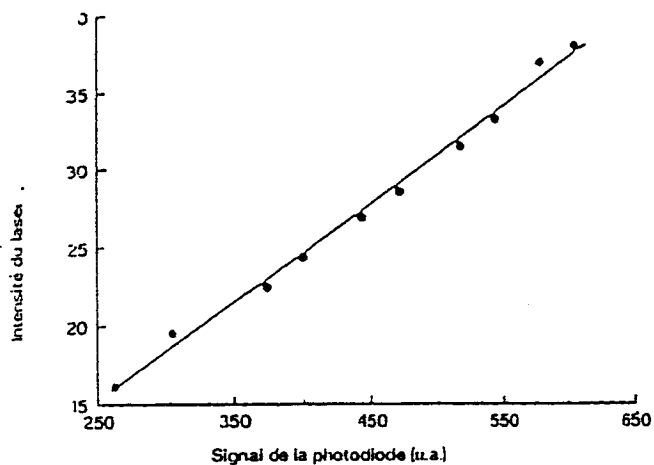


Figure 1. Courbe d'étalonnage de l'énergie du faisceau laser à l'aide d'un joulemètre.

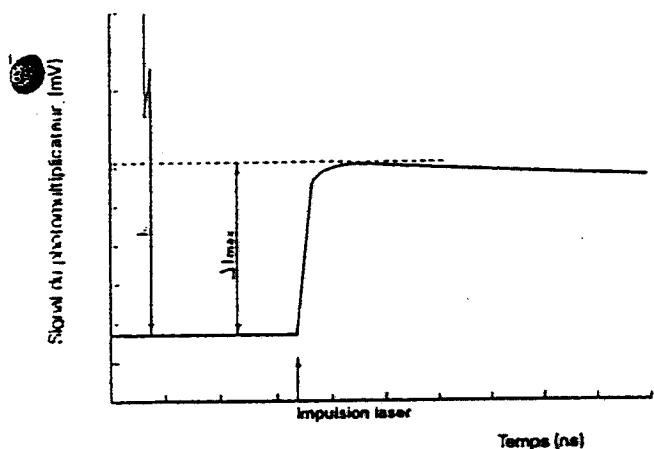


Figure 2. Absorption de MV<sup>•+</sup> (602 nm) après excitation de RuL<sub>3</sub><sup>2+</sup> par impulsion laser.

Résultats et discussion

D'une façon générale, on remarque que les complexes avec des ligands aromatiques diaza-1,2 ou -1,3 sont de moins bons sensibilisateurs que le Ru(II)-tris-bipyrazine (2). En particulier les complexes pyrimidiniques (3, 4 et 6) semblent favoriser la désactivation très efficace du complexe électroniquement excité, selon des processus non radiatifs.

La classification selon un cycle oxydant ou réducteur est obtenue à la suite de mesures photocinétiques d'inhibition de la luminescence; en effet les potentiels rédox pour les composés étudiés (tableau I) confirment nos résultats (tableau II).

Tableau I. - Potentiel rédox E<sup>0</sup> (V/SCE).

	1 <sup>a</sup>	2 <sup>a</sup>	3 <sup>a</sup>	5 <sup>a</sup>	6 <sup>a</sup>
(RuL <sub>3</sub> ) <sup>3+2+</sup>	1,26	1,98	1,69	1,58	1,38
(RuL <sub>3</sub> ) <sup>2+2+</sup>	0,84	1,40	1,00	1,06	0,93
(RuL <sub>3</sub> ) <sup>3+2+</sup>	-0,86	-0,10	-0,20	-0,48	-0,73
(RuL <sub>3</sub> ) <sup>2+2+</sup>	-1,28	-0,68	-0,91	-1,00	-1,18

Dans le cas où : E<sup>0</sup><sub>Ru<sup>3+</sup>/Ru<sup>2+</sup></sub> < E<sup>0</sup><sub>MV<sup>2+</sup>/MV<sup>•+</sup></sub> (-0,44 V) alors le mécanisme de l'inhibition est oxydant.

Tableau II. - Constantes d'inhibition ou de transfert d'électron et type de mécanisme<sup>a</sup>.

(RuL <sub>3</sub> ) <sup>2+</sup>	k <sub>2</sub> <sup>b</sup> [M <sup>-1</sup> s <sup>-1</sup> ]	k <sub>6</sub> <sup>c</sup> [M <sup>-1</sup> s <sup>-1</sup> ]	Cycle
1	1,17.10 <sup>4</sup>	-	Oxydant
2	-	3,9.10 <sup>7</sup>	Réducteur
3	-	<10 <sup>7</sup>	Réducteur
5	4,80.10 <sup>7</sup>	-	Oxydant
6	2,90.10 <sup>9</sup> <sup>f</sup>	-	Oxydant
	3,90.10 <sup>8</sup> <sup>g</sup>		

<sup>a</sup> Le complexe 4 n'est pas utilisé puisqu'il ne luminesce pas;

<sup>b</sup> A = méthylviologène (MV<sup>2+</sup>);

<sup>c</sup> D = sel de sodium de l'acide éthylènediaminotétracétique (EDTA);

<sup>d</sup> 1,03.10<sup>8</sup> M<sup>-1</sup> s<sup>-1</sup>;

<sup>e</sup> non déterminable dans le domaine de concentrations en inhibiteur choisi; le mécanisme est alors mis en évidence par des expériences qualitatives en utilisant des [EDTA] > 10<sup>-1</sup> M, sous irradiation continue;

<sup>f</sup> obtenu par inhibition de la luminescence (Stern-Volmer);

<sup>g</sup> sous d'autres conditions expérimentales, cf. référence<sup>2</sup>.

Si la constante d'inhibition de l'état électroniquement excité du complexe 3 n'a pas pu être déterminée en utilisant l'EDTA dans le domaine de concentrations indiqué, étant donné sa durée de vie relativement courte (τ<sub>LW</sub>: 190 ns; tableau III), une analyse qualitative du transfert d'électron selon un cycle réducteur (réaction 6, k<sub>6</sub> < 10<sup>7</sup> M<sup>-1</sup> s<sup>-1</sup>) est néanmoins rendue possible et confirme un rendement quantique de production d'hydrogène très faible (Φ<sub>1,2H<sub>2</sub></sub>: 0,005; tableau IV).

Tableau III. - Longueur d'onde maximale, durée de vie et rendement quantique de la luminescence des complexes (RuL<sub>3</sub>)<sup>2+</sup>. 1 à 6.

(RuL <sub>3</sub> ) <sup>2+</sup>	λ <sub>LW, max</sub> (nm)	τ <sub>LW</sub> [10 <sup>-6</sup> s]	Φ <sub>LW</sub>
1	610	0,61	0,040
2	603	0,75	0,043
3	639	0,19	0,002
4	Pas de luminescence		
5	622	0,58	0,014
6	613 <sup>a</sup>	0,19 <sup>a</sup>	0,008

Tableau IV. - Rendement quantique de production de radicaux MV<sup>•+</sup>, Φ<sub>MV<sup>•+</sup></sub>, comparé au rendement quantique de production d'hydrogène, Φ<sub>1,2H<sub>2</sub></sub>, à pH 5, avec EDTA comme agent réducteur<sup>a</sup>.

(RuL <sub>3</sub> ) <sup>2+</sup>	Φ <sub>MV<sup>•+</sup></sub>	Φ <sub>1,2H<sub>2</sub></sub>	Mécanisme
1	0,083	0,120 <sup>b</sup>	Oxydant
2	0,278	0,260	Réducteur
3	0,035	0,005	Réducteur
5	0,014	0,009	Oxydant

<sup>a</sup> [MV<sup>2+</sup>] = 2.10<sup>-3</sup> M, [EDTA] = 5.10<sup>-2</sup> M;

<sup>b</sup> 0,087<sup>2</sup>.

Les rendements quantiques  $\Phi_{1/2 H_2}$  indiqués respectivement dans les tableaux IV et V ont été mesurés dans des conditions identiques de pH et de concentration en accepteur et réducteur. Ces conditions ont été trouvées pour 1 et 2 en optimisant la production d'hydrogène sous un régime permanent et ne correspondent pas aux valeurs optimales pour chacun des systèmes. De plus, les rendements quantiques donnés sont des valeurs maximales et ne sont pas forcément les valeurs qu'on pourrait trouver sous un régime permanent<sup>11</sup>; le régime permanent n'est d'ailleurs atteint que si le système photochimique est stable, et la stabilité des différents composés utilisés n'a pas été prouvée dans cette étude<sup>12</sup>.

En principe  $\Phi_{MV^{\cdot+}}$  doit être supérieur ou égal au  $\Phi_{1/2 H_2}$ . Dans le tableau IV, on voit que le système contenant 1 ne remplit pas cette condition. Cette différence peut être expliquée par une nouvelle réduction de  $MV^{2+}$  par l'EDTA oxydée<sup>2, 13</sup> [ $D^{\cdot+}$ , équation (4)], EDTA étant présent en concentration relativement élevée ( $5 \cdot 10^{-2}$  M). Cette réduction secondaire de  $MV^{2+}$  apparaît dans la photolyse laser à une échelle de temps plus lente que celle de la réaction (2), et les deux réactions peuvent être différenciées. Dans le cas des systèmes suivant le cycle réducteur, cette différenciation n'est plus possible, et ainsi  $\Phi_{MV^{\cdot+}}$ , mesuré est toujours supérieur ou égal à  $\Phi_{1/2 H_2}$ . Une autre explication, mais nettement moins plausible, consiste à supposer que le catalyseur jouerait un rôle secondaire non négligeable de capteur d'électrons par inhibition du sensibilisateur excité; une telle supposition, facilement vérifiable, doit être rejetée, étant donné que ce phénomène devrait se répéter pour d'autres systèmes étudiés suivant un mécanisme oxydatif et ayant une durée de vie de  $(RuL_3)^{2+}$  comparable.

Le tableau V montre que les rendements quantiques de la production de radical  $MV^{\cdot+}$  sont en général meilleurs si EDTA est substitué par TEOA. Sous ces nouvelles conditions (pH 8), la réduction de  $MV^{2+}$  par le TEOA oxydé [ $D^{\cdot+}$ , équations (4) ou (6)] semble avoir une plus grande importance<sup>14</sup>.

Tableau V. — Rendement quantique de production de radicaux  $MV^{\cdot+}$ ,  $\Phi_{MV^{\cdot+}}$ , à pH 8 (système:  $RuL_3^{2+}$ ,  $MV^{2+}$ , TEOA) et à pH 5 (système:  $RuL_3^{2+}$ ,  $MV^{2+}$ , EDTA).

$(RuL_3)^{2+}$	$\Phi_{MV^{\cdot+}}$ (TEOA) <sup>a</sup>	$\Phi_{MV^{\cdot+}}$ (EDTA) <sup>b</sup>
1	0,190 <sup>c</sup>	0,083
2	0,301	0,278
3	0,021	0,035
5	0,036	0,014
6	0,020 <sup>d</sup>	-

<sup>a</sup>  $5 \cdot 10^{-2}$  M TEOA;

<sup>b</sup>  $5 \cdot 10^{-2}$  M EDTA;

<sup>c</sup>  $2 \cdot 10^{-1}$  M TEOA et  $6 \cdot 10^{-2}$  M  $MV^{2+}$ , sans tampon<sup>10</sup>;

<sup>d</sup>  $6 \cdot 10^{-1}$  M TEOA et  $2 \cdot 10^{-2}$  M  $MV^{2+}$ , sans tampon<sup>10</sup>.

*En conclusion*, les nouveaux complexes de ruthénium que nous avons caractérisés sont des sensibilisateurs nettement moins efficaces du point de vue de la production d'hydrogène, que les composés pris comme références (1 et 2). Cette constatation se base sur la comparaison des rendements quantiques ( $\Phi_{MV^{\cdot+}}$  et  $\Phi_{1/2 H_2}$ ) déterminés dans les mêmes condi-

tions expérimentales. Quelques travaux ont pourtant démontré que dans des conditions spécifiques pour un sensibilisateur donné, ces rendements quantiques peuvent considérablement varier; ainsi, en utilisant des concentrations très élevées de TEOA (0,6 M), des rendements quantiques de formation de  $MV^{\cdot+}$  de 0,77<sup>10</sup> et de 0,44<sup>9</sup> ont été trouvés respectivement pour les composés 2 et 3. Par ailleurs, cette comparaison indique que pour un mécanisme réducteur,  $\Phi_{MV^{\cdot+}}$  dépend de la concentration de l'agent réducteur<sup>15</sup>, dépendance qui a été rapportée pour le système éosine/TEOA/ $MV^{2+}$ <sup>16</sup>.

De plus, des rendements quantiques les plus élevés ont été observés dans des systèmes non tamponnés, c'est-à-dire dans des conditions où le radical intermédiaire de TEOA formé dans la réaction (6) peut être déprotoné et peut réduire une autre molécule de  $MV^{2+}$ <sup>14</sup>.

#### Remerciements

Les auteurs remercient le professeur M. Grätzel pour la mise à disposition des installations de photolyse laser. G. D. a pu faire un stage à l'École Polytechnique Fédérale de Lausanne grâce à une bourse de l'European Photochemistry Association. J.-M. C. remercie le Fonds de l'industrie chimique de Bâle pour son aide financière. Les travaux à l'E.P.F.L. ont été soutenus par le Fonds National Suisse (projet n° 4.397-0.80.04).

#### RÉFÉRENCES

- (a) Creutz C., Sutin N., *Proc. Nat. Acad. Sc. U.S.A.*, 1975, 72, 2858; (b) Moradpour A., Amouyal E., Keller P., Kagan H. B., *Nouv. J. Chim.*, 1978, 2, 547; (c) Kalyanasundaram K., Kiwi J., Grätzel M., *Helv. Chim. Acta*, 1978, 61, 2720; (d) Amouyal E., Koffi P., *J. Photochem.*, sous presse, et références citées.
- Amouyal E., Zidler B., *Israel J. Chem.*, 1982, 22, 117.
- Dürr H., Dürr G., Zengerle K., Reis B., Braun A. M., *Chimia*, 1983, 37, 245.
- Dürr H., Dürr G., Zengerle K., Curchod J. M., Braun A. M., *Helv. Chim. Acta*, 1983, 66, 2652.
- Van Haute J., Watts R. J., *J. Amer. Chem. Soc.*, 1976, 98, 4853.
- Curchod J. M., Braun A. M., en préparation.
- Balzani V., Bolletta F., Gandolfi M. T., Maestri M., *Topics in Current Chem.*, 1978, 75, 1.
- Rillema D. P., Allen G., Meyer T. J., Conrad D., *Inorg. Chem.*, 1983, 22, 1617.
- Kitamura N., Kawanishi Y., Tazuke S., *Chem. Lett.*, 1983, 1185; *Chem. Phys. Lett.*, 1983, 97, 103.
- Crutchley R. J., Lever A. B. P., *J. Amer. Chem. Soc.*, 1980, 102, 7128.
- Curchod J. M., Braun A. M., Dürr H., en préparation.
- (a) Johansen O., Launikonis A., Loder J. W., Mau A. W. H., Sasse W. H. F., Swift J. D., Wells D., *Aust. J. Chem.*, 1981, 34, 981; (b) Keller P., Moradpour A., Amouyal E., Kagan H. B., *J. Mol. Catal.*, 1980, 7, 539.
- Keller P., Moradpour A., Amouyal E., Kagan H. B., *Nouv. J. Chim.*, 1980, 4, 377; (b) Miller D., McLendon G., *Inorg. Chem.*, 1981, 20, 950; (c) Brugger P. A., Thèse n° 431, E.P.F. Lausanne, 1982; (d) Mulazza Q. G., Venturi M., Hoffman M. Z., *J. Phys. Chem.*, 1985, 89, 722.
- Hoffman M. Z., Prasad D. R., Jones II G., Malba V., *J. Amer. Chem. Soc.*, 1983, 105, 6360.
- Miedler K., Das P. K., *J. Amer. Chem. Soc.*, 1982, 104, 7462.
- Misawa H., Sakuragi H., Usui Y., Tokumaru K., *Chem. Lett.*, 1983, 10.

---

## TECHNICAL REPORT

---

### Photocatalytic Water Cleavage – A Simple Device for H<sub>2</sub>-Measurement

Sunlight or artificial light sources can be used for photochemical water cleavage to produce hydrogen and oxygen. Such a system consists of a sensitizer, an electron relay, and a catalyst. In a sacrificial system an electron donor (or acceptor) has to be added. A system like that produces hydrogen which ought to be measured quantitatively. The electron donor is used up in the reaction in a stoichiometric way. To obtain reproducible results an especially designed apparatus is needed. We have constructed such a simple device (Figs. 1 and 2).

A Xenon lamp (a) is used as a light source mounted on an optical bench (b). The combination of this lamp and a cut-off filter (c) provides visible light. Hydrogen evolved by the reaction is collected in a burette (d) which is connected to a flask containing Kolbe's solution (e) by a hose. Since the volume of the gas evolved is highly temperature dependent, constant temperature is needed in the whole set up. To ensure this the whole photolysis vessel (f) is immersed in a thermostatted bath (g). Irradiation is effected through a glass window (h) in the surrounding vessel. The burette is mounted outside the vessel being connected to the photolysis cell via a glass capillary. Prior to irradiation the photolysis chamber is purged with nitrogen to reduce O<sub>2</sub> to a minimum. This can be done using the glass capillary connected with a stopcock (j) of the photolysis cell. Nitrogen gets out of the photolysis cell via the capillary (i) of the burette, which involves a three-way cock. The Pt-catalyst can be injected through a septum (k) mounted on the photolysis vessel. This can also be used for a qualitative test of the gas evolved, for instance to detect H<sub>2</sub>. Constant temperature is controlled by an externally operating thermostat. The thermostatted water enters via the outer region of the burette into the outer vessel. A stirrer (l) ensures the same temperature in the whole system as well as stirring of the solution in the reaction vessel. In order to fill the photolysis vessel, the water in the thermostatted bath can be drained by a stopcock. The reaction vessel has a volume of 20 ml. Using capillaries for all connections reduces the dead volume to a minimum.

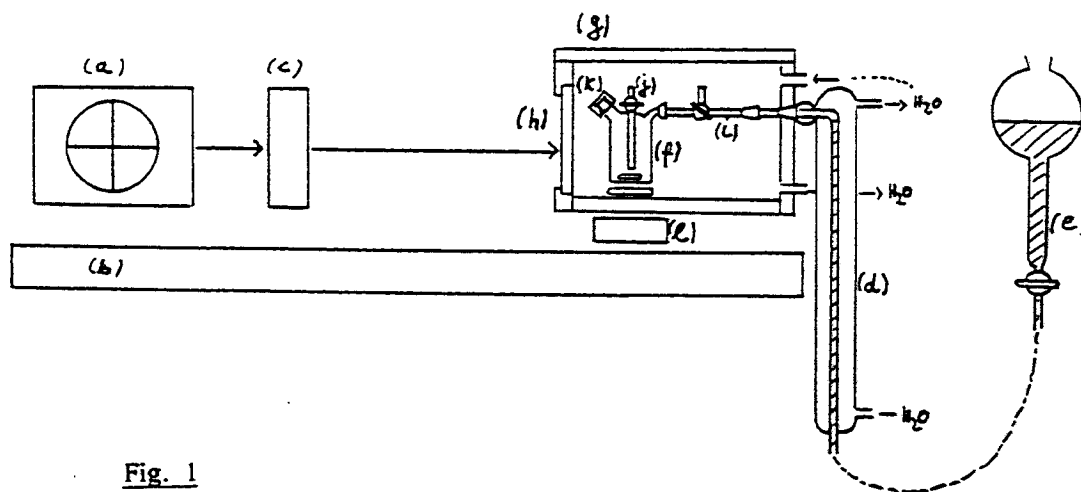


Fig. 1

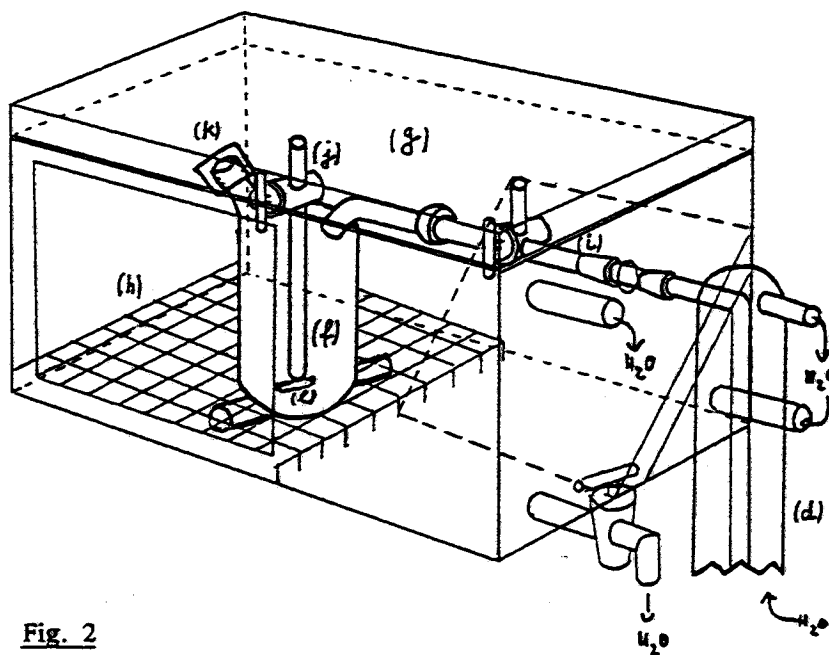


Fig. 2

- (a) Xenon lamp
- (b) optical bench
- (c) cut-off filter
- (d) burette
- (e) flask containing Kolbe's solution
- (f) photolysis cell

- (g) thermostatted bath
- (h) glass window
- (i) glass capillary
- (j) stopcock
- (k) septum
- (l) stirrer

H.Dürr, U.Thiery  
 FB 14 Organische Chemie, Universität des Saarlandes  
 D-6600 Saarbrücken  
 Fed. Rep. of Germany

received: 16.6.1986

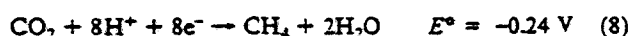
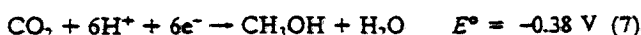
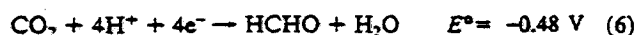
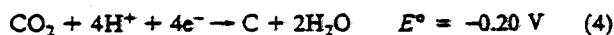
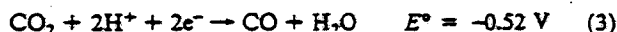
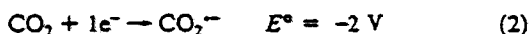
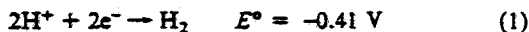
# Photosensitized Reduction of CO<sub>2</sub> to CH<sub>4</sub> and H<sub>2</sub> Evolution in the Presence of Ruthenium and Osmium Colloids: Strategies To Design Selectivity of Products Distribution<sup>1</sup>

Itamar Willner,<sup>\*†</sup> Ruben Maidan,<sup>†</sup> Daphna Mandler,<sup>†</sup> Heinz Dürr,<sup>‡</sup> Gisela Dörr,<sup>‡</sup> and Klaus Zengerle<sup>‡</sup>

Contribution from the Department of Organic Chemistry, The Hebrew University of Jerusalem, Jerusalem 91904, Israel, and Organische Chemie, Universität des Saarlandes, D-6000 Saarbrücken, Germany. Received March 5, 1987

**Abstract:** Photoreduction of CO<sub>2</sub> to methane and higher hydrocarbons is accomplished in aqueous solutions by using visible light and Ru or Os colloids as catalysts. One system is composed of Ru(II) tris(bipyridine), Ru(bpy)<sub>3</sub><sup>2+</sup>, as photosensitizer, triethanolamine, TEOA, as electron donor, and one of the following bipyridinium charge relays: *N,N'*-dimethyl-2,2'-bipyridinium, MQ<sup>2+</sup> (1), *N,N'*-trimethylene-2,2'-bipyridinium, TQ<sup>2+</sup> (2), *N,N'*-tetramethylene-2,2'-bipyridinium, DQ<sup>2+</sup> (3), or *N,N'*-bis-(3-sulfonatopropyl)-3,3'-dimethyl-4,4'-bipyridinium, MPVS<sup>0</sup> (4). Illumination of these systems under CO<sub>2</sub> in the presence of Ru or Os colloids results in the formation of methane and ethylene and in H<sub>2</sub> evolution. In the second system, illumination of an aqueous solution under CO<sub>2</sub> that includes Ru(II) tris(bipyrazine) as sensitizer, TEOA as electron donor, and the Ru colloids leads to the formation of methane, ethylene, and ethane, and no H<sub>2</sub> evolution occurs. The reduction process of CO<sub>2</sub> proceeds via electron transfer of metal-activated CO<sub>2</sub> rather than through a hydrogenation route. Detailed studies show that the H<sub>2</sub> evolution process can be inhibited by the addition of bipyrazine, while CO<sub>2</sub> reduction is inhibited in the presence of added thiols. Methanation of CO<sub>2</sub> by hydrogen proceeds in the dark in the presence of Pt and Ru or Os colloids and in the presence of MQ<sup>2+</sup> (1). The need for the electron relay implies that the methanation process occurs through an electron-transfer mechanism.

Photosensitized cleavage of water to hydrogen and oxygen and reduction of CO<sub>2</sub> to organic fuels are of substantial interest for the solar light-induced conversion of abundant materials to novel fuels.<sup>2,3</sup> Extensive efforts have been directed in recent years toward the development of photoinduced H<sub>2</sub> evolution systems.<sup>4-7</sup> Homogeneous photosensitizers such as Ru(II) tris(bipyridine), Ru(bpy)<sub>3</sub><sup>2+</sup>, or Zn porphyrins have been applied to photosensitize the reduction of various relay compounds that mediate H<sub>2</sub> evolution from aqueous solutions. For example, photoreduced *N,N'*-dialkyl-4,4'-bipyridinium radicals (viologen radicals), Co(III) sepulchurate, or Rh(bpy)<sub>3</sub><sup>3+</sup> mediate H<sub>2</sub> evolution from aqueous solutions in the presence of heterogeneous metal colloids such as Pt or Rh.<sup>8-10</sup> H<sub>2</sub> evolution has also been accomplished with semiconductor particles suspended in aqueous media in the form of powders or microheterogeneous colloids.<sup>11,12</sup> In these systems metals such as Pt or Rh immobilized on the particles catalyze H<sub>2</sub> evolution by conduction band electrons formed by excitation of the semiconductor. Several cyclic systems for the photocleavage of water have been reported,<sup>13,14</sup> although other studies questioned the cyclic activity of the systems.<sup>15</sup> Recent efforts were also directed toward the photoreduction of CO<sub>2</sub> to organic fuels.<sup>16-21</sup> Reduction of CO<sub>2</sub> might proceed to various products (eq 1-8).



The standard redox potentials of these reactions at pH 7 are given in the respective equations<sup>16,22</sup> and compared to that of H<sub>2</sub> evolution. It can be seen that, while the single-electron reduction

potential of CO<sub>2</sub> (eq 2) exhibits an extreme value, the multielectron reduction potentials of CO<sub>2</sub> to CO, formate, formaldehyde, and methanol exhibit comparable values to that of the H<sub>2</sub> evolution process. Furthermore, the reduction potential of CO<sub>2</sub> to CH<sub>4</sub> is thermodynamically more feasible than that required to reduce protons to H<sub>2</sub>. Nevertheless, despite the thermodynamic feasibility to reduce CO<sub>2</sub>, we anticipate kinetic difficulties in accomplishing

(1) For a preliminary report see: Maidan, R.; Willner, I. *J. Am. Chem. Soc.* 1986, 108, 8100-8101.

(2) Grätzel, M., Ed. *Energy Resources through Photochemistry and Catalysis*; Academic: New York, 1983.

(3) Calvin, M. *Acc. Chem. Res.* 1978, 11, 369-374.

(4) Harriman, A.; West, M. E., Eds. *Photogeneration of Hydrogen*; Academic: London, 1983.

(5) Sutin, N.; Creutz, C. *Pure Appl. Chem.* 1980, 52, 2717-2738.

(6) Grätzel, M. *Acc. Chem. Res.* 1981, 14, 376-384.

(7) Bard, A. J. *Science (Washington, D.C.)* 1980, 207, 139-144.

(8) (a) Kalyanasundaram, K.; Kiwi, J.; Grätzel, M. *Helv. Chim. Acta* 1978, 61, 2720-2730. (b) Moradpour, A.; Amouyal, E.; Keller, P.; Kagas, H. *Nouv. J. Chim.* 1978, 2, 547-549.

(9) Houlding, V.; Geiger, T.; Kolle, U.; Grätzel, M. *J. Chem. Soc., Chem. Commun.* 1982, 681-683.

(10) Kirch, M.; Lehn, J.-M.; Sauvage, J. P. *Helv. Chim. Acta* 1979, 62, 1345-1384.

(11) Reber, J.-F.; Meier, K. *J. Phys. Chem.* 1984, 88, 5903-5913.

(12) (a) Duonghong, D.; Borgarello, E.; Grätzel, M. *J. Am. Chem. Soc.* 1981, 103, 4685-4690. (b) Tricot, Y.-M.; Fendler, J. H. *J. Am. Chem. Soc.* 1984, 106, 7359-7366.

(13) Borgarello, E.; Kiwi, J.; Pelizzetti, E.; Visca, M.; Grätzel, M. *Nature (London)* 1981, 289, 158-160.

(14) Lehn, J.-M.; Sauvage, J.-P.; Ziessel, R. *Nouv. J. Chim.* 1980, 4, 623-627.

(15) Magliozzo, R. S.; Krasna, A. I. *Photochem. Photobiol.* 1983, 43, 15-21.

(16) (a) Lehn, J.-M.; Ziessel, R. *Proc. Natl. Acad. Sci. U.S.A.* 1982, 79, 701-704. (b) Ziessel, R.; Hawecker, J.; Lehn, J.-M. *Helv. Chim. Acta* 1980, 63, 1065-1084. (c) Hawecker, J.; Lehn, J.-M.; Ziessel, R. *J. Chem. Soc., Chem. Commun.* 1983, 536-538. (d) Hawecker, J.; Lehn, J.-M.; Ziessel, R. *Helv. Chim. Acta* 1986, 69, 1990-2012.

(17) Tazuke, S.; Kitamura, N. *Nature (London)* 1978, 275, 501-502.

(18) Legros, B.; Soumillion, J. Ph. *Tetrahedron Lett.* 1985, 26, 121-122.

(19) Hawecker, J.; Lehn, J.-M.; Ziessel, R. *J. Chem. Soc., Chem. Commun.* 1985, 56-58.

(20) Halmann, M. *Nature (London)* 1978, 275, 115-116.

(21) Willner, I.; Mandler, D.; Riklin, A. *J. Chem. Soc., Chem. Commun.* 1986, 1022-1024.

(22) (a) Halmann, M.; Aurián-Blajeni, B. Proceedings of the Seventh European Community Photovoltaic Solar Energy Conference, West Berlin, Federal Republic of Germany, 1979; pp 682-689. (b) Bard, A. J. *J. Electroanal. Chem.* 1977, 103, 1-12.

(23) *Encyclopedia of Electrochemistry of the Elements*; Dekker: New York, 1973; Vol. 7.

\*The Hebrew University of Jerusalem.

†Universität des Saarlandes.

processes due to the need to pursue multielectron reduction reactions. Thus, reduction of CO<sub>2</sub> in aqueous solutions is expected to be accompanied, or eventually obscured, by the kinetically favored H<sub>2</sub> evolution.

Several recent studies have explored the photoinduced fixation of CO<sub>2</sub>. Photoreduction of CO<sub>2</sub> to CO (eq 3) has been reported by Lehn and co-workers<sup>16</sup> in two different systems using Re(bpy)<sub>3</sub>(CO)<sub>2</sub>Cl as photocatalyst or using Ru(II) tris(bipyridine), Ru(bpy)<sub>3</sub><sup>2+</sup>, as sensitizer and cobalt(II) chloride as electron relay. In the latter system H<sub>2</sub> evolution is accompanied by CO<sub>2</sub> reduction. Photoreduction of CO<sub>2</sub> to formate (eq 5) has been claimed by Mizuki,<sup>17</sup> but later studies questioned the formation of formate by CO<sub>2</sub> reduction.<sup>18</sup> Reduction of CO<sub>2</sub> to HCO<sub>2</sub><sup>-</sup> has been reported by Lehn<sup>19</sup> using Ru(bpy)<sub>3</sub><sup>2+</sup> as photosensitizer in a dimethylformamide-triethanolamine-aqueous medium that contains CO<sub>2</sub>.

Fixation of CO<sub>2</sub> to various organic fuel products in very low yields has been reported by use of semiconductors.<sup>20</sup> We have recently reported on the specific photosensitized fixation of CO<sub>2</sub> to organic acids or formate using enzymes as specific CO<sub>2</sub>-fixation catalysts.<sup>21</sup> Similarly, in a primary note we have exemplified the application of Ru colloids as catalysts for the photoreduction of CO<sub>2</sub> to methane.<sup>1</sup>

Here we describe the photosensitized fixation of CO<sub>2</sub> to CH<sub>4</sub> and higher hydrocarbons using visible light. In these systems Ru and Os colloids act as CO<sub>2</sub>-fixation catalysts. We discuss two different systems for the reduction of CO<sub>2</sub> to CH<sub>4</sub>. One system involves the primary photosensitized reduction of *N,N'*-bipyridinium charge relays that mediate CO<sub>2</sub> reduction and H<sub>2</sub> evolution in the presence of Ru and Os colloids. The second system involves the selective reduction of CO<sub>2</sub> to CH<sub>4</sub> by using photogenerated Ru(I) tris(bipyridine) and a Ru metal catalyst. We also provide means to control the selectivities of CO<sub>2</sub> reduction vs. H<sub>2</sub> evolution by proper additives. As far as we are aware, these systems are the first examples for the photoinduced reduction of CO<sub>2</sub> to CH<sub>4</sub>.

### Experimental Methods

Absorption spectra were recorded with a Uvikon-860 (Kontron) spectrophotometer. Gas chromatography analyses were performed with a Packard 427 instrument (thermal conductivity detector) for H<sub>2</sub> analysis and Tracor 540 gas chromatograph (flame ionization detector) for methane, ethane, and ethylene analysis. For H<sub>2</sub> separation a 5-Å MS column and argon as the carrier gas were used. For hydrocarbon analysis a Porapak T-column and nitrogen as the carrier gas were used. Size and shape of Ru and Os colloids were determined with a Jeol 200 CX electron microscope. Elementary composition of particles was determined with a Link 860 energy-dispersion system. Atomic absorption measurements were carried out with a Perkin-Elmer 403 spectrophotometer. Continuous illuminations were performed with 150-W xenon arc lamps (PTI). Laser flash experiments were performed on a DL 200 (Molelectron) dye laser pumped by a UV-IU nitrogen laser (Molelectron). Flashes were recorded on a Biomation 8100, and pulse collection was carried out with a Nicolet 1170.

**Preparation of Metal Colloids.** Colloids were prepared by the reduction of the respective metal salts with citrate as reducing agent.<sup>22</sup> A 0.1% sodium citrate solution, 100 mL, that contains RuCl<sub>3</sub>, 16 mg, or OsO<sub>4</sub>, 15 mg, was heated to 100 °C overnight. The resulting colloid suspensions were centrifuged and dialyzed. Metal content of colloid suspension was determined by atomic absorption to be 60 mg L<sup>-1</sup> for Ru colloid and 95 mg L<sup>-1</sup> for Os colloid. The mean diameter of colloid particles was estimated by EM to be 400 Å for Ru colloid and 50 Å for Os colloid. An alternative procedure for the preparation of the Ru colloid involves the photochemical reduction of K<sub>3</sub>RuCl<sub>6</sub>. This colloid exhibits improved catalyst activity toward reduction of CO<sub>2</sub> to CH<sub>4</sub>. A 3-mL bicarbonate aqueous solution, pH 7.8, that includes Ru(II) tris(bipyridine), Ru(bpy)<sub>3</sub><sup>2+</sup>, 1 × 10<sup>-4</sup> M, K<sub>3</sub>RuCl<sub>6</sub>, 2 × 10<sup>-4</sup> M, and triethanolamine, 0.1 M, was illuminated for 20 min with a 150-W xenon arc lamp. To the resulting suspension a mixed-bed ion exchanger (Amberlite MB-3) was added to exclude all ions, and the colloid was filtered off. The mean diameter of the resulting colloid is estimated by EM to be 100 Å. *N,N'*-Dimethyl-2,2'-bipyridinium, MQ<sup>2+</sup> (1), *N,N'*-trimethylene-2,2'-bipyridinium, TQ<sup>2+</sup> (2), and *N,N'*-tetramethylene-2,2'-bipyridinium,

DQ<sup>2+</sup> (3), were prepared according to literature procedures.<sup>24</sup> *N,N'*-Bis(3-sulfonatopropyl)-3,3'-dimethyl-4,4'-bipyridine, MPVS<sup>9</sup> (4), was prepared by the reaction of 3,3'-dimethyl-4,4'-bipyridine with 1,3-propanesultone. To 100 mg of 3,3'-dimethyl-4,4'-bipyridine<sup>25</sup> was added 390 mg of 1,3-propanesultone. The resulting mixture was heated to 120 °C for 15 min without solvent under nitrogen. To the resulting semisolid was added 5 mL of DMF, and heating at 120 °C was continued for 3 h. After cooling, the white precipitate of 4 was filtered and washed three times with acetone; yield 89%. The product gave satisfactory elementary analysis.

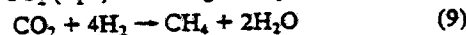
Continuous-illumination experiments were performed in a glass cuvette equipped with a valve and stopper. Samples of 3 mL each contained a ruthenium or osmium colloid, 20 mg/L; TEOA, 1.0 × 10<sup>-1</sup> M; NaHCO<sub>3</sub>, 5.0 × 10<sup>-2</sup> M; Ru(bpy)<sub>3</sub><sup>2+</sup>, 1.0 × 10<sup>-4</sup> M or Ru(bpy)<sub>3</sub><sup>2+</sup>, 1.4 × 10<sup>-4</sup> M; and one of the electron relays (MQ<sup>2+</sup>, TQ<sup>2+</sup>, DQ<sup>2+</sup>, or MPVS<sup>9</sup>), 1.4 × 10<sup>-3</sup> M; at pH 7.8 under a CO<sub>2</sub> atmosphere. Gas samples were taken out from the cuvette at time intervals of illumination and analyzed by the respective gas chromatography analyses.

Methane and hydrogen inhibition experiments were performed in similar cuvettes on 3-mL samples containing the ruthenium colloid, 20 mg/L; EDTA, 3.3 × 10<sup>-2</sup> M; NaHCO<sub>3</sub>, 5.0 × 10<sup>-2</sup> M; Ru(bpy)<sub>3</sub><sup>2+</sup>, 1.4 × 10<sup>-4</sup> M; and MQ<sup>2+</sup>, 1.0 × 10<sup>-3</sup> M; at pH 6.0 under a CO<sub>2</sub> atmosphere. The rates of formation of methane and hydrogen were followed at different bipyridine or 1,4-dimercapto-2,3-butanediol, dithiothreitol (DTT), concentrations.

Dark reduction of CO<sub>2</sub> was performed in a glass pressure-resistant reaction flask connected through a pressure gauge to a manifold enabling accurate control of the gaseous atmosphere composition. In a typical experiment, a solution containing Ru and Pt colloids, 20 mg/L each, NaHCO<sub>3</sub>, 5.0 × 10<sup>-2</sup> M, and MQ<sup>2+</sup>, 1.0 × 10<sup>-2</sup> M, was stirred under 0.75 atm of CO<sub>2</sub> and 0.75 atm of H<sub>2</sub>. Under these conditions methane and ethylene were formed as assayed by GC analysis. Exclusion of the relay from the reaction yielded no products.

### Results and Discussion

Photoreduction of *N,N'*-dialkylbipyridinium salts<sup>1,26</sup> in the presence of Ru(bpy)<sub>3</sub><sup>2+</sup>, metalloporphyrins, and organic dyes<sup>27</sup> in the presence of sacrificial electron donors and the subsequent evolution of H<sub>2</sub> with metal colloids<sup>3-10</sup> have been studied extensively. Various organometallic complexes such as Co(II) porphyrins<sup>28</sup> or Co and Ni macrocyclic complexes<sup>29</sup> exhibit catalytic activity in the electrochemical reduction of CO<sub>2</sub>. Nevertheless, the electrocatalytic potentials are usually far from being adequate to be applied in the photosensitized reduction of CO<sub>2</sub>. Ruthenium and osmium metals are used<sup>30,31</sup> as heterogeneous catalysts in the methanation of CO<sub>2</sub> (eq 9). Although this process proceeds at



elevated temperatures and pressures, it suggests that these metals activate CO<sub>2</sub> toward reduction. Recent electrochemical studies by Frese<sup>32</sup> have revealed that Ru electrodes catalyze the electrochemical reduction of CO<sub>2</sub> to CH<sub>4</sub> (eq 8). In these studies CO<sub>2</sub> reduction to CH<sub>4</sub> has been accomplished in aqueous solutions (pH 4.2–6.8) at electrode potentials (*E*<sup>0</sup>) as low as -0.55 V vs. SCE. Together with CO<sub>2</sub> reduction to CH<sub>4</sub>, hydrogen evolution is observed as well as reduction of CO<sub>2</sub> to CO. Thus, we have decided to examine the photosensitized reduction of CO<sub>2</sub> to methane in the presence of Ru and Os colloids.

(24) Homer, R. F.; Tomlinson, T. E. *J. Chem. Soc.* 1960, 2498–2503.

(25) Stoehr, C.; Wagner, M. *J. Prakt. Chem.* 1893, 48, 1–23.

(26) Amouyal, E.; Zidler, B.; Keller, P.; Moradpour, A. *Chem. Phys. Lett.* 1980, 74, 314–317.

(27) (a) Bock, C. R.; Meyer, T. J.; Whitten, D. G. *J. Am. Chem. Soc.* 1974, 96, 4710–4712. (b) Kalyanasundaram, K.; Grätzel, M. *Helv. Chim. Acta* 1980, 63, 478–485. (c) Krasna, A. I. *Photochem. Photobiol.* 1979, 29, 267–276.

(28) Takahashi, K.; Hiratsuka, K.; Sasaki, H.; Toshima, S. *Chem. Lett.* 1979, 305–308.

(29) (a) Fisher, B.; Eisenberg, R. *J. Am. Chem. Soc.* 1980, 102, 7361–7363. (b) Beley, M.; Collin, J.-P.; Ruppert, R.; Sauvage, J.-P. *J. Chem. Soc., Chem. Commun.* 1984, 1315–1316. (c) Pearce, D. J.; Pletcher, D. J. *Electroanal. Chem. Interfacial Electrochem.* 1986, 197, 317–330.

(30) (a) Solymosi, F.; Erdohelyi, A.; Kocsis, M. *J. Chem. Soc., Faraday Trans. 1* 1981, 77, 1003–1012. (b) Solymosi, F.; Erdohelyi, A. *J. Mol. Catal.* 1980, 8, 471–474. (c) Lunde, P. J.; Kester, F. L. *J. Catal.* 1973, 30, 423–429.

(31) (a) Yasukatsu, T.; Watanabe, H.; Akira, T. *Carbon* 1977, 15, 103–106. (b) Moggi, P.; Albanesi, G.; Predieri, G.; Sapa, E. *J. Organomet. Chem.* 1983, 252, C89–C92.

(32) Frese, K. W., Jr.; Leach, S. J. *Electrochem. Soc.* 1985, 135, 259–260.

(23) Furlong, D. N.; Launikonis, A.; Sasse, W. H. F.; Sanders, J. V. *J. Chem. Soc., Faraday Trans. 1* 1984, 80, 571–588.



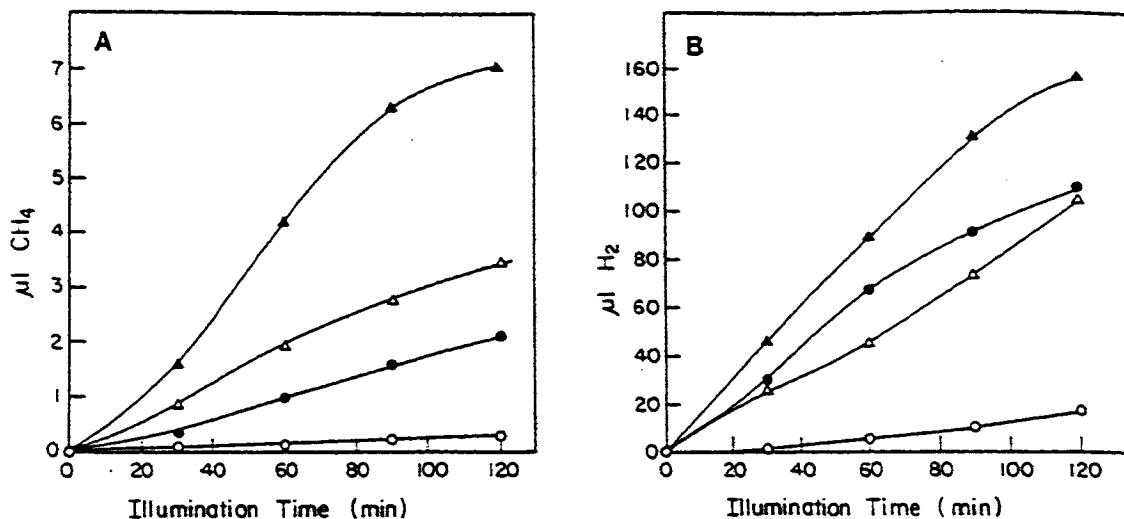
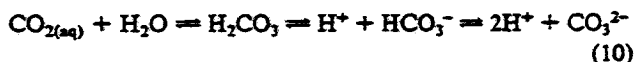
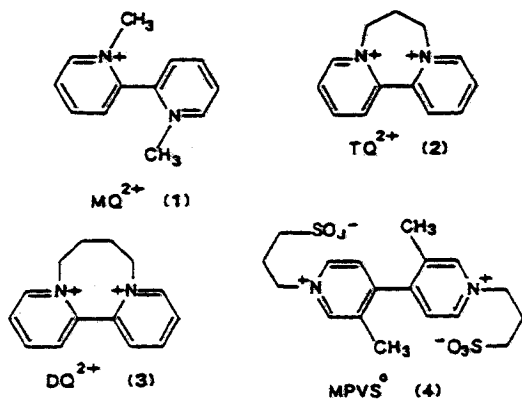


Figure 1. Rate of photosensitized  $\text{CH}_4$  formation (A) and  $\text{H}_2$  evolution (B) in the presence of the various charge relays and Ru colloid:  $[\text{Ru}(\text{bpy})_3]^{2+} = 1.4 \times 10^{-4} \text{ M}$ ,  $[\text{relay}] = 1.4 \times 10^{-3} \text{ M}$ ,  $[\text{TEOA}] = 1.0 \times 10^{-1} \text{ M}$ ,  $[\text{NaHCO}_3] = 5.0 \times 10^{-2} \text{ M}$ ,  $[\text{Ru colloid}] = 20 \text{ mg/L}$ , pH 7.8 under  $\text{CO}_2$  atmosphere. Key: ( $\Delta$ )  $\text{MQ}^{2+}$ ; ( $\bullet$ )  $\text{DQ}^{2+}$ ; ( $\circ$ )  $\text{TQ}^{2+}$ ; ( $\blacktriangle$ )  $\text{MPVS}^0$ .

**Photosensitized  $\text{H}_2$  Evolution and  $\text{CO}_2$  Reduction Using Bipyridinium Electron Relays.** The reduction potentials for  $\text{H}_2$  evolution and  $\text{CO}_2$  reduction depend on the pH of the aqueous media. Both of the processes are thermodynamically favored as the pH of the aqueous solution decreases. Yet, the reduction potentials for  $\text{H}_2$  formation decline to more positive values sharper than those of  $\text{CO}_2$  as the pH of the solution decreases.<sup>33</sup> Thus, to thermodynamically favor  $\text{CO}_2$  reduction over  $\text{H}_2$  evolution, it is advantageous to perform the reactions in basic aqueous media. However, since  $\text{CO}_2$  in aqueous solutions exhibits complex equilibria with  $\text{HCO}_3^-$  and  $\text{CO}_3^{2-}$  (eq 10) that are strongly affected by the pH, one is limited to the region employed. We have examined the photosensitized reduction of  $\text{CO}_2$  in aqueous solutions at pH 7.8 where  $\text{CO}_2$  consists of 3% of the total carbon dioxide introduced that corresponds to  $11.2 \mu\text{M}$ .<sup>34</sup>



We have studied the  $\text{CO}_2$ -reduction and  $\text{H}_2$ -evolution processes in aqueous solutions where photosensitized electron-transfer reactions result in reduced bipyridinium radical relays. In these systems Ru(II) tris(bipyridine) is used as photosensitizer and triethanolamine, TEOA, as sacrificial electron donor. As charge relays we have applied *N,N'*-dimethyl-2,2'-bipyridinium,  $\text{MQ}^{2+}$  (1), *N,N'*-trimethylene-2,2'-bipyridinium,  $\text{TQ}^{2+}$  (2), *N,N'*-tetra-



methylene-2,2'-bipyridinium,  $\text{DQ}^{2+}$  (3), or *N,N'*-bis(3-sulfonatopropyl)-3,3'-dimethyl-4,4'-bipyridinium,  $\text{MPVS}^0$  (4).

One of the colloids, Os or Ru, is included in the systems as a  $\text{CO}_2$ -reduction or a  $\text{H}_2$ -evolution catalyst. These charge relays were selected since their reduced forms exhibit more negative reduction potentials than *N,N'*-dialkyl-4,4'-bipyridinium (viologen) radicals. Previous studies have indicated that the reduction potentials of bipyridinium salts  $[E^\circ(\text{V}^{\bullet-}/\text{V}^{2+})]$ , are strongly affected by steric interactions in the molecular structure.<sup>35</sup> Reduction of the bipyridinium salts tends to bring the two pyridine rings into a planar structure to gain effective  $\pi$ - $\pi$  overlap and resonance delocalization. Hence, substitution of the ortho positions in the bipyridine structure distorts the two rings from planarity. Consequently, their reduction is more difficult, and the reduced form exhibits more negative reduction potentials as compared to the sterically unhindered relays. For example, the reduction potential of *N,N'*-bis(3-sulfonatopropyl)-4,4'-bipyridinium, PVS (5), corresponds<sup>36</sup> to  $E^\circ(\text{PVS}^{\bullet-}/\text{PVS}^0) = -0.41 \text{ V}$ , and introduction of the two methyl groups in the ortho positions to obtain the relay 4 introduces sufficient steric hindrance to decrease the reduction potential to the value of  $E^\circ(\text{MPVS}^{\bullet-}/\text{MPVS}^0) = -0.79 \text{ V}$ . The reduction potentials of the various relays used in our studies are summarized in Table I.

Illumination of these systems with visible light ( $\lambda > 400 \text{ nm}$ ) under a gaseous atmosphere of  $\text{CO}_2$  results in the formation of methane and ethylene,  $\text{C}_2\text{H}_4$ , as well as the evolution of  $\text{H}_2$ . Figure 1 shows the rates of  $\text{CH}_4$  formation and  $\text{H}_2$  evolution by the different relays and Ru colloid as catalyst for the reaction. Figure 2 exemplifies the rates of formation of  $\text{CH}_4$  and  $\text{C}_2\text{H}_4$  as a function of illumination time with MPVS as relay and Os as catalyst. The quantum yields for the formation of the various products with the different electron relays and the Os and Ru colloids as catalysts are summarized in Table I. It is evident that the yields of  $\text{H}_2$ -evolution and  $\text{CO}_2$ -reduction products increase as the reduction potentials of the relay is more negative. For example, by using the Ru colloid and MPVS as relay ( $E^\circ = -0.79 \text{ V}$ ), the quantum yields for  $\text{H}_2$  evolution and  $\text{CH}_4$  formation are  $\phi(\text{H}_2) = 2.6 \times 10^{-3}$  and  $\phi(\text{CH}_4) = 5.7 \times 10^{-4}$ , while with the relay TQ ( $E^\circ = -0.55 \text{ V}$ ) the respective quantum yields correspond to  $\phi(\text{H}_2) = 2.8 \times 10^{-4}$  and  $\phi(\text{CH}_4) = 2.0 \times 10^{-5}$ . When argon is used as the gaseous atmosphere instead of  $\text{CO}_2$ , only  $\text{H}_2$  evolution is observed. The quantum yields for  $\text{H}_2$  evolution in the presence of the different relays and metal catalysts are also summarized in Table I. Control experiments reveal that all of the components included in the systems are essential for  $\text{H}_2$  evolution as well as for  $\text{CO}_2$ -reduction. Exclusion of either the electron donor, charge relay or catalyst prohibits any photoproduct formation. Furthermore

(33) Keene, F. R.; Creutz, C.; Sutin, N. *Coord. Chem. Rev.* 1985, 64, 247-260.

(34) Asada, K. In *Organic and Bio-organic Chemistry of Carbon Dioxide*; Inoue, S., Yamazaki, N., Eds.; Kodansha: Tokyo, 1982.

(35) (a) Hünig, S.; Gross, J.; Schenk, W. *Justus Liebig's Ann. Chem.* 1967, 324-338. (b) Hünig, S.; Gross, J. *Tetrahedron Lett.* 1968, 2509-2512.

(36) Degani, Y.; Willner, I. *J. Am. Chem. Soc.* 1983, 105, 222-223.

Table I. Quantum Yields for H<sub>2</sub> Evolution and Hydrocarbon Formation in the Presence of Different Relays and Ru or Os Colloids as Catalysts<sup>a</sup>

relay	E <sup>0</sup> , V vs. SHE <sup>b,c</sup>	Ru colloid catalyst			Os colloid catalyst		
		10 <sup>3</sup> φ(H <sub>2</sub> )	10 <sup>3</sup> φ(CH <sub>4</sub> )	10 <sup>3</sup> φ(C <sub>2</sub> H <sub>4</sub> )	10 <sup>3</sup> φ(H <sub>2</sub> )	10 <sup>3</sup> φ(CH <sub>4</sub> )	10 <sup>3</sup> φ(C <sub>2</sub> H <sub>4</sub> )
MPVS <sup>0</sup>	-0.79	2.6 (80) <sup>d</sup>	5.7 (4.3)	1.9 (0.1)	1.9 (58)	2.1 (1.6)	1.04 (0.05)
MQ <sup>2+</sup>	-0.72	1.7 (51)	2.3 (1.7)	0.73 (0.03)	3.0 (91)	0.52 (0.4)	0.29 (0.014)
DQ <sup>2+</sup>	-0.65	1.8 (56)	1.4 (1.1)	1.08 (0.05)	9.2 (270)	0.61 (0.5)	0.67 (0.03)
TQ <sup>2+</sup>	-0.55	0.28 (8)	0.20 (0.15)	0.18 (0.01)	0.64 (19)	0.12 (0.1)	0.15 (0.008)

<sup>a</sup>In all systems [Ru(bpy)<sub>3</sub><sup>2+</sup>] = 1.4 × 10<sup>-4</sup> M, [TEOA] = 1 × 10<sup>-1</sup> M, [relay] = 1.4 × 10<sup>-3</sup> M, aqueous 0.1 M bicarbonate solution under CO<sub>2</sub>, <sup>b</sup>H. S. Kalyanasundaram, K. Coord. Chem. Rev. 1982, 46, 159-244. <sup>c</sup>Furlong, D. N.; Johansen, O.; Launikonis, A.; Loder, J. W.; Mau, A. H.; Sasse, W. H. F. Aust. J. Chem. 1985, 38, 363-367. <sup>d</sup>In parentheses volume (μL) of products formed per hour.

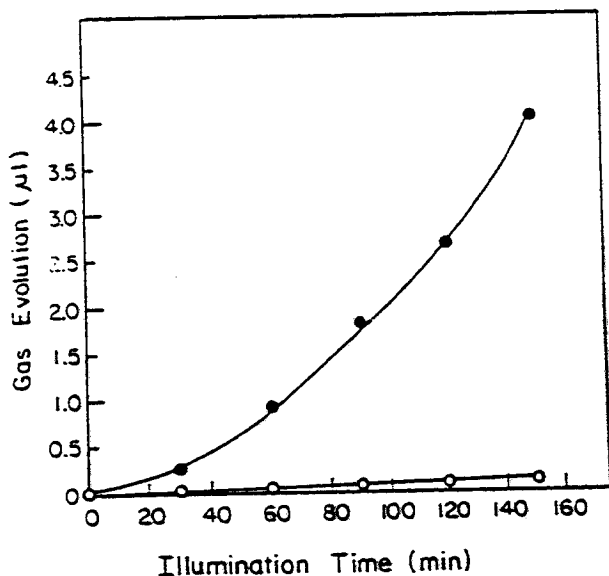


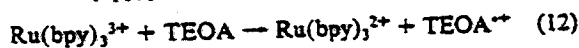
Figure 2. Yield of methane and ethylene formation as a function of illumination time with MPVS<sup>0</sup> as relay and Os colloid as catalyst: [Ru(bpy)<sub>3</sub><sup>2+</sup>] = 1.4 × 10<sup>-4</sup> M, [MPVS] = 1.4 × 10<sup>-3</sup> M, [TEOA] = 1.0 × 10<sup>-1</sup> M, [NaHCO<sub>3</sub>] = 5.0 × 10<sup>-2</sup> M, [Os colloid] = 20 mg/L, pH 7.8 under CO<sub>2</sub> atmosphere. Key: (●) methane; (○) ethylene.

other metal catalysts such as Pt or Pd are inactive toward the reduction of CO<sub>2</sub>, and only H<sub>2</sub> evolution is observed. Also, substitution of the charge relays by N,N'-dimethyl-4,4'-bipyridinium (methylviologen, MV<sup>2+</sup>) does not yield the reduction of CO<sub>2</sub>, and the blue radical cation (MV<sup>•+</sup>) is accumulated.

The lack of H<sub>2</sub> evolution and CH<sub>4</sub> formation with MV<sup>2+</sup> as charge relay suggests that the reduced relay MV<sup>•+</sup> does not exhibit the reduction potential required to evolve H<sub>2</sub> from the basic aqueous medium (pH 7.8) or to reduce metal-activated CO<sub>2</sub>.

The results clearly indicate that the photosensitized electron-transfer reaction leads to the reduction of CO<sub>2</sub> to methane and higher hydrocarbons. Thus, Ru and Os colloids are indeed heterogeneous catalysts that activate CO<sub>2</sub> toward the reduction. Nevertheless, the reduction of CO<sub>2</sub> in the aqueous media is nonspecific, and substantial amounts of H<sub>2</sub> are evolved. In fact H<sub>2</sub> evolution is the predominant product in the photosensitized transformations.

The mechanism that leads to H<sub>2</sub> evolution is well established.<sup>29</sup> It involves the oxidative quenching via electron transfer of the excited sensitizer Ru(bpy)<sub>3</sub><sup>2+</sup> by the relay (R<sup>2+</sup>), followed by charge separation (eq 11 and 12). Oxidation of the electron donor



TEOA by the oxidized sensitizer recycles the light-active compound, and the reduced relay is accumulated. Electron transfer from the reduced relay to the metal catalyst charges the colloid, and in the presence of protons, metal-bound H atoms are formed and their dimerization leads to H<sub>2</sub> evolution.<sup>37</sup> Figure 3 schematically represents the H<sub>2</sub>-evolution process. The fact that Ru

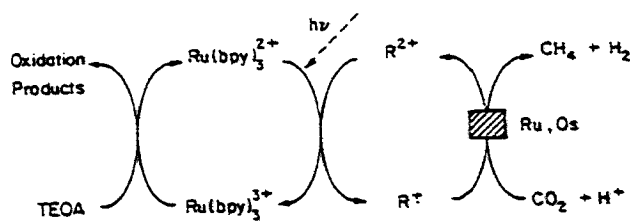
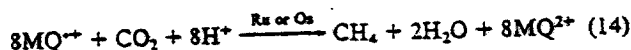
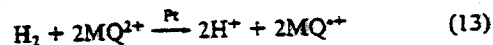


Figure 3. Schematic cycle for photosensitized H<sub>2</sub> evolution and CO<sub>2</sub> reduction using bipyridinium electron relays (R<sup>2+</sup>).

or Os colloids are essential catalysts for the reduction of CO<sub>2</sub> clearly indicates that CO<sub>2</sub> interacts with the metal surface and that it is activated toward the reduction process. The reduction might proceed via two alternative mechanisms: (i) hydrogenation of metal-activated CO<sub>2</sub> via in situ generated H atoms that lead to the methanation process (eq 9) [Similar photoinduced hydrogenation reactions and utilization of in situ generated hydrogen atoms have been exemplified with unsaturated substrates, i.e. ethylene and acetylene, and heterogeneous Pt or Pd colloids.<sup>37</sup>] and (ii) direct reduction of metal-activated CO<sub>2</sub> via electron transfer from the charge relay, independent to the H<sub>2</sub>-evolution system (Figure 3).

Dark experiments exclude the hydrogenation pathway as the mechanistic route for the reduction of CO<sub>2</sub> to CH<sub>4</sub> and imply that the reduction process proceeds through electron transfer from the reduced relay. In these experiments an aqueous bicarbonate solution (pH 7.8) that included the Ru or Os colloid was stirred in a sealed flask under a gaseous atmosphere that included H<sub>2</sub> (0.75 atm) and CO<sub>2</sub> (0.75 atm), and no hydrocarbons have been detected. Similarly, addition of the charge relay MQ<sup>2+</sup> to the system did not lead to any hydrocarbon products. Yet, addition of a Pt colloid to the system that included either Ru or Os colloid and the charge relay, MQ<sup>2+</sup>, resulted in the formation of methane and ethylene (C<sub>2</sub>H<sub>4</sub>). In a control experiment where MQ<sup>2+</sup> was excluded from the system, and Ru or Os and Pt colloids were present, no reduction of CO<sub>2</sub> occurred. Similarly, when the Ru or Os colloids were excluded and the Pt colloid and MQ<sup>2+</sup> were present, only MQ<sup>•+</sup> was formed and no CO<sub>2</sub>-reduction products were formed. This set of dark experiments clearly indicate that the reduction of CO<sub>2</sub> to hydrocarbons proceeds via electron transfer rather than through the hydrogenation route. The primary step involves the Pt-catalyzed reduction of the charge relay MQ<sup>2+</sup> (eq 13). The generation of the reduced relay, MQ<sup>•+</sup>, allows the subsequent reduction of Ru or Os metal-activated CO<sub>2</sub> to methane and higher hydrocarbons (eq 14).



It should be noted that these control dark reactions suggest a new important route for the methanation process of CO<sub>2</sub> (eq 9). At present, the reaction conditions using H<sub>2</sub> and CO<sub>2</sub> require high pressures and elevated temperatures.<sup>30,31</sup> Our results indicate that addition of an electron relay and proper electron-transfer mediating catalysts affects the process at an ambient temperature and low pressure.

**Photoreduction of CO<sub>2</sub> with Ru(bpy)<sub>3</sub><sup>2+</sup> as Photosensitizer.** The results discussed until now demonstrate that H<sub>2</sub> evolution occurs concomitantly to CO<sub>2</sub> reduction and the former process is the

(37) Degani, Y.; Willner, I. J. Chem. Soc., Perkin Trans. 2 1986, 37-41.

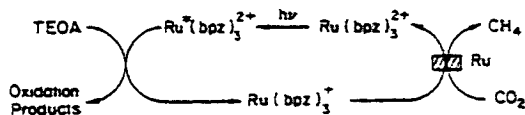


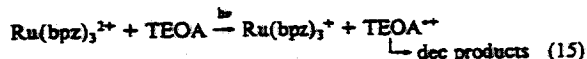
Figure 4. Schematic cycle for photosensitized reduction of  $\text{CO}_2$  to  $\text{CH}_4$  using  $\text{Ru}(\text{bpz})_3^{2+}$  as sensitizer.

Table II. Quantum Yields and Turnover Numbers (TN) for Hydrocarbon Formation Using  $\text{Ru}(\text{bpz})_3^{2+}$

system <sup>a</sup>	$\phi(\text{CH}_4)$	$\phi(\text{C}_2\text{H}_4)$	$\phi(\text{C}_2\text{H}_6)$	TN[ $\text{Ru}(\text{bpz})_3^{2+}$ ]
I	$2.5 \times 10^{-3}$ (0.15) <sup>b</sup>	$3.5 \times 10^{-6}$ (0.014)	$2 \times 10^{-6}$ (0.008)	1.8
II	$4.0 \times 10^{-4}$ (2.4)	$7.5 \times 10^{-3}$ (0.36)	$4 \times 10^{-3}$ (0.18)	15

<sup>a</sup> System components:  $[\text{Ru}(\text{bpz})_3^{2+}] = 1.0 \times 10^{-4}$  M,  $[\text{TEOA}] = 1 \times 10^{-1}$  M,  $[\text{Ru colloid}] = 20$  mg  $\text{L}^{-1}$ ,  $[\text{NaHCO}_3] = 0.05$  M. Systems: I, aqueous solution; II, water-ethanol, 2:1. <sup>b</sup> In parentheses volume ( $\mu\text{L}$ ) of products formed per hour.

predominating reaction. Assuming that  $\text{CO}_2$  reduction does not proceed through a hydrogenation mechanism suggests that specificity toward  $\text{CO}_2$  reduction might be designed. A strategy to induce selectivity into the process and favor  $\text{CO}_2$  reduction over  $\text{H}_2$  evolution will involve the design of a couple composed of a reduced relay-catalyst system that exhibits a kinetic barrier toward  $\text{H}_2$  evolution but still allows  $\text{CO}_2$  reduction.  $\text{Ru}(\text{II})$  tris(bipyrazine),  $\text{Ru}(\text{bpz})_3^{2+}$ , is a photosensitizer that absorbs in the visible region ( $\lambda_{\text{max}} = 443$  nm,  $\epsilon = 15000$   $\text{M}^{-1} \text{cm}^{-1}$ ) and exhibits a long excited-state lifetime ( $\tau = 1.04$   $\mu\text{s}$ ).<sup>38,39</sup> It is reductively quenched via electron transfer by various electron donors, i.e. triethanolamine, TEOA (eq 15). The reduced photoproduct,



$\text{Ru}(\text{bpz})_3^+$ , is a powerful reducing agent ( $E^\circ = -0.86$  V vs. SCE) capable thermodynamically to evolve  $\text{H}_2$  as well as to reduce  $\text{CO}_2$  to  $\text{CH}_4$ . Nevertheless, it has been reported that  $\text{Ru}(\text{bpz})_3^+$  does not mediate  $\text{H}_2$  evolution at pH 7.8 in the presence of heterogeneous catalysts such as Pt colloid.<sup>40</sup> Thus it exhibits the kinetic barrier for  $\text{H}_2$  evolution and meets the basic requirements to design selective  $\text{CO}_2$  reduction.

We therefore examined the reduction of  $\text{CO}_2$  in an aqueous system that includes  $\text{Ru}(\text{bpz})_3^{2+}$  as photosensitizer, TEOA as electron donor, and the Ru colloid as  $\text{CO}_2$  reduction catalyst. Illumination of this system (pH 7.8,  $\lambda > 400$  nm) results in the reduction of  $\text{CO}_2$  to  $\text{CH}_4$  and the formation of oligomerated hydrocarbons ethylene and ethane (Figure 4). No  $\text{H}_2$  formation is observed in these systems, and  $\text{CO}_2$ -reduction products are the sole products. Table II summarizes the quantum yield for the formation of the various hydrocarbons and the turnover numbers of the photosensitizer.

Control experiments reveal that indeed  $\text{CO}_2$  is photoreduced to methane, ethylene, and ethane. Illumination of a system that includes the colloids under argon instead of  $\text{CO}_2$  does not lead to any hydrocarbon products. Also, exclusion of the  $\text{Ru}(\text{bpz})_3^{2+}$  from the system does not yield upon illumination under  $\text{CO}_2$  any hydrocarbon products. Thus, it is evident that a photosensitized electron-transfer reaction in the visible absorption region leads to the reduction of  $\text{CO}_2$ .

A hydrogenation mechanism of  $\text{CO}_2$  to the hydrocarbons in these systems can be excluded since no  $\text{H}_2$  evolution occurs either in the presence of  $\text{CO}_2$  or under argon. That  $\text{CO}_2$  is reduced via electron transfer is evident from laser flash experiments as well as steady-state illumination. Excitation of an aqueous solution

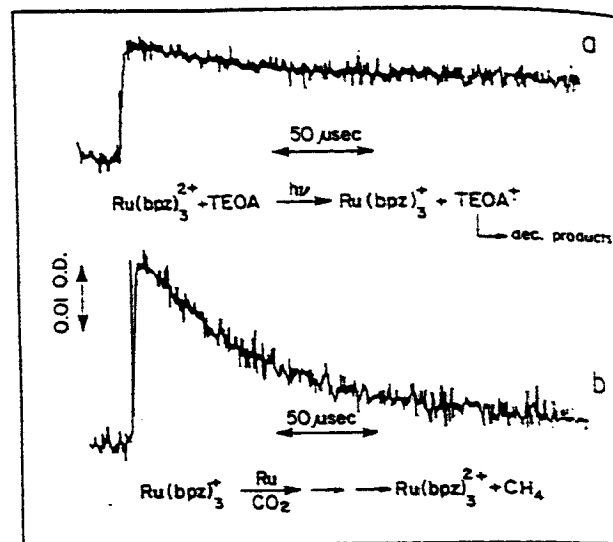


Figure 5. Transient spectra formed upon illumination of  $\text{Ru}(\text{bpz})_3^{2+}$ ,  $2.0 \times 10^{-5}$  M, and TEOA, 0.17 M solution, pH 9.5. Systems are flashed at  $\lambda = 440$  nm and product,  $\text{Ru}(\text{bpz})_3^+$ , is followed at  $\lambda = 500$  nm: (a) under argon or  $\text{CO}_2$ ; (b) in the presence of Ru colloid (20 mg/L) under  $\text{CO}_2$ .

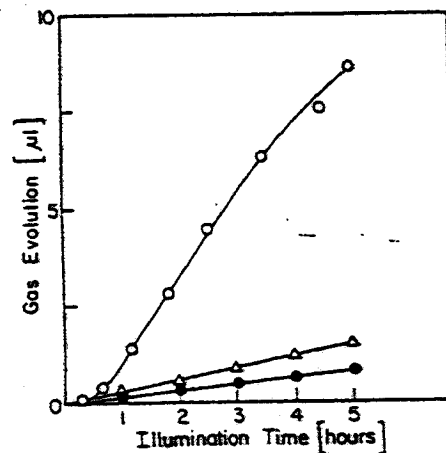


Figure 6. Rate of hydrocarbon formation as a function of illumination time in the  $\text{Ru}(\text{bpz})_3^{2+}$  system:  $[\text{Ru}(\text{bpz})_3^{2+}] = 1.0 \times 10^{-4}$  M,  $[\text{TEOA}] = 1.0 \times 10^{-1}$  M,  $[\text{NaHCO}_3] = 5.0 \times 10^{-2}$  M,  $[\text{Ru colloid}] = 20$  mg/L, pH 7.8, water-ethanol (2:1) solution under  $\text{CO}_2$  atmosphere. Key: (O) methane; ( $\Delta$ ) ethylene; ( $\bullet$ ) ethane.

that includes  $\text{Ru}(\text{bpz})_3^{2+}$  and TEOA under argon by a light pulse ( $\lambda_{\text{exc}} = 440$  nm) results in the trace displayed in Figure 5a. It corresponds to the reductive quenching of  $\text{Ru}(\text{bpz})_3^{2+}$  to form  $\text{Ru}(\text{bpz})_3^+$  (eq 15). The trace shows an initial decay for ca. 80  $\mu\text{s}$  and afterward a steady-state accumulation of  $\text{Ru}(\text{bpz})_3^+$ . The initial decay is due to a recombination of  $\text{Ru}(\text{bpz})_3^+$  with  $\text{TEOA}^{\bullet-}$ , but since  $\text{TEOA}^{\bullet-}$  is simultaneously decomposed, a net steady-state accumulation of  $\text{Ru}(\text{bpz})_3^+$  is observed. Addition of  $\text{CO}_2$  (instead of argon) does not alter the trace obtained upon flashing. Thus, no electron transfer from  $\text{Ru}(\text{bpz})_3^+$  to  $\text{CO}_2$  occurs. Addition of the Ru colloid to the system under argon results in the decay of  $\text{Ru}(\text{bpz})_3^+$  ( $\tau = 170$   $\mu\text{s}$ ), implying that electron transfer from  $\text{Ru}(\text{bpz})_3^+$  to the metal colloid occurs. In turn, flashing the system in the presence of  $\text{CO}_2$  and the Ru colloid results in the trace displayed in Figure 5b. It is evident that under these conditions a rapid decay ( $\tau = 50$   $\mu\text{s}$ ) of the photogenerated  $\text{Ru}(\text{bpz})_3^+$  occurs and  $\text{Ru}(\text{bpz})_3^{2+}$  is regenerated. Namely, photogenerated  $\text{Ru}(\text{bpz})_3^+$  is capable of affecting the electron transfer to Ru-activated  $\text{CO}_2$ , a process that ultimately yields the hydrocarbon products.

It is established that  $\text{Ru}(\text{bpz})_3^+$  can be photogenerated upon steady-state illumination of an aqueous ethanol solution that contains the photosensitizer  $\text{Ru}(\text{bpz})_3^{2+}$  and TEOA.<sup>40</sup> The accumulation of  $\text{Ru}(\text{bpz})_3^+$  in ethanol solutions is presumed to be due

(38) Crutchley, R. J.; Lever, A. B. P. *J. Am. Chem. Soc.* 1980, 102, 7128-7129.

(39) Crutchley, R. J.; Lever, A. B. P. *Inorg. Chem.* 1982, 21, 2276-2282.

(40) (a) Dürr, H.; Dörr, G.; Zengler, K.; Curchod, J.-M.; Braun, A. M. *Helv. Chim. Acta* 1984, 66, 2652-2655. (b) Dürr, H.; Dörr, G.; Zengler, K.; Mayer, E.; Curchod, J.-M.; Braun, A. M. *Nouv. J. Chim.* 1985, 9, 717-720.

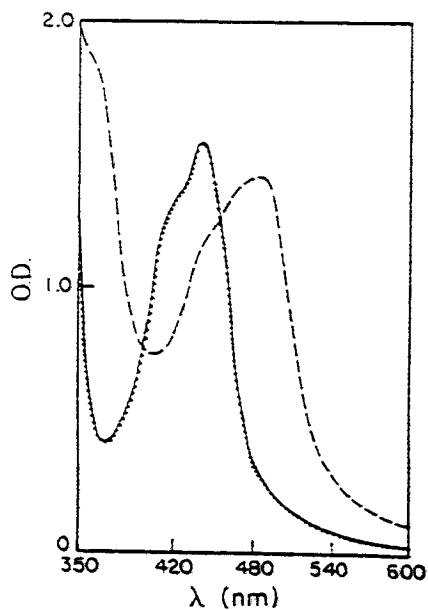


Figure 7. Effects of added CO<sub>2</sub> on photogenerated Ru(bpz)<sub>3</sub><sup>+</sup>. Absorption Spectra: (—) Ru(bpz)<sub>3</sub><sup>2+</sup>, 1.0 × 10<sup>-4</sup> M in water-ethanol (2:1) under argon; (---) photogenerated Ru(bpz)<sub>3</sub><sup>+</sup> prepared by illumination of Ru(bpz)<sub>3</sub><sup>2+</sup> in the presence of TEOA, 1.0 × 10<sup>-1</sup> M; (-·-) obtained upon injection of CO<sub>2</sub> to photogenerated Ru(bpz)<sub>3</sub><sup>+</sup>. In all samples [Ru colloid] = 20 mg/L.

to the rapid irreversible decomposition of TEOA<sup>•+</sup> in this medium (eq 15). Thus, the effective photogeneration of Ru(bpz)<sub>3</sub><sup>+</sup> in ethanol solutions suggests that enhanced quantum yields for CO<sub>2</sub> reduction to CH<sub>4</sub> could be accomplished in this medium. We have examined the photosensitized reduction of CO<sub>2</sub> to CH<sub>4</sub> in a water-ethanol (2:1) mixture using Ru(bpz)<sub>3</sub><sup>2+</sup> as sensitizer, TEOA as electron donor, and the Ru colloid as catalyst. Illumination of this system under CO<sub>2</sub> results in the formation of CH<sub>4</sub> and higher hydrocarbons. The rate of CH<sub>4</sub> formation (Figure 6) corresponds to a quantum yield of φ = 4.0 × 10<sup>-4</sup>. This value is 16-fold higher than the quantum yield for CH<sub>4</sub> formation in pure aqueous solutions and is mainly attributed to the effective photogeneration of Ru(bpz)<sub>3</sub><sup>+</sup> in the ethanol-water solution. Steady-state illumination experiments on this system in the absence and presence of CO<sub>2</sub> and the Ru colloid support the electron-transfer mechanism for reduction of CO<sub>2</sub>. Illumination of the ethanol-water solution that includes TEOA and the photosensitizer Ru(bpz)<sub>3</sub><sup>2+</sup> results in the photoreduction of Ru(bpz)<sub>3</sub><sup>2+</sup> to Ru(bpz)<sub>3</sub><sup>+</sup>, λ<sub>max</sub> = 470 nm (Figure 7, eq 15). Upon addition of the Ru colloid or CO<sub>2</sub> the photogenerated Ru(bpz)<sub>3</sub><sup>+</sup> is unaffected. Addition of both of the components, the Ru colloid and CO<sub>2</sub>, results in the reoxidation of Ru(bpz)<sub>3</sub><sup>2+</sup> and evolution of CH<sub>4</sub>, implying that the photosensitizer is recycled in the photosensitized evolution of CH<sub>4</sub> as well as supporting the electron-transfer mechanism. It should be noted that illumination of this system is performed in the region of λ = 420–450 nm. We find that illumination of the system with light of λ > 400 nm results in poor stability of the photosensitizer. The absorption spectra of Ru(bpz)<sub>3</sub><sup>2+</sup> and Ru(bpz)<sub>3</sub><sup>+</sup> (Figure 7) show that the two components exhibit an overlap in their absorption bands. The poor stability of the photosensitizer, under conditions where Ru(bpz)<sub>3</sub><sup>+</sup> is also excited, suggests that the photoproduct Ru(bpz)<sub>3</sub><sup>+</sup> is itself photoactive and transforms to a product inactive for CO<sub>2</sub> reduction. The relatively limited turnover number (TN) of the system, TN = 15, is thus attributed to the residual absorbance of Ru(bpz)<sub>3</sub><sup>+</sup> in the excitation region (λ = 420–450 nm) that causes photoconsumption of Ru(bpz)<sub>3</sub><sup>2+</sup>. We anticipate that development of Ru(bpz)<sub>3</sub><sup>2+</sup> derivatives where the 2+/1+ oxidation states exhibit distinct nonoverlapping absorption properties might increase the stability of the system toward CO<sub>2</sub> reduction.

**Selectivity in CO<sub>2</sub>-Reduction and H<sub>2</sub>-Evolution.** The two systems discussed for CO<sub>2</sub> reduction demonstrate that those systems that include a relay yield a mixture of H<sub>2</sub> and hydrocarbons while the

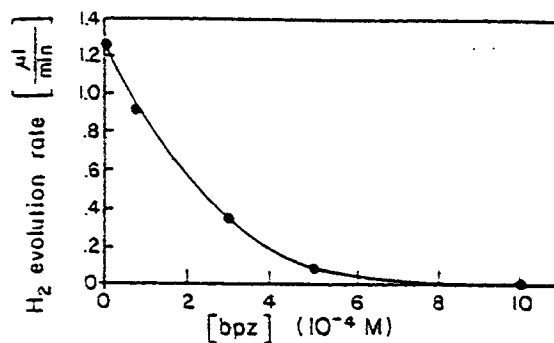


Figure 8. H<sub>2</sub>-Evolution rate as a function of bipyrazine concentration: [Ru(bpy)<sub>3</sub><sup>2+</sup>] = 1.4 × 10<sup>-4</sup> M, [MQ<sup>2+</sup>] = 1.0 × 10<sup>-3</sup> M, [Na<sub>2</sub>EDTA] = 3.3 × 10<sup>-2</sup> M, [NaHCO<sub>3</sub>] = 5.0 × 10<sup>-2</sup> M, [Ru colloid] = 20 mg/L, pH 6.0 under CO<sub>2</sub> atmosphere.

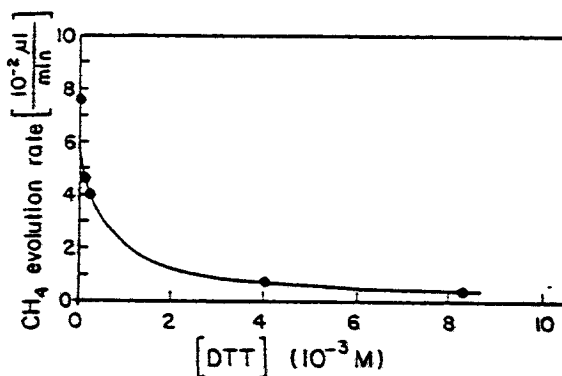


Figure 9. CH<sub>4</sub>-Evolution rate as a function of dithiothreitol concentration: [Ru(bpy)<sub>3</sub><sup>2+</sup>] = 1.4 × 10<sup>-4</sup> M, [MQ<sup>2+</sup>] = 1.0 × 10<sup>-3</sup> M, [Na<sub>2</sub>EDTA] = 3.3 × 10<sup>-2</sup> M, [NaHCO<sub>3</sub>] = 5.0 × 10<sup>-2</sup> M, [Ru colloid] = 20 mg/L, pH 6.0 under CO<sub>2</sub> atmosphere.

system that includes Ru(bpz)<sub>3</sub><sup>2+</sup> is specific for CO<sub>2</sub> reduction only. The laser flash studies (Figure 5) reveal that Ru(bpz)<sub>3</sub><sup>+</sup> exhibits a kinetic barrier toward H<sub>2</sub> evolution. We have speculated that the coordination sites on the ligands of Ru(bpz)<sub>3</sub><sup>2+</sup> might interact with the heterogeneous catalyst and consequently deactivate the catalyst toward the H<sub>2</sub>-evolution process. We thus examined the H<sub>2</sub>-evolution process under argon using Ru(bpy)<sub>3</sub><sup>2+</sup> as sensitizer, MQ<sup>2+</sup> as charge relay, Na<sub>2</sub>EDTA as electron donor, and the Ru colloid as catalyst in the presence and absence of bipyrazine. Figure 8 shows the quantum yield for H<sub>2</sub> evolution upon addition of the bipyrazine ligand. It is evident that H<sub>2</sub> evolution is retarded as the bipyrazine concentration increases, and at a concentration of 1 × 10<sup>-3</sup> M, no H<sub>2</sub> evolution occurs. Thus we conclude that H<sub>2</sub> evolution is prohibited by the bipyrazine ligand. It should be noted that no inhibitory effect in H<sub>2</sub> evolution is observed with 2,2'-bipyridine or 3,3'-bipyridine as additives. Under CO<sub>2</sub> the inhibition profile of H<sub>2</sub> evolution with added bipyrazine is similar to that observed under argon. Yet, also CO<sub>2</sub> reduction is inhibited to some extent by the addition of bipyrazine, and at [bipyrazine] = 1 × 10<sup>-3</sup> M H<sub>2</sub> evolution is totally blocked while the quantum yield of CO<sub>2</sub> reduction to CH<sub>4</sub> decreases to 30% of its value in the absence of bipyrazine.

Similarly, specificity toward H<sub>2</sub> evolution can be designed. CO<sub>2</sub> reduction can be eliminated in the two systems by the addition of thiols. In the presence of these additives H<sub>2</sub> evolution is not affected. We have examined the photosensitized reduction of CO<sub>2</sub> and H<sub>2</sub> evolution in a system composed of Ru(bpy)<sub>3</sub><sup>2+</sup> as sensitizer, MQ<sup>2+</sup> as electron relay, Na<sub>2</sub>EDTA as electron donor, and the Ru colloid as catalyst. Figure 9 shows the rates of CO<sub>2</sub> reduction to CH<sub>4</sub> at different concentrations of added dithiothreitol (DTT). It should be noted that the added thiols do not inhibit H<sub>2</sub> evolution. Furthermore, with DTT the quantum yield for H<sub>2</sub> reduction is slightly increased. It is evident that the added thiol inhibits CO<sub>2</sub> reduction and at 8 × 10<sup>-3</sup> M DTT CO<sub>2</sub> reduction to methane is prohibited while the H<sub>2</sub> evolution yield is unaffected.

This deactivation of the Ru colloid by thiols toward  $\text{CO}_2$  reduction is general, and cysteine or mercaptoethanol show similar inhibition effects. We thus conclude that thiols prevent the reduction of  $\text{CO}_2$ , and selective  $\text{H}_2$  evolution can be accomplished. Added bipyrazine shows inhibitoric effects toward  $\text{H}_2$  evolution as well as  $\text{CO}_2$  reduction although the deactivation is more pronounced toward the former process. We anticipate that other ligands might show higher selectivity in the degree of deactivation of these reactions. Also, the possibility to control the selective  $\text{CO}_2$ -reduction or  $\text{H}_2$ -evolution process suggests that on the Ru colloid exist distinct and different catalytic sites for the two reactions.

### Conclusions

We have discussed the novel application of Ru and Os colloids as catalysts for the photosensitized  $\text{CO}_2$  reduction to  $\text{CH}_4$ . The fixation of  $\text{CO}_2$  to  $\text{CH}_4$  in aqueous solutions is accompanied by the kinetically favored  $\text{H}_2$ -evolution process. Our results emphasize that selectivity toward  $\text{CO}_2$  reduction might be accomplished by proper design of a relay-catalyst configuration that exhibits overpotential properties toward  $\text{H}_2$  evolution. In this respect we find that bipyrazine acts as an inhibitor that eliminates  $\text{H}_2$  evolution. Similarly, thiols eliminate  $\text{CO}_2$  reduction but do not affect evolution of  $\text{H}_2$ . The multielectron fixation of  $\text{CO}_2$  to  $\text{CH}_4$  that involves eight electrons is certainly a stepwise process that involves various intermediates. We emphasize that no other reduction products of  $\text{CO}_2$ , i.e. formate, formaldehyde, or methanol, could be detected in the photosensitized transformation. We have shown that  $\text{C}_2$  hydrocarbons (ethane and ethylene) are also formed during the photoreduction of  $\text{CO}_2$ . The formation of these products suggests that  $\text{Ru}=\text{CH}_2$  (or  $\text{Os}=\text{CH}_2$ ) and  $\text{Ru}-\text{CH}_3$  act as intermediates along the photoreduction of  $\text{CO}_2$  since ethylene would be formed by the dimerization of the carbene species while ethane

is anticipated to originate from dimerization of the metal-methyl intermediate. It should be noted that similar intermediates have been suggested<sup>41</sup> in the methanation process of  $\text{CO}_2$ .

Our study has emphasized that photoreduction of  $\text{CO}_2$  occurs via electron transfer followed by protonation steps rather than by a hydrogenation mechanism. The control experiments that were applied to elucidate the mechanistic aspects of the photoreduction of  $\text{CO}_2$  revealed that the photochemically generated reduced relays  $\text{Ru}(\text{bpz})_3^+$  or the bipyridinium radicals mediate the reduction of  $\text{CO}_2$  to  $\text{CH}_4$  in the presence of Ru or Os colloids. Since bipyridinium radicals can be produced by  $\text{H}_2$  and heterogeneous catalysts, we might envisage routes to develop novel methanation reactions or electrocatalyzed methanation processes that proceed at ambient temperatures and atmospheric pressure via an electron-transfer pathway. Further attempts to characterize mechanistic aspects involved in the photoreduction of  $\text{CO}_2$  to methane, development of other  $\text{CO}_2$ -reduction catalysts, and the development of the dark electron-transfer reduction processes of  $\text{CO}_2$  are now under way in our laboratory.

**Acknowledgment.** This research is supported by a grant from the National Council for Research and Development, Israel, and the Kernforschung Anlage, Juelich, Germany.

**Registry No.** 1, 41491-80-9; 2, 7325-63-5; 3, 16651-68-6; 4, 86690-04-2; TEOA, 102-71-6;  $\text{CO}_2$ , 124-38-9;  $\text{Ru}(\text{bpy})_3^{3+}$ , 15158-62-0; Ru, 7440-18-8; Os, 7440-04-2; Pt, 7440-06-4;  $\text{H}_2$ , 1333-74-0; tris(bipyrazine)ruthenium(II), 75523-96-5; ethylene, 74-85-1; ethane, 74-82-0; methane, 74-82-8; dithiothreitol, 3483-12-3; 3,3'-dimethyl-4,4'-bipyrazine, 4479-73-6; 1,3-propanesultone, 1120-71-4.

(41) (a) Weatherbee, G. D.; Bartholomew, C. H. *J. Catal.* 1980, 77, 460-472. (b) Biloen, P.; Sachtler, W. M. H. *Adv. Catal.* 1981, 30, 165-216. (c) Baker, J. A.; Bell, A. T. *J. Catal.* 1982, 78, 165-181.

## Cyclobutene Photochemistry. Nonstereospecific Photochemical Ring Opening of Simple Cyclobutenes

K. Brady Clark and William J. Leigh\*<sup>1</sup>

Contribution from the Department of Chemistry, McMaster University, Hamilton, Ontario, Canada L8S 4M1. Received December 15, 1986

**Abstract:** The photochemistry of bicyclo[3.2.0]hept-6-ene, bicyclo[4.2.0]oct-7-ene, and *cis*- and *trans*-3,4-dimethylcyclobutene has been investigated in hydrocarbon solution with monochromatic far-ultraviolet (185 and 193 nm) light sources. All of these simple cyclobutene derivatives undergo ring opening to yield the isomeric 1,3-dienes, and the latter three open nonstereospecifically to yield mixtures of the possible geometric isomers. The isomeric 3,4-dimethylcyclobutenes yield different mixtures of the three 2,4-hexadiene isomers, and in each case the mixtures are weighted in favor of the orbital symmetry forbidden isomer(s). Attempts have been made to analyze the relative isomeric diene yields from ring opening of bicyclo[4.2.0]octene and the isomeric 3,4-dimethylcyclobutenes within the context of the purely disrotatory, adiabatic ring-opening mechanism that recent ab initio calculations suggest should be possible. While the results for the former compound are consistent with this mechanism, analysis of the relative yields of the isomeric 2,4-hexadienes from photolysis of the latter two compounds indicates that photochemical ring opening by the formally forbidden, conrotatory pathway may compete to some extent with disrotatory ring opening

In spite of the central role that the thermal<sup>2,3</sup> and photochemical<sup>3b,4,5</sup> interconversions of cyclobutene and 1,3-butadiene play

in our understanding of pericyclic reactions,<sup>6</sup> there are few reported examples that illustrate the photochemical electrocyclic ring-

(1) Natural Sciences and Engineering Research Council of Canada University Research Fellow, 1983-1988.

(2) (a) Winter, R. E. K. *Tetrahedron Lett.* 1965, 1207. (b) Brauman, J. I.; Golden, D. M. *J. Am. Chem. Soc.* 1968, 90, 1920. (c) Srinivasan, R. *J. Am. Chem. Soc.* 1969, 91, 7557. (d) Brauman, J. I.; Archie, W. C. *J. Am. Chem. Soc.* 1972, 94, 4262. (e) Jasinski, J. M.; Frisoli, J. K.; Moore, C. B. *J. Chem. Phys.* 1983, 79, 1312.

(3) (a) Doorakian, G. A.; Freedman, H. H. *J. Am. Chem. Soc.* 1968, 90, 5310, 6896. (b) Schumate, K. M.; Fonken, G. J. *J. Am. Chem. Soc.* 1965, 87, 3996; 1966, 88, 1073.

(4) (a) Dauben, W. G.; Cargill, R. G.; Coates, R. M.; Saitiel, J. *J. Am. Chem. Soc.* 1966, 88, 2742. (b) Srinivasan, R. *J. Am. Chem. Soc.* 1968, 90, 4498. (c) Chapman, O. L.; Pasto, D. J.; Borden, G. W.; Griswold, A. *J. Am. Chem. Soc.* 1962, 84, 1220. (d) Dauben, W. G.; Cargill, R. *J. Am. Chem. Soc.* 1962, 84, 1220. (e) Dauben, W. G.; Cargill, R. *J. Am. Chem. Soc.* 1962, 84, 1220.

# Podanden, Coronanden und Kryptanden als neue Komplex-Liganden für Photoelektronentransfer-Reaktionen Synthese und erste photophysikalische Studien

Podands, Coronands and Cryptands  
as New Complex-Ligands in Photoelectron Transfer Reactions  
Synthesis and Photophysical Studies

Heinz Dürr\*, Klaus Zengerle und Hans-Peter Trierweiler

Fachbereich 13.2. Organische Chemie, Universität des Saarlandes, D-6600 Saarbrücken

Herrn Prof. U. Schöllkopf zum 60. Geburtstag gewidmet

Z. Naturforsch. 43b, 361–367 (1988); eingegangen am 14. September/3. November 1987

Podands, Coronands, Cryptands, Photosensitizer, Photoanation

Podands, coronands and cryptands containing 2,2'-bipyridine-units were synthesized. These compounds can be used as ligands in Ru(II)-polypyridinecomplexes. This new route principally allows the preparation of tris-heteroleptic complexes using the appropriate cryptands. Ru(II)-polypyridines  $RuL_3^{2+}$  (e.g.  $Ru(bpy)_3^{2+}$ ) are interesting as sensitizers in photochemical water cleavage. Compared to  $Ru(bpy)_3^{2+}$ , the photoanationrate should be reduced in the  $Ru(cryp)^{2+}$  complex.

„Ru(II)-polypyridin-Komplexe spielen eine Schlüsselrolle bei der Entwicklung der Gebiete Photochemie, -physik, -katalyse, -elektrochemie, Chemilumineszenz und Elektronen- und Energietransfer“ [1]. Um die Eigenschaften von  $RuL_3^{2+}$ -Komplexen gezielt zu optimieren, müssen 1) die Orbital-Natur des niedrigsten Anregungszustandes, 2) dessen Energie und 3) die Redox Eigenschaften möglichst „maßgeschneidert“ sein. Darüber hinaus sind die neuartigen Liganden auch für die „Wirt-Gast-Chemie“ von Interesse. Als bisher bester Komplex hat sich  $Ru(bpy)_3^{2+}$  erwiesen [2]. Die trotzdem auch bei  $Ru(bpy)_3^{2+}$  mögliche Photoanation begrenzt die Photostabilität des Komplexes. Eine Verkettung der bpy-Untereinheiten sollte die Photoanation weitgehend unterdrücken.

In dieser Arbeit beschreiben wir die Synthese neuartiger, verketteter Pyridin- bzw. Bipyridin-Liganden vom Typ der Podanden, Coronanden und Kryptanden sowie erste photophysikalische Studien der Liganden und des  $Ru(cryp)^{2+}$ -Komplexes.

Zur Synthese der Podanden 14, Coronanden 13 und Kryptanden 12 wurden zunächst die Ausgangskomponenten, d. h. die Bausteine A = 3 und B = 6, nach zum Teil bekannten Routen dargestellt (s. Schema 1 und Tab. I).

Baustein A = 3 wurde ausgehend von 6,6'-Dibrom-2,2'-bipyridin 1 erhalten, das nach [4] zunächst in das Dicyan-Derivat 2 umgewandelt wurde. Katalytische Hydrierung ergab daraus Diamin, dessen Tosylierung 3 lieferte. B (=6) konnte durch Kopplung von 2-Brom-6-methylpyridin [5] mittels der  $Ni(TPP)_2$ -Methode in 5 (90%) übergeführt und hieraus nach l.c. [5] 6 dargestellt werden. Der Bipyridinkryptand 12, der Coronand 13 und Podand 14 wur-

Tab. I. Ausbeuten und Schmelzpunkte der aus 3 und 7 nach Schema 2 erhaltenen Kryptanden 12, Coronanden 13 und Podanden 14.

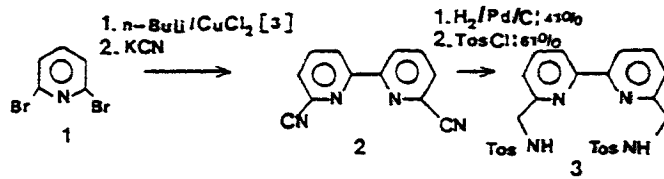
Verb.	Ausb. (%) diese Arbeit	Lit.	Schmp. (°C) diese Arbeit	Lit.
3	61		196	
7		98 [6]		91–93 [6]
9	64	57 [7.8]	>260	>260 [7.8]
10	68/77*	45 [6]	168	166–168 [6]
11	83		91–92	
9'	97	94 [6–8]	>260	>260 [6–8]
10'	98		farbl. Öl	
11	94		farbl. Öl	
12	52	62 [7.8]	>260	>260 [7.8]
13	10/65**		58	
14	53/54***		130	

\* Sonderdruckanforderungen an Prof. Dr. H. Dürr.

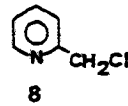
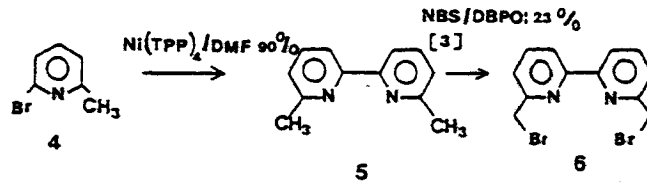
\*\* 4. Mitteilung: Photochemisch induzierte Elektronentransferreaktionen. 3. Mitteilung: H. Dürr, G. Dörr, K. Zengerle, E. Mayer, A. M. Braun und J. M. Curchod. *Nouv. J. Chim.* 9, 717 (1985).

Schema 1

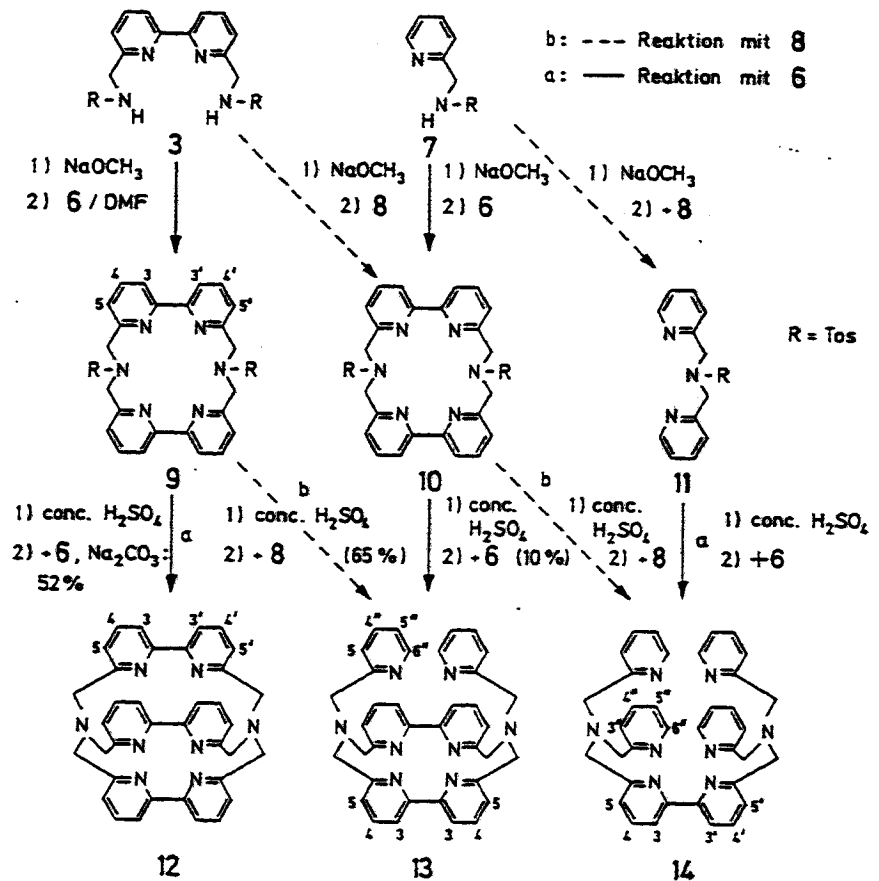
Baustein A:



Baustein B:



Schema 2



den daraus gemäß der Tosylamidmethode über folgende Route synthetisiert.

#### Umsetzung von 2-Chlormethylpyridin 8 mit 3, 7 mit 9', 11 mit 10'

Der besseren Übersichtlichkeit wegen sind die Reaktionen der Tosylamide 3 bzw. 7 mit dem Dibromid 6 durch ausgezogene Pfeile, die mit dem 2-Chlormethylpyridin 8 durch gestrichelte Pfeile gekennzeichnet. Aus gleichem Grund sind von den Podanden nicht die günstigsten Konformationen angegeben.

Das cyclische Bis-Tosylamid 9 wurde durch Lösen des Dinatriumsalzes 3' in DMF (ca. 1 mmol 3'/50 ml) und langsames Zutropfen des Dibromids 6 erhalten.

Die Reaktion des Dinatriumsalzes von 3 mit Monochlorid 8 in siedendem DMF lieferte das Tosylamid 10, analog wurde aus 7 das Tosylamid 11 hergestellt.

Zur Detosylierung wurden die Tosylamide 9–11 mit Schwefelsäure behandelt (2 h; 100 °C) [6], wobei in fast quantitativer Ausbeute der Coronand 9', das Bis-Amin 10' bzw. das Mono-Amin 11' anfielen (wobei in 9', 10' und 11' R=H ist).

Zur Synthese von 12–14 wurden zwei Alternativrouten (a) und (b) ausgewählt.

#### Route (a)

Die Reaktion des Coronanden 9 mit dem Dibromid 6 in Acetonitril ergab bei Zusatz von Natriumcarbonat (vgl. Lehn [7, 8]) den gewünschten Kryptanden 12 (52%) [4].

Auf die gleiche Weise war der Kryptand 12 erstmals aus 9 und 6 dargestellt worden [7, 8]. Der entscheidende Vorteil des von uns beschrittenen Syntheseweges zum Coronanden 9 besteht darin, daß das Brückenkopfstickstoffatom im Kryptanden 12 bereits im Tosylamid 3 (vgl. Schema 2) eingebaut worden ist. Daraus ergibt sich die Möglichkeit der selektiven Darstellung von bis- bzw. tris-heteroleptischen Rutheniumkryptanden.

Dies ist nach dem Lehn'schen Verfahren [7, 8] unmöglich, da dieses nur homoleptische und bis-heteroleptische Liganden bzw. Komplexe darzustellen erlaubt.

Die unter den gleichen Bedingungen vollzogene Cyclisierungsreaktion des Podanden 10' mit dem Di-

bromid 6 zum Coronanden 13 lieferte nur sehr unbefriedigende Ausbeuten (10%).

#### Route (b)

Analog durchgeführte Umsetzungen des Coronanden 9' mit 8 ergaben Coronand 13 in 65% und Podand 14 in 54% Ausbeute. Während 13 und 14 als reine „organische“ Verbindungen isoliert wurden, fällt der Kryptand 12 als NaBr-Komplex an [7–9].

Die neuen Synthesen von 13 und 14 sowie des bekannten 12 zeigen, daß mit Bis-Tosylamid 3 als zentralem Synthesebaustein der Aufbau von Bipyridinkryptanden, -coronanden und -podanden möglich ist. Darstellung des cyclischen Bis-Tosylamids (Coronand 9), ausgehend vom 6,6'-Bis(chlormethyl)-2,2'-bipyridin und 3 [6], ergab ein sehr komplexes, nicht trennbares Produktgemisch.

Von Vögtle wurde kürzlich ein verwandter Kryptand vorgestellt, bei dem drei Bipyridineinheiten über Benzolringe verbrückt sind [10].

#### NMR-Spektren

Die NMR-Spektren der neuen Verbindungen sind in Tab. II zusammengestellt.

Tab. II. <sup>1</sup>H-NMR-Daten von Pyridin- und Bipyridin-podanden, -coronanden und -kryptanden 12–14 in CDCl<sub>3</sub>.

	Bipyridin- und Pyridinteil				Tosylteil	
	H <sup>2</sup> , H <sup>3</sup> (H <sup>3</sup> )	H <sup>4</sup> , H <sup>4'</sup> (H <sup>4</sup> )	H <sup>5</sup> , H <sup>5'</sup> (H <sup>5</sup> )	(H <sup>6</sup> )	-CH <sub>2</sub> -	N-H
9'	7.71	7.50	7.03		4.08	2.88
10'	8.33 (7.37)	7.74 (7.62)	7.33 (7.14)	(8.41)	(4.07) <sup>a</sup> (4.06) <sup>a</sup>	3.10
11'	(7.35)	(7.61)	(7.13)	(8.54)	(4.00)	3.59
12	7.89	7.82	7.32		3.84	
13	7.77 (7.03)	7.74 (7.41)	7.26 (6.89)	(8.27)	3.93 (3.89)	
14	8.32 (7.64) <sup>a</sup>	7.78 (7.64) <sup>a</sup>	7.52 (7.12)	(8.51)	3.98 (3.98)	

( ) Verschiebung der Pyridinprotonen und deren benachbarter -CH<sub>2</sub>-Gruppe;

<sup>a</sup> nicht eindeutig zuzuordnen.

Die Verknüpfung der 2,2'-Bipyridin-Einheiten in 6,6'-Stellung (Teilstrukturen von 12–14) führt zu einer Fixierung der Bipyridine in „cisoider“ Konformation. Der daraus resultierende Hochfeld-shift der 3,3'-H im Vergleich zur transoiden Konformation ist



eindeutig. Auffallend ist auch die große Einfachheit der Spektren, insbesondere beim Kryptanden 12, die die hohe Symmetrie der Moleküle widerspiegelt.

#### UV- und Fluoreszenzspektren

**Liganden:** Die neuartigen Liganden 12 und 14 zeigen sehr einfache UV-Spektren. In Tab. III sind UV- und Fluoreszenzspektren einander gegenübergestellt. Wie Tab. III zeigt, sind die UV-Spektren mit denen des bpy vergleichbar und treten im gleichen Bereich auf.

Die  $\epsilon$ -Werte sind dagegen im Kryptand 12 etwa um den Faktor 3 größer als in bpy. Dies könnte auf die starre Anordnung in 12 zurückzuführen sein. Die Emission von Kryptand 12 und bpy liegen bei Raumtemperatur ( $H_2O$ ) im gleichen Bereich. Die Tieftemperaturfluoreszenz bei 12 ist jedoch bathochrom, bezogen auf bpy, verschoben.

#### Ru-Komplexe

$Ru^{2+}$  weist einen ähnlichen Ionenradius wie  $Na^+$  auf (1,13 Å vgl. mit 0,98 Å). Aus diesem Grunde sollte anstelle des  $Na^+$  in 12  $Ru^{2+}$  eingebaut werden können. Analog sollten sich 13 und 14 verhalten. Die Liganden 12 und 14 wurden daher nach der Standard-Methode [1, 2] mit  $Ru(DMSO)_4Cl_2$  in  $H_2O/EtOH$  umgesetzt. Dabei entstanden in allen Fällen rote Ru-Komplexe. Während nach  $^1H$ -NMR und UV-Spektren bei 13 und 14 höhermolekulare Komplexe möglich sind, die noch nicht genau charakterisiert werden konnten, wurde bei 12 ein Ru-Komplex  $Ru(kryp)^{2+}$  isoliert, dessen UV-Spektrum gut mit dem von  $Ru(bpy)_3Cl_2$  übereinstimmt (s. Abb. 1).

Der neue  $Ru(kryp)^{2+}$ -Komplex zeigt eine Lumineszenz bei 77 K, die je nach Anregungswellenlänge verschiedene Intensität aufweist. Die sehr schwache Lumineszenz im Falle der Anregung bei 480 nm könnte auf MLCT-Übergänge zurückzuführen sein, während die intensiven Lumineszenzbanden im Falle der energiereichsten Anregung wahrscheinlich auf innere Ligandenübergänge hindeuten (vgl. Tab. III):

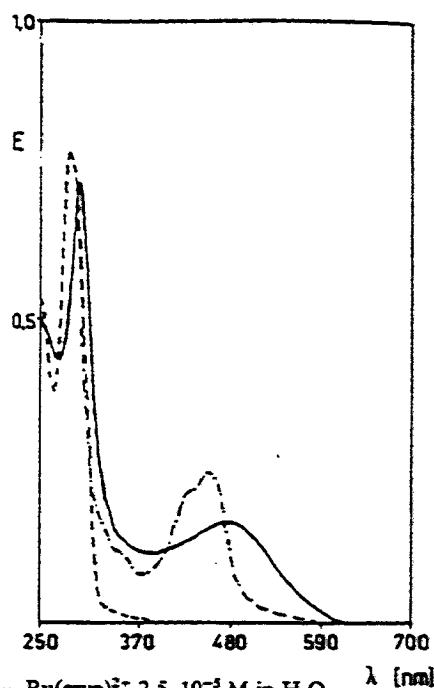


Abb. 1. UV/VIS-Spektrum des  $Ru(kryp)^{2+}$  aus der Umsetzung von 12 mit  $Ru(DMSO)_4Cl_2$ .

bei Raumtemperatur konnte keine Lumineszenz beobachtet werden. Offenbar ist die Metall-Ligand-Bindung zu schwach, so daß die Lebensdauer des angeregten Zustands zu gering wird. Andererseits könnte das freie Elektronenpaar als Donor fungieren und eine intramolekulare Löschung bewirken. Neue Komplexe mit veränderter Geometrie könnten hier eine Klärung ergeben.

#### Quench-Experimente

Um die Eigenschaften der neuen Liganden bei Elektronentransferreaktionen zu überprüfen, wurden bekannte oxidativ und reduktiv arbeitende Sensibilisatoren wie  $Ru(bpy)_3^{2+}$  und  $Ru(bpz)_3^{2+}$  einge-

Ligand bzw. Komplex	UV $\lambda_{max}$ [nm]	$\epsilon \cdot 10^{-4}$	Fluoreszenz RT [ $H_2O$ ]	$\lambda$ [nm] 77 K [EtOH]
Kryptand 12	280	3,08	422	487
bpy [11, 12]	232; 280 [11]	1,05; 1,34	424; 327 <sup>a</sup>	421; 453 <sup>a</sup>
$Ru(bpy)_3^{2+}$			613	580; 627
$Ru(kryp)^{2+}$	290; 478	1,61; 0,72	-	421; 453 <sup>a</sup> 474 <sup>c</sup> ; 726 <sup>d</sup>

Tab. III. Photophysikalische Studien an 12 und  $Ru(kryp)^{2+}$ .

Anregungswellenlängen [nm]<sup>a</sup> = 300; <sup>b</sup> = 310; <sup>c</sup> = 410; <sup>d</sup> = 480.

setzt. Als Quencher wurden die Liganden 12 und 14 verwandt. Wie die Ergebnisse einer Stern-Volmer-Studie zeigten, erhält man in einem derartigen Fluoreszenz-Lösch-Experiment eine Parallele zur Abszisse, d.h. die Emission von  $\text{Ru}(\text{bpy})_3^{2+}$  und  $\text{Ru}(\text{bpz})_3^{2+}$  wird nicht gequenchet.

Dies ist ein wichtiges Ergebnis, da das freie Elektronenpaar in den verbrückten Liganden 12–14 als Elektronendonatoren fungieren könnte und dies im bimolekularen Quenchprozeß offenbar nicht der Fall ist.

### Experimenteller Teil

Die Bestimmung der Schmelzpunkte erfolgte in einem Schmelzpunktapparat der Firma Büchi (Smp 20).

### Analytische Methoden

Säulenchromatographie: Kieselgel (MN-60, 0,05–0,20 mm)  $\text{Al}_2\text{O}_3$ , neutral (0,02–0,50 mm), (Macherey, Nagel & Co.). Analytische DC: DC-Mikroarten Polygram (Macherey, Nagel & Co.). CHN-Analysen: Ultramikroschnell-Methode nach Walisch [13] Elemental Analyser, Mod. 1106 Carlo Erba Strumentatione.

### Meßgeräte

NMR: AM-400 (Bruker); IR: Spektrometer IR-33, IR-4230 (Beckman); UV/VIS: DU-8 Spektrometer (Beckman), Uvikon 860 (Kontron); Fluoreszenz: Fluorescence Spectrophotometer F-3000 (Hitachi); MS: Massenspektrometer MAT-311 (Varian), Elektronenenergie 70 eV.

Die chemischen Verschiebungen der  $^1\text{H}$ -NMR- und  $^{13}\text{C}$ -NMR-Spektren wurden stets in  $\text{CDCl}_3$  mit TMS als innerem Standard gemessen und sind in  $\delta$  = (ppm) angegeben.

### *N,N'*-Ditosyl-6,6'-bis(aminomethyl)-2,2'-bipyridin (3)

Zu einer Lösung von 0,68 g (16,94 mmol) Natriumhydroxid in 10 ml Wasser wurden unter Eiskühlung 1,11 g (3,08 mmol) 6,6'-Bis(aminomethyl)-2,2'-bipyridin und 1,17 g (6,16 mmol) Tosylchlorid gelöst in 20 ml Ether gegeben. Die Reaktionslösung wurde 12 h bei Raumtemperatur gerührt, der ausgefallene weiße Niederschlag abfiltriert und mit 100 ml dest. Wasser nachgewaschen. Umkristallisation aus ca. 150 ml absol. Ethanol ergab 0,98 g (61%) farblose Kristalle vom Schmp. 196 °C. – IR (KBr): 3270 (=N–H), 3080 (Ar–H), 2940 (C–H), 1570, 1430, 1330, 1150, 900, 810, 790, 660  $\text{cm}^{-1}$ . –  $^{13}\text{C}$ -NMR:  $\delta$  =

154,7/154,2 ( $\text{C}^6$ ,  $\text{C}^{6'}/\text{C}^2$ ,  $\text{C}^{2'}$ ), 143,4 (Tos- $\text{C}^1$ ), 137,7 ( $\text{C}^4$ ,  $\text{C}^{4'}$ ), 136,7 (Tos- $\text{C}^4$ ), 129,6 (Tos- $\text{C}^3$ ), 127,2 (Tos- $\text{C}^3$ ), 122,0 ( $\text{C}^5$ ,  $\text{C}^{5'}$ ), 119,9 ( $\text{C}^3$ ,  $\text{C}^{3'}$ ), 47,3 ( $-\text{CH}_2-$ ), 21,5 ( $-\text{CH}_3$ ) ppm. – MS:  $m/e$  = 522 (100%,  $\text{M}^+$ ), 367 (35%,  $\text{M}^+$ -Tos), 210 (37%,  $\text{M}^+$ -2 Tos), 156 (28%,  $\text{bpy}^+$ ), 92 (52%,  $\text{C}_6\text{H}_6\text{N}^+$ ), 91 (100%,  $\text{C}_7\text{H}_7\text{OS}^+$ ).

$\text{C}_{26}\text{H}_{26}\text{N}_4\text{O}_4\text{S}_2$  (522,6)

Ber. C 59.75 H 5.01 N 10.72.

Gef. C 59.48 H 5.05 N 10.59.

### Natriumsalze (3') und (7') von

### *N,N'*-Ditosyl-6,6'-bis(aminomethyl)-2,2'-bipyridin

### (3) und *N*-Tosyl-2-(aminomethyl)pyridin (7)

(2,00 mmol) Tosylamid wurden mit der berechneten Menge Natriummethanolat 5 h in 30 ml absol. Ethanol zum Sieden erhitzt. Nach dem Einengen der Lösung und Abkühlen auf 0 °C wurde abfiltriert und mit Ether nachgewaschen.

### 8,21-Ditosyl-8,21,27,29,30-hexaazapentacyclo [21.3.1.1<sup>2,6</sup>.1<sup>10,14</sup>.1<sup>15,19</sup>]triaconto-1(30),2,4,6(27),10,12,14(28),15,17,19(29),23,25-dodecanen (9)

250 mg (0,44 mmol) Dinatriumsalz 3' wurde in 250 ml heißem DMF gelöst und 150 mg (0,44 mmol) 6,6'-Bis(brommethyl)-2,2'-bipyridin 6 in 50 ml DMF zugetropft. Die Lösung wurde 24 h unter Rückfluß erhitzt und anschließend abgekühlt. Nach dem Abfiltrieren und Waschen mit 20 ml dest. Wasser und 20 ml Ethanol wurden 200 mg (64%) weiße Kristalle vom Schmp. >260 °C erhalten. Da sich das Produkt in keinem Lösungsmittel löste, konnten keine spektroskopischen Daten ermittelt werden.

### *N,N'*-Ditosyl-6,6'-bis[(2-pyridylmethyl)amino]-methyl]-2,2'-2,2'-bipyridin (10)

560 mg (1,00 mmol) Dinatriumsalz 3' wurden in 30 ml heißem DMF gelöst und 250 mg (2,00 mmol) 2-Chlormethylpyridin 8 in 10 ml DMF zugetropft. Die Lösung wurde 6 h unter Rückfluß erhitzt und danach das Lösungsmittel i. Vak. abdestilliert. Umkristallisation aus Ethanol lieferte 530 mg (77%) weiße Kristalle an 10 vom Schmp. 168 °C (Lit. 167–168 °C).

$^{13}\text{C}$ -NMR:  $\delta$  = 156,7 ( $\text{C}^2$ ), 155,2/154,9 ( $\text{C}^6$ ,  $\text{C}^6'/\text{C}^2$ ,  $\text{C}^{2'}$ ), 148,9 ( $\text{C}^6$ ), 143,2 (Tos- $\text{C}^1$ ), 137,0/136,5 ( $\text{C}^4$ ,  $\text{C}^{4'}/\text{C}^5$ ), 136,8 (Tos- $\text{C}^4$ ), 129,5 (Tos- $\text{C}^3$ ), 127,3 (Tos- $\text{C}^3$ ), 122,6/122,5/122,3 ( $\text{C}^5$ ,  $\text{C}^{5'}/\text{C}^5/\text{C}^5$ ), 119,6 ( $\text{C}^3$ ,  $\text{C}^{3'}$ ), 54,1/53,5 ( $\text{C}^{\alpha}/\text{C}^{\beta}$ ), 21,4 ( $-\text{CH}_3$ ) ppm.

$\text{C}_{38}\text{H}_{36}\text{N}_6\text{O}_4\text{S}_2$  (704,9)

Ber. C 64.75 H 5.15 N 11.92.

Gef. C 64.53 H 5.25 N 11.85.

*N*-Tosyl-bis(2-pyridylmethyl)-amin (11)

2.00 g (7.05 mmol) Natriumsalz 7' wurden in 50 ml DMF in der Hitze gelöst und 0.89 g (7.05 mmol) 2-Chlormethylpyridin in 20 ml DMF zugetropft. Das Gemisch wurde 12 h bei 100 °C gehalten und das Lösungsmittel i. Vak. entfernt, der Rückstand in Methylenchlorid aufgenommen und abfiltriert. Entfernen des Lösungsmittels i. Vak. und Umkristallisieren aus Cyclohexan/Toluol (4:1) lieferte 2.06 g (83% bez. auf Natriumsalz) weiße Kristalle an 11 vom Schmp. 91–92 °C.

<sup>13</sup>C-NMR: δ = 156.1 (C<sup>2</sup>), 148.7 (C<sup>6</sup>), 143.1 (Tos-C<sup>4</sup>), 136.3 (Tos-C<sup>1</sup>), 136.1 (C<sup>4</sup>), 129.3 (Tos-C<sup>3</sup>), 127.1 (Tos-C<sup>3</sup>), 122.3/122.0 (C<sup>3</sup>/C<sup>5</sup>), 53.7 (–CH<sub>2</sub>–), 21.3 (–CH<sub>3</sub>) ppm.

C<sub>19</sub>H<sub>19</sub>N<sub>3</sub>O<sub>2</sub>S (353,4)

Ber. C 64.58 H 5.42 N 11.89,  
Gef. C 64.32 H 5.50 N 11.92.

*Allgemeine Arbeitsvorschrift  
zur Detosylierung der Sulfonamide*

Die Tosylamide 9–11 wurden jeweils mit konz. Schwefelsäure 2 h auf 100 °C erhitzt und nach Abkühlen unter Eiskühlung mit dest. Wasser verdünnt. Die erhaltene Lösung wurde unter Eiskühlung mit 100 ml Natronlauge neutralisiert, mit Methylenchlorid extrahiert, über Natriumsulfat getrocknet und das Lösungsmittel i. Vak. entfernt.

8,21,27,28,29,30-Hexaazapentacyclo-  
[21.3.1.1<sup>2,6</sup>.1<sup>10,14</sup>.1<sup>15,19</sup>]-triacont-  
1(30),2,4,6(27),10,12,14(28),15,17,19(29),23,25-  
dodecanen (9')

Ansatz: 110 mg (0.15 mmol) 9, 1 ml konz. Schwefelsäure. Ausbeute: 60 mg (97%) weißes Pulver vom Schmp. >260 °C.

<sup>13</sup>C-NMR: δ = 159.0 (C<sup>6</sup>, C<sup>6'</sup>), 155.8 (C<sup>2</sup>, C<sup>2'</sup>), 136.5 (C<sup>4</sup>, C<sup>4'</sup>), 122.5 (C<sup>5</sup>, C<sup>5'</sup>), 119.3 (C<sup>3</sup>, C<sup>3'</sup>), 56.0 (–CH<sub>2</sub>–) ppm.

C<sub>24</sub>H<sub>22</sub>N<sub>6</sub> (394,5)

Ber. C 73.07 H 5.62 N 21.30,  
Gef. C 72.81 H 5.54 N 21.01.

6,6'-Bis[(2-pyridylmethyl)amino)methyl]-  
2,2'-bipyridin (10')

Ansatz: 400 mg (0.57 mmol) 10, 5 ml konz. Schwefelsäure. Ausbeute: 220 mg (98%) schwach gelbes Öl an 10'.

<sup>13</sup>C-NMR: δ = 159.5 (C<sup>2</sup>), 158.6 (C<sup>6</sup>, C<sup>6'</sup>), 155.4 (C<sup>2</sup>, C<sup>2'</sup>), 149.0 (C<sup>6'</sup>), 136.9 (C<sup>4</sup>, C<sup>4'</sup>), 136.1 (C<sup>4'</sup>), 122.0/121.8/121.6 (C<sup>5</sup>/C<sup>5'</sup>, C<sup>5</sup>/C<sup>5'</sup>), 119.1 (C<sup>3</sup>, C<sup>3'</sup>), 54.5/54.4 (C<sup>5</sup>/C<sup>5'</sup>) ppm.

## Di(2-pyridylmethyl)amin (11')

Ansatz: 1.00 g (2.83 mmol) 11, 5 ml konz. Schwefelsäure. Ausbeute: 0.53 g (94%) schwach gelbes Öl an 11'.

<sup>13</sup>C-NMR: δ = 158.7 (C<sup>2</sup>), 148.6 (C<sup>6</sup>), 136.0 (C<sup>4</sup>), 121.8/121.5 (C<sup>5</sup>/C<sup>5'</sup>), 53.9 (–CH<sub>2</sub>–) ppm.

1,14,39,40,41,42,43,44-octaazaocytacyclo-  
[12.12.12<sup>1,14</sup>.1<sup>3,7</sup>.1<sup>8,12</sup>.1<sup>16,20</sup>.1<sup>21,25</sup>.1<sup>28,32</sup>.1<sup>33,37</sup>]-  
tetraetracont-3(39),4,6,8(40),9,11,16(42),  
17,19,21(41),22,24,28(43),29,31,33(44),34,36-octa-  
decanen (12)

Eine Suspension aus 75 mg (0.19 mmol) Coronand 9', 200 mg Natriumcarbonat und 50 ml Acetonitril wurde zum Sieden erhitzt und 60 mg (0.18 mmol) Bipyridin 6 in 50 ml Acetonitril zugetropft. Nach 24 h unter Rückfluß wurde abfiltriert und das Lösungsmittel i. Vak. entfernt. Säulenchromatographie an Al<sub>2</sub>O<sub>3</sub> mit CH<sub>2</sub>Cl<sub>2</sub>/EtOH (98:2) lieferte 60 mg (52%) farblose Kristalle (R<sub>f</sub> = 0.3) vom Schmp. >260 °C.

<sup>13</sup>C-NMR: δ = 158.6 (C<sup>6</sup>, C<sup>6'</sup>), 155.3 (C<sup>2</sup>, C<sup>2'</sup>), 138.1 (C<sup>4</sup>, C<sup>4'</sup>), 124.0 (C<sup>5</sup>, C<sup>5'</sup>), 120.0 (C<sup>3</sup>, C<sup>3'</sup>), 59.6 (–CH<sub>2</sub>–) ppm.

C<sub>36</sub>H<sub>30</sub>N<sub>8</sub>NaBr (677,6)

Ber. C 63.81 H 4.46 N 16.54,  
Gef. C 64.01 H 4.31 N 16.73.

8,21-Di(2-pyridylmethyl)-8,21,27,28,29,30-hexaaza-  
pentaacyclo[21.3.1.1<sup>2,6</sup>.1<sup>10,14</sup>.1<sup>15,19</sup>]-triacont-  
1(30),2,4,6(27),10,12,14(28),15,17,19(29),23,25-  
dodecanen (13)

Zu einer Suspension von 80 mg (0.20 mmol) Coronand 9' und 500 mg Natriumcarbonat in 50 ml Acetonitril wurden in der Siedehitze 55 mg (0,42 mmol) 2-Chlormethylpyridin in 20 ml Acetonitril zugetropft. Die Lösung wurde 24 h unter Rückfluß erhitzt, abfiltriert und das Lösungsmittel i. Vak. entfernt. Säulenchromatographie an Al<sub>2</sub>O<sub>3</sub> mit CH<sub>2</sub>Cl<sub>2</sub>/EtOH (95:5) lieferte 75 mg (65%) weiße Kristalle an 13 vom Schmp. 58 °C.

<sup>13</sup>C-NMR: δ = 158.5 (C<sup>6</sup>, C<sup>6'</sup>), 157.7 (C<sup>2</sup>), 154.4 (C<sup>2</sup>, C<sup>2'</sup>), 149.8 (C<sup>6'</sup>), 138.4 (C<sup>4</sup>, C<sup>4'</sup>), 136.7 (C<sup>4'</sup>), 124.2 (C<sup>5</sup>, C<sup>5'</sup>), 123.9/122.4 (C<sup>5</sup>/C<sup>5'</sup>), 120.3 (C<sup>3</sup>, C<sup>3'</sup>), 61.1 (C<sup>5</sup>), 60.5 (C<sup>6</sup>) ppm.

6,6'-Bis[(di(2-pyridylmethyl)amino)methyl]-  
2,2'-bipyridin (14)

Zu einer siedenden Suspension von 240 mg (0.61 mmol) Amin 10' und 400 mg Natriumcarbonat in 50 ml Acetonitril wurde langsam 160 mg

(1.30 mmol) 2-Chlormethyl-pyridin in 50 ml Acetonitril zugetropft und 20 h unter Rückfluß erhitzt. Nach dem Abkühlen wurde filtriert und das Lösungsmittel i. Vak. abdestilliert. Säulenchromatographie an  $\text{Al}_2\text{O}_3$  mit  $\text{CH}_2\text{Cl}_2/\text{EtOH}$  (90:10) lieferten 190 mg (54%) weiße Kristalle an 14 ( $R_f = 0.3$ ) vom Schmp. 130 °C.

$^{13}\text{C}$ -NMR:  $\delta = 159.6$  ( $\text{C}^2$ ), 158.6 ( $\text{C}^6, \text{C}^6$ ), 155.6 ( $\text{C}^2, \text{C}^2$ ), 148.9 ( $\text{C}^6$ ), 137.1 ( $\text{C}^4, \text{C}^4$ ), 136.3 ( $\text{C}^4$ ),

122.9/121.8 ( $\text{C}^3/\text{C}^5$ ), 122.8 ( $\text{C}^5, \text{C}^5$ ), 119.3 ( $\text{C}^3, \text{C}^3$ ), 60.3/60.1 ( $\text{C}^a/\text{C}^b$ ) ppm.

$\text{C}_{36}\text{H}_{34}\text{N}_8$  578,7

Ber. C 74,71 H 5,92 N 19,36.

Gef. C 74,54 H 6,05 N 19,15.

Dem BMFT sei für die finanzielle Unterstützung dieser Arbeit gedankt.

- [1] A. Juris, F. Barigelletti, S. Campagna, V. Balzani, P. Belser und A. v. Zelewsky. *Chem. Rev.* im Druck.
- [2] a) E. Seddon und K. R. Seddon. *Top. Inorg. a. Gen.* Vol. 19, Elsevier, Amsterdam (1984);  
b) N. Sutin und C. Creutz. *Pure Appl. Chem.* 52, 2717 (1980).
- [3] J. Parks, B. Wagner und R. Holm, *J. Organomet. Chem.* 56, 53 (1973).
- [4] F. Case. *J. Org. Chem.* 31, 2398 (1966).
- [5] G. Newkome, W. Puckett, G. Kiefer, V. Gupta, X. Xia, M. Coreil und M. Hackney. *J. Org. Chem.* 47, 4116 (1982).
- [6] G. Newkome, V. Gypta, F. Fronczek und S. Pappalardo. *Inorg. Chem.* 23, 2400 (1984) und 48, 4848 (1983).
- [7] J. C. Rodriguez-Ubis, B. Alpha, D. Blancherel und J. M. Lehn. *Helv. Chim. Acta* 67, 2264 (1984); die von uns entwickelte Synthese ist bereits beschrieben in: K. Zengerle. *Dissertation*, Universität des Saarlandes (1986).
- [8] B. Alpha, J. M. Lehn und G. Mathis. *Angew. Chem.* 99, 254 (1987).
- [9] J. M. Lehn. *Privatmitteilung*.
- [10] S. Grammenudi und F. Vögtle. *Angew. Chem.* 98, 1119 (1986).
- [11] J. H. Baxendale und P. George. *Trans. Faraday Soc.* 46, 55 (1955).
- [12] M. S. Henry und M. Z. Hoffman. *J. Phys. Chem.* 83, 618 (1979).
- [13] W. Walisch. *Chem. Ber.* 94, 2314 (1961).

# communications

## A SENSITIZER-RELAY ASSEMBLY WITH IMPROVED PROPERTIES IN ELECTRON TRANSFER PROCESSES

Heinz Dürr and Urs Thiery

Fachrichtung 13.2 Organische Chemie der Universität des Saarlandes, D-6600 Saarbrücken, F.R.G.

P.P. Infelta and A.M. Braun

Institut de Chimie Physique, EPFL, Ecublens, CH-1015 Lausanne, Switzerland.

Received December 15, 1988, accepted March 2, 1989.

**RÉSUMÉ.** — De nouveaux complexes homoleptiques et bis-hétéroleptiques de type  $RuL_3^{2+}$  et  $RuL_2L'^{2+}$  sont utilisés dans des réactions par transfert d'électrons. Le composé  $Ru(Me_2tepy)_3^{3+}$  est un nouveau sensibilisateur-relais qui produit de l'hydrogène avec un fort rendement en absence d'un réactif de transfert électronique.

**ABSTRACT.** — New homoleptic and bis-heteroleptic complexes of the type  $RuL_3^{2+}$  and  $RuL_2L'^{2+}$  are used in electron transfer reactions.  $Ru(Me_2tepy)_3^{3+}$  is a new sensitizer-relay assembly being highly efficient for hydrogen production in the absence of an electron transfer reagent.

Ru(II)-polypyridine complexes play an important role as sensitizers in the reduction of protons to hydrogen in the elementary process of the artificial photosynthesis<sup>1</sup>.

These ruthenium complexes, porphyrine derivatives and semiconductors ( $TiO_2$ ,  $SrTiO_3$ ) in microheterogeneous systems are the most important alternatives to photovoltaic solar energy conversion to the production of solar fuels<sup>2</sup>.

The major goal in the synthesis of these ruthenium complexes for solar energy conversion is to prepare molecules with tailor-made properties.

Such ruthenium complexes should possess the following properties :

- 1) absorption in the maximum of the solar spectrum,
- 2) a suitable lifetime of the excited state in the microsecond range,
- 3) show the thermodynamically desired redox potentials for electron transfer and,
- 4) diffusion controlled electron transfer quenching and effective separation of cage structure of photoproducts.

The sensitizer-relay assembly in one molecule should effect an especially efficient electron transfer as recent work of Balzani shows<sup>3</sup>.

$Ru(Me_2tepy)_3^{3+}$  5 (see Fig. 1) is an example of such a sensitizer-relay assembly.

It contains the structural properties of a ruthenium(II)-polypyridine complex with ferrioxo structure

( $=N-C-C-N=$ ) as well as the standard relay  $MV^{2+}$  (methyl-viologen = paraquat). On the other side, *tepy* (4, 4', 2', 2'', 4'', 4''')-tetrapyridine 1 can be regarded as a phenylogous

bipyrazine (see Fig. 2). Ruthenium(II)-tris-2,2'-bipyrazine showed a very high quantum yield of hydrogen evolution as was demonstrated previously<sup>4</sup>.

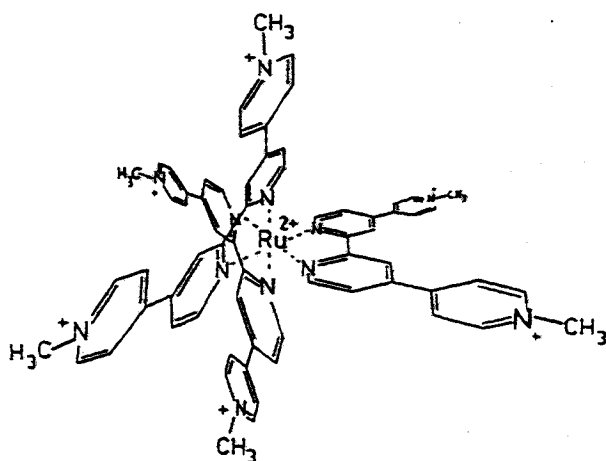
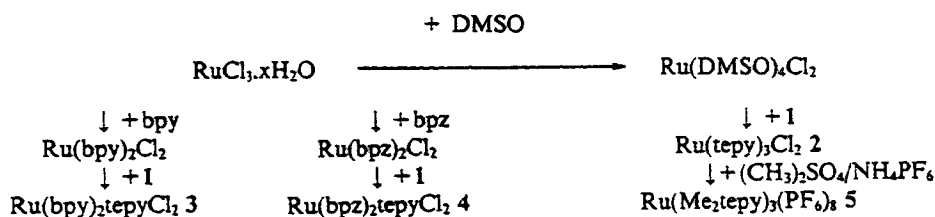


Figure 1. — Structure of  $Ru(Me_2tepy)_3^{3+}$  5

In this paper we report on :

- 1) the synthetic strategy of new homoleptic and bis-heteroleptic ruthenium(II)-polypyridine complexes,
- 2) the photophysical properties of these sensitizers and,
- 3) a sensitizer-relay assembly which allows hydrogen evolution in a sacrificial system without additional electron transfer reagent.

For the preparation of the ruthenium complexes the following synthetic strategy was used :



Scheme 1. — Preparation route for sensitizers 2 - 5; bpy = 2,2'-bipyridine, bpz = 2,2'-bipyrazine.

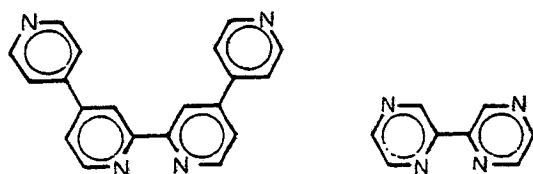


Figure 2. — Tepe 1 as phenyllogous 2,2'-bipyrazine.

In Table I the new homoleptic  $\text{RuL}_3^{2+}$  and heteroleptic  $\text{RuL}_2\text{L}'^{2+}$ -complexes, selected parameters of the UV-VIS spectra (MLCT-band) and luminescence spectra of 2-5 are collected.

The most important parameters of these new complexes are the luminescence lifetimes, which are determined by time resolved LASER-spectroscopy and luminescence quantum yields.

Table I. — Photophysical properties of the Ru-sensitizers at pH 7.

Compound	MLCT [nm] $\lambda_{\text{max}} \epsilon(\log)$	$\lambda_{\text{em,max}}(\text{RT})^a$ [nm]	$\lambda_{\text{em,max}}(77\text{K})^a$ [nm]
2	474(4.53)	638	615 665
3	468(4.18)	657	621 667sh
4	425(4.26)	643	600 648
5	487(4.20)	668	622sh 675

Solvent:  $\text{H}_2\text{O}$  in UV/VIS and luminescence spectra (RT); ethanol/ $\text{H}_2\text{O}$  (99/1) (v/v) in luminescence spectra (77K).

<sup>a</sup> For recording the luminescence spectra (RT; 77K) the sensitizers have been excited at the lowest energetic absorption band.

The lifetime  $\tau_0$  measured for 5 is in the microsecond range. The redox potentials for the excited states were calculated by standard procedures<sup>3</sup> from ground state potentials (obtained by cyclic voltammetry) and are given in Table II.

In presence of  $\text{MV}^{2+}$  the complexes 2 and 3 undergo oxidative electron transfer processes<sup>4</sup>, (see Table II). The excited states of compounds 4 and 5 are reductively deactivated by sacrificial donors such as EDTA or TEOA (triethanolamine).

The quantum yield of electron transfer processes (charge-relay =  $\text{MV}^{2+}$ ) are represented in Table II as well. The study of these new complexes in the sacrificial system  $\text{RuL}_3^{2+}/\text{TEOA}/2\text{-TMV}^{2+}/\text{Pt}$  at pH 7 (see Fig. 3;  $2\text{-TMV}^{2+} = 1,1', 2,2'$ -tetramethyl-4,4'-bipyridinium dichloride) indicates the improved properties of  $\text{Ru}(\text{Me}_2\text{tepy})_3^{2+}$  compared to the complexes shown in this paper as well as compounds that have been cited in the literature<sup>1,6</sup>.

The new sensitizer-relay assembly 5 shows in a sacrificial system in the absence of a relay (e.g.  $2\text{-TMV}^{2+}$ ) a significant hydrogen evolution (Fig. 3b).

This is an advantage in comparison to results obtained with  $\text{Ru}(\text{bpy})_3^{2+}$  and related  $\text{RuL}_3^{2+}$  complexes which do not lead to hydrogen evolution under similar conditions.

A combination of  $2\text{-TMV}^{2+}$  as electron transfer reagent with a sensitizer-relay assembly 5 shows under standard conditions (see Fig. 3a, 3b, 3c) the best quantum yield measured for hydrogen production mediated by ruthenium-complexes so far. Hydrogen production of the sensitizer-relay assembly in the absence of an electron transfer reagent opens the way to a very simple photochemical system for water reduction and related processes. Further work in this direction, especially with regard to the optimization of the system and the long term stability of 5 is under way.

Financial help of the BMFT is acknowledged.

Table II. — Luminescence lifetimes  $\tau_0$ , quenching constants  $k_q$ , quantum yields of viologen radical generation  $\Phi_{\text{MV}^{\cdot+}}$  and redox potentials of 2-5.

Compound	Lifetime $\tau_0(\text{ns})^f$	Quenching constant $k_q \times 10^6 [\text{M}^{-1}\text{s}^{-1}]^d$	Quantum yield $\Phi_{\text{MV}^{\cdot+}}^e$	$E^*_{\text{ox}}^a$ [V]	$E^*_{\text{red}}^b$ [V]
2	100	15	0.013	-0.60	1.00
3	55	14	0.020	-0.78	0.89
4	519	(red)	0.131	-0.63	—
5	444	(red)	(0.010)	-0.55	—

<sup>a</sup>  $E^*_{\text{ox}} = E^*(^*\text{RuL}_3^{2+}/\text{RuL}_3^{3+})$ ; <sup>b</sup>  $E^*_{\text{red}} = E^*(^*\text{RuL}_3^{2+}/\text{RuL}_3^{\cdot+})$ ; <sup>c</sup> obtained by LASER-flash-experiments; <sup>d</sup> measured at pH 6.88;  $[\text{NaCl}] = 0.1 \text{ M}$  (3 - 5); 0.033 2; Quencher:  $\text{MV}^{2+}$ ; (red) for 4 and 5: reductive deactivation of the excited sensitizer by a sacrificial donor; <sup>e</sup> argon degassed aqueous solution, phosphate buffer pH = 6.88  $[\text{MV}^{2+}] = 10^{-2} \text{ M}$ ;  $\Phi_{\text{MV}^{\cdot+}}$  was obtained by LASER-flash-experiments and can be regarded as a separation from the cage of photoproducts<sup>3</sup>; <sup>f</sup> measured vs. SCE in MeCN.

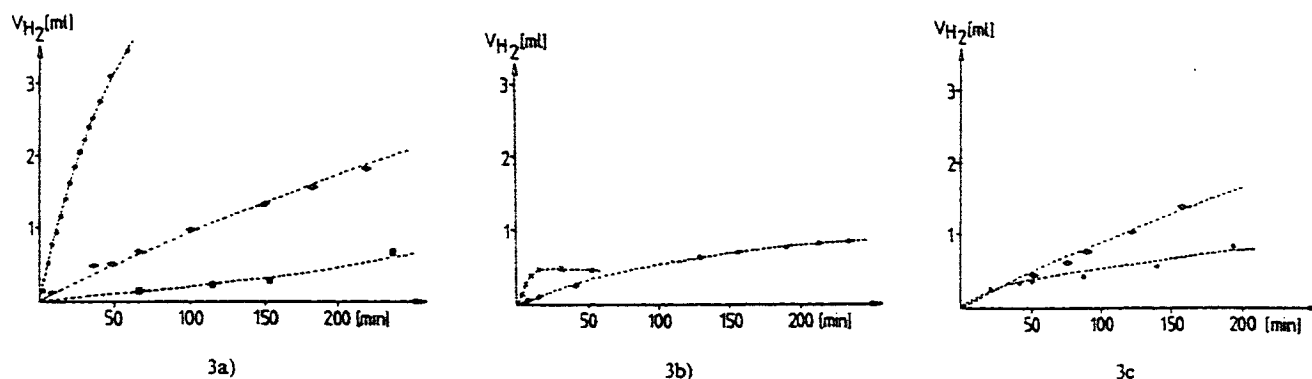


Figure 3a, 3b, 3c. — Hydrogen evolution in the sacrificial system containing 3 (=), 4 (◊) or 5 (●) as sensitizers and 2-TMV<sup>2+</sup> as charge relay at pH = 7.0 (a).

— Hydrogen evolution using 5 as sensitizer-relay assembly *without* external charge relay at pH = 4,7 (●) and pH = 7.0 (x); (b).

— Hydrogen evolution using 4 (◊) or 5 (●) as sensitizers and MV<sup>2+</sup> as charge relay at pH 4.7 (c).

Irradiation by 450 W xenon lamp combined by a 418 nm cut-off filter, 20 mL aqueous solution, catalyst Pt(polyvinylalcohol); 3, 4 and 5 as sensitizers. The sacrificial donor at pH 7.0 was TEOA, at pH 4.7 EDTA was used.

Electron transfer reactions. 5th paper see :

H. Dürr, K. Zengerle, H.P. Trierweiler, *Z. Naturforsch.*, 1988, 43b, 361-365.

#### REFERENCES

- Seddon S., Seddon K., « *Topics in Inorganic and General Chemistry, The Chemistry of Ruthenium* », Vol. 19, Elsevier, Amsterdam, 1984.
- Harriman A., West M.A., Eds., « *Photogeneration of Hydrogen* », Academic Press, London, 1982; Grätzel M., Ed., « *Energy Resources through Photochemistry and Catalysis* », Academic Press, New York, 1983; Rabani J., Ed., « *Photochemical Conversion and Storage of Solar Energy* », Weizman, Jerusalem, 1982; Connolly J.S., Ed., « *Photochemical Conversion and Storage of Solar Energy* », Academic Press, New York, 1981; Braun A.M., Ed., « *Photochemical Conversions* », Proceedings of the IOCD-UNESCO Seminar, Presses Polytechnique Romandes, Lausanne, 1983.
- Juris A., Barigelletti F., Campagna S., Balzani V., Belser P., von Zelewsky A., *Coord. Chem. Rev.*, 1988, 84, 85-277.
- Dürr H., Dörr G., Zengerle K., Reis B., Braun A.M., *Chimia*, 1983, 245-248; Dürr H., Dörr G., Zengerle K., Curchod J.-M., Braun A.M., *Helv. Chim. Acta.*, 1983, 66, 2652-2655; Dürr H., Dörr G., Zengerle K., Mayer E., Curchod J.-M., Braun A.M., *Nouv. J. Chim.*, 1985, 9, 717-720.
- Rillema D.P., Taghdiri D.G., Jones D.S., Keller C.D., Worl L.A., Meyer T.J., Levy H.A., *Inorg. Chem.*, 1987, 26, 578-585; Juris A., Belser P., Barigelletti F., von Zelewsky A., Balzani V., *Inorg. Chem.*, 1986, 25, 256-259.
- Meyer T.J., *Pure Appl. Chem.*, 1986, 58, 1193-1206; Kaiyanasundaram K., *Coord. Chem. Rev.*, 1982, 46, 159-244; DeArmond M.K., Carlin C.M., *Coord. Chem. Rev.*, 1981, 36, 325-355; Balzani V., Bolletta F., Gandolfi M.T., Maestri M., *Topics Curr. Chem.*, 1978, 75, 1-64.

# Artifizielle Photo-Synthese

## – Ein Beitrag zum Problem der Sonnenenergie-Konversion

Die Nutzung der regenerativen Energiequellen Wind, Wasser und Sonne hat sich in den letzten Jahren zum Gegenstand intensiver wissenschaftlicher Forschung entwickelt. Um Sonnenenergie im großen Maßstab für die Zukunft nutzbar zu machen, muß sie in geeigneter Weise umgewandelt und speicherbar gemacht werden. Dazu gibt es i.W. als Forschungsansätze das photobiologische Verfahren, die Photovoltaik, das solarthermische Verfahren und die in diesem Beitrag vorgestellte photochemische Methode oder artifizielle Photo-Synthese.

Photochemische Wasserspaltung kann als "künstliche Photosynthese" angesehen werden. Der Wirkungsgrad der Photosynthese beträgt maximal 1 %. Die photochemische Wasserspaltung erreicht heute 2,8 %, Wirkungsgrade von mehr als 10 % werden angestrebt.

Die letzten Jahre brachten dramatische Veränderungen für die Energieversorgung der Industrienationen. Die Energiekrise der 70er Jahre machte unsere Abhängigkeit vom Energieträger Erdöl auf sehr drastische Weise deutlich.

Inzwischen hat das Waldsterben die Öffentlichkeit auch auf das Problem der Umweltbelastung durch die Freisetzung von Luftschadstoffen wie Schwefel- und Stickoxide sensibilisiert.

Während die Emission von  $\text{NO}_x$  und  $\text{SO}_2$  der Kraftwerke durch geeignete Filtermaßnahmen reduziert werden kann, ist die Freisetzung von  $\text{CO}_2$ , die bei jeder Verbrennung fossiler Energieträger erfolgt, nicht zu beeinflussen. Schon heute ist ein Anstieg des  $\text{CO}_2$ -Gehaltes der Atmosphäre feststellbar, der in

Zukunft zu nicht abschätzbaren Klimaveränderungen führen kann (Treibhauseffekt).

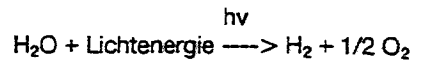
Nach heutiger Kenntnis werden die Erdölvorräte der Welt in wenigen Jahrzehnten verbraucht sein, womit nicht nur ein wichtiger Energieträger, sondern auch ein bedeutender Rohstofflieferant der chemischen Industrie unwiederbringlich verloren sein wird. Die Ereignisse der letzten Jahre (Harrisburg, Tschernobyl) zeigen, daß Kernenergie auf Dauer keinen Ersatz für fossile Energieträger darstellen kann, zumal das Problem der Behandlung radioaktiven Abfalls (Wiederaufarbeitung, Transport, Endlagerung) nicht zufriedenstellend gelöst ist und die Kosten zur Atomstromproduktion in keinem Verhältnis zur Betriebsdauer eines Kraftwerks stehen.

Wenn es gelänge, regenerative Energiequellen – vor allem Sonnenenergie – in großem Maßstab (Sonnenkraftwerke) nutzbar zu machen, würde die Menschheit über eine unerschöpfliche und zudem umweltfreundliche Energiequelle verfügen. Schon die Belegung von 0,1 % der Landfläche der Erde mit Solarzellen würde den Weltenergiebedarf vollständig decken. Den Energiebedarf der Bundesrepublik Deutschland könnte eine Fläche von 200 km x 225 km in der Sahara liefern.

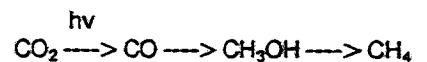
Unabdingbare Voraussetzung für die Nutzung der Sonnenenergie ist die Möglichkeit ihrer Speicherung in energiereichen, transport- und lagerfähigen Substanzen. Die Natur hat eine solche Umwandlungsmöglichkeit (Konversion) von Sonnenenergie in energiereiche Substanzen mit der Photosynthese geschaffen. Fossile Energieträger wie Kohle, Erdöl und Erdgas sind durch Photosynthese gebildete Speichersubstanzen der Sonnenenergie.

Als erfolgversprechende Lösungen des Speicherproblems bieten sich heute vor allem die Zerlegung

von Wasser in die Elemente Wasserstoff und Sauerstoff



sowie die Reduktion von  $\text{CO}_2$  zu Kohlenmonoxid, Methanol oder Methan an.



Die Wasserzerlegung besitzt den Vorteil, den Energieträger Wasserstoff zu liefern, der äußerst umweltfreundlich und vielseitig einsetzbar ist. Bei der Verbrennung von  $\text{H}_2$  entsteht nur  $\text{H}_2\text{O}$ , das Problem der Emission von  $\text{CO}_2$ ,  $\text{SO}_2$  wäre gelöst, die  $\text{NO}_x$ -Produktion stark reduziert.

$\text{H}_2$  kann als Brennstoff für Automobile und Kraftwerke eingesetzt werden, außerdem ist eine direkte Stromerzeugung in Brennstoffzellen möglich. Es gibt Vorschläge,  $\text{H}_2$  in großen Mengen durch geeignete Methoden der Sonnenenergiekonversion in den sonnenreichen Ländern zu produzieren und ihn dann (wie es vergleichbar derzeit mit Erdöl praktiziert wird) in die Industrieländer zu transportieren.

Abbildung 1 gibt einen schematischen Überblick über die Nutzungsmöglichkeiten des mit Hilfe der photochemischen Methode erzeugten Wasserstoffs.

### Methoden der Sonnenenergienutzung

Die Energie der Sonne wird von der Menschheit schon seit langem, etwa zur Salzgewinnung, in Wind- und Wasserkraftwerken genutzt. Ein Beispiel für die direkte Sonnenenergiekonversion wird uns von der Natur in der Photosynthese demonstriert. Dort wird mit Hilfe der Sonnenstrahlen Wasser und Kohlendioxid

\* Der Autor dankt Hans-P. Trierweiler, Thomas Röttsch, Armin Beuerlein, Andreas Guidner und Holger Kraus für ihre Mitarbeit



oxid in einem komplizierten Mechanismus, für dessen teilweise Aufklärung der Nobelpreis 1989 an Huber, Michel und Deisenhofer verliehen wurde, in energiereiche Kohlenhydrate und Sauerstoff umgewandelt. So entstanden über Jahrmillionen hinweg die heute genutzten fossilen Energieträger.

Der maximale Wirkungsgrad der Photosynthese liegt allerdings nur bei ca. 1% <sup>1)</sup>. Technologisch im großen Maßstab werden heute verschiedene Sonnenenergieumwandlungsverfahren untersucht:

### Solarthermische Verfahren:<sup>2)</sup>

Es existieren mittlerweile weltweit mehrere solarthermische Kraftwerke, wie Eulios in Sizilien, SEGS I + II in Kalifornien, die bei einem Wirkungsgrad von 10 % elektrischen Strom liefern.

### Photovoltaische Verfahren:<sup>3)</sup>

Dabei wird mit Solarzellen (Si-Halbleiter) mit hohem Wirkungsgrad (10-20 %) Elektrizität erzeugt. Eine speicherfähige Energieform ist erst mit nachgeschalteter Wasserelektrolyse (Wirkungsgrad 60-80 %) zu erreichen, wodurch der Gesamtwirkungsgrad herabgesetzt wird. Photovoltaische Großanlagen, wie das Solarkraftwerk Carriso Plains in Kalifornien, liefern jährlich schon über 14 Mio. kWh elektrische Energie<sup>4)</sup>.

### Photoelektrochemische Verfahren:<sup>5)</sup>

Hier werden bei Bestrahlung mit Hilfe von Photohalbleitern (CdS, MoSe<sub>2</sub>) in wässrigen Elektrolytlösungen Strom oder chemische Energiespeicherprodukte, beispielsweise Wasserstoff und Sauerstoff, erzeugt.

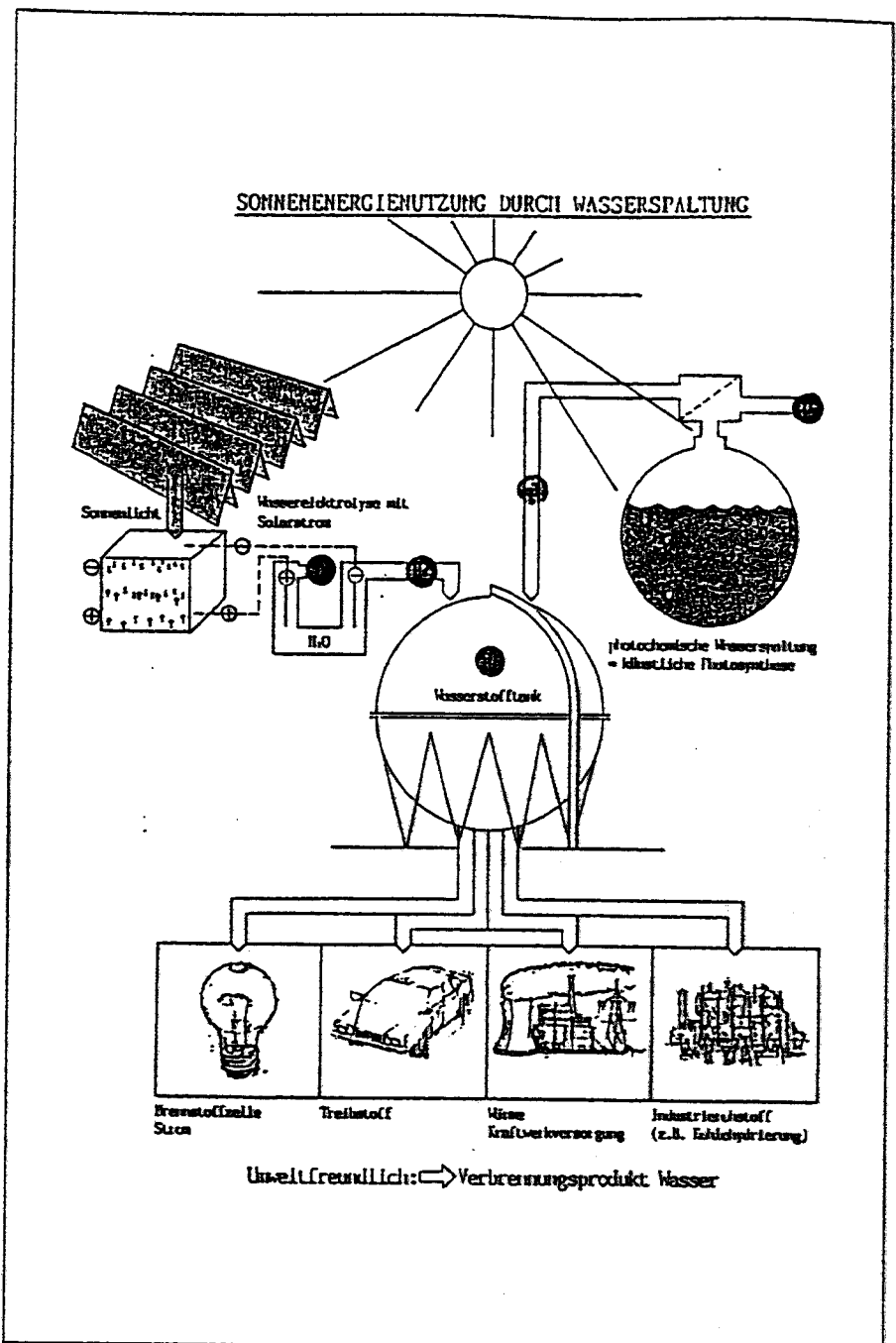


Abbildung 1: schematische Darstellung der Erzeugung und Nutzung des mittels der photochemischen Sonnenenergiekonversion gebildeten Wasserstoffs.

AC.PRESS

**Wir engagieren uns für Energie und Umwelt . . .**

Für eine langfristig sichere Elektrizitätsversorgung und zur Sicherung saarländischer Arbeitsplätze verstromen wir heimische Steinkohle.

Zum Schutz unserer Umwelt haben wir in diesem Jahr in unserem Kraftwerk Ensdorf eine Rauchgasentschwefelungsanlage nach dem abwasserfreien Sprühabsorptionsverfahren in Betrieb genommen.

**... für das Saarland**

**VSE**

Partner für Energie und Umwelt

Vereinigte Saar-Elektrizitäts-AG  
Heinrich-Böcking-Straße 10-14  
6600 Saarbrücken  
Tel. 06811/607-1

Beratungszentrum  
Gymnasialstraße 72a  
6688 Illingen  
Tel. 06825/44011

Beratungszentrum  
Hochwaldstraße 70  
6640 Merzig  
Tel. 06861/5016

## Photobiologische Verfahren:<sup>6</sup>

Neben der Anwendung von Algenkulturen zur Erzeugung von Biomasse wird die Gewinnung von Sauerstoff und Wasserstoff durch Algen oder phototrophe Bakterien in speziellen Nährlösungen untersucht.

## Photochemische Verfahren:<sup>7a,b)</sup>

Hierzu gehören unimolekulare Umlagerungsreaktionen (z.B. Norcaradien in Quadricyclan), Photodissoziation von Molekülen ( $\text{NO}_2 \rightarrow \text{NO} + 1/2\text{O}_2$ ) sowie die photochemische Wasserspaltung oder artifizielle Photosynthese, die Thema dieses Beitrags ist.

## Mechanismus der Reduktion von Wasser und Kohlendioxid

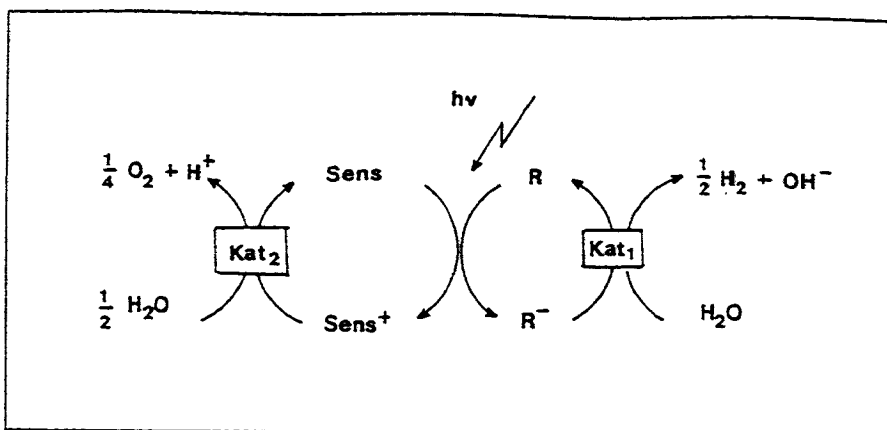
Sowohl Wasser als auch Kohlendioxid absorbieren kein sichtbares Licht; eine direkte photochemische Aktivierung von  $\text{H}_2\text{O}$  bzw.  $\text{CO}_2$  gelingt nur im Vakuum-UV. Um die Sonnenenergie auf die zu reduzierende Spezies ( $\text{H}_2\text{O}$  bzw.  $\text{CO}_2$ ) zu übertragen, ist ein komplexes System aus Lichtfänger (Sensibilisator) und Elektronenüberträger (Relais) sowie ein oder mehrere Katalysatoren erforderlich.

### a) Wasserspaltung

Aufbauend auf den Arbeiten von Sutin<sup>8a,b,c)</sup> wurde ein cyclisches System zur Wasserspaltung (artifizielle Photosynthese) vorgeschlagen<sup>9</sup> (Schema 1):

Die Reproduzierbarkeit dieses Systems ist allerdings nicht in eindeutiger Weise möglich, insbesondere der  $\text{O}_2$ -liefernde Schritt stellt hohe Reinheits- und Selektivitätsanforderungen an den dazu erforderlichen  $\text{RuO}_2$ -Katalysator. Unsere Arbeitsgruppe<sup>10,11,12)</sup> konzentriert sich daher auf die Entwicklung von sogenannten sacrificiellen Systemen zur Wasserspaltung, d.h. der Trennung des Gesamtprozesses in Wasserstoff- bzw. Sauerstoffherzeugung. Hierbei wird der  $\text{O}_2$ -liefernde Schritt in diesem System simuliert ( $\text{Ru}^{3+}$  wird durch einen "aufzuopfernden" Donor (Ethylendiamintetraessigsäure EDTA, Triethanolamin TEOA) oder erneut zu  $\text{Ru}^{2+}$  regeneriert) (Schema 2):

Neben diesem sogenannten photooxidativen Mechanismus (der an-



Schema 1: Cyclische Wasserspaltung

Sens. =  $\text{Ru}(\text{bpy})_3^{2+}$  (Ruthenium-trisbipyridin)  
 $\text{R} = \text{MV}^{2+}$  (Methylviologen);

$\text{Kat}_1 = \text{Pt}$  (Platin);  
 $\text{Kat}_2 = \text{RuO}_2$  (Ruthenium-(IV)-oxid)

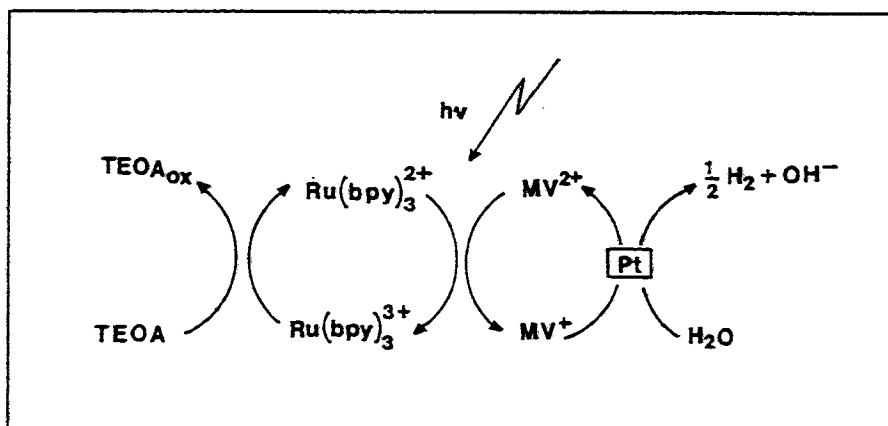
geregte Sensibilisator wird im ersten Schritt oxidiert) kann die sacrificielle Wasserstoffentwicklung auch photo-reduktiv geführt werden.

### b) Kohlendioxidreduktion

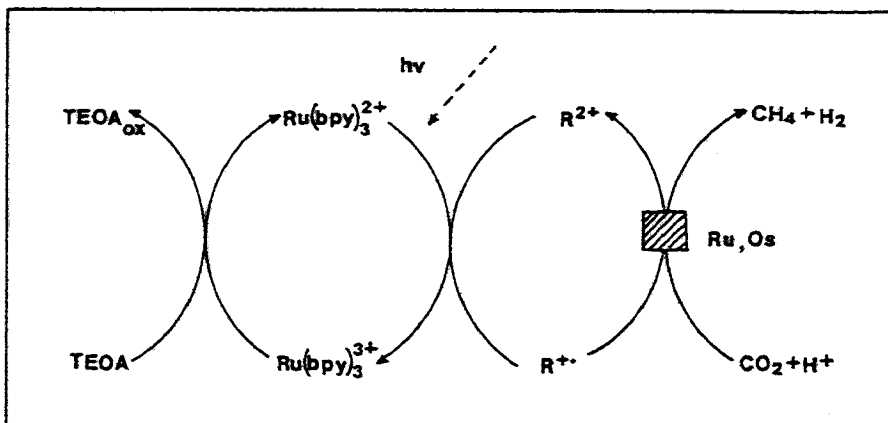
Der sehr intensiv untersuchte Sensibilisator  $\text{Ru}(\text{bpy})_3^{2+}$  eignet sich darüber hinaus auch zur sacrificiellen

Reduktion von Kohlendioxid<sup>13,14,15)</sup> (Schema 3):

Durch Variation des Katalysators (Ersatz von Platin durch Ruthenium oder Osmium) und Verwendung eines stärker reduzierend wirkenden Elektronenrelais (negativeres Potential) ist die Bildung von Methan und Ethan realisiert worden. Diese als



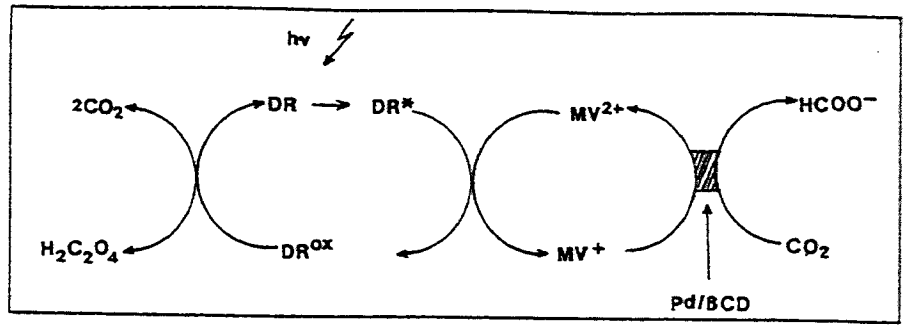
Schema 2: Sacrificielle Wasserspaltung (oxidatives System)  
 (Die Liganden sind der besseren Übersichtlichkeit halber weggelassen)



Schema 3: Sacrificielle Reduktion von Kohlendioxid

Brennstoffe einsetzbaren organischen Verbindungen (Methan ist Hauptbestandteil von Erdgas) werden auch als "Solar Fuels" (durch Sonnenenergie erzeugte Brennstoffe) bezeichnet. Ein weiterer, sehr effektiver Sensibilisator auf Naturstoffbasis ist das Deazariboflavin, welches als Vitamin B<sub>2</sub>-Derivat aufzufassen ist.

Dieses System enthält darüber hinaus Oxalsäure als sacrificiellen Donor sowie das bereits bei der Wasserreduktion vorgestellte Elektronenrelais MV<sup>2+</sup>. Als Katalysator fungiert hier Palladium, stabilisiert durch  $\beta$ -Cyclodextrin; als Reduktionsprodukt des Kohlendioxids wird das Salz der Ameisensäure – Natriumformiat – erhalten.



Schema 4: Sacrificielle Kohlendioxidreduktion mit Deazariboflavin - DR als Sensibilisator.

Besonders vorteilhaft wirkt sich in diesem System aus, daß das Oxidationsprodukt des Donors – Kohlendioxid – als Oxidationsmittel des MV<sup>+</sup> wirkt. Die einzelnen Parameter dieser Gesamtsysteme (Sensibilisa-

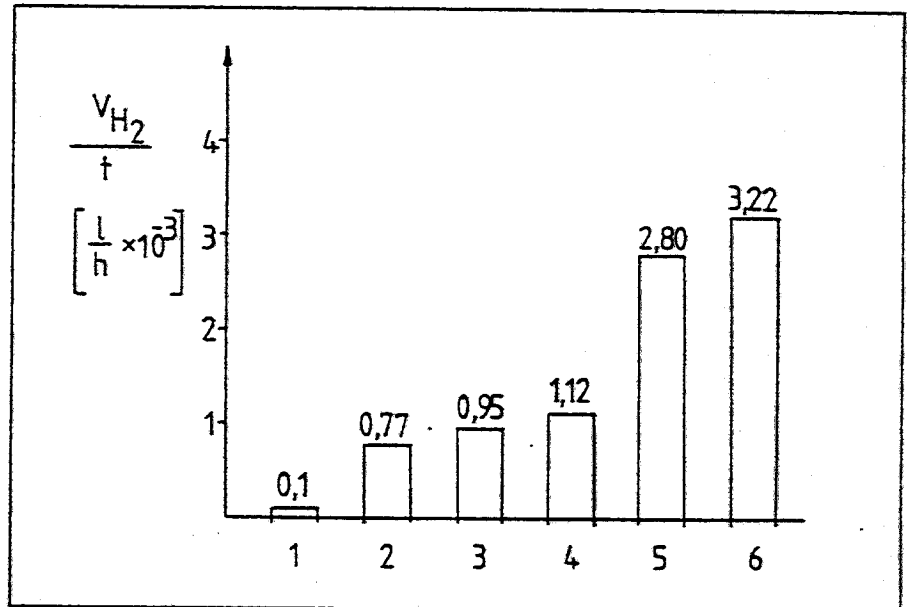
tor im photochemischen Zyklus; Elektronenrelais und Katalysator im thermischen Zyklus) können getrennt optimiert und so zu einer möglichst effektiven Einheit kombiniert werden.

## Eigene Arbeiten und Forschungsergebnisse<sup>10,11,12,13</sup>

Da, wie schon erwähnt, die Einzelkomponenten eines photochemischen Systems getrennt untersucht werden können, sind in unserer Arbeitsgruppe insbesondere Sensibilisatoren, Katalysatoren und Elektronenrelais (Quencher) Gegenstand intensivster Forschung. Als geeignete Modelle werden die schon erwähnten sacrificiellen Systeme bearbeitet.

Ein Schwerpunkt liegt auf der Untersuchung der Sensibilisatoren. Sie werden auf ihre Eignung nach den Kriterien des reversiblen Redoxverhaltens, der geeigneten Potentiale, der photochemischen und thermischen Stabilität, der Absorptionseigenschaften und der Lebensdauer des angeregten Zustandes untersucht.

Schema 5 zeigt die Wasserstoffproduktion einer Auswahl von Sensibilisatoren, die von uns zum Teil erstmals synthetisiert und studiert worden sind.



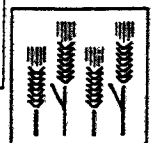
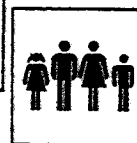
Schema 5: Wasserstoffproduktion durch Sensibilisatoren (1)-(6)

(1) Ru(bpy)<sub>2</sub>PPBCl<sub>2</sub>  
 (3) Ru(bpz)<sub>2</sub>bpdzCl<sub>2</sub>  
 (5) Ru(bpz)<sub>2</sub>2-bpmCl<sub>2</sub>  
 (bpz-Bipyrazin)

(2) Ru(bpz)<sub>2</sub>PPCl<sub>2</sub>  
 (4) Ru(bpy)<sub>3</sub>Cl<sub>2</sub>  
 (6) Ru(bpz)<sub>3</sub>Cl<sub>2</sub>  
 (2 bpm-Bipyrimidin)

# Lebensmittel info

Fachinformationen für Hygiene und Verbraucherschutz



Gesundheit

Ernährung

Wie Schema 5 zeigt, wurde insbesondere in (6) ein besonders wirksamer Sensibilisator zur Wasserstoffzeugung gefunden.

Eine von dem Ru-Komplexen abweichende Spezies stellt die Klasse der Zinnporphyrine dar. Sie ist strukturell mit den in der Natur vorkommenden Sensibilisatoren, den Chlorophyllen, verwandt. Es konnte festgestellt werden, daß es sich zwar um photoredoxaktive Substanzen handelt, die aber kein zyklisches System ergeben, da bei der Photoreduktion dieser Substanzen Hydrierungsprodukte der eingesetzten Sensibilisatoren gebildet werden.

Ein allgemeines Problem aller Sensibilisatoren stellt die photochemische Zerstörung durch Abspaltung eines Liganden dar (Photoanation). So ist z.B.  $\text{Ru}(\text{bpz})_3\text{Cl}_2$  zu Beginn der Bestrahlung ein sehr aktiver  $\text{H}_2$ -Produzent, vermindert dann aber nach ca. 3 Stunden die Produktion aus oben genanntem Grund. Unsere Arbeitsgruppe beschäftigt sich intensiv mit der Suche nach der möglichen Unterdrückung solcher Photoanationen. Ein verbrücktes Ligandensystem sollte keine Photoanation mehr zeigen. Diese Überlegung führt zur Verbindungsklasse der Podanden, Coronanden und Kryptanden, die Moleküle mit komplexer Struktur darstellen. Abbildung 2 zeigt die Struktur des Kryptanden.

Insbesondere solche Kryptanden sollten wegen ihrer allseitigen Fixierung keine Photoanation mehr zeigen. Bei diesem Verbindungstyp werden die Liganden mit Ferroinstruktur

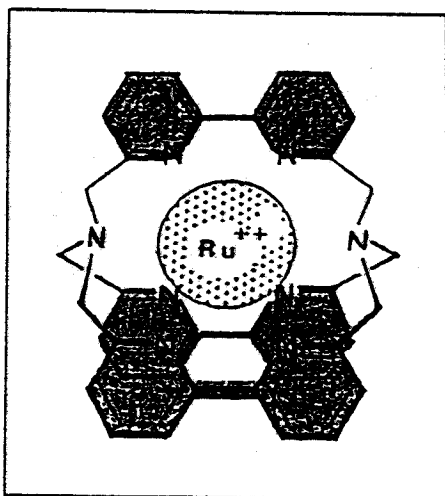
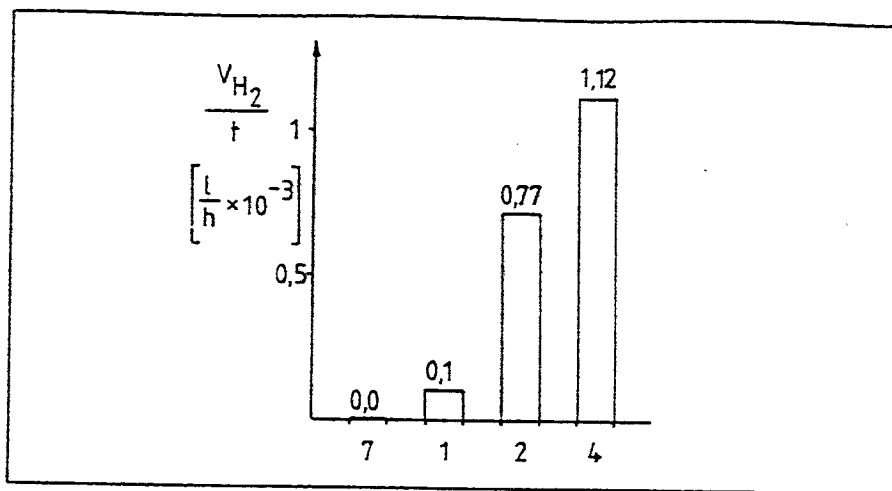


Abbildung 2:  
Im Kryptandmolekül sind die Bipyridineinheiten käfigartig miteinander verbunden; ein Verlust einer Untereinheit ist nicht mehr möglich (Methode zur Langzeitstabilisierung von Sensibilisatoren).



Schema 6: Änderung der Wasserstoffproduktion von Sensibilisatoren durch schrittweise Variation im Molekül.

(1)  $\text{Ru}(\text{bpy})_2\text{PPCl}_2$   
(4)  $\text{Ru}(\text{bpy})_3\text{Cl}_2$

(2)  $\text{Ru}(\text{bpy})_2\text{PPCl}_2$   
(7)  $\text{Ru}(\text{bpz})_2\text{PPCl}_2$

über zwei  $(\text{CH}_2)_3\text{-N}$  Einheiten miteinander verbunden. Parallel zu J. M. Lehn (Nobelpreisträger in Chemie 1987) wurde von uns eine Route zur Synthese solcher Verbindungen entwickelt. Sie weist gegenüber der Methode von Lehn zahlreiche Vorteile auf. Ihr größter Vorzug besteht darin, eine Kombination verschiedener Liganden vorzunehmen, um somit die Eigenschaften des Komplexes zu optimieren<sup>14)</sup>. Dazu ist es notwendig, die Skala der zur Verfügung stehenden Liganden zu erweitern, um Änderungen und Einflüsse eines Liganden auf die Komplexcharakteristik zu untersuchen. Es wird deshalb zur Zeit eine Gruppe von Liganden synthetisiert, die sich nur durch ihr Substitutionsmuster voneinander unterscheiden. Durch ihren Einbau in herkömmliche Komplexe kann abgeschätzt werden, ob sie die geforderten Eigenschaften in den Verbindungen besitzen. Da die Synthese eines Kryptanden sehr aufwendig ist, werden erst bei Erfüllung der Anforderungen neue Liganden in eine Kryptandenstruktur eingebaut werden. Wie die Komplexeigenschaften durch Austausch nur eines Liganden beeinflusst werden, zeigt Schema 6.

Wie Schema 6 zu entnehmen ist, wird die Wasserstoff-Produktion entscheidend durch die Änderung nur eines Liganden beeinflusst. Die Volumenangaben des entwickelten Wasserstoffs beziehen sich auf eine Photolysezelle von 20 ml Fassungsvermögen. Die dabei in unserer Arbeitsgruppe entwickelte Photolysezelle<sup>15)</sup> ist in Abbildung 3 schematisch dargestellt.

Diese Apparatur wurde im Rahmen der Messe Energie und Umwelt 87 in Saarbrücken einer breiteren Öffentlichkeit vorgestellt. Durch diese Präsentation wurden auch die Medien (WDR) angeregt, den gesamten Themenkomplex am 13.12.1987 im Rahmen der Sendung "Globus – die Welt von der wir leben" einer bundesweiten Öffentlichkeit vorzustellen.

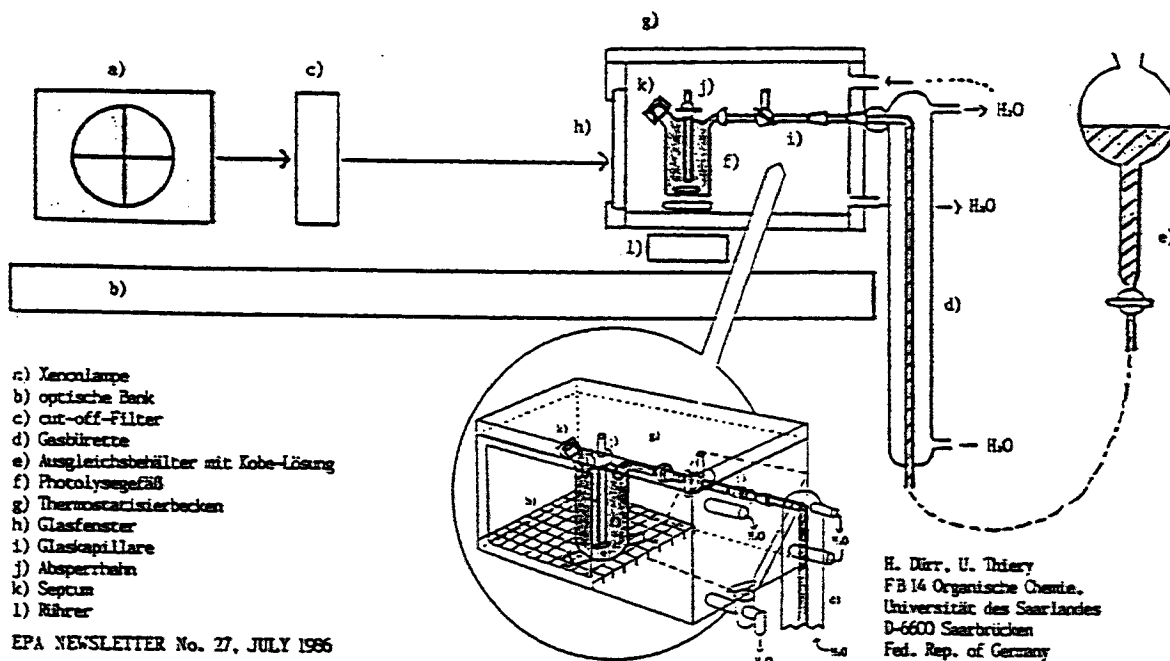
## Elektronenrelais

Die von einem Sensibilisator absorbierte Strahlungsenergie kann nicht direkt auf Protonen übertragen werden. Elektronenrelais (Quencher) übernehmen die Aufgabe dieses Energietransfers. Elektronenrelais sollen sowohl thermisch als auch photochemisch stabil sein und reversibel ein Elektron austauschen können. Auch dürfen keine Zersetzungsreaktionen in Konkurrenz zur Elektronenübertragung auftreten.

Basierend auf der Stammverbindung Dimethylviologen wurden in unserer Arbeitsgruppe mehrere Viologene synthetisiert und auf ihre Eignung zum Energietransfer untersucht. Die vorangegangene Abbildung zeigt die Wasserstoffproduktion in Abhängigkeit des verwendeten Elektronenrelais bei sonst unveränderten Versuchsbedingungen.

Der unterschiedliche Methylierungsgrad bewirkt eine Änderung der Redoxpotentiale. Als beste Relais erwiesen sich dabei (8) und (9), ((8) =  $\text{MV}^{2+}$ ; (9) =  $2\text{-TMV}^{2+}$  Tetramethylviologen). Eine wichtige Erkenntnis erhielt man durch Untersuchung ver-

## PHOTOCHEMISCHE WASSERSPALTUNG



EPA NEWSLETTER No. 27, JULY 1986

Abbildung 3: schematische Darstellung der Photolyseapparatur<sup>15)</sup>; mit dieser Apparatur wurden o.g. Werte der Wasserstoffproduktion ermittelt.

schiedener Relais bei Variation des pH-Wertes. Es zeigte sich, daß unterschiedliche Überträger bei Variation des pH-Wertes verschiedene Effektivitäten bezüglich der Wasserstoffproduktion aufweisen. Es gibt also kein unter jeder Bedingung ideales Relais, sondern es muß den Erfordernissen des Systems angepaßt werden.

### Katalysatoren

Katalysatoren haben die Aufgabe, die Elektronenübertragung vom redu-

zierten Relais zum Wasserstoffion  $H^+$  zu ermöglichen. Aufgrund der verwendeten Katalysatoren können prinzipiell zwei Systeme, ein quasihomogenes und ein mikroheterogenes, unterschieden werden. Im quasihomogenen System liegt der Katalysator als Übergangsmetallsol (Ru, Pt, Os), im mikroheterogenen System auf einem Träger (oft ein Halbleiter, wie z.B.  $TiO_2$ ) vor.

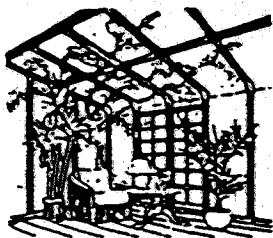
In unserem Arbeitskreis wurden bisher verschiedene Metallsole (Ru-, Os-, Pt-, Pd-Sol), die auf unter-

schiedlichste Weise hergestellt und stabilisiert werden, auf ihre Tauglichkeit zur photochemischen Wasserreduktion getestet. Bei den untersuchten Katalysatoren auf Trägern (mikroheterogenes System) wurden die reproduzierbare Herstellung und Charakterisierung des Trägers ( $TiO_2$ ) sowie dessen reproduzierbare Beschichtung mit Platin in den Vordergrund gestellt. Die Ergebnisse der bisher erfolgten Untersuchungen an  $TiO_2$ -Pt-Katalysatoren zeigen, daß die benötigte Katalysatormenge gegenüber den Solen bei gleicher Effizienz drastisch reduziert wurde, die Reproduzierbarkeit der Darstellung gewährleistet und damit die industrielle Herstellung möglich und ein Recycling des Katalysators gegeben ist.

### Ausblick

Es bleibt im Bereich der artifiziellen Photo-Synthese mit Ru-Sensibilisatoren das Ziel, verbrückte Systeme nach Art der Kryptanden zu synthetisieren. Es muß sich dabei um Verbindungen handeln, die über optimale Liganden bzw. Ligandenkombinationen verfügen. Wir sind zuversichtlich, daß es in naher Zukunft gelingt, die sacrificiellen Teil-Systeme der Wasserstoff- und Sauerstoffproduktion zu effizienten voll-cyclischen Systemen zur gleichzeitigen Wasserstoff- und Sauerstoffherzeugung zu kombinieren.

# nom



**Wintergarten-Systeme**  
 Wintergärten aus Holzern  
 nach Wahl mit Isolier-  
 und Acrylglas

Rufen Sie uns an.  
 Wir beraten Sie gerne.

## Ihr Platz an der Sonne

Neu im Programm: **Möbel aus Plexiglas**  
**Markisen**

Norbert Müller · Primswelderstr. 40 · 6612 Schmelz-Hüttersdorf  
 Telefon: (0 68 87) 36 76



Professor Dr. rer. nat. **Heinz Dürr**, geb. 1934 in Pforzheim; von 1954 bis 1959 Studium der Chemie in Stuttgart, Innsbruck und Heidelberg. 1959 Diplom, 1961 Promotion an der Universität

Heidelberg bei Prof. Wittig. Von 1961 bis 1962 Research associate bei Prof. H. E. Zimmermann, University of Wisconsin, Madison; von 1962 bis 1963 NATO-Stipendiat bei Prof. G. Ourisson, ULP, Strasbourg. Von 1963 bis 1964 Farberforschungslabor der BASF in Ludwigshafen, danach wiss. Assistent an der Universität des Saarlandes bei Prof. B. Eistert. 1969 Habilitation, seit 1971 Professor der Chemie an der Universität des Saarlandes.

Gastprofessuren in Ibandan, Nigeria, und an der Universität Marseille; Forschungs- und Vortragsaufenthalte an der Universität Kairo, der University of Florida/Gainesville und der Columbia University, New York. Seit 1984 Gastvorlesungen an der EHCS in Straßburg.

Parallel dazu wird die Forschung zur Produktion energiereicher Roh- oder Brennstoffe, also den "Solar Fuels" forciert werden, da diese Systeme

in ihrer Flexibilität der Energiespeicherung den nur zur Strom- oder Wasserstoffherzeugung geeigneten photovoltaischen Methoden überlegen sind.

#### Literaturverzeichnis:

1. R. Dahlgren, Bild der Wissenschaft, Sonderheft: Energie aus Sonne und Wind, Deutsche Verlagsanstalt, Stuttgart.
2. J. Bolton, Science, 202, 705, 1978.
3. M. Selders, D. Bonnet, Physik in unserer Zeit, 10, 3, (1979).
4. B. Kobbe, Bild der Wissenschaft 11, 1986
5. M. Wrighton, J. Chem. Educ., 60, 877, (1983).
6. "Möglichkeiten der verstärkten energetischen Nutzung photochemischer, photoelektrochemischer und biologischer Umwandlungsverfahren", BMFT-Studie, H. Möhwald, E. Hamer, B. Obkircher, W. Schäfer und B. Schröder, 1982.
- 7a. E. Schumacher, Chimia, 32, 193, (1978).
- 7b. H.D. Scharf, J. Fleischauer, H. Leismann, J. Ressler, W. Schläger, R. Weitz, Angew. Chem., 91, 696, (1979).
- 8a. C. Creutz, N. Sutin, Proc. Natl. Acad. Sci. USA, 72, 2858, (1975).
- 8b. K. Chandrasekaran, T. Foreman, D. Whitten, Nouv. J. Chim., 5, 275, (1981).
- 8c. V. Balzani, L. Moggi, M. Manfrim, F. Bolletta, M. Gleria, Science, 189, 852, (1975).
9. K. Kalyanasundaram, M. Grätzel, Angew. Chem., 91, 759, (1979).
10. H. Dürr, G. Dörr, K. Zengerle, A.M. Braun, Chimia, 37, 245, (1983).
11. H. Dürr, G. Dörr, K. Zengerle, J.M. Curchod, A.M. Braun, Helv. Chim. Acta, 66, 2652, (1983).
12. H. Dürr, G. Dörr, K. Zengerle, E. Mayer, J.M. Curchod, A.M. Braun, Nouv. J. Chim., 9, 717, (1985).
13. I. Wäliker, R. Maidan, D. Mandler, H. Dürr, G. Dörr, K. Zengerle, J. Am. Chem. Soc. 109, 6080, (1987).
14. H. Dürr, K. Zengerle, H.P. Trierweiler, Zeitschr. f. Naturforsch., 43b, 361, (1988).
15. H. Dürr, U. Thiery, EPA-Newsletters, 6, 39, (1986).

AC-PRESS

**Wir engagieren uns für Energie und Umwelt . . .**

Für eine langfristig sichere Elektrizitätsversorgung und zur Sicherung saarländischer Arbeitsplätze verstromen wir heimische Steinkohle.

Zum Schutz unserer Umwelt haben wir in diesem Jahr in unserem Kraftwerk Ensdorf eine Rauchgasentschweelungsanlage nach dem abwasserfreien Sprühabsorptionsverfahren in Betrieb genommen.

**... für das Saarland**

**VSE**

**Partner für Energie und Umwelt**

Vereinigte Saar-Elektrizitäts-AG  
Heinrich-Böcking-Straße 10-14  
6600 Saarbrücken  
Tel. 06 61 / 607-1

Beratungszentrum  
Gymnasialstraße 72 a  
6688 Illingen  
Tel. 0 68 25 / 4 40 11

Beratungszentrum  
Hochwaldstraße 70  
6640 Merzig  
Tel. 0 68 61 / 50 16



**Blankstahl und Qualitätsstahl**  
**Blanker Rund- und Flachstahl in allen Güten,**  
**Automatenstahl, Keilstahl, Silberstahl.**  
**Rostfreie und hochfeste Stähle,**  
**Werkzeugstahl, Metalle.**

**WEINMANN & CO - IHRE STAHLHANDLUNG**

ZWEIBRÜCKEN  
☎ (0 63 32) 20 45  
Fax: (0 63 32) 1 42 73

WALDMOHR  
☎ (0 63 73) 30 15  
Fax: (0 63 73) 44 43

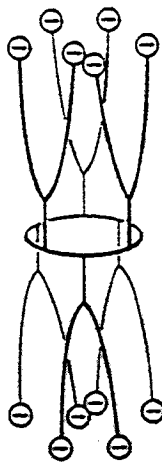
# Supramolekulare Chemie in Saarbrücken

Den „supramolekularen Chemikern“, die sich in Saarbrücken zu einem international besetzten Workshop trafen, geht es bald wie den Molekularbiologen: Ihre Systeme sind so komplex, daß eine Darstellung in der klassischen chemischen Formelsprache, die Atom für Atom registriert, zu optischem Chaos führen muß. Über den Zwang zu einer neuen Symbolik – bis jetzt hat jeder, ungestört von IUPAC-Direktiven, seine eigene – tröstet eine Fülle neuer Perspektiven und potentieller Anwendungen hinweg.

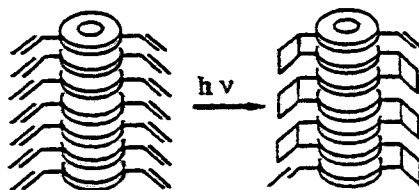
Unter dem Titel „Supramolecular Organic Chemistry and Photochemistry“ wurde vom 27. August bis 1. September 1989 an der Universität des Saarlandes ein internationaler Workshop veranstaltet, der zeitweilig mehr als 300 Zuhörer anlockte. Die unerwartet hohe Zahl von über 220 Voranmeldungen aus 22 Ländern zeigt das zunehmende Gewicht dieses relativ neuen Forschungsgebiets, dessen interdisziplinären Charakter mehrere Redner hervorhoben. Aus den Hauptvorträgen, welche durch kürzere Darstellungen und durch sehr instruktive und vielfältige Poster ergänzt wurden, seien hier nur einige Glanzlichter herausgegriffen, die Spannweite und Anwendungsmöglichkeiten des Gebiets illustrieren.

## Strukturen und Funktionen

In einem umfassenden Überblick zeigte J.-M. Lehn, wie iono-, chemo- oder photoaktive molekulare Komponenten zur Informations- und Signalverarbeitung benutzt werden können, so zur bereits anwendungsreifen Markierung von Antikörpern in der medizinischen Diagnostik durch lumineszenzverstärkende Metallkomplexe. Für den Ionen-transport durch Membranen wurden in Straßburg Systeme wie (1) mit Kronen-



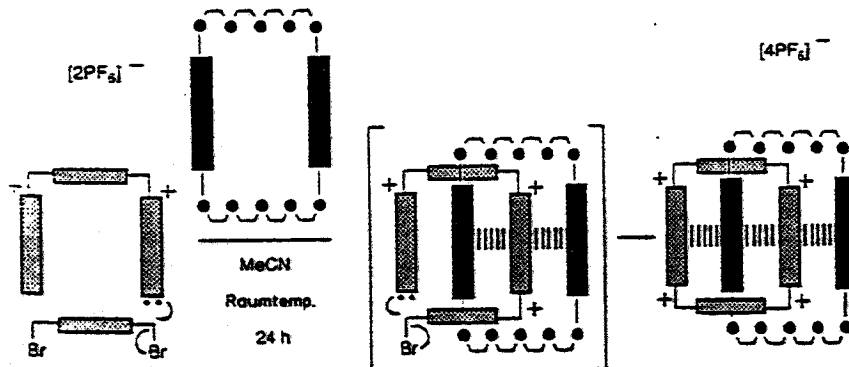
(1)



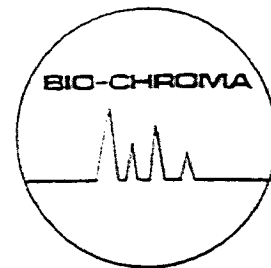
(2)

ethern als Basisring aufgebaut. H. Ringsdorf stellte u. a. ein anderes Konzept (2) vor, dem die photochemische Vernetzung von zimtsäuresubstituierten Azakronen zugrundeliegt.

Fraser Stoddart lieferte eindrucksvolle Beispiele zur Synthese polymolekularer Makrocyclen durch Templateffekte organischer Edukte, wodurch Catenane (3a), Rotaxane (3b) wie auch „Abacus“-Strukturen mit verschiebbaren Ringen (3c) zugänglich werden. Solche Verbindungen erlauben ebenso wie die von A. Collet vorgestellten Einschlußkomplexe (4) das Studium der dominierenden nichtkovalenten Wechselwirkungen.



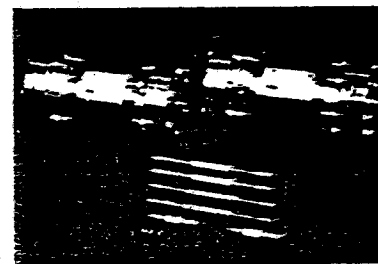
(3a)



Labormeßtechnik GmbH  
Talstr. 64 6905 Schriesheim

## HPLC-SÄULEN

- analytische Stahlsäulen
- analytische Glassäulen im Kartuschensystem
- präparative Stahlsäulen
- Kieselgel-Sorbents
- HEMA-BIO-Sorbents



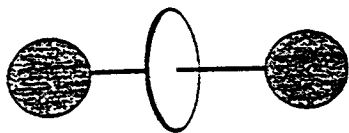
Kostenloser Applikationsservice aus unserer Datenbank.

Fordern Sie auch Unterlagen über unser sonstiges Lieferprogramm an:

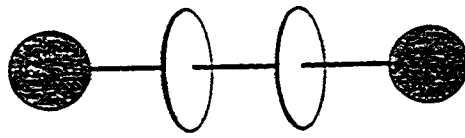
- HPLC-Pumpen
- HPLC-Detektoren
- HPLC-Auswertesysteme
- HPLC-Zubehör
- HPLC-Software BIO-SOFT für Aufzeichnung, Auswertung und Steuerung von HPLC-Anlagen.

## BIO-CHROMA

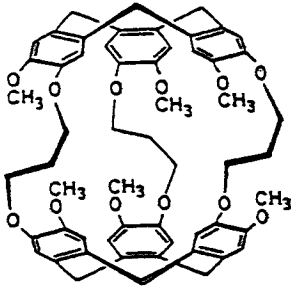
Labormeßtechnik GmbH  
Talstr. 64 6905 Schriesheim  
Tel: 06203-6659 Fax: 06203-68429



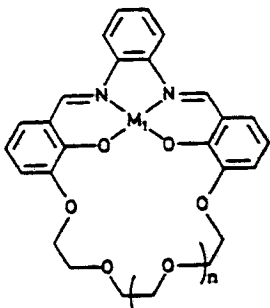
(3b)



(3c)



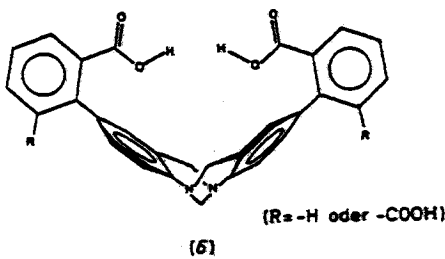
(4)



(5),  $M_1 = UO_2$

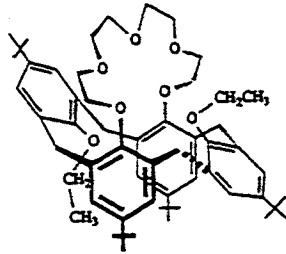
Die optimalen Abstände scheinen in Lösung kleiner als die entsprechenden Van-der-Waals-Kontakte zu sein.

In den von C. Wilcox vorgestellten halboffenen „cleft“-Verbindungen (5) führen Wasserstoffbrücken zu hohen Bindungskonstanten (bis 45 000) mit Adenin-, Biotin- oder Barbitursäure-Derivaten, während D. N. Reinhoudt in ditopischen Rezeptormolekülen (6) durch Co-Komplexierung mit eingebauten Metallen eine starke und vielleicht medizinisch interessante Bindung, z. B. von Harnstoff, erzielt.



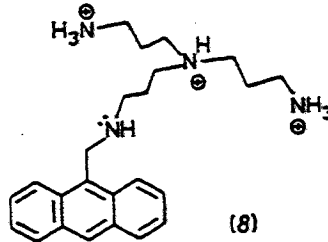
(6)

Metalle, auch  $Na^+$  oder  $K^+$ , werden unter konformativer Steuerung durch Substituenten R mit kronenetherüberbrückten Calixarenen (7) selektiv komplexiert, wie im Vor-



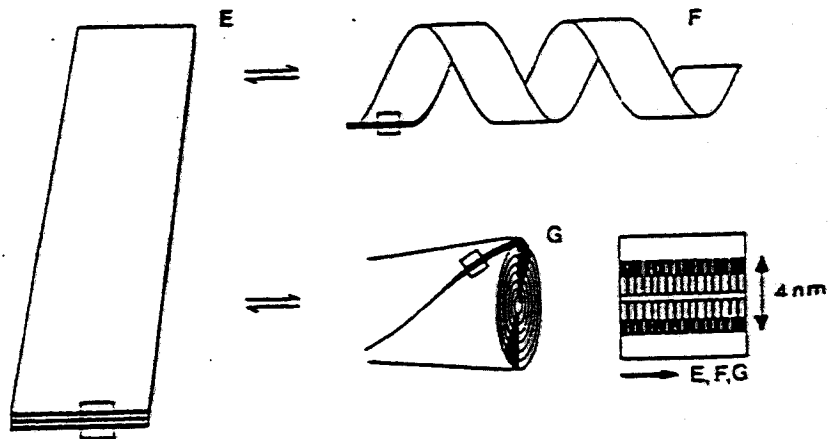
(7)

trag von R. Ungaro sowie auf mehreren Postern gezeigt wurde. A. W. Czarnik demonstrierte, wie mit Anthrylpolyaminen (8) durch Chelatbildung mit dem Benzylaminstickstoff sowohl Kationen wie auch DNA, Heparin etc. durch Fluoreszenzerhöhung analysiert werden können.



(8)

Enzymanaloga standen im Vordergrund der Vorträge von F. Toda und vor allem von F. Diederich, der Thiazole, Flavine und Porphyrine als Coenzym-Vertreter in Cyclophane einbaut, um damit die Voraussetzung zur

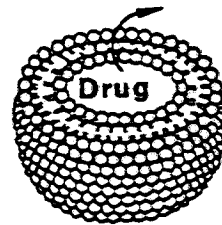


(9)

Katalyse, z. B. von Benzoinkondensationen und Redoxreaktionen, zu schaffen – ein wichtiger Schritt zu biomimetischen Synthesen.

Methodischen Aspekten der supramolekularen Chemie galt der Vortrag von G. Wipff über computergestützte Modellierung von Molekülen einschließlich ihrer Dynamik. Ebenfalls methodischen Fragen galt ein ebenso neues wie erfolgreiches Experiment, eine Panelpräsentation, bei der von sechs Fachleuten kurz Anwendungen und Entwicklungstendenzen wichtiger Techniken vorgestellt wurden.

Über höhermolekulare Aggregate berichtete neben Lehn und Ringsdorf auch J. Fuhrhop, dem die spontane Bildung makroskopischer chiraler Superstrukturen wie (9) aus chiralen Monomeren gelang. Y. Hui stellte die helicalen Strukturen von Amylosen vor, welche in China seit langem für therapeutische Zwecke eingesetzt werden. Interessante Perspektiven u. a. zur Krebschemotherapie



(10)

deutete F. M. Menger an: Bei Anwendung entsprechend „verpackter“ Pharmaka kostete ein spezifisches Enzym der Tumorzellen die Vesikel (10) selektiv öffnen und ein Cytostatikum freisetzen – eine in der anschließenden Diskussion heftig umstrittene Vorstellung.

VE Außen- und Binnenhandelsbetrieb  
 Robert-Rossie-Str. 10  
 Berlin  
 DDR-1115  
 Telefon: 3400111  
 Telex: 113148

1964-1989  
 Isocommerz  
 Ihr Partner

isocommerz

SPEZIALREINE CHEMIKALIEN FÜR  
 DIE OPTISCHE ANALYTIK

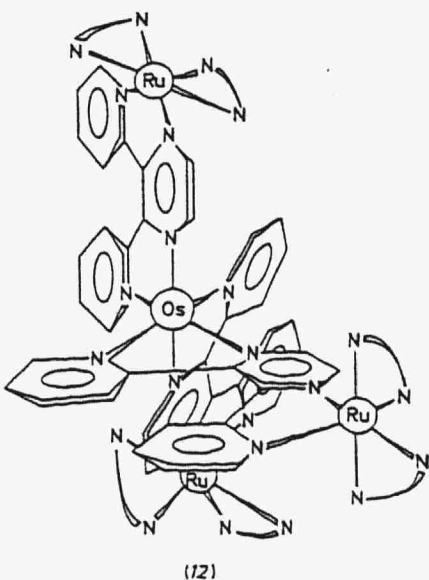
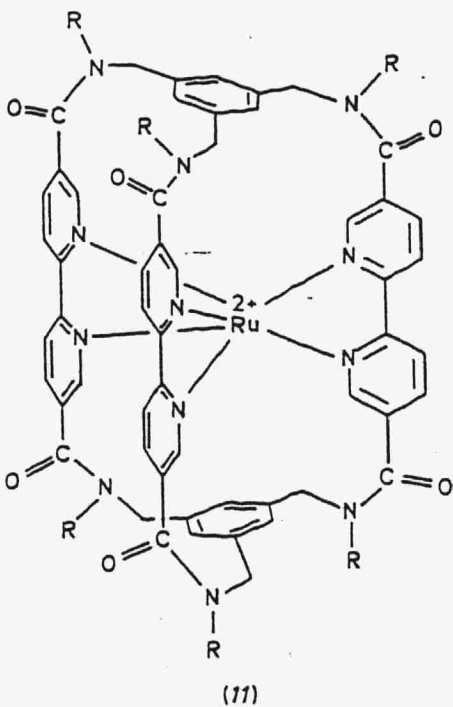
Chromatographie · HPLC ·  
 UV-Spektroskopie · IR-Spektroskopie



## Photochemie

Der zweite Teil des Workshops, der sich mit supramolekularer Photochemie beschäftigte, war im wesentlichen den Themen „Energie-transfer, Elektronentransfer und Konfigurationsänderungen“ gewidmet.

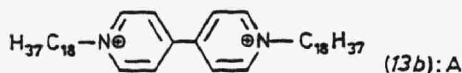
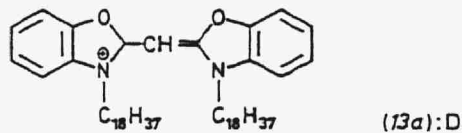
Von V. Balzani wurden die grundlegenden Phänomene supramolekularer Photochemie und besonders die Beziehung zwischen Chemie, Physik und Biologie an den Beispielen kovalent oder durch Wirt-Gast-Wechselwirkungen verknüpfter Systeme vorgestellt. Besonders beeindruckten dabei die neuartigen hochstabilen Ru-Cryptanden (11) sowie die auf der Basis geeigneter Podanden (12) synthetisierten Ru-Os-Metallkomplexe und deren Chemie in angeregten Zuständen. Ein wichtiger Punkt war die Anwendung entsprechender Systeme als „Photochemical Molecular Devices (PMD)“.



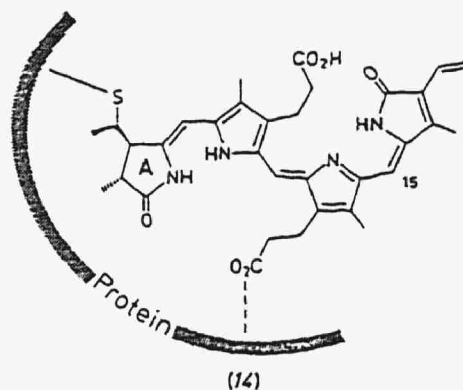
Von I. Willner wurde in hervorragender Weise das zentrale Problem des photoinduzierten Ladungstransfers bei der artifiziellen Photosynthese behandelt. Eine effiziente Ladungstrennung im Zn-Porphyrin/Viologen-System wird durch Cyclodextrin im homogenen sowie im heterogenen System vermittelt. Willner beschrieb den Aufbau eines supramolekularen Systems, das letztlich die Funktion des photosynthetischen Apparates der Pflanzen imitiert.

Von A. M. Braun wurde der Effekt micellarer Systeme auf die Ladungstrennung bei photoinduzierten Elektronentransfer-Reaktionen beleuchtet sowie die Photochemie SiO<sub>2</sub>-fixierter Sensibilisatoren und Katalysatoren vorgestellt. Ferner ging es um die interessante Frage nach der Rolle des Singulett-Sauerstoffs bei der Phototoxizität von Pharmaka und um Modellstudien zur Photodynamischen Therapie.

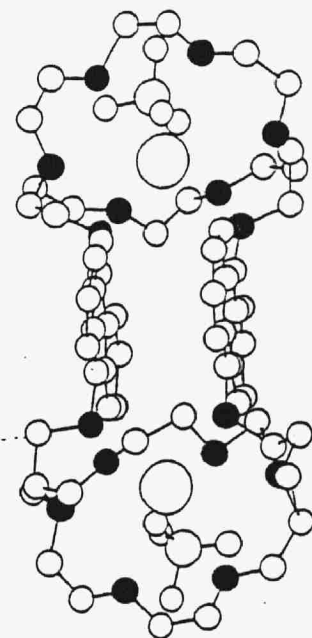
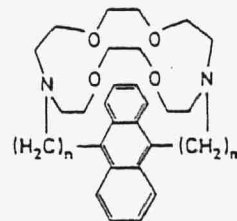
Mit dem Schlagwort „Molecular Engineering“ können neueste Ergebnisse zur Photochemie mono- und biomolekularer Schichten gekennzeichnet werden, über die D. Möbius am Beispiel des Energie- und Elektronentransfers in Cyanin/Viologen-Systemen (13a/b) berichtete. Die komplexen in



der Natur realisierten Elektronen- und Energietransfer-Prozesse, die Basis allen pflanzlichen Lebens, wurden von K. Schaffner am Beispiel des Phycobilisoms und der Phytochrome (14) erläutert. Die komplexen licht sammelnden und - z. B. Pflanzenwuchs und -entwicklung - lichtinduziert-steuern Systeme in Algen und grünen Pflanzen und die Aufklärung der Einzelreaktionen und -mechanismen mußten auch bei dieser Tagung den Zuhörer in Staunen versetzen.



Von F. de Schryver wurden die neuartigen Eigenschaften supramolekularer, angeregter Zustände am Beispiel kationischer Micellen, funktionalisierter Pyrene auf Ton sowie an dem Enzym Chymotrypsin behandelt. H. Bouas-Laurent stellte neue kation-komple-



xierende makrocyclische Fluorophore mit ihren photochemischen und physikalischen Eigenschaften vor. Ein Beispiel ist Verbindung (15) mit Ag<sup>+</sup> als komplexiertem Kation. Der makrocyclische Kryptand (16), das sogenannte „Tonneler“ (Fäßchen), zeigt, komplexiert mit zwei Rb<sup>+</sup>-Ionen, typische Excimerenfluoreszenz.

Den krönenden Abschluß und zukunftsweisenden Ausklang des Workshops brachte schließlich der Vortrag von U. Wild. Sein neuartiges holographisches Aufzeichnungssystem, basierend auf dem Lochbrennprozeß von Chlorin in Polyvinylbutyral bei extrem hohen Temperaturen, stellt im Prinzip eine extrem hohe Speicherkapazität zur Verfügung. Eine Diskette von 10 cm Durchmesser könnte 10 Stunden Fernsehen oder 100 Jahre Musikproduktion speichern - eine phantastische Vorstellung, deren Realisierung bei Raumtemperatur heiß diskutiert wurde.

Wie viele Teilnehmer bestätigten, war dieser erste Versuch, supramolekulare Chemie und Photochemie einander näher zu bringen, außerordentlich stimulierend. Viele neue Kontakte zwischen den Wissenschaftlern wurden aufgebaut. Für Interessenten, die sich vor allem auch für den Inhalt der hochaktuellen Poster interessieren, sei das noch verfügbare „Book of Abstracts“ des Workshops empfohlen.

Hans-Jörg Schneider und Heinz Dürr  
Fachrichtung Organische Chemie  
Universität des Saarlandes

## APPLICATION OF Ru-(II)-POLYPYRIDINE SENSITIZERS IN THE REDUCTION OF CO<sub>2</sub> TO CH<sub>4</sub> AND H<sub>2</sub>-EVOLUTION USING Ru-COLLOIDS

H. Dürr and H.-P. Trierweiler

Fachrichtung 11.2 Organische Chemie, Universität des Saarlandes, D-6600 Saarbrücken, F.R.G.

I. Willner and R. Maidan

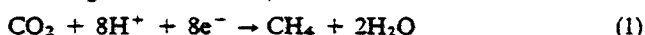
Department of Organic Chemistry, The Hebrew University of Jerusalem, Jerusalem 91904, Israel.

Received August 28, accepted December 6, 1989.

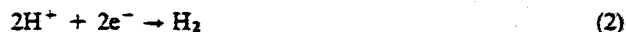
**ABSTRACT.** — The favourable photophysical properties of Ru(phen)<sub>3</sub><sup>2+</sup> compared to Ru(bpy)<sub>3</sub><sup>2+</sup> allow to realize an improved photochemical system for carbon dioxide reduction and hydrogen evolution.

The photosensitized reduction of carbon dioxide is of substantial interest as a means of mimicking natural photosynthesis as well as generation of carbon fuel products<sup>1</sup>. Two different approaches to reduce CO<sub>2</sub> by photochemical means have been extensively developed in recent years: One approach involves the application of semiconductor electrodes, powders or colloids as photocatalysts for the processes mentioned<sup>2-4</sup>. These systems are usually inefficient and yield a mixture of reduced photoproducts. The immobilization of Pd metal onto TiO<sub>2</sub> powders results however in the selective photoreduction of CO<sub>2</sub>/HCO<sub>3</sub><sup>-</sup> to formate<sup>5</sup>. A second approach involves the application of homogeneous photosensitizers such as Ru(II)-tris-bipyridine, Ru(bpy)<sub>3</sub><sup>2+</sup>, and tailored homogeneous<sup>6-8</sup>, heterogeneous<sup>9,10</sup> specific catalysts, or enzymes<sup>11,12</sup> for CO<sub>2</sub>-reduction. Photoreduction of CO<sub>2</sub> to formate has been accomplished in assemblies that include Ru(bpy)<sub>3</sub><sup>2+</sup> as photosensitizer and Ru(bpy)<sub>2</sub>L<sub>2</sub> as catalysts<sup>6</sup>. Photoreduction of CO<sub>2</sub> to carbon monoxide has been accomplished using Co(II), CO-(II)-bipyridine complexes or Re(I)bpy(CO)<sub>3</sub>X as homogeneous catalysts. Heterogeneous Pd and Ru-colloids have been applied as catalysts for the selective photosensitized reduction of CO<sub>2</sub> to formate<sup>9</sup> and methane<sup>10</sup> respectively. Biocatalysts have been coupled to photosensitized electron transfer reactions to effect direct fixation of CO<sub>2</sub> to formate<sup>11</sup> or alternatively to insert CO<sub>2</sub> into C-H bonds (carboxylation processes)<sup>12</sup>.

The photoinduced reduction of CO<sub>2</sub> to methane in aqueous media [equation (1)] is of specific interest. It involves a multi-electron reduction of CO<sub>2</sub>, and thus a catalyst that acts as an electron-sink, and concomitantly is capable of activating CO<sub>2</sub> towards the process desired. Metal colloids act as electron-sinks and were successfully applied in the photosensitized H<sub>2</sub>-evolution<sup>13,14</sup>,



hydrogenation of unsaturated substrates<sup>15</sup> and reduction of CO<sub>2</sub>/HCO<sub>3</sub><sup>-</sup>.



Interestingly, Ru-colloids were found as proper catalysts for the specific activation of CO<sub>2</sub> towards photoreduction to methane<sup>10</sup>. Nevertheless, this metal colloid simultaneously catalyses H<sub>2</sub> evolution from aqueous media [equation (2)]. Although the overall reduction of CO<sub>2</sub> to methane is thermodynamically favoured, the H<sub>2</sub> evolution process is kinetically favoured. Addition of bipyrazine ligand specifically blocks H<sub>2</sub>-evolution and introduces a kinetic barrier for the process. Application of Ru-(II)-tris-bipyrazine as photosensitizer generates an intrinsic « built-in » inhibition site for H<sub>2</sub>-evolution and results in the selective reduction of CO<sub>2</sub> to methane<sup>10</sup>.

The synthesis of photosensitizers with different photophysical and redox properties as well as photosensitizers with functional groups in the ligand backbone has been widely examined in our laboratory<sup>16,17</sup>. Here we report on the application of Ru-(II)-tris-phenanthroline 1 and Ru-(II)-bis-bipyridine-pyridyl-3-methylpyrimidine, Ru(bpy)<sub>2</sub>(Py-MPym)<sup>2+</sup>, 2, as photosensitizers in the reduction of CO<sub>2</sub> to CH<sub>4</sub> in the presence of Ru-colloid. We compare the photophysical properties and effectiveness of these photosensitizers to those of Ru(bpy)<sub>3</sub><sup>2+</sup>.

### Experimental Section

The illumination experiments were carried out in a glass cuvette equipped with a valve and a stopper.

The samples contain RuL<sub>3</sub><sup>2+</sup> (L = 2,2'-bipyridine or 1,10-phenanthroline), 1.4 × 10<sup>-4</sup> M; MPVS, 7.0 × 10<sup>-3</sup> M; TEOA, 1.0 × 10<sup>-1</sup> M; NaHCO<sub>3</sub>, 2.0 × 10<sup>-1</sup> M and ruthenium colloid, 20 mg/L

Table I. — Photophysical and Redox Properties of Photosensitizers.

Photosensitizer	$T_F$ ( $\mu\text{sec}$ )	$E^*$ ( $S^*/S_{\text{red}}$ ) (V) <sup>d</sup>	$E^*$ ( $S^*/S_{\text{ox}}$ ) (V) <sup>d</sup>	$E(S/S_{\text{ox}})$ (V) <sup>e, c</sup>	$E(S/S_{\text{red}})$ (V) <sup>e</sup>
$\text{Ru}(\text{bpy})_3^{2+}$	0.61 <sup>(18)</sup>	0.77 <sup>(19)</sup>	-0.81 <sup>(19)</sup>	1.29 <sup>(19)</sup>	-1.33 <sup>(19)</sup>
$\text{Ru}(\text{phen})_3^{2+}$	0.96 <sup>(18)</sup>	0.77	-0.78	1.40 <sup>(20)</sup>	-1.41 <sup>(20)</sup>
$\text{Ru}(\text{bpy})_2(\text{PyMPy})^{2+}$	0.11 <sup>(21)</sup>	1.20	-0.71 <sup>(21)</sup>	1.39 <sup>(21)</sup>	-0.90 <sup>(21)</sup>

<sup>a</sup> Calculated from the ground state redox potentials and the excitation energy  $E^{0-0}$ . <sup>b</sup> vs. SCE. Solvent MeCN. <sup>c</sup> See experimental section.

at pH 7.8 under  $\text{CO}_2$  atmosphere. The total amount of the aqueous solution was 3 mL. The light source for performing continuous illumination experiments was a 150 W xenon arc lamp (PTI). For detection of the evolved synthesis gas (hydrogen and hydrocarbons) the gas samples were taken out from the cuvettes and analyzed by gas chromatography (Packard 427 instrument with thermal conductivity detector for hydrogen and a Tracor 540 gas chromatograph with flame ionization detector for hydrocarbons).

Redox potentials of the sensitizers at the ground-state were determined by cyclic voltammetry<sup>21</sup> using the corresponding  $\text{RuL}_2$  ( $L$ ) ( $\text{PF}_6$ )<sub>2</sub> complexes of  $\text{Ru}(\text{bpy})_3^{2+}$  ( $L = L$ ),  $\text{Ru}(\text{phen})_3^{2+}$  1, ( $L = L$ ) and  $\text{Ru}(\text{bpy})_2(\text{PyMPy})^{2+}$  2. Excited state potentials were calculated from the ground-state potentials and the zero-zero excitation energy  $E^{0-0}$ , which was taken from UV-data. The resulting data were compared to literature values, which are given in Table I.

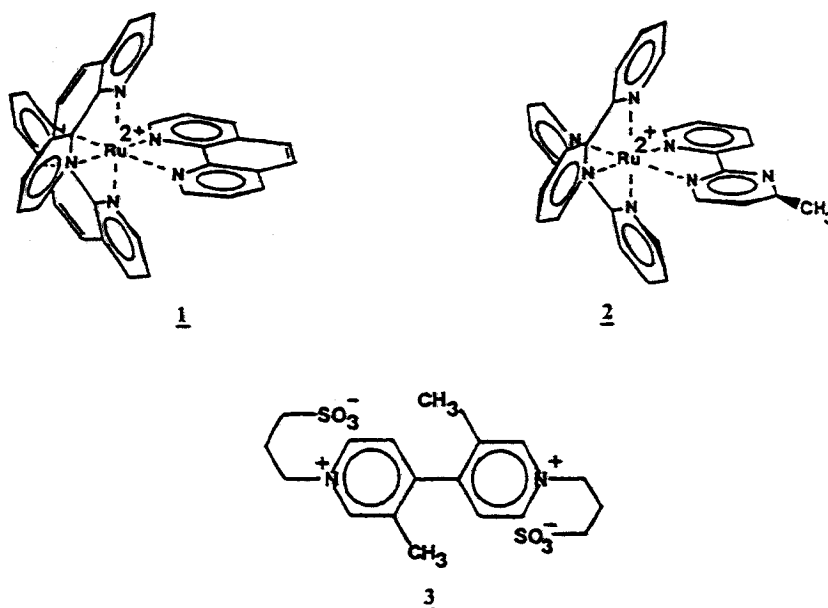
## Results and Discussion

The electron acceptor that was applied in this study as electron carrier is  $N,N'$ -3-propylsulfonato-(3,3'-dimethyl)-4,4'-bipyridinium, MPVS, 3. The reduction potential of this charge relay ( $E^0$  ( $\text{MPVS}^-/\text{MPVS}^0$ ) = -0.79 V) is substantially more negative than that of  $\text{PVS}^-$ , 4,  $E^0$  ( $\text{PVS}^-/\text{PVS}^0$ ) = -0.41 V. The lower reduction potential of 3 as compared to that of 4, originates from steric hindrance of the methyl substituents that introduce a barrier to planarity of the two rings and resonance delocalization of the resulting reduced radical. Consequently, reduction of  $\text{MPVS}^0$  is more difficult

than reduction of  $\text{PVS}^0$ , and therefore the reduced photoproduct is a more powerful reductant.

Illumination of an aqueous solution that includes  $\text{Ru}(\text{phen})_3^{2+}$  as photosensitizer, MPVS as primary electron acceptor and triethanolamine as sacrificial electron donor under an atmosphere of  $\text{CO}_2$  in the presence of the Ru-colloid, results in the reduction of  $\text{CO}_2$  to methane and concomitant  $\text{H}_2$ -evolution. Fig. 1 displays the rate of methane formation as a function of illumination time. Fig. 2 shows the rate of  $\text{H}_2$ -evolution from the system. For comparison, the rates of  $\text{CH}_4$ -formation and  $\text{H}_2$ -evolution from a similar system that applies  $\text{Ru}(\text{bpy})_3^{2+}$  as photosensitizer are also displayed. In addition to the formation of methane, minor amounts of ethane,  $\text{C}_2\text{H}_6$ , are also formed ( $0.01 \mu\text{L}\cdot\text{h}^{-1}$ ).

Exclusion of  $\text{CO}_2$  from the system results in only  $\text{H}_2$ -evolution and no methane or ethane is formed. Exclusion of  $\text{MPVS}^0$ , the electron donor or the Ru-colloid eliminates the formation of  $\text{H}_2$  and  $\text{CO}_2$  reduction products. Furthermore, substitution of  $\text{MPVS}^0$  by  $\text{MV}^{2+}$  (methyl viologen) or  $\text{PVS}^0$  eliminates the formation of  $\text{CH}_4$  and  $\text{C}_2\text{H}_6$  but the activity of the system towards  $\text{H}_2$ -evolution is maintained. These results indicate that  $\text{CH}_4$  and  $\text{C}_2\text{H}_6$  originate from the reduction of  $\text{CO}_2$  substrate. Also, the results imply that the reduction of ruthenium colloid activated  $\text{CO}_2$  requires a charge relay ( $\text{MPVS}^-$ ) that exhibits a more negative reduction potential than that required for  $\text{H}_2$ -evolution. Substitution of the photosensitizer  $\text{Ru}(\text{phen})_3^{2+}$  by  $\text{Ru}(\text{bpy})_2(\text{PyMPy})^{2+}$ ,



Structures of Ru-(II)-tris-phenanthroline 1; Ru-(II)-bis-bipyridine-pyridyl-3-methylpyrimidine,  $\text{Ru}(\text{bpy})_2(\text{PyMPy})^{2+}$  2 and  $N,N'$ -3-propylsulfonato-(3,3'-dimethyl)-4,4'-bipyridinium, MPVS, 3.

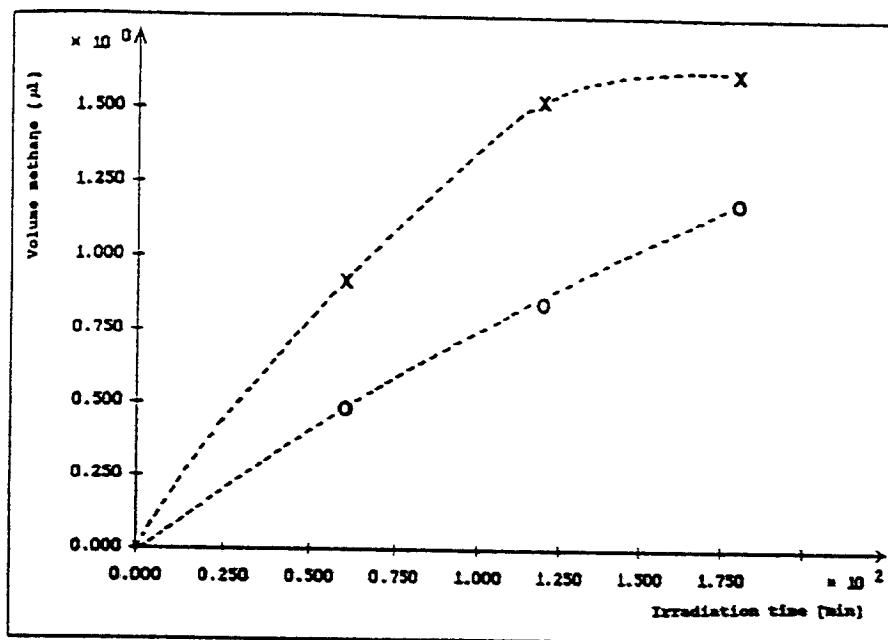


Figure 1. — Rate of photosensitized CH<sub>4</sub> formation in the presence of the sensitizers Ru(phen)<sub>3</sub><sup>2+</sup> (X) or Ru(bpy)<sub>3</sub><sup>2+</sup> (O). [sensitizer] = 1.4 × 10<sup>-4</sup> M; [MPVS] = 7.0 × 10<sup>-3</sup> M; [NaHCO<sub>3</sub>] = 5.0 × 10<sup>-2</sup> M; [Ru colloid] = 20 mg/L; pH = 7.8 under CO<sub>2</sub> atmosphere.

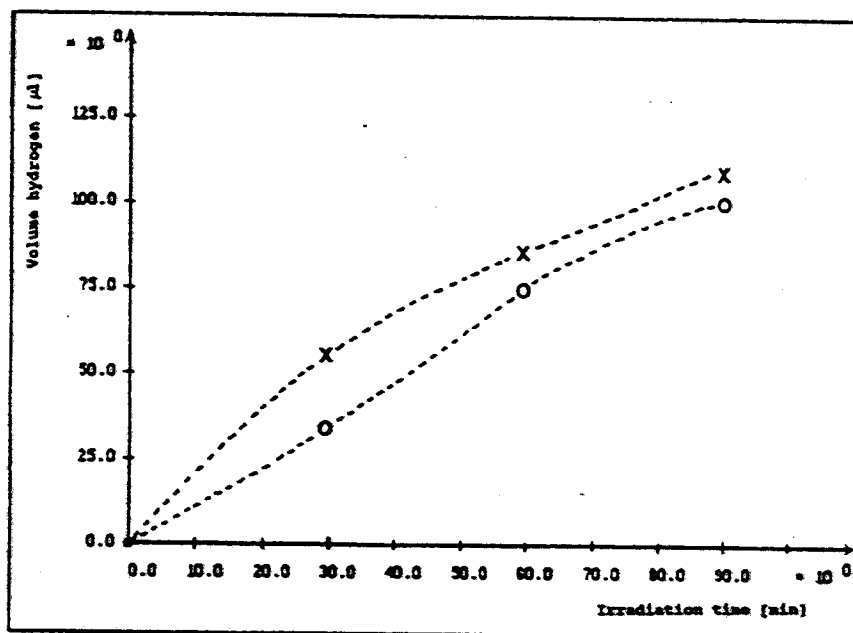


Figure 2. — Rate of photosensitized hydrogen evolution in the presence of the sensitizers Ru(phen)<sub>3</sub><sup>2+</sup> (X) or Ru(bpy)<sub>3</sub><sup>2+</sup> (O). [sensitizer] = 1.4 × 10<sup>-4</sup> M; [MPVS] = 7.0 × 10<sup>-3</sup> M; [NaHCO<sub>3</sub>] = 5.0 × 10<sup>-2</sup> M; [Ru colloid] = 20 mg/L; pH = 7.8 under CO<sub>2</sub> atmosphere.

does yield upon illumination neither CO<sub>2</sub> reduction nor H<sub>2</sub>-evolution. Table I summarizes the photophysical properties and redox characteristics of the photosensitizers, Ru(phen)<sub>3</sub><sup>2+</sup> and Ru(bpy)<sub>2</sub>(PyMPy)<sup>2+</sup> in comparison to those of Ru(bpy)<sub>3</sub><sup>2+</sup>. The fluorescence quenching processes of the excited photosensitizers by MPVS<sup>0</sup> [see equation (3)] have been examined. The quenching rate constants are summarized in Table II together with the excitation and emission wavelengths. It is evident that the quenching of



Ru(phen)<sub>3</sub><sup>2+</sup> and Ru(bpy)<sub>2</sub>(PyMPy)<sup>2+</sup> by MPVS<sup>0</sup> is respectively ca. 3 and 12 times more effective than the electron transfer quenching of Ru(bpy)<sub>3</sub><sup>2+</sup> by MPVS<sup>0</sup>. The charge separation yield of the encounter cage structure of photopro-

ducts ( $\Phi_S$ ) and the back electron transfer rate of the separated photoproducts [equation (4)] have been determined by means of laser flash photolysis. These values are also summarized in Table II. It is evident that the charge separation yield in the presence of Ru(phen)<sub>3</sub><sup>2+</sup> is improved as compared to Ru(bpy)<sub>3</sub><sup>2+</sup>. Also, the recombination of the intermediate photoproducts is about 55 % slower in the system that applies Ru(phen)<sub>3</sub><sup>2+</sup>. In turn, no separation of the encounter cage complex of photoproducts takes place in the system with Ru(bpy)<sub>2</sub>(PyMPy)<sup>2+</sup>. Thus, the absence of H<sub>2</sub> evolution and CO<sub>2</sub> reduction products in the system that applies Ru(bpy)<sub>2</sub>(PyMPy)<sup>2+</sup> as photosensitizer, is due to rapid recombination of the electron transfer products in the primary encounter complex that eliminates the subsequent reduction processes by MPVS<sup>-</sup>.



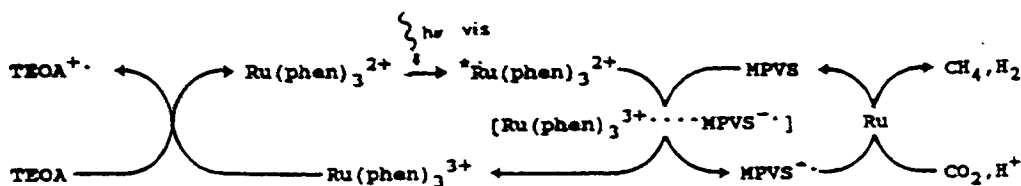


Figure 3. — Mechanism of the photoinduced reduction of carbon dioxide to methane and simultaneous water reduction by using  $\text{Ru}(\text{phen})_3\text{Cl}_2$  I as sensitizer, MPVS 3 as charge relays, TEOA as sacrificial donor and Ru colloid as catalyst.

Table II. — Quenching Rates and Back Electron Transfer of the Different Photosensitizers and Electron Transfer Products.

Compound	$\lambda_{\text{ex}}$ (nm)	$\lambda_{\text{em}}$ (nm)	$k_q^a \times 10^{-9}$ ( $\text{M}^{-1} \cdot \text{sec}^{-1}$ )	$\Phi_s^b$	$k_b^c \times 10^{-9}$ ( $\text{M}^{-1} \cdot \text{sec}^{-1}$ )
$\text{Ru}(\text{bpy})_3^{2+}$	456	618	0.18	$0.9 \times 10^{-2}$	3.8
$\text{Ru}(\text{phen})_3^{2+}$	451	601	0.76	$1.3 \times 10^{-2}$	2.1
$\text{Ru}(\text{bpy})_2$	452	649	2.24	0	—
$(\text{PyMPym})^{2+}$					

<sup>a</sup> Static quenching; decreasing luminescence of the sensitizer by increasing concentration of quenching compound.  $k_q$  was calculated from the slope of correlating the ratio  $I_0/I$  ( $I_0$  = luminescence intensity without quencher,  $I$  = luminescence with defined concentration of quencher) vs the concentration of the quencher and the luminescence lifetime of the sensitizer. Quencher: MPVS:3 in aqueous solution  $[\text{KCl}] = 0.5 \text{ M}$ . <sup>b</sup>  $\Phi_s$  = charge separation yield of the encounter cage structure of photoproducts estimated by the amount of optical density of the reduced relay MPVS at  $\lambda_{\text{max}} = 602 \text{ nm}$  after laser-flash excitation of the photolysis system containing sensitizer, charge relay and the sacrificial donor in accurately degassed solution under argon atmosphere. <sup>c</sup>  $k_b$  = back reaction constant of the primary photogenerated oxidized sensitizer and reduced charge relay [see equation (4)].  $k_b$  was determined by time resolved laser-flash-photolysis.

We conclude that  $\text{Ru}(\text{phen})_3^{2+}$  acts as a superior photosensitizer as compared to  $\text{Ru}(\text{bpy})_3^{2+}$  in  $\text{H}_2$ -evolution and  $\text{CO}_2$ -reduction in the presence of Ru-colloid as catalyst. The improved activity originates from additive effects: Improved quenching of the excited state and effective charge separation of the primary encounter cage complex and slower back electron transfer of the intermediate photoproducts. The overall sequential process that leads to the reduction of  $\text{CO}_2$  and  $\text{H}_2$ -evolution is schematically displayed in Fig. 3. Interestingly, the formation of ethane through reduction of  $\text{CO}_2$  might suggest the intermediate formation  $\text{Ru} = \text{CH}_2$  and  $\text{Ru} - \text{CH}_3$  surface species. Dimerization of the first species followed by hydrogenation or dimerization of the second species might be the source of ethane.

#### REFERENCES

- (a) Willner I., Mandler D., Maidan R., *New J. Chem.*, 1987, 11, 109-121; (b) Inoue S. in « *Organic and Bioorganic Chemistry of Carbon Dioxide* », Inoue S. and Yamazaki N., Eds., Kodsanska, Tokyo, Wiley, New York, 1982, pp. 253; (c) Ziesel R., *Nouv. J. Chim.*, 1983, 7, 613-633.
- (a) Aurian-Blanjeni B., Halmann M., Manassen J., *J. Sol. Energy*, 1980, 25, 165; (b) Inoue T., Fujishima A., Konishi S., Honda K., *Nature*, 1979, 277, 637-638.
- Bradley M. G., Tysak T., Graves D. J., Vlachopoulos N. A., *J. Chem. Soc., Chem. Commun.*, 1983, 349-350.
- Halmann M., *Nature*, 1978, 275, 115-116.
- Goren Z., Willner I., Neison A. J., Frank A. J., Submitted for publication, 1989.
- (a) Hawecker J., Lehn J. M., Ziesel R., *J. Chem. Soc., Chem. Commun.*, 1985, 56-58; (b) Ishida H., Tanaka K., Tanaka T., *Chem. Lett.*, 1983, 1035-1038; (c) Kitamura N., Tazuke S., *Chem. Lett.*, 1983, 1109-1112.
- (a) Lehn J. M., Ziesel R., *Proc. Natl. Acad. Sci., USA*, 1982, 79, 701-704; (b) Hawecker J., Lehn J. M., Ziesel R., *J. Chem. Soc., Chem. Commun.*, 1983, 536-538.
- (a) Ziesel R., Hawecker J., Lehn J. M., *Helv. Chim. Acta*, 1986, 69, 1065-1084; (b) Hawecker J., Lehn J. M., Ziesel R., *Helv. Chim. Acta*, 1986, 69, 1990-2012.
- (a) Mandler D., Willner I., *J. Am. Chem. Soc.*, 1987, 109, 7884-7885; (b) Willner I., Mandler D., *J. Am. Chem. Soc.*, in press 1989.
- (a) Maidan R., Willner I., *J. Am. Chem. Soc.*, 1986, 108, 8100-8101; (b) Willner I., Maidan R., Mandler D., Dürr H., Dörr G., Zengerle K., *J. Am. Chem. Soc.*, 1987, 109, 6080-6086.
- Mandler D., Willner I., *J. Chem. Soc., Perkin Trans. II*, 1988, 997-1003.
- Willner I., Mandler D., Riklin A., *J. Chem. Soc., Chem. Commun.*, 1986, 1022-1024.
- (a) Willner I., Mandler D., Steinberger-Willner B., *Int. J. Hydrogen Energy*, 1988, 13, 593; (b) Grätzel M., *Acc. Chem. Res.*, 1981, 14, 376-384.
- (a) Grätzel M., Ed. « *Energy Resources Through Photochemistry and Catalysis* », Academic Press, New York, 1983; (b) Harriman A., West M. E., Ed. « *Photogeneration of Hydrogen* », Academic Press, London, 1989.
- Degani Y., Willner I., *J. Chem. Soc. Perkin Trans. II*, 1986, 37-41.
- Dürr H., Dörr G., Zengerle K., Reis B., Braun A. M., *Chimia*, 1983, 245-248.
- Dürr H., Dörr G., Zengerle K., Mayer E., Curchod J. M., Braun A. M., *Nouv. J. Chim.*, 1985, 9, 717-720.
- (a) Van Houten J., Watts R. J., *J. Am. Chem. Soc.*, 1976, 98, 4853-4858; (b) Juris A., Barigelletti F., Campagna S., Balzani V., Belser P., von Zelewsky A., *Coord. Chem. Rev.*, 1988, 84, 85-277.
- Bock C. R., Connor J. A., Gutierrez A. R., Meyer T. J., Whitten D. G., Sullivan B. P., Nagle J. K., *J. Am. Chem. Soc.*, 1979, 101, 4815-4824.
- Kirsch-DeMesmaeker A., Nasielski-Hinkens R., Maetens D., Nasielski J., *Inorg. Chem.*, 1984, 23, 377-379.
- Dürr H., Meyer E., unpublished results.

# SYNTHESIS

Journal of  
Synthetic Organic  
Chemistry

REPRINT

1990  
No. 9  
September

---

*With Compliments of the Author.*

GEORG THIEME VERLAG · STUTTGART · NEW YORK

## Compound 3:

IR (neat):  $\nu = 1710, 1740$  (CO),  $970 \text{ cm}^{-1}$  (C=C).

$^1\text{H-NMR}$  ( $\text{CDCl}_3/\text{TMS}$ ):  $\delta = 1.14$  (t,  $J = 7.1 \text{ Hz}$ ,  $\text{CH}_3\text{CH}_2$ ), 1.18 (s,  $\text{CH}_3\text{CCO}$ ), 1.52 (dd,  $J = 6.4, 1.5 \text{ Hz}$ ,  $\text{CH}_3\text{CH}$ ), 2.02 (s,  $\text{CH}_3\text{CO}$ ), 2.38 (m,  $J = 7.2, 1.1 \text{ Hz}$ ,  $\text{CH}_2\text{CH}$ ), 4.07 (q,  $J = 7.1 \text{ Hz}$ ,  $\text{CH}_2\text{O}$ ), 5.14 (m,  $J = 15.1, 7.2, 1.5 \text{ Hz}$ ,  $\text{CH}_2\text{CH}$ ), 5.39 (m,  $J = 15.4, 6.4, 1.1 \text{ Hz}$ ,  $\text{HCCH}_3$ ).

MS:  $m/z = 198$  ( $\text{M}^+$ ).

## Compound 4:

IR (neat):  $\nu = 1715, 1740$  (CO),  $705 \text{ cm}^{-1}$  (C=C).

$^1\text{H-NMR}$  ( $\text{CDCl}_3/\text{TMS}$ ):  $\delta = 1.20$  (t,  $J = 7.1 \text{ Hz}$ ,  $\text{CH}_3\text{CH}_2$ ), 1.26 (s,  $\text{CH}_3\text{CCO}$ ), 1.56 (dd,  $J = 6.8, 1.8 \text{ Hz}$ ,  $\text{CH}_3\text{CH}$ ), 2.09 (s,  $\text{CH}_3\text{CO}$ ), 2.53 (m,  $J = 7.5, 1.6 \text{ Hz}$ ,  $\text{CH}_2\text{CH}$ ), 4.13 (q,  $J = 7.1 \text{ Hz}$ ,  $\text{CH}_2\text{O}$ ), 5.17 (m,  $J = 10.8, 7.5, 1.8 \text{ Hz}$ ,  $\text{CH}_2\text{CH}$ ), 5.54 (m,  $J = 10.8, 6.8, 1.6 \text{ Hz}$ ,  $\text{HCCH}_3$ ).

MS:  $m/z = 198$  ( $\text{M}^+$ ).

## Compound 5:

IR (neat):  $\nu = 1710-1730$  (CO),  $1635 \text{ cm}^{-1}$  (C=C).

$^1\text{H-NMR}$  ( $\text{CDCl}_3/\text{TMS}$ ):  $\delta = 1.19, 1.2$  (m,  $J = 7.1 \text{ Hz}$ ,  $\text{CH}_3\text{CH}_2$ ), 1.21, 1.22 (s,  $\text{CH}_3\text{CCO}$ ), 2.10, 2.08 (s,  $\text{CH}_3\text{CO}$ ), ca. 3 (m br,  $J = 8, 1.1, 0.8 \text{ Hz}$ ,  $\text{HCCH}_3$ ), 4.13, 4.10 (m,  $J = 7.1 \text{ Hz}$ ,  $\text{CH}_2\text{O}$ ), 4.96 (m,  $J = 16.2, 1.8 \text{ Hz}$ ,  $\text{HCCH}=\text{}$ ), 5.0 (m,  $J = 7, 1.8, 1.1 \text{ Hz}$ ,  $\text{HCCH}=\text{}$ ), 5.70, 5.61 (m,  $J = 16.2, 7, 8 \text{ Hz}$ ,  $\text{HCCH}_2$ ).

MS:  $m/z = 198$  ( $\text{M}^+$ ).

The other compounds shown in the Tables were prepared similarly, separated by preparative GC and identified spectroscopically.

Received: 23 January 1990; revised: 26 April 1990

- (1) See for example: Keim, W.; Behr, A.; Röper, M., in: *Comprehensive Organometallic Chemistry*, Vol. 8, Wilkinson, G., Stone, F.G.A., Abel, E.W. (eds.), Pergamon Press, Oxford, 1982, p. 371.  
Behr, A. *Aspects Homogen. Cat.* 1984, 5, 3.
- (2) Jolly, P.W. *Angew. Chem.* 1985, 97, 279; *Angew. Chem., Int. Ed. Engl.* 1985, 24, 283; and references therein.  
Jolly, P.W.; Mynott, R.; Raspel, B.; Schick, K.P. *Organometallics* 1986, 5, 473.  
Benn, R.; Jolly, P.W.; Mynott, R.; Raspel, B.; Schenker, G.; Schick, K.P.; Schroth, G. *Organometallics* 1985, 4, 1945.  
Benn, R.; Jolly, P.W.; Mynott, R.; Schenker, G. *Organometallics* 1985, 4, 1136.
- (3) Gaube, W.; Stegemann, H. *J. Prakt. Chem.* 1984, 326, 947.  
Baker, R.; Popplestone, R.J. *Tetrahedron Lett.* 1978, 3575.  
Symon, T.; Christensen, N.J. *US Patent* 3998872 (1976), Universal Oil Prod. Co.; *C.A.* 1977, 86, 89174.  
Commereuc, D.; Chauvin, Y. *Bull. Soc. Chim. Fr.* 1974, 652.  
Watanabe, S.; Suga, K.; Fujita, T. *Can. J. Chem.* 1973, 51, 848.  
Takahashi, K.; Miyake, A.; Hata, G. *Bull. Chem. Soc. Jpn.* 1972, 45, 1183.
- (4) Benn, R.; Jolly, P.W.; Joswig, T.; Mynott, R.; Schick, K.P. *Z. Naturforsch.* 1986, 41b, 680.
- (5) Betz, P.; Krüger, C., unpublished results (1988).
- (6) Dzhemilev, U.M.; Kunakova, R.V.; Gaisin, R.L. *Bull. Acad. Sci. USSR Div. Chem.* 1981, 2213.
- (7) Karim, A.; Mortreux, A.; Petit, F.; Buono, G.; Peiffer, G.; Siv, C. *J. Organometal. Chem.* 1986, 317, 93.
- (8) Köhler, J.; Schomburg, G. *J. Chromatogr.* 1983, 255, 311.

## Efficient Synthesis of Crown Ester-Linked Ruthenium Complexes. A New Class of a Supramolecular Sensitizer-Crown Ester Assembly for Electron Transfer<sup>1</sup>

Heinz Dürr,\* Heike Kilburg, Stefan Bossmann

Fachbereich 11.2, Organische Chemie der Universität des Saarlandes, 6600 Saarbrücken, Federal Republic of Germany

Dedicated to Professor W. Krimse on the occasion of his 60th birthday

The synthesis of a novel class of supramolecular ruthenium-sensitizers directly linked to new heterocyclic crown ethers, as well as their IR-, UV- and fluorescence spectroscopic data are described.

Ruthenium ( $\text{L}_3$ )<sup>2+</sup> complexes are important light harnessing materials used in photoinduced electron-transfer reactions, and consequently important components for solar light conversion and storage devices.<sup>2,3</sup> Effective electron transfer quenching of the excited species is essential for light/chemical energy conversion processes.<sup>4</sup> An effective quenching of excited species has been accomplished in organized microheterogeneous environments by locations of the photosensitizer-relay components at the interface.<sup>5-7</sup> Localization of the relay component at the photosensitizer site can be accomplished also at the molecular level through linkage of the two components.<sup>8,9</sup> Nevertheless, such an assembly also assists the back electron-transfer process of the intermediate chemically linked photoproducts. A second approach involves the design of photosensitizer receptor systems.<sup>10-12</sup> Association of the relay to the receptor site is anticipated to allow effective electron

transfer properties, but nevertheless enable consequent dynamic flexibility for subsequent charge separation.<sup>13-17</sup>

The first heterocyclic crown ethers including 2,2'-bipyridine were synthesized by Rebeck.<sup>18,19</sup> The design of efficient energy storage systems using these compounds as ligands in ruthenium-polypyridyl complexes is not possible, because the expected lifetime of these complexes (with electron donor substituents) are relatively short and the binding properties of the crown ether unit cannot be modified (e. g. by structural changes of the electron relays or solvation effects), which is also the case for crown esters.<sup>20</sup>

In this paper we describe the preparation of a new sensitizer-relay assembly combining ruthenium( $\text{bpy}$ )<sub>3</sub><sup>2+</sup> and crown ester functions. The crown ester is supposed to bind the ions to the appropriate relay in a dynamic process.

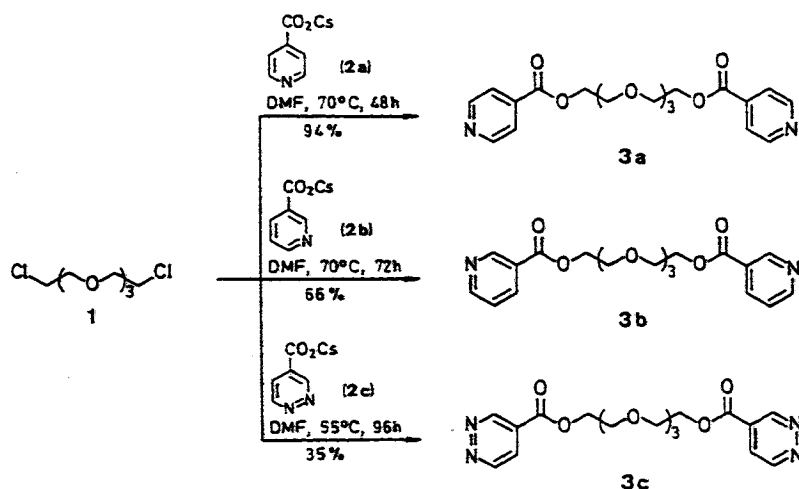
For the preparation of suitably functionalized crown esters the esterification method of Wang et al.<sup>21</sup> coupled with the modification of Piepers and Kellogg,<sup>22</sup> by reacting

dicesium salts of the corresponding carboxylic acids with polyglycol dihalides in dimethylformamide was chosen. Accordingly, the heterocyclic podands **3a–c** and coronands **6–10** were synthesized (Schemes A and B) (Tables 1 and 2).

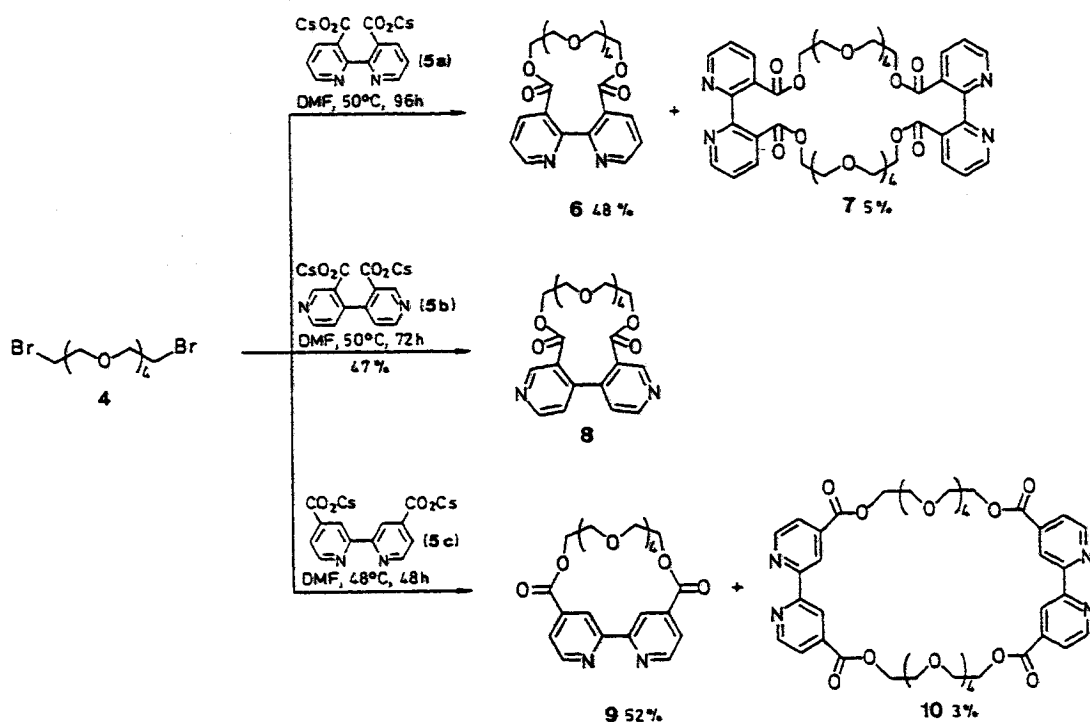
Using the new heterocyclic podands **3** and coronands **6–10** three types of ruthenium complexes were prepared by treating them with  $[\text{Ru}(\text{bpy})_2]\text{Cl}_2$  (**11**) ( $\text{bpy} = 2,2'$ -bipyridine),  $[\text{Ru}(\text{bpz})_2]\text{Cl}_2$  (**16**) ( $\text{bpz} = 2,2'$ -bipyrazine) and  $[\text{Ru}(\text{DMSO})_4]\text{Cl}_2$  (**21**) in aqueous ethanol under reflux conditions. Bis-heteroleptic complexes  $[\text{Ru}(\text{bpy}_2)(\text{L}')]\text{Cl}_2$  [**12**, **13** ( $\text{L}' = 3\text{a}$ ), **14**, **15** ( $\text{L}' = 3\text{b}$ )] containing the podands **3a** and **3b**, bis-heteroleptic com-

plexes  $[\text{Ru}(\text{bpy}_2)(\text{L}'')]\text{Cl}_2$  (**17**, **19**  $\text{L}'' = 6$ , **9**) and  $[\text{Ru}(\text{bpz})_2(\text{L}'')]\text{Cl}_2$  (**18**, **20**  $\text{L}'' = 6$ , **9**) possessing in both cases the coronands **6** and **9** were thus obtained (Schemes C and D). The tris-heteroleptic complexes  $[\text{Ru}(\text{L}''')_3]\text{Cl}_2$  (**22**, **23**  $\text{L}''' = 6$ , **9**) were formed similarly from **21** (Scheme E).

The reaction of  $[\text{Ru}(\text{bpy})_2]\text{Cl}_2$  (**11**) and the podands **3a, b** lead to mononuclear **12**, **14** and binuclear ruthenium complexes **13**, **15** respectively. The complexes were separated by column chromatography using Sephadex LH100 and ethanol/methanol (5:1) as eluent. In all cases, the IR, UV, NMR, mass spectra and elemental analyses were in agreement with the structures proposed (Tables 3–5).



Scheme A



Scheme B



Table 1. Compounds 3, 6-10 Prepared

Dicesium Salt (mol)	Polyethylene Glycol Dihalide (mol)	Reaction Time (h)	Product	Yield (%)	mp (°C)	Molecular Formula <sup>a</sup>	IR (film/KBr) $\nu$ (cm <sup>-1</sup> )	UV(CH <sub>2</sub> Cl <sub>2</sub> ) $\lambda_{max}$ (nm) (log $\epsilon$ )	MS (FAB) $m/z$ (%)
2a (0.02)	1 (0.01)	48	3a	94	oil	C <sub>20</sub> H <sub>24</sub> N <sub>2</sub> O <sub>7</sub> (404.4)	3050, 2940, 1735, 1290	269 (3.63)	-
2b (0.039)	1 (0.019)	72	3b	66	48	C <sub>20</sub> H <sub>24</sub> N <sub>2</sub> O <sub>7</sub> (404.4)	3060, 2970, 1740, 1250	262 (3.52)	-
2c (0.028)	1 (0.014)	96	3c	35	oil	C <sub>18</sub> H <sub>22</sub> N <sub>4</sub> O <sub>7</sub> (406.4)	3070, 2900, 1730, 1250	328 (2.44), 257 (3.24)	-
5a (0.01)	4 (0.01)	96	6	48	oil	C <sub>22</sub> H <sub>26</sub> N <sub>2</sub> O <sub>8</sub> (446.5)	3070, 2940, 1730, 1450	265 (3.56)	447 (0.5), 96 (100)
			7	5	113	C <sub>44</sub> H <sub>52</sub> N <sub>4</sub> O <sub>16</sub> (892.9)	3074, 2952, 1730, 1455	268 (3.42)	894 (0.1), 447 (0.6), 96 (100)
5b (0.016)	4 (0.016)	72	8	47	oil	C <sub>22</sub> H <sub>26</sub> N <sub>2</sub> O <sub>8</sub> (446.5)	3070, 2900, 1475, 1460	264 (2.69)	448 (1.2), 112 (100)
5c (0.01)	4 (0.01)	48	9a	52	oil	C <sub>22</sub> H <sub>26</sub> N <sub>2</sub> O <sub>8</sub> (446.5)	3100, 2900, 1730, 1490	295 (3.59)	447 (2.1), 95 (100)
			10	3	127	C <sub>44</sub> H <sub>52</sub> N <sub>4</sub> O <sub>16</sub> (892.9)	3100, 2905, 1736,	297 (3.88)	893 (0.3), 95 (100)

<sup>a</sup> Satisfactory microanalyses obtained: C  $\pm$  0.3, H  $\pm$  0.1, N  $\pm$  0.1.

Table 2. NMR Data of Compounds 3, 6-10

Compound	<sup>1</sup> H-NMR (CDCl <sub>3</sub> /TMS) $\delta$ , J(Hz)	<sup>13</sup> C-NMR (CDCl <sub>3</sub> /TMS)
3a	3.73 (mc, 8H), 3.85 (mc, 4H), 4.50 (mc, 4H), 7.87 (dd, 4H, <sup>3</sup> J = 5.7, <sup>4</sup> J = 0.9, 4H), 8.78 (dd, 4H, <sup>3</sup> J = 5.7, <sup>4</sup> J = 0.9)	63.74, 69.67, 70.11, 121.71, 136.20, 149.46, 163.75
3b	3.70 (mc, 8H), 3.85 (mc, 4H), 4.50 (mc, 4H), 7.44 (td, 2H, <sup>3</sup> J = 4.8, <sup>4</sup> J = 1.6), 8.31 (mc, 2H), 8.76 (dd, 2H, <sup>3</sup> J = 4.8, <sup>4</sup> J = 1.6), 9.20 (dm, 2H, <sup>3</sup> J = 4.8)	63.80, 68.28, 69.96, 122.71, 125.23, 136.44, 150.07, 152.70, 164.41
3c	3.69 (mc, 8H), 3.80 (mc, 4H), 4.51 (mc, 4H), 8.03 (dd, 2H, <sup>3</sup> J = 5.2, <sup>4</sup> J = 1.1), 9.43 (dd, 2H, <sup>3</sup> J = 5.2, <sup>4</sup> J = 1.1), 9.45 (s, 2H)	62.57, 70.46, 71.35, 125.64, 128.05, 149.66, 152.17, 164.38
6	3.62 (mc, 12H), 3.79 (mc, 4H), 4.20 (mc, 4H), 7.51 (td, 2H, <sup>3</sup> J = 7.7, <sup>4</sup> J = 1.6), 8.39 (dd, 2H, <sup>3</sup> J = 7.7, <sup>4</sup> J = 1.6), 8.74 (mc, 2H)	63.77, 69.62, 121.83, 125.08, 137.30, 150.40, 157.83, 164.48
7	3.58 (mc, 24H), 3.74 (mc, 8H), 4.24 (mc, 8H), 7.50 (td, 4H, <sup>3</sup> J = 7.6, <sup>4</sup> J = 1.7), 8.37 (dd, 4H, <sup>3</sup> J = 7.6, <sup>4</sup> J = 1.7), 8.76 (mc, 4H)	63.56, 68.18, 120.64, 124.97, 138.02, 148.11, 157.67, 164.42
8	3.62 (mc, 12H), 3.79 (mc, 4H), 4.20 (mc, 4H), 7.49 (dd, 2H, <sup>3</sup> J = 7.9, <sup>4</sup> J = 1.7), 8.40 (dd, 2H, <sup>3</sup> J = 7.9, <sup>4</sup> J = 1.7), 9.02 (s, 2H)	64.07, 69.38, 70.65, 122.50, 125.13, 138.36, 151.05, 155.31, 164.03
9	3.67 (mc, 12H), 3.88 (mc, 4H), 4.55 (mc, 4H), 7.92 (d, 2H, <sup>3</sup> J = 5.2), 8.86 (d, 2H, <sup>3</sup> J = 5.2), 8.96 (mc, 2H)	64.01, 70.16, 70.88, 122.85, 124.98, 138.21, 149.70, 155.99, 164.62
10	3.65 (mc, 24H), 3.85 (mc, 8H), 4.53 (mc, 8H), 7.87 (d, 4H, <sup>3</sup> J = 5.5), 8.89 (d, 4H, <sup>3</sup> J = 5.5), 8.98 (mc, 4H)	64.13, 70.44, 70.56, 70.78, 123.05, 125.03, 138.16, 149.78, 127.47, 164.62

Table 3. Ruthenium Complexes 12-15, 17-20, 22 and 23 Prepared

Starting Ru(II) Complex (mmol)	Podand/Coronand (mmol)	Reaction Time	Product <sup>a</sup>	Color of the Crystals	Yield (%)	Molecular Formula <sup>b</sup>	MS (FAB) $m/z$ (%)
11 (0.18)	3a (0.29)	12	12	orange red	34	C <sub>60</sub> H <sub>40</sub> Cl <sub>2</sub> N <sub>6</sub> O <sub>7</sub> Ru (888.8)	889 (0.8), 195 (100)
			13	red	58	C <sub>80</sub> H <sub>80</sub> Cl <sub>4</sub> N <sub>12</sub> O <sub>14</sub> Ru <sub>2</sub> · 11 H <sub>2</sub> O (1777.6)	1778 (0.06), 195 (100)
11 (0.18)	3b (0.29)	12	14	orange red	37	C <sub>60</sub> H <sub>40</sub> Cl <sub>2</sub> N <sub>6</sub> O <sub>7</sub> Ru · 8 H <sub>2</sub> O (832.8)	890 (1.4), 195 (100)
			15	red	47	C <sub>80</sub> H <sub>80</sub> Cl <sub>4</sub> H <sub>12</sub> O <sub>14</sub> Ru <sub>2</sub> · 8 H <sub>2</sub> O (1777.6)	1778 (0.12), 195 (100)
11 (0.18)	6 (0.29)	48	17	red	67	C <sub>42</sub> H <sub>44</sub> Cl <sub>2</sub> N <sub>6</sub> O <sub>8</sub> Ru · 8 H <sub>2</sub> O (932.8)	-
11 (0.18)	9 (0.29)	36	19	red	95	C <sub>42</sub> H <sub>44</sub> Cl <sub>2</sub> N <sub>6</sub> O <sub>8</sub> Ru · 10 H <sub>2</sub> O (932.8)	-
16 (0.18)	6 (0.29)	124	18	dark red	21	C <sub>38</sub> H <sub>38</sub> Cl <sub>2</sub> N <sub>10</sub> O <sub>8</sub> Ru · 6 H <sub>2</sub> O (934.8)	-
16 (0.18)	9 (0.29)	48	20	dark red	43	C <sub>38</sub> H <sub>38</sub> Cl <sub>2</sub> N <sub>10</sub> O <sub>8</sub> Ru · 6 H <sub>2</sub> O (937.8)	-
21 (0.25)	6 (0.29)	72	22	black	45	C <sub>66</sub> H <sub>78</sub> Cl <sub>2</sub> N <sub>6</sub> O <sub>24</sub> Ru · 9 H <sub>2</sub> O (1511.4)	-
21 (0.25)	9 (0.29)	112	23	dark red	53	C <sub>66</sub> H <sub>78</sub> Cl <sub>2</sub> N <sub>6</sub> O <sub>24</sub> Ru · 8 H <sub>2</sub> O (1511.4)	-

<sup>a</sup> All products had melting points > 280°C.

<sup>b</sup> Satisfactory microanalyses obtained: C  $\pm$  0.4, H  $\pm$  0.14, N  $\pm$  0.2. Exceptions; 13, 14: C + 0.5.

Table 4. UV Data of Complexes 12–15, 17–20, 22 and 23<sup>a</sup>

Compound	$\lambda_{LC}$ (nm)	$\log \epsilon$	$\lambda_{MLCT}$ (nm)	$\log \epsilon$	$\lambda_{EX}$ (nm)	$\lambda_{EM}$ (nm)
12	291.0	4.73	460.5	4.09	415.8	505.0
13	289.0	5.02	461.5	4.38	416.2	504.7
14	292.0	4.96	466.5	4.21	466.2	652.0
15	291.6	5.28	468.2	4.54	468.4	652.5
17	287.2	4.45	427.7	3.75	456.0	652.4
			505.0	3.53	531.0	728.2
			(sh)			
18	295.5	4.54	379.5	3.78	351.0	646.0
			471.0	4.05	480.2	646.2
19	289.6	4.57	464.0	3.81	428.4	495.0
					468.4	680.0
20	303.0	4.52	421.4	3.92	471.0	659.0
			481.0	3.70		
			(sh)			
22	299.7	4.31	451.0	3.52	513.0	712.2
23	309.5	4.41	404.2	3.49	350.0	656.2
			531.0	3.29	474.0	657.4

<sup>a</sup> LC = Ligand centered; MLCT = Metal to ligand charge transfer, EX = Excitation, EM = Emission.

Table 5. <sup>1</sup>H-NMR Data of Complexes 12–15, 17–20, 22 and 23 (CDCl<sub>3</sub>/TMS)

Compound	$\delta$ , J(Hz)
12	3.56 (mc, 4H), 3.66 (mc, 4H), 3.76 (mc, 4H), 4.06 (mc, 4H), 7.18 (mc, 4H), 7.58 (d, 2H, <sup>3</sup> J = 6.2), 7.61 (d, 2H, <sup>3</sup> J = 6.2), 7.86 (mc, 4H), 8.13 (mc, 4H), 8.44 (mc, 4H), 8.62 (d, 2H, <sup>3</sup> J = 5.4), 9.28 (d, 2H, <sup>3</sup> J = 5.4)
13	2.84 (mc, 8H), 2.75 (mc, 8H), 2.84 (mc, 8H), 2.88 (mc, 8H), 6.03 (mc, 8H), 6.44 (mc, 8H), 6.57 (d, 4H, <sup>3</sup> J = 5.5), 7.04 (d, 4H, <sup>3</sup> J = 5.5), 7.33 (mc, 8H), 7.41 (d, 4H, <sup>3</sup> J = 5.2), 7.67 (mc, 8H), 8.23 (d, 6H, <sup>3</sup> J = 5.2)
14	3.64 (mc, 4H), 3.85 (mc, 8H), 3.89 (mc, 4H), 7.29 (mc, 2H), 7.71 (mc, 4H), 7.84 (d, 2H, <sup>3</sup> J = 5.8), 7.95 (mc, 4H), 8.22 (t, 2H, <sup>3</sup> J = 5.8), 8.47 (mc, 4H), 9.68 (mc, 4H), 9.34 (mc, 2H)
15	2.57 (mc, 16H), 2.62 (mc, 8H), 2.68 (mc, 8H), 6.17 (mc, 8H), 6.79 (mc, 4H), 6.90 (mc, 8H), 7.11 (mc, 8H), 7.34 (mc, 8H), 7.38 (d, 4H, <sup>3</sup> J = 5.0), 7.55 (t, 4H, <sup>3</sup> J = 5.0), 8.31 (mc, 4H)
17	CL <sub>2</sub> 3.48 (mc, 12H), 3.53 (mc, 4H), 3.62 (mc, 4H), 7.16 (mc, 4H), 3.62 (mc, 4H), 7.16 (mc, 4H), 7.20 (mc, 4H), 7.48 (d, 4H, <sup>3</sup> J = 6.8), 7.84 (d, 2H, <sup>3</sup> J = 6.2), 8.31 (t, 2H, <sup>3</sup> J = 6.2), 8.45 (mc, 4H), 8.67 (mc, 2H)
18	3.48 (mc, 12H), 3.67 (mc, 4H), 3.78 (mc, 4H), 6.71 (mc, 2H), 7.15 (mc, 4H), 7.38 (d, 2H, <sup>3</sup> J = 7.4), 7.57 (mc, 4H), 7.64 (d, 2H, <sup>3</sup> J = 7.4), 7.83 (mc, 4H), 8.32 (mc, 4H)
19	3.49 (mc, 12H), 3.55 (mc, 4H), 3.68 (mc, 4H), 7.86 (d, 2H, <sup>3</sup> J = 6.6), 7.92 (mc, 4H), 8.56 (mc, 4H), 8.67 (mc, 2H), 8.75 (d, 2H, <sup>3</sup> J = 6.6), 9.71 (mc, 4H)
20	3.51 (mc, 12H), 3.67 (mc, 4H), 3.71 (mc, 4H), 6.74 (mc, 2H), 7.41 (d, 2H, <sup>3</sup> J = 6.8), 7.72 (d, 2H, <sup>3</sup> J = 6.8), 7.88 (mc, 4H), 8.48 (mc, 4H), 9.68 (mc, 4H)
22	3.48 (mc, 12H), 3.52 (mc, 12H), 3.58 (mc, 12H), 8.24 (mc, 6H), 8.82 (mc, 6H), 9.01 (mc, 6H)
23	3.44 (mc, 12H), 3.51 (mc, 12H), 3.60 (mc, 12H), 7.76 (mc, 6H), 7.82 (mc, 6H), 8.92 (mc, 6H)

The polyoxyethylene 3 or macrocyclic ligands 6, 8, 9 were studied with regard to their properties as hosts for alkali (Li<sup>+</sup>, Na<sup>+</sup>, K<sup>+</sup>, Rb<sup>+</sup>) and earth-alkali ions (Mg<sup>2+</sup>, Ca<sup>2+</sup>, Sr<sup>2+</sup>, Ba<sup>2+</sup>) as guests. The binding properties shows a clear effect in the series Rb<sup>+</sup>, Mg<sup>2+</sup>, Ca<sup>2+</sup>, Sr<sup>2+</sup>, Ba<sup>2+</sup>. The extinction coefficients increase, and the absorption maxima do not show a remarkable shift (Table 6).

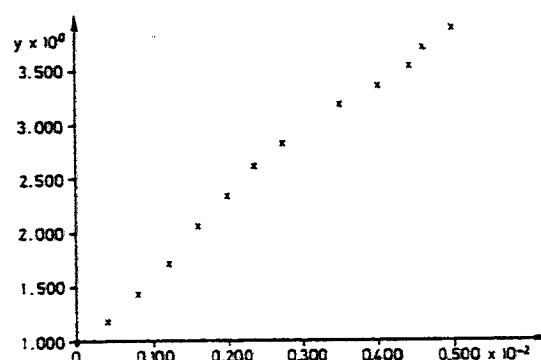
Table 6. Absorption Maxima and Extinction Coefficients of the Crown Esters 3, 8 and 9

Ion	3b		8		9	
	$\lambda_{max}$ (nm)	$\log \epsilon$	$\lambda_{max}$ (nm)	$\log \epsilon$	$\lambda_{max}$ (nm)	$\log \epsilon$
–	262	3.77	263	2.18	289	3.54
Rb <sup>+</sup>	262	4.06	270	3.01	272	3.78
			(sh)			
Mg <sup>2+</sup>	262	4.04	267	2.99	283	3.80
Ca <sup>2+</sup>	264	4.16	266	3.00	286	3.80
Sr <sup>2+</sup>	268	4.15	267	3.00	286	3.81
Ba <sup>2+</sup>	263	4.13	268	2.90	283	3.81

The crown ester modified ruthenium polypyridyls compared with the standard sensitizer [Ru(bpy)<sub>3</sub>Cl<sub>2</sub>] [ $\lambda_{MLCT} = 452.0$  (nm),  $\lambda_{EX} = 452$  (nm),  $\lambda_{EM} = 613$  (nm)] give rise to bathochromic shifts in absorption as well as in emission.

The large Stokes shifts of the UV and emission maxima of the tris-homoleptic sensitizers can be explained by higher internal conversion rates caused by the flexibility of the crown ester function and the lowering of the <sup>3</sup>MLCT-level of the complexes.<sup>23</sup>

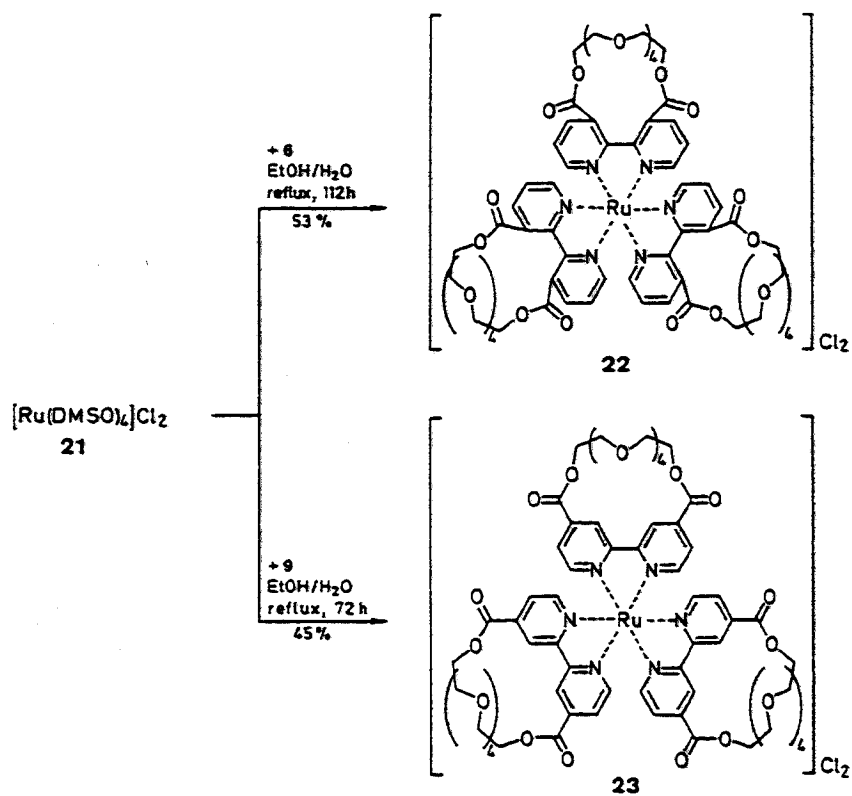
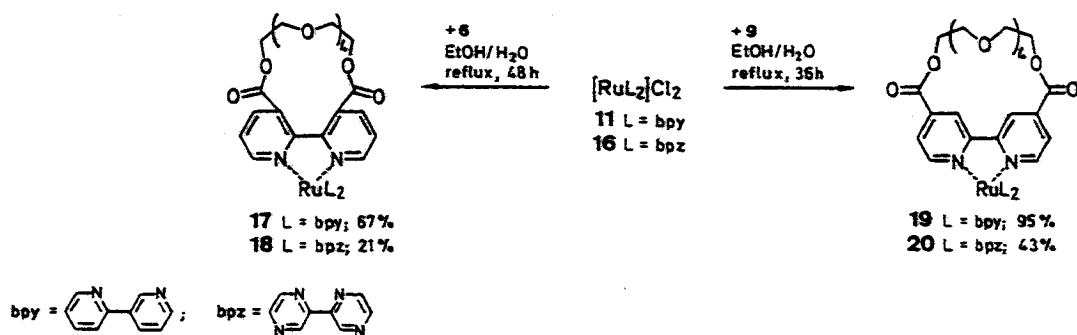
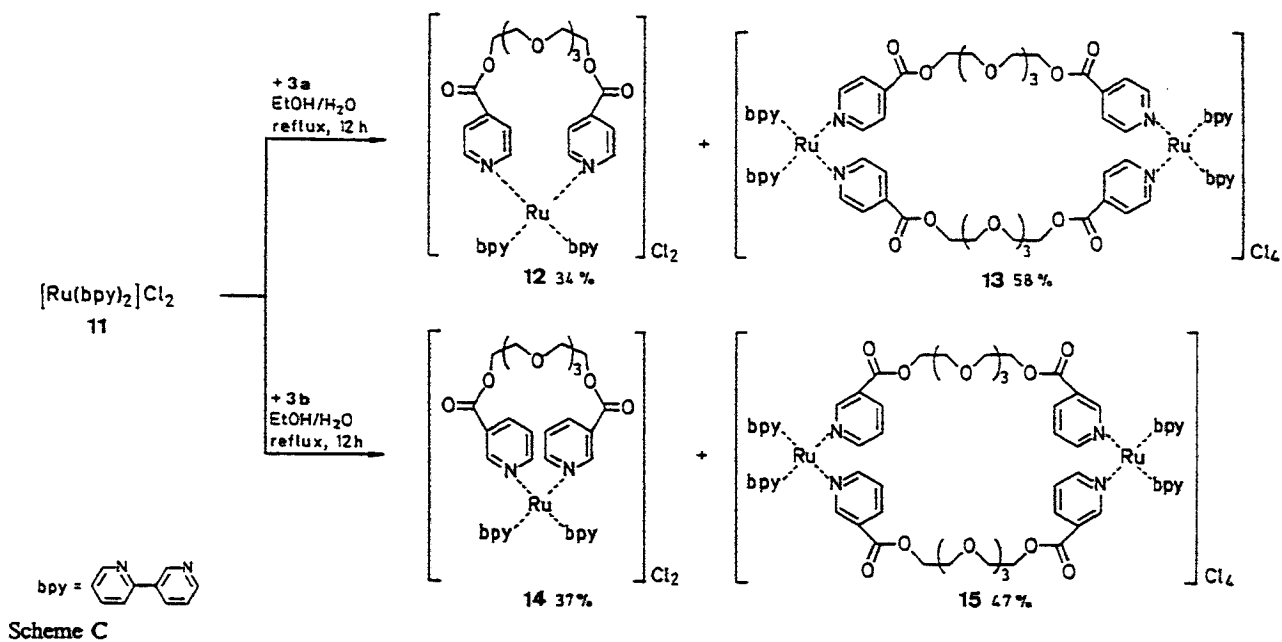
An experiment under steady state irradiation using the ruthenium complex 19 and methylviologen (MV<sup>2+</sup>) as electron relay in acetonitrile/water (95:5) was carried out.



Sensitizer: Ruthenium bis(2,2'-bipyridine) (oxybis(ethylenoxyethyl-oxymethylene) (2,2'-bipyridine-4,4'-dicarboxylate)dichloride;  $c = 3 \cdot 10^{-3}$  mol L<sup>-1</sup>.

Charge relay: Methylviologen dichloride.  
Solvent: Acetonitrile/Water (95/5).

Figure. Stern-Volmer Plot of the Complex 19 and Methylviologen as Electron Relay in Acetonitrile/Water (95:5).



The non-linear Stern-Volmer plot (Figure) indicates an attraction between the crown ether modified bipyridine ligand of the complex and the relay, leading to a very rapid decrease of the luminescence and thus to a very fast intramolecular electron transfer. This is an important process which opens up a possibility to reduce back electron transfer in energy storing systems.

In summary, we have demonstrated that pyridines and bipyridines linked by a polyoxyethylene or a crown ether moiety can be prepared in good yields. The ruthenium complexes containing these ligands were synthesized in average to good yield. The new ligands 3, 6, 8 and 9 show interesting binding properties with alkali ions, which are promising for the binding efficiencies of the ruthenium complexes. The quenching experiment using the ruthenium complex 19 and the electron relay methylviologen prove a very fast intramolecular electron transfer.

Further results analog these lines comprising mechanistic studies will be reported elsewhere.

The following instruments were used for spectral and analytical measurements: IR-Beckman IR spectrophotometer, UV-Kontron Uvikon spectrophotometer, <sup>1</sup>H- and <sup>13</sup>C-NMR-Bruker 400 MHz spectrometer, MS Varian and C,H,N-Carlo Erba.

Pyridine-3-carboxylic acid, pyridine-4-carboxylic acid, tetraethylene glycol dichloride, 2,2'-bipyridine, 4,4'-dimethyl-2,2'-bipyridine, 1,10-phenanthroline and Sephadex LH100 were obtained from Aldrich and used as such. Pyridazine-4-carboxylic acid,<sup>24</sup> 2,2'-bipyridine-3,3'-dicarboxylic acid,<sup>25</sup> 2,2'-bipyridine-4,4'-dicarboxylic acid,<sup>26</sup> pentaethyleneglycoldibromide,<sup>27</sup> ruthenium-bis-bipyridine-dichloride,<sup>28</sup> ruthenium-bis-bipyridine-dichloride,<sup>29</sup> and ruthenium-tetrakis-dimethylsulfoxide-dichloride<sup>30</sup> were prepared as described in the literature.

**Dicesium-4,4'-bipyridine-3,3'-dicarboxylate (5b); Typical Procedure:** 3,3'-Dimethyl-4,4'-bipyridine<sup>31</sup> (5.0 g,  $2.7 \times 10^{-2}$  mol) is oxidized in water with an excess of KMnO<sub>4</sub> (15.8 g, 0.1 mol). After filtration the solvent is removed. The potassium salt is dissolved in water and precipitated as the barium salt using Ba(OH)<sub>2</sub>.

The barium salt (7.1 g,  $1.9 \times 10^{-2}$  mol) is treated with Cs<sub>2</sub>CO<sub>3</sub> and H<sub>2</sub>SO<sub>4</sub> and then filtered. Removal of the solvent affords dicesium-4,4'-bipyridine-3,3'-dicarboxylate (5b); yield: 9.7 g ( $1.87 \times 10^{-2}$  %).

**Heterocyclic Crown Podands 3 and Coronands 6–10; General Procedure:**

A heterogeneous solution of the corresponding cesium salt 5 and the appropriate polyethylene glycol dihalide 1 or 4 in dry DMF (2 L) is stirred 48–96 h at 50–70°C (see Tables 1 and 2 for molar equivalents and reaction conditions). After removing the solvent *in vacuo*, the residue is extracted with CH<sub>2</sub>Cl<sub>2</sub> and filtered. The organic phase is concentrated and, the product is purified by column chromatography on aluminum oxide using EtOAc/CH<sub>2</sub>Cl<sub>2</sub> (1:1) as eluent.

The dimers 7 and 10 are eluted in a second fraction by chromatography on aluminum oxide using EtOAc/CH<sub>2</sub>Cl<sub>2</sub>/EtOH (7:1:1) as eluent (Tables 1 and 2).

**Ruthenium Complexes 12–15, 17–20, 22, 23; General Procedure:** A mixture of the appropriate podand 3, coronand 6 or 9 and the corresponding ruthenium complex 11, 16 or 22 is refluxed in EtOH/H<sub>2</sub>O (3:1) for 12–24 h (see Table 4 for molar equivalents and reaction conditions). After removing the solvent *in vacuo*, water (100 mL) is added and the mixture is extracted with CH<sub>2</sub>Cl<sub>2</sub> (4 × 100 mL). The water is removed again *in vacuo* and the complexes are precipitated by adding MeOH (5 mL) and Et<sub>2</sub>O (20 mL). The precipitate is dissolved in MeOH and the complexes are

separated in monomers and dimers (in the case of 12–15) and/or separated from the bis-complexes by column chromatography on Sephadex LH100 using EtOH/MeOH (5:1 as eluent. The solvent is removed and the complexes are dried at 50°C *in vacuo* and stored over P<sub>2</sub>O<sub>5</sub> (Tables 3–5).

We acknowledge financial support from BMFT, from the Landesgraduiertenförderung des Saarlandes (HK) and from the Stiftung Stipendien Fonds der Chemischen Industrie e. V. (StB).

Received: 4 December 1989; revised: 9 April 1990

- (1) Electron Transfer Reactions Part 7. For Part 6, see: Dürr, H. *Nouv. J. Chem.* 1990. Trierweiler, H.P., in press.
- (2) *Supramolecular Photochemistry*, Balzani, V. (ed.), D. Reidel, Publ. Co., Dordrecht and Boston, 1987.
- (3) Juris, A.; Barigeletti, F.; Compagna, F.; Balzani, V.; Zelewsky, A. v. *Coord. Chem. Rev.* 1988, 84, 85.
- (4) Rau, H.; Franck, R.; Greiner, G. *J. Phys. Chem.* 1986, 90, 2476.
- (5) Willner, I.; Otvos, J.W.; Calvin, M. *J. Am. Chem. Soc.* 1981, 103, 3203.
- (6) Willner, I.; Yang, J.M.; Laane, C.; Otvos, J.M.; Calvin, M. *J. Phys. Chem.* 1981, 85, 3277.
- (7) Frank, A.J.; Willner, I.; Goren, Z.; Degani, Y. *J. Am. Chem. Soc.* 1987, 109, 3568.
- (8) Krueger, J.S.; Mayer, J.E. *J. Am. Chem. Soc.* 1988, 110, 8232.
- (9) Dürr, H.; Thiery, U.; Infelta, P.P.; Braun, A.M. *Nouv. J. Chim.* 1989, 13, 575.
- (10) Lehn, J.M. *Angew. Chem.* 1988, 100, 91; *Angew. Chem., Intl. Ed. Engl.* 1988, 27, 89.
- (11) Alpha, B.; Lehn, J.M.; Mathis, G. *Angew. Chem.* 1987, 99, 259; *Angew. Chem., Intl. Ed. Engl.* 1987, 26, 266.
- (12) Chambron, J.C.; Sauvage, J.P. *Tetrahedron Lett.* 1986, 27, 865.
- (13) Maier, V.E.; Shafirovich, V.Ya. *Izv. Akad. Nauk. SSSR*, 1989, 3, 700; *C.A.* 1989, 111, 125629.
- (14) Zhilina, Z.I.; Mel'nik, V.I.; Andronati, S.A.; Abramovich, A.E. *Zh. Org. Khim.* 1989, 25, 1063, 1070; *C.A.* 1989, 111, 240014.
- (15) Danielson, E.; Elliot, C.M.; Merkert, J.W.; Meyer, T.J. *J. Am. Chem. Soc.* 1987, 109, 2519.
- (16) Meyer, T.J. *Acc. Chem. Res.* 1989, 22, 163.
- (17) Collin, J.P.; Guilleres, St.; Sauvage, J.P. *J. Chem. Soc., Chem. Commun.* 1989, 776.
- (18) Rebeck, J.; Trend, J.F.; Wattley, R.V.; Chakravorti, S. *J. Am. Chem. Soc.* 1979, 101, 4333.
- (19) Rebeck, J.; Trend, J.F. *J. Am. Chem. Soc.* 1980, 102, 4853.
- (20) Lin, C.T.; Boettcher, W.; Chou, M.; Creutz, C.; Sutin, N. *J. Am. Chem. Soc.* 1976, 98, 6536.
- (21) Wang, S.S.; Gisin, B.F.; Winter, D.P.; Makofske, R.; Kulesha, I.D.; Tzougraki, C.; Meienhofer, J. *J. Org. Chem.* 1977, 42, 1286.
- (22) Piepers, O.; Kellogg, R.M. *J. Chem. Soc., Chem. Commun.* 1978, 383.
- (23) Barigeletti, F.; De Cola, L.; Balzani, V.; Belser, P.; v. Zelewsky, A.; Vögtle, F.; Gramenudi, S. *J. Am. Chem. Soc.* 1989, 111, 4662.
- (24) Heinisch, G. *Monatsh. Chem.* 1973, 104, 958.
- (25) Wimmer, F.L.; Wimmer, S. *Org. Prep. Proced. Int.* 1983, 15, 368.
- (26) Case, F.H. *J. Am. Chem. Soc.* 1946, 68, 2574.
- (27) Dann, J.R.; Chiesa, P.P.; Gates, J.W. *J. Org. Chem.* 1961, 26, 1991.
- (28) Sprintschnik, G.; Sprintschnik, H.; Kirsch, P.P.; Whitten, D.G. *J. Am. Chem. Soc.* 1977, 99, 4947.
- (29) Crutchley, R.J. *Inorg. Chem.* 1961, 22, 2647.
- (30) Evans, I.; Spencer, A.; Wilkinson, G. *J. Chem. Soc., Dalton Trans.* 1973, 203.
- (31) Stoeckl, C.; Wagner, M. *J. Prakt. Chem.* 1893, 48, 1.

Reprint from:

# **Frontiers in Supramolecular Organic Chemistry and Photochemistry**

Edited by  
Hans-Jörg Schneider and Heinz Dürr

With an Introductory Chapter  
by Jean-Marie Lehn



Weinheim · New York · Basel · Cambridge

© VCH Verlagsgesellschaft mbH, D-6940 Weinheim, 1991

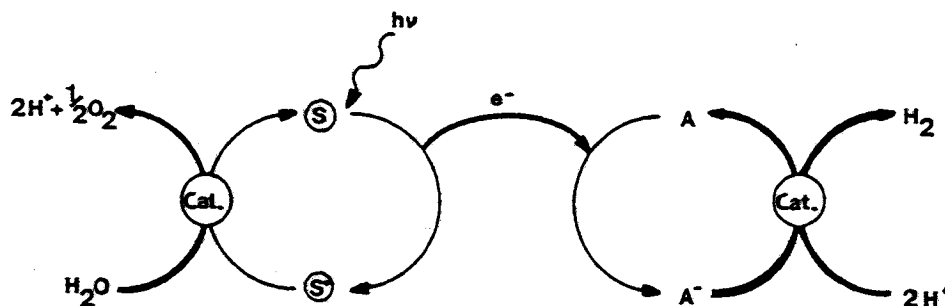
# Supramolecular Sensitizers and Sensitizer/Relay Assemblies

A Novel Approach to Electron Transfer Reactions

*H. Dürr, S. Bossmann, H. Kilburg, H. P. Trierweiler, and R. Schwarz*

Artificial photosynthesis involves a truly supramolecular system [1]. The key step—as in natural photosynthesis—is an electron-transfer process. In the recent past, numerous papers [1-9] have been devoted to the study of such systems, the results of which can be summarized as follows:

An artificial photosynthesis system consists basically of a light absorber (sensitizer), an electron carrier (relay), and catalysts to mediate  $H_2$  and  $O_2$ -production from water. As sensitizer, metal-pyridine complexes [2], metal porphyrines [3], and semiconductors [4] have all been employed. Relays have included bis-ammonium salts like methylviologen [5], or more complex molecules like cobalt-sepulchrate [6]. The kinetic barrier represents a major obstacle to generating hydrogen or oxygen, and it has been circumvented by catalysts such as Pt, Ru, Os [7] and  $RuO_2$ ,  $IrO_2$  [8], etc. Such a supramolecular system can in principle generate  $H_2$  and  $O_2$  during irradiation of an aqueous solution (Scheme 1).



Scheme 1. Artificial photosynthesis.

However, to facilitate the study of the reduction and oxidation steps, the two processes have frequently been separated, thus giving rise to simpler systems [2, 9].

In order to achieve the final goal, efficient cleavage of water to hydrogen and oxygen, optimization is essential for each component: sensitizer, relay, and catalyst.

In this contribution the focus is on the development of new, efficient supramolecular sensitizers based on a Ru(L<sub>3</sub>) complex. Three topics associated with this very general problem are presented:

1. Development and characterization of a new Ru(L<sub>3</sub>)-cage complex.
2. Test of a new supramolecular sensitizer/relay assembly with respect to H<sub>2</sub> production from water and CH<sub>4</sub> generation from CO<sub>2</sub>, and
3. Experimental results from novel sensitizer/relay-crown assemblies with regard to electron transfer.

## Development and Characterization of a Supramolecular Ru(L<sub>3</sub>)-Cage Complex

The principal problem in electron transfer reactions employing Ru(L<sub>3</sub>) complexes (or other metals) is the need for optimal photophysical parameters with respect to the complexes themselves. The requirements for a good sensitizer are:

- absorption in the region of solar emission
- excited states with long lifetimes
- suitable redox potentials
- photostability
- fast bimolecular electron transfer.

Many papers have dealt with the optimization of these parameters [1, 2, 3], but photostability remains a major problem to be solved. A very elegant idea for increasing photostability and overcoming "photoanation" (the photo-dissociation of a complex ligand) was first presented by Sargeson [10]. He demonstrated that cage structures are apparently 1) more stable to photoanation and 2) unchanged with respect to ligand properties when coordinated to metals [11]. In the case of Ru-polypyridines, internal conversion (ic) processes were also reduced as evidenced by luminescence (quantum yield) and the lifetime of the metal-to-ligand charge transfer (MLCT) state (see below). Typical complexes in which this idea has been further pursued include those shown in Figure 1.

The metal (Eu/Tb)(cryp)<sup>3+</sup> **2a/2b** prepared by Lehn were useful only for energy production, not for electron transfer [12]. Synthesis of the caged Ru-cryptate **3** in small amounts has been reported by Vögtle and Balzani [13].

We recently synthesized the new supramolecular Ru(cryp)<sup>2+</sup> **4** [14]. The novel complex **4** was expected to be subject to slightly more geometrical constraint than

o hydrogen and  
relay, and cata-

icient supramo-  
ociated with this

plex.  
spect to H<sub>2</sub> pro-

olies with regard

amolecular

ng Ru(L<sub>3</sub>) com-  
parameters with  
d sensitizer are:

ters [1, 2, 3], but  
gant idea for in-  
oto-dissociation  
onstrated that  
d 2) unchanged  
reduced as evi-  
metal-to-ligand  
which this idea

ful only for en-  
ged Ru-cryptate

[14]. The novel  
constraint than

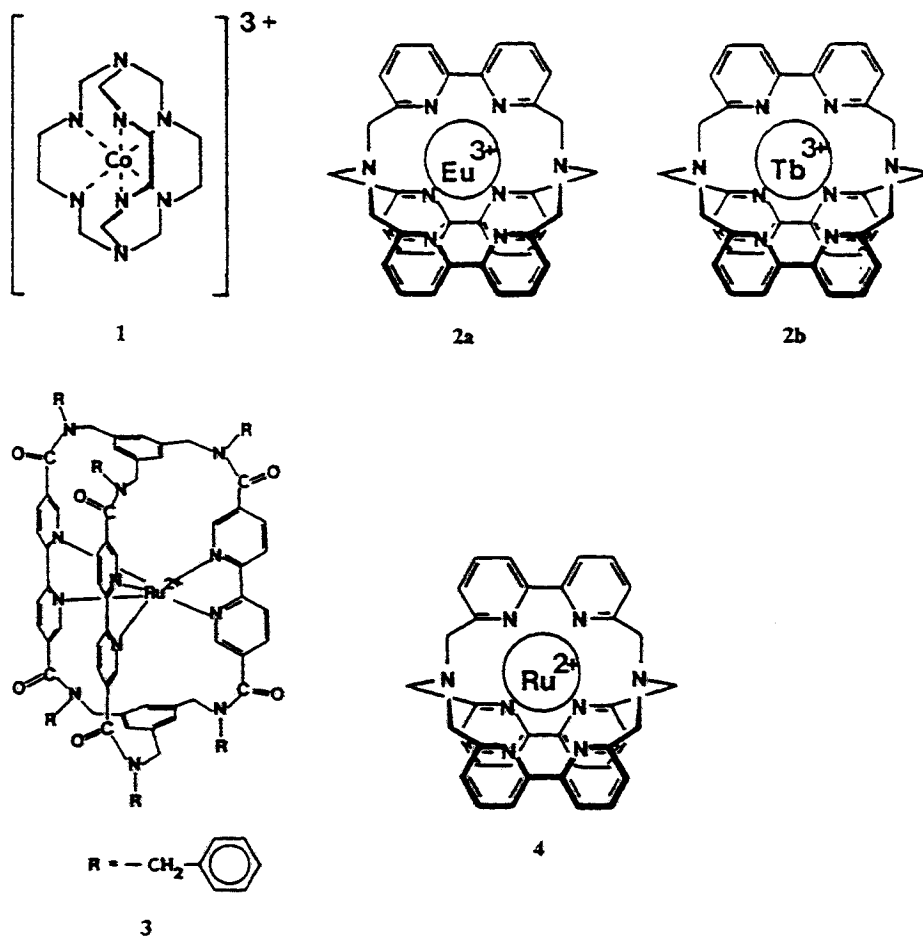
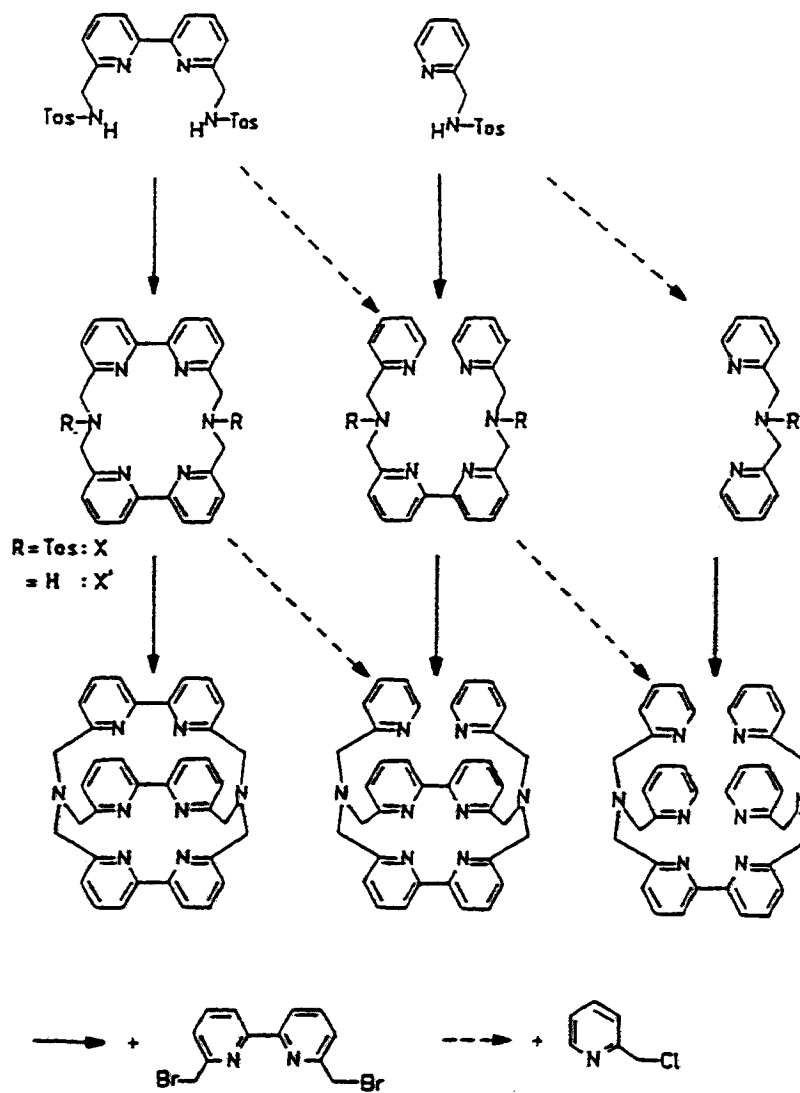


Figure 1. Cryptates described by Sargeson 1, Lehn 2a, b, Balzani 3 and Dürre 4 (the different structures of 3 and 4 are indicated by the endings Ru(cryptate)<sup>2+</sup>: 3 and Ru(cryp)<sup>2+</sup>: 4.

3, and it was of interest to see how the photophysical data for 4 would compare with those from 3. The synthetic route to the Na(cryp)<sup>+</sup> represented a modification of Lehn's [12] procedure, as outlined schematically in Scheme 2 [14].





**Scheme 2.** The synthesis of pyridine- and bipyridinecoronands and -cryptands.

A new chromatographic work-up technique (isotachopheresis) permitted the  $\text{Ru}(\text{cryp})^{2+}$  4 to be both isolated in low yield (3%) and characterized [15].

The result of the isotachopheresis is shown in Figure 2.

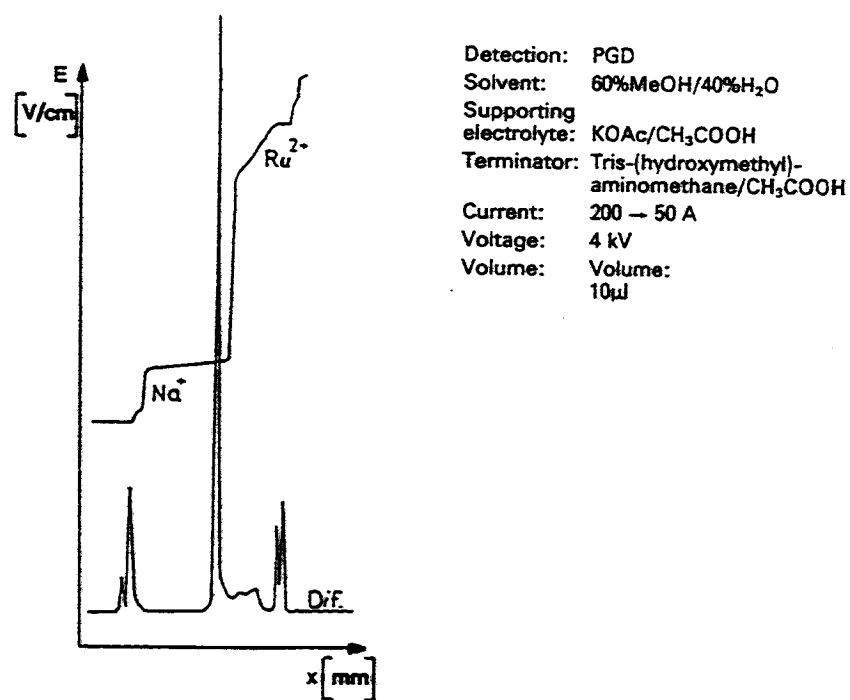


Figure 2. Isotachopheresis of the reaction mixture after removal of solvent of  $\text{Ru}(\text{cryp})^{2+}$ .

Structural proof is provided by NMR data for the  $\text{Na}(\text{cryp})^+$  and  $\text{Ru}(\text{cryp})^{2+}$  4, as summarized in Table 1 and illustrated in Figure 3.

Table 1. <sup>1</sup>H-NMR data for the  $\text{Na}^+$ - and the  $\text{Ru}(\text{cryp})^{2+}$  4 (δ in ppm).

	H <sup>3</sup> , H <sup>3'</sup>	H <sup>4</sup> , H <sup>4'</sup>	H <sup>5</sup> , H <sup>5'</sup>	—CH <sub>2</sub> —
$\text{Na}(\text{cryp})^+$	8.19	7.96	7.46	3.77
$\text{Ru}(\text{cryp})^{2+}$	8.05	8.01	7.47	4.85

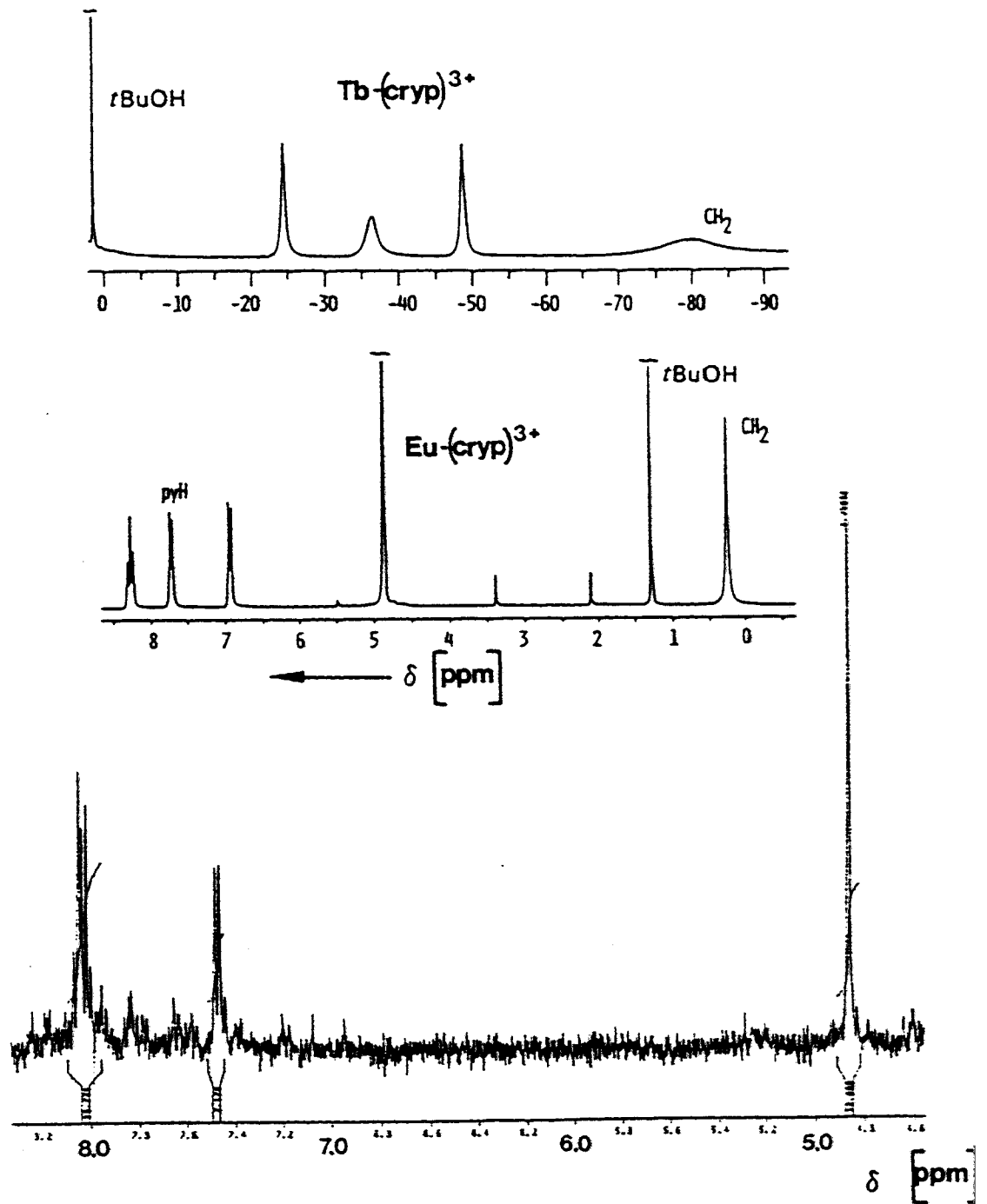


Figure 3. NMR-spectra for the  $Eu/Tb(cryp)^{3+}$  2a, b and the  $Ru^{2+}(cryp)4$ .

Photophysical data for  $\text{Ru}(\text{cryp})^{2+}$  4

Most important for the quality of a sensitizer, including a  $\text{Ru}(\text{L})_3^+$  complex, are the corresponding photophysical data.

UV-spectra:

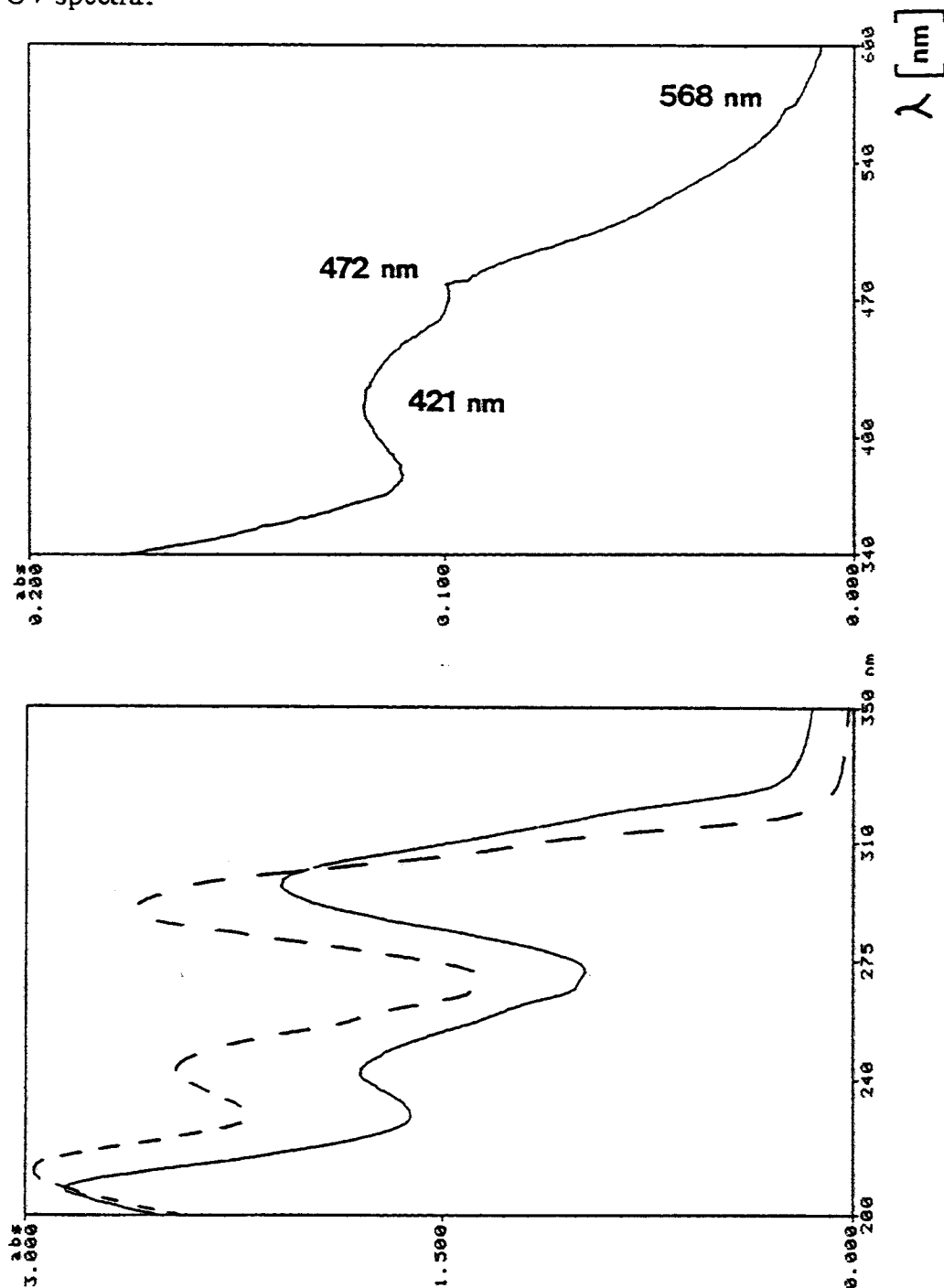


Figure 4. Comparison of the UV-data obtained for the  $\text{Na}^+$ - and the  $\text{Ru}(\text{cryp})^{2+}$  4 (---  $\text{Na}(\text{cryp})^+$ ; (—  $\text{Ru}(\text{cryp})^{2+}$ ).

UV spectra for the  $\text{Ru}(\text{cryp})^{2+}$  **4** are shown in Figure 4 in comparison with a spectrum from the  $\text{Na}(\text{cryp})^+$ .

UV and fluorescence data for  $\text{Ru}(\text{bpy})_3^{2+}$  and the cage complex **3** relative to the  $\text{Ru}(\text{cryp})^{2+}$  **4** are clearly distinct, as seen from Table 2.

The new absorption band of **4** at 421 nm is assigned to MLCT excitation (see below).

**Table 2.** UV/VIS and fluorescence data for  $\text{Ru}(\text{bpy})_3^{2+}$ ;  $\text{Ru}(\text{cryptate})^{2+}$  **3** and  $\text{Ru}(\text{cryp})^{2+}$  **4**.

	$\lambda_{\text{max}}$ (nm)	$\Delta\lambda$ (nm)	emission $\lambda$ (nm)	
			77 K	298 K
$\text{Ru}(\text{bpy})_3^{2+}$	452 300, 350 (sh)		582	615
$\text{Ru-cryptate}$ <b>3</b>	455 355 (sh)	+ 3 + 3	597	612
$\text{Ru}(\text{cryp})^{2+}$ <b>4</b>	421 472, 568 (sh)	- 31 +170, +216	568	604

### Emission spectra

The emission spectra for **4** are provided in Figure 5 and Table 2. In contrast to our earlier findings prior to the availability of a clean sample,  $\text{Ru}(\text{cryp})^{2+}$  **4** shows clear emission, albeit of low intensity. At 77 K the emission intensity is increased.

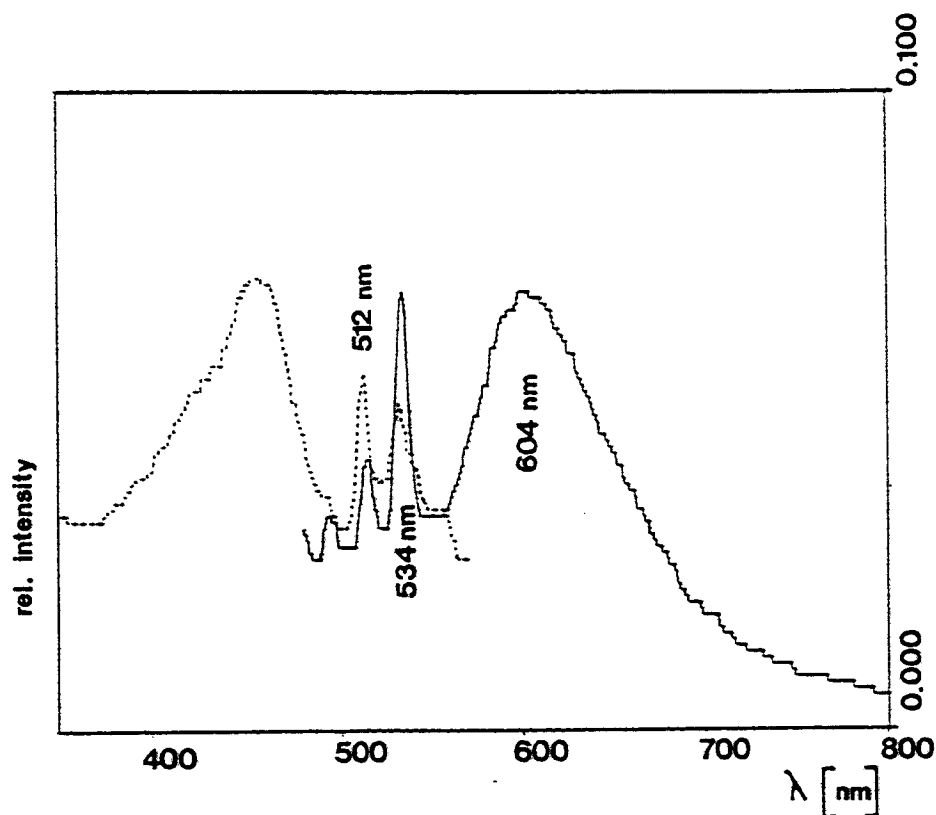


Figure 5. Excitation (·····) and emission (—) spectra for Ru(cryp)<sup>2+</sup> at 298 K.

## Discussion

A typical excitation scheme for tris-homoleptic Ru(L)<sub>3</sub><sup>2+</sup> complexes possessing an ideal octahedral coordination sphere is given by Balzani [13] (Figure 6a).

From this scheme the differences in the transitions become clear. Decisive for the lifetime of these complexes is the relative ordering of the <sup>3</sup>MLCT and <sup>3</sup>MC hypersurfaces.

Figure 6b shows simplified hypersurfaces for the various excited states of the cage complex 3. Deactivation of the excited Ru(L)<sub>3</sub><sup>2+</sup> and 3 is due mainly to emission from the <sup>3</sup>MLCT state. From <sup>3</sup>MC, internal conversion leads to thermal deactivation of the excited state. In this case  $k_b$  is larger than  $k_c$ . The complex 3 possesses the same energy gap between <sup>3</sup>MLCT and <sup>3</sup>MC, but here the hypersurface of <sup>3</sup>MC is slightly modified so that the reaction <sup>3</sup>MC → <sup>3</sup>MLCT is faster, and a further reaction from <sup>3</sup>MC ( $k_b > k_c$ ) is no longer possible.

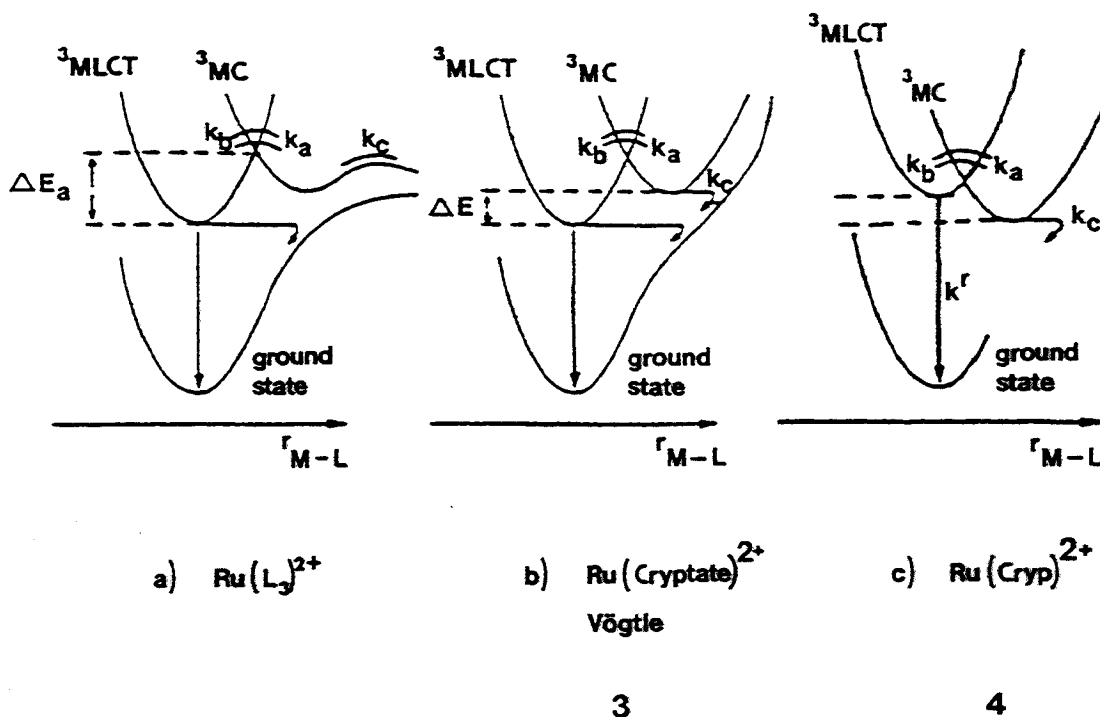


Figure 6. Typical excitation schemes for tris-homoleptic  $\text{Ru}(\text{L})_3^{2+}$  complexes [13]. a)  $\text{Ru}(\text{L})_3^{2+}$ , b) 3, c) 4.

A completely different situation applies to  $\text{Ru}(\text{cryp})^{2+}$  4 (cf. Figure 6c and Table 2). From Figure 6b, c (and Table 2) it is evident that the excited states of 3 and 4 are quite distinct. In 4, the d-d band is shifted bathochromically, so the bands at 472 and 568 nm can be assigned to the MC transition. The  $^3\text{MLCT}$  transition is seen in the band at 421 nm.

This means that the latter transition requires slightly more energy than excitation to the  $^3\text{MLCT}$  state in 3. The energy profile assumed for 4 thus most probably resembles Figure 4c, putting the MC state at lower energy. Excitation of  $\text{Ru}(\text{cryp})^{2+}$  4 leads via intersystem crossing (isc) directly from the  $^3\text{MLCT}$  to the  $^3\text{MC}$  state. The low population of  $^3\text{MLCT}$  is presumably responsible for the weak fluorescence of 4 ( $\Phi_F < 10^{-3}$ ).

The corresponding emission spectrum shows two additional bands at 512 and 534 nm. These have been tentatively assigned to the  $^1\text{MLCT}$  transitions.

The basis for the differences in the photophysical data obtained for  $\text{Ru}(\text{cryp})^{2+}$  4 relative to 3 is most probably the distorted geometry in 4. The perfect octahedral geometry achieved in  $\text{Ru}(\text{bpy})_3^{2+}$  is obviously not possible in 4. Slightly weaker overlap between metal and ligand orbitals accompanying a distorted octahedral geometry could account for all the spectral data described above.

Comparisons of  $\text{Ru}(\text{bpy})_3^{2+}$ , 3, and 4 permit the following conclusions to be drawn:

- a)  $\text{Ru}(\text{bpy})_3^{2+}$  shows:
  - fast radiationless decay of the lowest  $^3\text{MLCT}$  state
  - photoanation
- b) 3 possesses:
  - a longer lifetime compared to  $\text{Ru}(\text{bpy})_3^{2+}$ , and
  - great photostability due to caging
- c) 4 has:
  - weak fluorescence and a  $^3\text{MLCT}$  lifetime comparable to that of  $\text{Ru}(\text{bpy})_3\text{Cl}_2$
  - potential for photoanation due to distorted geometry.

## A Sensitizer-Relay Assembly for Electron Transfer

A second approach to efficient systems for electron transfer is to employ a covalently linked sensitizer-relay assembly [16] (Scheme 3).

In the sensitizer-relay molecule 7, the fragment 2,2'-bipyridine (5) (bpy) together with relays (modified 4,4'-viologens (6) are combined in one molecule. Complex 7 has special properties that are reflected in electrochemical and photo-physical data.

The lifetime of 7 in its MLCT state is in the microsecond range. Redox potentials were calculated by standard procedures. Table 3 provides a summary of absorption and emission data as well as the redox properties of 7.

Such a system slightly simplifies the supramolecular arrangement of the components necessary for light-induced electron transfer. The excited state of compound 7 is reductively deactivated by sacrificial donors (ones that are irreversibly deac-

Table 3. Luminescence lifetime and redox potential of the sensitizer/relay assembly 7.

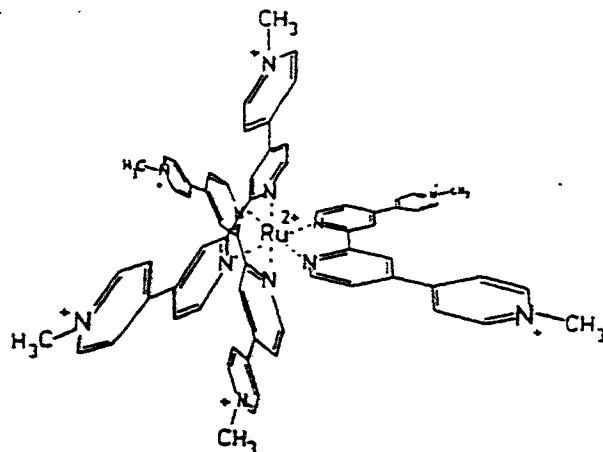
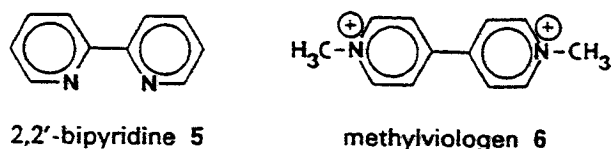
	$\lambda_{\text{max}}$ (nm)	$\log \epsilon$	$\text{EM}^{\text{a)}}$ (nm)	$\Phi_{\text{L}}$	Lifetime <sup>b)</sup> $\tau$ (ns)	$E^{+/2+c)}$ (V)
sensitizer-relay assembly 7	487.0	4.20	668 <sup>a</sup>	0.024	444	-0.55

<sup>a)</sup> Luminescence at 298 K

<sup>b)</sup> of the MLCT-state

<sup>c)</sup>  $\text{H}_2\text{O}$  phosphate buffer, pH=6.88





sensitizer-relay assembly 7

Scheme 3. The structures of 2,2'-bipyridine, methylviologen, and the sensitizer/relay assembly 7.

tivated) such as EDTA (ethylenediamine tetraacetic acid) or TEOA (triethanolamine) [17].

A study of this new complex in the sacrificial system  $\text{RuL}_3^{2+}/\text{TEOA}/2\text{-TMV}^{2+}/\text{Pt}$  at  $\text{pH}=7$  clearly indicates the advantages of  $\text{Ru}(\text{Me}_2\text{tepy})_3^{8+}$  (7) relative to the standard complexes that have been cited in the literature. In particular, and with a sacrificial system in the absence of a relay (e.g.  $2\text{-TMV}^{2+}$ ), the new sensitizer-relay assembly 7 shows a significant amount of hydrogen evolution in contrast to  $\text{Ru}(\text{bpy})_3^{2+}$  and related  $\text{Ru}(\text{L})_3^{2+}$  complexes, which do not lead to hydrogen evolution under similar conditions.

A combination of  $2\text{-TMV}^{2+}$  as electron-transfer reagent with the sensitizer-relay assembly 7 under standard conditions affords the best quantum yield so far observed for hydrogen production mediated by ruthenium complexes. Hydrogen production of the sensitizer-relay assembly 7 in the absence of an electron-transfer reagent opens the way to a very simple photochemical system for water reduction and related processes.

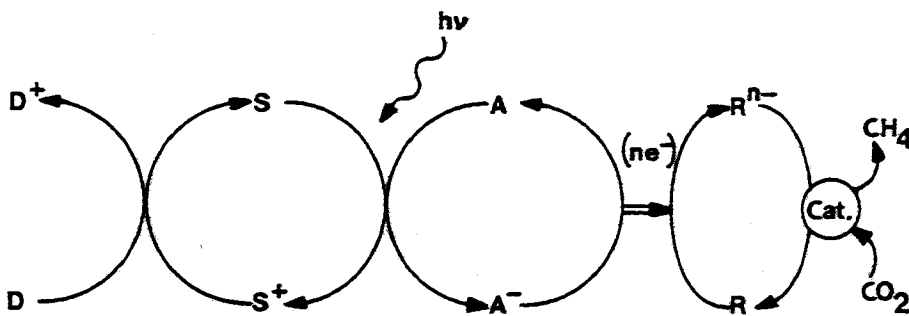
CO<sub>2</sub>-Reduction

Another interesting process is the reduction of CO<sub>2</sub>. The various possible reactions, together with the associated redox potentials [18], are given in Scheme 4:

Scheme 4. Various reduction reactions of CO<sub>2</sub> and the corresponding potentials.

(1)	$2\text{H}^+ + 2\text{e}^- \longrightarrow \text{H}_2$	$E^\circ = -0.41 \text{ V}$
(2)	$\text{CO}_2 + 1\text{e}^- \longrightarrow \text{CO}_2^-$	$E^\circ = -2.0 \text{ V}$
(3)	$\text{CO}_2 + 2\text{e}^- \longrightarrow \text{CO} + \text{H}_2\text{O}$	$E^\circ = -0.52 \text{ V}$
(4)	$\text{CO}_2 + 4\text{e}^- \longrightarrow \text{C} + \text{H}_2\text{O}$	$E^\circ = -0.20 \text{ V}$
(5)	$\text{CO}_2 + 2\text{e}^- \longrightarrow \text{HCOOH}$	$E^\circ = -0.61 \text{ V}$
(6)	$\text{CO}_2 + 4\text{e}^- \longrightarrow \text{HCHO} + \text{H}_2\text{O}$	$E^\circ = -0.48 \text{ V}$
(7)	$\text{CO}_2 + 6\text{e}^- \longrightarrow \text{CH}_3\text{OH} + \text{H}_2\text{O}$	$E^\circ = -0.38 \text{ V}$
(8)	$\text{CO}_2 + 8\text{e}^- \longrightarrow \text{CH}_4 + \text{H}_2\text{O}$	$E^\circ = -0.24 \text{ V}$

The new complex 7 was tested for this purpose just as it was in reduction [19]. According to Willner, ruthenium metal can be used as an efficient catalyst for generating CH<sub>4</sub> [20] (Scheme 5).



Scheme 5. Scheme for sacrificial CO<sub>2</sub>-reduction to methane.

The results are shown in Figure 7, from which it can be seen that CH<sub>4</sub> was produced very efficiently, as compared to Ru(bpy)<sub>3</sub><sup>2+</sup>.

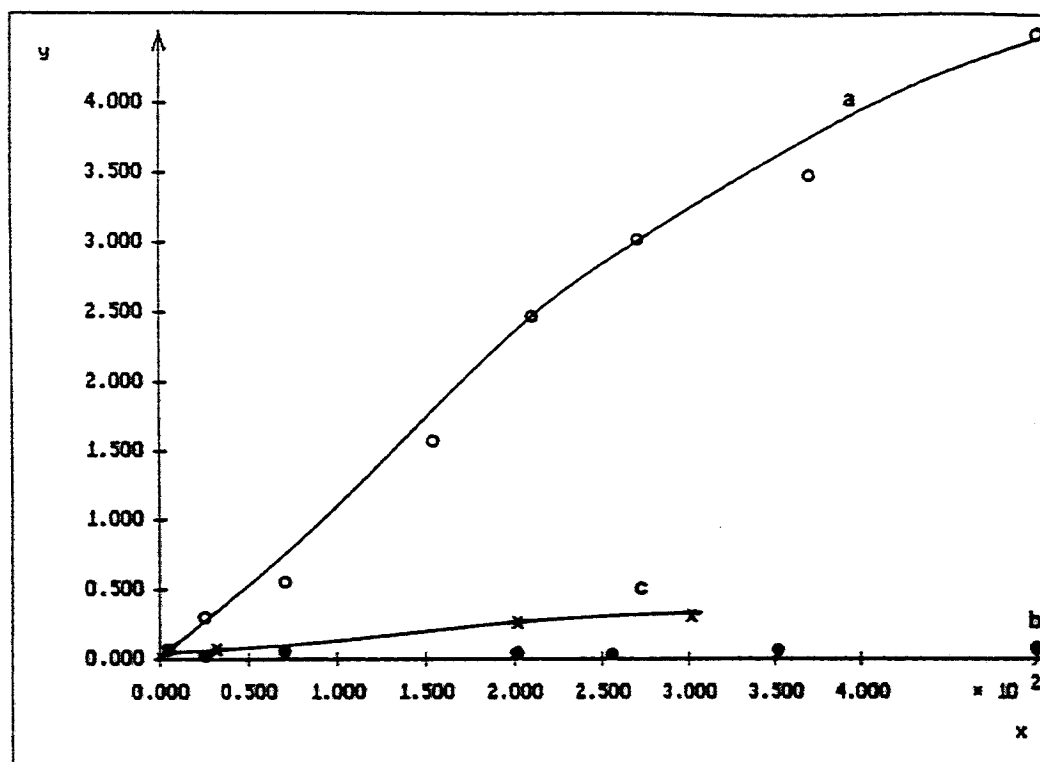
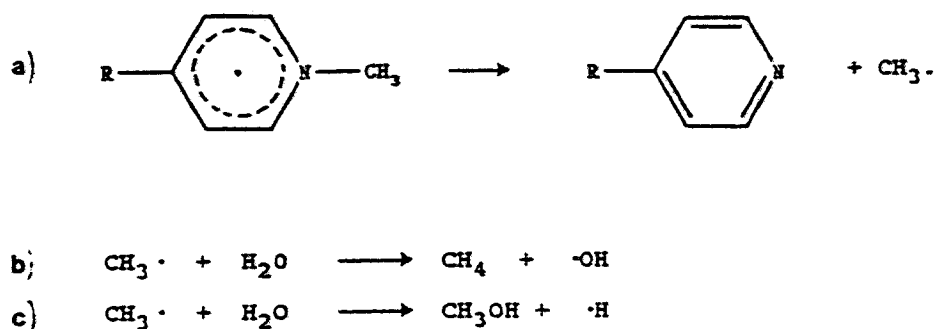
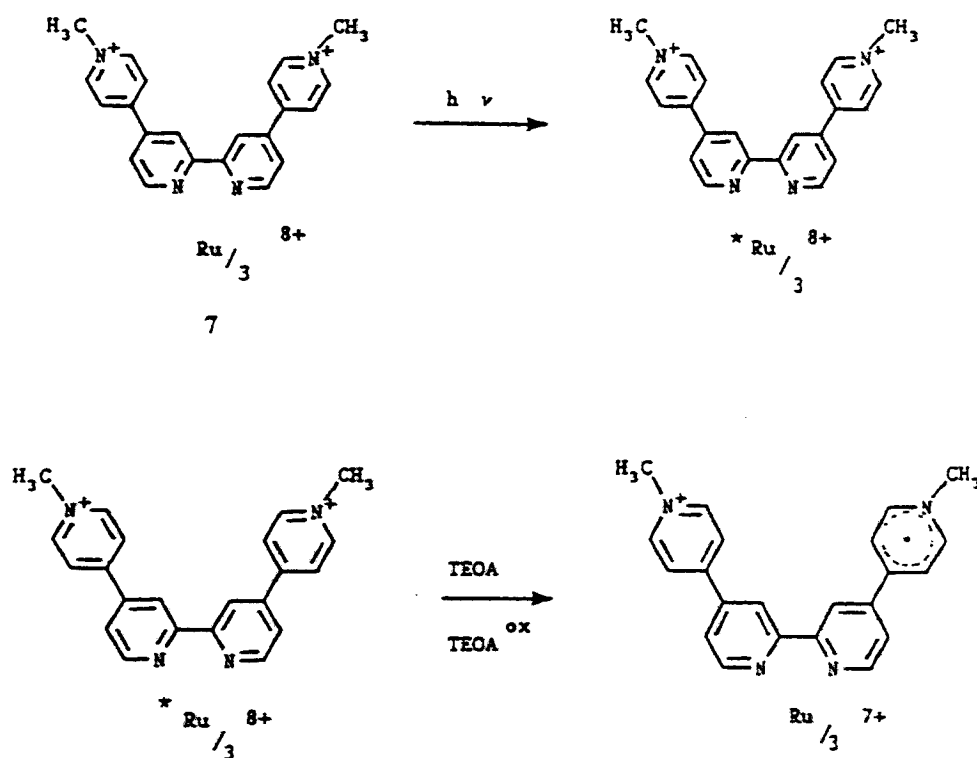


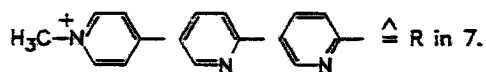
Figure 7. CH<sub>4</sub>-evolution using the sensitizer/relay assembly 7; TEOA as sacrificial electron donor and Ru-metal as catalyst. a) Methane-evolution using a CO<sub>2</sub>/NaHCO<sub>3</sub>-buffer. b) Methane-evolution in the absence of CO<sub>2</sub>/NaHCO<sub>3</sub>-buffer. c) Methane-evolution using Ru(bpy)<sub>3</sub><sup>2+</sup> as sensitizer; (3-sulfonato-propyl)-3,3'-dimethyl-4,4'-bipyridinium (MPVS) as electron relay; TEOA as sacrificial electron donor; Ru-metal as catalyst and a CO<sub>2</sub>/NaHCO<sub>3</sub>-buffer.

In this process, however, 7 is obviously subject to photochemical demethylation [19]. This is apparent from the lower trace b. Nevertheless, CH<sub>4</sub> production by demethylation of 7 is clearly a process of minor importance. The demethylation can be explained by equations a)–c) (Scheme 6).





Scheme 6. The demethylation of 7;



## A Novel Sensitizer-Relay Assembly with Regard to Electron Transfer

A further important factor—apart from the long-term stability of an artificial photosynthetic system—is the effectiveness of electron transfer between sensitizer and electron relay.

Effective quenching of excited species has previously been accomplished by appropriate placement of the photosensitizer and the electron relay in an organized microheterogeneous environment [21].

One example of the realization of this concept is the sensitizer-relay assembly of type 7 described above.

A second example involves covalent connection of the sensitizer and relay components using methylene groups **8**, an approach demonstrated by T. J. Meyer and by Shafirovich and by J. P. Sauvage [22] **9** (Figure 8).

Nevertheless, such an assembly is also capable of assisting the back-electron transfer of intermediate photoredox products. A third concept, due to Lehn [23], requires a photosensitizer-receptor system so designed as to allow effective elec-

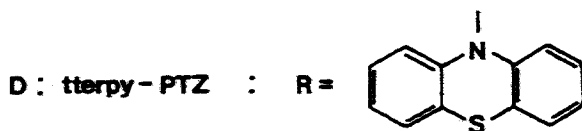
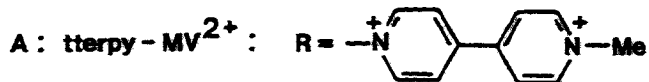
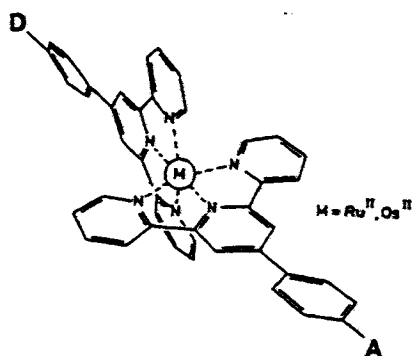
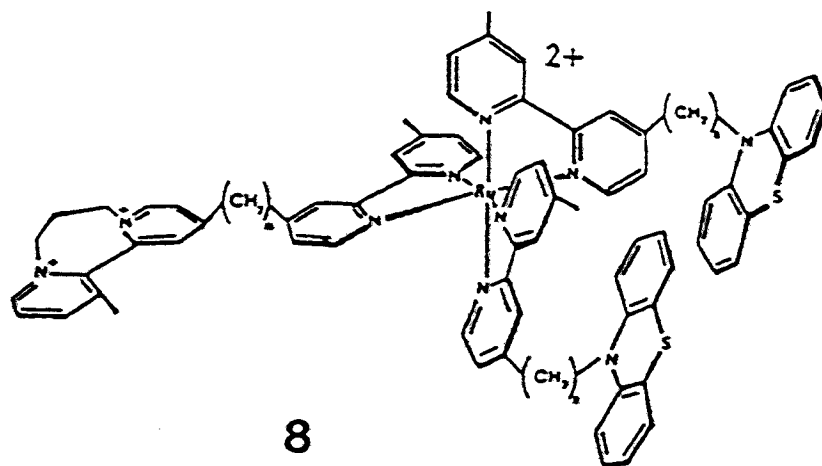
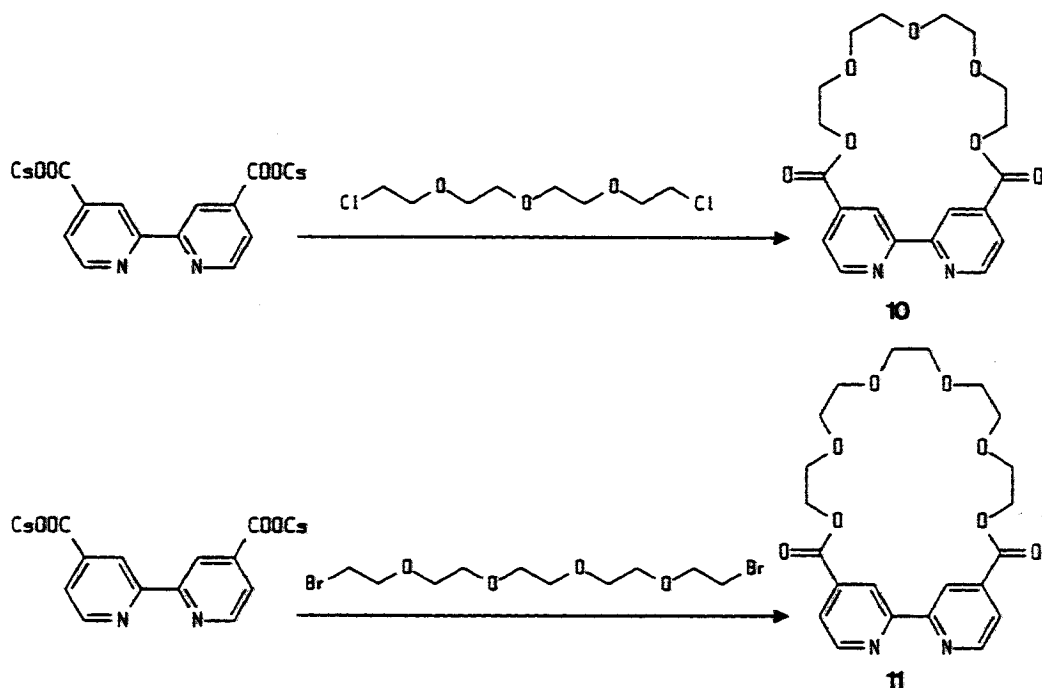


**Figure 8.** The combination of sensitizer-donor and relay components developed by T. J. Meyer and J.-P. Sauvage.

tron transfer, but retaining sufficient flexibility to also facilitate the decisive charge-separation step.

We were interested in constructing new sensitizer-relay assemblies with reversible binding properties allowing a) the binding of an electron relay, b) very fast electron transfer, and c) exchange of reduced relay for a bis-cationic (unreduced) species. Our approach was to synthesize crown ether-modified 2,2'-bipyridines. The crown ether groups were intended to bind cationic species like bis-ammonium salts in a dynamic process.

The first crown ether-modified 2,2'-bipyridines were synthesized by Rebeck [24]. The preparation of mononuclear ruthenium complexes using this compounds proved impossible, because the binding properties of the heterolytic and the crown ether parts to the ruthenium are similar. We chose the method of Wang in the modification by Piepers and Kellogg [25] for the preparation of suitably functionalized crown ethers. Target structures were the substances **10** and **11** (Scheme 7) where the crown ether unit is linked by ester groups.



Scheme 7. The novel heterocyclic crown ethers **10** and **11**.

These macrocyclic hosts were tested with regard to binding properties for alkali metal and alkaline earth ions ( $\text{Li}^+$ ,  $\text{Na}^+$ ,  $\text{K}^+$ ,  $\text{Rb}^+$ ,  $\text{Mg}^{2+}$ ,  $\text{Ca}^{2+}$ ,  $\text{Sr}^{2+}$ ,  $\text{Ba}^{2+}$ ) as guests. Binding was shown to give rise to hyperchromic shifts with the ions:  $\text{Mg}^{2+}$ ,  $\text{Ca}^{2+}$ ,  $\text{Sr}^{2+}$ ,  $\text{Ba}^{2+}$ . No remarkable bathochromic or hypsochromic shifts were detected (Table 4).

Starting with the new heterocyclic crown ethers **10** and **11**, the bisheteroleptic Ru-complexes  $\text{Ru}(\text{bpy})_2(\mathbf{10})^{2+}$  **12** and  $\text{Ru}(\text{bpy})_2(\mathbf{11})^{2+}$  **13** and the tris-homoleptic

**Table 4.** Absorption maxima and absorption coefficients for the heterocyclic crown ethers **10** and **11** in the presence of metal ions.

Ion	$\lambda_{\text{max}}$ (nm) <b>10</b>	log $\epsilon$	$\lambda_{\text{max}}$ (nm) <b>11</b>	log $\epsilon$
/	263	2.18	289	3.54
Rb <sup>+</sup>	270 (sh)	3.01	272	3.78
Mg <sup>2+</sup>	267	2.99	283	3.80
Ca <sup>2+</sup>	266	3.00	286	3.80
Sr <sup>2+</sup>	267	3.00	286	3.81
Ba <sup>2+</sup>	268	2.90	283	3.81

**Table 5.** UV-VIS, fluorescence data, lifetimes and quenching constants of the crown ether–ruthenium complexes **12**, **13**, **15** and **16** as well as the “reference compounds” **14** and **17**.

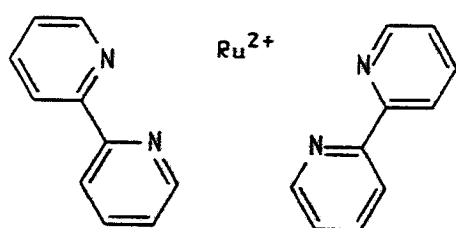
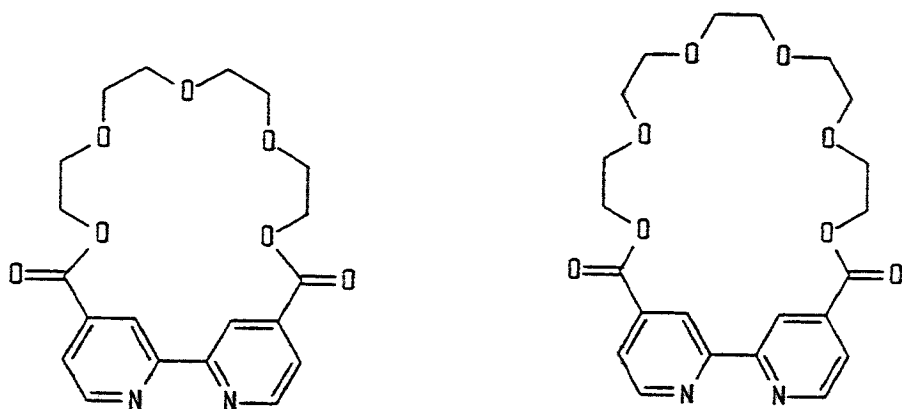
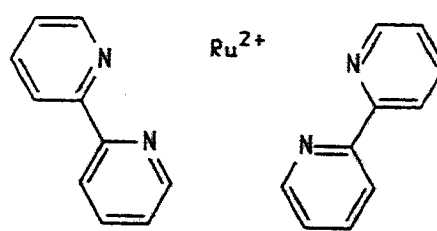
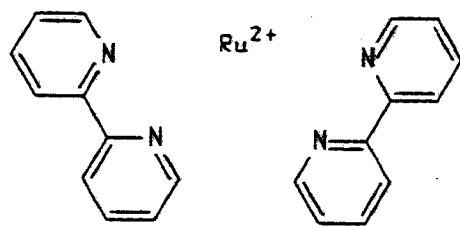
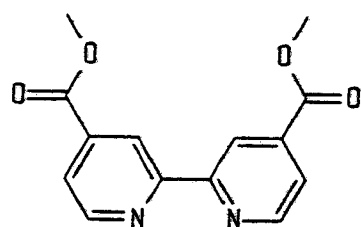
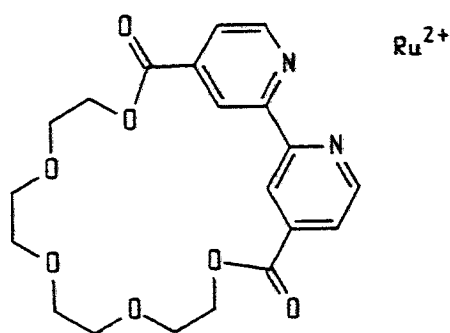
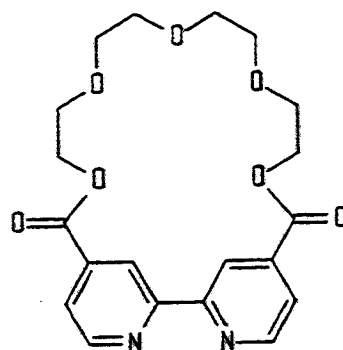
Compound	$\lambda_{\text{max}}$ , MLCT (nm)	lg $\epsilon$	luminescence lifetime $\tau$ (ns)	emission 298 K $\lambda$ (nm)
<b>12</b>	366.4, 481.4	3.84, 4.07	457 <sup>a)</sup>	641.2
<b>13</b>	379.5, 471.0	3.78, 4.05	495 <sup>a)</sup>	646.2
<b>14</b>	423.8, 481.4	3.92, 4.13	332 <sup>a)</sup>	694.0
<b>15</b>	398.4, 474.5	4.27, 4.12	1318	638.8
<b>16</b>	402.2, 531.0 (w)	3.49, 3.29	1527	657.4
<b>17</b>	354.0, 469.0	4.12, 4.29	822	646.0

<sup>a)</sup> phosphate buffer; pH = 6.88.**Table 6.** Quenching constants for the crown ether–ruthenium complexes **12**, **13**, **15** and **16** as well as the “reference compounds” **14** and **17**.

Compound	$k_q \times 10^{-9} \text{ ms}^{-1}$		
	MV <sup>2+</sup>	BV <sup>2+</sup>	TEOA
<b>12</b>	4.96 ( $r=0.9999$ )	0.24 ( $r=0.9996$ )	/
<b>13</b>	11.23* ( $r=0.9936$ )	1.94* ( $r=0.9982$ )	/
<b>14</b>	0.88 ( $r=0.9998$ )	0.13 ( $r=0.9996$ )	/
<b>15</b>	/	/	0.52 ( $r=0.980$ )
<b>16</b>	/	/	0.12 ( $r=0.990$ )
<b>17</b>	/	/	1.24 ( $r=0.982$ )

c(sensitizers) =  $1 \times 10^{-5}$  mol/lc(MV<sup>2+</sup>, BV<sup>2+</sup>) =  $0-3.5 \times 10^{-3}$  mol/l

\* calculated using the first three values measured

**12****13****14****15**



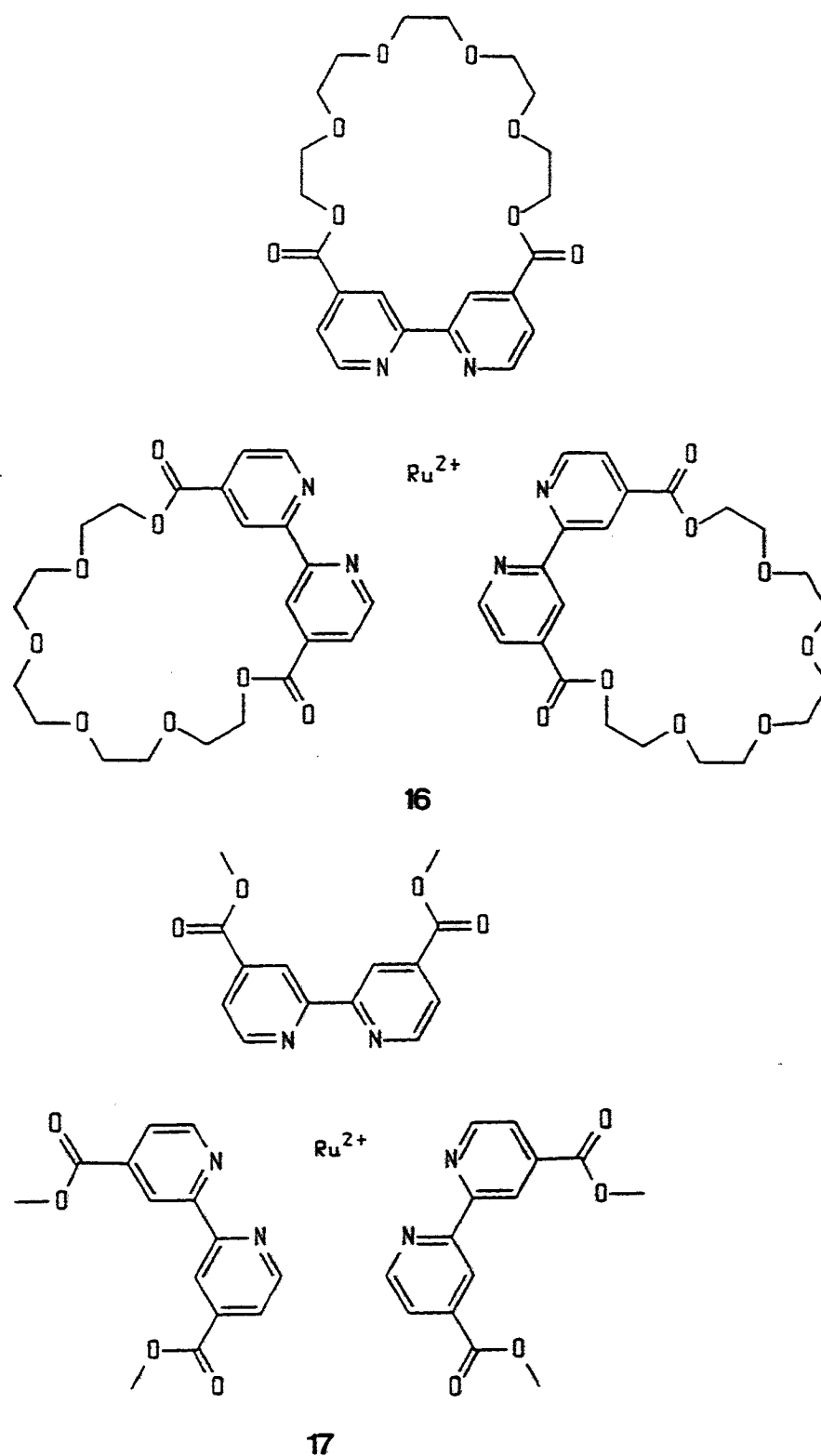


**Figure 9.** The structure of the crown ether-modified ruthenium-trisbipyridine complexes **12**, **13**, **15** and **16** as well as the "reference compounds" **14** and **17**.

compounds  $\text{Ru}(10)_3^{2+}$  15 and  $\text{Ru}(11)_3^{2+}$  16 were then synthesized [26] (Figure 9).

These new crown ether-modified ruthenium polypyridines produced bathochromic shifts (compared to  $\text{Ru}(\text{bpy})_3^{2+}$ ) in both absorption and emission.

The relevant photophysical data are summarized in Tables 5 and 6.

The photochemical behavior of the bis-heteroleptic Ru complexes 12 and 13 possessing one crown ether-modified ligand is very similar to that of the complex 14, which contains the ligand bis-methoxy-2,2'-bipyridine-4,4'-dicarboxylate. The large Stokes shifts can be explained by a lower  $^3\text{MLCT}$  state in the case of an ester-substituted 2,2'-bipyridine ligand and the resulting distortion of the complex geometry. It can be seen that the exchange of two methoxy functions for one penta- or tetraethylene bis-ester function occurs without loss of valuable photophysical properties. No remarkable shifts were seen when alkali metal or alkaline earth ions were used as guests.

Quenching experiments employing Ru complex 13 and the electron relay methylviologen ( $\text{MV}^{2+}$ ) under steady-state irradiation gave rise to a non-linear Stern-Volmer plot. This indicates an attraction between the crown ether function

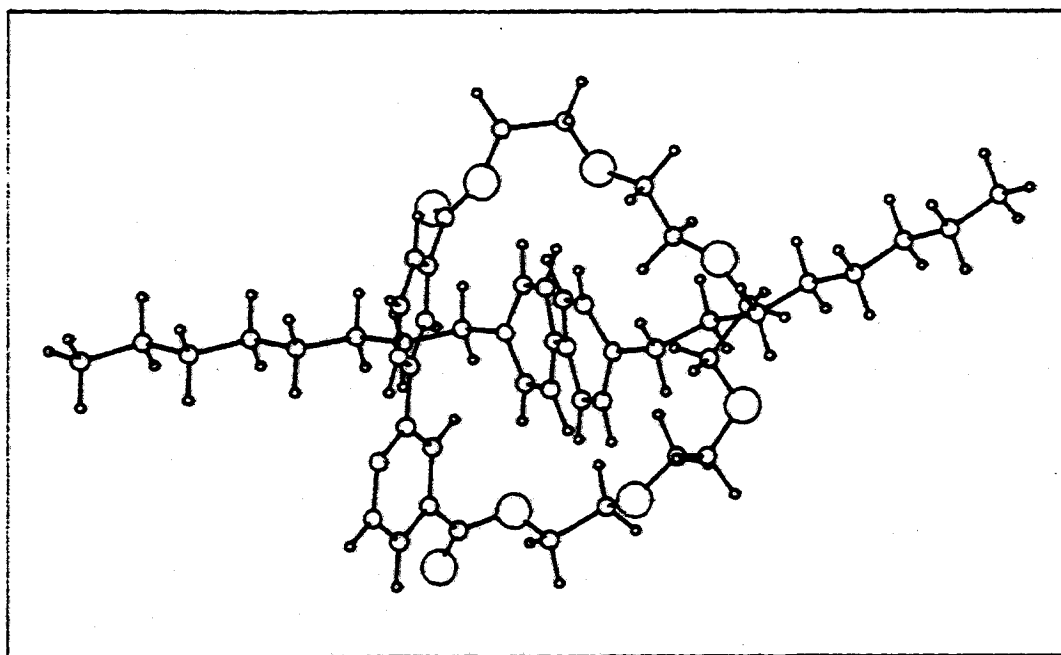


**Figure 10.** The result of a force-field calculation (CHARMm, Polygen) of a supramolecular assembly using the crown ether 11 in the bis-heteroleptic complex 13 is shown. The charges and the space demand of the complex are calculated but not plotted. Only in the case of the heterocyclic crown ester 11 containing five ethylene glycol units is the binding of the electron relay possible. (Chains containing less than five ethylene glycol units are too small.)

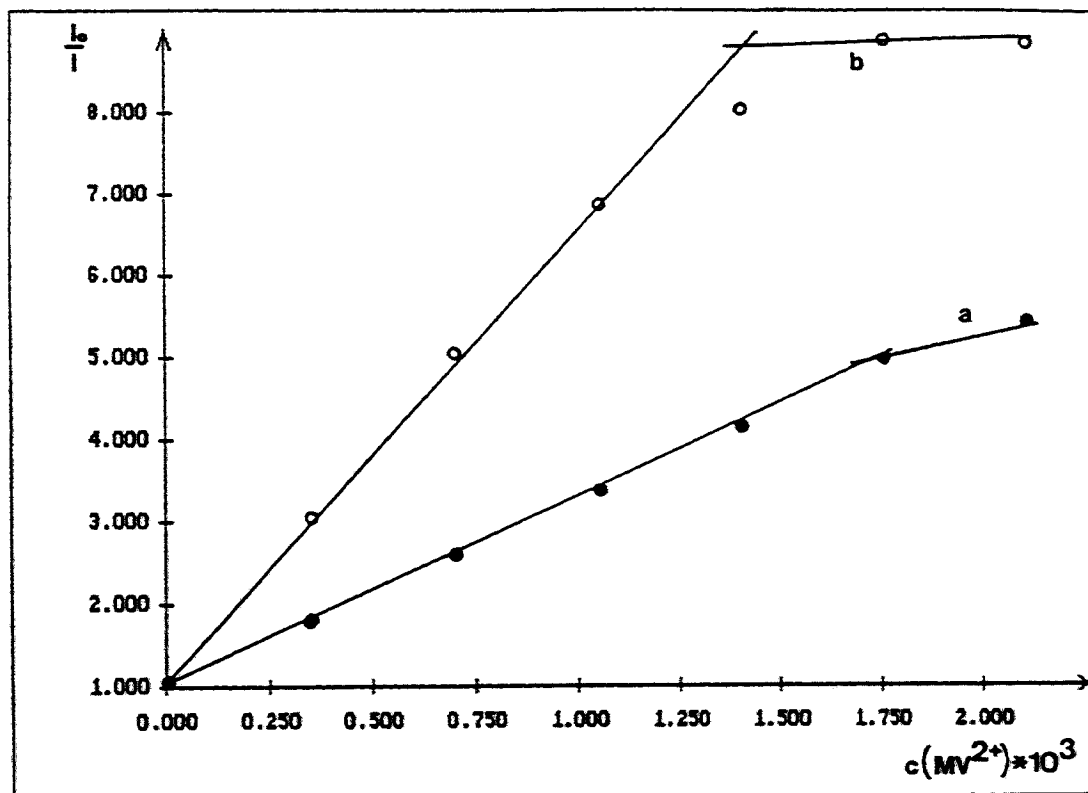


Figure 11. Stern-Volmer plots using the crown ether-ruthenium complexes 12 and 13 and the electron relay methylviologen. a)  $c(12) = 10^{-4}$  mol/l,  $c(\text{MV}^{2+}) = 0.230 \cdot 10^{-3}$  mol/l; b)  $c(13) = 10^{-4}$  mol/l,  $c(\text{MV}^{2+}) = 0.230 \cdot 10^{-3}$  mol/l.

and the bis-cationic electron relay, leading to a very rapid decrease in luminescence. With benzylviologen this effect is weaker because of enhanced steric demand. In contrast to these results, Ru complex 12 containing both relays shows nearly linear Stern-Volmer plots. The corresponding quenching constants are relatively low. These effects indicate that Ru complex 12 cannot bind the relays  $\text{MV}^{2+}$  and  $\text{BV}^{2+}$ , a conclusion supported by molecular models and force field calculations (see Fig. 10). The Stern-Volmer plots are shown in Figure 11.

No quenching of the excited states for methylviologen and benzylviologen was observed when the tris-homoleptic complexes 15 and 15 and the "reference compound" 17 were used as sensitizers. These complexes undergo reductive electron-transfer processes. Deactivation of the excited states in 15 and 16 can be effected by electron donors like TEOA. For the tris-homoleptic sensitizers a similar behavior is found for the absorption and emission properties, but the (reductive) quenching is hindered in the presence of crown ether groups.

## Summary:

1) New routes to efficient supramolecular sensitizers have been opened, resulting in Ru complexes with high or improved stability to photoanation. Geometrical parameters are decisive for the efficient realization of this concept.

2) A sensitizer-relay assembly has proven to be a powerful electron-transfer system not only for the production of H<sub>2</sub> but also methane.

3) Supramolecular crown ether-ruthenium sensitizers show interesting binding effects with respect to relays, suggesting a new approach to an efficient charge-separation step in electron transfer reactions.

Financial support from the BMFT is gratefully acknowledged, as is a Fonds Stipendium (St. B.) and LGFG support (H. K.).

## References

- [1] Energy Resources through Photochemistry and Catalysis, Edited by Grätzel, M., Academic Press, New York, 1987.
- [2] Juris, A., Barigoletti, F., Campagna, S., Balzani, V., Belser, P., von Zelewsky, A., *Coord. Chem. Rev.* 1988, 84, 85. Sutin, N., Creutz, C., *Pure Appl. Chem.* 1980, 52, 2717.
- [3] Harriman, A., Nahor, G., Mosseri, S., Neita, P., *J. Chem. Soc. Farad. Tr.* 1988, 84, 2821. Harriman, A., *J. Photochem.* 1985, 29, 139. Danverat, J., Douglas, P., Harriman, A., Porter, G., *Coord. Chem. Rev.* 1982, 44, 83.
- [4] Borgarello, E., Kiwi, J., Pelizzetti, E., Visca, M., Grätzel, M., *Nature* 1981, 289, 158. Lehn, J.-M., Sauvage, J.-P., Ziessel, R., *Nouv. J. Chim.* 1980, 4, 355. Lehn, J.-M., Sauvage, J.-P., Ziessel, R., *Nouv. J. Chim.* 1980, 4, 623.
- [5] Bock, C. R., Meyer, T. J., Whitten, D. G., *J. Am. Chem. Soc.* 1974, 96, 4710. Sasse, W., *Aust. J. Chem.* 1982, 35, 1341.
- [6] Houlding, V., Geiger, T., Kölle, U., Grätzel, M., *J. Chem. Soc. Chem. Commun.* 1982, 681. Lehn, J.-M., Sauvage, J.-P., Ziessel, R., *Nouv. J. Chim.* 1980, 4, 377.
- [7] Willner, I., Steinberger, B., ISES Solar World Congress, Hamburg, 1987. Kalyanasundaram, K., Kiwi, J., Grätzel, M., *Helv. Chim. Acta* 1978, 61, 2720. Kirsch, M., Lehn, J.-M., Sauvage, J.-P., *Helv. Chim. Acta* 1979, 62, 1345. Houlding, V., Geiger, T., Kölle, U., Grätzel, M., *J. Chem. Soc. Chem. Commun.* 1982, 681.
- [8] Harriman, A., Pickering, L., Thomas, J. M., *J. Chem. Soc. Farad. Tr. I* 1988, 84, 2795. Harriman, A., Thomas, J. M., Millward, G. R., *Nouv. J. Chim.* 1987, 11, 757. Kalyanasundaram, K., Grätzel, M., *Angew. Chem. Int. Ed. Engl.* 1979, 18, 701 [*Angew. Chem.* 1979, 91, 759].
- [9] Hennig, H., Rehorek, D., "Photochemische und Photokatalytische Reaktionen von Koordinationsverbindungen", Akademie Verlag, Berlin 1987. Case, F. H., *J. Am. Chem. Soc.* 1946, 68, 2574. Bos, K. D., Kraaijkamp, J. G., Noltes, J. G., *Synth. Comm.* 1979, 9, 497. Sprintschnik, G., Sprintschnik, H. W., Kirsch, P. P., Whitten, D. G., *J. Am. Chem. Soc.* 1977, 99, 4947. Dürr, H., Dörr, G., Braun, A., *Helv. Chim. Acta* 1983, 66, 2653. Dürr, H., Dörr, G., Zengerle, K., Mayer, E., *Nouv. J. Chim.*

- 1985, 66, 2653. Rotzinger, F. P., Munavalli, S., Comte, P., Hurst, J. K., Grätzel, M., Pern, F.-J., Frank, A. J., *J. Am. Chem. Soc.* 1987, 109, 6619.
- [10] Sargeson, A. M., *Chem. Br.* 1979, 15, 23. Sargeson, A. M., *Pure Appl. Chem.* 1984, 56, 1603.
- [11] Tazuke, S., Kitamura, N., *Pure Appl. Chem.* 1984, 56, 1296.
- [12] Alpha, B., Lehn, J.-M., Mathis, G., *Angew. Chem. Int. Ed. Engl.* 1987, 26, 6 [*Angew. Chem.* 1987, 99, 269]. Rodriguez-Ubis, J. C., Alpha, B., Plancherel, D., Lehn, J.-M., *Helv. Chim. Acta* 1984, 67, 2264. Lehn, J.-M. in *Supramolecular Photochemistry*, Edited by Balzani, V., Reidel, Dordrecht, The Netherlands, 1987; p. 29.
- [13] Barigeletti, F., De Cola, L., Balzani, V., Belsen, P., von Zelewsky, A., Vögtle, F., Ebmeyer, F., Grammenudi, S., *Angew. Chem. Int. Ed. Engl.* 1986, 25, 1122 [*Angew. Chem.* 1986, 98, 1119]. Beiser, P., De Cola, L., von Zelewsky, A., *J. Chem. Soc. Chem. Commun.* 1988, 1057.
- [14] Dürre, H., Zengerle, K., Trierweiler, H. P., *Z. Naturforsch.* 1988, 43B, 361.
- [15] Schwarz, R., Diplomarbeit, University of Saarbrücken 1989.
- [16] Crutchley, R. J., *Inorg. Chem.* 1961, 22, 4947.
- [17] Dürre, H., Thiery, U., Infelta, P. P., Braun, A. M., *Nouv. J. Chim.* 1989, 13, 575.
- [18] Willner, I., Maidan, R., Dürre, H., Dörr, G., Zengerle, K., *J. Am. Chem. Soc.* 1987, 109, 6080.
- [19] Trierweiler, H. P., Thesis, University of Saarbrücken 1989.
- [20] Willner, I., Mandler, D., Riklin, A. J., *J. Chem. Soc. Chem. Commun.* 1985, 1022.
- [21] Willner, I., Otvos, J. W., Calvin, M., *J. Am. Chem. Soc.* 1981, 103, 3203. Willner, I., Yang, J. M., Laane, C., Otvos, J. M., Calvin, M., *J. Phys. Chem.* 1981, 85, 3277. Frank, A. J., Willner, I., Goren, Z., Degani, Y., *J. Am. Chem. Soc.* 1987, 109, 3568.
- [22] Danielson, E., Elliot, C. M., Merkert, J. W., Meyer, T. J., *J. Am. Chem. Soc.* 1987, 109, 2519. Meyer, T. J., *Acc. Chem. Res.* 1989, 22, 163. Mayer, V. E., Shafirovich, V. Y., *IzK. Akad. Nauk. SSSR* 1989, 3, 700. Chambron, J. C., Sauvage, J.-P., *Tetrahedron Lett.* 1986, 27, 865. Collin, J. P., Guillerez, S., Sauvage, J.-P., *J. Chem. Soc. Chem. Commun.* 1989, 776.
- [23] Lehn, J.-M., *Angew. Chem. Int. Ed. Engl.* 1988, 27, 89 [*Angew. Chem.* 1988, 100, 91]. *Supramolecular Photochemistry*, Edited by Balzani, V., Reidel, D. Publ. Co., Dordrecht and Boston 1987.
- [24] Rebeck, J., Trend, J. F., Wattle, R. V., Charkravorti, S., *J. Am. Chem. Soc.* 1979, 101, 4333. Rebeck, J., Trend, J. F., *J. Am. Chem. Soc.* 1980, 102, 4853.
- [25] Wang, S.-S., Gisin, B. F., Winter, D. P., Makofske, R., Kulesha, I. D., Tzougraki, C., Meienhofer, J., *J. Org. Chem.* 1977, 42, 1286. Piepers, O., Kellogg, R. M., *J. Chem. Soc. Chem. Commun.* 1978, 383.
- [26] Kilburg, H., Thesis, University of Saarbrücken 1990. Dürre, H., Kilburg, H., Boßmann, S., *Synthesis* 1990, 773.

Forschungsgebiet:

- |  |  |
|--|--|
| <input type="checkbox"/> Solarthermik (Wärmeerzeugung) | <input type="checkbox"/> Windenergie                           |
| <input type="checkbox"/> Solarthermik (Stromerzeugung) | <input type="checkbox"/> Biomasse                              |
| <input type="checkbox"/> Speichertechnik               | <input type="checkbox"/> Kleinwasserkraftanlagen               |
| <input type="checkbox"/> Solararchitektur              | <input type="checkbox"/> Meeresenergie                         |
| <input type="checkbox"/> Fotovoltaik                   | <input checked="" type="checkbox"/> Fixierung von Kohlendioxid |

Thema des Projektes:

Synthese neuer Sensibilisatoren

Durchführende Stelle:

FB 13.2 Org. Chemie  
Universität des Saarlandes

Leiter:

Prof. Dr. H. Dürr

Beginn der Arbeiten: 1986

Ende der Arbeiten (voraussichtl.):  
1989

Fördermittel von:

BMFT

Projektbeschreibung:

Neben der photochemischen Wasserspaltung<sup>1)</sup> ist auch die Photoreduktion von Kohlendioxid als Teilschritt der artifiziellen Photosynthese von ständig steigendem Interesse.

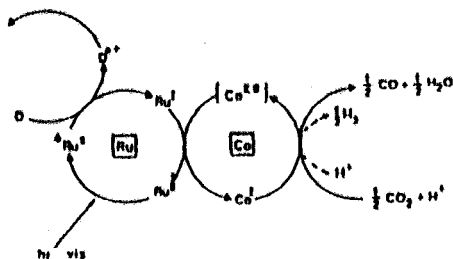
Kohlendioxid ist wie Wasser für sichtbares Licht transparent. Um Kohlendioxid photochemisch zu spalten ist daher ein Photosensibilisator notwendig, der die eingestrahlte Lichtenergie aufnimmt und über ein komplexes Redoxsystem (Elektronenrelais, Donor) letztlich die Kohlendioxidreduktion bewirkt<sup>2)</sup>.

Das Photoredoxsystem sollte zyklisch sein, damit alle Komponenten wieder in den Ausgangszustand zurückgeführt werden.

Neben Rutheniumkomplexen eignen sich auch Rheniumcarbonylkomplexe als Photosensibilisatoren<sup>2)</sup>.

Schema 1 zeigt einen photochemischen Reaktionszyklus auf der Basis von  $\text{Ru}(\text{bpy})_3\text{Cl}_2 = \text{Ru}(\text{II})$  als Photosensibilisator, der nach Anregung durch den Donor Triethanolamin = TEOA reduziert wird und

in einem nachgeschalteten thermischen Zyklus mit  $\text{Co}(\text{bpy})_3\text{Cl}_2$  =  $\text{Co}(\text{II})$  als Elektronenrelais wieder oxidiert wird. Die Reduktion von Kohlendioxid zu Kohlenmonoxid wird durch  $\text{Co}(\text{I})$  bewirkt.



Neben Kohlenmonoxid entsteht aus Wasser bei dieser Photoreduktion auch Wasserstoff; das Ausbeuteverhältnis  $\text{CO}/\text{H}_2$  kann durch Variation von Komplexliganden (Synthesziel) zugunsten von  $\text{CO}$  verschoben werden.

Ein von Lehn<sup>2)</sup> vorgestelltes System der Photoreduktion von Kohlendioxid verwendet  $\text{Re}(\text{CO})_3\text{bpyCl} = \text{Re}(\text{I})$  als Photosensibilisator. Neben Bpy = 2,2'-Bipyridin sollen auch andere von uns dargestellte Liganden (insbesondere Bisdiazinderivate) in den Komplex eingebaut werden:



- |                                      |                      |
|--------------------------------------|----------------------|
| 2,9-Dimethyl-1,10-phenanthrolin = 1; | 3,3'-Bipyridazin = 2 |
| 2,2'-Bipyrazin = 3;                  | 2,2'-Bipyrimidin = 4 |
| 4,5-Diazafluorenon = 5               |                      |

Die Liganden 2-5 wurden bereits von uns hergestellt. Zur Zeit überprüfen wir verschiedene publizierte Photoredoxsysteme um sie dann bezüglich ihrer Rentabilität einzuschätzen und gegebenenfalls verbessern zu können.

- 1) V. Balzani, L. Moggi, M. Manfrin, M. Gleria, Science, 189, 852 (1975).
- 2) J. Hawecker, J. M. Lehn, R. Ziessel, J. Chem. Soc., Chem. Commun., 536 (1983).

Forschungsgebiet:

- |                                   |                               |
|-----------------------------------|-------------------------------|
| ( ) Solarthermik (Wärmeerzeugung) | ( ) Windenergie               |
| ( ) Solarthermik (Stromerzeugung) | ( ) Biomasse                  |
| ( ) Speichertechnik               | ( ) Kleinwasserkraftanlagen   |
| ( ) Solararchitektur              | ( ) Meeresenergie             |
| ( ) Fotovoltaik                   | (X) photochem. Wasserspaltung |

Thema des Projektes:

Synthese neuer Sensibilisatoren

Durchführende Stelle:

FB 13.2 Org. Chemie  
Universität des Saarlandes

Leiter:

Prof. Dr. H. Dürr

Beginn der Arbeiten: 1986

Ende der Arbeiten (voraussichtl.):  
1989

Fördermittel von:

BMFT

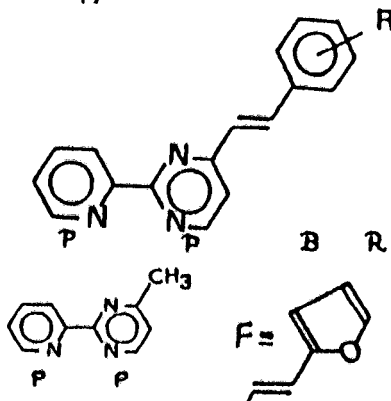
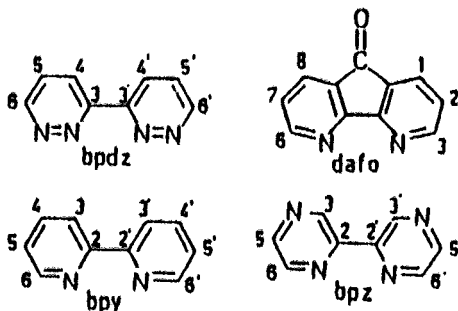
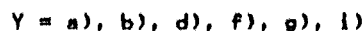
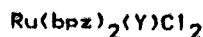
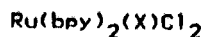
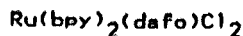
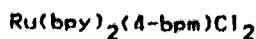
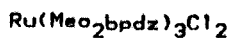
Projektbeschreibung:

Die zur Zeit bekannten Systeme zur photochemischen Wasserspaltung beinhalten einen Sensibilisator, der die Energie des eingestrahelten Lichtes zunächst aufnimmt und dann einen Elektronentransfer mit einem Elektronenrelais eingeht, neben Katalysatoren wie Platin und Rutheniumoxid an denen sich danach die eigentliche Wasserspaltung vollzieht. Der Reaktionsweg muß zyklisch geführt werden, um Sensibilisator und Elektronenrelais wieder in die Ausgangsform zu bringen.<sup>1)</sup> Die bisher bekannten Sensibilisatoren weisen unzureichende Quantenausbeuten und zu geringe Stabilitäten auf. Es ist daher notwendig neue Verbindungen zu synthetisieren und auf ihre Tauglichkeit als Sensibilisator zu untersuchen. In den letzten Jahren beschäftigten sich weltweit eine Reihe von Arbeitskreisen<sup>2)</sup> mit dieser Problematik und stellten neue Sensibilisatoren vor. Eine Verbesserung konnte jedoch nur in Teilbereichen erzielt werden, so daß die weiterführenden Forschungsar-



beiten sich damit befassen müssen Teilerfolge in einer Verbindung zu vereinen. Schwerpunkte stellen die Vergrößerung des Absorptionsbereiches, Optimierung des Redoxpotentials und die Verbesserung der Stabilität dar.

Im letzten Jahr wurden unter diesen Gesichtspunkten in unserem Arbeitskreis folgende Verbindungen synthetisiert:



1) K. Kalyanasundaram, M. Grätzel, Angew. Chem., 91, (1979) 759.

2) a) H. Dürr, G. Dürr, K. Zengerle, B. Reis, A.M. Braun, Chimia, 37, (1983) 245.

b) H. Dürr, G. Dürr, K. Zengerle, J.M. Curchod, A.M. Braun, Hel. Chim. Akta, 66, (1983) 2652.

c) H. Dürr, G. Dürr, K. Zengerle, E. Meyer, J.M. Curchod, A.M. Braun, Nouv. J. Chimie, 9, (1985).

Forschungsgebiet:

- |                                   |                               |
|-----------------------------------|-------------------------------|
| ( ) Solarthermik (Wärmeerzeugung) | ( ) Windenergie               |
| ( ) Solarthermik (Stromerzeugung) | ( ) Biomasse                  |
| ( ) Speichertechnik               | ( ) Kleinwasserkraftanlagen   |
| ( ) Solararchitektur              | ( ) Meeresenergie             |
| ( ) Fotovoltaik                   | (X) Photochem. Wasserspaltung |

Thema des Projektes:

Synthese neuer Sensibilisatoren zur O<sub>2</sub> Entwicklung

Durchführende Stelle:

FB 13.2. Org. Chemie  
Universität des Saarlandes

Leiter:

Prof. Dr. H. Dürr

Beginn der Arbeiten: 1986

Ende der Arbeiten (voraussichtl.):  
1989

Fördermittel von: BMFT

Projektbeschreibung:

Die photochemische Wasserspaltung ist zur Energieerzeugung nur dann interessant, wenn gleichzeitig Wasserstoff und Sauerstoff produziert werden. Bisher war der Zweig der Wasserstoffentwicklung Gegenstand intensiver Forschung.

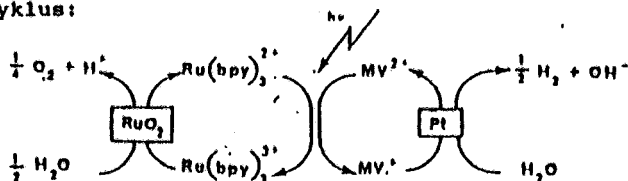
Photosensibilisatoren, die in der Regel Rutheniumkomplexe des Typs  $RuL_3Cl_2$  (L=Ligand mit Ferriinstruktur) sind, absorbieren die eingestrahlte Energie und treten in einen komplizierten Redoxprozeß ein, an dessen Ende die Wasserstoffentwicklung steht. Um diesen Prozeß zyklisch zu gestalten, arbeitete man bislang in sogenannten sakrifiziellen Systemen. Dabei überträgt der Sensibilisator Elektronen auf die Protonen (H<sub>2</sub>-Entwicklung) und wird in einem anschließenden Reduktionsschritt von einem irreversibel oxidierten Elektronendonator reduziert.

Sakrifizielle Systeme sind wirtschaftlich uninteressant, da

teuere Elektronendonatoren eingesetzt werden.

Deshalb wird zunehmend die Oxidation des im Wasser gebundenen Sauerstoffs zur Schließung des Zyklus diskutiert.

Der Sauerstoff des Wassers soll an geeigneten Katalysatormaterialien den Elektronentransfer zum Sensibilisator vollziehen. Das nachfolgende Schema zeigt den angestrebten vollständigen Zyklus:



Ein in der Literatur ( ) beschriebener Katalysator ist das  $\text{RuO}_2$ . Lehn konnte mit dieser Substanz schon eine Sauerstoffentwicklung durchführen.

Steigendes Interesse gewinnen homogene Katalysatoren auf der Basis zweikerniger Rutheniumkomplexe vom Typ  $\text{Ru}_2\text{LL}'_4$ . Photosensibilisatoren mit unterschiedlichen Liganden werden im sakrifiziellen System schon seit einiger Zeit in unserer Arbeitsgruppe untersucht. Sie sollen nun mit  $\text{RuO}_2$ -Katalysatoren auch auf ihre Verwendbarkeit im vollzyklischen System getestet werden. Mit der Synthese zweikerniger Rutheniumkomplexe als Katalysatoren zur  $\text{O}_2$ -Entwicklung ist bereits begonnen worden.

#### Literatur:

- (1) M.Grätzel, J.McLendon, J.Phys.Chem., **86**, (1982), 944
- (2) H.Dürr, A.M.Braun, G.Dörr, B.Reis, K.Zengerle, *Chimia* **17**, (1983), 245
- (3) J.M.Lehn, R.Ziessel, Proc.Nat.Acad.Sci. USA, **79**(1982), 707

be confirmed by emergence of the u.v. absorption peak at 243 nm in the  $\text{CH}_2\text{Cl}_2$  layer. Moreover,  $\text{Pt}^{\text{II}}$  can be *selectively* extracted at pH 3 from a mixture of  $\text{Pt}^{\text{II}}$ ,  $\text{Cu}^{\text{II}}$ , and  $\text{Ni}^{\text{II}}$  using our system (see Run 12 in Table 1). This is due to the more favourable deprotonation of amide nitrogens in forming  $[\text{Pt}^{\text{II}}\text{L}]^0$  than in forming other metal-dioxocyclam complexes where the deprotonation pH's are observed to be higher:  $\text{Cu}^{\text{II}}$ , pH 5–6;  $\text{Ni}^{\text{II}}$ , pH 8–9. It is shown in Run 13, Table 1, that the  $\text{Pt}^{\text{II}}$  ion is transferred from the aqueous solution of  $\text{Pt}^{\text{II}}$ -glycylglycylglycine (prepared by the method of Margerum<sup>6</sup>) to the  $\text{CH}_2\text{Cl}_2$  solution containing dioxocyclam (1b). The  $\text{Pt}^{\text{II}}$ -macrocyclic complex (2) should be thermodynamically more stable than the  $\text{Pt}^{\text{II}}$ -linear-glycylglycylglycine complex. This may suggest that the macrocyclic ligands (1) are potentially useful as a drug for excretion of  $\text{Pt}^{\text{II}}$  which is accumulated in the body as  $\text{Pt}^{\text{II}}$ -peptide complexes. Platinum(II) complexed with a ten fold excess of adenine, guanine, thymine, or cytosine can also be extracted (more than 50%) with (1b) at pH 7, indicating that nucleic acid-bound  $\text{Pt}^{\text{II}}$  can be removed by our method. Finally, it is to be noted that the lipophilic cyclam [(1b)-analogue with reduced amides] is ineffective for selective extraction of  $\text{Pt}^{\text{II}}$ .

The efficiency and selectivity of (1) for  $\text{Pt}^{\text{II}}$  also demonstrate

the potential usefulness of macrocyclic oxopolyamines in analytical and mineralogical applications.

Received, 11th April 1986; Com. 477

### References

- (a) B. Rosenberg, 'Metal Ions in Biological Systems,' ed. H. Sigel, Marcel Dekker, New York, 1980, vol. 11, pp. 127–196; (b) M. J. Cleare and P. C. Hydes, *ibid.*, pp. 1–62; (c) M. E. Howe-Grant and S. J. Lippard, *ibid.*, pp. 63–125.
- Review article; E. Kimura, *J. Coord. Chem.*, 1986, 15, 1.
- (a) M. Kodama and E. Kimura, *J. Chem. Soc., Dalton Trans.*, 1979, 325; (b) p. 1783; (c) 1981, 694.
- R. Machida, E. Kimura, and M. Kodama, *Inorg. Chem.*, 1983, 22, 2055.
- E. Kimura and R. Machida, unpublished results.
- G. E. Kirvan and D. W. Margerum, *Inorg. Chem.*, 1985, 24, 3017.
- D. F. Evans, *J. Chem. Soc.*, 1959, 2003.
- F. A. Cotton and G. Wilkinson, 'Advanced Inorganic Chemistry,' Fourth Edition, Wiley, New York, 1980, pp. 951ff.
- E. Kimura, C. A. Dalimunte, A. Yamashita, and R. Machida, *J. Chem. Soc., Chem. Commun.*, 1985, 1041.
- M. Di Case, L. Fabbri, A. Perotti, A. Poggi, and P. Tundo, *Inorg. Chem.*, 1985, 24, 1610.

## Photoinduced Carbon Dioxide Fixation forming Malic and Isocitric Acid

Itamar Willner,\* Daniel Mandler, and Azalia Riklin

Department of Organic Chemistry, The Hebrew University of Jerusalem, Jerusalem 91904, Israel

Photoinduced  $\text{CO}_2$ -fixation into organic substrates is accomplished *via* enzyme-catalysed reactions.

Carbon dioxide fixation into the form of organic compounds is a major challenge of chemistry. Of particular interest is visible-light induced  $\text{CO}_2$  fixation as a means of mimicking natural photosynthesis. Photosensitized NADPH regeneration cycles can be utilized in  $\text{CO}_2$  fixation to form malic and isocitric acid. Photosensitized  $\text{CO}_2$ -fixation into organic compounds such as formic and oxalic acid has been reported recently. In these reports semiconductors<sup>1–4</sup> or homogeneous catalysts<sup>5,6</sup> mediate  $\text{CO}_2$  reduction. The specificity and efficiency of these processes is limited. The photoinduced fixation of  $\text{CO}_2$  to formic acid has also been reported using a semiconductor-enzyme catalysed system.<sup>7</sup> We have recently reported<sup>8</sup> on the enzyme catalysed photosensitized regeneration of NADPH. In this system photogenerated methylviologen radical,  $\text{MV}^{\cdot+}$ , mediates the reduction of  $\text{NADP}^+$  to NADPH in the presence of ferredoxin-NADP<sup>+</sup> reductase (E.C. 1.18.1.2).

Here we report successful  $\text{CO}_2$  fixation forming malic acid (1) and isocitric acid (2), using NADPH dependent enzymes coupled to the photosensitized NADPH regeneration system. The system for malic acid formation is composed of an aqueous solution (4.2 ml; Tris buffer, 0.2 M; pH 8.0) that includes trisbipyridineruthenium,  $\text{Ru}(\text{bpy})_3^{2+}$  ( $2.1 \times 10^{-5}$  M) as sensitizer, methyl viologen,  $\text{MV}^{2+}$  ( $1.9 \times 10^{-4}$  M), as primary electron acceptor,  $\text{NADP}^+$  ( $1.8 \times 10^{-4}$  M),  $\text{MnCl}_2$  ( $9.5 \times 10^{-5}$  M),  $\text{NaHCO}_3$  (0.2 M), pyruvic acid ( $4.7 \times 10^{-2}$  M), and the electron donor mercaptoethanol ( $1.9 \times 10^{-2}$  M, initial

concentration). Two enzymes are included in the system: ferredoxin-NADP<sup>+</sup> reductase (FDR, E.C. 1.18.1.2, 0.2 Units) and the malic enzyme (E.C. 1.1.1.40, 1.33 Units). Illumination of this system ( $\lambda > 400$  nm) under a  $\text{CO}_2$  atmosphere (1.01 atm) results in the formation of malic acid (1).

The rate of malic acid formation as a function of illumination time was followed by h.p.l.c. [Figure 1(A)]. In the absence of malic enzyme no malic acid was formed and NADPH accumulated in the system as a photoproduct. Introduction of the malic enzyme resulted in the disappearance of NADPH and formation of (1).

In view of our previous observations,<sup>8</sup> we suggest the schematic cycle outlined in Figure 2 as the multi-step process leading to the formation of malic acid. The primary photochemical process involves the photosensitized reduction of  $\text{MV}^{2+}$  by the electron donor using  $\text{Ru}(\text{bpy})_3^{2+}$  as sensitizer. The characterization of the photosensitized reduction of viologens by various sensitizers such as  $\text{Ru}(\text{bpy})_3^{2+}$  or Zn-porphyrins has been established in numerous studies.<sup>9,10</sup> The subsequent reaction involves the enzyme catalysed reduction of  $\text{NADP}^+$  by  $\text{MV}^{\cdot+}$  to form NADPH.  $\text{NADP}^+$  can be reduced by two alternative routes:<sup>11</sup> a single-electron-transfer reduction ( $E^\circ = 0.85$  V vs. normal hydrogen electrode, N.H.E.) that leads to  $\text{NAD}^{\cdot}$  which can undergo dimerization to a biologically inactive reduction product,<sup>11,12</sup> or hydride reduction to form the biologically active NADPH

Table 1. Turnover numbers of components involved in the CO<sub>2</sub> fixation processes.

	Ru(bpy) <sub>3</sub> <sup>2+</sup>	MV <sup>2+</sup>	NADP <sup>+</sup>	FDR <sup>a</sup>	Malic enzyme <sup>b</sup>	ICDH <sup>c</sup>	% Conversion
Malic acid	1074	117	62.2	2.5 × 10 <sup>4</sup>	7.4 × 10 <sup>5</sup>		24
Isocitric acid	272	23	11.4	2.5 × 10 <sup>3</sup>		5.5 × 10 <sup>4</sup>	4.6

<sup>a</sup> M<sub>t</sub> = 40 000; cf.: M. Shin, *Methods Enzymol.*, 1971, 23, 441. <sup>b</sup> M<sub>t</sub> = 280 000; cf.: R. Y. Hsu and H. A. Lardy, *J. Biol. Chem.*, 1967, 242, 520. <sup>c</sup> M<sub>t</sub> = 58 000; cf.: R. F. Colman, *J. Biol. Chem.*, 1968, 243, 2454.

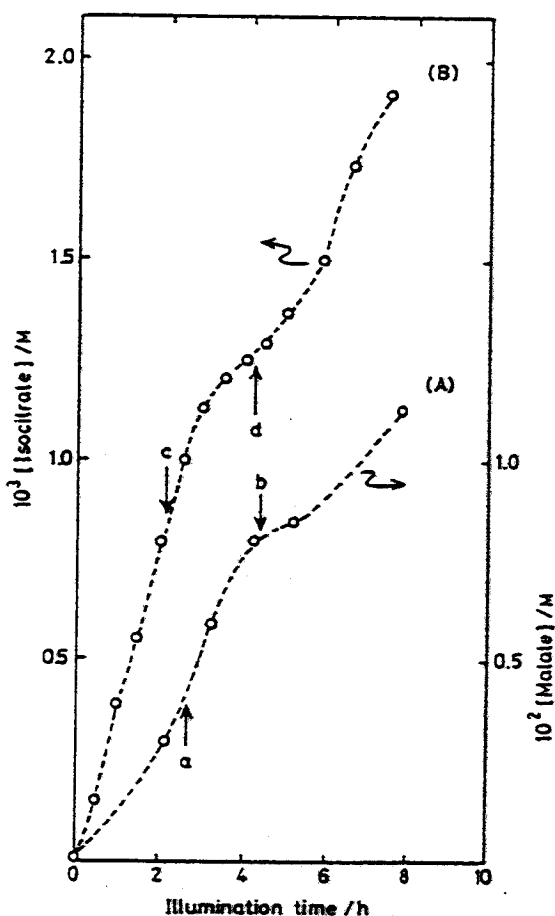


Figure 1. Rate of CO<sub>2</sub> fixation as a function of illumination time. (A) Pyruvic acid: a, addition of mercaptoethanol (2.2 × 10<sup>-2</sup> M); b, addition of mercaptoethanol (2.7 × 10<sup>-2</sup> M); (B) oxoglutaric acid: c and d addition of DTT (5 × 10<sup>-3</sup> M).

(E° = 0.32 V vs. N.H.E.). Previous studies have indicated that hydride compounds such as NaBH<sub>4</sub><sup>11</sup> or hydrido-Rh complexes<sup>13,14</sup> are capable of reducing NADP<sup>+</sup> to NADPH via the second route. Other reports have shown<sup>15,16</sup> that the enzyme FDR catalyses the reduction of NADP<sup>+</sup> by MV<sup>2+</sup>. Since MV<sup>2+</sup> is thermodynamically unable to reduce NADP<sup>+</sup> to its radical (E° = 0.44 V vs. N.H.E.), we presume that the process is accomplished via a hydride intermediate formed at the active site of the enzyme. The photoproduct NADPH mediates the fixation of CO<sub>2</sub> into pyruvic acid forming malic acid in the presence of the malic enzyme, and NADP<sup>+</sup> is recycled for the photochemical reaction.

The net reaction accomplished in this system corresponds to CO<sub>2</sub> fixation into pyruvic acid using mercaptoethanol as electron donor (equation 1). The thermodynamic balance of this reaction shows that it is endoenergetic by ca. 11.5 kcal per mole of mercaptoethanol consumed (1 cal = 4.184 J).

The system for the photogeneration of isocitric acid (2) is composed of an aqueous solution (4.2 ml; Tris buffer, 0.2 M; pH 7.2) that includes Ru(bpy)<sub>3</sub><sup>2+</sup> (1.4 × 10<sup>-5</sup> M), NaHCO<sub>3</sub> (0.17 M), oxoglutaric acid (4.15 × 10<sup>-2</sup> M), D,L-dithiothreitol (DTT, 8.3 × 10<sup>-3</sup> M initial concentration) as electron donor, and the two enzymes ferredoxin-NADP<sup>+</sup> reductase (FDR, E.C. 1.18.1.2, 0.2 Units) and isocitrate dehydrogenase (ICDH, E.C. 1.1.1.42, 0.47 Units immobilized on PAN<sup>17</sup>).

Illumination of this system (λ > 420 nm) under an atmosphere of CO<sub>2</sub> (1.08 atm) results in the fixation of CO<sub>2</sub> into oxoglutaric acid and formation of isocitric acid (2). The rate of isocitrate formation as a function of illumination time is shown in Figure 1(B).

Control experiments reveal that all components are required in the system. The sequence of reactions that lead to the formation of isocitric acid are summarized in Figure 2 and involve the utilization of photogenerated NADPH in the fixation of CO<sub>2</sub> into oxoglutaric acid in the presence of isocitrate dehydrogenase. The net reaction forming (2) corresponds to the light-induced fixation of CO<sub>2</sub> into oxoglutaric acid using D,L-dithiothreitol (DTT) as electron donor (equation 2). The thermodynamic balance of this process is approximately zero. [E° (DTT) -0.3 V vs. N.H.E.]

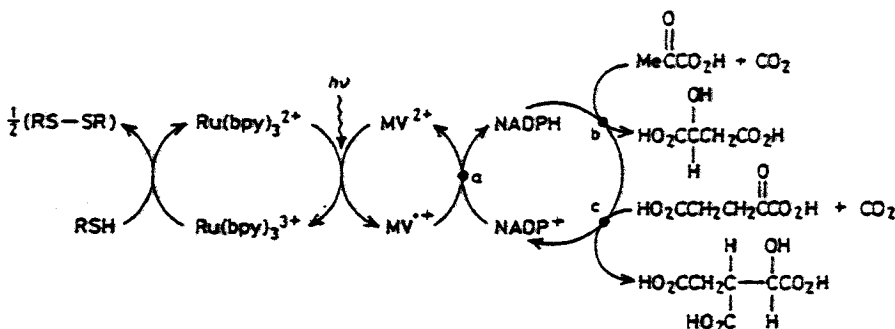
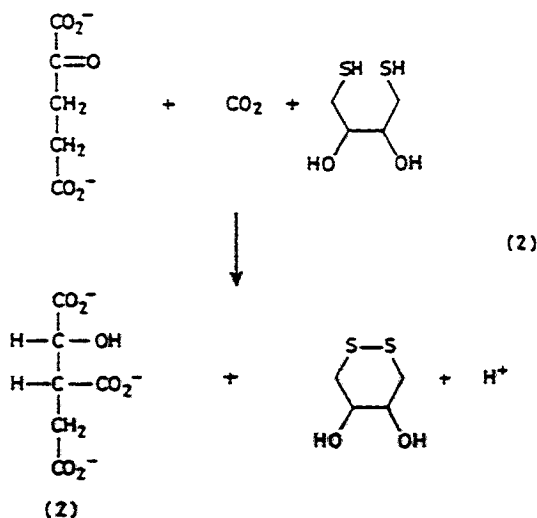
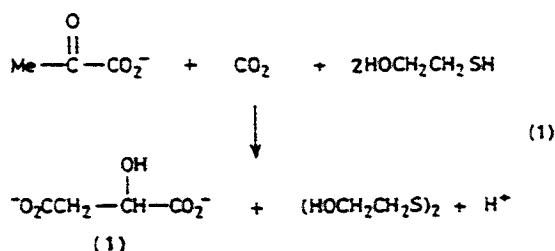


Figure 2. Cyclic scheme for the photoinduced regeneration of NADPH and CO<sub>2</sub> fixation into keto acids. a, Ferredoxin-NADP<sup>+</sup> reductase; b, malic enzyme; c, isocitrate dehydrogenase.



The stability of the different components involved in the formation of (1) and (2) was examined and the turnover numbers of the different components are summarized in Table 1. These data correspond to 24% conversion of pyruvic acid into (1) and 4.6% conversion of oxoglutaric acid into (2).

It should be noted that in the two processes the efficiency of NADPH production must be tuned to a low level since the  $\text{CO}_2$  fixation reactions are the rate determining steps.

Accumulation of NADPH results in substantial decomposition of this ingredient.

In conclusion, we have accomplished the enzyme catalysed fixation of  $\text{CO}_2$  into organic substrates using the photosensitized NADPH regeneration cycle. One of these processes is endoenergetic and represents a process that converts light energy into chemical potential.

We thank the Belfer Center for Energy Research for support.

Received, 29th November 1985; Com. 1693

## References

- 1 B. Aurian-Blajeni, M. Halman, and J. Manassen, *Solar Energy*, 1980, 25, 165.
- 2 M. Halman, *Nature (London)*, 1978, 275, 115.
- 3 T. Inoue, A. Fujishima, S. Konishi, and K. Honda, *Nature (London)*, 1979, 277, 637.
- 4 N. G. Bradley, T. Tysak, D. J. Graves, and N. A. Vlachopoulos, *J. Chem. Soc., Chem. Commun.*, 1983, 349.
- 5 R. Ziessel, *Nouv. J. Chem.*, 1983, 7, 613.
- 6 J. Hawecker, J.-M. Lehn, and R. Ziessel, *J. Chem. Soc., Chem. Commun.*, 1985, 56.
- 7 B. A. Parkinson and P. F. Weaver, *Nature (London)*, 1984, 148.
- 8 D. Mandler and I. Willner, *J. Am. Chem. Soc.*, 1984, 106, 5352.
- 9 J. R. Kalyasundaram, *Coord. Chem. Rev.*, 1982, 46, 159.
- 10 J. R. Darwent, P. Douglas, A. Harriman, G. Porter, and M.-C. Richoux, *Coord. Chem. Rev.*, 1982, 44, 83.
- 11 P. Hemmerich, H. Michel, C. Schug, and V. Massey, *Struct. Bonding (Berlin)*, 1982, 48, 93.
- 12 C. O. Schmackel, K. S. V. Santhanam, and P. J. Elving, *J. Am. Chem. Soc.*, 1975, 97, 5083.
- 13 R. Weinkamp and E. Steckham, *Angew. Chem., Int. Ed. Engl.*, 1983, 22, 497.
- 14 P. Cuendet and M. Grätzel, *Photochem. Photobiol.*, 1984, 39, 609.
- 15 D. J. Day, S. J. Kinsey, E. T. Ses. N. Weliky, and H. P. Silverman, *Trans. N.Y. Acad. Sci.*, 1972, 587.
- 16 M. Ito and T. Kuwana, *J. Electroanal. Chem.*, 1971, 32, 415.
- 17 The enzyme was immobilized by the procedure of A. Pollack, H. Blumenfeld, M. Wax, R. L. Baughn, and G. M. Whitesides, *J. Am. Chem. Soc.*, 1980, 102, 6324. Without immobilization the enzyme is destroyed under the experimental conditions.

## Recognition of the *threo* and *erythro* Isomers of 1-C-Substituted Glycerols†

El Sayed H. El Ashry‡

Chemistry Department, Faculty of Science, Alexandria University, Alexandria, Egypt

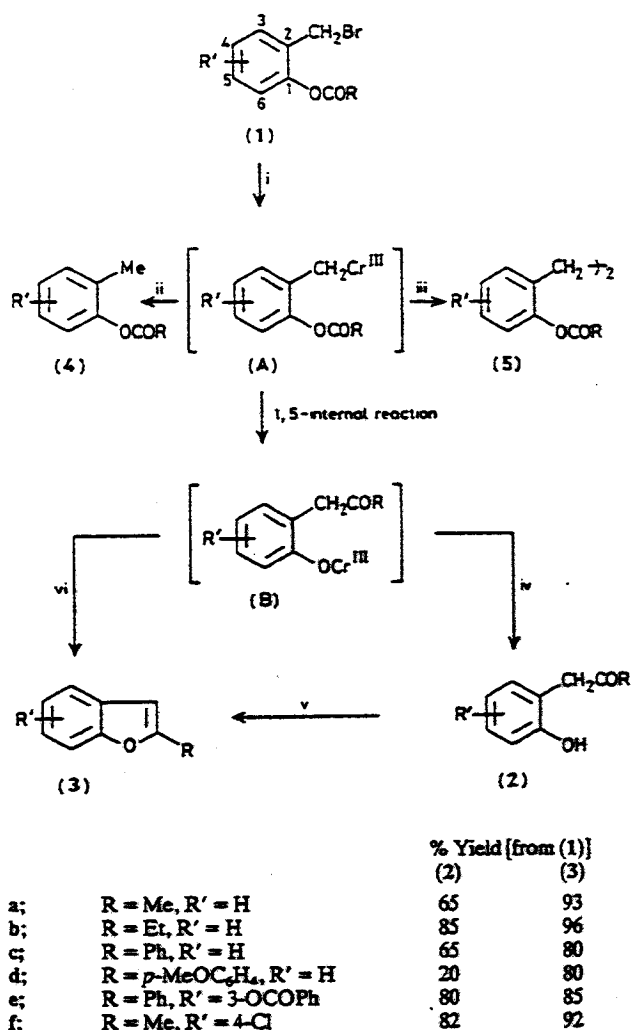
A method for the differentiation of the *threo* and *erythro* isomers of 1-C-substituted glycerols has been developed, based on the difference in the chemical shift ( $\Delta\delta$ ) between the proton resonances of the two methyl groups of the corresponding isopropylidene as a criterion of the location of the isopropylidene group on a polyol residue, as well as the regioselective formation of the isopropylidene.

A method has been developed to recognise the configuration of hydroxy groups, whether *threo* or *erythro*, in 1-C-

substituted glycerols which may form a part of acyclic sugar derivatives or acyclic nucleosides. The method was based on (i) the difference in the chemical shift ( $\Delta\delta$ ) between the  $^1\text{H}$  n.m.r. signals for two methyl groups of an isopropylidene group, which has been found to be a criterion for its location on a polyol residue, and (ii) the regioselectivity of the isopropylidene<sup>1-5</sup> under thermodynamic control of various 1-C-substituted glycerols.

† For part 1 in the series 'Acetals,' see ref. 1.

‡ Address during 1986-87: Chemistry Department, Faculty of Applied Sciences and Engineering, Umm Alquara University, Makkah, P.O. 3711, Saudi Arabia.



Scheme 1. Reagents: i, 2 CrCl<sub>2</sub>; ii, H<sub>2</sub>O; iii, (1); iv, H<sub>2</sub>O, NH<sub>4</sub>Cl; v, AcOH-HCl, heat, -H<sub>2</sub>O; vi, Et<sub>2</sub>O-BF<sub>3</sub>, heat, -HOCr<sup>III</sup>.

Unavoidable losses of (2), especially (2d), occurred during isolation-purification, by conversion into (3) in solution and even in the dry state but much more slowly.

mmol), (2) were obtained in good yields. On the other hand the direct conversion of (1) into (3) could be realized when the reduction was performed in the presence of a Lewis acid, the method for preparation of (2) being modified by addition of Et<sub>2</sub>O-BF<sub>3</sub> (1.25 mmol) to the reducing reagent.

Since similar conversions could not be accomplished with other usual reducing reagents (Mg, Zn, Al), the present methodology therefore constitutes a good route to the unmasked (2) and a new access to (3) from the readily available benzylic bromides (1)<sup>3</sup> and an inexpensive Cr<sup>III</sup> salt.<sup>10</sup>

We thank the Agence Nationale de Valorisation de la Recherche for financial support.

Received, 1st October 1985; Com. 1419

#### References

- H. Muth and M. Sauerbier, 'Methoden der Organische Chemie Houben-Weyl,' G. Thieme Verlag, Stuttgart-New York, 1981, vol. IV-1d, p. 506; see also R. P. A. Sneeden, 'Organochromium Compounds,' Academic Press, New York, 1975.
- D. Stephan, A. Gorgues, and A. Le Coq, *Tetrahedron Lett.*, 1984, 25, 5649 and ref. cited.
- A. Hercouet and M. Le Corre, *Tetrahedron*, 1981, 37, 2867; see also M. Le Corre, *Jarssen Chim. Acta*, 1985, 3, 4.
- (a) J. W. Schulenberg and S. Archer, *J. Am. Chem. Soc.*, 1960, 82, 2035; (b) R. Royer and E. Bisagni, *Bull. Soc. Chim. Fr.*, 1960, 395.
- Y. Okude, S. Hirano, T. Hiyama, and H. Nozaki, *J. Am. Chem. Soc.*, 1977, 99, 3179.
- For some papers involving OH-blocked derivatives of (2), see: L. Christiaens and H. Renson, *Bull. Soc. Chim. Belg.*, 1970, 79, 235; R. E. Moengkramer and H. Zimmer, *J. Org. Chem.*, 1980, 45, 3994; R. Beugelmans and H. Ginsburg, *J. Chem. Soc., Chem. Commun.*, 1980, 508.
- R. Royer, *Acta Chim. Therap.*, 1975, 3, 3.
- P. Cagniant and D. Cagniant, *Adv. Heterocycl. Chem.*, 1975, 18, 337; A. Mustapha, 'Benzofurans,' vol. 29 in 'Chemistry of Heterocyclic Compounds,' Wiley-Interscience, London, 1974.
- F. Delbecq, R. Baudouy, and J. Goré, *Nouv. J. Chim.*, 1979, 3, 321.
- Instead of the expensive CrCl<sub>2</sub> (Merck) or of the Hiyama's reagent, we used the crude salt (80–85% Cr<sup>II</sup> content) simply obtained after dissolution of Cr powder into aq. HCl, slow evaporation of the water and then dehydration, through a progressive heating from 40 to 160 °C *in vacuo*, according to W. A. Knight and E. M. Rich, *J. Chem. Soc.*, 1911, 87.

## Photodecomposition of Formic Acid by Cadmium Sulphide Semiconductor Particles

Itamar Willner\* and Zafir Goren

Department of Organic Chemistry, The Hebrew University of Jerusalem, Jerusalem 91904, Israel

CdS semiconductor particles induce the photodecomposition of formate; photogenerated Cd metal acts as an H<sub>2</sub> evolution catalyst.

Formic acid is formed by certain plants and can be obtained by alkaline hydrolysis of glucose. It is considered to be a valuable hydrogen carrier,<sup>1</sup> and various hydrogenation processes have utilized this product as hydrogen donor.<sup>2</sup> The decomposition of formic acid [equation (1)] is exoenergetic by  $\Delta G^\circ = ca. -38.5$  kJ mol<sup>-1</sup> and is accomplished by the use of Pd-carbon

catalysts.<sup>3</sup> The photo-Kolbe reaction has been induced by various platinumized semiconductor particles.<sup>4,5</sup> Recently, the photodecomposition of formic acid to hydrogen and CO<sub>2</sub> has been reported using a homogeneous porphyrin photosensitizer.<sup>6</sup> Here we report on the photocatalysed decomposition of formic acid by CdS semiconductor particles.

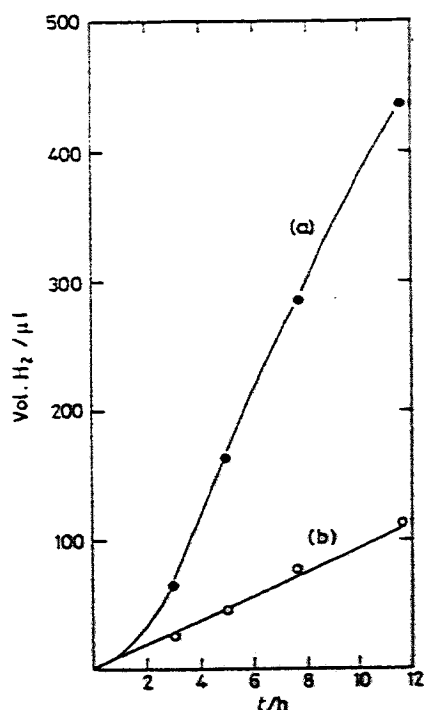


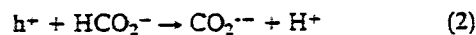
Figure 1. Photodecomposition of formic acid by CdS: H<sub>2</sub> evolution as a function of illumination time at pH 6.4: (a) HCO<sub>2</sub><sup>-</sup>, H<sub>2</sub>O; (b) DCO<sub>2</sub><sup>-</sup>, H<sub>2</sub>O.



The system is composed of an aqueous suspension (pH 6.4) that includes CdS powder (20 mg) and potassium formate (0.5 M). Illumination of the deaerated system with visible light,  $\lambda > 400$  nm, results in the decomposition of formate to H<sub>2</sub> and CO<sub>2</sub>. The rate of H<sub>2</sub> evolution as a function of illumination time is displayed in Figure 1.† Recently, we applied<sup>7</sup> Pt-coated CdS particles for the photodecomposition of H<sub>2</sub>S. We have shown that 'in situ' photogenerated H<sub>2</sub> can be utilized for hydrogenation of ethylene or acetylene with elimination of H<sub>2</sub> evolution. Introduction of Pt-CdS particles<sup>7</sup> into the formate system results upon illumination in H<sub>2</sub> evolution with efficiency similar to that obtained with unplatized CdS particles. Thus, no Pt catalyst is needed for the photodecomposition of formate with CdS particles. When acetylene is introduced as the gaseous atmosphere in the presence of Pt-CdS particles, the major product is H<sub>2</sub> and only traces of ethylene are obtained. These results imply that the hydrogenation process is inhibited in the presence of formate and that 'in situ' H<sub>2</sub> is scarcely formed on the Pt catalyst.

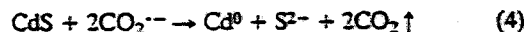
To account for the photodecomposition of formate by CdS semiconductor particles we have performed the reaction using DCO<sub>2</sub><sup>-</sup>-K<sup>+</sup> as substrate in H<sub>2</sub>O. We find that the major product (> 90%) is H<sub>2</sub>. The rate of H<sub>2</sub>-evolution using [H]formate as substrate is shown in Figure 1(b). It can be seen that the rate of H<sub>2</sub> evolution is substantially decreased

( $k_{\text{H}}/k_{\text{D}} = 5.1$ ). These results allow us to conclude that the oxidation of formate by the semiconductor photogenerated holes [equation (2)] is the rate limiting process in H<sub>2</sub>-evolution [equation (3)]. Furthermore, the results show that the source of the evolved H<sub>2</sub> is water rather than the formate-linked hydrogen.



Recent studies have shown that the photo-decarboxylation of acetic acid with semiconductor particles can proceed by two alternative mechanisms, depending on the pH of the aqueous medium: (i) homolytic decarboxylation<sup>4</sup> that yields methane, ethane, and CO<sub>2</sub>; (ii) oxidative decarboxylation,<sup>5</sup> that yields methanol and CO<sub>2</sub>. Since H<sub>2</sub> is the major product with DCO<sub>2</sub><sup>-</sup> as substrate, the oxidative pathway outlined in equation (2) is supported.

Finally, the fact that Pt does not affect the H<sub>2</sub> evolution yield and the lack of hydrogenation products in the presence of acetylene, are attributed to the 'in situ' formation of Cd metal in the photodecomposition of formate. The oxidized product, CO<sub>2</sub><sup>-</sup>, is a powerful reductant ( $E^\circ -0.97$  V)<sup>6</sup> capable of reducing CdS [equation (4)]. Indeed, upon illumination of CdS in the presence of formate, the yellow CdS powder adopts a grey tint suggesting that the powder is coated by Cd metal. This Cd metal offers an effective catalyst for H<sub>2</sub>-evolution,<sup>10</sup> though the catalysed hydrogenation is eliminated.



In conclusion, we have demonstrated that CdS semiconductor particles induce the photodecomposition of formate without added catalyst, and that photogenerated Cd metal offers a catalytic site for H<sub>2</sub> evolution. Application of other semiconductor particles for photodecomposition of formate and other hydrogen donors is under way in our laboratory.

This research was supported by the Israel Research and Development Council and by the Kernforschung Stiftung Juelich, Germany.

Received, 21st October 1985; Com. 1499

#### References

- 1 A. M. Klibanov, B. N. Alberti, and S. E. Zale, *Biotechnol. Bioeng.*, 1982, 26, 25.
- 2 H. B. Hart, *Nature (London)*, 1979, 277, 15.
- 3 R. Williams, R. S. Crandall, and A. Bloom, *Appl. Phys. Lett.*, 1978, 33, 381.
- 4 B. Krautler and A. J. Bard, *J. Am. Chem. Soc.*, 1978, 100, 2239, 5989.
- 5 S. Sato, *J. Chem. Soc., Chem. Commun.*, 1982, 26.
- 6 A. Harriman and M. C. Richoux, *J. Photochem.*, 1984, 27, 205.
- 7 A. J. Frank, Z. Goren, and I. Willner, *J. Chem. Soc., Chem. Commun.*, 1985, 1029.
- 8 T. Sakata, T. Kawai, and K. Hashimoto, *J. Phys. Chem.*, 1984, 88, 2344.
- 9 J. F. Endicott, in 'Concepts of Inorganic Photochemistry,' eds. A. W. Adamson and P. D. Fleischauer, Wiley-Interscience, New York, 1975, p. 81.
- 10 A. Henglein, B. Lindig, and J. Westerhausen, *J. Phys. Chem.*, 1981, 85, 1627.

† H<sub>2</sub> analysis was performed by gas chromatography using an M.S. 5Å column, with argon as carrier gas at 30 °C.



# Photosensitized Electron-Transfer Reactions in $\beta$ -Cyclodextrin Aqueous Media: Effects on Dissociation of Ground-State Complexes, Charge Separation, and H<sub>2</sub> Evolution

Eti Adar, Yinon Degani, Zafrir Goren, and Itamar Willner\*

Contribution from the Department of Organic Chemistry and The Fritz Haber Center for Molecular Research, The Hebrew University of Jerusalem, Jerusalem 91904, Israel.  
Received December 23, 1985

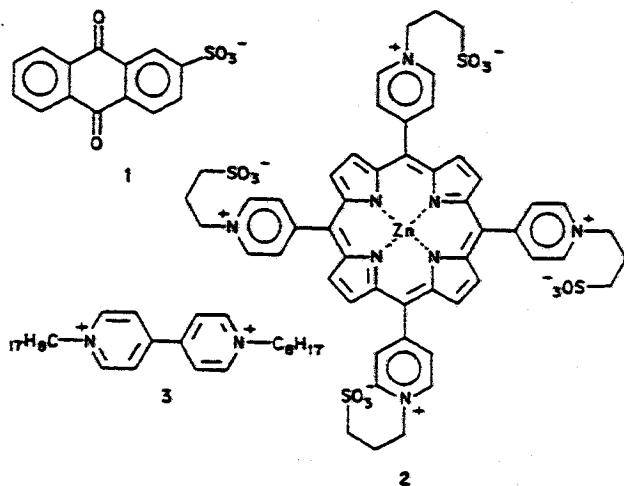
**Abstract:** Zinc(II) *meso*-tetrakis[1-(3-sulfonatopropyl)-4-pyridino]porphyrin, ZnTPSPyP (2), forms a ground state complex with anthraquinone-2-sulfonate, AQS<sup>-</sup> (1). The formation of the complex results in internal static quenching of the excited S state of the sensitizer and recombination of the photoproducts in the cage structure. In the presence of  $\beta$ -cyclodextrin ( $\beta$ -CD), the complex is separated due to selective association of AQS<sup>-</sup> to the receptor cavity. This process leads to the effective decay of excited ZnTPSPyP to the T state that undergoes diffusional quenching by  $\beta$ -CD-bound AQS<sup>-</sup>. The electron-transfer photoproducts are stabilized against back-electron-transfer reaction and AQS<sup>-</sup> can be accumulated under continuous illumination in the presence of cysteine as the electron donor. Photoreduction of *N,N'*-dioctyl-4,4'-bipyridinium, C<sub>4</sub>V<sup>2+</sup>, with Ru(bpy)<sub>3</sub><sup>2+</sup> as the sensitizer and Na<sub>2</sub>EDTA as the donor leads to the formation of a dimer aggregate (C<sub>4</sub>V<sup>•+</sup>)<sub>2</sub>. The aggregate is inactive in H<sub>2</sub> evolution. In the presence of  $\beta$ -CD, the aggregate formation is prevented due to the selective association of C<sub>4</sub>V<sup>•+</sup> monomer to the cyclodextrin cavity. High quantum yields for H<sub>2</sub> evolution in the presence of a Pt-colloid are observed with  $\beta$ -CD,  $\phi = 4 \times 10^{-2}$ . Flash photolysis studies reveal that the association of C<sub>4</sub>V<sup>•+</sup> to the  $\beta$ -CD stabilizes the intermediate photoproducts against back-electron-transfer reactions.

Photosensitized electron-transfer reactions are of substantial interest as a means of solar energy conversion and storage.<sup>1-4</sup> Serious efforts have been devoted in studying photoinduced electron-transfer reactions in organized microenvironments such as micelles,<sup>5-7</sup> charged colloids,<sup>8,9</sup> microemulsions,<sup>10,11</sup> and vesicles.<sup>12</sup> With these organized systems, control of the photosensitized electron-transfer processes has been accomplished. Namely, the quenching process could be improved, charge separation has been facilitated, and the stabilization of photoproducts against back-electron-transfer reactions has been accomplished. Cyclodextrins (CD) are cyclic polysugars composed of glucose units linked by 1-4 $\alpha$ -glycoside bonds.<sup>11,13</sup> The cyclic structure forms a hydrophobic cavity capable of associating organic substrates.<sup>14</sup>

Application of cyclodextrins as an organizing microenvironment in photochemical reactions has been initiated recently and revealed selectivity in products distribution.<sup>15,16</sup> In principle, one could apply the association properties of cyclodextrins for controlling the recombination process between photoproducts by the selective binding of one of the electron-transfer products.

Here we wish to report on the effects of  $\beta$ -CD on photosensitized electron-transfer reactions in aqueous media. We find that in the presence of  $\beta$ -CD, the photosensitized reduction of anthraquinone-2-sulfonate, AQS<sup>-</sup> (1) using the neutral zinc porphyrin, zinc(II) *meso*-tetrakis[1-(3-sulfonatopropyl)-4-pyridino]porphyrin, ZnTPSPyP (2), and cysteine as the electron donor is possible. Without CD the process is prevented due to the formation of a

- (1) (a) *Energy Resources Through Photochemistry and Catalysis*; Gratzel, M., Ed.; Academic: New York, 1983. (b) Bard, A. J. *Science (Washington, D.C.)* 1980, 207, 138.
- (2) (a) Gratzel, M. *Acc. Chem. Res.* 1981, 14, 376-384. (b) Maverick, A. W.; Gray, B. H. *Pure Appl. Chem.* 1980, 52, 2339-2348.
- (3) Whitten, D. G.; Russel, J. C.; Schmill, R. H. *Tetrahedron* 1982, 38, 2455-2487.
- (4) (a) Sutin, N.; Creutz, C. *Pure Appl. Chem.* 1980, 52, 2717-2738. (b) Kalyanasundaram, K. *Coord. Chem. Rev.* 1982, 46, 159-244.
- (5) Turro, N. J.; Gratzel, M.; Braun, A. M. *Angew. Chem., Int. Ed. Engl.* 1980, 19, 675-696.
- (6) (a) Brugger, P. A.; Infelta, P. P.; Braun, A. M.; Gratzel, M. *J. Am. Chem. Soc.* 1981, 103, 320-326. (b) Evans, C. A.; Bolton, J. R. *Photochem. Photobiol.* 1979, 30, 697-707.
- (7) (a) Matsuo, T.; Takama, K.; Tsusui, Y.; Nishigima, T. *Coord. Chem. Rev.* 1980, 10, 195-216. (b) Moroi, Y.; Infelta, P. P.; Gratzel, M. *J. Am. Chem. Soc.* 1979, 101, 573-579. (c) Moroi, Y.; Braun, M. A.; Gratzel, M. *J. Am. Chem. Soc.* 1979, 101, 567-572.
- (8) (a) Willner, I.; Otvos, J. W.; Calvin, M. *J. Am. Chem. Soc.* 1981, 103, 3203-3205. (b) Willner, I.; Yang, J. M.; Otvos, J. W.; Calvin, M. *J. Phys. Chem.* 1981, 85, 3277-3282. (c) Degani, Y.; Willner, I. *J. Am. Chem. Soc.* 1983, 105, 6228-6233.
- (9) Willner, I.; Laane, C.; Otvos, J. W.; Calvin, M. In *Inorganic Reactions in Organized Media*; Holt, S. L., Ed.; ACS Symposium Series 177; American Chemical Society: Washington, DC, 1982; pp 71-95.
- (10) Mandler, D.; Degani, Y.; Willner, I. *J. Phys. Chem.* 1984, 88, 4366-4370.
- (11) Jones, C. A.; Weaner, L. E.; Mackay, R. A. *J. Phys. Chem.* 1980, 84, 1495-1500.
- (12) (a) Sudo, Y.; Toda, F. *Nature (London)* 1979, 279, 808. (b) Matsuo, T.; Itoh, K.; Takuma, K.; Hashimoto, K.; Nagamura, T. *Chem. Lett.* 1980, 1009-1012. (c) Fendler, J. H. *J. Phys. Chem.* 1980, 84, 1485-1491. (d) Infelta, P. P.; Gratzel, M.; Fendler, J. H. *J. Am. Chem. Soc.* 1980, 102, 1497.
- (13) (a) Saenger, A. Q. *Angew. Chem., Int. Ed. Engl.* 1980, 19, 344. (b) Cramer, F.; Hettler, H. *Naturwissenschaften* 1967, 54, 625. (c) Bender, M. L.; Kamiyama, M. *Cyclodextrin Chemistry*; Springer: Berlin, 1978.
- (14) (a) Tabushi, I. *Acc. Chem. Res.* 1982, 15, 66. (b) Breslow, R. *Science (Washington, D.C.)* 1982, 218, 532. (c) Tabushi, I.; Yamamura, K. *Topp. Curr. Chem.* 1983, 113, 145. (d) Willner, I.; Goren, Z. *J. Chem. Soc., Chem. Commun.* 1983, 1469-1470.



ground-state complex between the sensitizer and the anthraquinone acceptor. This complex avoids the separation of electron-transfer photoproducts. Also, we report on the photosensitized reduction of *N,N'*-dioctyl-4,4'-bipyridinium (octylviologen), C<sub>4</sub>V<sup>2+</sup> (3), using ruthenium(II) tris(bipyridine), Ru(bpy)<sub>3</sub><sup>2+</sup>, as the sensitizer in the presence and absence of  $\beta$ -CD. Without cyclodextrin, photoreduction of C<sub>4</sub>V<sup>2+</sup> yields a dimer aggregate of the reduced

- (15) (a) Okuno, Y.; Chiba, Y.; Yonemitsu, O. *J. Chem. Soc., Chem. Commun.* 1984, 1638-1639. (b) Sidney, G. C.; Hauptman, P. J.; Turro, N. J. *Photochem. Photobiol.* 1984, 39, 597-601.
- (16) Kano, K.; Takenoshita, I.; Ogawa, T. *Abstr. Pap.—Am. Chem. Soc.* 1982, 186, 1833-1838.

photoproduct  $C_3V^{2+}$ . This aggregate is inactive in subsequent  $H_2$  evolution. In the presence of  $\beta$ -CD, the formation of the aggregate is prevented due to the association of  $C_3V^{2+}$  monomer to the CD cavity. Consequently, subsequent effective  $H_2$  evolution in the presence of a Pt catalyst is possible. The studies reveal that the cyclodextrins stabilize effectively the intermediate photoproducts, formed in the different reactions, against back-electron-transfer reactions.

### Experimental Section

Absorption spectra were recorded with a Uvikon-820 (Kontron) spectrophotometer equipped with a  $\psi$ -80 computer (Kontron) for spectra accumulation and manipulation. Fluorescence spectra were recorded with a SEM-25 spectrophotometer (Kontron). Flash photolysis experiments were performed with a DL200 (Molelectron) dye laser pumped by a UV-IL (Molelectron) nitrogen laser. Flashes were recorded on Bio-Radation S100, and pulse collection was performed with a Nicolet-1170. Steady-state illuminations were performed with a 1000-W halogen quartz lamp. Light was filtered through a 400-nm cut-off filter. Photon flux was determined by Reinecke salt actinometry<sup>17</sup> to be  $2 \times 10^{-2}$  einsteins  $L^{-1} \cdot min^{-1}$ . Hydrogen analysis was performed with a Hewlett-Packard 427 gas chromatograph, 5-Å molecular sieve column.

Zinc(II) meso-tetrakis[1-(3-sulfonatopropyl)-4-pyridino]porphyrin (2) was prepared as described previously.<sup>18</sup> *N,N'*-Dioctyl-4,4'-bipyridinium dibromide (3) was prepared by refluxing 4,4'-bipyridine with a 6-fold excess of octyl bromide in dimethylformamide. To the cool solution, acetone was added and the precipitate was washed several times with acetone. All compounds gave satisfactory elementary analysis.

For steady-state illumination, photoreduction of  $AQS^-$  was performed in a system composed of an aqueous 0.02 M phosphate buffer, pH 6, that included the sensitizer ZnTPSPyP,  $7 \times 10^{-6}$  M, the electron acceptor,  $AQS^-$ ,  $3.0 \times 10^{-4}$  M, and the electron donor L-cysteine,  $2.0 \times 10^{-3}$  M. Photoreduction of  $C_3V^{2+}$  was performed in an aqueous system composed of a phosphate buffer, pH 5.5, that included ruthenium(II) tris(bipyridine),  $Ru(bpy)_3^{2+}$ ,  $5.5 \times 10^{-5}$  M, as the sensitizer, octylviologen  $C_8V^{2+}$ ,  $5 \times 10^{-3}$  M, as the electron acceptor, and disodiumethylenediaminetetraacetic acid,  $Na_2EDTA$ ,  $1.0 \times 10^{-1}$  M, as the electron donor.  $\beta$ -Cyclodextrin (Aldrich) was dissolved in the different systems at the specified concentrations. For  $H_2$  evolution a Pt colloid ( $12 \text{ mg} \cdot L^{-1}$ ) was introduced into the system. The Pt colloid was prepared by the citrate reduction method (particle size  $\sim 10 \text{ \AA}$ ).<sup>19,20</sup> The Pt colloids were dialyzed before use. Samples (3 mL) of the aqueous solutions of the systems were transferred into  $1 \times 1 \text{ cm}$  Pyrex glass cuvettes equipped with a valve and serum stopper. Samples were deaerated by repeated evacuation followed by flushing with oxygen-free argon. The samples were illuminated with a 1000-W halogen quartz lamp, and the formation of products was followed spectroscopically.  $AQSH^-$  formation was followed<sup>21</sup> at  $\lambda = 384$  ( $\epsilon 12,000 \text{ M}^{-1} \text{ cm}^{-1}$ ).  $C_3V^{2+}$  was followed at  $\lambda = 602 \text{ nm}$  ( $\epsilon 13,800 \text{ M}^{-1} \text{ cm}^{-1}$ ), and the dimer ( $C_3V^{2+}$ )<sub>2</sub> was followed at  $\lambda = 569 \text{ nm}$  ( $\epsilon 6200 \text{ M}^{-1} \text{ cm}^{-1}$ ). Fluorescence measurements were performed in aqueous 0.02 M phosphate buffer samples (3 mL) that included the sensitizer, ZnTPSPyP,  $5 \times 10^{-6}$  M, and the decay of fluorescence upon addition of  $AQS^-$  was measured at  $\lambda = 622 \text{ nm}$ . Quenching of the triplet  $^3ZnTPSPyP$  by  $AQS^-$  was followed by its decay at  $\lambda = 790 \text{ nm}$  (excitation at  $\lambda = 448 \text{ nm}$ ). Charge separation and recombination of ZnTPSPyP<sup>+</sup> was followed at  $\lambda = 680 \text{ nm}$ . Quenching of  $^3Ru(bpy)_3^{2+}$  by  $C_3V^{2+}$  was followed by steady-state fluorescence quenching ( $\lambda = 602 \text{ nm}$ ). Charge separation of  $C_3V^{2+}$  and its recombination with  $Ru(bpy)_3^{2+}$  was measured by following the formation and decay of  $C_3V^{2+}$  at  $\lambda = 602\text{-nm}$  excitation at  $\lambda = 455 \text{ nm}$ .  $H_2$  evolution was followed by injection of 300  $\mu\text{L}$  of the gaseous atmosphere of the flask into the gas chromatograph at time intervals of illumination.

### Results and Discussion

**Photosensitized Reduction of Anthraquinone-2-sulfonate in the Presence of  $\beta$ -CD.** Zinc(II) meso-tetrakis[1-(3-sulfonatopropyl)-4-pyridino]porphyrin, ZnTPSPyP (1), is an aqueous soluble neutral metalloporphyrin. Its photophysical properties have been previously characterized.<sup>22,23</sup> It exhibits a fluorescence

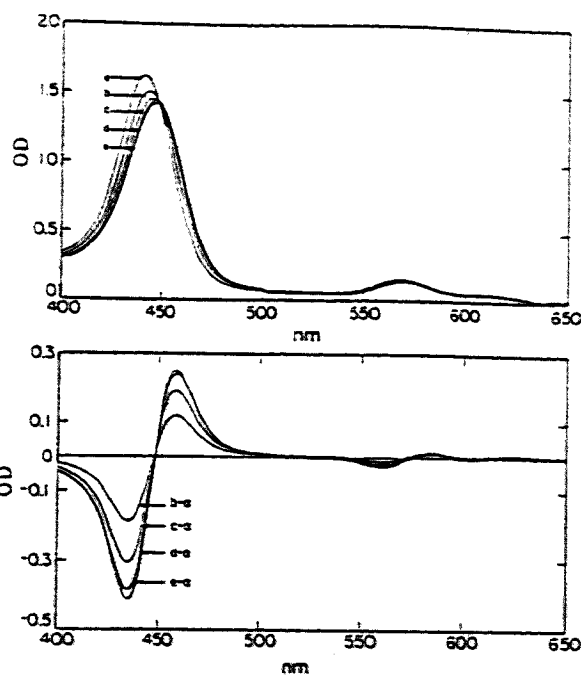
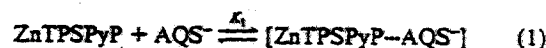


Figure 1. Absorption spectra (top) and differential absorption spectra (bottom) of ZnTPSPyP ( $7 \times 10^{-6}$  M) obtained after addition of  $AQS^-$ : (a) no added  $AQS^-$ ; (b)  $[AQS^-] = 2 \times 10^{-4}$  M; (c)  $[AQS^-] = 4 \times 10^{-4}$  M; (d)  $[AQS^-] = 6 \times 10^{-4}$  M.

emission at  $\lambda = 622 \text{ nm}$  and a short-lived singlet state ( $\tau \sim 10 \times 10^{-9} \text{ s}$ ) that undergoes effective crossing to a long-lived triplet state ( $\tau = 0.5 \text{ ms}$ ,  $\phi = 0.9$ ). Addition of anthraquinone-2-sulfonate,  $AQS^-$  (1), to an aqueous solution of ZnTPSPyP,  $5 \times 10^{-6}$  M, results in substantial changes in the absorption spectrum and emission properties of the metalloporphyrin. In the absorption spectrum (Figure 1), the Soret absorption band of 2 is shifted from  $\lambda = 439$  to  $444 \text{ nm}$  in the presence of  $AQS^-$ . The effects of added  $AQS^-$  on the emission of ZnTPSPyP are shown in Figure 2. It can be seen that the fluorescence emission is totally quenched at  $[AQS^-] = 5.0 \times 10^{-5}$  M. Laser flash studies reveal that under these conditions the singlet excited state is totally quenched and no formation of the T state is observed.

These results are attributed to the formation of a ground-state complex between ZnTPSPyP and  $AQS^-$  (eq 1), where the S state is being quenched in the complex structure. From the changes in the absorption spectrum of ZnTPSPyP upon addition of  $AQS^-$ , the association constant of the complex  $[ZnTPSPyP-AQS^-]$ , eq 2, is estimated to be  $K_1 = 4.35 \pm 0.5 \times 10^5 \text{ M}^{-1}$ . Furthermore,



$$K_1 = [ZnTPSPyP-AQS^-] / [ZnTPSPyP][AQS^-] \quad (2)$$

assuming that the metalloporphyrin does not emit, then the fluorescence intensity is proportional to the concentration of free porphyrin. This allows us to determine the concentration of free and bound metalloporphyrin at each concentration of  $AQS^-$ . When this method is used, the association constant of the complex is estimated to be  $K_1 = 4.5 \pm 1 \times 10^5 \text{ M}^{-1}$ , a value that is in good agreement to the value obtained by the changes in the absorption spectrum.

It is well established<sup>14</sup> that cyclodextrins bind aromatic compounds into the hydrophobic cavity of the CD. Indeed, addition of  $\beta$ -CD to an aqueous solution ZnTPSPyP and  $AQS^-$ , under conditions where the metalloporphyrin is in the complex structure, restores the emission properties of ZnTPSPyP (Figure 2). This

(22) Harriman, A.; Porter, G.; Richoux, M. C. J. Chem. Soc., Faraday Trans. 2 1982, 78, 1955-1970.

(23) Houlding, V. H.; Kalyanasundaram, K.; Gratzel, M.; Milgrom, L. R. J. Phys. Chem. 1983, 87, 3175-3179.

(17) Wegner, E. E.; Adamson, A. W. J. Am. Chem. Soc. 1966, 88, 394.

(18) (a) Willner, I.; Degani, Y. J. Chem. Soc., Chem. Commun. 1982, 1249-1251. (b) Degani, Y.; Willner, I. J. Phys. Chem. 1985, 89, 56859

(19) Furlong, D. A.; Launikonis, A.; Sasse, H. F.; Wolfgang, H. F. J. Chem. Soc., Faraday Trans. 1 1984, 80, 571-588.

(20) Aika, K.; Ban, L. L.; Okura, I.; Namba, S.; Turkerich, J. J. Res. Inst. Catal. Hokkaido Univ. 1976, 24, 55.

(21) Rao, P. S.; Hayon, E. J. Phys. Chem. 1973, 77, 2274-2276.

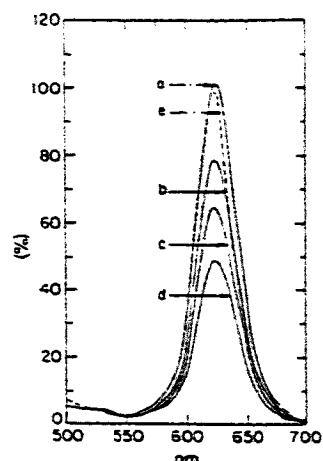


Figure 2. Fluorescence spectra of ZnTPSPyP ( $5 \times 10^{-6}$  M) upon addition of AQS<sup>-</sup>: (a) no added AQS<sup>-</sup>; (b) [AQS<sup>-</sup>] =  $2 \times 10^{-6}$  M; (c) [AQS<sup>-</sup>] =  $4 \times 10^{-6}$  M; (d) [AQS<sup>-</sup>] =  $8 \times 10^{-6}$  M; (e) [AQS<sup>-</sup>] =  $8 \times 10^{-6}$  M and [ $\beta$ -CD] =  $1 \times 10^{-2}$  M.

implies that upon addition of  $\beta$ -CD the complex of the two components is separated by the selective association of AQS<sup>-</sup> to the CD cavity (eq 3). The restoration of the emission properties of the zinc porphyrin in the presence of  $\beta$ -CD allows one to determine the association constant of AQS<sup>-</sup> to  $\beta$ -CD (eq 3 and 4). Since



$$K_2 = [\text{AQS}^- \text{-} \beta\text{-CD}] / [\text{AQS}^-][\beta\text{-CD}] \quad (4)$$

the fluorescence intensity is only due to free porphyrin ZnTPSPyP, the concentration of free quinone and  $\beta$ -CD-bound AQS<sup>-</sup> can be derived from eq 2a and 5, where [AQS<sup>-</sup>]<sub>f</sub> and [AQS<sup>-</sup>]<sub>0</sub> correspond to the free and total concentration of the quinone. When this analysis is used, the derived association constant of AQS<sup>-</sup> to  $\beta$ -CD is  $K_2 = 3 \pm 0.5 \times 10^3 \text{ M}^{-1}$ .

$$[\text{AQS}^-]_f = K_1 [\text{ZnTPSPyP}] / [\text{ZnTPSPyP-AQS}^-] \quad (2a)$$

$$[\text{AQS}^- \text{-} \beta\text{-CD}] = [\text{AQS}^-]_0 - [\text{AQS}^-]_f - [\text{ZnTPSPyP-AQS}^-] \quad (5)$$

The separation of the complex structure between the metal-porphyrin and AQS<sup>-</sup> by  $\beta$ -CD allows the accumulation of electron-transfer products upon illumination. Irradiation of an aqueous solution ( $\lambda > 400$  nm) that includes ZnTPSPyP ( $7.0 \times 10^{-6}$  M), AQS<sup>-</sup> ( $3.0 \times 10^{-6}$  M), and cysteine ( $2.0 \times 10^{-3}$  M) as the electron donor does not yield any photoproducts in the absence of  $\beta$ -CD. In turn, in the presence of  $\beta$ -CD,  $1 \times 10^{-2}$  M, the reduced hydroquinone radical, AQHS<sup>-</sup> is formed upon illumination,  $\phi = 1.35 \times 10^{-3}$ . Exclusion of cysteine from the composition that includes  $\beta$ -CD prohibits the formation of AQHS<sup>-</sup> upon illumination. This implies that cysteine acts as the electron donor in the photosensitized reduction of AQS<sup>-</sup>.

The functions of  $\beta$ -CD in the photosensitized reduction of AQS<sup>-</sup> have been elucidated by means of laser flash photolysis.

The sensitizer, ZnTPSPyP<sup>0</sup>, decays upon excitation to the long-lived T state ( $\tau = 0.5$  ms,  $\phi = 0.9$ ). Addition of AQS<sup>-</sup> (1) results in a decrease in the T state yield, and at a [AQS<sup>-</sup>] =  $4 \times 10^{-6}$ , the T-state yield corresponds to 0.5 of the value obtained in the absence of AQS<sup>-</sup>. This is in accordance with our previous results that indicated the formation of the complex ZnTPSPyP-AQS<sup>-</sup>, where the excited sensitizer is quenched in the S state. This intramolecular quenching prohibits the formation of the long-lived triplet state. Addition of  $\beta$ -CD to the solution of ZnTPSPyP and AQS<sup>-</sup> restores the effective formation of the T state and shortening of the T state lifetime. This result implies that a different quenching mechanism occurs where the ZnTPSPyP T state is quenched by AQS<sup>-</sup> (eq 6). The quenching rate constant corresponds to  $k_q = 3.3 \times 10^6 \text{ M}^{-1} \text{ s}^{-1}$ . This quenching process leads to separated electron-transfer products

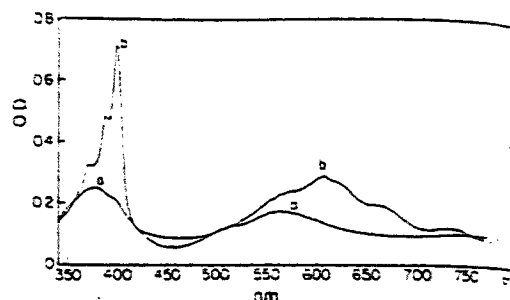
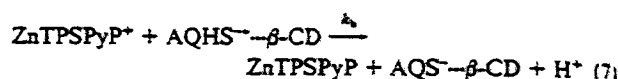
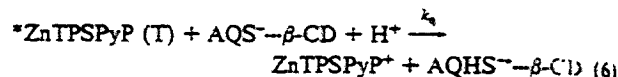


Figure 3. Absorption spectra of the photoreduced product of  $\text{C}_{12}\text{V}^{2+}$  ( $5.0 \times 10^{-3}$  M) in the presence of  $\text{Ru}(\text{bpy})_3^{2+}$ ,  $1.0 \times 10^{-3}$  M, and  $\text{Na}_2\text{EDTA}$ ,  $1.0 \times 10^{-1}$  M: (a) in the absence of  $\beta$ -CD; (b) in the presence of  $\beta$ -CD,  $1.0 \times 10^{-2}$  M.

(eq 6) that recombine (eq 7) with a bimolecular recombination rate constant of  $k_b = 2.5 \times 10^7 \text{ M}^{-1} \text{ s}^{-1}$ . Comparison of the



recombination rate of the electron-transfer products in the presence of  $\beta$ -CD to the value obtained in the absence of  $\beta$ -CD<sup>24</sup> indicates that the back-electron-transfer process is 10-fold retarded in the presence of  $\beta$ -CD.

Thus, in view of the flash photolysis results, we can conclude that the added  $\beta$ -CD participates in the electron-transfer process in two routes: (i) it separates the complex structure ZnTPSPyP-AQS<sup>-</sup> and allows the formation of the T state of the excited sensitizer, and (ii) it stabilizes the electron-transfer products against back-electron-transfer reactions, by the selective association of AQHS<sup>-</sup> within the cyclodextrin cavity. These two functions of  $\beta$ -CD allow the effective accumulation of AQHS<sup>-</sup> under continuous illumination.

**Photoreduction of Octylviologen and H<sub>2</sub> Evolution in the Presence of  $\beta$ -CD.** Photoreduction of alkylviologens in the visible spectrum has been extensively examined using various sensitizers<sup>25-27</sup> and organized microenvironments.<sup>28,29</sup> Emphasis has been directed to the utilization of the photoproducts, viologen radicals, in H<sub>2</sub> evolution in the presence of metal colloids such as Pt catalysts.<sup>30-32</sup> Interestingly, illumination of an aqueous solution, pH 5.5, that includes the sensitizer, ruthenium(II) tris(bipyridine),  $\text{Ru}(\text{bpy})_3^{2+}$ , *N,N'*-dioctyl-4,4'-bipyridinium, octylviologen,  $\text{C}_{12}\text{V}^{2+}$ , as the electron acceptor and disodioethylenediaminetetraacetic acid,  $\text{Na}_2\text{EDTA}$ , as the electron donor, results in the formation

(24) At low AQS<sup>-</sup> concentration electron-transfer products are formed inefficiently via quenching of uncomplexed sensitizer in the T state. The recombination rate is estimated to be  $k_b = 2.9 \times 10^7$ .

(25) Okura, I.; Takeuchi, M.; Kim-Thuan, N. *J. Mol. Catal.* 1979, 6, 227.

(26) Kalyanasundaram, K.; Gratzel, M. *Helv. Chim. Acta* 1980, 63, 478.

(27) Okura, I.; Aono, S.; Takeuchi, M.; Kusunoki, S. *Bull. Chem. Soc. Jpn.* 1982, 55, 3637-3638.

(28) (a) Brugger, P. A.; Gratzel, M. *J. Am. Chem. Soc.* 1980, 102, 2461-2463. (b) Kamogawa, H.; Masui, T.; Nanasawa, M. *Chem. Lett.* 1980, 1145-1148.

(29) (a) Brugger, P. A.; Infelta, P. P.; Braun, A. M.; Gratzel, M. *J. Am. Chem. Soc.* 1981, 103, 320-326. (b) Wheeler, J.; Thomas, K. J. *J. Phys. Chem.* 1982, 86, 4540-4544. (c) Maidan, R.; Goren, Z.; Becker, J. Y.; Willner, I. *J. Am. Chem. Soc.* 1984, 106, 6217-6222.

(30) (a) Kiwi, J.; Gratzel, M. *Angew. Chem., Int. Ed. Engl.* 1979, 18, 624-626. (b) Okura, I.; Nakamura, S.; Nakamura, K. I. *J. Mol. Catal.* 1979, 6, 71-73. (c) Koritsin, B. V.; Dzhabiev, T. S.; Shilon, A. *Dokl. Akad. Nauk SSSR* 1977, 233, 620.

(31) (a) Keller, P.; Moradpour, A.; Amouyal, E.; Kagan, H. B. *Nouv. J. Chim.* 1980, 4, 377-384; *J. Am. Chem. Soc.* 1980, 102, 7193-7196. (b) Harriman, A.; Porter, G.; Richoux, M. C. *J. Chem. Soc., Faraday Trans. 2* 1981, 77, 1939-1948. (c) Harriman, A.; Porter, G.; Richoux, M. C. *J. Chem. Soc., Faraday Trans. 2* 1981, 77, 833-844.

(32) (a) Krassa, A. I. *Photochem. Photobiol.* 1980, 31, 75-81. (b) Frank, A. J. *J. Chem. Soc., Chem. Commun.* 1981, 593-594. (c) Okura, I.; Kim-Thuan, N. *J. Chem. Soc., Faraday Trans. 1* 1981, 77, 1411-1415. (d) Keller, P.; Moradpour, A.; Amouyal, E. *Ibid.* 1982, 78, 3331-3340.

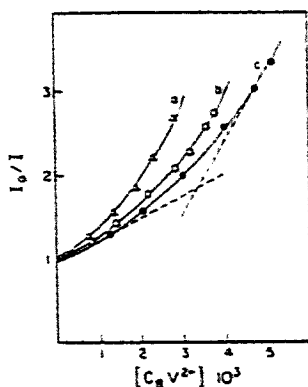
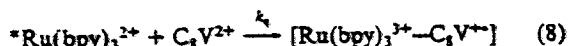


Figure 4. Fluorescence quenching of  $\text{Ru}(\text{bpy})_3^{2+}$ ,  $4 \times 10^{-5}$  M, by  $\text{C}_8\text{V}^{2+}$  in the presence of  $\beta$ -CD: (a)  $[\beta\text{-CD}] = 1 \times 10^{-3}$  M; (b)  $[\beta\text{-CD}] = 5 \times 10^{-3}$  M;  $[\text{C}_8\text{V}^{2+}] = 7.5 \times 10^{-3}$  M.

of a violet solution of the octylviologen radical in its dimer form  $(\text{C}_8\text{V}^{\bullet+})_2$  (Figure 3).<sup>33</sup> The quantum yield for the octylviologen radical dimer formation corresponds to  $\phi = 10.6 \times 10^{-2}$ . It is well established<sup>33</sup> that viologen radicals tend to aggregate at high concentrations of the radicals. With octylviologen, the dimer aggregate is the predominating species, even at very low concentrations of the reduced photoproduct. Further illumination of the system results in the precipitation of a deep violet product from the aqueous solution that is presumably a higher aggregate form of the single electron-transfer product  $\text{C}_8\text{V}^{\bullet+}$ . We believe that due to the hydrophobic character of  $\text{C}_8\text{V}^{\bullet+}$ , the aggregation process is favored as a result of intermolecular hydrophobic interactions. Similar hydrophobic interactions have been previously discussed<sup>28</sup> in the photoreduction of *N*-methyl-*N'*-dodecyldecyl-4,4'-bipyridinium,  $\text{MeC}_{14}\text{V}^{2+}$ . With this charge relay, the reduced photoproduct,  $\text{MeC}_{14}\text{V}^{\bullet+}$  forms micellar aggregates as a result of hydrophobic interactions. The absorption pattern of the micellar aggregate of  $\text{MeC}_{14}\text{V}^{\bullet+}$  resembles that of the  $\text{C}_8\text{V}^{\bullet+}$  dimer complex.

Previous studies have indicated that cyclodextrins induce deaggregation of dyes such as thionine<sup>34</sup> or rhodamine B<sup>35</sup> by the selective association of the monomer dye form to the CD cavity. We have examined the possibility to prevent the aggregation of  $\text{C}_8\text{V}^{\bullet+}$  in the presence of  $\beta$ -CD. Illumination of the previously described system,  $\lambda > 400$  nm, in the presence of  $\beta$ -CD,  $1 \times 10^{-2}$  M, results in the formation of the monomer photoproduct,  $\text{C}_8\text{V}^{\bullet+}$  (Figure 3). The quantum yield of  $\text{C}_8\text{V}^{\bullet+}$  formation in the presence of  $\beta$ -CD is  $\phi = 8.8 \times 10^{-2}$ . The formation of the monomer  $\text{C}_8\text{V}^{\bullet+}$  in the presence of  $\beta$ -CD is attributed to the binding of the reduced photoproduct to the hydrophobic cavity of the cyclodextrin (vide infra). The size of the CD cavity (6.2-Å diameter, 7-Å height)<sup>13c</sup> limits the accommodation of the monomer form only, and consequently aggregation is prevented.

The mechanistic steps leading to the photoreduction of  $\text{C}_8\text{V}^{2+}$  in the absence and presence of  $\beta$ -CD have been studied in detail using laser flash photolysis. The primary process involves the electron-transfer quenching of the excited sensitizer by  $\text{C}_8\text{V}^{2+}$  (eq 8). In the absence of  $\beta$ -CD, the Stern-Volmer plot following



the quenching process is linear and the quenching rate constant corresponds to  $k_1 = 2.5 \times 10^9 \text{ M}^{-1} \text{ s}^{-1}$ , a value very similar to that reported for other viologen charge relays.<sup>26,36</sup> The Stern-Volmer plots following the quenching process in the presence of  $\beta$ -CD show a nonlinear behavior and depend on the  $\beta$ -CD concentration (Figure 4). It can be seen that the quenching curves exhibit a hyperbolic shape and that the curvatures rises at a lower  $\text{C}_8\text{V}^{2+}$

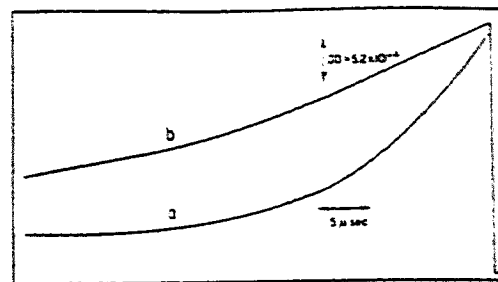
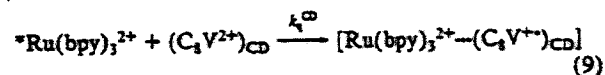


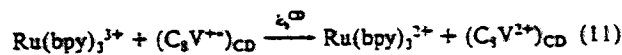
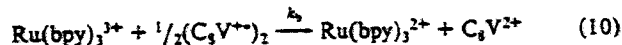
Figure 5. Transient decay of the photoreduced product of  $\text{C}_8\text{V}^{2+}$  followed at  $\lambda = 600$  nm. Excitation of  $\text{Ru}(\text{bpy})_3^{2+}$ ,  $4 \times 10^{-5}$  M, at  $\lambda = 455$  nm.  $[\text{C}_8\text{V}^{2+}] = 2.0 \times 10^{-3}$  M; (a) without  $\beta$ -CD; (b) in the presence of  $\beta$ -CD  $= 1 \times 10^{-2}$  M.

concentration when the  $\beta$ -CD concentration decreases. Furthermore, it is evident that for each  $\beta$ -CD concentration the quenching plots rise with an asymptotic slope similar to the value observed in the absence of  $\beta$ -CD. These results suggest that the quenching plots can be interpreted by two complementary quenching processes: at low  $\text{C}_8\text{V}^{2+}$  concentrations, the charge relay is mainly associated with the  $\beta$ -CD, and the quenching of the excited species occurs by CD-bound  $\text{C}_8\text{V}^{2+}$ ,  $(\text{C}_8\text{V}^{2+})_{\text{CD}}$  (eq 9). From the different curves the calculated quenching rate



constant for  $\beta$ -CD-bound  $\text{C}_8\text{V}^{2+}$  corresponds to  $k_1^{\text{CD}} = 8.5 \times 10^8 \text{ M}^{-1} \text{ s}^{-1}$ . At high  $\text{C}_8\text{V}^{2+}$  concentration, the binding sites of  $\beta$ -CD are saturated, and consequently the quenching process occurs by free  $\text{C}_8\text{V}^{2+}$  with a rate constant similar to that observed in the absence of  $\beta$ -CD. Certainly, the amount of free  $\text{C}_8\text{V}^{2+}$  needed to saturate the cyclodextrin cavities will depend on the  $\beta$ -CD concentration and will be controlled by the association constant of  $\text{C}_8\text{V}^{2+}$  to  $\beta$ -CD. This is consistent with the result that the quenching plots are curved at lower  $\text{C}_8\text{V}^{2+}$  concentrations, when the  $\beta$ -CD concentration decreases. The curved parts of the quenching plots are thus representing stages where the excited sensitizer is quenched by the free and bound quencher concomitantly. The studies reveal that the effectiveness of the quenching process of the excited sensitizer by  $\beta$ -CD-bound  $\text{C}_8\text{V}^{2+}$  is ca. 3-fold decreased as compared to the similar process by the free quencher.

Nevertheless, the quantum yields of the reduced photoproducts,  $(\text{C}_8\text{V}^{\bullet+})_2$  and  $(\text{C}_8\text{V}^{\bullet+})_{\text{CD}}$ , under continuous illumination are very similar ( $\phi \sim 10\%$ ), despite the inefficient primary process involved in the electron transfer in the presence of  $\beta$ -CD. This phenomenon suggests that an additional reaction participating in the overall process is improved in the presence of  $\beta$ -CD and compensates for the inefficient quenching process. We have thus examined the recombination process of the separated photoproducts. These reactions were characterized by following the decay of the photogenerated products  $(\text{C}_8\text{V}^{\bullet+})_2$  or  $(\text{C}_8\text{V}^{\bullet+})_{\text{CD}}$ , eq 10 and 11 (Figure 5). The recombination rate constant of the photoproducts in the



absence of  $\beta$ -CD is  $k_2 = 3.2 \times 10^8 \text{ M}^{-1} \text{ s}^{-1}$ . It should be noted that the value of the back-electron-transfer rate constant using  $\text{C}_8\text{V}^{2+}$  as the charge relay is ca. 1 order of magnitude lower than the recombination rates of the alkylviologen radical and  $\text{Ru}(\text{bpy})_3^{3+}$  that are almost diffusion controlled. This might be attributed to electrostatic repulsion of the oxidized product by the positively charged octylviologen radical aggregate.<sup>28,29</sup> Yet, in the presence of  $\beta$ -CD, the back-electron-transfer rate constant of the photoproducts is  $k_2^{\text{CD}} = 3.2 \times 10^7 \text{ M}^{-1} \text{ s}^{-1}$ . These results imply that the back-electron-transfer process is 10-fold retarded as compared to the system without cyclodextrin and ca. 2 orders of magnitude slower than a diffusion-controlled process. Thus, we conclude that the separated photoproducts are stabilized against

(33) Kosower, E. M.; Cotter, J. L. *J. Amer. Chem. Soc.* 1964, 86, 5524.

(34) Dan, P.; Willner, I. *J. Chem. Soc., Perkin Trans. 2* 1984, 455-459.

(35) Degani, Y.; Willner, I.; Haas, Y. *Chem. Phys. Lett.* 1984, 104, 496-499.

(36) Bock, O. R.; Meyer, T. J.; Whitten, D. G. *J. Am. Chem. Soc.* 1974, 96, 1-10.

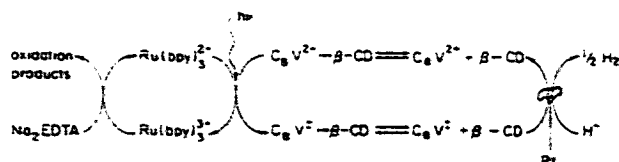
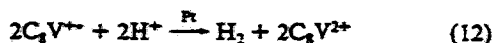


Figure 6. Schematic function of  $\beta$ -CD in photogeneration of  $C_9V^{2+}$  monomer and subsequent  $H_2$  evolution.

the back-electron-transfer reaction in the presence of  $\beta$ -CD. This stabilization is attributed to the selective binding of the photoproduct  $C_9V^{2+}$  to the hydrophobic cavity of the cyclodextrin. This stabilization allows the effective subsequent regeneration of the sensitizer by the electron donor,  $Na_2EDTA$  (Figure 6). Therefore, the high quantum yields observed in the photoreduction of  $C_9V^{2+}$  in the presence of  $\beta$ -CD are mainly attributed to the stabilization of the photoproducts against destructive back-electron-transfer processes. Previous studies have shown that organized microenvironments such as micelles,<sup>5-7</sup> colloids,<sup>8,9</sup> polyelectrolytes,<sup>37</sup> vesicles,<sup>12</sup> and microemulsions<sup>10,11</sup> can control electron-transfer reactions and stabilize the photoproducts against back reactions. The present study reveals a novel approach for retardation of the recombination rate that uses cyclodextrins for controlling the process. These host receptors associate selectively with one of the photoproducts, and consequently, the photoproduct is being stabilized toward the back-electron-transfer process.

It is well established that  $N,N'$ -dialkyl-4,4'-bipyridinium radicals act as charge relays that mediate  $H_2$  evolution in the presence of metal colloids such as Pt.<sup>30-32</sup> Introduction of a Pt colloid to an aqueous solution that includes the sensitizer,  $Ru(bpy)_3^{2+}$ , the electron acceptor,  $C_9V^{2+}$ , and  $Na_2EDTA$  does not yield any hydrogen upon illumination although the reduced photoproduct  $(C_9V^{2+})_2$  is formed efficiently. This implies that the aggregate,  $(C_9V^{2+})_2$ , is not active as a charge relay for  $H_2$  evolution. Yet, in the presence of  $\beta$ -CD, where the reduced product is in the monomer form,  $C_9V^{2+}$ , effective  $H_2$  evolution is accomplished,  $\phi = 4 \times 10^{-2}$  (eq 12).



The reason for the inertness of the dimer aggregate  $(C_9V^{2+})_2$  is still questionable. The redox properties of  $C_9V^{2+}$  have been

(37) (a) Meisel, D.; Matheson, M. *J. Am. Chem. Soc.* 1977, 99, 6577. (b) Meisel, D.; Matheson, M.; Rabani, J. *J. Am. Chem. Soc.* 1978, 100, 117.

examined in aqueous solutions in the presence and absence of  $\beta$ -CD using cyclic voltammetry. In the presence of  $\beta$ -CD, the reduction potential of  $C_9V^{2+}$  corresponds to  $E^\circ = -0.36$  V (vs. NHE). In the absence of  $\beta$ -CD the reduction potential is more positive by ca. 0.05 V.<sup>38</sup> For  $H_2$  formation at pH 5.5, the charge relay must exhibit a limiting redox potential of  $E^\circ = -0.33$  V, excluding overpotential needs. Thus, the relatively positive redox potential of the dimer aggregate  $(C_9V^{2+})_2$ , together with its low solubility in water, might eliminate  $H_2$  evolution.

### Conclusions

We have studied different photosensitized electron-transfer reactions in aqueous media containing  $\beta$ -cyclodextrins. We find several functions of the CD receptor in the photoinduced process.  $\beta$ -Cyclodextrin could destroy a ground-state complex between a neutral zwitterionic zinc porphyrin and anthraquinone-2-sulfonate. Similarly  $\beta$ -CD separates the dimer photoproduct  $(C_9V^{2+})_2$ . This separation ability of  $\beta$ -CD toward aggregated forms is a result of the binding properties of the cyclodextrin receptor. The different separation processes that were studied have significant consequences on the photosensitized electron-transfer reactions in the  $\beta$ -CD microenvironments. In the former system, the restoration of the photophysical properties of the zinc porphyrin has been accomplished. In the latter system the formation of an active charge relay,  $C_9V^{2+}$ , that mediates  $H_2$  evolution was established. Further effects of  $\beta$ -CD are apparent in controlling the photosensitized electron-transfer process. Substantial stabilization of the intermediate photoproducts against back-electron-transfer reactions is achieved, by selective binding of one of the photoproducts to the CD cavity.

**Acknowledgment.** This research is supported by a grant from the National Council for Research and Development, Israel, and the Kernforschung Anlage, Juelich, Germany.

Registry No. 1, 5776-56-7; 2, 84431-54-9; 3, 36437-30-6;  $\beta$ -CD, 7585-39-9;  $Ru(bpy)_3^{2+}$ , 15158-62-0.

(38) The reduction potentials of  $C_9V^{2+}$  in water and in the presence of  $\beta$ -CD should be related by  $E_{\beta-CD}^\circ = E_{CD}^\circ + 0.029 \log K_{dim}$  where  $E_{\beta-CD}^\circ$  and  $E_{CD}^\circ$  are the standard reduction potentials of  $C_9V^{2+}$  in water and in the presence of  $\beta$ -CD, respectively, and  $K_{dim}$  is the equilibrium constant of the dimerization process  $2C_9V^{2+} \rightleftharpoons (C_9V^{2+})_2$ . The observed difference in the reduction potential in water and  $\beta$ -CD media allows us to estimate the equilibrium constant of the dimerization process to be  $K_{dim} = 52.98 \pm 4.8 M^{-1}$ . We thank one of the referees for pointing out the possibility to estimate the dimerization constant by this approach.

resents a rare example<sup>15</sup> of clean chirality induction to an sp<sup>2</sup> carbon which is not part of a ring, during a carbon-centered free-radical cyclization. Furthermore, the highly efficient insertion of the oxygen atom at C-22 into the C-Si bond<sup>16</sup> of the heterocyclic units 4 and 9 has provided a novel entry to the synthesis of the 22-hydroxylated natural and 20-iso-steroid side chains.

The results described herein have considerable implications beyond the synthesis of the steroid side chains. We believe that this type of chirality transmission approach employing the  $\alpha$ -silyl radical-mediated cyclization should have the potential to be effectively applied in the synthesis of various acyclic molecules or their equivalents.

**Acknowledgment.** We are grateful for financial support from the National Institutes of Health (DK30025) and to the Michigan Cancer Institute for a fellowship to I.A.G.

(15) For previously reported examples involving 5- $\alpha$  cyclization, see ref 1c, 4p, and 4ee.

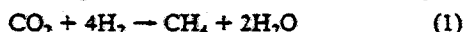
(16) (a) Tamao, K.; Ishida, N.; Tanaka, T.; Kumada, M. *Organometallics* 1983, 2, 1694. (b) Tamao, K.; Ishida, N.; Kumada, M. *J. Org. Chem.* 1983, 48, 2120. (c) Tamao, K.; Ishida, N. *J. Organomet. Chem.* 1984, 269, C37. See also ref 1f and 4p.

### Photoreduction of CO<sub>2</sub> to CH<sub>4</sub> in Aqueous Solutions Using Visible Light

Ruben Maidan and Itamar Willner\*

Department of Organic Chemistry  
The Hebrew University of Jerusalem  
Jerusalem 91904, Israel  
Received May 27, 1986

Reduction of CO<sub>2</sub> to combustible organic products by means of solar light is of substantial interest as a means for solar energy conversion and storage.<sup>1-3</sup> Serious attempts have recently been directed toward the development of light-induced CO<sub>2</sub>-fixation processes.<sup>4-7</sup> Reduction of CO<sub>2</sub> to carbon monoxide,<sup>4</sup> formate,<sup>5,6</sup> and other organic acids<sup>7</sup> has been reported, using homogeneous catalysts,<sup>4,5</sup> semiconductor particles,<sup>6</sup> or artificially enzyme catalyzed coupled systems.<sup>7</sup> Reduction of CO<sub>2</sub> to methane, the methanation process (eq 1), is of substantial industrial impor-



tance.<sup>8,9</sup> This reaction proceeds at high temperatures and pressures and is catalyzed by metal catalysts such as Ru, Mo, and Ni. Electrocatalyzed reduction of CO<sub>2</sub> using Ru electrodes has been reported.<sup>10</sup> Here we wish to report on the photocatalyzed reduction of CO<sub>2</sub> to methane using tris(bipyrazine)ruthenium(II), Ru(bpz)<sub>3</sub><sup>2+</sup>, as sensitizer<sup>11</sup> and a Ru metal colloid as catalyst for the process.

The system is composed of an aqueous solution, pH 9.5, that includes NaHCO<sub>3</sub>, 0.05 M, Ru(bpz)<sub>3</sub><sup>2+</sup>, 1 × 10<sup>-4</sup> M, triethanolamine, TEOA, 0.17 M, as electron donor, and a Ru colloid, 20 mg·L<sup>-1</sup>, prepared by the citrate reduction method.<sup>12</sup> Illu-

(1) Calvin, M. *Acc. Chem. Res.* 1978, 11, 369-374.

(2) *Organic and Bio-Organic Chemistry of Carbon Dioxide*; Inoue, S., Yamazaki, N., Eds.; Wiley: New York, 1982.

(3) Ulman, M.; Aurian-Blajeni, B.; Halmann, M. *ChemTech* 1984, 1, 235-239.

(4) Lehn, J.-M.; Zissel, R. *Proc. Natl. Acad. Sci. U.S.A.* 1982, 79, 701-704.

(5) Hawcker, J.; Lehn, J.-M.; Zissel, R. *J. Chem. Soc., Chem. Commun.* 1985, 56-58.

(6) Halmann, M. *Nature (London)* 1978, 275, 115-116.

(7) Willner, I.; Mandler, D.; Riklin, A. *J. Chem. Soc., Chem. Commun.* 1986, 1022-1024.

(8) *Methanation of Synthesis Gas*; Seglia, L., Ed.; American Chemical Society: Washington, DC.

(9) Mills, G. A.; Steffgen, F. W. *Catal. Rev.* 1973, 8, 159-210.

(10) Frese, K. W., Jr.; Leach, S. J. *Electrochem. Soc.* 1985, 133, 259-260.

(11) Crutchley, R. J.; Lever, A. B. P. *Inorg. Chem.* 1982, 21, 2276-2282.

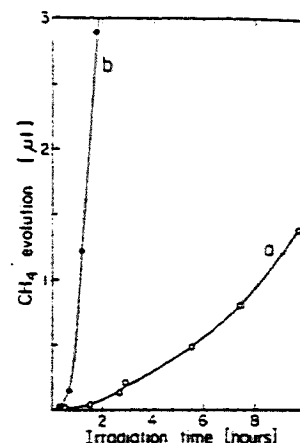


Figure 1. Rate of CH<sub>4</sub> formation as a function of illumination time: (a) in H<sub>2</sub>O; (b) in water-ethanol 2:1 solution.

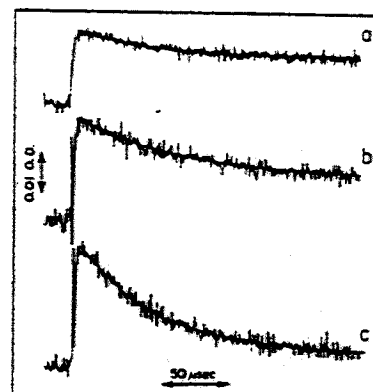


Figure 2. Transient spectra formed upon illumination of Ru(bpz)<sub>3</sub><sup>2+</sup>, 2 × 10<sup>-5</sup> M and TEOA, 0.17 M solution pH 9.5. Systems are flashed at λ = 440 nm and product is followed at λ = 500 nm: (a) under CO<sub>2</sub>, argon; (b) in the presence of Ru colloid (20 mg·L<sup>-1</sup>) under argon; (c) in the presence of Ru colloid (20 mg·L<sup>-1</sup>) under CO<sub>2</sub>.

mination of this system under a gaseous atmosphere of CO<sub>2</sub>, > 420 nm, results in the formation of methane. Methane analysis was performed by gas chromatography (Porapak T column) by comparison to an authentic sample as well as by mass spectrometry. The rate of CH<sub>4</sub> formation at time intervals of illumination is displayed in Figure 1a and corresponds to a quantum yield of φ = 0.0025%. Exclusion from the system of the sensitizer, Ru(bpz)<sub>3</sub><sup>2+</sup>, or the Ru colloid prevents the formation of CH<sub>4</sub>. Similarly, exclusion of NaHCO<sub>3</sub> and CO<sub>2</sub> eliminates any production of methane. These results imply that all of the components are essential for the reduction of CO<sub>2</sub> to CH<sub>4</sub>. The turnover number of Ru(bpz)<sub>3</sub><sup>2+</sup> is 15, implying a cyclic activity of the system.

The photophysical properties of Ru(bpz)<sub>3</sub><sup>2+</sup> have been studied in detail.<sup>11,13</sup> It exhibits a long-lived excited state (τ = 1.04 μs) that is reductively quenched by triethanolamine, TEOA (eq 2)



$k_q = 2 \times 10^8 \text{ M}^{-1} \text{ s}^{-1}$ . The photoproduct, Ru(bpz)<sub>3</sub><sup>+</sup>, formed by the electron-transfer process is a powerful reductant,  $E^\circ[\text{Ru}(\text{bpz})_3^+/\text{Ru}(\text{bpz})_3^{2+}] = -0.86 \text{ V vs. SCE}$ .

The reduction potential for half-cell reaction of CO<sub>2</sub> reduction to CH<sub>4</sub> (eq 2) at pH 7 corresponds to  $E^\circ = -0.24 \text{ V vs. NHE}$ . Electrochemical studies<sup>10</sup> have indicated that CO<sub>2</sub> is reduced to CH<sub>4</sub> at a Ru electrode at an applied potential that corresponds to -0.5 V vs. SCE. Thus, photogenerated Ru(bpz)<sub>3</sub><sup>+</sup> is thermo-

(12) Furlong, D. N.; Launikonis, A.; Sasse, W. H.; Sanders, J. V. *J. Chem. Soc., Faraday Trans. 1* 1984, 80, 571-588.

(13) Crutchley, R. J.; Lever, A. B. P. *J. Am. Chem. Soc.* 1980, 102, 7128-7129.

(14) (a) Lehn, J.-M.; Zissel, R. *Proc. Natl. Acad. Sci. U.S.A.* 1982, 79, 701-704. (b) *Encyclopedia of Electrochemistry of the Elements*; Bard, A. J., Ed.; Dekker: New York, 1976; Vol. 7.

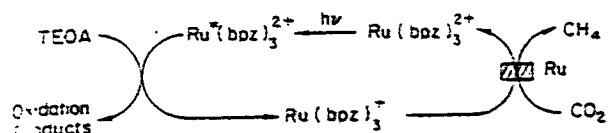


Figure 3. Schematic cycle for the photosensitized reduction of  $\text{CO}_2$  to  $\text{CH}_4$ .

dynamically capable of reducing  $\text{CO}_2$  to  $\text{CH}_4$ . To account for the functions of the different components included in the system that leads to the reduction of  $\text{CO}_2$ , a laser flash photolysis study was performed (Figure 2). Flashing a system that includes  $\text{Ru}(\text{bpz})_3^{2+}$  and TEOA under an inert Ar atmosphere results in the trace displayed in Figure 2a. Namely, flashing of the system results in the formation of  $\text{Ru}(\text{bpz})_3^+$ . This photoproduct decays for ca. 80  $\mu\text{s}$ , as a result of back reaction with  $\text{TEOA}^{\cdot+}$ , and later is accumulated as a result of irreversible decomposition of the latter photoproduct. A similar trace is observed under a  $\text{CO}_2$  atmosphere, implying that  $\text{Ru}(\text{bpz})_3^+$  is unaffected by  $\text{CO}_2$  in the absence of the catalyst. Introduction of the Ru colloid to the  $\text{Ru}(\text{bpz})_3^{2+}$ -TEOA system under Ar atmosphere results upon flashing in the trace displayed in Figure 2b. It is evident that in the presence of the Ru colloid, the photoproduct  $\text{Ru}(\text{bpz})_3^+$  decays ( $\tau = 170 \mu\text{s}$ ), implying that electron transfer to the colloid occurs. We attribute this decay process to a charging process of the Ru colloid<sup>15</sup> by  $\text{Ru}(\text{bpz})_3^+$ . Even more interesting is the behavior of flash-photogenerated  $\text{Ru}(\text{bpz})_3^+$  in the presence of the Ru colloid and  $\text{CO}_2$  (Figure 2c). It can be seen that in the presence of these two components  $\text{Ru}(\text{bpz})_3^+$  rapidly decays and its lifetime is considerably shortened ( $\tau = 50 \mu\text{s}$ ), as compared to the system in the absence of  $\text{CO}_2$  or the system where the Ru colloid is excluded. These results clearly indicate that electron transfer from  $\text{Ru}(\text{bpz})_3^+$  is very rapid in the presence of the Ru colloid and  $\text{CO}_2$  together. This effect might be attributed to either improvement of the charging capability of the Ru colloid (via, for example, electron transfer from the colloid to adsorbed  $\text{CO}_2$ ), or to direct reduction of  $\text{CO}_2$  adsorbed to the metal colloid. Nevertheless, the decay curve of  $\text{Ru}(\text{bpz})_3^+$  in the presence of the Ru metal and  $\text{CO}_2$  shows a single exponential decay, and thus the first possibility is preferred. In view of these results, we suggest the schematic cycle presented in Figure 3 as a possible route for the photoreduction of  $\text{CO}_2$  to  $\text{CH}_4$ .

Previous studies have shown that  $\text{Ru}(\text{bpz})_3^{2+}$  can be effectively reduced by TEOA in ethanol.<sup>10</sup> Thus, we have studied the reduction of  $\text{CO}_2$  to methane using  $\text{Ru}(\text{bpz})_3^{2+}$  as sensitizer, TEOA as electron donor, and the Ru colloid in a mixture of  $\text{H}_2\text{O}$ -ethanol (2:1). The rate of  $\text{CH}_4$  formation is displayed in Figure 1b and corresponds to a quantum yield of  $\phi = 0.04\%$ . The higher quantum yield obtained under these conditions is mainly attributed to the effectiveness of  $\text{Ru}(\text{bpz})_3^+$  formation in this medium. Introduction of the Ru colloid to the photogenerated  $\text{Ru}(\text{bpz})_3^+$  in the water-ethanol mixture results in the evolution of  $\text{CH}_4$  and recovery of  $\text{Ru}(\text{bpz})_3^{2+}$ . These results are consistent with the previously described mechanistic cycle outlined in Figure 3. It should be noted that in the absence of  $\text{CO}_2$ , no  $\text{H}_2$  evolution is detected. Thus, the conversion to methane is not considered to proceed via hydrogenation of  $\text{CO}_2$  but rather via electron transfer to metal-activated  $\text{CO}_2$  followed by protonation. In the electrochemical reduction of  $\text{CO}_2$  to  $\text{CH}_4$ , it has been observed<sup>10</sup> that the Ru electrode undergoes partial oxidation by  $\text{CO}_2$  to form CO. In our system no CO formation is detected, yet such partial oxidative corrosion of the Ru colloid is not excluded.

In conclusion, we have demonstrated that the photosensitized reduction of  $\text{CO}_2$  to  $\text{CH}_4$  can be accomplished with photogenerated  $\text{Ru}(\text{bpz})_3^+$  in the presence of colloidal Ru. The functions of the metal colloid in this process clearly indicate that in the presence of  $\text{CO}_2$ , electron transfer from  $\text{Ru}(\text{bpz})_3^+$  to the colloid-associated  $\text{CO}_2$  is effective. Further experiments utilizing other catalysts and attempts to further characterize mechanistic aspects of the process are now under way in our laboratory.

### Neutral Gas-Phase Analogs of Condensed-Phase Post-Transition-Metal Cluster Ions: Laser Vaporization and Photoionization of Sn/Bi and Pb/Sb Alloys

R. G. Wheeler, K. LaiHing, W. L. Wilson, J. D. Allen, R. B. King, and M. A. Duncan\*

Department of Chemistry  
School of Chemical Sciences, University of Georgia  
Athens, Georgia 30602

Received August 18, 1986

The recent development of laser vaporization/molecular beam technology<sup>1</sup> has resulted in numerous studies of gas-phase metal cluster molecules.<sup>2</sup> Various experiments have examined the structures of diatomic<sup>3</sup> and triatomic<sup>4</sup> species, as well as size-dependent properties such as ionization potentials,<sup>5</sup> chemical reactivity,<sup>6</sup> and fragmentation.<sup>7</sup> Semiconductors<sup>8</sup> and other materials<sup>9</sup> have also been included in this growing area of research. Prior to the development of these rather exotic techniques, however, cluster systems had already been studied for many years in condensed phases. For example, borane,<sup>10,11</sup> carborane,<sup>10-12</sup> transition-metal carbonyl,<sup>13</sup> and post-transition-metal ion<sup>14-17</sup> cluster systems are well characterized. In general, condensed-phase clusters have limited volatility and are coordinatively saturated with external ligands so that detailed comparisons with bare-metal gas-phase species are not possible. However, ionic clusters of the post-transition elements ( $\text{Sn}_n^{2+}$ ,  $\text{Pb}_n^{4+}$ ,  $\text{Bi}_n^{5+}$ , etc.)<sup>15</sup> are ligand-free, consisting of charged metal polyhedral networks accompanied by counterions. These systems have been investigated extensively through NMR and X-ray diffraction experiments<sup>15</sup> and theoretical treatments using molecular orbital methods as well as less rigorous electron counting techniques.<sup>13,14</sup> In this report we describe the observation of neutral gas-phase counterparts to these condensed-phase ionic clusters. These results establish one of the few existing links between cluster research in these different environments.

- (1) (a) Dietz, T. G.; Duncan, M. A.; Powers, D. E.; Smalley, R. E. *J. Chem. Phys.* 1981, 74, 6511. (b) Bondybey, V. E.; English, J. H. *J. Chem. Phys.* 1981, 74, 6978. (c) Hopkins, J. B.; Langridge-Smith, P. R. R.; Morse, M. D.; Smalley, R. E. *J. Chem. Phys.* 1983, 78, 1627.
- (2) Morse, M. D. *Chem. Rev.*, in press.
- (3) Weltner, W.; van Zee, R. *J. Atmos. Res. Phys. Chem.* 1984, 35, 291.
- (4) (a) Morse, M. D.; Hopkins, J. B.; Langridge-Smith, P. R. R.; Smalley, R. E. *J. Chem. Phys.* 1983, 79, 5316. (b) Rohlfing, E. A.; Valentini, J. J. *J. Chem. Phys. Lett.* 1986, 126, 113. (c) Crumley, W. H.; Hayden, J. S.; Gole, J. L. *J. Chem. Phys.* 1986, 84, 5250.
- (5) (a) Rohlfing, E. A.; Cox, D. M.; Kaldor, A.; Johnson, K. *J. Chem. Phys.* 1984, 81, 3846. (b) Whetten, R. L.; Zakin, M. R.; Cox, D. M.; Trevor, D. J.; Kaldor, A. *J. Chem. Phys.* 1986, 85, 1697.
- (6) (a) Geusic, M. E.; Morse, M. D.; O'Brien, S. C.; Smalley, R. E. *J. Chem. Phys.* 1985, 82, 590. (b) Morse, M. D.; Geusic, M. E.; Heath, J. R.; Smalley, R. E. *J. Chem. Phys.* 1985, 83, 2293. (c) Whetten, R. L.; Cox, D. M.; Trevor, D. J.; Kaldor, A. *Phys. Rev. Lett.* 1985, 54, 1494. (d) Trevor, D. J.; Whetten, R. L.; Cox, D. M.; Kaldor, A. *J. Am. Chem. Soc.* 1985, 107, 518. (e) Richtsmeier, S. C.; Parix, E. K.; Liu, K.; Pobo, L. G.; Riley, S. J. *J. Chem. Phys.* 1985, 82, 3659.
- (7) Brucat, P. J.; Zheng, L. S.; Pettiette, C. L.; Yang, S.; Smalley, R. E. *J. Chem. Phys.* 1986, 84, 3078.
- (8) (a) Bloomfield, L. A.; Freeman, R. R.; Brown, W. A. *Phys. Rev. Lett.* 1985, 20, 2246. (b) Geusic, M. E.; McIlrath, T. J.; Jarrold, M. F.; Bloomfield, L. A.; Freeman, R. R.; Brown, W. L. *J. Chem. Phys.* 1986, 84, 2421. (c) Mandich, M. L.; Reents, W. D., Jr.; Bondybey, V. E. *J. Phys. Chem.* 1986, 90, 2315.
- (9) Bondybey, V. E.; Schwartz, G. P.; English, J. H. *J. Chem. Phys.* 1983, 78, 11.
- (10) (a) Muetterties, E. L.; Knoth, W. H. *Polyhedral Boranes*; Marcel Dekker: New York, 1968. (b) Rudolph, R. W. *Acc. Chem. Res.* 1976, 9, 446.
- (11) Wade, K. *Adv. Inorg. Chem. Radiochem.* 1976, 18, 1.
- (12) Grimes, R. N. *Carboranes*; Academic: New York, 1970.
- (13) (a) Muetterties, E. L.; Rhodin, T. N.; Bond, E.; Bruckner, C. F.; Pretzer, W. R. *Chem. Rev.* 1979, 79, 91. (b) Cotton, F. A.; Walton, R. A. *Multiple Bonds Between Metal Atoms*; Wiley: New York, 1982. (c) Schmid, G. *Struct. Bonding (Berlin)* 1985, 62, 51.
- (14) King, R. B. *Inorg. Chim. Acta* 1982, 57, 79.
- (15) Corbett, J. D. *Chem. Rev.* 1985, 85, 383.
- (16) Lohr, L. L. *Inorg. Chem.* 1981, 20, 4229.
- (17) Burns, R. C.; Gillespie, R. J.; Barnes, J. A.; McGlinchey, M. J. *Inorg. Chem.* 1982, 21, 799.

\*Delcourt, M. O.; Keghouche, N. *Nouv. J. Chim.* 1985, 9, 235-240.

These structures consist of alkyl groups which, on average, experience a crystalline-like environment, are canted from the surface normal, and packed to high densities sufficient to form high-quality barriers for both electron- and ion-transfer processes. Defects in these structures would be expected because of the complex surface morphology of the polycrystalline gold including crystallographic faceting and surface roughness as well as the complexities of the thiol head-group attachment chemistry and mismatches of ideal lattice parameters for the alkyl chains and the substrate-bound head groups. However, for the case of the long-chain thiols, the van der Waals interactions of the chains appear to sustain a structure which is a very effective dielectric barrier. Shorter chain lengths promote a loss of film organization. This results in a decreased packing density and the onset of permeability by  $\text{Cl}^-$  and  $\text{ClO}_4^-$ .

This study clearly shows that significant potential exists to adapt these *n*-alkyl thiol monolayer assemblies for use as model systems for fundamental studies of heterogeneous charge-transfer, ion transport and double-layer phenomena. There are several po-

tentially fruitful modifications, not considered in this first study that could lead to improve the properties of this model system. These include the use of smooth, single-crystal gold substrate and the optimization of adsorption conditions as well as variation in the molecular structures of the thiols. Utilization of these approaches for various applications is presently underway.

**Acknowledgment.** The authors gratefully acknowledge many valuable discussions with G. Whitesides, B. Troughton, and the co-workers at Harvard University. We thank B. Troughton for the gift of  $\text{CH}_3(\text{CH}_2)_{21}\text{SH}$ . Also acknowledged are discussions with H. Finklea and J. Sagiv in the initial stages of this study. We are particularly grateful to R. Nuzzo for critical discussion during the course of this study. The useful comments of one reviewer are acknowledged.

Registry No.  $\text{CH}_3\text{CH}_2\text{SH}$ , 75-08-1;  $\text{CH}_3(\text{CH}_2)_5\text{SH}$ , 109-79-5;  $\text{CH}_3(\text{CH}_2)_9\text{SH}$ , 111-31-9;  $\text{CH}_3(\text{CH}_2)_{11}\text{SH}$ , 111-88-6;  $\text{CH}_3(\text{CH}_2)_{13}\text{SH}$ , 143-10-2;  $\text{CH}_3(\text{CH}_2)_{15}\text{SH}$ , 1322-36-7;  $\text{CH}_3(\text{CH}_2)_{17}\text{SH}$ , 2917-26-2;  $\text{CH}_3(\text{CH}_2)_{19}\text{SH}$ , 2885-00-9;  $\text{CH}_3(\text{CH}_2)_{21}\text{SH}$ , 7773-83-3; Au, 7440-57-5.

## Improved Charge Separation and Photosensitized $\text{H}_2$ Evolution from Water with $\text{TiO}_2$ Particles on Colloidal $\text{SiO}_2$ Carriers

Arthur J. Frank,<sup>\*†</sup> Itamar Willner,<sup>\*‡</sup> Zafrir Goren,<sup>‡</sup> and Yinon Degani<sup>‡</sup>

Contribution from the Solar Energy Research Institute, Golden, Colorado 80401, and The Department of Organic Chemistry, The Hebrew University of Jerusalem, Jerusalem 91904, Israel. Received September 25, 1986

**Abstract:** Laser flash photolysis and steady-state photolysis studies show that electrostatic interactions have a dramatic influence on the kinetics for charge separation and hydrogen production in aqueous systems (pH 9.8) of 20-nm diameter  $\text{TiO}_2$ -modified  $\text{SiO}_2$  colloids in various combinations with an electron relay, a photosensitizer, and a Pt catalyst. Either direct excitation of the semiconductor or the photosensitizer  $\text{Ru}(\text{bpy})_3^{2+}$  ( $\text{bpy} = 2,2'$ -bipyridine), electrostatically adsorbed to the colloid, initiate electron transfer to either the zwitterionic electron relay, *N,N'*-bis(3-sulfonatopropyl)-4,4'-bipyridinium ( $\text{PVS}^0$ ), or *N,N'*-bis(3-sulfonatopropyl)-2,2'-bipyridinium ( $\text{DQS}^0$ ), or methyl viologen ( $\text{MV}^{2+}$ ). The rates and quantum yields for the formation of the radical  $\text{PVS}^{\cdot-}$  anion in both the  $\text{TiO}_2\text{-SiO}_2/\text{PVS}^0$  and the  $\text{TiO}_2\text{-SiO}_2/\text{Ru}(\text{bpy})_3^{2+}/\text{PVS}^0$  systems decline with increasing ionic strength. The rate and quantum yields for  $\text{H}_2$  production in both the  $\text{TiO}_2\text{-SiO}_2/\text{DQS}^0/\text{Pt}$  and the  $\text{TiO}_2\text{-SiO}_2/\text{Ru}(\text{bpy})_3^{2+}/\text{DQS}^0/\text{Pt}$  systems also show a similar ionic strength dependence. Kinetic analysis of the data infers that repulsion of the reduced zwitterionic relay  $\text{PVS}^{\cdot-}$  and  $\text{DQS}^{\cdot-}$  from the negatively charged colloidal interface inhibits back electron transfer to both the semiconductor and the surface-attached oxidized photosensitizer  $\text{Ru}(\text{bpy})_3^{2+}$ . Formation of the cation  $\text{MV}^{\cdot+}$  radical and its back electron transfer to the semiconductor are rapid and imply that the  $\text{MV}^{2+}$  electron relay is in close proximity to the colloid. Both the photogenerated valence-band holes and the oxidized photosensitizer  $\text{Ru}(\text{bpy})_3^{2+}$  oxidize surface  $\text{Ti-O}^-$  groups of  $\text{TiO}_2$ . This redox process has the important effect of recycling the photosensitizer for further reaction. The addition of the superoxide dismutase enzyme to the oxidized  $\text{TiO}_2\text{-(SiO}_2)$  system regenerates, in part, the activity of the semiconductor to evolve  $\text{H}_2$  and to release molecular oxygen.

Light-induced electron-transfer reactions in colloidal and particulate semiconductor dispersions have become an active area of research in photochemistry.<sup>1</sup> Extensive studies have demonstrated the potential utility of semiconductor particles as light-harvesting units in the photochemical conversion and storage of solar energy. Semiconductor particles of minute size (diameters of 5–50 nm) can have high efficiencies for the photogeneration of electron-hole pairs because of the short transit time of charge carriers from the particle interior to the surface compared with the long relaxation time for charge recombination in the bulk of the semiconductor.<sup>2</sup> A crucial problem inherent to microheterogeneous systems is, however, the rapid surface recombination of photogenerated electrons and holes as well as the back electron transfer between the semiconductor and reactive intermediates formed at the semiconductor particle-liquid interface. A second obstacle to the exploitation of small semiconductor particles for photochemical solar energy conversion is the absence of materials

that not only form colloids but also have good photostability and high solar spectral response. One approach that addresses this

(1) See, for example: (a) Kraeutler, B.; Bard, A. J. *J. Am. Chem. Soc.* 1978, 100, 2239. (b) Duonghong, D.; Borgarello, E.; Grätzel, M. *J. Am. Chem. Soc.* 1981, 103, 4685. (c) Henglein, A. *Ber. Bunsenges. Phys. Chem.* 1982, 86, 301. (d) Fox, M. A.; Lindig, B.; Chen, C. C. *J. Am. Chem. Soc.* 1982, 104, 5828. (e) Grätzel, M., Ed. *Energy Resources Through Photochemistry and Catalysis*; Academic Press: New York, 1983. (f) Meissner, D.; Memming, R.; Kastening, B. *Chem. Phys. Lett.* 1983, 96, 34. (g) Brus, L. E. *J. Chem. Phys.* 1984, 80, 4403. (h) Nenadović, M. T.; Rajh, T.; Mičić, O.; Nozik, A. J. *J. Phys. Chem.* 1984, 88, 5827. (i) Yesodharan, E.; Yesodharan, S.; Grätzel, M. *Solar Energy Materials* 1984, 10, 287. (j) Mau, A. W.-H.; Huang, C.-B.; Kakuta, N.; Bard, A. J.; Campion, A.; Fox, M. A.; White, J. M.; Webber, S. E. *J. Am. Chem. Soc.* 1984, 106, 6537. (k) Fojtík, A.; Weller, M.; Koch, U.; Henglein, A. *Ber. Bunsenges. Phys. Chem.* 1984, 88, 969. (l) Kuczynski, J. P.; Milosajević, B. H.; Thomas, J. K. *J. Phys. Chem.* 1984, 88, 980. (m) Ramsden, J. J.; Webber, S. E.; Grätzel, M. *J. Phys. Chem.* 1985, 89, 2740. (n) Tricot, Y.-M.; Emeren, A.; Fendler, J. H. *J. Phys. Chem.* 1985, 89, 4721. (o) Harada, H.; Sakata, T.; Ueda, T. *J. Am. Chem. Soc.* 1985, 107, 1773. (p) Serpone, N.; Sharma, K. D.; Jamieson, M. A.; Grätzel, M.; Ramsden, J. *Chem. Phys. Lett.* 1985, 115, 473. (q) Kamat, P. V. *Langmuir* 1985, 1, 608. (r) Yanagida, S.; Mizumoto; Pac, C. J. *J. Am. Chem. Soc.* 1986, 108, 647. (s) Pelizzetti, E.; Serpone, N., Eds. *Homogeneous and Heterogeneous Photocatalysis*; D. Reidel Publishing Co.: Dordrecht, 1986.

<sup>\*</sup>Solar Energy Research Institute.

<sup>†</sup>The Hebrew University of Jerusalem.



latter problem is to develop new materials (e.g., molecular semiconductors<sup>3</sup>) having the appropriate properties. Another strategy is to use known materials that form colloids and then to modify them to obtain the other desired properties. Toward this end, a considerable amount of work has been concerned with the photo-sensitization of stable wide-bandgap semiconductors such as TiO<sub>2</sub><sup>4,5</sup> with chromophores that absorb strongly in the visible and near-infrared regions of the solar spectrum. Photosensitizers have also been used in nonsemiconductor-based systems to bring about the cleavage of water,<sup>6</sup> CO<sub>2</sub> fixation,<sup>7</sup> and other chemical transformations.<sup>8,9</sup> Efficient conversion of light energy requires that back charge transfer to the oxidized (or reduced) photosensitizer be suppressed. Charged colloids such as SiO<sub>2</sub> and ZrO<sub>2</sub> have been shown to provide effective microenvironments for controlling electron-transfer reactions between photosensitizers and electron relays.<sup>10,11</sup> With SiO<sub>2</sub> colloids, for example, good charge separation between the oxidized photosensitizer and the reduced electron relay has been accomplished. The mechanism involves the selective electrostatic association of one of the redox products with the charged colloid and the specific repulsion of the partner product from the colloid interface. In these photochemical systems, a sacrificial electron donor is generally required to recycle the photosensitizer. Hydrogen is evolved upon reaction of the reduced electron relay with an appropriate catalyst under suitable conditions.

We report here the first example of the application of electrostatic effects to control electron transfer in a colloidal or a particulate semiconductor-based system. Electrostatic effects are found to produce a marked improvement in the kinetics for charge separation and hydrogen production in aqueous media. The representative system consisted of TiO<sub>2</sub> particles immobilized on negatively charged SiO<sub>2</sub> colloids in various combinations with a zwitterionic electron relay, a photosensitizer, and a colloidal Pt catalyst. The photosensitizer was Ru(bpy)<sub>3</sub><sup>2+</sup> (bpy = 2,2'-bipyridine) and the zwitterionic electron relay was either *N,N'*-

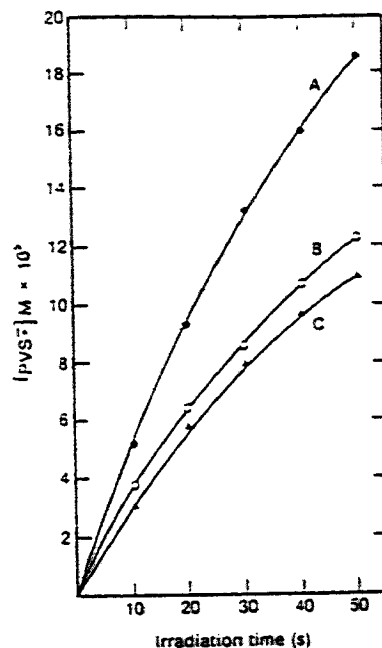
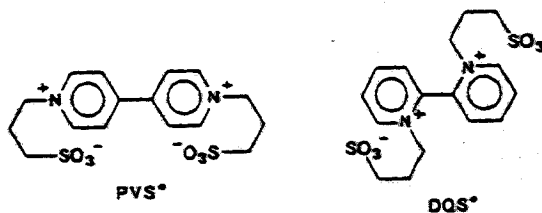


Figure 1. Production of PVS<sup>-</sup> with irradiation time ( $\lambda > 305$  nm) for  $2 \times 10^{-3}$  M PVS<sup>0</sup> with 0.5% TiO<sub>2</sub>-SiO<sub>2</sub> colloids in aqueous solutions at pH 9.8 with (A) no added salt, (B) 0.06 M NaCl, and (C) 0.14 M NaCl.

bis(3-sulfonatopropyl)-4,4'-bipyridinium (PVS<sup>0</sup>) or *N,N'*-bis(3-sulfonatopropyl)-2,2'-bipyridinium (DQS<sup>0</sup>).



### Experimental Section

**Materials.** *N,N'*-Bis(3-sulfonatopropyl)-4,4'-bipyridinium (PVS<sup>0</sup>) and *N,N'*-bis(3-sulfonatopropyl)-2,2'-bipyridinium (DQS<sup>0</sup>) were prepared as described elsewhere.<sup>11a,12</sup> The titania-modified silica (TiO<sub>2</sub>-SiO<sub>2</sub>) colloids (24.2% (w/w)) were obtained from Nalco Chemical Co. The colloids were dialyzed for 10 h and diluted to the desired concentrations. Transmission electron microscopy (TEM), measurements of the TiO<sub>2</sub>-SiO<sub>2</sub> dispersion show that the TiO<sub>2</sub> particles (4-nm diameter) are distributed nonhomogeneously onto spherical SiO<sub>2</sub> colloids (30-nm diameter). Some SiO<sub>2</sub> particles have no TiO<sub>2</sub> sites, whereas others have one or more TiO<sub>2</sub> particles on the surface. Still others have a cluster of TiO<sub>2</sub> particles present at the interface of several SiO<sub>2</sub> colloids. Whether the latter type of aggregation also exists in aqueous solution is speculative. Although both TiO<sub>2</sub> and SiO<sub>2</sub> are each charged negatively at the pH of the solution (pH 9.8), the TEM indicates that they are present as colloids. In other words, the TiO<sub>2</sub> is associated with the silica and is not free in solution. Colloidal Pt (12 mg l<sup>-1</sup>; 2 nm particle diameter) was prepared by the citrate reduction of H<sub>2</sub>PtCl<sub>6</sub><sup>13</sup> and dialyzed just prior to use.

**Apparatus.** Laser photolysis experiments employed a Molelectron UV-IU nitrogen-pumped Molelectron DL200 dye laser combined with fast kinetic spectroscopy to detect transient species. Continuous illumination was carried out with a PTI Model A-1000 Xe lamp equipped with a 3 cm path length copper sulfate solution to remove IR radiation and a cutoff filter ( $\lambda > 400$  nm, incident photon flux =  $1.8 \times 10^{-7}$  einstein s<sup>-1</sup> cm<sup>-2</sup>;  $\lambda > 305$  nm, incident photon flux =  $2.3 \times 10^{-7}$  einstein s<sup>-1</sup> cm<sup>-2</sup>). Absorption spectra were recorded on a Uvikon-820 (Kontron) spectrophotometer equipped with a  $\psi$ -80 computer (Kontron) for data acquisition and reduction. Hydrogen and oxygen were measured with a

- (2) Grätzel, M.; Frank, A. J. *J. Phys. Chem.* 1982, 86, 2964.  
 (3) Houlding, V. H.; Frank, A. J. *Inorg. Chem.* 1985, 24, 3664.  
 (4) (a) Clark, W. D. K.; Sutin, N. *J. Am. Chem. Soc.* 1977, 99, 4676. (b) Fujihara, M.; Oshishi, H.; Osa, T. *Nature (London)* 1977, 268, 226. (c) Spitzer, M.; Calvin, M. *J. Chem. Phys.* 1977, 66, 4294. (d) Hammett, A.; Dare-Edwards, M. P.; Wright, R. D.; Seddon, K. R.; Goodenough, J. P. *J. Phys. Chem.* 1979, 83, 3280. (e) Dare-Edwards, M. P.; Goodenough, J. P.; Hammett, A.; Seddon, K. R.; Wright, R. D. *Faraday Discuss. Chem. Soc.* 1980, 70, 285. (f) Girardeau, A.; Fan, F.-R. F.; Bard, A. J. *J. Am. Chem. Soc.* 1980, 102, 5137. (g) Gulino, D. A.; Drickamer, H. G. *J. Phys. Chem.* 1984, 88, 1173.  
 (5) (a) Fan, F. R. F.; Bard, A. J. *J. Am. Chem. Soc.* 1979, 101, 6139. (b) Duonghong, D.; Borgarello, E.; Grätzel, M.; Pelizzetti, E.; Visca, M. *J. Am. Chem. Soc.* 1981, 103, 4685. (c) Borgarello, E.; Kiwi, J.; Grätzel, M.; Pelizzetti, E.; Visca, M. *J. Am. Chem. Soc.* 1982, 104, 2996. (d) Houlding, V. H.; Grätzel, M. *J. Am. Chem. Soc.* 1983, 105, 5695. (e) Hashimoto, K.; Iwai, T.; Sakata, T. *Nouv. J. Chim.* 1983, 7, 249. (f) Duonghong, D.; Sorpone, N.; Grätzel, M. *Helv. Chim. Acta* 1984, 67, 1012. (g) Moser, J.; Grätzel, M. *J. Am. Chem. Soc.* 1984, 106, 6557. (h) Borgarello, E.; Pelizzetti, E.; Ballardini, R.; Scandola, F. *Nouv. J. Chim.* 1984, 8, 567. (i) Desilvestro, J.; Grätzel, M.; Kavan, L.; Moser, J. *J. Am. Chem. Soc.* 1985, 107, 2988. (j) Shimidzu, T.; Iyoda, T.; Koide, Y. *J. Am. Chem. Soc.* 1985, 107, 35. (k) Kamat, P. V. *J. Chem. Soc., Faraday Trans.* 1985, 81, 509. (l) Kamat, P. V.; Chauvet, J.-P.; Fessenden, R. W. *J. Phys. Chem.* 1986, 90, 1389. (m) Fessenden, R. W.; Kamat, P. V. *Chem. Phys. Lett.* 1986, 123, 233. (n) Furlong, D. N.; Wells, D.; Sasse, W. H. F. *J. Phys. Chem.* 1986, 90, 1107.  
 (6) (a) Borgarello, E.; Kiwi, J.; Pelizzetti, E.; Visca, M.; Grätzel, M. *Nature (London)* 1981, 289, 158. (b) Kalyanasundaram, K.; Grätzel, M. *Angew. Chem., Int. Ed. Engl.* 1979, 18, 701. (c) Kiwi, J.; Borgarello, E.; Pelizzetti, E.; Visca, M.; Grätzel, M. *Angew. Chem., Int. Ed. Engl.* 1980, 19, 647.  
 (7) Willner, I.; Mandler, D.; Riklin, A. *J. Chem. Soc., Chem. Commun.* 1986, 1022.  
 (8) Wheeler, J.; Thomas, K. J. *J. Phys. Chem.* 1982, 86, 4540.  
 (9) (a) Degani, Y.; Willner, I. *J. Chem. Soc., Chem. Commun.* 1985, 648. (b) Mandler, D.; Willner, I. *J. Chem. Soc., Perkin Trans. 2* 1986, 805.  
 (10) (a) Willner, I.; Otvos, J. W.; Calvin, M. *J. Am. Chem. Soc.* 1981, 103, 3203. (b) Willner, I.; Yang, J. M.; Otvos, J. W.; Calvin, M. *J. Phys. Chem.* 1981, 85, 3277. (c) Willner, I.; Laane, C.; Otvos, J. W.; Calvin, M. In *Inorganic Reactions in Organized Media*; Holt, S. L., Ed.; American Chemical Society: Washington, DC, 1982; ACS Symp. Ser. No. 177, pp 71. (d) Furlong, D. A. *Aust. J. Chem.* 1982, 35, 911.  
 (11) (a) Degani, Y.; Willner, I. *J. Am. Chem. Soc.* 1983, 105, 6228. (b) Willner, I.; Degani, Y. *Isr. J. Chem.* 1982, 22, 163.

- (12) Willner, I.; Ford, W. E. *J. Heterocycl. Chem.* 1983, 20, 1113.  
 (13) (a) Furlong, D. A.; Lannikonis, A.; Sasse, W. H. F. *J. Chem. Soc., Faraday Trans. 1* 1984, 80, 571. (b) Aika, K.; Ban, L. L.; Okura, I.; Namba, S.; Turkevich, J. *J. Res. Inst. Catal., Hokkaido Univ.* 1976, 24, 55.

Packard Model 427 gas chromatograph equipped with a 5-Å molecular sieve column, a thermal conductivity detector, and argon or helium as the carrier gas for H<sub>2</sub> or O<sub>2</sub> analyses, respectively.

**General Photolysis Samples and Procedures.** In the UV-photolysis studies of PVS<sup>0</sup>, the samples consisted of 0.5% (w/w) TiO<sub>2</sub>-SiO<sub>2</sub> colloids and 2 × 10<sup>-3</sup> M PVS<sup>0</sup> in 3 mL of aqueous solutions at pH 9.8. In the investigation of H<sub>2</sub> production in the ultraviolet region, the samples contained 2.4% (w/w) TiO<sub>2</sub>-SiO<sub>2</sub> colloids and 2 × 10<sup>-3</sup> M DQS<sup>0</sup> in 3 mL of aqueous solutions at pH 9.8. In the photosensitization studies of H<sub>2</sub> evolution, 6 × 10<sup>-3</sup> M Ru(bpy)<sub>3</sub><sup>2+</sup> was added to the above samples and the concentrations of the TiO<sub>2</sub>-SiO<sub>2</sub> were either 1.2% or 0.6% (w/w). The photolysis vessel was a 1-cm cuvette fitted with a microvalve and rubber septum. Prior to photolysis, the solutions were deaerated by repeated evacuation and argon bubbling cycles. During irradiation, the cuvette was maintained at 23.6 °C. The absorbed light intensity was determined with the Reinecke's salt actinometer.<sup>14</sup> Quantum yields for the formation of the methyl viologen MV<sup>2+</sup> and PVS<sup>-</sup> radical ions were determined from the knowledge of the concentrations of the species at 602 nm (MV<sup>2+</sup>, ε = 12 800 M<sup>-1</sup> cm<sup>-1</sup>; PVS<sup>-</sup>, ε = 13 800 M<sup>-1</sup> cm<sup>-1</sup>). The amount of light absorbed by Ru(bpy)<sub>3</sub><sup>2+</sup> was determined from its absorption spectrum. In the case of the TiO<sub>2</sub>-SiO<sub>2</sub> colloids, the amount of light absorbed was estimated from the difference in light intensity that was transmitted through a reaction vessel containing only water and then water plus TiO<sub>2</sub>-SiO<sub>2</sub> particles. In studies in which H<sub>2</sub>/O<sub>2</sub> production was investigated, gas samples were taken at regular intervals during photolysis and injected into the gas chromatograph for analysis.

## Results and Discussion

### Electron Transfer and H<sub>2</sub> Production in the Ultraviolet Region.

Figure 1 describes the effect of ionic strength on the generation of PVS<sup>-</sup> radical anions in the bandgap-illuminated (λ > 305 nm) TiO<sub>2</sub>-SiO<sub>2</sub>/PVS<sup>0</sup> systems in aqueous solution at pH 9.8. At this pH, the TiO<sub>2</sub>-SiO<sub>2</sub> colloids are negatively charged, since TiO<sub>2</sub> and the silanol groups of SiO<sub>2</sub><sup>15</sup> are ionized at pH 9.8. Figure 1 shows that the rate and the yield of PVS<sup>-</sup> production decline with increasing ionic strength. In the absence of added salt, the quantum yield φ for the formation of PVS<sup>-</sup> is 2.3 × 10<sup>-2</sup>. At 0.06 and 0.14 M NaCl, the quantum yields are 1.5 × 10<sup>-2</sup> and 1.2 × 10<sup>-2</sup>, respectively. The dependence of the quantum yield for PVS<sup>-</sup> formation on the ionic strength is attributed to electrostatic interactions between the colloids and the PVS<sup>-</sup> radical anion. Also, since no photoreduction of the PVS<sup>0</sup> charge relay occurs in the SiO<sub>2</sub>/PVS<sup>0</sup> system (i.e., in a system without TiO<sub>2</sub>), we infer that TiO<sub>2</sub> is the photoactive component involved in the electron transfer to PVS<sup>0</sup>. Thus, at low ionic strength, the surface potential of the TiO<sub>2</sub>-SiO<sub>2</sub> colloid is sufficiently negative to inhibit the approach of PVS<sup>-</sup> radical anions to the immobilized TiO<sub>2</sub> sites. With increasing ionic strength, the electrical field of TiO<sub>2</sub>-SiO<sub>2</sub> is screened and the rate of reaction of the PVS<sup>-</sup> radicals with the photogenerated valence-band holes of TiO<sub>2</sub> increases.



It is important to note that the photoreduction of PVS<sup>0</sup> in the TiO<sub>2</sub>-SiO<sub>2</sub>/PVS<sup>0</sup> system occurs without the addition of a sacrificial electron donor (or hole acceptor) such as triethanolamine for reasons that are discussed below.

To further investigate the role of electrostatic forces in controlling electron transfer, methyl viologen was substituted for PVS<sup>0</sup>. Whereas PVS<sup>0</sup> is a zwitterion that becomes negatively charged when reduced, methyl viologen MV<sup>2+</sup> forms the positively charged MV<sup>•+</sup> radical upon reduction. Several studies<sup>16,17</sup> have examined the photoreduction of MV<sup>2+</sup> by TiO<sub>2</sub> colloids. In the case of TiO<sub>2</sub>-SiO<sub>2</sub> colloids, we have found that the quantum yield for

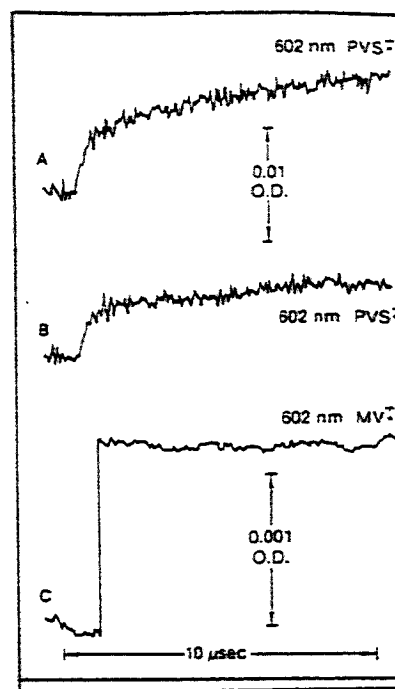


Figure 2. Absorption transients for the production of PVS<sup>-</sup> (A and B) and MV<sup>2+</sup> (C) for aqueous solutions (pH 9.8) of 0.5% TiO<sub>2</sub>-SiO<sub>2</sub> colloid with 2 × 10<sup>-3</sup> M PVS<sup>0</sup> or 2 × 10<sup>-3</sup> M MV<sup>2+</sup>, respectively. Ionic strength effects: no added salt in part A and 0.11 M NaCl in part B. 337-nm laser excitation.

reduction of MV<sup>2+</sup> (φ = 9.6 × 10<sup>-3</sup>) without added salt is close to that observed for PVS<sup>0</sup> (φ = 1.2 × 10<sup>-2</sup>) at high ionic strength (μ = 0.14 M = [NaCl]). Furthermore, in contrast to the absorption spectrum of the reduction product of PVS<sup>0</sup> which corresponds to that of the monomeric PVS<sup>-</sup> radical anion (λ = 602 nm; ε = 13 800 M<sup>-1</sup> cm<sup>-1</sup>), the absorption spectrum of the photoproduct of MV<sup>2+</sup> corresponds to that of the dimeric cation radical (MV<sup>•+</sup>)<sub>2</sub> (λ<sub>max</sub> = 550 nm), even when MV<sup>2+</sup> is present at low bulk concentrations in aqueous solutions. Dimer formation is, however, observed only at high concentrations of MV<sup>•+</sup>,<sup>18</sup> suggesting the buildup of a high local concentration of the MV<sup>•+</sup> radical cation at the negatively charged TiO<sub>2</sub>-SiO<sub>2</sub> colloid interface. The electrostatic attraction between the oppositely charged species also favors oxidation of the viologen radical cation by the valence-band holes of TiO<sub>2</sub> and accounts for the relatively low quantum yield for reduction of MV<sup>2+</sup> compared to that of PVS<sup>0</sup>.

Figure 2 shows the respective transient absorption spectra of MV<sup>•+</sup> and PVS<sup>-</sup>, following the pulsed 337-nm laser excitation of TiO<sub>2</sub> in the TiO<sub>2</sub>-SiO<sub>2</sub>/MV<sup>2+</sup> and the TiO<sub>2</sub>-SiO<sub>2</sub>/PVS<sup>0</sup> systems. The upper and middle traces indicate that the growth of the PVS<sup>-</sup> radical anion occurs over a period of 10 μs. The lower trace shows that the MV<sup>•+</sup> radical cation (λ = 602 nm) is present immediately after the laser pulse. One can infer from these results that the prompt reduction of MV<sup>2+</sup> is due to its close association with the TiO<sub>2</sub>-SiO<sub>2</sub> interface. The slower growth kinetics of PVS<sup>-</sup> indicates that subsequent to excitation of the semiconductor, PVS<sup>0</sup> must diffuse to the particle surface before electron transfer occurs. A comparison of the absorption transients in Figure 2, A and B, shows that the ionic strength of the solutions affects the steady-state concentration of PVS<sup>-</sup>. At low ionic strength, the back-reaction of PVS<sup>-</sup> with the photogenerated valence-band holes of TiO<sub>2</sub> is impeded by the establishment of an electrostatic barrier between PVS<sup>-</sup> and the negatively charged TiO<sub>2</sub>-SiO<sub>2</sub> colloids. At high ionic strength, the negative surface potential of TiO<sub>2</sub>-SiO<sub>2</sub> is screened and the relative rate of the reverse process (reaction 1) is accelerated, thus decreasing the net yield of PVS<sup>-</sup>. The

(14) Wegner, E. E.; Adamson, A. W. *J. Am. Chem. Soc.* 1966, 88, 394.

(15) (a) Iler, R. K. *The Chemistry of Silica*; Wiley: New York, 1979. (b) Iler, R. K. *The Colloid Chemistry of Silica and Silicates*; Cornell University Press: Ithaca, NY, 1955.

(16) (a) Duonghong, D.; Ramsden, J.; Grätzel, M. *J. Am. Chem. Soc.* 1982, 104, 2977. (b) Moser, J.; Grätzel, M. *J. Am. Chem. Soc.* 1983, 105, 6547.

(17) (a) Dimitrijevic, M. M.; Savic, D.; Micic, O. I.; Nozik, A. J. *J. Phys. Chem.* 1984, 88, 4278. (b) Brown, G. T.; Darwent, J. R. *J. Chem. Soc., Chem. Commun.* 1985, 98. (c) Brown, G. T.; Darwent, J. R.; Fletcher, P. D. I. *J. Am. Chem. Soc.* 1985, 107, 6446.

(18) Kosower, E. M.; Cotter, J. L. *J. Am. Chem. Soc.* 1964, 86, 5524.

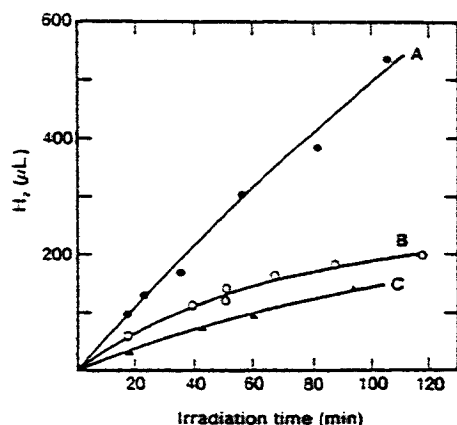


Figure 3. Production of H<sub>2</sub> with irradiation time ( $\lambda_{\text{exc}} > 305$  nm) for aqueous solutions (pH 9.8) of 2.4% TiO<sub>2</sub>-SiO<sub>2</sub> colloids,  $2 \times 10^{-3}$  M DQS<sup>0</sup>, and 12 mg L<sup>-1</sup> Pt colloids with (A) no salt, (B) 0.08 M NaCl, and (C) 0.11 M NaCl.

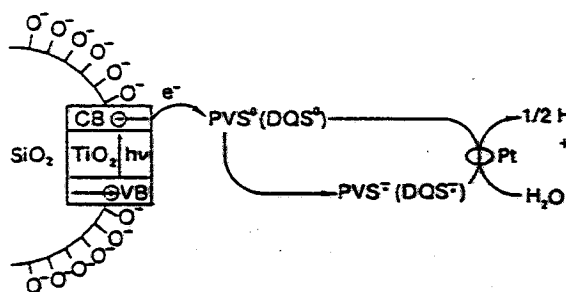


Figure 4. Representation of electrostatic effects: Following photoinitiated electron transfer from TiO<sub>2</sub> to an electron relay PVS<sup>0</sup> or DQS<sup>0</sup>, the negatively charged SiO<sub>2</sub> colloidal support repels PVS<sup>-</sup> or DQS<sup>-</sup> from the semiconductor, thus inhibiting the back reaction. The escaped DQS<sup>-</sup> is recycled through a reaction with a colloidal Pt catalyst to evolve H<sub>2</sub>.

transient and steady-state photolysis data illustrate the influence of electrostatic forces in controlling both the forward and the reverse electron transfer between the two-electron relays (PVS<sup>0</sup> and MV<sup>2+</sup>) and the TiO<sub>2</sub>-modified SiO<sub>2</sub> colloids.

The possibility that the negative surface charge of the TiO<sub>2</sub>-SiO<sub>2</sub> particles might be effective in promoting the redox chemistry for H<sub>2</sub> production was also explored. In these experiments, *N,N'*-bis(3-sulfonatopropyl)-2,2'-bipyridinium (DQS<sup>0</sup>) was used as an electron relay. The redox potential of the DQS<sup>0</sup>/DQS<sup>-</sup> couple in aqueous solutions is -0.65 V (vs. NHE) and the radical anion DQS<sup>-</sup> can reduce water to H<sub>2</sub> at pH 9.8.<sup>19</sup> The flatband potential of TiO<sub>2</sub> is pH dependent.<sup>16,20</sup> At this pH, the flatband potential of colloidal TiO<sub>2</sub> is -0.70 V (vs. NHE)<sup>16</sup> which is sufficiently negative, thermodynamically, to reduce DQS<sup>0</sup>. Figure 3 demonstrates that bandgap illumination ( $\lambda > 305$  nm) of the TiO<sub>2</sub>-SiO<sub>2</sub> colloids with DQS<sup>0</sup> and a catalytic Pt sol (12 mg/L) in aqueous solution at pH 9.8 does indeed produce molecular hydrogen. The quantum yield for H<sub>2</sub> production is  $1.6 \times 10^{-3}$ . However, the H<sub>2</sub> production exhibits a strong dependence on the ionic strength, indicating electrostatic interaction between DQS<sup>-</sup> and the negatively charged TiO<sub>2</sub>-SiO<sub>2</sub> colloids. On decreasing the ionic strength, both the yield and rate of H<sub>2</sub> production increase, implying that the DQS<sup>-</sup> radical anion was repelled from the surface of the colloid before back reaction with the valence-band holes of TiO<sub>2</sub> could take place. Inhibition of the back reaction stabilizes DQS<sup>-</sup> for subsequent reaction with the Pt catalyst and H<sub>2</sub> production. Figure 4 summarizes schematically the respective mechanisms for electron transfer and H<sub>2</sub> production in the TiO<sub>2</sub>-SiO<sub>2</sub>/PVS<sup>0</sup> and the TiO<sub>2</sub>-SiO<sub>2</sub>/DQS<sup>0</sup>/Pt systems.

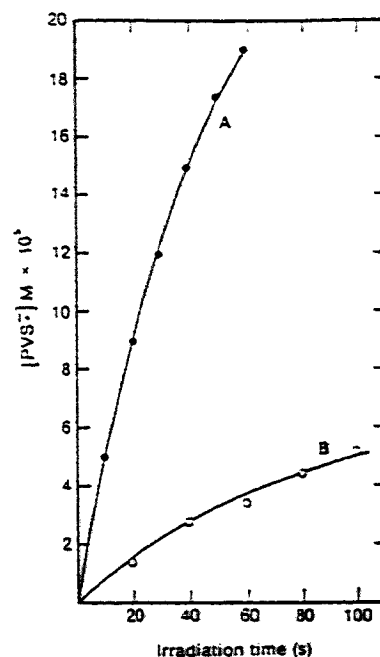


Figure 5. Production of PVS<sup>-</sup> with irradiation time ( $\lambda_{\text{exc}} > 400$  nm) for  $6 \times 10^{-3}$  M Ru(bpy)<sub>3</sub><sup>2+</sup>,  $2 \times 10^{-3}$  M PVS<sup>0</sup>, and 0.5% TiO<sub>2</sub>-SiO<sub>2</sub> colloids with (A) no added salt and (B) 0.12 M NaCl.

**Electron Transfer and H<sub>2</sub> Production in the Visible Region.** Several studies<sup>5</sup> have dealt with the photosensitization of TiO<sub>2</sub> particles to visible light by employing chromophores that can serve as electron donors to the semiconductor. It has been found<sup>5</sup> that the Ru(bpy)<sub>3</sub><sup>2+</sup> complex is a relatively poor sensitizer for TiO<sub>2</sub> compared to the carboxylic acid derivative of Ru(bpy)<sub>3</sub><sup>2+</sup> which is electrostatically attached to the semiconductor surface. The close association of the latter complex with the semiconductor surface is presumed to facilitate charge injection into the conduction band of TiO<sub>2</sub>. It has been shown<sup>10a,d</sup> that Ru(bpy)<sub>3</sub><sup>2+</sup> may be electrostatically adsorbed to the interface of colloidal SiO<sub>2</sub>. We anticipated therefore that a similar electrostatic association of Ru(bpy)<sub>3</sub><sup>2+</sup> with the TiO<sub>2</sub>-SiO<sub>2</sub> particle interface might lead to effective electron transfer from the excited state of the complex to the conduction band of TiO<sub>2</sub>. Steady-state fluorescence quenching and laser flash photolysis studies indicated, however, that the emission from excited Ru(bpy)<sub>3</sub><sup>2+</sup> is not quenched and that no photoinitiated electron transfer to TiO<sub>2</sub>(-SiO<sub>2</sub>) takes place, suggesting that the Ru(bpy)<sub>3</sub><sup>2+</sup> may be associated with the SiO<sub>2</sub> colloidal support and not with the TiO<sub>2</sub> sites.

We thought that the presence of a zwitterionic electron relay such as PVS<sup>0</sup> or DQS<sup>0</sup> might promote electron transfer in the TiO<sub>2</sub>-SiO<sub>2</sub>/Ru(bpy)<sub>3</sub><sup>2+</sup> system. For example, the reduction of PVS<sup>0</sup> or DQS<sup>0</sup> by excited Ru(bpy)<sub>3</sub><sup>2+</sup> occurs rapidly in the presence of SiO<sub>2</sub> and a sacrificial electron donor.<sup>10a,11</sup> In this system, the negatively charged SiO<sub>2</sub> colloid stabilizes the intermediate viologen radical anion against back electron transfer by repelling the reduced PVS<sup>-</sup> or DQS<sup>-</sup> from Ru(bpy)<sub>3</sub><sup>2+</sup> species adsorbed to the colloidal SiO<sub>2</sub> interface. Similar electrostatic effects are anticipated to inhibit the reverse electron transfer between the viologen radical anion and Ru(bpy)<sub>3</sub><sup>2+</sup> in the presence of TiO<sub>2</sub>-SiO<sub>2</sub> colloids. Figure 5 shows the production of PVS<sup>-</sup> in aqueous solution at pH 9.8 when Ru(bpy)<sub>3</sub><sup>2+</sup> is excited by sub-bandgap light ( $\lambda > 400$  nm).



The quantum yield  $\phi$  for PVS<sup>-</sup> formation declines with increasing ionic strength. With no added salt,  $\phi = 2.4 \times 10^{-2}$ , and at 0.12 M NaCl, the quantum yield for PVS<sup>-</sup> formation decreases to  $4.6 \times 10^{-3}$ . The ionic strength dependence implicates electrostatic effects in controlling the electron transfer. The ionic strength effects suggest that the PVS<sup>-</sup> radical anion is repelled from the TiO<sub>2</sub>-SiO<sub>2</sub> surface to which the oxidized sensitizer Ru(bpy)<sub>3</sub><sup>2+</sup>

(19) Furlong, D. N.; Johansen, O.; Launikonis, A.; Loder, J. W.; Mau, A. W.-H.; Sasse, W. H. F. *Aust. J. Chem.* 1983, 38, 363.

(20) Ward, M. D.; White, J. R.; Bard, A. J. *J. Am. Chem. Soc.* 1983, 105, 27.

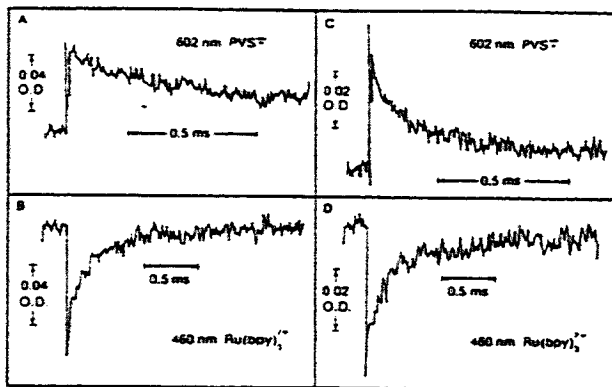


Figure 6. Absorption transients for the decay of PVS<sup>-</sup> (A and C) and the recovery of bleached Ru(bpy)<sub>3</sub><sup>3+</sup> (B and D) for aqueous solutions (pH 9.8) of 0.5% TiO<sub>2</sub>-SiO<sub>2</sub> colloids, 3 × 10<sup>-3</sup> M Ru(bpy)<sub>3</sub><sup>2+</sup>, 2 × 10<sup>-3</sup> M PVS<sup>0</sup>, with no added salt in parts A and B and 0.11 M NaCl in parts C and D. 457-nm laser excitation.

is bound. With increasing ionic strength, the electrostatic effects diminish and the back electron transfer becomes increasingly favorable.



The efficient photoproduction of PVS<sup>-</sup> in the aqueous TiO<sub>2</sub>-SiO<sub>2</sub>/Ru(bpy)<sub>3</sub><sup>2+</sup>/PVS<sup>0</sup> system was unexpected since no sacrificial electron donor was added to the solution to recycle Ru(bpy)<sub>3</sub><sup>3+</sup> to Ru(bpy)<sub>3</sub><sup>2+</sup>. To determine whether TiO<sub>2</sub> was the source of electrons for the reduction of Ru(bpy)<sub>3</sub><sup>3+</sup>, additional experiments were carried out. We found that in either the absence of the TiO<sub>2</sub>-SiO<sub>2</sub> colloids or a system in which the TiO<sub>2</sub>-SiO<sub>2</sub> colloids were replaced by a SiO<sub>2</sub> sol, no photoreduction of PVS<sup>0</sup> occurred. These results suggest that TiO<sub>2</sub> did indeed participate in the conversion of Ru(bpy)<sub>3</sub><sup>3+</sup> to Ru(bpy)<sub>3</sub><sup>2+</sup> in basic media. These studies also infer that TiO<sub>2</sub> is the source of electrons for the reduction of Ru(bpy)<sub>3</sub><sup>3+</sup> and is, in turn, oxidized presumably by means of a surface reaction.



The surface oxidation of TiO<sub>2</sub> by photogenerated valence-band holes has been suggested to occur during the photooxidation of water.<sup>21</sup>

Figure 6 provides information on the temporal behavior of PVS<sup>-</sup> and Ru(bpy)<sub>3</sub><sup>3+</sup> in aqueous solutions with TiO<sub>2</sub>-SiO<sub>2</sub> colloids at different ionic strengths. With no added salt, the transient absorption of PVS<sup>-</sup> (λ = 602 nm; ε = 13 800 M<sup>-1</sup> cm<sup>-1</sup>) is present immediately after the laser pulse but then decays to a nonbaseline level in 1 ms (Figure 6A). The transient behavior of Ru(bpy)<sub>3</sub><sup>3+</sup> is more complex than that of PVS<sup>-</sup>. Figure 6B records the bleaching and recovery of the absorption of Ru(bpy)<sub>3</sub><sup>2+</sup> (λ = 460 nm; ε = 14 600 M<sup>-1</sup> cm<sup>-1</sup>), following the laser pulse. The bleaching and recovery of the absorption of Ru(bpy)<sub>3</sub><sup>2+</sup> corresponds to the growth and disappearance of Ru(bpy)<sub>3</sub><sup>3+</sup>, respectively. In contrast to the decay kinetics of PVS<sup>-</sup>, Ru(bpy)<sub>3</sub><sup>3+</sup> decays to baseline within 1 ms, indicating that Ru(bpy)<sub>3</sub><sup>3+</sup> is consumed by more than one pathway as may be anticipated by reactions 3 and 4. A comparison of the transient absorptions in Figure 6, A and B, shows that after Ru(bpy)<sub>3</sub><sup>3+</sup> is completely consumed, no further reaction of PVS<sup>-</sup> takes place over the period of observation. From the residual absorption of PVS<sup>-</sup> obtained after steady state (Figure 6A), one can estimate that 42% of Ru(bpy)<sub>3</sub><sup>3+</sup> is reduced by the surface groups of TiO<sub>2</sub>, according to reaction 4. In other words, 58% of Ru(bpy)<sub>3</sub><sup>3+</sup> back reacts with PVS<sup>-</sup> via reaction 3. Figure 6C shows that at high ionic strength (0.11 M NaCl), the decay rate of PVS<sup>-</sup> is substantially accelerated and a lower steady-state concentration is reached compared

(21) Manuera, G.; Gonzalez-Elipe, A. R.; Espinos, J. P.; Navio, A. *J. Mol. Struct.* 1986, 143, 227.

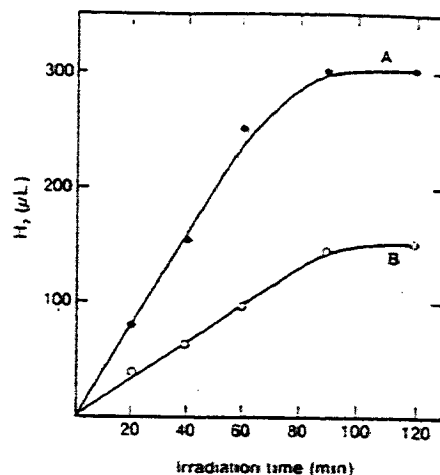


Figure 7. Production of H<sub>2</sub> with irradiation time (λ > 400 nm) for aqueous solutions of 6 × 10<sup>-3</sup> M Ru(bpy)<sub>3</sub><sup>2+</sup>, 2 × 10<sup>-3</sup> M DQS<sup>0</sup>, and 12 mg L<sup>-1</sup> Pt colloids with (A) 1.2% TiO<sub>2</sub>-SiO<sub>2</sub> colloids and (B) 0.5% TiO<sub>2</sub>-SiO<sub>2</sub> colloids.

to the system without added salt. The rate constant<sup>22</sup> for recombination of PVS<sup>-</sup> and Ru(bpy)<sub>3</sub><sup>3+</sup> at 0.11 M NaCl is

$$k_3 = 3 \times 10^9 \text{ M}^{-1} \text{ s}^{-1}$$

which is a factor of 6 higher than the system without added salt, which has a rate constant of

$$k_3' = 5 \times 10^8 \text{ M}^{-1} \text{ s}^{-1}$$

Furthermore, from the residual absorption of PVS<sup>-</sup> after reaching steady state, one can conclude that about 19% of Ru(bpy)<sub>3</sub><sup>3+</sup> is consumed by reaction with the TiO<sub>2</sub> surface (reaction 4) in the presence of 0.11 M NaCl. Thus, the effect of the increased ionic strength is to promote the back electron transfer between PVS<sup>-</sup> and Ru(bpy)<sub>3</sub><sup>3+</sup> at the expense of the oxidation of the TiO<sub>2</sub> surface (reaction 4). The kinetics for electron transfer in the TiO<sub>2</sub>-SiO<sub>2</sub>/Ru(bpy)<sub>3</sub><sup>2+</sup>/PVS<sup>0</sup> system are in marked contrast to those in the Ru(bpy)<sub>3</sub><sup>2+</sup>/PVS<sup>0</sup> system. In the homogeneous media, flash photolysis studies indicate that the back reaction of PVS<sup>-</sup> and Ru(bpy)<sub>3</sub><sup>3+</sup> is diffusion controlled with a rate constant of

$$k_3'' = 3 \times 10^9 \text{ M}^{-1} \text{ s}^{-1}$$

This value of the rate constant for recombination of PVS<sup>-</sup> and Ru(bpy)<sub>3</sub><sup>3+</sup> in homogeneous media is identical with k<sub>3</sub> obtained in the microheterogeneous TiO<sub>2</sub>-SiO<sub>2</sub>/Ru(bpy)<sub>3</sub><sup>2+</sup>/PVS<sup>0</sup> system at high ionic strength. However, in the homogeneous system, the decay kinetics of PVS<sup>-</sup> are concomitant with and match those of Ru(bpy)<sub>3</sub><sup>3+</sup>, indicating the absence of side reactions. The results of these studies suggest that the negatively charged TiO<sub>2</sub>-SiO<sub>2</sub> colloids improve the stability of the intermediate photoproducts PVS<sup>-</sup> and Ru(bpy)<sub>3</sub><sup>3+</sup> against back electron transfer at low ionic strength. In addition, the data indicate that TiO<sub>2</sub>-SiO<sub>2</sub> colloids provides electrons to the oxidized intermediate, Ru(bpy)<sub>3</sub><sup>3+</sup>, thus recycling the complex for further reaction.

The possibility that the TiO<sub>2</sub>-SiO<sub>2</sub>/Ru(bpy)<sub>3</sub><sup>2+</sup>/Pt system with an appropriate electron relay could be used to photogenerate H<sub>2</sub> from water with visible light was also investigated. For these studies, the DQS<sup>0</sup> zwitterion was employed as the electron relay. Figure 7 shows the H<sub>2</sub> production with illumination time in the TiO<sub>2</sub>-SiO<sub>2</sub>/Ru(bpy)<sub>3</sub><sup>2+</sup>/DQS<sup>0</sup>/Pt system in aqueous media at pH 9.8. When the TiO<sub>2</sub>-SiO<sub>2</sub> colloids are present at a concentration of 1.2%, a total of 300 μL of H<sub>2</sub> was generated in 90 min with an initial rate of 230 μL/h (Figure 7; curve A). When

(22) The recombination rate constant was determined with use of eqs. 1 and 2.

$$d[\text{PVS}^-]/dt = k_3[\text{PVS}^-][\text{Ru(bpy)}_3^{3+}] \quad (1)$$

$$\ln \{d[\text{PVS}^-]_0/[\text{PVS}^-]_t\} = k_3 \int [\text{Ru(bpy)}_3^{3+}]_t dt \quad (2)$$

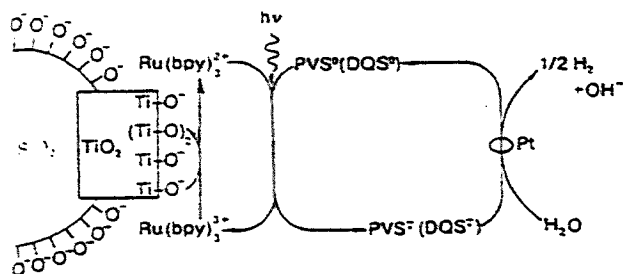


Figure 8. Representation of mechanisms: Following photoinduced electron transfer from sensitizer  $\text{Ru}(\text{bpy})_3^{2+}$  to an electron relay  $\text{PVS}^0$  or  $\text{DQS}^0$ , the negatively charged  $\text{SiO}_2$  colloidal support repels  $\text{PVS}^-$  or  $\text{DQS}^-$  from  $\text{Ru}(\text{bpy})_3^{2+}$  at colloidal interface, thus inhibiting the back electron transfer. The escaped  $\text{DQS}^-$  is recycled through reaction with a colloidal Pt catalyst to evolve  $\text{H}_2$ . The oxidized sensitizer,  $\text{Ru}(\text{bpy})_3^{3+}$ , is recycled through the oxidation of the  $\text{TiO}_2$  surface.

concentration of  $\text{TiO}_2\text{-SiO}_2$  was decreased by one-half, the  $\text{H}_2$  yield was also cut by one-half (Figure 7, curve B). Furthermore, when the enzyme superoxide dismutase was added to the system after cessation of hydrogen generation, the photoproduction of  $\text{H}_2$  resumed. Along with the hydrogen production, oxygen was also formed. The role of superoxide dismutase to catalyze  $\text{O}_2$  production in biological systems has been well studied.<sup>23</sup> Superoxide dismutase catalyzes the disproportionation of two molecules of superoxide  $\text{O}_2^-$  to  $\text{O}_2$  and hydrogen peroxide in two steps that are in equilibrium. The catalytic reaction of the enzyme is highly specific to superoxide. In the case of  $\text{TiO}_2$ , the mechanism suggests the possibility for the interconversion of peroxide and superoxide. Since the equilibrium favors peroxide in the biological system, it seems reasonable that only a small fraction of the oxidized surface groups of  $\text{TiO}_2$  would be present in the superoxo form. Consistent with this notion is the observation that in the  $\text{TiO}_2\text{-SiO}_2$  system to which superoxide dismutase had been added, the amount of  $\text{O}_2$  produced represented about 15% of the expected 1:2 stoichiometric ratio of  $\text{O}_2/\text{H}_2$ . Several other studies<sup>21,24</sup> also implicate peroxo or superoxo compounds as the oxidized product of surface  $\text{TiO}_2$  groups. The dependence of the  $\text{H}_2$  production on the concentration of the  $\text{TiO}_2\text{-SiO}_2$  colloids can thus be explained by the decline in the number of surface  $\text{Ti-O}^-$  groups available for the reduction of  $\text{Ru}(\text{bpy})_3^{3+}$ . Similarly, the leveling off of the  $\text{H}_2$  production with illumination time is likely due to the exhaustion of  $\text{Ti-O}^-$  groups available for the reduction (or recycling) of the oxidized  $\text{Ru}(\text{bpy})_3^{3+}$  species.

In the absence of  $\text{Ru}(\text{bpy})_3^{2+}$ , sub-bandgap irradiation ( $\lambda_{\text{ex}} > 400$  nm) of the  $\text{TiO}_2\text{-SiO}_2/\text{DQS}^0/\text{Pt}$  system did not produce molecular  $\text{H}_2$ . However, illumination of the  $\text{TiO}_2\text{-SiO}_2/\text{DQS}^0/\text{Pt}$

system with bandgap irradiation ( $\lambda > 305$  nm) did generate  $\text{H}_2$ . The  $\text{Ru}(\text{bpy})_3^{2+}$  sensitizer was thus an essential component for the visible-light-induced production of hydrogen. The quantum yield for  $\text{H}_2$  production was markedly dependent on the ionic strength. With no added salt, the quantum yield  $\phi$  for  $\text{H}_2$  formation was  $1.4 \times 10^{-3}$ . At 0.12 M NaCl, the quantum yield was  $2 \times 10^{-4}$ , representing a factor of 7 decrease with respect to the solution with no added salt. The dependence of the quantum yields for  $\text{H}_2$  production on ionic strength illustrates the importance of electrostatic effects in controlling electron transfer and the subsequent photogeneration of molecular hydrogen. Figure 8 is a conceptual representation of the mechanism at low ionic strength. The negative surface charge of the  $\text{TiO}_2\text{-SiO}_2$  colloid stabilizes the  $\text{DQS}^-$  and  $\text{Ru}(\text{bpy})_3^{3+}$  intermediates against back electron transfer, thus allowing the  $\text{DQS}^-$  reaction with the catalytic Pt colloid to produce  $\text{H}_2$ .  $\text{Ru}(\text{bpy})_3^{3+}$  is converted to  $\text{Ru}(\text{bpy})_3^{2+}$  by oxidation of the  $\text{TiO}_2$  surface. The oxidation of the  $\text{TiO}_2$  surface thus recycles the sensitizer for further reaction. The decrease of the quantum yield for  $\text{H}_2$  production at high ionic strength is due to the dampening of the negative surface potential of the  $\text{TiO}_2\text{-SiO}_2$  colloids, resulting in the facile recombination of the intermediate photoproducts  $\text{DQS}^-$  and  $\text{Ru}(\text{bpy})_3^{3+}$ .

#### Final Remarks

This study has demonstrated that electrostatic effects produce a dramatic improvement in the kinetics for charge separation and fuel generation in illuminated colloidal or particulate semiconductor systems. Titanium dioxide was immobilized on negatively charged  $\text{SiO}_2$  colloids. Direct excitation of the semiconductor or an electrostatically bound sensitizer initiates electron transfer to a neutrally charged zwitterionic relay. Repulsion of the negatively charged reduced electron relay inhibits the reverse electron transfer. The reducing power of the reduced electron relay serves to generate molecular hydrogen in the presence of a Pt catalyst. Surface redox reactions between  $\text{Ti-O}^-$  groups of  $\text{TiO}_2$  and the photogenerated valence-band holes or the oxidized sensitizer probably form peroxo or superoxo groups. The ability of  $\text{TiO}_2$  to store  $\text{O}_2$  as an intermediate peroxide provides a potentially important mechanism for achieving the separation of  $\text{H}_2$  and  $\text{O}_2$  in dispersed systems. Heat treatment and additives such as metal oxides have been employed to regenerate the surface-oxidized  $\text{TiO}_2$  with the accompanying release of molecular oxygen.<sup>25</sup> The use of enzymes such as superoxide dismutase is an alternative approach for the regeneration of  $\text{TiO}_2$  and the discharge of surface bound oxygen. Further studies are now in progress to characterize the surface oxidation product of  $\text{TiO}_2$  and to determine the effectiveness of enzymes to decompose it to molecular oxygen.

**Acknowledgment.** We are grateful to Dr. B. B. Keiser at Nalco Chemical Co. for kindly providing the  $\text{TiO}_2\text{-SiO}_2$  colloids and Kim Jones at SERI for the TEM measurements. This work was supported by Contract No. 5083-260-0796 from the Gas Research Institute.

(23) Malmstrom, B. G.; Andreasson, L. E.; Reinhammer, B. In *The Enzymes*; Boyer, P. D., Ed.; Academic Press: New York, 1975; Vol. 12B, p 1. (a) Bickley, R. L.; Jayanti, R. K. M. *Discuss. Faraday Soc.* 1978, 58, 194. (b) Manuera, G.; Rives-Arnaud, V.; Sancedo, A. *J. Chem. Soc., Faraday Trans. 1*, 1979, 75, 736. (c) Duonghong, D.; Grätzel, M. *J. Chem. Soc., Chem. Commun.* 1984, 1597. (d) Oosawa, Y.; Grätzel, M. *J. Chem. Soc., Chem. Commun.* 1984, 1629.

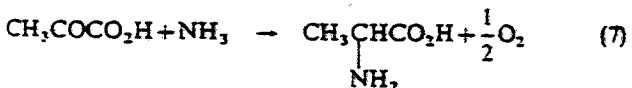
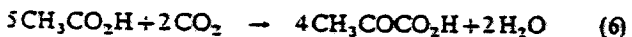
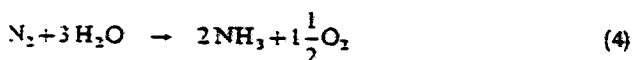
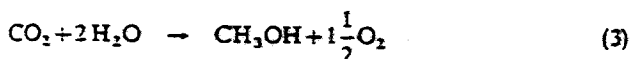
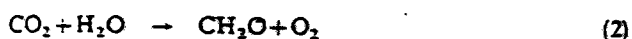
(25) Gu, B.; Kiwi, J.; Grätzel, M., unpublished results.

# BIO-MODELS AND ARTIFICIAL MODELS FOR PHOTOSYNTHESIS

Itamar Willner\*, Daniel Mandler and Ruben Maidan

Department of Organic Chemistry and the Fritz Haber Research Center for Molecular Dynamics, The Hebrew University of Jerusalem, Jerusalem 91904 (Israel).

The production of fuels and useful chemicals with the aid of solar light energy is a long-term challenge in chemistry<sup>1-5</sup>. The use of light energy to drive endoergic processes such as photocleavage of water (1) carbon dioxide reduction [(2) and (3)] and nitrogen fixation (4) exemplifies possibilities to convert abundant raw materials to fuel products. One could also envisage more complicated pathways to utilize solar energy in synthetic routes. For example, the stepwise reduction of CO<sub>2</sub> to acetic acid and pyruvic acid [(5) and (6)] followed by reductive amination (7) to form alanine, demonstrates an endoergic synthesis of an amino acid. Thus, development of such solar light driven process might have a substantial impact on fuel and feedstock resources.



Nature has developed impressively sophisticated mechanisms for utilizing solar light in the energy storage and for synthetic purposes.<sup>6,7</sup> The photosynthetic cycle coupled to the heterotrophic cycle (Fig. 1) reveals the fundamental pathways for light storage and subsequent synthesis of products. In the photosynthetic cycle, the formation of carbohydrates from CO<sub>2</sub> is induced by light energy. The coupled catabolic cycle uses the products of the primary cycle as an energy source and origin to construct the building blocks required by the heterotrophic organism for synthesis. Photosynthetic model systems aim to mimic the natural system to the extent that solar light is used to drive the conversion of abundant compounds to fuels and useful chemicals. Photosensitized electron transfer reactions using visible light (Fig. 2) offer the basis for the conversion of light energy to chemical energy. Application of artificial photosensitizers<sup>8,9</sup> to accomplish electron transfer reactions and means to stabilize the photoproducts in organized microenvironments<sup>10-14</sup> have been extensively investigated in recent years. Although most of the efforts have been directed to the utilization of the photoproducts in the photodecomposition of water (i. e. hydrogen evolution), no general approach to apply the electron transfer process for synthetic purposes is available.

A scheme for the constituents of a photosynthetic model system is suggested in Figure 2, where fixation of CO<sub>2</sub> to methane is exemplified. In this system the primary photosensitized electron transfer process yields the single electron transfer product, A<sup>-</sup>, exhibiting thermodynamic capability

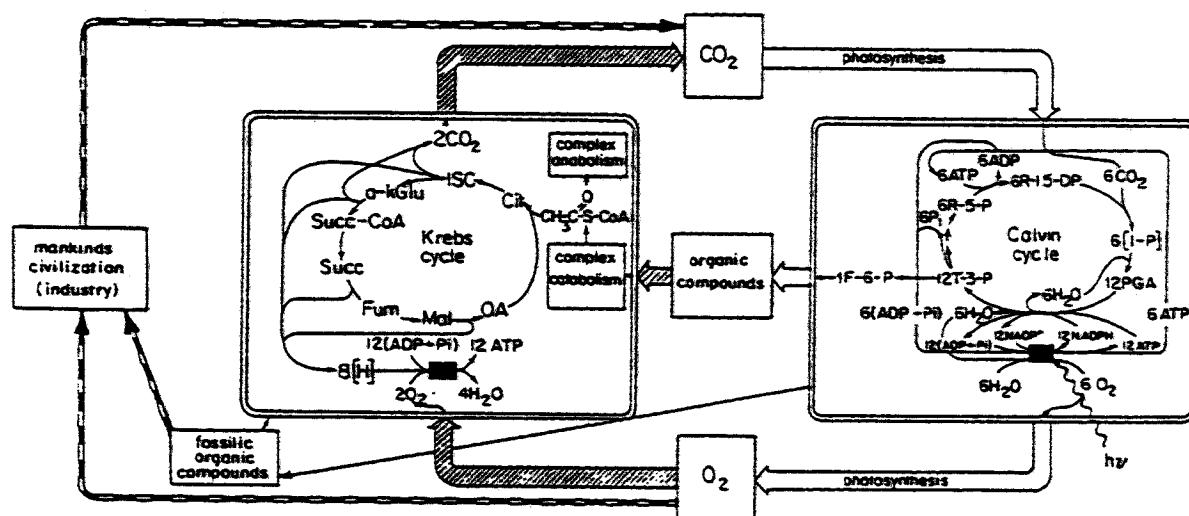


Figure 1. - Scheme of the biological photosynthetic and heterotrophic cycles. The following abbreviations are used: ADP=adenosine diphosphate, ATP=adenosine triphosphate, Pi=inorganic phosphate, F-6-P=fructose-6-phosphate, PGA=phosphoglyceric acid, NADP<sup>+</sup>/NADPH=nicotinamide adenoindinucleotide phosphate couple, R-5-P=ribose-5-phosphate, R-1,5-DP=ribose-1,5-diphosphate, T-3-P=triose-3-phosphate, α-Kglu=α-ketoglutarate, Cit=citrate, Fum=fumarate, [H]=metabolically bound hydrogen, ISC=isocitrate, Mal=malate, OA=oxaloacetate, Succ=succinate, Succ-CoA=succinate bound to coenzyme A.

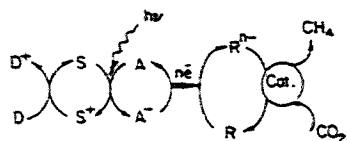
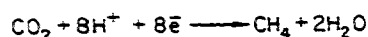
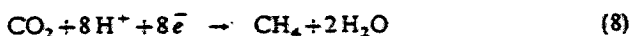


Figure 2. — Scheme for the constituents of a photosynthetic model system.

to reduce CO<sub>2</sub>. Nevertheless, the system should also exhibit favoured kinetics to allow the process. This is accomplished by the introduction of two constituents: a charge relay, (R), and a catalyst, (Cat). The function of the catalyst is to activate the substrate, i.e. CO<sub>2</sub>. The charge relay, R, accumulates electrons from the single electron transfer product, A<sup>-</sup>. Proper coupling of the reduced relay, R (ne<sup>-</sup>), and the catalyst activated substrate might then result in the multi-electron reduction of CO<sub>2</sub> to methane (8).



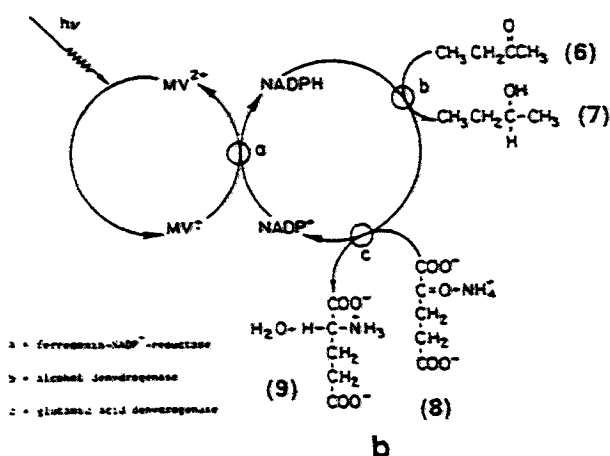
Thus, the construction of photosynthetic models involves the design and selection of constituents that operate in a synchronic mode to accomplish the desired process. Nature has constructed such organized systems, where enzymes and specific cofactors function in substrate activation and charge accumulation.

Recent studies in our laboratory attempt to construct bio-models and artificial models for photosynthesis. The bio-model attempts to regenerate natural cofactor by a photosensitized electron transfer process initiated by synthetic ingredients. The regenerated cofactor is then coupled to enzymatic synthesis. The artificial models represent attempts to construct tailored constituents that mimic the natural systems by artificial means. This report is aimed to summarize the progress in these complementary subjects and to emphasize future perspectives.

Photosynthetic bio-models

PHOTOSENSITIZED NAD(P)H REGENERATION SYSTEMS AND THEIR SYNTHETIC APPLICATION

1,4-Dihyronicotinamide adenine dinucleotide, NADH, and 1,4-dihyronicotinamide adenine dinucleotide phosphate



- a • ferredoxin-NADP<sup>+</sup>-reductase
- b • alcohol dehydrogenase
- c • glutamate acid dehydrogenase

(NADPH) are essential cofactors in many enzymatic oxidation-reduction processes. Specifically, in natural photosynthesis, NAD(P)H acts as a charge relay that accumulates the electrons transferred by photosystem II and participates as cofactor in the enzymatic CO<sub>2</sub>-fixation. Therefore, the development of photoinduced NAD(P)H regeneration processes coupled to enzymatic reaction might establish a general synthetic route.

We have developed<sup>15, 16</sup> photosensitized regeneration systems for NADH and NADPH (Fig. 3). The regeneration processes are based on the photoinduced production of N, N'-dimethyl-4, 4'-bipyridinium radical cation, methyl viologen radical (MV<sup>•-</sup>). For the regeneration of NADH (Fig. 3a), Zn(II)-meso-tetramethyl pyridinium porphyrin, Zn-TMPyP<sup>4+</sup>, is used as photosensitizer and mercaptoethanol as an electron donor. Upon illumination by visible light (λ > 400 nm) the photosensitized reduction of MV<sup>2+</sup> pro-

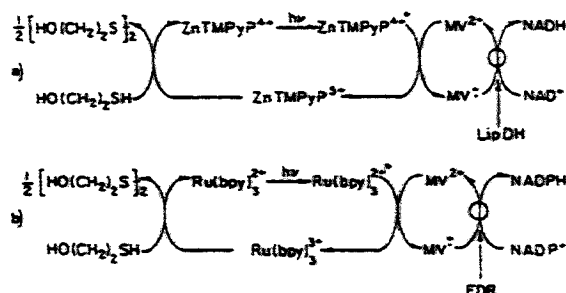
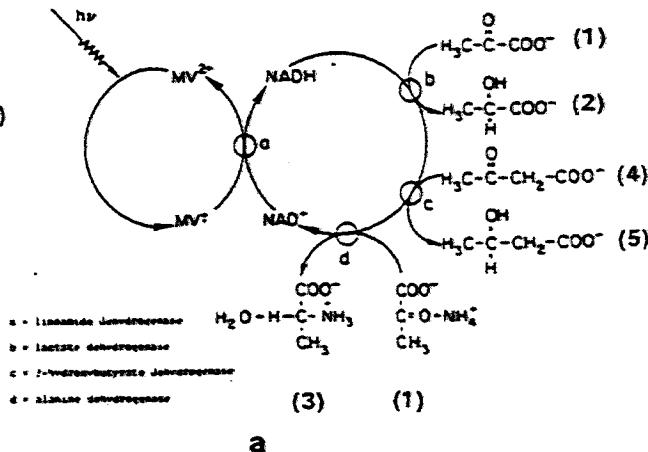


Figure 3. — Photosensitized regeneration scheme for (a) NADH (b) NADPH.

ceeds. In the presence of the enzyme lipoamide dehydrogenase (LipDH, E.C. 1.6.4.3), the artificial charge relay MV<sup>•-</sup> mediates the reduction of NAD<sup>+</sup> to NADH. The second cofactor, NADPH, could be similarly regenerated by a photosensitized electron transfer process. For NADPH regeneration (Fig. 3b) Ru(II)-tris-bipyridine, Ru(bpy)<sub>3</sub><sup>2+</sup>, or Zn-TMPyP<sup>4+</sup> are used as photosensitizers and mercaptoethanol or (NH<sub>4</sub>)<sub>3</sub>EDTA are used as electron donors. In this system photogenerated MV<sup>•-</sup> mediates the reduction of NADP<sup>+</sup> to NADPH in the presence of the enzyme ferredoxin-NADP<sup>+</sup>-reductase, (FDR, E.C. 1.18.1.2). The quantum yield for NADH formation is φ = 5 × 10<sup>-3</sup>, while that for NADPH production correspond to φ = 1.9 × 10<sup>-2</sup>. It should be noted that NADH regeneration could not be accomplished with

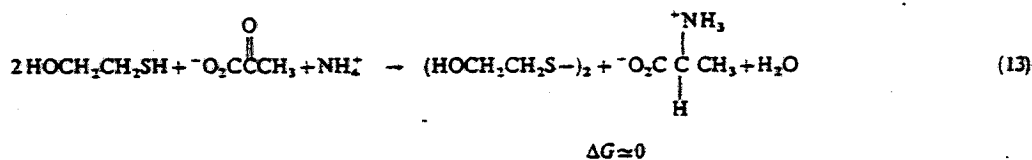
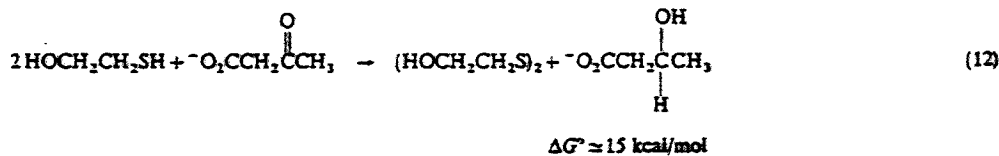
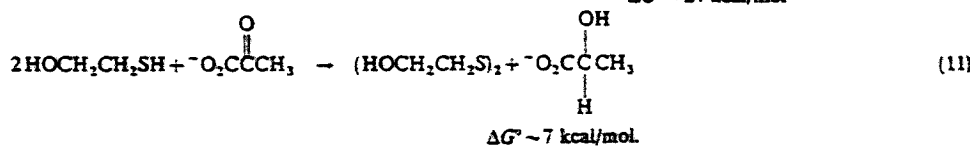
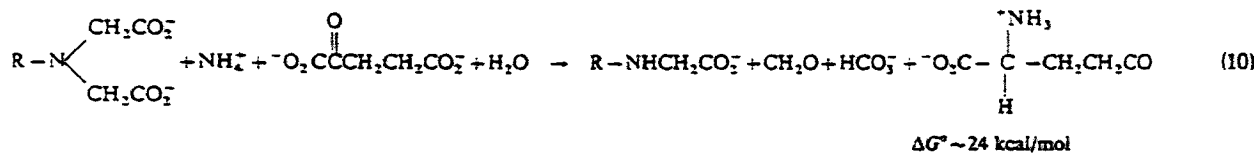
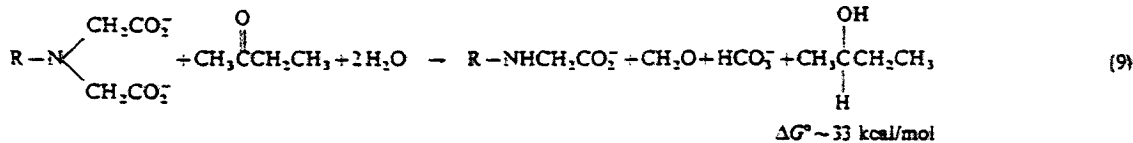


- a • lipoamide dehydrogenase
- b • lactate dehydrogenase
- c • 2-hydroxybutyrate dehydrogenase
- d • alanine dehydrogenase

Figure 4. — Application of MV<sup>•-</sup> regeneration cycles in synthetic routes: (a) NADH coupled synthesis; (b) NADPH coupled synthesis.

Ru(bpy)<sub>3</sub><sup>2+</sup> as a photosensitizer. A detailed study reveals that NADH acts as an electron donor for the oxidized photoproduct, Ru(bpy)<sub>3</sub><sup>2+</sup>, resulting in a short circuit in the system, that prevents the accumulation of NADH.<sup>17</sup>

been coupled (Fig. 4a) to the reduction of pyruvic acid (1) to lactic acid (2), in the presence of the enzyme lactate dehydrogenase (LacDH, E.C. 1.1.1.27), to the reductive amination of pyruvic acid (1) to alanine, (3), with the enzyme



The photosensitized regeneration of NAD(P)H enables the coupling of these systems to enzymatic synthesis.<sup>16, 18</sup> Figure 4 presents several of the accomplished photosynthetic processes: The photoinduced NADH regeneration system has

alanine dehydrogenase (AlaDH, E.C. 1.4.1.1) and to the reduction of acetoacetate (4) to β-hydroxybutyrate (5). Similarly, the photosensitized NADPH regeneration cycle has been coupled (Fig. 4b) to the reduction of 2-butanone (6)

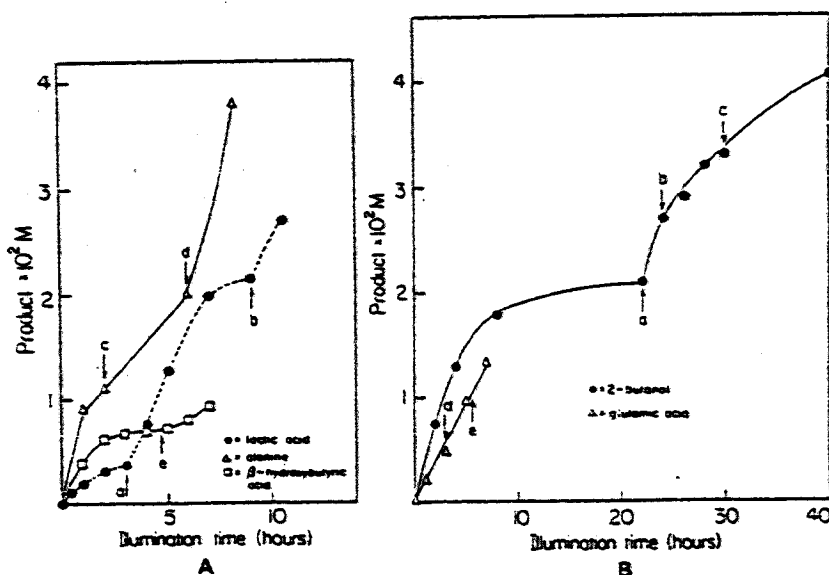


Figure 5. — Rates of products formation as function of illumination time via photosensitized NAD(P)H regeneration cycles: A. Products formed by NADH: Δ—alanine; at point c—addition of 2-mercaptoethanol, 4 × 10<sup>-2</sup> mol.l<sup>-1</sup>; at point d—addition of 2-mercaptoethanol, 2.5 × 10<sup>-2</sup> mol.l<sup>-1</sup>; ●—lactic acid; at point e and b—addition of 2-mercaptoethanol, 3.3 × 10<sup>-2</sup> mol.l<sup>-1</sup>; □—β-hydroxybutyric acid. B. Products formed by NADPH: ●—2-butanol; at point a—addition of (NH<sub>4</sub>)<sub>2</sub>EDTA, 2 × 10<sup>-2</sup> mol.l<sup>-1</sup>; at points b and c—addition of (NH<sub>4</sub>)<sub>2</sub>EDTA, 1.7 × 10<sup>-2</sup> mol.l<sup>-1</sup>; Δ—glutamic acid; at point d—addition of 2-mercaptoethanol, 1.2 × 10<sup>-2</sup> mol.l<sup>-1</sup>; at point e—addition of 2-mercaptoethanol, 1.9 × 10<sup>-2</sup> mol.l<sup>-1</sup>



to 2-butanol (7), with the enzyme alcohol dehydrogenase (AlaDH, E.C. 1.1.1.2), and to the reductive amination of ketoglutaric acid (8) to glutamic acid (9) in the presence of the enzyme glutamate dehydrogenase (GluDH, E.C. 1.4.1.4). The net light induced processes mediated by the NAD(P)H regeneration cycles and their energetic balance are summarized in equations (9)-(13). It can be seen that most of the processes are endoergic photosynthetic routes.

Whenever enzymes are excluded from their native environments and especially when introduced into media that include chemical ingredients the stability of the enzymes must be considered. The rate of formation of the different products as a function of illumination time is displayed in Figure 5. As an example, the photoreduction of 2-butanone (6) to (7) will be discussed: It can be seen [Fig. 5 B—(●)—] that the formation of (7) levels off as illumination proceeds. This is a result of consumption of the electron donor required for the photochemical reaction. Readdition of the electron donor to the system at the marked time intervals restores the original activity of the system towards the reduction of (6), and by stepwise introduction of the electron donor the activity of the system is maintained for prolonged illumination. Similar long term activities of the other photosynthetic systems are also observed.

The turnover numbers (TN = number of moles of product/number of moles of ingredient) of the different ingredients included in the enzyme catalysed reactions, are summarized in Table I. It is evident that high conversion yields are obtained, and that all of the components and particularly the enzymes are effectively recycled in the photoinduced chemical transformations. Furthermore, since enzymes are applied, chiroselectivity in products formation is anticipated. The optical purity of the different products is also summarized in Table I. As expected the optimal purity of the products is close to 100% in most of the reactions.

Enzyme catalysed synthesis through the regeneration of the NAD(P)H cofactors has been a subject of extensive research in recent years. Specific efforts have been directed towards the chemical regeneration to NAD(P)H. This method of chemical regeneration of the cofactor is exemplified in Figure 6a, where alanine is synthesized via regeneration of NADH by an alcohol and the enzyme alcohol

dehydrogenase. Yet, the cyclic process reveals its disadvantages and limitations. Since the enzymes are reversibly active, product accumulation will result in the reverse reactions and the system will reach an equilibrium state controlled by the specific thermodynamics of the process. Thus, for endoergic synthesis ( $\Delta G^{\circ} \gg 0$ ), a composite of equilibrium products is obtained and limited amounts of the desired product can be accumulated. These disadvantages are resolved by the photochemical regeneration approach. Supply of light energy (Fig. 6b) constantly forms the reduced cofactor and products are accumulated as long as illumination proceeds. Consequently, the photosensitized regeneration of NAD(P)H allows us to drive endoergic photosynthetic processes.

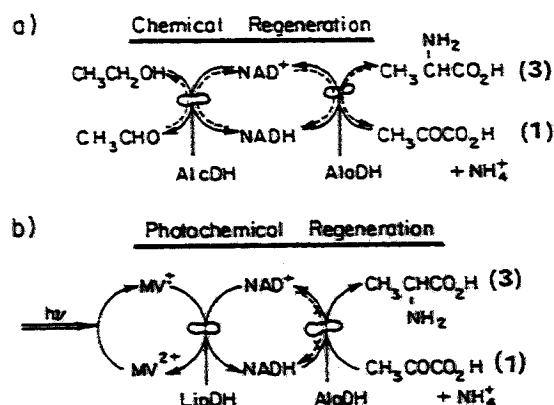


Figure 6. — Chemical and photochemical regeneration of NAD(P)H: (a) chemical regeneration and application in synthesis; (b) photochemical regeneration and application in endoergic synthesis.

The light active compounds used for the regeneration of the NAD(P)H cofactor were homogeneous, water soluble, photosensitizers. In a slightly different approach we have applied semiconductors<sup>19</sup> in the form of powders or colloids as the photosystem that induces the regeneration of these cofactors. The photosensitized regeneration of NAD(P)H was accomplished with CdS-semiconductor powders or colloids ( $\lambda > 400$  nm) or by wide band gap excitation ( $\lambda > 400$  nm) of TiO<sub>2</sub>. The regeneration system with CdS

Table I. — Turnover numbers (TN) of the components in the different enzyme catalysed reactions.

	Ru(bpy) <sub>3</sub> <sup>2+</sup>	ZnTMP <sub>4</sub> P <sup>4+</sup>	MV <sup>2+</sup>	NAD(P) <sup>+</sup>	Enzymes	% Conversion	% Optical purity	Final product (M)	Initial Substrate (M)
2-butanol	530		40	40	FDR <sup>a</sup> 2.4 × 10 <sup>4</sup>	27	100 ± 10	4.05 × 10 <sup>-2</sup>	0.15
Glutamic acid			15	15	FDR 9.75 × 10 <sup>3</sup>	13	99 ± 7	1.3 × 10 <sup>-2</sup>	0.1
Lactic acid		4,500	13.5	27	LipDH <sup>b</sup> 5.67 × 10 <sup>4</sup>	27	94 ± 7	2.7 × 10 <sup>-2</sup>	0.1
Alanine		7,900	19	27	LipDH 1.7 × 10 <sup>4</sup>	38	78 ± 7	3.8 × 10 <sup>-2</sup>	0.1
β-hydroxy-butyric acid		1,900	2.4	10	LipDH 5.2 × 10 <sup>3</sup>	21	105 ± 10	9.4 × 10 <sup>-3</sup>	4.52 × 10 <sup>-2</sup>

<sup>a</sup> F.W. ≈ 40,000; Shin M., *Methods Enzymol.*, 1971, 23, 441. <sup>b</sup> F.W. ≈ 70,000; Straub F.B., *Biochem. J.*, 1939, 33, 787. <sup>c</sup> F.W. ≈ 40,000 (ref. 11). <sup>d</sup> F.W. ≈ 2,200,000; Sund H., Burchard W., *Eur. J. Biochem.*, 1968, 6, 202. <sup>e</sup> F.W. ≈ 140,000; Jaenicke R., Knof S., *Eur. J. Biochem.*, 1968, 4, 157. <sup>f</sup> F.W. ≈ 228,000; Yoshida A., Freese E., *Biochim. Biophys. Acta*, 1964, 92, 33. <sup>g</sup> F.W. ≈ 85,000; Bergmeyer H.U. et al., *Biochem. J.*, 1967, 102, 423.

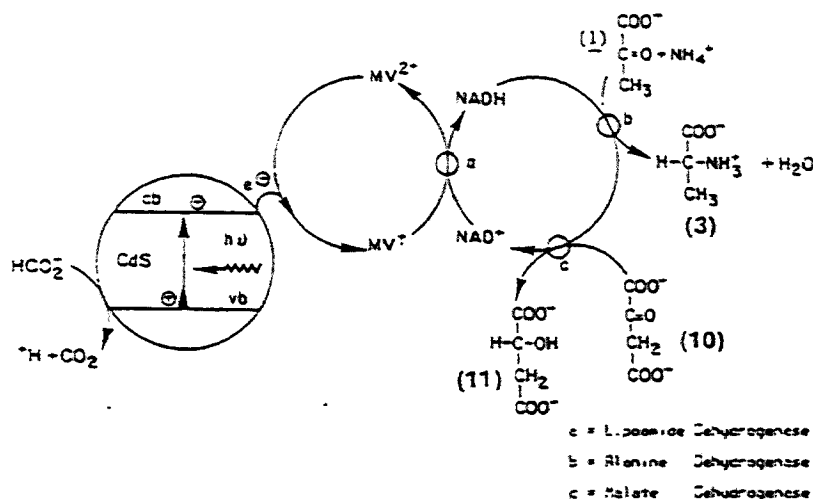
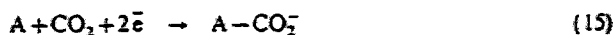
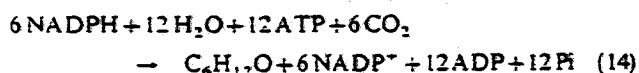


Figure 7. — Photosensitized NADH regeneration with CdS semiconductor particles and their synthetic application.

schematically presented in Figure 7. In this system conduction band electrons generate  $MV^+$  while formate is used as the electron donor that scavenges valence band holes. The photogenerated  $MV^+$  mediates the formation of NADH or NADPH with the specific enzymes described previously. Similarly, these photoinduced regeneration cycles have been coupled to synthetic routes, i.e., the photoreduction of oxaloacetic acid (10) to malic acid (11) and the reductive amination of pyruvic acid (1) to alanine (3) have been accomplished by the light driven NADPH regeneration cycle.

BIO-MODELS FOR PHOTOINDUCED  $CO_2$ -FIXATION

Carbon dioxide fixation in the photosynthetic apparatus is a complex sequence of enzyme catalysed reactions. The net process corresponds to the reduction of  $CO_2$  by NADPH with the participation of ATP (14). The NADPH cofactor is formed in the light induced electron transfer process and acts as a charge relay for electrons tunnelled by photosystem II. The primary step in the  $CO_2$ -fixation mechanism involves the reductive incorporation of  $CO_2$  in an acceptor molecule (A), (15). In turn, various decarboxylation reactions occur in the catabolic degradation pathway of the heterotrophic cycle.



For example, isocitric acid (12) is decarboxylated to ketoglutaric acid (8), in the Krebs Cycle (16), or malate (11) formed in this cycle is decarboxylated to pyruvic acid (1) (17). Both of the decarboxylation reactions involve the concomitant conversion of  $NADP^+$  to NADPH. Thus, we realize that  $CO_2$  incorporation in photosynthesis and  $CO_2$ -elimination in the catabolic degradation process is accompanied by the utilization or production of the NAD(P)H cofactor. The capability to regenerate photochemically the NAD(P)H cofactors and to couple the photogenerated cofactor to endoergic enzymatic synthesis, might establish a means to reverse the catabolic decarboxylation process to  $CO_2$  photosynthetic reactions. That is, photochemically regenerated NAD(P)H might act as cofactor for the enzymatic  $CO_2$  incorporation to organic acceptor molecules similarly to the  $CO_2$ -fixation mechanism in nature.

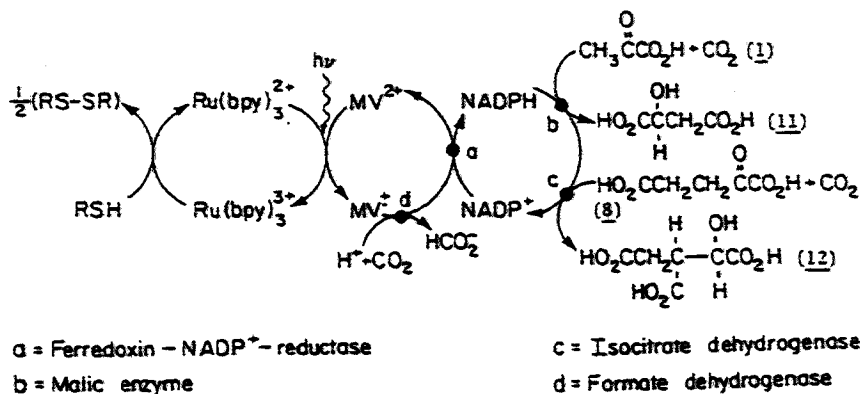
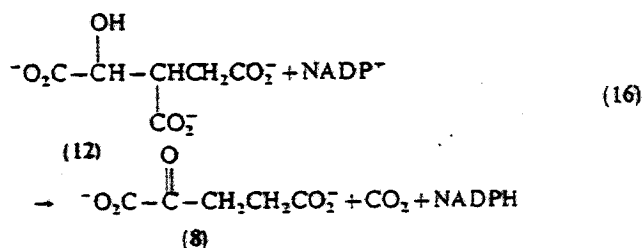
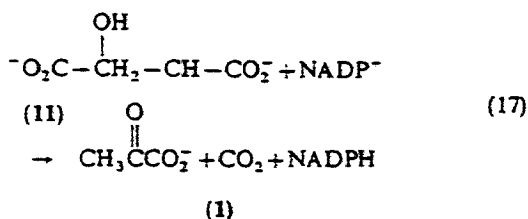


Figure 8. — Cyclic scheme for the photosensitized  $CO_2$ -fixation to form malic acid, isocitric acid and formic acid.



We have succeeded in developing these  $\text{CO}_2$ -fixation processes by photo-induced regeneration of NADPH (Fig. 8).<sup>20</sup> The photochemical system consists of Ru(II)-tris-bipyridine as photosensitizer, N, N'-dimethyl-4,4'-bipyridinium,  $\text{MV}^{2+}$ , as primary charge relay and two different thiolates as sacrificial electron donors: for malic acid production, 2-mercaptoethanol (13) is used as electron donor, while for isocitric formation dithiothreitol (14) is used as an ultimate donor. The light induced generated  $\text{MV}^{\cdot-}$  mediates the reduction of  $\text{NADP}^+$  to NADPH in the presence of ferredoxin-NADP<sup>+</sup>-reductase (FDR, E.C. 1.18.1.2). The photogenerated NADPH cofactor is coupled to the appropriate  $\text{CO}_2$ -incorporation

rating enzymes: isocitrate dehydrogenase (ICDH, E.C. 1.1.1.42), or malic enzyme (ME, E.C. 1.1.1.40). Illumination of these systems in the presence of the organic acceptors: pyruvic acid (1) or ketoglutaric acid (8) under  $\text{CO}_2$  results in the formation of malic acid (11) and isocitric acid (12). The rates of formation of malic acid (11) and isocitric acid (12) are displayed in Figure 9. The turnover numbers of the different components included in the  $\text{CO}_2$ -fixation cycles are summarized in Table II. It should be mentioned that the enzyme ICDH had to be immobilized on a polymer support to eliminate its rapid deactivation in an aqueous solution. The enzyme was immobilized<sup>21</sup> into a cross-linked polyacrylamide gel and exhibited high stability in this form. It is evident from Table II and Figure 9 that the enzymatic  $\text{CO}_2$ -fixation processes exhibit high stability, and products are accumulated as long as the systems are illuminated.

The net processes accomplished by the light induced reactions correspond to the reductive  $\text{CO}_2$ -incorporation into keto-acids via oxidation of the thiols. The thermodynamic balance of these reactions is summarized in equations (18) and (19). We conclude that the formation of malate (11) ( $\text{C}_4$ -compound) from pyruvic acid ( $\text{C}_3$ ) and  $\text{CO}_2$  represents an energy storage  $\text{CO}_2$ -photosynthetic process.

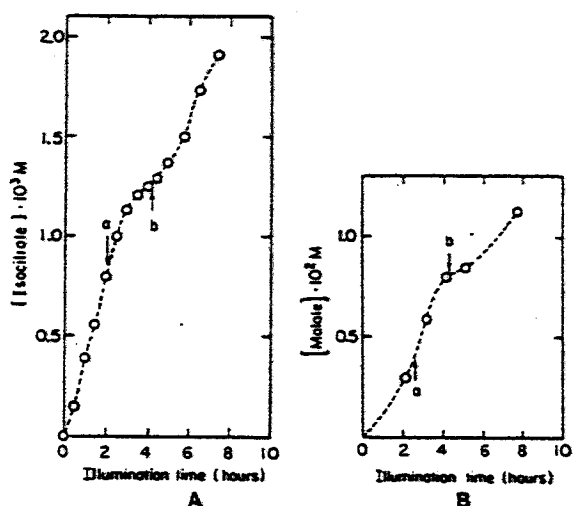
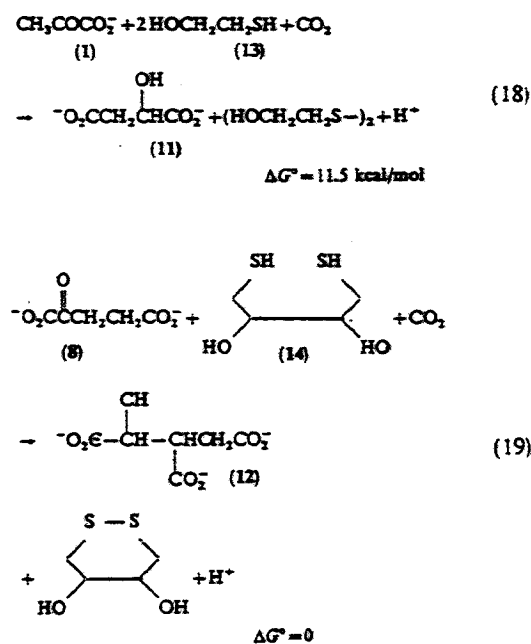


Figure 9. — Rate of  $\text{CO}_2$ -fixation products formation as a function of illumination time:  $[\text{Ru}(\text{bpy})_3^{2+}] = 2.1 \times 10^{-3} \text{ mol.l}^{-1}$ ,  $[\text{MV}^{2+}] = 1.9 \times 10^{-4} \text{ mol.l}^{-1}$ ,  $[\text{NADP}^+] = 1.7 \times 10^{-4} \text{ mol.l}^{-1}$ , FDR = 0.2 units. A. Isocitric acid formation: [ketoglutaric acid] =  $4.1 \times 10^{-2} \text{ mol.l}^{-1}$ , [dithiothreitol] =  $8.3 \times 10^{-3} \text{ mol.l}^{-1}$ , ICDH = 0.47 units (immobilized on PAN). (a) and (b) = addition of  $5 \times 10^{-3} \text{ mol.l}^{-1}$  dithiothreitol. B. Malic acid formation: [pyruvic acid] =  $4.7 \times 10^{-2} \text{ mol.l}^{-1}$ , [mercaptoethanol] =  $1.9 \times 10^{-2} \text{ mol.l}^{-1}$ , malic enzyme = 1.33 units. (a) and (b) = addition of  $2.3 \times 10^{-2} \text{ mol.l}^{-1}$  mercaptoethanol.



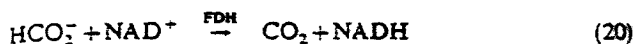
Finally, we were able<sup>22</sup> to reduce  $\text{CO}_2$  to formate,  $\text{HCO}_2^-$ , using an artificial photosystem and the enzyme formate dehydrogenase (FDH, E.C. 1.2.1.2) as biocatalyst. This

Table II. — Turnover numbers (TN) of components involved in the  $\text{CO}_2$ -fixation processes.

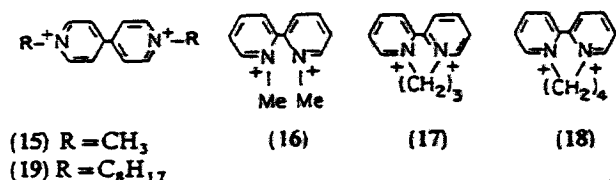
	Ru (bpy) <sub>3</sub> <sup>2+</sup>	MV <sup>2+</sup>	NADP <sup>+</sup>	FDR <sup>a</sup>	Malic enzyme <sup>b</sup>	ICDH <sup>c</sup>	% Conversion
Malic acid	118	58.6	62.2	$2.3 \times 10^4$	$7.4 \times 10^5$		24
Isocitric acid	136	11.4	11.4	$2.5 \times 10^3$		$5.5 \times 10^4$	4.6

<sup>a</sup> FW  $\approx$  40,000; cf.: Shin M., *Methods Enzymol.*, 1971, 23, 441. <sup>b</sup> FW  $\approx$  280,000; cf.: Hsu R. Y., Lardy H. A., *J. Biol. Chem.*, 1967, 242, 520. <sup>c</sup> FW  $\approx$  58,000; cf.: Colman R. F., *J. Biol. Chem.*, 1968, 243, 2454.

enzyme is NADH dependent and catalyses the oxidation of  $\text{HCO}_2^-$  to  $\text{CO}_2$  (20). Thus, the photoinduced regeneration of NADH might provide



a light induced process to reverse this reaction and drive the reduction of  $\text{CO}_2$  to formate. Studies along this direction reveal interesting observations. We find that the enzyme FDH is non-specific and various photogenerated bipyridinium radical cations mediate the reduction of  $\text{CO}_2$  to formate directly without the participation of the NADH cofactor but in the presence of the enzyme FDH. In these systems  $\text{Ru}(\text{bpy})_3^{2+}$  is used as photosensitizer, cysteine is used as sacrificial electron donor and one of the following bipyridinium salts as primary electron acceptor: N, N'-dimethyl-4, 4'-bipyridinium,  $\text{MV}^{2+}$ , (15 a), N, N'-dimethyl-2, 2'-bipyridinium,  $\text{DM}^{2+}$  (16), N,N'-trimethylene-2, 2'-bipyridinium,  $\text{DT}^{2+}$  (17), and N, N'-tetramethylene-2, 2'-bipyridinium,  $\text{DQ}^{2+}$  (18).



Illumination of these systems under  $\text{CO}_2$  and in the presence of FDH results in the formation of formate (Fig. 10). The highest quantum yields are observed with  $\text{MV}^{2+}$  and  $\text{DT}^{2+}$  as charge relays,  $\phi = 1.6 \times 10^{-2}$ . The net process accomplished in these systems corresponds to the reduction of  $\text{CO}_2$  by cysteine [(21) and Fig. 8], a process being endoergic by ca. 12.5 kcal/mol.

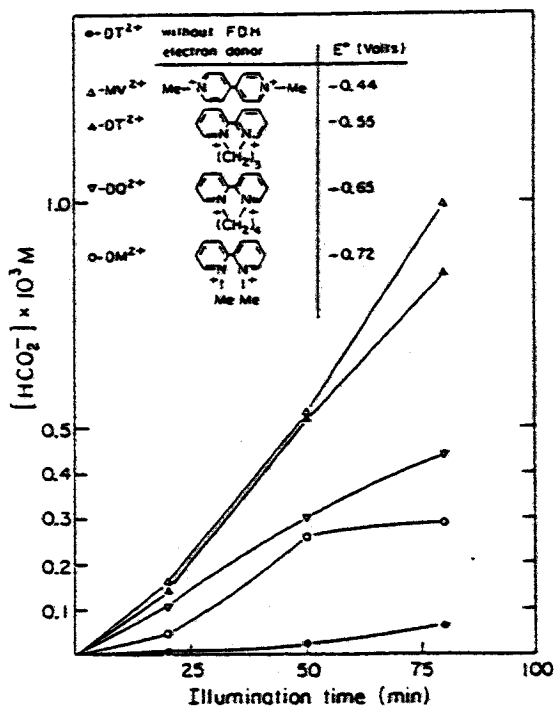
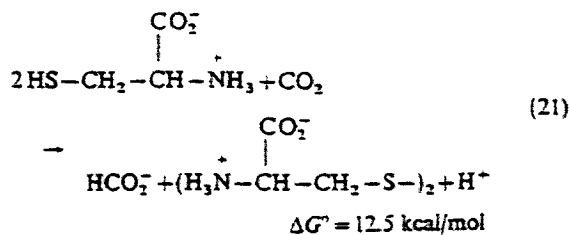


Figure 10. - Rate of formate,  $\text{HCO}_2^-$ , formation as a function of illumination time using different charge relays: [relay] =  $1 \times 10^{-3}$  mol.l<sup>-1</sup>,  $[\text{Ru}(\text{bpy})_3^{2+}] = 3 \times 10^{-5}$  mol.l<sup>-1</sup>, [cysteine] =  $1 \times 10^{-2}$  mol.l<sup>-1</sup>, FDH = 0.89 units.



We conclude that bio-models consisting of an artificial photo-system conjugated to biocatalysts provide photosynthetic systems.

ARTIFICIAL PHOTOSYNTHETIC SYSTEMS

The construction of photosynthetic bio-models reveals important guidelines to develop entirely artificial photosynthetic models. The design of an artificial photosynthetic system is schematically presented in Figure 11. The system is constituted of two units: one unit acts as charge relay that accumulates electron from the single electron transfer photoproduct,  $\text{A}^-$ , and forms the multi-electron reduced relay,  $\text{R}(\text{ne})$ . The second unit is a catalytic site, where the substrate is activated towards the specific reduction process. Coupling of these two units in one configuration might resemble the enzyme-cofactor relationship, and lead to the desired photosynthesis by reduction of the activated substrate by the charge relay  $\text{R}(\text{ne})$ .

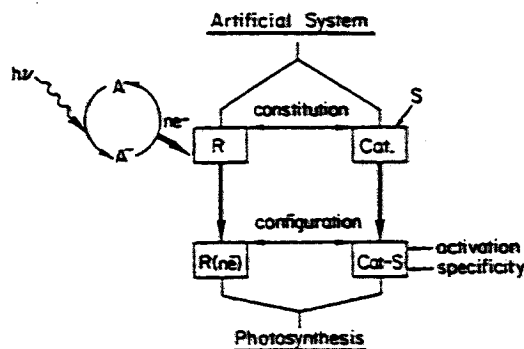


Figure 11. - Schematic constitution of an artificial photosynthetic system.

We were able to construct artificial photosynthetic systems along these guidelines. The approach involved the development of the separated relay and catalyst units. These were then organized in united photosynthetic devices exhibiting various characteristics of the natural system.

FORMATION OF MULTI-ELECTRON CHARGE RELAYS BY PHOTOINDUCED SINGLE ELECTRON TRANSFER REACTIONS

A simple mechanism to envisage the transformation of a single electron transfer product to a multi-electron charge relay is the disproportionation of the former species (22). The equilibrium constant,  $K_d$ , of this process is controlled by the reduction potentials of the single electron transfer product,  $\text{A}^\cdot$ , and the doubly reduced species  $\text{A}^{2+}$ , [ $E_1^0$  and  $E_2^0$  respectively, (23)].



$$K_d = \exp(-n\Delta E^0/RT)$$

Usually, the reduction potential to form the doubly reduced species,  $A^{\cdot -}$ , is substantially more negative than that for the single electron reduction product,  $A^{\cdot}$ . Hence, the equilibrium lies overwhelmingly towards the single electron transfer product and the formation of the two electron transfer charge relay is unfavoured. Nevertheless, this situation is valid only in a homogeneous phase and might be rather altered in a properly organized two-phase system<sup>23</sup> (Fig. 12). Assume that we design a water-oil two phase system, where the oxidized form,  $A^{2+}$ , is hydrophilic and merely water soluble, while the single electron transfer product exhibits hydrophobic character and prefers solubilization in the oil media. Under these conditions, photoreduction of  $A^{2+}$  in the aqueous phase will result in the formation of the single electron transfer product,  $A^{\cdot}$ , that is extracted to the organic phase. Disproportionation of the single electron transfer product in the organic phase will result in two products of opposite solubility properties. While  $A^{\cdot}$  is soluble in the oil phase,  $A^{2+}$  is extracted back to the aqueous medium. Consequently, the disproportionation equilibrium will be shifted toward towards the formation of the two electron charge relays. Thus, by proper design of the hydrophobic-hydrophilic character of the acceptor and its reduced products, induced disproportionation of the single electron transfer product to the two electron reduced relay might occur in a water-oil two phase system.

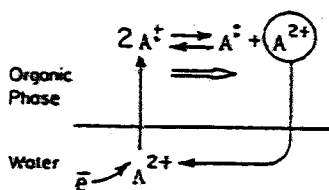


Figure 12. — Induced disproportionation of a single electron transfer product in a water-oil two phase system.

We have found that N, N'-dioctyl-4, 4'-bipyridinium, octyl viologen,  $C_8V^{2+}$ , (19), and its reduced products meet the desired hydrophilic-hydrophobic balance.<sup>23</sup> That is, the oxidized form  $C_8V^{2+}$  is merely soluble in water, while the reduced product  $C_8V^{\cdot}$  is hydrophobic since one of the positive charges is removed. The results of illumination of a water-oil two phase system that includes the photosystem Ru(bpy)<sub>3</sub><sup>2+</sup> as photosensitizer, octylviologen,  $C_8V^{2+}$ , as electron acceptor and ammonium ethylenediamine tetraacetic acid, (NH<sub>4</sub>)<sub>2</sub>EDTA, as electron donor are shown in Figure 13. This photosystem is soluble only in the aqueous phase. Illumination of the unstirred two-phase system produces octylviologen radical,  $C_8V^{\cdot}$  in the aqueous phase. Yet, upon stirring, this radical is extracted to the organic phase, and a new species is formed. The absorption spectrum of this photoproduct is consistent with the formation of the two electron charge relay  $C_8V^{\cdot -}$ .

We conclude that a photogenerated single electron transfer product undergoes induced disproportionation in a water-oil two phase system, provided that the proper hydrophilic-hydrophobic properties of the electron transfer products exists. The advantages of such system seem obvious:

- (i) The induced disproportionation product,  $C_8V^{\cdot -}$ , is a powerful reducing agent as compared to the single electron transfer photoproduct,  $C_8V^{\cdot}$ .
- (ii) The formation of the two electron charge relay in the organic phase allows its coupling to specific catalysts

solubilized in the organic phase and thus the construction of the proposed configuration of relay-catalyst can be envisaged.

Furthermore, induced disproportionation of a single electron transfer product in a two phase system might offer a model for the formation of the multi-electron charge relays in nature. Since reactions in natural systems occur in hydrophilic-hydrophobic microenvironments, we believe that similar induced disproportionation mechanisms might play an important role in the formation of the electron relays.

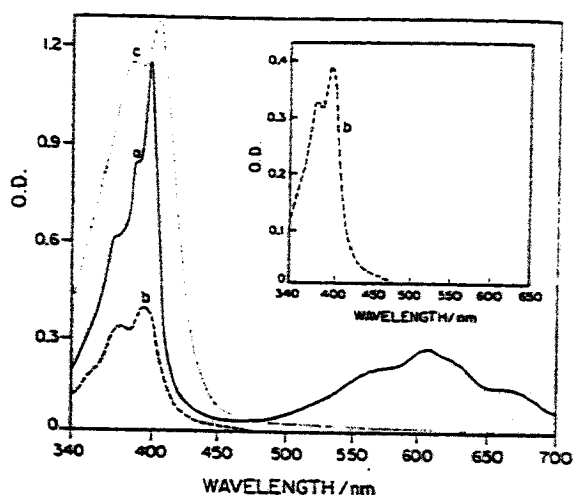
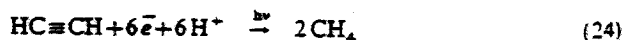


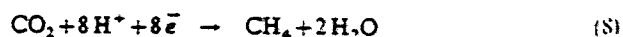
Figure 13. — Absorption spectra of disproportionation products of photogenerated  $C_8V^{\cdot -}$ : (a) Composite spectrum of  $C_8V^{\cdot -}$  and  $C_8V$  in ethyl acetate; (b) spectrum of  $C_8V$  in ethyl acetate, after subtraction of the  $C_8V^{\cdot -}$  spectrum; (c) spectrum of photoproduct in toluene.

#### PHOTOREDUCTION OF CO<sub>2</sub> TO CH<sub>4</sub>

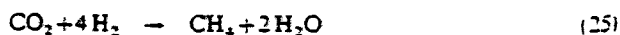
The development of specific catalysts for photosynthetic processes is certainly a most challenging subject. Homogeneous and heterogeneous catalysts were applied in various photosensitized transformations. For example, H<sub>2</sub>-evolution has been extensively studied using photogenerated viologen radicals in the presence of Pt or Rh colloids.<sup>24-27</sup> Similarly, homogeneous ruthenium complexes of the type [RuL<sub>3</sub>(H<sub>2</sub>O)]<sup>2+</sup> have been applied<sup>28</sup> as multi-electron charge relays for the reductive photocleavage of acetylene to methane (24).



The subject of CO<sub>2</sub> photoreduction is particularly interesting since it simulates natural photosynthesis. Recently, we were able to accomplish the photoreduction of CO<sub>2</sub> to methane (25). The problematicity in developing catalysts for artificial photosynthetic systems, will be exemplified in relation to this process.



Carbon dioxide is activated by ruthenium metal. This property of the Ru-catalyst is the basis for the methanation process (25) as well as for the electrocatalysed reduction of CO<sub>2</sub> to CH<sub>4</sub>. Thus, we attempted<sup>29</sup> to reduce Ru-activated CO<sub>2</sub> by a photogenerated relay compound.



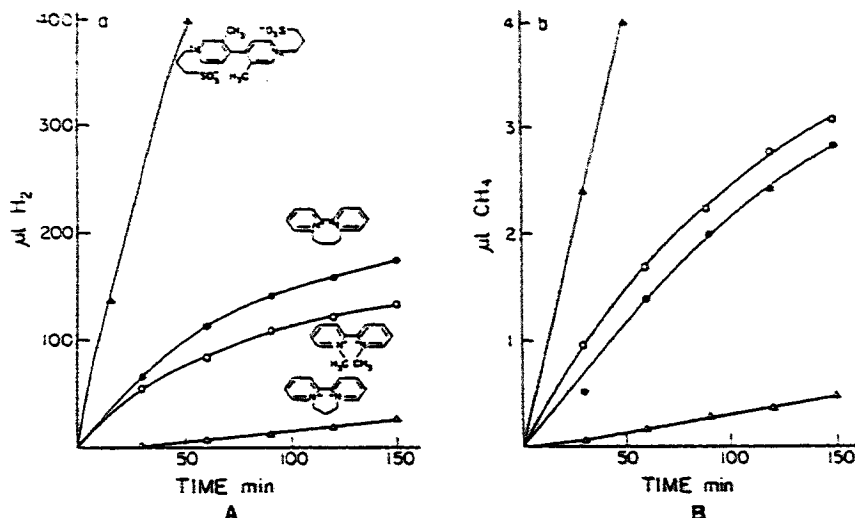


Figure 14. — Rate of H<sub>2</sub> and CH<sub>4</sub> formation using different charge relays: [Ru(bpy)<sub>3</sub><sup>2+</sup>]=1.4 × 10<sup>-4</sup> mol.l<sup>-1</sup>, [TEOA]=0.17 mol.l<sup>-1</sup>, [Relay]=1.4 × 10<sup>-3</sup> M; Ru-colloid=20 mg/l: A—H<sub>2</sub>-formation, B—CH<sub>4</sub>-formation.

Illumination of an aqueous solution that includes Ru(bpy)<sub>3</sub><sup>2+</sup> as photosensitizer, triethanolamine, TEOA, as electron donor and one of the electron acceptors (16)-(18) and (20) yields a mixture of gaseous products (Fig. 14). The major product is H<sub>2</sub> while a minor amount of methane (CH<sub>4</sub>) and higher hydrocarbons (ethylene and ethane) are also formed. The formation of the hydrocarbons is accomplished only in the presence of the Ru-colloid, and in the presence of other metal colloids, i.e., Pd, Pt or Rh-colloids only H<sub>2</sub>-formation is observed.

Thus, the Ru-colloid exhibits non-specificity in its catalytic activity, and H<sub>2</sub> evolution as well as CO<sub>2</sub> reduction occur simultaneously. Yet, an important conclusion is that CO<sub>2</sub> is indeed activated towards reduction in the presence of the Ru-metal. The reduction of protons to H<sub>2</sub> is thermodynamically favoured over the reduction of CO<sub>2</sub>. Therefore, to increase specificity towards CO<sub>2</sub> reduction, introduction of a kinetic barrier (overpotential) towards H<sub>2</sub>-formation is desirable. This approach might be accomplished either by substitution of the catalyst or the relay in the system.

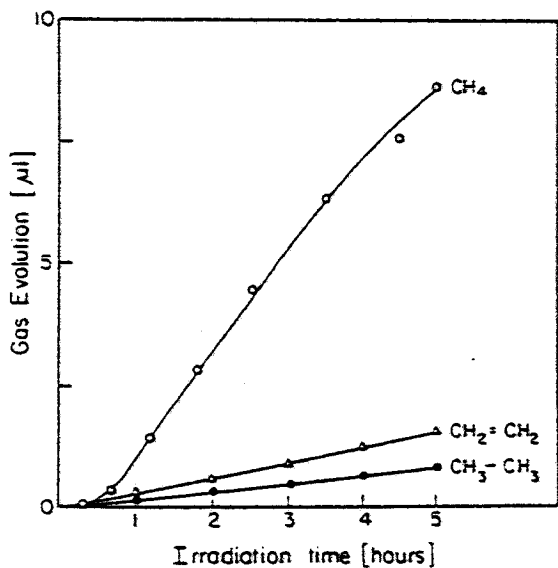
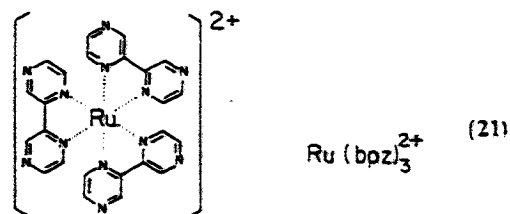


Figure 15. — Rate of hydrocarbons formation as a function of illumination time: [Ru(bpz)<sub>3</sub><sup>2+</sup>]=1 × 10<sup>-4</sup> mol.l<sup>-1</sup>, [TEOA]=0.17 mol.l<sup>-1</sup>, Ru-colloid=20 mg/l.

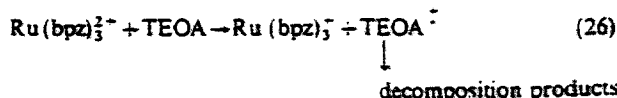
It is well established that Ru(II)-tris-bipyrazine, (21), Ru(bpz)<sub>3</sub><sup>2+</sup>, is oxidatively quenched by various electron donors<sup>30</sup> to form Ru(bpz)<sub>3</sub><sup>+</sup>. The reduced product is a powerful reductant,

$$E^0[\text{Ru}(\text{bpz})_3^+][\text{Ru}(\text{bpz})_3^{2+}] = -0.86 \text{ V vs. SCE,}$$

capable of reducing CO<sub>2</sub>. Interestingly, Ru(bpz)<sub>3</sub><sup>+</sup> does not mediate H<sub>2</sub>-evolution in the presence of Pt-colloids,<sup>31</sup> and so it meets the overpotential properties towards H<sub>2</sub>-evolution. Illumination of an aqueous system that includes Ru(bpz)<sub>3</sub><sup>2+</sup> as photosensitizer, triethanolamine as electron donor and Ru-colloid as catalyst under a gaseous CO<sub>2</sub> atmosphere results in the reduction of CO<sub>2</sub> and formation of hydrocarbons: methane, CH<sub>4</sub>, is the major product while ethylene and ethane are also formed (Fig. 15). The quantum



yield for methane formation is φ=0.04%. No H<sub>2</sub>-evolution is observed concomitant to methane evolution or in the absence of CO<sub>2</sub>. The origin for the specificity of the system towards CH<sub>4</sub> formation by the reduced relay Ru(bpz)<sub>3</sub><sup>+</sup> has been elucidated by laser flash photolysis experiments (Fig. 16). Flashing of a solution that includes Ru(bpz)<sub>3</sub><sup>2+</sup> and TEOA results in the steady state accumulation of the reduced relay since the oxidized photoproduct, TEOA<sup>•+</sup> decomposes irreversibly (26). Introduction of the Ru-colloid and CO<sub>2</sub>



results upon flashing in the rapid decay of photogenerated Ru(bpz)<sub>3</sub><sup>+</sup>. No decay of Ru(bpz)<sub>3</sub><sup>+</sup> occurs under CO<sub>2</sub> in the

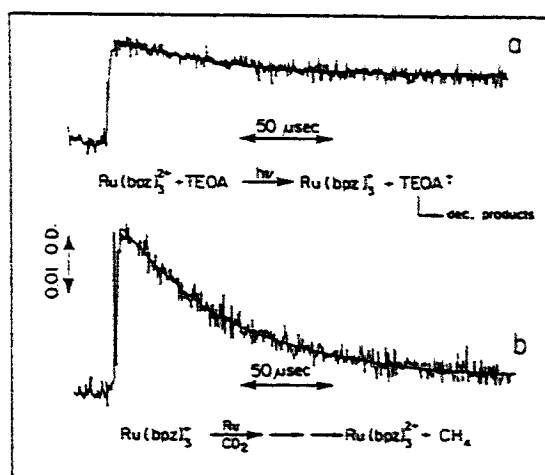
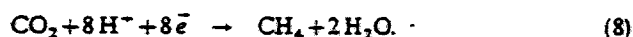


Figure 16. — Transient spectra formed upon illumination of  $\text{Ru}(\text{bpz})_3^{2+}$ ,  $2.2 \times 10^{-5} \text{ mol.l}^{-1}$  and TEOA,  $0.17 \text{ mol.l}^{-1}$  solution, pH 9.5. Systems are flashed at  $\lambda = 440 \text{ nm}$  and product is followed at  $\lambda = 500 \text{ nm}$ : (a) under  $\text{CO}_2$  or argon; (b) in the presence of Ru-colloid (20 mg/l) under  $\text{CO}_2$ .

absence of the Ru-colloid, and similarly the decay of  $\text{Ru}(\text{bpz})_3^{2+}$  is very inefficient in the presence of the Ru-colloid and absence of  $\text{CO}_2$ . These results clearly imply that the reduced relay is effectively oxidized only in the presence of the catalyst and  $\text{CO}_2$ . Thus, the formation of  $\text{CH}_4$  under steady state illumination is a result of the electron transfer from  $\text{Ru}(\text{bpz})_3^{2+}$  to Ru-metal activated  $\text{CO}_2$ . The inefficient electron exchange between the reduced relay and the Ru-colloid in the absence of  $\text{CO}_2$ , confirms the existence of an overpotential towards  $\text{H}_2$ -evolution. We thus conclude that the assembly of Ru-metal activated  $\text{CO}_2$  and the relay  $\text{Ru}(\text{bpz})_3^{2+}$  provides a proper relay-catalyst configuration for the multi electron reduction process of  $\text{CO}_2$  to  $\text{CH}_4$  (8).



We know that together with  $\text{CH}_4$  formation, ethylene,  $\text{C}_2\text{H}_4$ , and ethane,  $\text{C}_2\text{H}_6$ , are also formed (Fig. 15). The formation of these products can be rationalized in terms of metal carbene  $\text{Ru}=\text{CH}_2$  and methyl-ruthenium  $\text{Ru}-\text{CH}_3$  intermediates that lead to the formation of  $\text{CH}_4$  and upon dimerization yield ethylene and ethane. Yet, other mechanistic aspects such as the mode of  $\text{CO}_2$  activation by the Ru-colloid and the identification of the different intermediates involved in  $\text{CO}_2$  reduction process need further insight.

#### PHOTOINDUCED HYDROGENATION OF UNSATURATED COMPOUNDS. A RELAY-CATALYST COMBINED SYSTEM

The previous section emphasized that interaction between the reduced relay and the metal catalyst results in a mixture of products due to the competitive  $\text{H}_2$ -evolution process. To increase specificity towards the desired process, elimination of  $\text{H}_2$ -formation was suggested. A different conceptual approach might be developed, where the hydrogen generation system is used for the reduction of the substrate. The photosensitized evolution of  $\text{H}_2$  in the presence of a reduced relay, i.e., viologen radical, and an heterogeneous catalyst such as Pt, involves electron transfer from the relay to the catalyst and production of Pt-bound hydrogen atoms. These surface bound atoms dimerize to evolve molecular  $\text{H}_2$ . Hydrogenation processes of unsaturated compounds such as olefins or acetylenes by hydrogen proceed at high pressures in the

presence of heterogeneous catalysts similar to those used for  $\text{H}_2$ -evolution. The heterogeneous catalyst in the hydrogenation processes participates in two complementary functions: It activates the unsaturated substrate towards hydrogenation and it fragments molecular hydrogen into surface bound atoms generating the same intermediate that leads to  $\text{H}_2$ -evolution in the photochemical process. Thus, one might envisage the possibility to conduct photosensitized hydrogenation of unsaturated substrates at ambient pressures by trapping the *in situ* generated hydrogen atom formed by the reduced charge relay and the metal colloid.<sup>32</sup>

Illumination of an aqueous solution that includes the photosensitizer  $\text{Ru}(\text{bpy})_3^{2+}$ , the electron acceptor, N, N'-dimethyl-4, 4'-bipyridinium,  $\text{MV}^{2+}$ ,  $\text{Na}_2\text{EDTA}$  as sacrificial electron donor and a Pt colloid, under an atmosphere of ethylene results in the formation of ethane,  $\text{C}_2\text{H}_6$ , and no hydrogen is formed. The quantum yield of  $\text{C}_2\text{H}_6$ -formation is  $\phi = 9.9 \times 10^{-2}$ , a value identical to the  $\text{H}_2$ -evolution quantum yield in the absence of ethylene. These results clearly indicate that ethylene is activated by the Pt-colloid towards hydrogenation and all surface bound hydrogen atoms are trapped by the unsaturated substrate.<sup>32</sup>

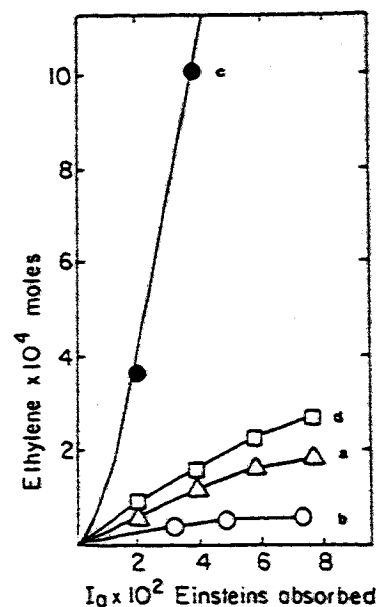


Figure 17. — Quantum yields for  $\text{C}_2\text{H}_2$  photohydrogenation in the presence of different catalysts: (a) Pt-colloid 43.0 mg/l (b) Pd-colloid, 4.2 mg/l, (c) Pt-colloid coated with Pd, Pt 43.0 mg/l, Pd 4.2 mg/l, (d) mixture of Pt-colloid 43.0 mg/l and Pd-colloid 4.2 mg/l.

A different situation is observed in the hydrogenation of acetylene,  $\text{C}_2\text{H}_2$ . When acetylene is substituted for ethylene as substrate,<sup>32</sup> and Pt is used as catalyst, inefficient hydrogenation of  $\text{C}_2\text{H}_2$  to ethylene is observed, ( $\phi = 3.2 \times 10^{-3}$ , Fig. 17 a), but no  $\text{H}_2$ -evolution is observed. The low quantum yield of  $\text{C}_2\text{H}_2$ -hydrogenation is rationalized in terms of poor activation of the substrate towards hydrogenation. The elimination of  $\text{H}_2$ -formation in the presence of  $\text{C}_2\text{H}_2$  is attributed to a "poisoning effect" of strongly associated acetylene to the metal surface that prevents H-atoms dimerization and  $\text{H}_2$ -evolution. Indeed, it is well established that Pd metal is superior to the Pt-catalyst for activation of acetylenes in hydrogenation processes. When the Pt colloid is substituted by a Pd colloid in the photochemical hydrogenation system, an improved quantum yield of  $\text{C}_2\text{H}_2$  hydrogenation is observed ( $\phi = 1.4 \times 10^{-2}$ , Fig. 17 b). It is evident that the quantum

yield for  $C_2H_2$ -hydrogenation is improved in the presence of the Pd catalyst, although it is substantially lower than that of  $H_2$ -evolution yield in the absence of the unsaturated substrate. The catalyst in the photohydrogenation process participates in two complementary functions (Fig. 18 a): (i) it interacts with the photoreduced relay, accepts electrons and forms surface bound hydrogen atoms, and (ii) it activates the unsaturated substrate towards the hydrogenation reaction. The effectiveness of the catalyst in accepting the electrons from the reduced relay,  $V^-$ , can be easily determined by laser flash photolysis, by following the decay of the reduced relay in the presence of the specific catalyst. Such studies reveal that electron transfer from photogenerated  $MV^-$  to the Pt colloid is substantially more effective than to the Pd colloid.

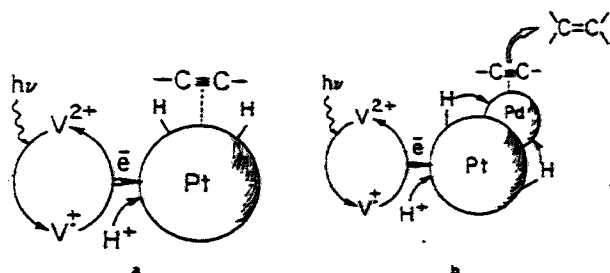


Figure 18. — (a) Functions of a heterogeneous catalyst in the photohydrogenation of  $C_2H_2$ . (b) Design of a bimetallic heterogeneous catalyst for improved photohydrogenation of  $C_2H_2$ .

To obtain high yields in photohydrogenation processes, optimum conditions to meet both functions of the catalyst should be fulfilled. The hydrogenation of  $C_2H_2$  in the presence of Pd-colloid improved activation of the substrate but concomitantly perturbed the former function of the catalyst in accepting electrons from the relay. A general approach to design a catalyst that meets both catalytic functions is schematically presented in Figure 18 b and involves the application of bimetallic heterogeneous catalysts. In the specific example the bimetallic catalyst is composed of one unit that includes a Pt-colloid coated by spots of Pd-metal. The Pt-center is aimed to participate in the efficient acceptance of electrons from the reduced relay. The Pd-catalytic sites are designed to activate effectively the acetylene substrate. With this combination of metals, migration of H-atoms from the Pt-surface to the Pd component, where  $C_2H_2$  is activated is anticipated to yield improved hydrogenation yields. The results of photohydrogenation of acetylene in the presence of the bifunctional Pt-Pd colloid are shown in Figure 17 c. For comparison, the photohydrogenation of  $C_2H_2$  has been examined using a mixture of the two separated Pd colloids (Fig. 17 d). It is evident that the mixture of colloids shows an additive effect of the hydrogenation yields in the presence of each of the catalysts. Yet, with the bifunctional constructed catalyst a synergistic effect is evident: The quantum yield for  $C_2H_2$ -hydrogenation is  $\phi = 3.2 \times 10^{-2}$  with a Pt colloid coated with Pd. These results imply that optimal yields in the sequestered steps of hydrogenation of  $C_2H_2$  have been accomplished using the bifunctional catalyst.

This approach where a bifunctional catalyst is used in photosynthetic processes simulates the cofactor-enzyme activity in natural photosynthesis. The Pt-component of the bifunctional catalyst mimics the cofactor functions in charge accumulation and generation of the reducing equivalents, [H]-atoms. The Pd-site resembles the function of the enzyme

to the extent that the substrate is activated towards the hydrogenation process. Only the spatial configuration of the two components in one unit results in the desired catalytic activity, similarly to the high ordered configuration of the enzyme-cofactor required in nature.

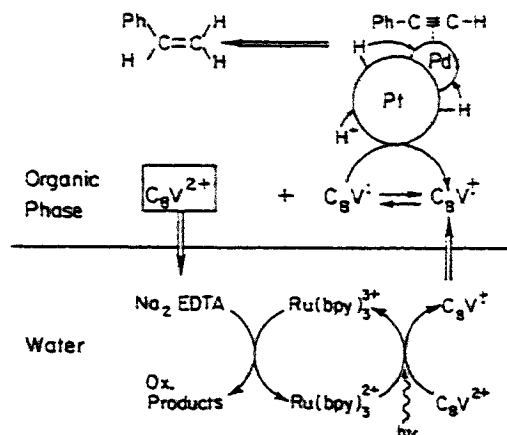


Figure 19. — Schematic cycle for the photohydrogenation of phenylacetylene in a water-oil two phase system.

The hydrogenation process of unsaturated substrates is of substantial importance in organic synthesis. Yet, organic compounds are insoluble in aqueous solutions, and therefore the applicability of the photohydrogenation process is limited. To overcome this difficulty we have combined the concepts of photoinduced generation of multielectron charge relays in water-oil two phase systems, with the design of bifunctional catalysts into one synchronically operative system.<sup>33</sup> This system is schematically presented in Figure 19. It includes a water-oil (cyclohexane) two phase system. The photosystem is solubilized in the aqueous phase and is composed of  $Ru(bpy)_3^{2+}$  as photosensitizer, dioctylviologen (19),

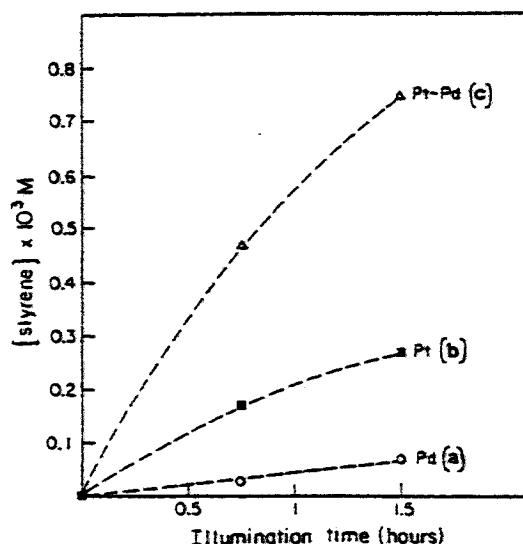


Figure 20. — Rates of photosensitized hydrogenation of  $PhC\equiv CH$  in a water-hexane two phase system:

$[Ru(bpy)_3^{2+}] = 1.9 \times 10^{-3} \text{ mol.l}^{-1}$ ,  
 $[C_8V^{2+}] = 2 \times 10^{-3} \text{ mol.l}^{-1}$ ,  
 $[Na_2EDTA] = 2 \times 10^{-2} \text{ mol.l}^{-1}$ .

(a) Pd-colloid 5.9 mg/l (b) Pt-colloid 12.3 mg/l; (c) Pt-Pd colloid: Pt 12.3 mg/l, Pd 5.9 mg/l.



$C_8V^{2-}$ , as electron acceptor and  $Na_2EDTA$  as electron donor. Methods to prepare metal colloids in organic solutions were developed. The Pt or Pd-metal colloids or a combination of the two metals is introduced into the organic phase where phenylacetylene,  $Ph-C\equiv CH$  is solubilized as substrate. Illumination of this system results in the photosensitized formation of  $C_8V^-$  in the aqueous phase. This hydrophobic reduced photoproduct is extracted from the aqueous phase to the organic phase where hydrogenation of phenylacetylene occurs. The rates of hydrogenation of  $Ph-C\equiv CH$  to styrene in the presence of the various metal catalysts are displayed in Figure 20. It is evident that while the Pd-colloid is inefficient in the hydrogenation process, and the Pt-colloid exhibits moderate activity, the combination of the two catalysts reveals high effectiveness. This synergistic effect is attributed to the two complementary functions of the metals as discussed previously: i.e. formation of active [H]-atoms on the Pt surface and activation of the substrate on the Pt component. A detailed mechanistic study using cyclic voltammetry has revealed that the reduced photoproduct  $C_8V^-$  is inactive in charging the Pt-colloid presents in the organic phase. In turn, the two electron charge relay,  $C_8V^-$ , formed by induced disproportionation in the water-oil two phase system is the active species in the production of [H]-atoms on the colloid surface.

We conclude that photohydrogenation of phenylacetylene in the two phase system exemplifies the photosynthetic potential of properly composed and organized systems. The two phase system provides a means to separate the photosystem from the catalytic site. The stabilization of composed metal colloids in the organic phase allows to design multi-purpose catalysts in the oil phase. The hydrophobic nature of the reduced relay and the induced disproportionation process provides a means to link the photochemical and catalytic sites.

### Conclusions

We have exemplified the perspectives of bio-models and artificial models for photosynthesis. Bio-models are a composite of an artificial photosystem linked to biocatalysts. The photoinduced regeneration of the natural cofactors by artificial means provides a general approach for driving endoergic enzyme catalysed synthesis. The remarkable stability of the enzymes in the artificial environments, and the specificity in reactions, opens a broad array of possibilities to apply visible light and enzymes in biotechnology.

Artificial photosynthetic models attempt to design and construct artificially tailored systems that mimic natural photosynthesis. In our view an artificial photosynthetic system should be composed of two separate sub-components: A multi-electron charge relay that simulates the functions of the natural cofactor, and a catalytic site that activates the substrates towards the specific reaction. Proper configurational linkage of these two components in an organized manner provides a means for simulating natural photosynthesis. We have discussed examples where this approach is successfully applied, i.e. photoreduction of  $CO_2$  to methane and photohydrogenation of unsaturated compounds.

The design of specificity in artificial photosynthetic systems is a major subject for consideration. Heterogeneous metal colloids designed for specific reactions act also as  $H_2$ -evolution catalysts. Consequently,  $H_2$ -formation accompanies and

eventually eliminates the desired fixation (reduction) process. Two alternative approaches were suggested to resolve this difficulty. One approach has suggested the use of charge relays exhibiting overpotential properties, in the presence of the catalyst, towards  $H_2$ -evolution. The second approach suggested effective activation of the substrate towards hydrogenation and utilization of *in situ* generated H-atoms to induce the reduction (hydrogenation) of the desired process. Both approaches are essentially mimicking the cofactor-enzyme configuration of the natural system. Significant progress in underlining the conceptual approaches for photosynthetic devices has been accomplished. Application of such bio-models and artificial models for the reduction of other substrates and design of other specific catalysts remain future challenging goals.

### Acknowledgement

This research is supported by a grant from the National Council for Research and Development, Israel, the Kernforschung Anlage Juelich, Germany, and the Belfer Foundation, Israel.

### REFERENCES

- Bard A. J., *Science*, 1980, 207, 139.
- "Photogeneration of Hydrogen", Harriman A. and West M. A. Eds., Academic Press, London, 1983.
- "Energy Resources through Photochemistry and Catalysis", Gratzel M. Ed., Academic Press, New York, 1983.
- (a) Sutin N., Creutz C., *Pure Appl. Chem.*, 1980, 52, 2717; (b) Gratzel M., *Acc. Chem. Res.*, 1981, 14, 376.
- (a) "Solar Power and Fuels", Bolton J. R. Ed., Academic Press, New York, 1977; (b) Bolton J. R., *Science*, 1978, 202, 105.
- Hall D. O., Rao K. K., "Photosynthesis", Edward Arnold, London, 1972.
- "Topics in Photosynthesis-Photosynthesis in Relation to Model Systems", Barber J. Ed., Vol. 3, Elsevier/North Holland, Biochemical Press, Amsterdam 1979.
- Kalyanasundaram K., *Coord. Chem. Rev.*, 1982, 46, 159.
- (a) Darwent J. R., Douglass P., Harriman A., Porter G., Richoux M. C., *Coord. Chem. Rev.*, 1982, 44, 83; (b) Balzani V., Boletta F., Scandola F., Ballardini R., *Pure Appl. Chem.*, 1979, 51, 299.
- Turro N., Gratzel M., Braun A. M., *Angew. Chem. Int. Ed. Engl.*, 1980, 19, 675.
- Matsuo T., Takuma K., Tsusui Y., Nishigima T., *Coord. Chem. Rev.*, 1980, 10, 195.
- (a) Willner I. in "Organic Phototransformations in Nonhomogeneous Media", Fox M.-A. Ed., A.C.S. Symposium Series No. 278, 1985, p. 191; (b) Fendler J. H., *J. Phys. Chem.*, 1980, 84, 1485.
- (a) Brugger P. A., Infelta P. P., Braun A. M., Gratzel M., *J. Amer. Chem. Soc.*, 1981, 103, 320; (b) Degani Y., Willner I., *J. Phys. Chem.*, 1985, 89, 5685; (c) Mandler D., Degani Y., Willner I., *J. Phys. Chem.*, 1984, 88, 4366.
- (a) Willner I., Yang J. M., Otvos J. W., Calvin M., *J. Phys. Chem.*, 1981, 85, 3277; (b) Willner I., Otvos J. W., Calvin M., *J. Amer. Chem. Soc.*, 1981, 103, 3203; (c) Degani Y., Willner I., *J. Phys. Chem.*, 1985, 89, 5685.
- Mandler D., Willner I., *J. Amer. Chem. Soc.*, 1984, 106, 5352.
- Mandler D., Willner I., *J. Chem. Soc., Perkin Trans. 2*, 1986, 805.
- Maidan R., Willner I., Unpublished results.
- Mandler D., Willner I., *J. Chem. Soc., Chem. Commun.*, 1986, 851.
- Goren Z., Lapidot N., Willner I., Submitted for publication.
- Willner I., Mandler D., Riklin A., *J. Chem. Soc., Chem. Commun.*, 1986, 1022.

- Pollak A., Blumenfeld H., Wax M., Baughn B. L., Whitesides G. M., *J. Amer. Chem. Soc.*, 1980, 102, 6324.
- 22 Mandler D., Unpublished results.
- 23 (a) Goren Z., Willner I., *J. Amer. Chem. Soc.*, 1983, 105, 7764; (b) Maidan R., Goren Z., Becker J. Y., Willner I., *J. Amer. Chem. Soc.*, 1984, 106, 6217.
- 24 (a) Keller P., Moradpour A., Amouyal E., Kagan H. B., *Nouv. J. Chim.*, 1980, 4, 377; *J. Amer. Chem. Soc.*, 1980, 102, 7193; (b) Harriman A., Porter G., Richoux M. C., *J. Chem. Soc., Faraday Trans. 2*, 1981, 77, 1939; (c) Harriman A., Porter G., Richoux M. C., *J. Chem. Soc., Faraday Trans. 2*, 1981, 77, 833.
- 25 (a) Kirsch M., Lehn J.-M., Sauvage J.-P., *Helv. Chim. Acta*, 1979, 62, 1345; (b) Krasna A. I., *Photochem. Photobiol.*, 1980, 31, 75.
- 26 (a) Okura I., Kim-Thuan N., *J. Chem. Soc., Faraday Trans.*, 1981, 77, 1; (b) Keller P., Moradpour A., Amouyal E., *J. Chem. Soc., Faraday Trans.*, 1982, 78, 3531.
- 27 Degani Y., Willner I., *J. Amer. Chem. Soc.*, 1983, 105, 6228.
- 28 Degani Y., Willner I., *J. Chem. Soc., Chem. Commun.*, 1985, 648.
- 29 Maidan R., Willner I., *J. Amer. Chem. Soc.*, 1986, 108, 8100.
- 30 (a) Crutchley R. J., Lever A. B. P., *Inorg. Chem.*, 1982, 21, 2276; (b) Crutchley R. J., Lever A. B. P., *J. Amer. Chem. Soc.*, 1980, 102, 7128.
- 31 Dürr H., Dörr G., Zengerle K., Curchod J.-M., Braun A. M., *Helv. Chim. Acta*, 1984, 2652; (b) Dürr H., Dörr G., Zengerle K., Mayer E., Curchod J.-M., Braun A. M., *Nouv. J. Chim.*, 1985, 9, 717.
- 32 Degani Y., Willner I., *J. Chem. Soc., Perkin Trans. 2*, 1986, 57.
- 33 Mandler D., Willner I., Unpublished results.

conclusion being supported by studies with  $[5-^{13}\text{C}]\text{Glu-bR}$ . Possible changes of the four Asp residues are proposed in Table I. It is interesting to note that the currently favored models<sup>12</sup> for the folding of bR show that of the nine Asp residues, four reside within the interior of the membrane. Groups which change protonation state concomitantly with the proton-pumping process might be involved as a conducting wire.<sup>13</sup> In addition to Asp, we have observed protonation/deprotonation steps in the following changes: DA (Tyr-OH)  $\rightarrow$  LA (Tyr-O<sup>-</sup>)  $\rightarrow$  (Tyr-OH)  $\rightarrow$  L (Tyr-OH)  $\rightarrow$  M (Tyr-O<sup>-</sup>),<sup>4,5</sup> while Rothschild and co-workers have also shown<sup>22</sup> that a tyrosinate protonates in LA  $\rightarrow$  K. Clearly the technique of difference FTIR provides a powerful method which will contribute to the understanding of subtle dynamic processes exemplified by proton translocation.

**Acknowledgment.** This work has been supported by PHS GM 32455 (to L.E.), PHS IS10RR2298 (to L.E., for purchase of Mattson Sirius 100), and NSF CHE 84-12513 (to K.N.).

**Supplementary Material Available:** The DA/LA, K/LA, L/LA, and M/LA difference spectra of the entire region and of the expanded carboxylate region for native and  $[4-^{13}\text{C}]\text{Asp-bR}$ ; the DA/LA, K/LA, L/LA, and M/LA difference spectra for native and  $[5-^{13}\text{C}]\text{Glu-bR}$  (12 pages). Ordering information is given on any current masthead page.

- (12) (a) Huang, K.-S.; Radhakrishnan, R.; Bayley, H.; Khorana, H. G. *J. Biol. Chem.* 1982, 257, 13616-13623. (b) Trehub, J.; Anderson, S.; Fox, R.; Gogol, E.; Khan, S.; Engelman, D. *Biophys. J.* 1983, 42, 233-241.  
(13) Nagle, J. F. *J. Membrane Biol.* 1983, 74, 1-14.

### TiO<sub>2</sub> and CdS Colloids Stabilized by $\beta$ -Cyclodextrins: Tailored Semiconductor-Receptor Systems as a Means to Control Interfacial Electron-Transfer Processes

Itamar Willner\* and Yoav Eichen

Department of Organic Chemistry  
The Hebrew University of Jerusalem  
Jerusalem 91904, Israel

Received April 17, 1987

The photocatalytic activity of semiconductor particles is of substantial interest in synthesis<sup>1</sup> as well as a means of solar energy conversion and storage.<sup>2,3</sup> Electron-transfer reactions such as charge ejection or charge injection at semiconductor-solution interfaces are important factors that control the photocatalytic activity of the semiconductors.<sup>4,5</sup> Electrostatic attraction of solute to the semiconductor surface has improved charge ejection from the excited semiconductor to solute relays.<sup>6</sup> Adsorption of dyes to the semiconductor surface, i.e., by hydrophobic interactions, resulted in effective charge injection to the semiconductor and consequently the photocatalytic activity of semiconductors operative in the UV region could be shifted to the visible absorption spectrum.<sup>5,7</sup> Substantial efforts have also been directed in recent

- (1) Fox, M. A. *Acc. Chem. Res.* 1983, 16, 314.  
(2) (a) *Energy Resources Through Photochemistry and Catalysis*; Gratzel, M., Ed.; Academic: New York, 1983. (b) Bard, A. J. *Science (Washington, D.C.)* 1980, 207, 1380. (c) Gratzel, M. *Acc. Chem. Res.* 1981, 14, 376.  
(3) *Photochemical Conversion and Storage of Solar Energy*; Connolly, J. S., Ed.; Academic: New York, 1981.  
(4) (a) Kamat, P. V.; Dimitrijevic, N. M.; Fessenden, R. W. *J. Phys. Chem.* 1987, 91, 396. (b) Kamat, P. V.; Fox, M. A. *Chem. Phys. Lett.* 1983, 102, 379.  
(5) (a) Fan, F. R. F.; Bard, A. J. *J. Am. Chem. Soc.* 1979, 101, 6139. (b) Borgarello, E.; Kiwi, J.; Gratzel, M.; Pelizzetti, E.; Visca, M. *J. Am. Chem. Soc.* 1985, 107, 2996. (c) Dealverstro, J.; Gratzel, M.; Kavan, L.; Moser, J. *J. Am. Chem. Soc.* 1985, 107, 2988.  
(6) Frank, A. J.; Willner, I.; Goren, Z.; Degani, Y. *J. Am. Chem. Soc.* 1987, 109, 3568.

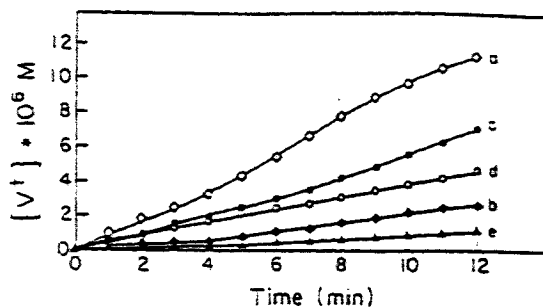


Figure 1. Rate of  $\text{C}_4\text{V}^{2+}$  and  $\text{MV}^{2+}$  formation at time intervals of illumination in the presence of  $\text{TiO}_2$ - $\beta$ -CD colloid. All experiments include  $[\text{C}_4\text{V}^{2+}]$  or  $[\text{MV}^{2+}] = 5 \times 10^{-5}$  M, 2 mL of  $\text{TiO}_2$ , 2 g-L<sup>-1</sup>, stabilized by 1%  $\beta$ -CD: (a)  $\text{C}_4\text{V}^{2+}$  formation, (b)  $\text{MV}^{2+}$  formation, (c) rate of  $\text{C}_4\text{V}^{2+}$  formation, with  $[\text{phenol}] = 0.018$  M, (d)  $\text{C}_4\text{V}^{2+}$  formation with  $[\text{phenol}] = 0.024$  M, (e)  $\text{C}_4\text{V}^{2+}$  formation, with  $[\text{phenol}] = 0.05$  M.

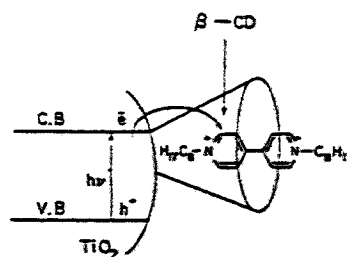


Figure 2. Schematic function of the receptor-semiconductor colloid in improving interfacial electron transfer.

years toward the preparation of semiconductor particles in colloidal forms to improve their light harvesting and interfacial electron-transfer properties.<sup>8-10</sup> Stabilization of semiconductor colloids by polymers, microemulsions, and vesicle encapsulation<sup>10</sup> has been reported. Here we report on a novel method for stabilizing semiconductor colloids by  $\beta$ -cyclodextrin ( $\beta$ -CD).

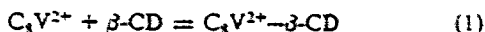
Cyclodextrins have been extensively examined as molecular receptors that bind solutes to their hydrophobic cavities.<sup>11-12</sup> Thus, the tailored semiconductor-receptor configuration allows the association of solutes to the  $\beta$ -CD cavity and consequently improves the interfacial electron transfer process at the semiconductor-solution interface.

We have stabilized CdS and  $\text{TiO}_2$  colloids in aqueous solutions with  $\beta$ -CD. The CdS colloid has been prepared by slow addition of  $\text{Cd}(\text{NO}_3)_2$  into the solution of 1%  $\beta$ -CD +  $\text{Na}_2\text{S}$ . The  $\text{TiO}_2$  colloid was prepared by the slow addition of  $\text{TiCl}_4$  to the  $\beta$ -CD solution at 0 °C. The mean diameter of the CdS and  $\text{TiO}_2$  particles was determined by TEM to be 80 and 100 Å, respectively. In the absence of  $\beta$ -cyclodextrin the semiconductors precipitate out of solution.

$N,N'$ -Diocetyl-4,4'-bipyridinium (octyl viologen,  $\text{C}_4\text{V}^{2+}$ ) associates with the  $\beta$ -CD cavity<sup>13</sup> (eq 1),  $K_{\text{ass}} = 5.6 \times 10^3$  M<sup>-1</sup>. Illumination of the  $\text{TiO}_2$ - $\beta$ -CD colloid ( $\lambda > 335$  nm), pH 2.5, in the presence of  $\text{C}_4\text{V}^{2+}$ ,  $5 \times 10^{-5}$  M, and 2-propanol,  $5 \times 10^{-3}$  M, as electron donor results in the formation of  $\text{C}_4\text{V}^{•+}$  in its monomer form. Figure 1a shows the rate of  $\text{C}_4\text{V}^{•+}$  formation at time intervals of illumination that corresponds to a quantum yield of  $\phi = 1.1 \times 10^{-3}$ .<sup>14</sup> Similarly, illumination of the CdS- $\beta$ -CD colloid

- (7) Houding, V. H.; Gratzel, M. *J. Am. Chem. Soc.* 1983, 105, 5695.  
(8) Hradah, H.; Udea, T. *Chem. Phys. Lett.* 1984, 106, 229.  
(9) Mayer, M.; Wallberg, C.; Karihara, K.; Fendler, H. J. *J. Chem. Soc., Chem. Commun.* 1984, 90.  
(10) (a) Tricot, M. Y.; Fendler, H. J. *J. Am. Chem. Soc.* 1984, 106, 2475.  
(b) Tricot, M. Y.; Emren, A.; Fendler, H. J. *J. Phys. Chem.* 1985, 89, 4721.  
(c) Tricot, M. Y.; Fendler, H. J. *J. Am. Chem. Soc.* 1984, 106, 7359.  
(11) (a) *Cyclodextrin Chemistry*; Bender, M.; Kamiyama, L., Eds.; Springer, 1978. (b) Sanger, A. Q. *Angew. Chem., Int. Ed. Engl.* 1980, 19, 344. (c) Breslow, R. *Science (Washington D.C.)* 1982, 218, 532.  
(12) Tabushi, I. *Acc. Chem. Res.* 1982, 15, 66.  
(13) Adar, E.; Degani, Y.; Goren, Z.; Willner, I. *J. Am. Chem. Soc.* 1986, 108, 4696.

in the presence of  $C_3V^{2+}$ , pH 6, and  $Na_2S$ ,  $5 \times 10^{-2}$  M, as donor, results in the monomer photoproduct,  $C_3V^{++}$ ,  $\phi = 0.2$ .<sup>14</sup> When



methyl viologen,  $MV^{2+}$ , is used as charge relay instead of  $C_3V^{2+}$ , substantially lower quantum yields of  $MV^{++}$  are observed. Figure 1b shows the rate of  $MV^{++}$  formation at time intervals of illumination with the  $TiO_2$ - $\beta$ -CD colloid. The quantum yield corresponds to  $\phi = 2.6 \times 10^{-4}$  and is 4.4 times lower than that for  $C_3V^{++}$  formation in the analogous system. Similarly, the quantum yield for  $MV^{++}$  formation with  $CdS$ - $\beta$ -CD is 3.6 times lower as compared to  $C_3V^{++}$  production. It should be noted that methyl viologen ( $MV^{2+}$ ) is not associated with  $\beta$ -cyclodextrin.<sup>15</sup> Thus, the high quantum yields for  $C_3V^{++}$  formation in the presence of the  $\beta$ -CD semiconductor stabilized colloids, as compared to that of  $MV^{2+}$  photoreduction, is attributed to improved interfacial electron transfer from the excited semiconductor to the relay substrate,  $C_3V^{2+}$  (Figure 2). Association of  $C_3V^{2+}$  to the  $\beta$ -CD hydrophobic cavity increases the local concentration of the relay in proximity with the semiconductor interface. Consequently, the interfacial electron-transfer rates and reduction of the relay  $C_3V^{2+}$  by conduction band electrons are improved. Indeed, the photoreduction process of  $C_3V^{2+}$  using the semiconductor- $\beta$ -CD stabilized colloids is strongly inhibited in the presence of phenol, which associates with the  $\beta$ -CD hydrophobic cavity. Figure 1(c-e) shows the rate of  $C_3V^{++}$  formation at time intervals of illumination and different concentrations of added phenol. It is evident that the quantum yield for  $C_3V^{++}$  production decreases as the concentration of phenol increases. Thus, phenol that associates to  $\beta$ -CD expels the charge relay  $C_3V^{2+}$  from the receptor and consequently the superior configuration for electron transfer is destroyed. Similarly,  $TiO_2$  colloids were stabilized with  $\alpha$ -cyclodextrins. The association properties of  $C_3V^{2+}$  to  $\alpha$ -CD are weaker than those to  $\beta$ -CD ( $K_a = 4500 \text{ M}^{-1}$ ). Accordingly, the specificity toward  $C_3V^{2+}$  photoreduction as compared to  $MV^{2+}$  reduction decreases,  $\phi(C_3V^{++})/\phi(MV^{++}) = 4.0$ .

We have compared the photoreduction reactions of  $C_3V^{2+}$  and  $MV^{2+}$  using  $TiO_2$ - $\beta$ -CD colloids to the similar reactions induced by  $TiO_2$  colloids stabilized by poly(vinyl alcohol), PVA. With  $TiO_2$ -PVA colloids the quantum yield ratio  $\phi(C_3V^{++})/\phi(MV^{++})$  is 1:1, implying similar efficiencies. With the  $TiO_2$ - $\beta$ -CD colloids the ratio is 4.4:1 and it demonstrates selectivity in the reduction of the  $C_3V^{2+}$  relay system.

Laser flash experiments confirm that improved electron transfer occurs to  $C_3V^{2+}$  in the presence of  $TiO_2$ - $\beta$ -CD. Flashing the systems that include  $TiO_2$ - $\beta$ -CD and  $MV^{2+}$  or  $C_3V^{2+}$  at  $\lambda = 337.1$  nm results in the formation of  $MV^{++}$  or  $C_3V^{++}$ . With  $MV^{2+}$  as charge relay, instantaneous accumulation of  $MV^{++}$  is observed that results from electrostatically associated  $MV^{2+}$  to the  $TiO_2$ -colloid.<sup>2c</sup> With  $C_3V^{2+}$  as relay, the instantaneous formation of  $C_3V^{++}$  is followed by a diffusional charge ejection to  $C_3V^{2+}$  associated with the  $\beta$ -CD, and the total amount of accumulated  $C_3V^{++}$  is ca. 4 times larger than that of  $MV^{++}$ .

In conclusion we have stabilized  $TiO_2$  and  $CdS$  semiconductor colloids with  $\beta$ -cyclodextrins. The tailored semiconductor-receptor configuration and proper design of the charge relay provide means to control interfacial electron transfer and introduce selectivity in the reduction of relay substrates. The association of the relay to the receptor sites increases the local concentration of the relay at the colloid interface and consequently improves the interfacial electron-transfer process. Further applications of semiconductor-receptor colloids could be envisaged. These include effective and selective charge injection via the selective association of chromophores to  $\beta$ -CD or selective synthesis through immobilization of catalysts on the semiconductor sites. These aspects are now being examined in our laboratory.

**Acknowledgment.** The support of the Singer Foundation is gratefully acknowledged.

(14) Light intensity was determined by using Reinecke's salt actinometry. cf.: Wanger, E. E.; Adamson, A. W. *J. Am. Chem. Soc.* 1966, 88, 394.  
(15) Maisue, T.; Kato, T.; Akiba, U.; Osa, T. *Chem. Lett.* 1985, 1825.

## Spectroscopic and Structural Evidence of Temperature Dependent Charge Localization and Structural Differentiation of the Fe Sites within the $[Fe_6S_6X_6]^{2-}$ Clusters (X = Cl, Br)

D. Coucouvanis,\* M. G. Kanatzidis, A. Salifoglou, and W. R. Dunham

Department of Chemistry, University of Michigan  
Ann Arbor, Michigan 48109

A. Simopoulos, J. R. Sams,<sup>1</sup> V. Papaefthymiou, and A. Kostikas

Nuclear Research Center Demokritos  
Aghia Paraskevi, Attiki, Greece

C. E. Strouse

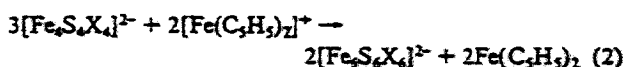
Department of Chemistry and Biochemistry and the  
Solid State Science Center, University of California  
Los Angeles, California 90024

Received May 8, 1987

The recently reported  $[Fe_6S_6L_6]^{2-}$  clusters<sup>2</sup> are new members in the general series of the synthetic Fe/S clusters that contain the  $[Fe_2S_2]_n^{++}$  cores. They are metastable species and thermally or catalytically can be converted quantitatively to the  $[Fe_6S_6X_6]^{2-}$  "cubanes" (eq 1).



The oxidized,  $[Fe_6S_6X_6]^{2-}$ , prismatic clusters can be obtained in nearly quantitative yields by chemical oxidation of the  $[Fe_6S_6X_6]^{2-}$  clusters<sup>2c</sup> (eq 2) (X = Cl, Br) with  $[(C_2H_5)_2Fe]^+-[PF_6]^-$ .



The Mossbauer spectra of the  $[Fe_6S_6X_6]^{2-}$  clusters for X = Cl, I [or Br, II], were examined at various temperatures in the range from 1.6 K to ambient temperature (AT). The spectra (Figure 1) generally show two broad lines of unequal intensities at temperatures above 100 K. The average values of the isomer shift (IS) and quadrupole splitting ( $\Delta_{eq}$ ) for these doublets above 100 K are 0.44 (I), 0.62 (I) and 0.44 (I), 0.70 (I) mm/s, respectively, for I and II. These values, which represent iron atoms in a formal +2.66 oxidation state, as expected, are somewhat smaller than corresponding values for the  $[Fe_6S_6X_6]^{2-}$  clusters, which contain iron atoms in a +2.5 formal oxidation state.<sup>2b</sup> For the latter, IS and  $\Delta_{eq}$  values of 0.52 (I) and 0.95 (I) mm/s for X = Cl and 0.54 (I) and 1.00 (I) mm/s for X = Br have been observed at 125 K. At 1.6 K the high velocity line clearly shows partially resolved structure that suggests at least three peaks. The structure persists to about 50 K and gradually becomes obscure at higher temperatures. The spectra for both I and II at 4.2 K were fitted by the superposition of three symmetric quadrupole doublets constrained to equal intensities and line widths. This model implies the grouping of the iron ions into three pairs characterized by different IS and  $\Delta_{eq}$  values with the irons within each pair being equivalent. Two realistic combinations of six peaks into quadrupole doublets can be chosen.<sup>3</sup> For combination (a) in the low tem-

(1) On leave of absence, Chemistry Department, University of British Columbia, Vancouver, British Columbia, Canada.

(2) (a) Kanatzidis, M. G.; Dunham, W. R.; Hagen, W. R.; Coucouvanis, D. *J. Chem. Soc., Chem. Commun.* 1984, 356. (b) Kanatzidis, M. G.; Hagen, W. R.; Dunham, W. R.; Lester, R. K.; Coucouvanis, D. *J. Am. Chem. Soc.* 1985, 107, 953. (c) Coucouvanis, D.; Kanatzidis, M. G.; Dunham, W. R.; Hagen, W. R. *J. Am. Chem. Soc.* 1984, 106, 7998. (d) Kanatzidis, M. G.; Salifoglou, A.; Coucouvanis, D. *J. Am. Chem. Soc.* 1985, 107, 3358. (e) Kanatzidis, M. G.; Salifoglou, A.; Coucouvanis, D. *Inorg. Chem.* 1986, 25, 2460.

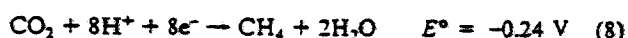
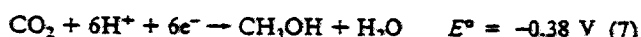
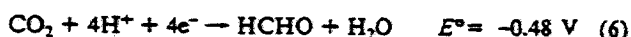
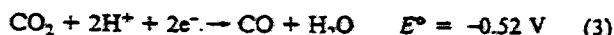
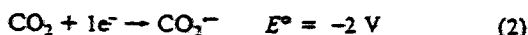
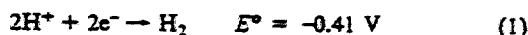
# Photosensitized Reduction of CO<sub>2</sub> to CH<sub>4</sub> and H<sub>2</sub> Evolution in the Presence of Ruthenium and Osmium Colloids: Strategies To Design Selectivity of Products Distribution<sup>1</sup>

Itamar Willner,\*† Ruben Maida,† Daphna Mandler,† Heinz Dürr,‡ Gisela Dörr,‡ and Klaus Zengerle‡

Contribution from the Department of Organic Chemistry, The Hebrew University of Jerusalem, Jerusalem 91904, Israel, and Organische Chemie, Universität des Saarlandes, D-6000 Saarbrücken, Germany. Received March 5, 1987

**Abstract:** Photoreduction of CO<sub>2</sub> to methane and higher hydrocarbons is accomplished in aqueous solutions by using visible light and Ru or Os colloids as catalysts. One system is composed of Ru(II) tris(bipyridine), Ru(bpy)<sub>3</sub><sup>2+</sup>, as photosensitizer, triethanolamine, TEOA, as electron donor, and one of the following bipyridinium charge relays: *N,N'*-dimethyl-2,2'-bipyridinium, MQ<sup>2+</sup> (1), *N,N'*-trimethylene-2,2'-bipyridinium, TQ<sup>2+</sup> (2), *N,N'*-tetramethylene-2,2'-bipyridinium, DQ<sup>2+</sup> (3), or *N,N'*-bis-(3-sulfonatopropyl)-3,3'-dimethyl-4,4'-bipyridinium, MPVS<sup>0</sup> (4). Illumination of these systems under CO<sub>2</sub> in the presence of Ru or Os colloids results in the formation of methane and ethylene and in H<sub>2</sub> evolution. In the second system, illumination of an aqueous solution under CO<sub>2</sub> that includes Ru(II) tris(bipyrazine) as sensitizer, TEOA as electron donor, and the Ru colloids leads to the formation of methane, ethylene, and ethane, and no H<sub>2</sub>-evolution occurs. The reduction process of CO<sub>2</sub> proceeds via electron transfer of metal-activated CO<sub>2</sub> rather than through a hydrogenation route. Detailed studies show that the H<sub>2</sub>-evolution process can be inhibited by the addition of bipyrazine, while CO<sub>2</sub> reduction is inhibited in the presence of added thiols. Methanation of CO<sub>2</sub> by hydrogen proceeds in the dark in the presence of Pt and Ru or Os colloids and in the presence of MQ<sup>2+</sup> (1). The need for the electron relay implies that the methanation process occurs through an electron-transfer mechanism.

Photosensitized cleavage of water to hydrogen and oxygen and reduction of CO<sub>2</sub> to organic fuels are of substantial interest for the solar light-induced conversion of abundant materials to novel fuels.<sup>2,3</sup> Extensive efforts have been directed in recent years toward the development of photoinduced H<sub>2</sub>-evolution systems.<sup>4-7</sup> Homogeneous photosensitizers such as Ru(II) tris(bipyridine), Ru(bpy)<sub>3</sub><sup>2+</sup>, or Zn porphyrins have been applied to photosensitize the reduction of various relay compounds that mediate H<sub>2</sub> evolution from aqueous solutions. For example, photoreduced *N,N'*-dialkyl-4,4'-bipyridinium radicals (viologen radicals), Co(III) sepulchurate, or Rh(bpy)<sub>3</sub><sup>3+</sup> mediate H<sub>2</sub> evolution from aqueous solutions in the presence of heterogeneous metal colloids such as Pt or Rh.<sup>8-10</sup> H<sub>2</sub> evolution has also been accomplished with semiconductor particles suspended in aqueous media in the form of powders or microheterogeneous colloids.<sup>11,12</sup> In these systems metals such as Pt or Rh immobilized on the particles catalyze H<sub>2</sub> evolution by conduction band electrons formed by excitation of the semiconductor. Several cyclic systems for the photocleavage of water have been reported,<sup>13,14</sup> although other studies questioned the cyclic activity of the systems.<sup>15</sup> Recent efforts were also directed toward the photoreduction of CO<sub>2</sub> to organic fuels.<sup>16-21</sup> Reduction of CO<sub>2</sub> might proceed to various products (eq 1-8).



The standard redox potentials of these reactions at pH 7 are given in the respective equations<sup>16,22</sup> and compared to that of H<sub>2</sub> evolution. It can be seen that, while the single-electron reduction

potential of CO<sub>2</sub> (eq 2) exhibits an extreme value, the multicenter reduction potentials of CO<sub>2</sub> to CO, formate, formaldehyde, and methanol exhibit comparable values to that of the H<sub>2</sub>-evolution process. Furthermore, the reduction potential of CO<sub>2</sub> to CH<sub>4</sub> is thermodynamically more feasible than that required to reduce protons to H<sub>2</sub>. Nevertheless, despite the thermodynamic feasibility to reduce CO<sub>2</sub>, we anticipate kinetic difficulties in accomplishing

- (1) For a preliminary report see: Maida, R.; Willner, I. *J. Am. Chem. Soc.* 1986, 108, 8100-8101.
- (2) Grätzel, M., Ed. *Energy Resources through Photochemistry and Catalysis*; Academic: New York, 1983.
- (3) Calvin, M. *Acc. Chem. Res.* 1978, 11, 369-374.
- (4) Harriman, A.; West, M. E., Eds. *Photogeneration of Hydrogen*; Academic: London, 1983.
- (5) Sutin, N.; Crestz, C. *Pure Appl. Chem.* 1980, 52, 2717-2738.
- (6) Grätzel, M. *Acc. Chem. Res.* 1981, 14, 376-384.
- (7) Bard, A. J. *Science (Washington, D.C.)* 1980, 207, 139-144.
- (8) (a) Kalyanasundaram, K.; Kiwi, J.; Grätzel, M. *Helv. Chim. Acta* 1978, 61, 2720-2730. (b) Moradpour, A.; Amouyal, E.; Keller, P.; Kagan, H. *Nouv. J. Chim.* 1978, 2, 547-549.
- (9) Houlding, V.; Geiger, T.; Kolle, U.; Grätzel, M. *J. Chem. Soc., Chem. Commun.* 1982, 681-683.
- (10) Kirch, M.; Lehn, J.-M.; Sauvage, J. P. *Helv. Chim. Acta* 1979, 62, 1345-1384.
- (11) Reber, J.-F.; Meier, K. *J. Phys. Chem.* 1984, 88, 5903-5913.
- (12) (a) Duonghong, D.; Borgarello, E.; Grätzel, M. *J. Am. Chem. Soc.* 1981, 103, 4685-4690. (b) Tricot, Y.-M.; Fendler, J. H. *J. Am. Chem. Soc.* 1984, 106, 7359-7366.
- (13) Borgarello, E.; Kiwi, J.; Pelizzetti, E.; Visca, M.; Grätzel, M. *Nature (London)* 1981, 289, 158-160.
- (14) Lehn, J.-M.; Sauvage, J.-P.; Ziessel, R. *Nouv. J. Chim.* 1980, 4, 623-627.
- (15) Magliozzo, R. S.; Krasna, A. I. *Photochem. Photobiol.* 1983, 39, 15-21.
- (16) (a) Lehn, J.-M.; Ziessel, R. *Proc. Natl. Acad. Sci. U.S.A.* 1982, 79, 701-704. (b) Ziessel, R.; Hawecker, J.; Lehn, J.-M. *Helv. Chim. Acta* 1980, 69, 1065-1084. (c) Hawecker, J.; Lehn, J.-M.; Ziessel, R. *J. Chem. Soc., Chem. Commun.* 1983, 536-538. (d) Hawecker, J.; Lehn, J.-M.; Ziessel, R. *Helv. Chim. Acta* 1986, 69, 1990-2012.
- (17) Tazuke, S.; Kitamura, N. *Nature (London)* 1978, 275, 301-302.
- (18) Legros, B.; Soumillion, J. Ph. *Tetrahedron Lett.* 1985, 26, 2599-2600.
- (19) Hawecker, J.; Lehn, J.-M.; Ziessel, R. *J. Chem. Soc., Chem. Commun.* 1985, 56-58.
- (20) Halmann, M. *Nature (London)* 1978, 275, 115-116.
- (21) Willner, I.; Mandler, D.; Riklin, A. *J. Chem. Soc., Chem. Commun.* 1986, 1022-1024.
- (22) (a) Halmann, M.; Aurian-Blajeni, B. Proceedings of the Second European Community Photovoltaic Solar Energy Conference, West Berlin, Federal Republic of Germany, 1979; pp 682-689. (b) Bard, A. J., Ed. *Encyclopedia of Electrochemistry of the Elements*; Dekker: New York, 1973; Vol. 7.

\*The Hebrew University of Jerusalem.  
†Universität des Saarlandes.

processes due to the need to pursue multielectron reduction reactions. Thus, reduction of CO<sub>2</sub> in aqueous solutions is expected to be accompanied, or eventually obscured, by the kinetically favored H<sub>2</sub> evolution.

Several recent studies have explored the photoinduced fixation of CO<sub>2</sub>. Photoreduction of CO<sub>2</sub> to CO (eq 3) has been reported by Lehn and co-workers<sup>16</sup> in two different systems using Re(III)(Cl) as photocatalyst or using Ru(II) tris(bipyridine), (bpy)<sub>3</sub><sup>2+</sup>, as sensitizer and cobalt(II) chloride as electron relay. In the latter system H<sub>2</sub> evolution is accompanied by CO<sub>2</sub> reduction. Photoreduction of CO<sub>2</sub> to formate (eq 5) has been claimed by Mizuki,<sup>17</sup> but later studies questioned the formation of formate in CO<sub>2</sub> reduction.<sup>18</sup> Reduction of CO<sub>2</sub> to HCO<sub>2</sub><sup>-</sup> has been reported by Lehn<sup>19</sup> using Ru(bpy)<sub>3</sub><sup>2+</sup> as photosensitizer in a dimethylformamide-triethanolamine-aqueous medium that contains CO.

Fixation of CO<sub>2</sub> to various organic fuel products in very low yields has been reported by use of semiconductors.<sup>20</sup> We have recently reported on the specific photosensitized fixation of CO<sub>2</sub> to organic acids or formate using enzymes as specific CO<sub>2</sub>-fixation catalysts.<sup>21</sup> Similarly, in a primary note we have examined the application of Ru colloids as catalysts for the photoreduction of CO<sub>2</sub> to methane.<sup>1</sup>

Here we describe the photosensitized fixation of CO<sub>2</sub> to CH<sub>4</sub> and higher hydrocarbons using visible light. In these systems Ru and Os colloids act as CO<sub>2</sub>-fixation catalysts. We discuss two different systems for the reduction of CO<sub>2</sub> to CH<sub>4</sub>. One system involves the primary photosensitized reduction of *N,N'*-bipyridinium charge relays that mediate CO<sub>2</sub> reduction and H<sub>2</sub> evolution in the presence of Ru and Os colloids. The second system involves the selective reduction of CO<sub>2</sub> to CH<sub>4</sub> by using photo-generated Ru(I) tris(bipyrazine) and a Ru metal catalyst. We also provide means to control the selectivities of CO<sub>2</sub> reduction vs. H<sub>2</sub> evolution by proper additives. As far as we are aware, these systems are the first examples for the photoinduced reduction of CO<sub>2</sub> to CH<sub>4</sub>.

### Experimental Methods

Absorption spectra were recorded with a Uvikon-860 (Kontron) spectrophotometer. Gas chromatography analyses were performed with a Packard 427 instrument (thermal conductivity detector) for H<sub>2</sub> analysis and Tracor 540 gas chromatograph (flame ionization detector) for methane, ethane, and ethylene analysis. For H<sub>2</sub> separation a 5-Å MS column and argon as the carrier gas were used. For hydrocarbon analyses a Porapak T-column and nitrogen as the carrier gas were used. Size and shape of Ru and Os colloids were determined with a Jeol 200 CX electron microscope. Elementary composition of particles was determined with a Link 860 energy-dispersion system. Atomic absorption measurements were carried out with a Perkin-Elmer 403 spectrophotometer. Continuous illuminations were performed with 150-W xenon arc lamps (PTI). Laser flash experiments were performed on a DL 200 (Moletron) dye laser pumped by a UV-IU nitrogen laser (Moletron). Flashes were recorded on a Biomaster 8100, and pulse collection was carried out with a Nicolet 1170.

**Preparation of Metal Colloids.** Colloids were prepared by the reduction of the respective metal salts with citrate as reducing agent.<sup>22</sup> A 21% sodium citrate solution, 100 mL, that contains RuCl<sub>3</sub>, 16 mg, or OsO<sub>4</sub>, 15 mg, was heated to 100 °C overnight. The resulting colloid suspensions were centrifuged and dialyzed. Metal content of colloid suspension was determined by atomic absorption to be 60 mg L<sup>-1</sup> for Ru colloid and 95 mg L<sup>-1</sup> for Os colloid. The mean diameter of colloid particles was estimated by EM to be 400 Å for Ru colloid and 50 Å for Os colloid. An alternative procedure for the preparation of the Ru colloid involves the photochemical reduction of K<sub>2</sub>RuCl<sub>6</sub>. This colloid exhibits improved catalyst activity toward reduction of CO<sub>2</sub> to CH<sub>4</sub>: A 3-mL carbonate aqueous solution, pH 7.8, that includes Ru(II) tris(bipyrazine), Ru(bpz)<sub>3</sub><sup>2+</sup>, 1 × 10<sup>-4</sup> M, K<sub>2</sub>RuCl<sub>6</sub>, 2 × 10<sup>-4</sup> M, and triethanolamine, 0.1 M, was illuminated for 20 min with a 150-W xenon lamp. To the resulting suspension a mixed-bed ion exchanger (Amberlite MB-1) was added to exclude all ions, and the colloid was filtered off. The mean diameter of the resulting colloid is estimated by EM to be 100 Å. *N,N'*-Dimethyl-2,2'-bipyridinium, MQ<sup>2+</sup> (1), *N,N'*-trimethylene-2,2'-bipyridinium, TQ<sup>2+</sup> (2), and *N,N'*-tetramethylene-2,2'-bipyridinium,

DQ<sup>2+</sup> (3), were prepared according to literature procedures.<sup>24</sup> *N,N'*-Bis(3-sulfonatopropyl)-3,3'-dimethyl-4,4'-bipyridine, MPVS<sup>9</sup> (4), was prepared by the reaction of 3,3'-dimethyl-4,4'-bipyridine with 1,3-propanesultone. To 100 mg of 3,3'-dimethyl-4,4'-bipyridine<sup>25</sup> was added 390 mg of 1,3-propanesultone. The resulting mixture was heated to 120 °C for 15 min without solvent under nitrogen. To the resulting semisolid was added 5 mL of DMF, and heating at 120 °C was continued for 3 h. After cooling, the white precipitate of 4 was filtered and washed three times with acetone; yield 89%. The product gave satisfactory elementary analysis.

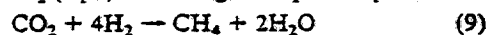
Continuous-illumination experiments were performed in a glass cuvette equipped with a valve and stopper. Samples of 3 mL each contained a ruthenium or osmium colloid, 20 mg/L; TEOA, 1.0 × 10<sup>-1</sup> M; NaHCO<sub>3</sub>, 5.0 × 10<sup>-2</sup> M; Ru(bpz)<sub>3</sub><sup>2+</sup>, 1.0 × 10<sup>-4</sup> M or Ru(bpy)<sub>3</sub><sup>2+</sup>, 1.4 × 10<sup>-4</sup> M; and one of the electron relays (MQ<sup>2+</sup>, TQ<sup>2+</sup>, DQ<sup>2+</sup>, or MPVS<sup>9</sup>), 1.4 × 10<sup>-3</sup> M; at pH 7.8 under a CO<sub>2</sub> atmosphere. Gas samples were taken out from the cuvette at time intervals of illumination and analyzed by the respective gas chromatography analyses.

Methane and hydrogen inhibition experiments were performed in similar cuvettes on 3-mL samples containing the ruthenium colloid, 20 mg/L; EDTA, 3.3 × 10<sup>-2</sup> M; NaHCO<sub>3</sub>, 5.0 × 10<sup>-2</sup> M; Ru(bpy)<sub>3</sub><sup>2+</sup>, 1.4 × 10<sup>-4</sup> M; and MQ<sup>2+</sup>, 1.0 × 10<sup>-3</sup> M; at pH 6.0 under a CO<sub>2</sub> atmosphere. The rates of formation of methane and hydrogen were followed at different bipyrazine or 1,4-dimercapto-2,3-butanediol, dithiothreitol (DTT), concentrations.

Dark reduction of CO<sub>2</sub> was performed in a glass pressure-resistant reaction flask connected through a pressure gauge to a manifold enabling accurate control of the gaseous atmosphere composition. In a typical experiment, a solution containing Ru and Pt colloids, 20 mg/L each, NaHCO<sub>3</sub>, 5.0 × 10<sup>-2</sup> M, and MQ<sup>2+</sup>, 1.0 × 10<sup>-3</sup> M, was stirred under 0.75 atm of CO<sub>2</sub> and 0.75 atm of H<sub>2</sub>. Under these conditions methane and ethylene were formed as assayed by GC analysis. Exclusion of the relay from the reaction yielded no products.

### Results and Discussion

Photoreduction of *N,N'*-dialkylbipyridinium salts<sup>2,26</sup> in the presence of Ru(bpy)<sub>3</sub><sup>2+</sup>, metalloporphyrins, and organic dyes<sup>27</sup> in the presence of sacrificial electron donors and the subsequent evolution of H<sub>2</sub> with metal colloids<sup>2-10</sup> have been studied extensively. Various organometallic complexes such as Co(II) porphyrins<sup>28</sup> or Co and Ni macrocyclic complexes<sup>29</sup> exhibit catalytic activity in the electrochemical reduction of CO<sub>2</sub>. Nevertheless, the electrocatalytic potentials are usually far from being adequate to be applied in the photosensitized reduction of CO<sub>2</sub>. Ruthenium and osmium metals are used<sup>30,31</sup> as heterogeneous catalysts in the methanation of CO<sub>2</sub> (eq 9). Although this process proceeds at



elevated temperatures and pressures, it suggests that these metals activate CO<sub>2</sub> toward reduction. Recent electrochemical studies by Frese<sup>32</sup> have revealed that Ru electrodes catalyze the electrochemical reduction of CO<sub>2</sub> to CH<sub>4</sub> (eq 8). In these studies CO<sub>2</sub> reduction to CH<sub>4</sub> has been accomplished in aqueous solutions (pH 4.2–6.8) at electrode potentials (E<sup>0</sup>) as low as -0.55 V vs. SCE. Together with CO<sub>2</sub> reduction to CH<sub>4</sub>, hydrogen evolution is observed as well as reduction of CO<sub>2</sub> to CO. Thus, we have decided to examine the photosensitized reduction of CO<sub>2</sub> to methane in the presence of Ru and Os colloids.

(24) Homer, R. F.; Tomlinson, T. E. *J. Chem. Soc.* 1960, 2498–2503.

(25) Stoehr, C.; Wagner, M. *J. Prakt. Chem.* 1893, 48, 1–23.

(26) Amouyal, E.; Zidler, B.; Keller, P.; Moradpour, A. *Chem. Phys. Lett.* 1980, 74, 314–317.

(27) (a) Bock, C. R.; Meyer, T. J.; Whitten, D. G. *J. Am. Chem. Soc.* 1974, 96, 4710–4712. (b) Kalyanasundaram, K.; Grätzel, M. *Helv. Chim. Acta* 1980, 63, 478–485. (c) Krasna, A. I. *Photochem. Photobiol.* 1979, 29, 267–276.

(28) Takahashi, K.; Hiratsuka, K.; Sasaki, H.; Toshima, S. *Chem. Lett.* 1979, 305–308.

(29) (a) Fisher, B.; Eisenberg, R. *J. Am. Chem. Soc.* 1980, 102, 7361–7363. (b) Beley, M.; Collin, J.-P.; Ruppert, R.; Sauvage, J.-P. *J. Chem. Soc., Chem. Commun.* 1984, 1315–1316. (c) Pearce, D. J.; Pletcher, D. J. *Electroanal. Chem. Interfacial Electrochem.* 1986, 197, 317–330.

(30) (a) Solymosi, F.; Erdohelyi, A.; Kocsis, M. *J. Chem. Soc., Faraday Trans. 1* 1981, 77, 1003–1012. (b) Solymosi, F.; Erdohelyi, A. *J. Mol. Catal.* 1980, 8, 471–474. (c) Lunde, P. J.; Kester, F. L. *J. Catal.* 1973, 30, 423–429.

(31) (a) Yasukatsu, T.; Watanabe, H.; Akira, T. *Carbon* 1977, 15, 103–106. (b) Moggi, P.; Albanesi, G.; Predieri, G.; Sapa, E. *J. Organomet. Chem.* 1983, 252, C89–C92.

(32) Frese, K. W., Jr.; Leach, S. J. *Electrochem. Soc.* 1985, 135, 259–260.

(23) Furlong, D. N.; Launikonis, A.; Sasse, W. H. F.; Sanders, J. V. *J. Chem. Soc., Faraday Trans. 1* 1984, 80, 571–588.

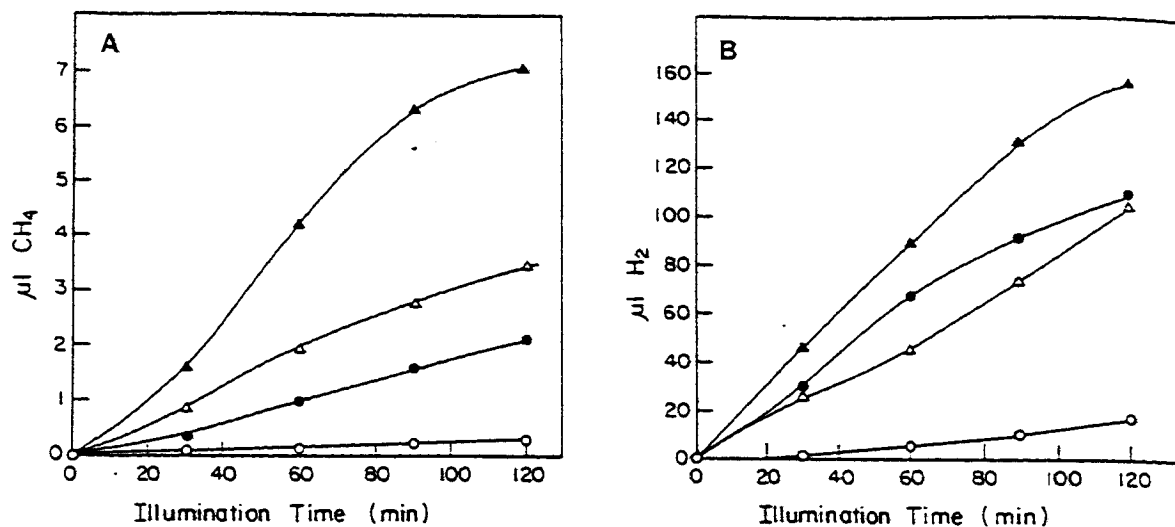
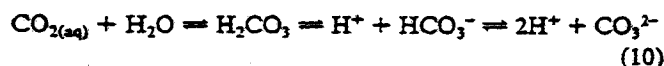
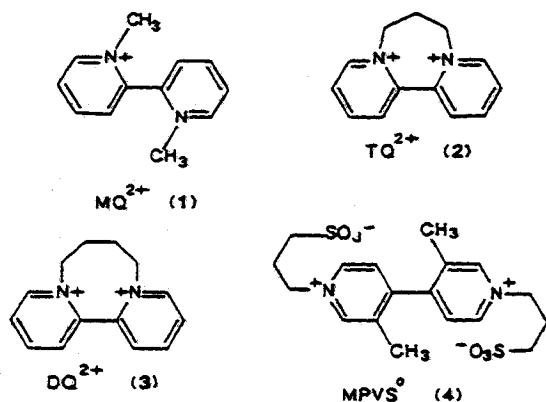


Figure 1. Rate of photosensitized  $\text{CH}_4$  formation (A) and  $\text{H}_2$  evolution (B) in the presence of the various charge relays and Ru colloid:  $[\text{Ru}(\text{bpy})_3]^{2+} = 1.4 \times 10^{-4} \text{ M}$ ,  $[\text{relay}] = 1.4 \times 10^{-3} \text{ M}$ ,  $[\text{TEOA}] = 1.0 \times 10^{-3} \text{ M}$ ,  $[\text{NaHCO}_3] = 5.0 \times 10^{-2} \text{ M}$ ,  $[\text{Ru colloid}] = 20 \text{ mg/L}$ , pH 7.8 under  $\text{CO}_2$  atmosphere. Key: ( $\Delta$ )  $\text{MQ}^{2+}$ ; ( $\bullet$ )  $\text{DQ}^{2+}$ ; ( $\circ$ )  $\text{TQ}^{2+}$ ; ( $\blacktriangle$ )  $\text{MPVS}^0$ .

**Photosensitized  $\text{H}_2$  Evolution and  $\text{CO}_2$  Reduction Using Bipyridinium Electron Relays.** The reduction potentials for  $\text{H}_2$  evolution and  $\text{CO}_2$  reduction depend on the pH of the aqueous media. Both of the processes are thermodynamically favored as the pH of the aqueous solution decreases. Yet, the reduction potentials for  $\text{H}_2$  formation decline to more positive values sharper than those of  $\text{CO}_2$  as the pH of the solution decreases.<sup>33</sup> Thus, to thermodynamically favor  $\text{CO}_2$  reduction over  $\text{H}_2$  evolution, it is advantageous to perform the reactions in basic aqueous media. However, since  $\text{CO}_2$  in aqueous solutions exhibits complex equilibria with  $\text{HCO}_3^-$  and  $\text{CO}_3^{2-}$  (eq 10) that are strongly affected by the pH, one is limited to the region employed. We have examined the photosensitized reduction of  $\text{CO}_2$  in aqueous solutions at pH 7.8 where  $\text{CO}_2$  consists of 3% of the total carbon dioxide introduced that corresponds to  $11.2 \mu\text{M}$ .<sup>34</sup>



We have studied the  $\text{CO}_2$ -reduction and  $\text{H}_2$ -evolution processes in aqueous solutions where photosensitized electron-transfer reactions result in reduced bipyridinium radical relays. In these systems Ru(II) tris(bipyridine) is used as photosensitizer and triethanolamine, TEOA, as sacrificial electron donor. As charge relays we have applied *N,N'*-dimethyl-2,2'-bipyridinium,  $\text{MQ}^{2+}$  (1), *N,N'*-trimethylene-2,2'-bipyridinium,  $\text{TQ}^{2+}$  (2), *N,N'*-tetra-



methylene-2,2'-bipyridinium,  $\text{DQ}^{2+}$  (3), or *N,N'*-bis(3-sulfonatopropyl)-3,3'-dimethyl-4,4'-bipyridinium,  $\text{MPVS}^0$  (4).

One of the colloids, Os or Ru, is included in the systems as  $\text{CO}_2$ -reduction or a  $\text{H}_2$ -evolution catalyst. These charge relay were selected since their reduced forms exhibit more negative reduction potentials than *N,N'*-dialkyl-4,4'-bipyridinium (viologen) radicals. Previous studies have indicated that the reduction potentials of bipyridinium salts [ $E^\circ(\text{V}^-/\text{V}^{2+})$ ], are strongly affected by steric interactions in the molecular structure.<sup>35</sup> Reduction of the bipyridinium salts tends to bring the two pyridine rings into a planar structure to gain effective  $\pi$ - $\pi$  overlap and resonance delocalization. Hence, substitution of the ortho positions in the bipyridine structure distorts the two rings from planarity. Consequently, their reduction is more difficult, and the reduced form exhibits more negative reduction potentials as compared to the sterically unhindered relays. For example, the reduction potential of *N,N'*-bis(3-sulfonatopropyl)-4,4'-bipyridinium, PVS (5), corresponds<sup>36</sup> to  $E^\circ(\text{PVS}^-/\text{PVS}^0) = -0.41 \text{ V}$ , and introduction of the two methyl groups in the ortho positions to obtain the relay 4 introduces sufficient steric hindrance to decrease the reduction potential to the value of  $E^\circ(\text{MPVS}^-/\text{MPVS}^0) = -0.79 \text{ V}$ . The reduction potentials of the various relays used in our studies are summarized in Table I.

Illumination of these systems with visible light ( $\lambda > 400 \text{ nm}$ ) under a gaseous atmosphere of  $\text{CO}_2$  results in the formation of methane and ethylene,  $\text{C}_2\text{H}_4$ , as well as the evolution of  $\text{H}_2$ . Figure 1 shows the rates of  $\text{CH}_4$  formation and  $\text{H}_2$  evolution by the different relays and Ru colloid as catalyst for the reaction. Figure 2 exemplifies the rates of formation of  $\text{CH}_4$  and  $\text{C}_2\text{H}_4$  as a function of illumination time with MPVS as relay and Os as catalyst. The quantum yields for the formation of the various products with the different electron relays and the Os and Ru colloids as catalysts are summarized in Table I. It is evident that the yields of  $\text{H}_2$ -evolution and  $\text{CO}_2$ -reduction products increase as the reduction potentials of the relay is more negative. For example, by using the Ru colloid and MPVS as relay ( $E^\circ = -0.79 \text{ V}$ ), the quantum yields for  $\text{H}_2$  evolution and  $\text{CH}_4$  formation are  $\phi(\text{H}_2) = 2.6 \times 10^{-3}$  and  $\phi(\text{CH}_4) = 5.7 \times 10^{-4}$ , while with the relay TQ ( $E^\circ = -0.55 \text{ V}$ ) the respective quantum yields correspond to  $\phi(\text{H}_2) = 2.8 \times 10^{-4}$  and  $\phi(\text{CH}_4) = 2.0 \times 10^{-5}$ . When argon is used as the gaseous atmosphere instead of  $\text{CO}_2$ , only  $\text{H}_2$  evolution is observed. The quantum yields for  $\text{H}_2$  evolution in the presence of the different relays and metal catalysts are also summarized in Table I. Control experiments reveal that all of the components included in the systems are essential for  $\text{H}_2$  evolution as well as for  $\text{CO}_2$ -reduction. Exclusion of either the electron donor, charge relay, or catalysts prohibits any photoproduct formation. Furthermore,

(33) Keene, F. R.; Creutz, C.; Sutin, N. *Coord. Chem. Rev.* 1985, 64, 247-260.

(34) Asada, K. In *Organic and Bio-organic Chemistry of Carbon Dioxide*; Inoue, S., Yamazaki, N., Eds.; Kodansha: Tokyo, 1982.

(35) (a) Hünig, S.; Gross, J.; Schenk, W. *Justus Liebig's Ann. Chem.* 1973, 324-338. (b) Hünig, S.; Gross, J. *Tetrahedron Lett.* 1968, 2599-2602.

(36) Degani, Y.; Willner, I. *J. Am. Chem. Soc.* 1983, 105, 6228-6231.

Table I. Quantum Yields for H<sub>2</sub> Evolution and Hydrocarbon Formation in the Presence of Different Relays and Ru or Os Colloids as Catalysts<sup>a</sup>

relay	E <sup>o</sup> , V vs. SHE <sup>b,c</sup>	Ru colloid catalyst			Os colloid catalyst		
		10 <sup>3</sup> φ(H <sub>2</sub> )	10 <sup>4</sup> φ(CH <sub>4</sub> )	10 <sup>5</sup> φ(C <sub>2</sub> H <sub>4</sub> )	10 <sup>3</sup> φ(H <sub>2</sub> )	10 <sup>4</sup> φ(CH <sub>4</sub> )	10 <sup>5</sup> φ(C <sub>2</sub> H <sub>4</sub> )
MPVS <sup>d</sup>	-0.79	2.6 (80) <sup>d</sup>	5.7 (4.3)	1.9 (0.1)	1.9 (58)	2.1 (1.6)	1.04 (0.05)
MQ <sup>2+</sup>	-0.72	1.7 (51)	2.3 (1.7)	0.73 (0.03)	3.0 (91)	0.52 (0.4)	0.29 (0.014)
R <sup>2+</sup>	-0.65	1.8 (56)	1.4 (1.1)	1.08 (0.05)	9.2 (270)	0.61 (0.5)	0.67 (0.03)
R <sup>2+</sup>	-0.55	0.28 (8)	0.20 (0.15)	0.18 (0.01)	0.64 (19)	0.12 (0.1)	0.15 (0.008)

<sup>a</sup>In all systems [Ru(bpy)<sub>3</sub><sup>2+</sup>] = 1.4 × 10<sup>-4</sup> M, [TEOA] = 1 × 10<sup>-1</sup> M, [relay] = 1.4 × 10<sup>-3</sup> M, aqueous 0.1 M bicarbonate solution under CO<sub>2</sub>, pH 7.8. <sup>b</sup>Kalyanasundaram, K. *Coord. Chem. Rev.* 1982, 46, 159-244. <sup>c</sup>Furlong, D. N.; Johansen, O.; Launikonis, A.; Loder, J. W.; Mau, A. W.-H.; Sasse, W. H. F. *Aust. J. Chem.* 1985, 38, 363-367. <sup>d</sup>In parentheses volume (μL) of products formed per hour.

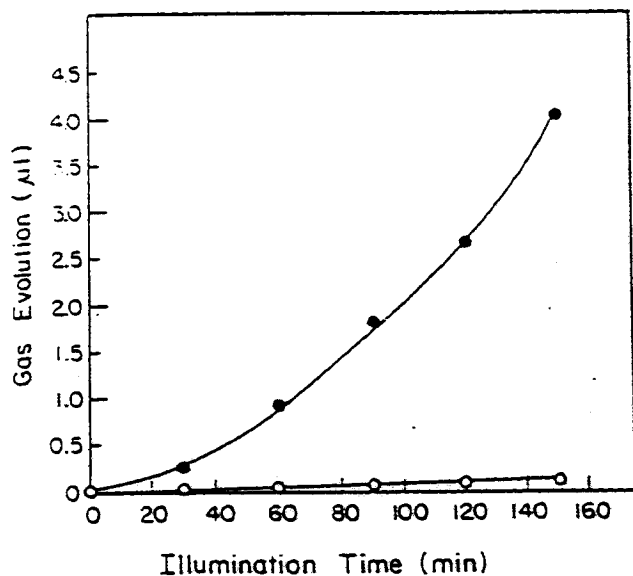


Figure 2. Yield of methane and ethylene formation as a function of illumination time with MPVS<sup>d</sup> as relay and Os colloid as catalyst: [Ru(bpy)<sub>3</sub><sup>2+</sup>] = 1.4 × 10<sup>-4</sup> M, [MPVS] = 1.4 × 10<sup>-3</sup> M, [TEOA] = 1.0 × 10<sup>-1</sup> M, [NaHCO<sub>3</sub>] = 5.0 × 10<sup>-2</sup> M, [Os colloid] = 20 mg/L, pH 7.8 under CO<sub>2</sub> atmosphere. Key: (●) methane; (○) ethylene.

other metal catalysts such as Pt or Pd are inactive toward the reduction of CO<sub>2</sub>, and only H<sub>2</sub> evolution is observed. Also, substitution of the charge relays by *N,N'*-dimethyl-4,4'-bipyridinium (methylviologen, MV<sup>2+</sup>) does not yield the reduction of CO<sub>2</sub>, and the blue radical cation (MV<sup>•+</sup>) is accumulated.

The lack of H<sub>2</sub> evolution and CH<sub>4</sub> formation with MV<sup>2+</sup> as charge relay suggests that the reduced relay MV<sup>•+</sup> does not exhibit the reduction potential required to evolve H<sub>2</sub> from the basic aqueous medium (pH 7.8) or to reduce metal-activated CO<sub>2</sub>.

The results clearly indicate that the photosensitized electron-transfer reaction leads to the reduction of CO<sub>2</sub> to methane and higher hydrocarbons. Thus, Ru and Os colloids are indeed heterogeneous catalysts that activate CO<sub>2</sub> toward the reduction. Nevertheless, the reduction of CO<sub>2</sub> in the aqueous media is nonspecific, and substantial amounts of H<sub>2</sub> are evolved. In fact H<sub>2</sub> evolution is the predominant product in the photosensitized transformations.

The mechanism that leads to H<sub>2</sub> evolution is well established.<sup>8,9</sup> It involves the oxidative quenching via electron transfer of the excited sensitizer Ru(bpy)<sub>3</sub><sup>2+</sup> by the relay (R<sup>2+</sup>), followed by charge separation (eq 11 and 12). Oxidation of the electron donor



TEOA by the oxidized sensitizer recycles the light-active compound, and the reduced relay is accumulated. Electron transfer from the reduced relay to the metal catalyst charges the colloid, and in the presence of protons, metal-bound H atoms are formed and their dimerization leads to H<sub>2</sub> evolution.<sup>37</sup> Figure 3 schematically represents the H<sub>2</sub>-evolution process. The fact that Ru

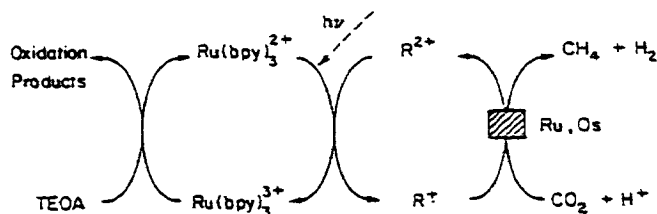
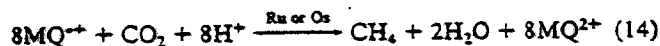
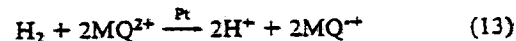


Figure 3. Schematic cycle for photosensitized H<sub>2</sub> evolution and CO<sub>2</sub> reduction using bipyridinium electron relays (R<sup>2+</sup>).

or Os colloids are essential catalysts for the reduction of CO<sub>2</sub> clearly indicates that CO<sub>2</sub> interacts with the metal surface and that it is activated toward the reduction process. The reduction might proceed via two alternative mechanisms: (i) hydrogenation of metal-activated CO<sub>2</sub> via in situ generated H atoms that lead to the methanation process (eq 9) [Similar photoinduced hydrogenation reactions and utilization of in situ generated hydrogen atoms have been exemplified with unsaturated substrates, i.e. ethylene and acetylene, and heterogeneous Pt or Pd colloids.<sup>37</sup>] and (ii) direct reduction of metal-activated CO<sub>2</sub> via electron transfer from the charge relay, independent to the H<sub>2</sub>-evolution system (Figure 3).

Dark experiments exclude the hydrogenation pathway as the mechanistic route for the reduction of CO<sub>2</sub> to CH<sub>4</sub> and imply that the reduction process proceeds through electron transfer from the reduced relay. In these experiments an aqueous bicarbonate solution (pH 7.8) that included the Ru or Os colloid was stirred in a sealed flask under a gaseous atmosphere that included H<sub>2</sub> (0.75 atm) and CO<sub>2</sub> (0.75 atm), and no hydrocarbons have been detected. Similarly, addition of the charge relay MQ<sup>2+</sup> to the system did not lead to any hydrocarbon products. Yet, addition of a Pt colloid to the system that included either Ru or Os colloid and the charge relay, MQ<sup>2+</sup>, resulted in the formation of methane and ethylene (C<sub>2</sub>H<sub>4</sub>). In a control experiment where MQ<sup>2+</sup> was excluded from the system, and Ru or Os and Pt colloids were present, no reduction of CO<sub>2</sub> occurred. Similarly, when the Ru or Os colloids were excluded and the Pt colloid and MQ<sup>2+</sup> were present, only MQ<sup>•+</sup> was formed and no CO<sub>2</sub>-reduction products were formed. This set of dark experiments clearly indicate that the reduction of CO<sub>2</sub> to hydrocarbons proceeds via electron transfer rather than through the hydrogenation route. The primary step involves the Pt-catalyzed reduction of the charge relay MQ<sup>2+</sup> (eq 13). The generation of the reduced relay, MQ<sup>•+</sup>, allows the subsequent reduction of Ru or Os metal-activated CO<sub>2</sub> to methane and higher hydrocarbons (eq 14).



It should be noted that these control dark reactions suggest a new important route for the methanation process of CO<sub>2</sub> (eq 9). At present, the reaction conditions using H<sub>2</sub> and CO<sub>2</sub> require high pressures and elevated temperatures.<sup>30,31</sup> Our results indicate that addition of an electron relay and proper electron-transfer mediating catalysts affects the process at an ambient temperature and low pressure.

Photoreduction of CO<sub>2</sub> with Ru(bpz)<sub>3</sub><sup>2+</sup> as Photosensitizer. The results discussed until now demonstrate that H<sub>2</sub> evolution occurs concomitantly to CO<sub>2</sub> reduction and the former process is the

(37) Degani, Y.; Willner, I. *J. Chem. Soc., Perkin Trans. 2* 1986, 37-41.



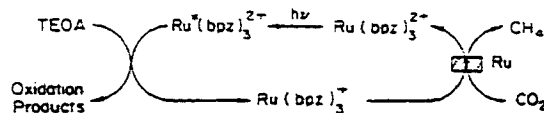


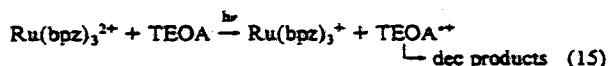
Figure 4. Schematic cycle for photosensitized reduction of  $\text{CO}_2$  to  $\text{CH}_4$  using  $\text{Ru}(\text{bpz})_3^{2+}$  as sensitizer.

Table II. Quantum Yields and Turnover Numbers (TN) for Hydrocarbon Formation Using  $\text{Ru}(\text{bpz})_3^{2+}$

system <sup>a</sup>	$\phi(\text{CH}_4)$	$\phi(\text{C}_2\text{H}_4)$	$\phi(\text{C}_2\text{H}_6)$	TN[ $\text{Ru}(\text{bpz})_3^{2+}$ ]
I	$2.5 \times 10^{-5}$ (0.15) <sup>b</sup>	$3.5 \times 10^{-6}$ (0.014)	$2 \times 10^{-6}$ (0.008)	1.8
II	$4.0 \times 10^{-4}$ (2.4)	$7.5 \times 10^{-5}$ (0.36)	$4 \times 10^{-5}$ (0.18)	15

<sup>a</sup> System components:  $[\text{Ru}(\text{bpz})_3^{2+}] = 1.0 \times 10^{-4}$  M,  $[\text{TEOA}] = 1 \times 10^{-1}$  M,  $[\text{Ru colloid}] = 20$  mg  $\text{L}^{-1}$ ,  $[\text{NaHCO}_3] = 0.05$  M. Systems: I, aqueous solution; II, water-ethanol, 2:1. <sup>b</sup> In parentheses volume ( $\mu\text{L}$ ) of products formed per hour.

predominating reaction. Assuming that  $\text{CO}_2$  reduction does not proceed through a hydrogenation mechanism suggests that specificity toward  $\text{CO}_2$  reduction might be designed. A strategy to induce selectivity into the process and favor  $\text{CO}_2$  reduction over  $\text{H}_2$  evolution will involve the design of a couple composed of a reduced relay-catalyst system that exhibits a kinetic barrier toward  $\text{H}_2$  evolution but still allows  $\text{CO}_2$  reduction.  $\text{Ru}(\text{II})$  tris(bipyrazine),  $\text{Ru}(\text{bpz})_3^{2+}$ , is a photosensitizer that absorbs in the visible region ( $\lambda_{\text{max}} = 443$  nm,  $\epsilon = 15000$   $\text{M}^{-1} \text{cm}^{-1}$ ) and exhibits a long excited-state lifetime ( $\tau = 1.04$   $\mu\text{s}$ ).<sup>38,39</sup> It is reductively quenched via electron transfer by various electron donors, i.e. triethanolamine, TEOA (eq 15). The reduced photoproduct,



$\text{Ru}(\text{bpz})_3^+$ , is a powerful reducing agent ( $E^\circ = -0.86$  V vs. SCE) capable thermodynamically to evolve  $\text{H}_2$  as well as to reduce  $\text{CO}_2$  to  $\text{CH}_4$ . Nevertheless, it has been reported that  $\text{Ru}(\text{bpz})_3^+$  does not mediate  $\text{H}_2$  evolution at pH 7.8 in the presence of heterogeneous catalysts such as Pt colloid.<sup>40</sup> Thus it exhibits the kinetic barrier for  $\text{H}_2$  evolution and meets the basic requirements to design selective  $\text{CO}_2$  reduction.

We therefore examined the reduction of  $\text{CO}_2$  in an aqueous system that includes  $\text{Ru}(\text{bpz})_3^{2+}$  as photosensitizer, TEOA as electron donor, and the Ru colloid as  $\text{CO}_2$  reduction catalyst. Illumination of this system (pH 7.8,  $\lambda > 400$  nm) results in the reduction of  $\text{CO}_2$  to  $\text{CH}_4$  and the formation of oligomerated hydrocarbons ethylene and ethane (Figure 4). No  $\text{H}_2$  formation is observed in these systems, and  $\text{CO}_2$ -reduction products are the sole products. Table II summarizes the quantum yield for the formation of the various hydrocarbons and the turnover numbers of the photosensitizer.

Control experiments reveal that indeed  $\text{CO}_2$  is photoreduced to methane, ethylene, and ethane. Illumination of a system that includes the colloids under argon instead of  $\text{CO}_2$  does not lead to any hydrocarbon products. Also, exclusion of the  $\text{Ru}(\text{bpz})_3^{2+}$  from the system does not yield upon illumination under  $\text{CO}_2$  any hydrocarbon products. Thus, it is evident that a photosensitized electron-transfer reaction in the visible absorption region leads to the reduction of  $\text{CO}_2$ .

A hydrogenation mechanism of  $\text{CO}_2$  to the hydrocarbons in these systems can be excluded since no  $\text{H}_2$  evolution occurs either in the presence of  $\text{CO}_2$  or under argon. That  $\text{CO}_2$  is reduced via electron transfer is evident from laser flash experiments as well as steady-state illumination. Excitation of an aqueous solution

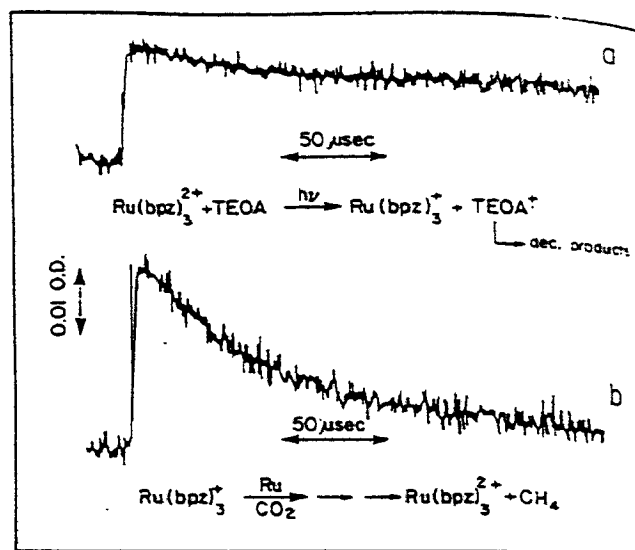


Figure 5. Transient spectra formed upon illumination of  $\text{Ru}(\text{bpz})_3^{2+}$ ,  $2.2 \times 10^{-5}$  M, and TEOA, 0.17 M solution, pH 9.5. Systems are flushed at  $\lambda = 440$  nm and product,  $\text{Ru}(\text{bpz})_3^+$ , is followed at  $\lambda = 500$  nm: (a) under argon or  $\text{CO}_2$ ; (b) in the presence of Ru colloid (20 mg/L) under  $\text{CO}_2$ .

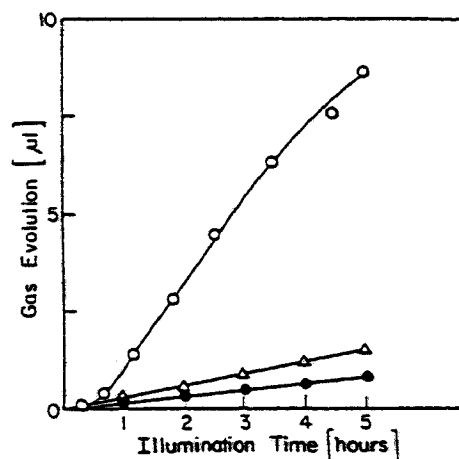


Figure 6. Rate of hydrocarbon formation as a function of illumination time in the  $\text{Ru}(\text{bpz})_3^{2+}$  system:  $[\text{Ru}(\text{bpz})_3^{2+}] = 1.0 \times 10^{-4}$  M,  $[\text{TEOA}] = 1.0 \times 10^{-1}$  M,  $[\text{NaHCO}_3] = 5.0 \times 10^{-2}$  M,  $[\text{Ru colloid}] = 20$  mg/L, pH 7.8, water-ethanol (2:1) solution under  $\text{CO}_2$  atmosphere. Key: (O) methane; ( $\Delta$ ) ethylene; ( $\bullet$ ) ethane.

that includes  $\text{Ru}(\text{bpz})_3^{2+}$  and TEOA under argon by a light pulse ( $\lambda_{\text{exc}} = 440$  nm) results in the trace displayed in Figure 5a. It corresponds to the reductive quenching of  $\text{Ru}(\text{bpz})_3^{2+}$  to form  $\text{Ru}(\text{bpz})_3^+$  (eq 15). The trace shows an initial decay for ca. 80  $\mu\text{s}$  and afterward a steady-state accumulation of  $\text{Ru}(\text{bpz})_3^+$ . The initial decay is due to a recombination of  $\text{Ru}(\text{bpz})_3^+$  with  $\text{TEOA}^{\cdot+}$ , but since  $\text{TEOA}^{\cdot+}$  is simultaneously decomposed, a no steady-state accumulation of  $\text{Ru}(\text{bpz})_3^+$  is observed. Addition of  $\text{CO}_2$  (instead of argon) does not alter the trace obtained upon flashing. Thus, no electron transfer from  $\text{Ru}(\text{bpz})_3^+$  to  $\text{CO}_2$  occurs. Addition of the Ru colloid to the system under argon results in the decay of  $\text{Ru}(\text{bpz})_3^+$  ( $\tau = 170$   $\mu\text{s}$ ), implying that electron transfer from  $\text{Ru}(\text{bpz})_3^+$  to the metal colloid occurs. In turn, flashing the system in the presence of  $\text{CO}_2$  and the Ru colloid results in the trace displayed in Figure 5b. It is evident that under these conditions a rapid decay ( $\tau = 50$   $\mu\text{s}$ ) of the photogenerated  $\text{Ru}(\text{bpz})_3^+$  occurs and  $\text{Ru}(\text{bpz})_3^{2+}$  is regenerated. Namely, photogenerated  $\text{Ru}(\text{bpz})_3^+$  is capable of affecting the electron transfer to Ru-activated  $\text{CO}_2$ , a process that ultimately yields the hydrocarbon products.

It is established that  $\text{Ru}(\text{bpz})_3^+$  can be photogenerated upon steady-state illumination of an aqueous ethanol solution that contains the photosensitizer  $\text{Ru}(\text{bpz})_3^{2+}$  and TEOA.<sup>40</sup> This accumulation of  $\text{Ru}(\text{bpz})_3^+$  in ethanol solutions is presumably due

(38) Crutchley, R. J.; Lever, A. B. P. *J. Am. Chem. Soc.* 1980, 102, 7128-7129.

(39) Crutchley, R. J.; Lever, A. B. P. *Inorg. Chem.* 1982, 21, 2276-2282.

(40) (a) Dürr, H.; Dörr, G.; Zengerle, K.; Curcbod, J.-M.; Braun, A. M. *Helv. Chim. Acta* 1984, 66, 2652-2655. (b) Dürr, H.; Dörr, G.; Zengerle, K.; Mayer, E.; Curcbod, J.-M.; Braun, A. M. *Nouv. J. Chim.* 1985, 9, 717-720.

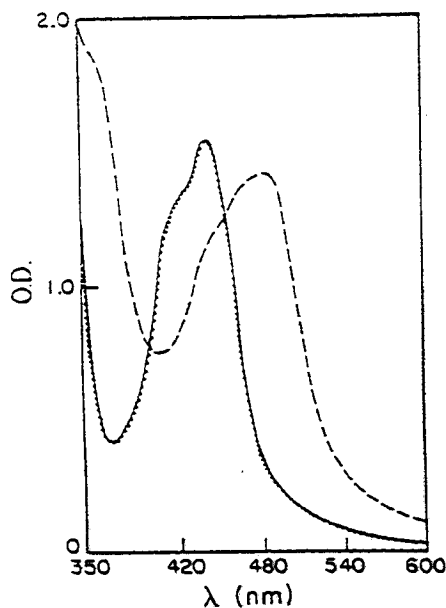


Figure 7. Effects of added CO<sub>2</sub> on photogenerated Ru(bpz)<sub>3</sub><sup>2+</sup>. Absorption Spectra: (—) Ru(bpz)<sub>3</sub><sup>2+</sup>, 1.0 × 10<sup>-4</sup> M in water-ethanol (2:1) under argon; (---) photogenerated Ru(bpz)<sub>3</sub><sup>2+</sup> prepared by illumination of Ru(bpz)<sub>3</sub><sup>2+</sup> in the presence of TEOA, 1.0 × 10<sup>-1</sup> M; (—) obtained upon injection of CO<sub>2</sub> to photogenerated Ru(bpz)<sub>3</sub><sup>2+</sup>. In all samples [Ru colloid] = 20 mg/L.

to the rapid irreversible decomposition of TEOA<sup>•+</sup> in this medium (eq 15). Thus, the effective photogeneration of Ru(bpz)<sub>3</sub><sup>2+</sup> in ethanol solutions suggests that enhanced quantum yields for CO<sub>2</sub> reduction to CH<sub>4</sub> could be accomplished in this medium. We have examined the photosensitized reduction of CO<sub>2</sub> to CH<sub>4</sub> in a water-ethanol (2:1) mixture using Ru(bpz)<sub>3</sub><sup>2+</sup> as sensitizer, TEOA as electron donor, and the Ru colloid as catalyst. Illumination of this system under CO<sub>2</sub> results in the formation of CH<sub>4</sub> and higher hydrocarbons. The rate of CH<sub>4</sub> formation (Figure 6) corresponds to a quantum yield of  $\phi = 4.0 \times 10^{-4}$ . This value is 16-fold higher than the quantum yield for CH<sub>4</sub> formation in pure aqueous solutions and is mainly attributed to the effective photogeneration of Ru(bpz)<sub>3</sub><sup>2+</sup> in the ethanol-water solution. Steady-state illumination experiments on this system in the absence and presence of CO<sub>2</sub> and the Ru colloid support the electron-transfer mechanism for reduction of CO<sub>2</sub>. Illumination of the ethanol-water solution that includes TEOA and the photosensitizer Ru(bpz)<sub>3</sub><sup>2+</sup> results in the photoreduction of Ru(bpz)<sub>3</sub><sup>2+</sup> to Ru(bpz)<sub>3</sub><sup>•+</sup>,  $\lambda_{\max} = 470$  nm (Figure 7, eq 15). Upon addition of the Ru colloid or CO<sub>2</sub> the photogenerated Ru(bpz)<sub>3</sub><sup>2+</sup> is unaffected. Addition of both of the components, the Ru colloid and CO<sub>2</sub>, results in the reoxidation of Ru(bpz)<sub>3</sub><sup>2+</sup> and evolution of CH<sub>4</sub>, implying that the photosensitizer is recycled in the photosensitized evolution of CH<sub>4</sub> as well as supporting the electron-transfer mechanism. It should be noted that illumination of this system is performed in the region of  $\lambda = 420$ –450 nm. We find that illumination of the system with light of  $\lambda > 400$  nm results in poor stability of the photosensitizer. The absorption spectra of Ru(bpz)<sub>3</sub><sup>2+</sup> and Ru(bpz)<sub>3</sub><sup>•+</sup> (Figure 7) show that the two components exhibit an overlap in their absorption bands. The poor stability of the photosensitizer, under conditions where Ru(bpz)<sub>3</sub><sup>•+</sup> is also excited, suggests that the photoproduct Ru(bpz)<sub>3</sub><sup>•+</sup> is itself photoactive and transforms to a product inactive for CO<sub>2</sub> reduction. The relatively limited turnover number (TN) of the system, TN = 15, is thus attributed to the residual absorbance of Ru(bpz)<sub>3</sub><sup>•+</sup> in the excitation region ( $\lambda = 420$ –450 nm) that causes photoconsumption of Ru(bpz)<sub>3</sub><sup>2+</sup>. We anticipate that development of Ru(bpz)<sub>3</sub><sup>2+</sup> derivatives where the 2+/1+ oxidation states exhibit distinct nonoverlapping absorption properties might increase the stability of the system toward CO<sub>2</sub> reduction.

**Selectivity in CO<sub>2</sub>-Reduction and H<sub>2</sub>-Evolution.** The two systems discussed for CO<sub>2</sub> reduction demonstrate that those systems that include a relay yield a mixture of H<sub>2</sub> and hydrocarbons while the

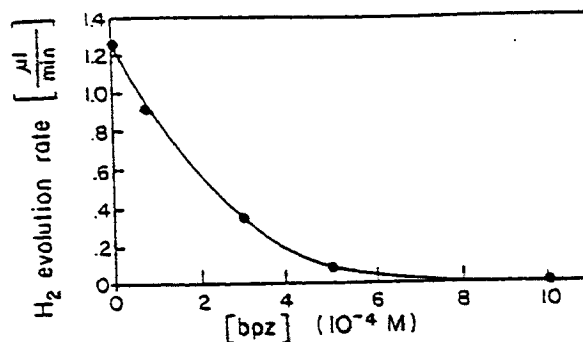


Figure 8. H<sub>2</sub>-Evolution rate as a function of bipyrazine concentration: [Ru(bpy)<sub>3</sub><sup>2+</sup>] = 1.4 × 10<sup>-4</sup> M, [MQ<sup>2+</sup>] = 1.0 × 10<sup>-3</sup> M, [Na<sub>2</sub>EDTA] = 3.3 × 10<sup>-2</sup> M, [NaHCO<sub>3</sub>] = 5.0 × 10<sup>-2</sup> M, [Ru colloid] = 20 mg/L, pH 6.0 under CO<sub>2</sub> atmosphere.

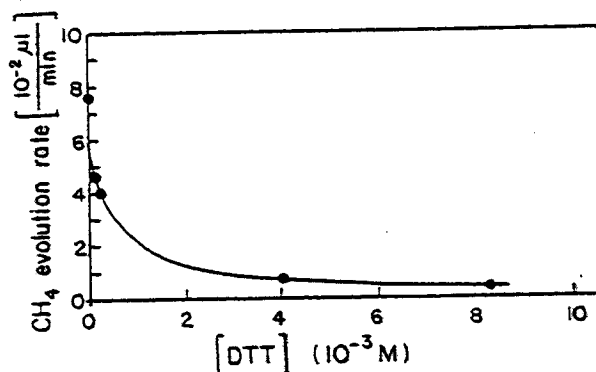


Figure 9. CH<sub>4</sub>-Evolution rate as a function of dithiothreitol concentration: [Ru(bpy)<sub>3</sub><sup>2+</sup>] = 1.4 × 10<sup>-4</sup> M, [MQ<sup>2+</sup>] = 1.0 × 10<sup>-3</sup> M, [Na<sub>2</sub>EDTA] = 3.3 × 10<sup>-2</sup> M, [NaHCO<sub>3</sub>] = 5.0 × 10<sup>-2</sup> M, [Ru colloid] = 20 mg/L, pH 6.0 under CO<sub>2</sub> atmosphere.

system that includes Ru(bpz)<sub>3</sub><sup>2+</sup> is specific for CO<sub>2</sub> reduction only. The laser flash studies (Figure 5) reveal that Ru(bpz)<sub>3</sub><sup>2+</sup> exhibits a kinetic barrier toward H<sub>2</sub> evolution. We have speculated that the coordination sites on the ligands of Ru(bpz)<sub>3</sub><sup>2+</sup> might interact with the heterogeneous catalyst and consequently deactivate the catalyst toward the H<sub>2</sub>-evolution process. We thus examined the H<sub>2</sub>-evolution process under argon using Ru(bpy)<sub>3</sub><sup>2+</sup> as sensitizer, MQ<sup>2+</sup> as charge relay, Na<sub>2</sub>EDTA as electron donor, and the Ru colloid as catalyst in the presence and absence of bipyrazine. Figure 8 shows the quantum yield for H<sub>2</sub> evolution upon addition of the bipyrazine ligand. It is evident that H<sub>2</sub> evolution is retarded as the bipyrazine concentration increases, and at a concentration of 1 × 10<sup>-3</sup> M, no H<sub>2</sub> evolution occurs. Thus we conclude that H<sub>2</sub> evolution is prohibited by the bipyrazine ligand. It should be noted that no inhibitory effect in H<sub>2</sub> evolution is observed with 2,2'-bipyridine or 3,3'-bipyridine as additives. Under CO<sub>2</sub> the inhibition profile of H<sub>2</sub> evolution with added bipyrazine is similar to that observed under argon. Yet, also CO<sub>2</sub> reduction is inhibited to some extent by the addition of bipyrazine, and at [bipyrazine] = 1 × 10<sup>-3</sup> M H<sub>2</sub> evolution is totally blocked while the quantum yield of CO<sub>2</sub> reduction to CH<sub>4</sub> decreases to 30% of its value in the absence of bipyrazine.

Similarly, specificity toward H<sub>2</sub> evolution can be designed. CO<sub>2</sub> reduction can be eliminated in the two systems by the addition of thiols. In the presence of these additives H<sub>2</sub> evolution is not affected. We have examined the photosensitized reduction of CO<sub>2</sub> and H<sub>2</sub> evolution in a system composed of Ru(bpy)<sub>3</sub><sup>2+</sup> as sensitizer, MQ<sup>2+</sup> as electron relay, Na<sub>2</sub>EDTA as electron donor, and the Ru colloid as catalyst. Figure 9 shows the rates of CO<sub>2</sub> reduction to CH<sub>4</sub> at different concentrations of added dithiothreitol (DTT). It should be noted that the added thiols do not inhibit H<sub>2</sub> evolution. Furthermore, with DTT the quantum yield for H<sub>2</sub> reduction is slightly increased. It is evident that the added thiol inhibits CO<sub>2</sub> reduction and at 8 × 10<sup>-3</sup> M DTT CO<sub>2</sub> reduction to methane is prohibited while the H<sub>2</sub> evolution yield is unaffected.

This deactivation of the Ru colloid by thiols toward  $\text{CO}_2$  reduction is general, and cysteine or mercaptoethanol show similar inhibition effects. We thus conclude that thiols prevent the reduction of  $\text{CO}_2$ , and selective  $\text{H}_2$  evolution can be accomplished. Added bipyrazine shows inhibitoric effects toward  $\text{H}_2$  evolution as well as  $\text{CO}_2$  reduction although the deactivation is more pronounced toward the former process. We anticipate that other ligands might show higher selectivity in the degree of deactivation of these reactions. Also, the possibility to control the selective  $\text{CO}_2$ -reduction or  $\text{H}_2$ -evolution process suggests that on the Ru colloid exist distinct and different catalytic sites for the two reactions.

### Conclusions

We have discussed the novel application of Ru and Os colloids as catalysts for the photosensitized  $\text{CO}_2$  reduction to  $\text{CH}_4$ . The fixation of  $\text{CO}_2$  to  $\text{CH}_4$  in aqueous solutions is accompanied by the kinetically favored  $\text{H}_2$ -evolution process. Our results emphasize that selectivity toward  $\text{CO}_2$  reduction might be accomplished by proper design of a relay-catalyst configuration that exhibits overpotential properties toward  $\text{H}_2$  evolution. In this respect we find that bipyrazine acts as an inhibitor that eliminates  $\text{H}_2$  evolution. Similarly, thiols eliminate  $\text{CO}_2$  reduction but do not affect evolution of  $\text{H}_2$ . The multielectron fixation of  $\text{CO}_2$  to  $\text{CH}_4$  that involves eight electrons is certainly a stepwise process that involves various intermediates. We emphasize that no other reduction products of  $\text{CO}_2$ , i.e. formate, formaldehyde, or methanol, could be detected in the photosensitized transformation. We have shown that  $\text{C}_2$  hydrocarbons (ethane and ethylene) are also formed during the photoreduction of  $\text{CO}_2$ . The formation of these products suggests that  $\text{Ru}=\text{CH}_2$  (or  $\text{Os}=\text{CH}_2$ ) and  $\text{Ru}-\text{CH}_3$  act as intermediates along the photoreduction of  $\text{CO}_2$  since ethylene would be formed by the dimerization of the carbene species while ethane

is anticipated to originate from dimerization of the metal-methyl intermediate. It should be noted that similar intermediates have been suggested<sup>41</sup> in the methanation process of  $\text{CO}_2$ .

Our study has emphasized that photoreduction of  $\text{CO}_2$  occurs via electron transfer followed by protonation steps rather than by a hydrogenation mechanism. The control experiments that were applied to elucidate the mechanistic aspects of the photo-reduction of  $\text{CO}_2$  revealed that the photochemically generated reduced relays  $\text{Ru}(\text{bpy})_3^{2+}$  or the bipyridinium radicals mediate the reduction of  $\text{CO}_2$  to  $\text{CH}_4$  in the presence of Ru or Os colloid. Since bipyridinium radicals can be produced by  $\text{H}_2$  and heterogeneous catalysts, we might envisage routes to develop novel methanation reactions or electrocatalyzed methanation processes that proceed at ambient temperatures and atmospheric pressure via an electron-transfer pathway. Further attempts to characterize mechanistic aspects involved in the photoreduction of  $\text{CO}_2$  to methane, development of other  $\text{CO}_2$ -reduction catalysts, and the development of the dark electron-transfer reduction processes of  $\text{CO}_2$  are now under way in our laboratory.

**Acknowledgment.** This research is supported by a grant from the National Council for Research and Development, Bonn, and the Kernforschung Anlage, Juelich, Germany.

Registry No. 1, 41491-80-9; 2, 7325-63-5; 3, 16651-68-6; 4, 86690-04-2; TEOA, 102-71-6;  $\text{CO}_2$ , 124-38-9;  $\text{Ru}(\text{bpy})_3^{2+}$ , 15158-62-0;  $\text{Ru}$ , 7440-18-8;  $\text{Os}$ , 7440-04-2;  $\text{Pt}$ , 7440-06-4;  $\text{H}_2$ , 1333-74-0; tris(bipyrazine)ruthenium(II), 75523-96-5; ethylene, 74-85-1; ethane, 74-84-0; methane, 74-82-8; dithiothreitol, 3483-12-3; 3,3'-dimethyl-4,4'-bipyridine, 4479-73-6; 1,3-propanesultone, 1120-71-4.

(41) (a) Weatherbee, G. D.; Bartholomew, C. H. *J. Catal.* 1980, 77, 460-472. (b) Biloen, P.; Sachtler, W. M. H. *Adv. Catal.* 1981, 30, 105-216. (c) Baker, J. A.; Bell, A. T. *J. Catal.* 1982, 78, 165-181.

## Cyclobutene Photochemistry. Nonstereospecific Photochemical Ring Opening of Simple Cyclobutenes

K. Brady Clark and William J. Leigh\*<sup>1</sup>

Contribution from the Department of Chemistry, McMaster University, Hamilton, Ontario, Canada L8S 4M1. Received December 15, 1986

**Abstract:** The photochemistry of bicyclo[3.2.0]hept-6-ene, bicyclo[4.2.0]oct-7-ene, and *cis*- and *trans*-3,4-dimethylcyclobutene has been investigated in hydrocarbon solution with monochromatic far-ultraviolet (185 and 193 nm) light sources. All of these simple cyclobutene derivatives undergo ring opening to yield the isomeric 1,3-dienes, and the latter three open nonstereospecifically to yield mixtures of the possible geometric isomers. The isomeric 3,4-dimethylcyclobutenes yield different mixtures of the three 2,4-hexadiene isomers, and in each case the mixtures are weighted in favor of the orbital symmetry forbidden isomer(s). Attempts have been made to analyze the relative isomeric diene yields from ring opening of bicyclo[4.2.0]octene and the isomeric 3,4-dimethylcyclobutenes within the context of the purely disrotatory, adiabatic ring-opening mechanism that recent ab initio calculations suggest should be possible. While the results for the former compound are consistent with this mechanism, analysis of the relative yields of the isomeric 2,4-hexadienes from photolysis of the latter two compounds indicates that photochemical ring opening by the formally forbidden, conrotatory pathway may compete to some extent with disrotatory ring opening.

In spite of the central role that the thermal<sup>2,3</sup> and photochemical<sup>3b,4,5</sup> interconversions of cyclobutene and 1,3-butadiene play

in our understanding of pericyclic reactions,<sup>6</sup> there are few reported examples that illustrate the photochemical electrocyclic ring-

(1) Natural Sciences and Engineering Research Council of Canada University Research Fellow, 1983-1988.

(2) (a) Winter, R. E. K. *Tetrahedron Lett.* 1965, 1207. (b) Brauman, J. L.; Golden, D. M. *J. Am. Chem. Soc.* 1968, 90, 1920. (c) Srinivasan, R. *J. Am. Chem. Soc.* 1969, 91, 7557. (d) Brauman, J. L.; Archie, W. C. *J. Am. Chem. Soc.* 1972, 94, 4252. (e) Jasinski, J. M.; Frisoli, J. K.; Moore, C. B. *J. Chem. Phys.* 1983, 79, 1312.

(3) (a) Doorkian, G. A.; Freedman, H. H. *J. Am. Chem. Soc.* 1968, 91, 5310, 6896. (b) Schumate, K. M.; Fonken, G. J. *J. Am. Chem. Soc.* 1965, 87, 3996; 1966, 88, 1073.

(4) (a) Dauben, W. G.; Cargill, R. G.; Coates, R. M.; Saltiel, J. J. *J. Am. Chem. Soc.* 1966, 88, 2742. (b) Srinivasan, R. *J. Am. Chem. Soc.* 1968, 90, 4498. (c) Chapman, O. L.; Pasto, D. J.; Borden, G. W.; Griswold, A. A. *J. Am. Chem. Soc.* 1962, 84, 1220. (d) Dauben, W. G.; Cargill, R. L. *J. Org. Chem.* 1962, 27, 1910.

**Acknowledgment.** We would like to acknowledge the help of Drs. Gwen Bauman, Asbed Vassilian, and Bruno van Hemeleer in the early stages of this work. We also gratefully acknowledge the support of the National Institutes of Health by Grant GM 26234. S.S.I. is the recipient of a National Institutes of Health Career Development Award (AM 00732) (1980-1985) and a Camille and Henry Dreyfus Teacher-Scholar Award (1981-1985).

## Effective Photoreduction of $\text{CO}_2/\text{HCO}_3^-$ to Formate Using Visible Light

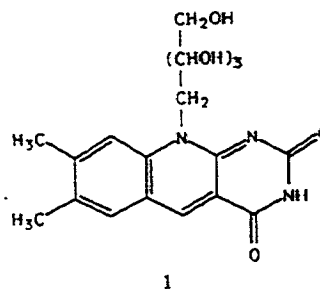
Daniel Mandler and Itamar Willner\*

Department of Organic Chemistry  
The Hebrew University of Jerusalem  
Jerusalem 91904, Israel

Received April 6, 1987

Photoreduction of  $\text{CO}_2$  and its aqueous forms to organic products is a challenging subject as a means of mimicking photosynthesis and solar energy conversion and storage.<sup>1,2</sup> Photoreduction of  $\text{CO}_2$  to formate has been reported with use of homogeneous catalysts,<sup>3</sup> semiconductor powders<sup>4</sup> or electrodes,<sup>5</sup> and the enzyme formate dehydrogenase.<sup>6</sup> Recently, we were able to photoreduce  $\text{CO}_2$  to methane,<sup>7</sup> although in low yields. Electrocatalyzed reductions of  $\text{CO}_2$  have been extensively studied,<sup>8,9</sup> but these do not occur at the thermodynamic potential for formate formation. Wrighton et al. have examined<sup>10</sup> the reduction of  $\text{HCO}_3^-$  to formate by hydrogen and the electroreduction of  $\text{HCO}_3^-$ , in the presence of various supported palladium catalysts, in which effective formate production has been accomplished at room temperature close to the thermodynamic potential. Interestingly, the photosensitized reduction of  $\text{CO}_2/\text{HCO}_3^-$  using Pd-based heterogeneous catalysts has not been reported. Here we wish to report on the design of a novel heterogeneous Pd colloid stabilized by  $\beta$ -cyclodextrin ( $\beta$ -CD)<sup>11</sup> and its application in the effective reduction of  $\text{CO}_2/\text{HCO}_3^-$  to formate. High quantum yields,  $\phi = 1.1$  are reported for formate production. We find that the  $\beta$ -CD support strongly affects the catalyst activity.

Photoreduction of  $N,N'$ -dimethyl-4,4'-bipyridinium salt, methyl viologen,  $\text{MV}^{2+}$ , with various sensitizers and sacrificial electron donors, has been extensively explored in recent years.<sup>12,13</sup> Krasna has found<sup>14</sup> that deazariboflavin, dRFI (1), acts as an effective

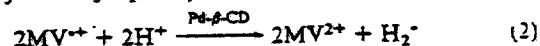


1

photosensitizer for the reduction of  $\text{MV}^{2+}$ . For example, in the presence of oxalate as electron donor,  $\text{MV}^{2+}$  is photogenerated in quantum yields  $\phi > 1$ . Comparison of the reduction potential of  $\text{MV}^{2+}$  ( $E^\circ(\text{MV}^{2+}/\text{MV}^{\bullet+}) = -0.45$  V vs NHE<sup>15</sup>) to the thermodynamic potential for formate formation ( $E^\circ(\text{HCO}_3^-/\text{HCO}_2^-) = -0.42$  V vs NHE,<sup>16</sup> at pH 7) suggests that the thermodynamic balance for the process outlined in eq 1 corresponds to  $\Delta G^\circ \approx 2\text{MV}^{\bullet+} + \text{HCO}_3^- + 2\text{H}^+ \rightleftharpoons 2\text{MV}^{2+} + \text{HCO}_2^- + \text{H}_2\text{O}$  (1)

0. Thus, by the light-driven generation of  $\text{MV}^{\bullet+}$  high concentrations of formate could, in principle, be accumulated. Yet, this process is kinetically unfavored, and no formate is formed in systems that include  $\text{CO}_2/\text{HCO}_3^-$  and photogenerated  $\text{MV}^{\bullet+}$ .

We find that Pd supported on  $\beta$ -CD acts as an effective catalyst for the photoreduction of  $\text{CO}_2/\text{HCO}_3^-$ , by  $\text{MV}^{\bullet+}$ . The system was composed of an aqueous sodium bicarbonate solution (3 mM), 0.06 M, that included deazariboflavin, dRFI (1), as photosensitizer,  $8 \times 10^{-5}$  M,  $\text{MV}^{2+}$ ,  $2 \times 10^{-3}$  M, as primary electron acceptor, and oxalate as sacrificial electron donor, 0.06 M. Pd- $\beta$ -CD colloid (30 mg-L<sup>-1</sup>) was added to the solution, and  $\text{CO}_2$  was bubbled through the system (final pH 6.8). Illumination of the system ( $\lambda > 400$  nm), at 30 °C, results in the formation of formate,  $\text{HCO}_2^-$ , and trace amounts of hydrogen. Figure 1 shows the rate of  $\text{HCO}_2^-$  and  $\text{H}_2$  formation at time intervals of illumination.<sup>17</sup> The quantum yields correspond to  $\phi(\text{HCO}_2^-) = 1.1$  and  $\phi(\text{H}_2) = 0.03$ . Control experiments reveal that in the absence of  $\text{CO}_2/\text{HCO}_3^-$  the major photoproduct is  $\text{H}_2$  (eq 2),  $\phi = 0.12$ , and



only trace amounts of  $\text{HCO}_2^-$  are formed by in situ generation of  $\text{CO}_2$  by the oxidation of oxalate (vide infra). Also, in the absence of the Pd- $\beta$ -CD colloid no  $\text{HCO}_2^-$  or  $\text{H}_2$  are produced, and  $\text{MV}^{\bullet+}$  is the only photoproduct,  $\phi(\text{MV}^{\bullet+}) \approx 3.5$ . Illumination of an aqueous system that includes dRFI (1),  $\text{MV}^{2+}$  as electron acceptor, oxalate as electron donor, and a Pt colloid stabilized by  $\beta$ -CD results in the formation of  $\text{H}_2$ , and no formate is formed. These results clearly indicate that formate is not formed by the sacrificial oxidation of oxalate and that Pd- $\beta$ -CD is a specific catalyst for the photoreduction of  $\text{CO}_2/\text{HCO}_3^-$  to formate.<sup>18</sup> Comparison of the amount of photogenerated formate to the

(1) (a) Inoue, S.; Yamazaki, N. *Organic and Bio-organic Chemistry of Carbon Dioxide*; Kodansha Ltd.: Tokyo, Wiley: New York, 1982. (b) Ziessel, R. *Nouv. J. Chim.* 1983, 7, 613.

(2) (a) Keene, F. R.; Creutz, C.; Sutin, N. *Coord. Chem. Rev.* 1985, 64, 247. (b) Hawecker, J.; Lehn, J.-M.; Ziessel, R. *J. Chem. Soc., Chem. Commun.* 1985, 56. (c) Hawecker, J.; Lehn, J.-M.; Ziessel, R. *J. Chem. Soc., Chem. Commun.* 1983, 536. (d) Kitamura, N.; Tazuke, S. *Chem. Lett.* 1983, 1109.

(3) Ziessel, R.; Hawecker, J.; Lehn, J.-M. *Helv. Chim. Acta* 1986, 69, 1065.

(4) (a) Aurian-Blanjani, B.; Halmann, M.; Manassen, J. *Sol. Energy* 1980, 25, 165. (b) Halmann, M. *Nature (London)* 1978, 275, 115.

(5) Bradley, M. G.; Tysak, T.; Graves, D. J.; Vlachopoulos, N. A. *J. Chem. Soc., Chem. Commun.* 1983, 349.

(6) Parkinson, B. A.; Weaver, P. F. *Nature (London)* 1984, 148.

(7) Mandler, R.; Willner, I. *J. Am. Chem. Soc.* 1986, 108, 8100.

(8) (a) Russell, P. G.; Kovac, N.; Srinivasan, S.; Steinberg, M. *J. Electrochem. Soc.* 1977, 124, 1329. (b) Amatore, C.; Saveant, J.-M. *J. Am. Chem. Soc.* 1981, 103, 5021. (c) Kaiser, V.; Heitz, E. *Ber. Bunsen. Gesell.* 1973, 77, 818.

(9) (a) Tezuka, M.; Yajima, T.; Tsuchiya, A. *J. Am. Chem. Soc.* 1982, 104, 6834. (b) Slater, S.; Wagenknecht, J. H. *J. Am. Chem. Soc.* 1984, 106, 5367. (c) Hawecker, J.; Lehn, J.-M.; Ziessel, R. *J. Chem. Soc., Chem. Commun.* 1984, 328.

(10) (a) Stalder, C. J.; Chao, S.; Summers, D. P.; Wrighton, M. S. *J. Am. Chem. Soc.* 1983, 105, 6318. (b) Chao, S.; Stalder, C. J.; Summers, D. P.; Wrighton, M. S. *J. Am. Chem. Soc.* 1984, 106, 2723.

(11) The colloid of Pd stabilized by  $\beta$ -CD was prepared by heating a 1.5  $\times 10^{-3}$  M  $\text{PdCl}_2$  solution that included  $\beta$ -CD (1% w/w) at 70 °C for several minutes till the color changed. Heating was continued another 2-3 min. The colloid was then deionized (with Amberlite MB-1) and centrifugated (5000 rpm, 30 min). The mean particle diameter of the colloid was estimated to be 150 Å by electron microscopy measurements. Preparation of metal colloids stabilized by cyclodextrins has been previously reported. Cf. Komiyama M.; Hirai, H. *Bull. Chem. Soc. Jpn.* 1983, 56, 2833.

(12) (a) Willner, I.; Ford, W. E.; Orvos, J. W.; Calvin, M. In *Bioelectrochemistry*; Keyser, H.; Gutmann, F., Eds.; Plenum Press: New York, 1980. (b) Moradpour, A.; Amouyal, E.; Keller, P.; Kagan, H. *Nouv. J. Chim.* 1978, 2, 547. (c) Kalyanasundaram, K.; Gratzel, M. *Helv. Chim. Acta* 1978, 61, 2720.

(13) (a) Amouyal, E.; Zidler, B.; Keller, P. *Nouv. J. Chim.* 1983, 7, 725. (b) Kalyanasundaram, K. *Coord. Chem. Rev.* 1982, 46, 159.

(14) Krasna, A. I. *Photochem. Photobiol.* 1980, 31, 75.

(15) Ito, M.; Kuwana, T. *J. Electroanal. Chem. Interfac. Electrochem.* 1971, 32, 415.

(16) Latimer, In *The Oxidation States of the Elements and Their Potentials in Aqueous Solutions*, 2nd ed.; Prentice Hall: New York, 1952.

(17) Formate was analyzed by two complementary methods: ion chromatography (Wescan ion exclusion column,  $2 \times 10^{-3}$  N  $\text{H}_2\text{SO}_4$  as eluent) and by an enzymatic assay with use of formate dehydrogenase.

(18) At pH  $\leq 5$  no formate is photogenerated, and the only photoproduct is  $\text{H}_2$ . This suggests that  $\text{HCO}_3^-$  is the substrate being reduced to formate rather than  $\text{CO}_2$ . In the specified systems, pH 6.8,  $\text{CO}_2$  is included to maintain constant pH and  $\text{HCO}_3^-$  concentration.

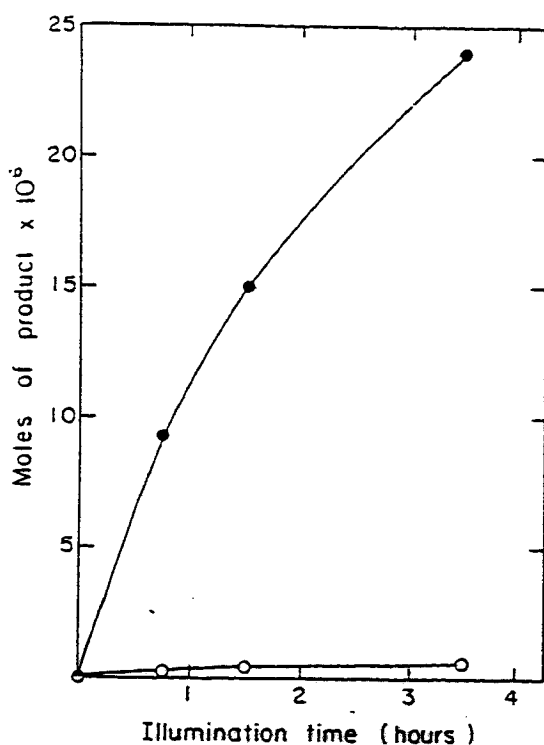


Figure 1. Rate of formate (●) and hydrogen (○) formation as a function of illumination time.

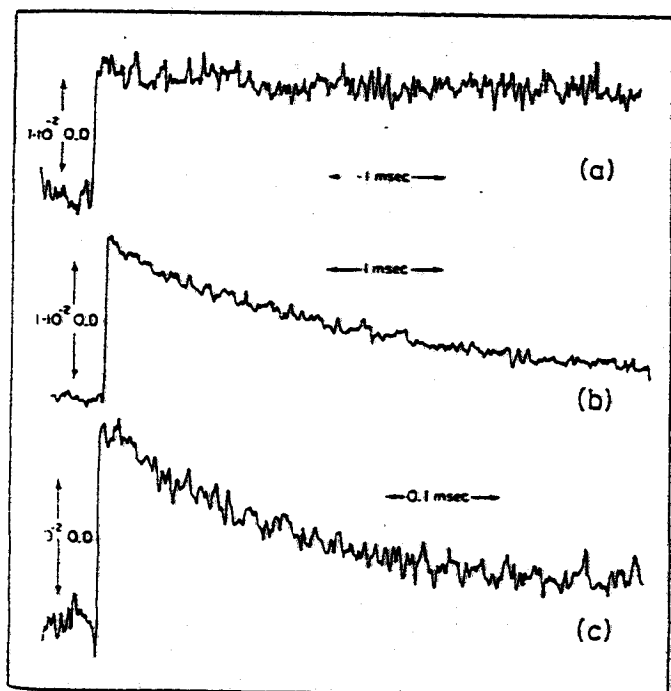


Figure 2. Transient decay of  $MV^{2+}$  followed at  $\lambda = 602$  nm in systems composed of dRFL,  $4 \times 10^{-5}$  M;  $MV^{2+}$ ,  $1 \times 10^{-3}$  M; and oxalic acid,  $6.7 \times 10^{-2}$  M. (a) Without  $CO_2/HCO_3^-$  or Pd- $\beta$ -CD. (b) Without  $CO_2/HCO_3^-$  and with Pd- $\beta$ -CD (30 mg-L<sup>-1</sup>). (c) With  $CO_2/HCO_3^-$  ( $6.7 \times 10^{-2}$  M) and with Pd- $\beta$ -CD (30 mg-L<sup>-1</sup>). All systems were adjusted to pH 7 and degassed by either  $CO_2$  (b) and (c) or by Ar (a).

amount of Pd- $\beta$ -CD catalyst included reveals that the catalyst performs ca. 10 turnovers.

It is evident that the Pd- $\beta$ -CD colloid is a poor catalyst for  $H_2$  evolution. Comparison of the quantum yields obtained under steady-state illumination of  $MV^{2+}$  production to those of  $HCO_3^-$  and  $H_2$  formation suggests that the catalytic processes are the rate-limiting steps. Laser flash photolysis studies have confirmed that Pd- $\beta$ -CD is a superior catalyst for  $CO_2/HCO_3^-$  reduction as compared to  $H_2$  evolution (Figure 2). Flashing the system

that includes dRFL,  $MV^{2+}$ , and oxalate results in the steady-state accumulation of  $MV^{2+}$  (Figure 2a) as a result of the photoreduction of  $MV^{2+}$ . Addition of Pd- $\beta$ -CD in the absence of  $CO_2/HCO_3^-$  (Figure 2b) induced a slow decay of  $MV^{2+}$  due to  $H_2$  evolution. Addition of  $CO_2/HCO_3^-$  (Figure 2c) to the system effects a rapid decay of  $MV^{2+}$ , implying that the rate of  $CO_2/HCO_3^-$  reduction is substantially faster than  $H_2$  evolution.

Formate,  $HCO_2^-$ , reduces  $MV^{2+}$  in the dark in the presence of Pd- $\beta$ -CD (eq 1). This allows us to examine the catalytic activity of the Pd colloid in the presence of various additives, and particularly in the presence of sacrificial electron donors, by means of the reverse formate decomposition process. We find that common electron donors such as thiols and the photodecomposition products of EDTA (formaldehyde) inhibit the catalytic activity of Pd- $\beta$ -CD toward formate decomposition. Accordingly, no photoreduction of  $CO_2/HCO_3^-$  is observed in the presence of these electron donors. Oxalate does not inhibit the catalytic activity of Pd- $\beta$ -CD and explains the success to photoinduce the reduction of  $CO_2$  in the present system.

In conclusion, we have developed an effective system for the photoreduction of  $CO_2/HCO_3^-$  to formate by visible light. It should be noted that the  $\beta$ -CD support for the Pd colloid is extremely important to its catalyst activity and Pd colloids prepared by the reduction with citrate or stabilized by polymers, i.e. poly vinyl alcohol, are inactive toward formate production. Previous studies<sup>19</sup> have indicated that hydroxyl-containing supports, i.e., alumina, participate cooperatively in the activation of  $CO_2$  by Pd metal. Similarly, cyclodextrins have been claimed<sup>20</sup> to associate  $CO_2$ , and derivatized cyclodextrins catalyze the hydration of  $CO_2$ .<sup>21</sup> The possible cooperative activation of  $CO_2/HCO_3^-$  by  $\beta$ -CD and Pd are now being investigated.

**Acknowledgment.** This research is supported by the Belfer Center for Energy Research, Israel.

**Registry No.** 1, 19342-73-5;  $CO_2$ , 124-38-9;  $HCO_3^-$ , 71-52-3;  $HCOO^-$ , 64-18-6.

- (19) (a) Solymosi, F.; Erdohelyi, A.; Lancz, M. *J. Catal.* 1985, 95, 567.  
 (b) Solymosi, F.; Erdohelyi, A. *J. Mol. Catal.* 1980, 8, 471.  
 (20) (a) Hadley, J. H.; Hsu, F. H.; Yei, W. *J. Chem. Phys.* 1979, 70, 3702.  
 (b) Cramer, F.; Henglein, F. M. *Angew. Chem.* 1956, 20, 649.  
 (21) Tabushi, I.; Kuroda, Y.; Mochizuki, A. *J. Am. Chem. Soc.* 1980, 102, 1152.

#### Incorporation of D-Amino Acids into Peptides via Enzymatic Condensation in Organic Solvents

Alexey L. Margolin, Dar-Fu Tai, and Alexander M. Klivanov\*

Department of Applied Biological Sciences  
 Massachusetts Institute of Technology  
 Cambridge, Massachusetts 02139  
 Received August 4, 1987

A number of biologically active peptides, including important antibiotics, synthetic vaccines, and enkephalins and other hormones, contain D-amino acid residues.<sup>1</sup> Although enzymes, namely proteases, are becoming increasingly popular as catalysts of peptide bond formation,<sup>2</sup> this synthetic methodology (as well

- (1) Shoji, J. *Adv. Appl. Microbiol.* 1978, 24, 187-214. Hansen, P. E.; Morgan, B. A. In *The Peptides: Analysis, Synthesis, Biology*; Udenfriend, S.; Meienhofer, J., Eds.; Academic Press: Orlando, 1984; Vol. 6, pp 269-321.  
 Blanc, J. P.; Kaiser, E. T. *J. Biol. Chem.* 1984, 259, 9549-9556. Wolfe, S.; Demain, A. L.; Jensen, S. E.; Westlake, D. W. *S. Science (Washington, D. C.)* 1984, 226, 1386-1392. Geysen, H. M.; Rodda, S. J.; Mason, T. J. In *Synthetic Peptides as Antigens*; Ciba Foundation Symposium No. 119; Wiley: Chichester, 1986; pp 130-149.  
 (2) Fruton, J. S. *Adv. Enzymol.* 1982, 53, 239-306. Chaiken, I. M.; Komoriya, A.; Ohno, M.; Widmer, F. *Appl. Biochem. Biotechnol.* 1982, 7, 385-399. Jakubke, H.-D.; Kuhl, P.; Konnecke, A. *Angew. Chem., Int. Ed. Engl.* 1985, 24, 85-93. Kullmann, W. *Enzymatic Peptide Synthesis*; CRC Press: Boca Raton, FL, 1987.

# PHOTOSENSITIZED REDUCTION OF BENZYL AND OCTYL VIOLOGENS IN $\beta$ -CD AQUEOUS MEDIA

Itamar Willner\*, Eti Adar, Zafir Goren and Bilha Steinberger

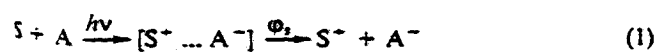
Department of Organic Chemistry and The Fritz Haber Research Center for Molecular Dynamics, The Hebrew University of Jerusalem, Jerusalem 91904 (Israel).

Received March 23, 1987, accepted for publication June 3, 1987.

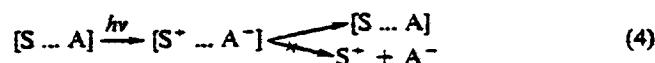
**RÉSUMÉ.** — Le N,N'-dioctylbipyridinium 4,4' (octyl viologène,  $C_8V^{2+}$ ), ainsi que le N,N'-dibenzylbipyridinium 4,4' (benzyl viologène,  $BV^{2+}$ ), forment des complexes à l'état fondamental avec le photosensibilisateur Zn(II)-mésotétraphényl sulfonate porphyrine, Zn-TPPS $^{4-}$ . La formation de ces complexes supprime la photoréduction des  $C_8V^{2+}$  et  $BV^{2+}$ , à cause de la recombinaison des photoproduits dans la structure des complexes. En présence de  $\beta$ -cyclodextrine ( $\beta$ -CD), la photoréduction de  $C_8V^{2+}$  et de  $BV^{2+}$  se passe de désactivation de l'état triplet du Zn-TPPS $^{4-}$  excité. On démontre que le  $\beta$ -CD prend part à la réduction photosensibilisée des  $BV^{2+}$  et  $C_8V^{2+}$  de 3 façons complémentaires. 1° Il sépare les complexes destructifs à l'état fondamental; 2° Il aide à la séparation des charges, et stabilise les photoproduits contre les réactions en retour de transfert d'électrons; 3° Il empêche l'agrégation des relais réduits  $C_8V^{\cdot-}$  et  $BV^{\cdot-}$ . Ces effets résultent de l'association sélective des  $C_8V^{2+}$  et  $BV^{2+}$ , ainsi que des variantes réduites correspondantes, à la cavité hydrophobe du  $\beta$ -CD.

**ABSTRACT.** — N,N'-dioctyl-4,4'-bipyridinium, octyl viologen,  $C_8V^{2+}$ , and N,N'-dibenzyl-4,4'-bipyridinium, benzyl viologen,  $BV^{2+}$ , form ground state complexes with the photosensitizer, Zn(II)-meso-tetraphenyl sulfonato porphyrin, Zn-TPSS $^{4-}$ . The formation of this complex eliminates photoreduction of  $C_8V^{2+}$  and  $BV^{2+}$  since the photoproducts recombine in the complex structure. In the presence of  $\beta$ -cyclodextrin, ( $\beta$ -CD), photoreduction of  $C_8V^{2+}$  and  $BV^{2+}$  occurs *via* quenching of the triplet state of excited Zn-TPSS $^{4-}$ . It is demonstrated that  $\beta$ -CD participates in three complementary functions in the photosensitized reduction of  $BV^{2+}$  and  $C_8V^{2+}$ : i) It separates destructive ground state complexes; ii) It assists charge separation and stabilizes the photoproducts against back electron transfer reactions and iii) It prevents aggregation of the reduced relays  $C_8V^{\cdot-}$  and  $BV^{\cdot-}$ . These effects are a result of the selective association of  $C_8V^{2+}$  and  $BV^{2+}$  and their reduced forms to the hydrophobic cavity of  $\beta$ -CD.

Photosensitized electron transfer reactions using visible light are of substantial interest as a means of solar energy conversion and storage<sup>1,3</sup>. To accomplish high quantum yields in the photosensitized transformations, effective charge separation of the initial « encounter cage complex » (1) and stabilization of the photoproducts against back electron transfer reactions (2) are required<sup>4</sup>. Various organized microheterogeneous environments such as micelles<sup>5,6</sup>, polyelectrolytes<sup>7</sup>, charged colloids<sup>8,9</sup>, vesicles<sup>10</sup> and microemulsions<sup>11</sup> have been utilized to assist charge separation and retard the recombination reactions. Recently, we have applied  $\beta$ -cyclodextrins ( $\beta$ -CD) in aqueous media as molecular receptors that stabilize the intermediate photoproducts against recombination reactions<sup>12</sup>.



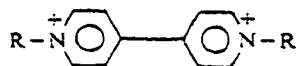
$\beta$ -CD are cyclic polysugars composed of glucose units linked by 1-4- $\alpha$ -glycoside bonds. The cyclic structure includes an hydrophobic cavity capable of accommodating organic substrates<sup>13-15</sup>. Thus, by the selective association of one of the photoproducts to the  $\beta$ -CD cavity stabilization of the photoproducts against back reactions could be accomplished. A second difficulty often encountered in photosensitized reactions is the formation of sensitizer-acceptor ground state complexes (3). The formation of these complexes has destructive consequences on the net photosensitized electron transfer process. As the photoproducts are stabilized by similar interactions rapid recombination reactions occur and no charge separation is accomplished (4).



Here we wish to report on the photosensitized reduction of N,N'-dioctyl-4,4'-bipyridinium,  $C_8V^{2+}$ , (1), and N,N'-dibenzyl-4,4'-bipyridinium,  $BV^{2+}$ , (2), in aqueous media in the

\* To whom all correspondence should be addressed.

absence and presence of  $\beta$ -CD, using Zn(II)-*meso*-tetraphenyl sulfonato porphyrin, Zn-TPPS<sup>4-</sup>, as sensitizer. We discuss three separate functions of  $\beta$ -CD in the photosensitized electron transfer reactions: *i*) Separation of ground state complexes between Zn-TPPS<sup>4-</sup> and the electron relays  $C_8V^{2-}$  and  $BV^{2-}$  and its consequences on the photosensitized transformations; *ii*) Stabilization of the photoproducts against back electron transfer reactions, and *iii*) Stabilization of the monomeric forms of the reduced photoproducts  $C_8V^{\cdot-}$  and  $BV^{\cdot-}$  and elimination of aggregated reduced relays.



- (1) R = C<sub>6</sub>H<sub>17</sub>  
 (2) R = PhCH<sub>2</sub>

### Experimental section

Absorption spectra were recorded with a Uvikon-820 (Kontron) Spectrophotometer equipped with a  $\psi$ -80 computer for spectra accumulation and manipulation. Fluorescence spectra were recorded with a SEM-25 spectrophotometer (Kontron). Flash photolysis experiments were performed with a DL 200 (Molelectron) dye laser pumped by a UV-IU (Molelectron) nitrogen laser. Flashes were recorded on biomatron 8100, and pulse collection was performed with a Nicolet 1170. Steady state illuminations were performed with a 1 000 W — halogen quartz lamp. Light was filtered through a 400 nm cut-off filter. Photon flux was determined by Reinecke salt actinometry<sup>16</sup> to be  $2 \times 10^{-2}$  Einsteins  $L^{-1} \cdot min^{-1}$ .

For steady state illumination an aqueous phosphate buffer solution, pH = 8.5, 3 mL that includes the photosensitizer, Zn-TPPS<sup>4-</sup>,  $3.2 \times 10^{-6}$  mol  $L^{-1}$ , the electron acceptor  $C_8V^{2-}$  or  $BV^{2-}$ ,  $5 \times 10^{-4}$  mol  $L^{-1}$  and the sacrificial electron donor (NH<sub>4</sub>)<sub>2</sub>EDTA  $1.0 \times 10^{-1}$  mol  $L^{-1}$  was used. In the desired systems  $\beta$ -CD (Aldrich) was added at the specified concentration. The solutions were introduced into a glass cuvette equipped with a stirrer, valve and septum stopper. The solutions were deaerated with oxygen free argon and illuminated.  $C_8V^{\cdot-}$  and  $BV^{\cdot-}$  were followed spectroscopically at  $\lambda = 602$  nm ( $\epsilon = 13\,800$  mol<sup>-1</sup> L $\cdot$ cm<sup>-1</sup>), ( $C_8V^{\cdot-}$ )<sub>2</sub> and ( $BV^{\cdot-}$ )<sub>2</sub> were followed at  $\lambda = 569$  nm ( $\epsilon = 6\,200$  mol<sup>-1</sup> L $\cdot$ cm<sup>-1</sup>). For flash photolysis experiments buffer solutions, pH = 8.5, that include Zn-TPPS<sup>4-</sup>,  $7.6 \times 10^{-6}$  mol  $L^{-1}$  and the electron relay  $C_8V^{2-}$  or  $BV^{2-}$ ,  $4 \times 10^{-6}$ , were used.  $\beta$ -CD was added,  $1 \times 10^{-2}$  mol  $L^{-1}$ , to the desired systems and the deaerated solutions were flashed with argon. To follow the T<sub>Zn-TPPS<sup>4-</sup></sub> formation and quenching, the system was excited at  $\lambda = 555$  nm and the triplet yield and lifetime were followed at  $\lambda = 840$  nm. Photoproducts were followed at  $\lambda = 602$  nm for  $C_8V^{\cdot-}$  and  $BV^{\cdot-}$  and at  $\lambda = 580$  nm for ( $C_8V^{\cdot-}$ )<sub>2</sub> and ( $BV^{\cdot-}$ )<sub>2</sub>. For steady state fluorescence measurements the photosensitizer was followed at  $\lambda = 600$  nm.

### Results and Discussion

#### COMPLEX FORMATION BETWEEN Zn-TPPS<sup>4-</sup> AND THE RELAYS $C_8V^{2-}$ AND $BV^{2-}$

Ground state complex formation between metalloporphyrins and charged electron acceptors is well established. For example, Pd-TPPS<sup>4-</sup> forms a complex structure with methylviologen, MV<sup>2+</sup>, and the zwitterionic Zn(II)-*meso*-tetrapropylsulfonato-pyridinium porphyrin, Zn-TPSPyP forms a complex with anthraquinone-2,6-disulfonate<sup>12</sup>. These complexes are essentially a result of electrostatic attractions between the oppositely charged components, although additional stabilization by charge-transfer interactions cannot be excluded.

Stepwise addition of  $C_8V^{2-}$  or  $BV^{2-}$  to an aqueous solution of the sensitizer Zn-TPPS<sup>4-</sup> results in substantial changes in the absorption spectrum of the sensitizer (Fig. 1). The gradual changes in the absorption spectra upon addition of the

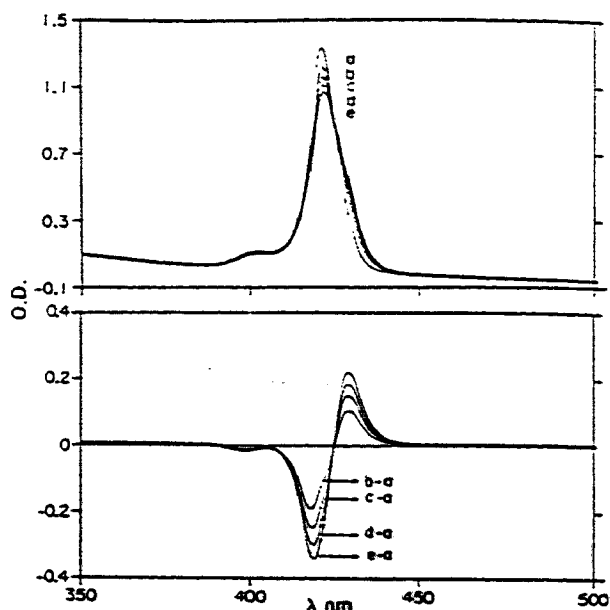
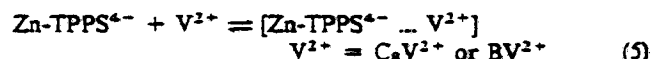


Figure 1. — Absorption spectra (top) and differential absorption spectra (bottom) of Zn-TPPS<sup>4-</sup> ( $4.2 \times 10^{-7}$  mol  $L^{-1}$ ) obtained after addition of  $BV^{2+}$ : (a) no added  $BV^{2+}$ ; (b) [ $BV^{2+}$ ] =  $6.6 \times 10^{-6}$  mol  $L^{-1}$ ; (c) [ $BV^{2+}$ ] =  $9.9 \times 10^{-6}$  mol  $L^{-1}$ ; (d) [ $BV^{2+}$ ] =  $1.3 \times 10^{-5}$  mol  $L^{-1}$ ; (e) [ $BV^{2+}$ ] =  $1.6 \times 10^{-5}$  mol  $L^{-1}$ .

electron acceptor and the presence of isosbestic points suggest the formation of a sensitizer acceptor complex (5). From the absorption spectra changes, and using the Benesi-Hildebrand equation<sup>17</sup>, the association constants,  $K_a$  (6) were estimated to be  $K_a = (2.0 \pm 0.3) \times 10^4$  mol<sup>-1</sup> L for  $C_8V^{2-}$  and  $K_a = (2.5 \pm 0.4) \times 10^4$  mol<sup>-1</sup> L for  $BV^{2-}$ .



$$K_a = \frac{[Zn-TPPS^{4-} \dots V^{2+}]}{[Zn-TPPS^{4-}][V^{2+}]} \quad (6)$$

The addition of  $C_8V^{2-}$  or  $BV^{2-}$  to an aqueous solution of Zn-TPPS<sup>4-</sup> has also a substantial effect on the emission properties of the sensitizer. The solution of the free sensitizer exhibits a fluorescence band at  $\lambda = 600$  nm. Upon addition of  $C_8V^{2-}$  or  $BV^{2-}$  the fluorescence emission is quenched (Fig. 2). Assuming that only the free Zn-TPPS<sup>4-</sup> exhibits fluorescence properties, while the sensitizer in the complex structure does not emit, the concentration of free and associated Zn-TPPS<sup>4-</sup> can be determined (7). Using these assumptions, the derived association constants for the complexes [Zn-TPPS<sup>4-</sup> ... V<sup>2+</sup>] correspond to  $K_a = (2.3 \pm 0.4) \times 10^4$  mol<sup>-1</sup> L for  $C_8V^{2-}$  and  $K_a = (1.9 \pm 0.3) \times 10^4$  mol<sup>-1</sup> L for  $BV^{2-}$ , values that are in good agreement to those obtained from the absorption spectra changes.

$$[Zn-TPPS^{4-}]_{free} = [Zn-TPPS^{4-}]_0 - [Zn-TPPS^{4-} \dots V^{2+}] \quad (7)$$

Addition of  $\beta$ -CD to an aqueous solution of Zn-TPPS<sup>4-</sup> and  $C_8V^{2-}$  or  $BV^{2-}$  has a significant effect on the stability of complex [Zn-TPPS<sup>4-</sup> ... V<sup>2+</sup>], (Fig. 2). The fluorescence intensity of Zn-TPPS<sup>4-</sup> decreases upon addition of  $C_8V^{2-}$  or  $BV^{2-}$  due to the formation of the complex that lacks

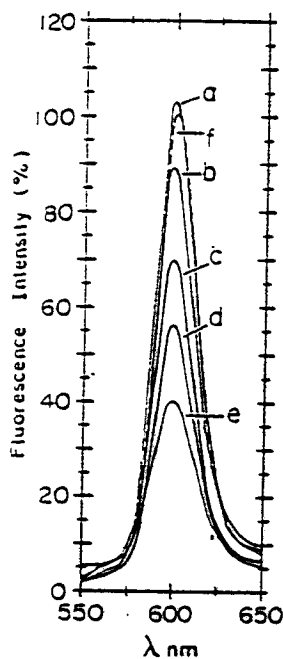
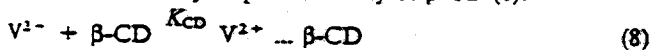


Figure 2. — Fluorescence spectra of Zn-TPPS<sup>4-</sup> ( $2.8 \times 10^{-6}$  mol L<sup>-1</sup>) upon addition of BV<sup>2+</sup>: (a) no added BV<sup>2+</sup>; (b) [BV<sup>2+</sup>] =  $6.6 \times 10^{-6}$  mol L<sup>-1</sup>; (c) [BV<sup>2+</sup>] =  $9.9 \times 10^{-6}$  mol L<sup>-1</sup>; (d) [BV<sup>2+</sup>] =  $1.3 \times 10^{-5}$  mol L<sup>-1</sup>; (e) [BV<sup>2+</sup>] =  $1.6 \times 10^{-5}$  mol L<sup>-1</sup>; (f) [BV<sup>2+</sup>] =  $1.6 \times 10^{-5}$  mol L<sup>-1</sup> and [β-CD] =  $1.0 \times 10^{-2}$  mol L<sup>-1</sup>.

luminescence characteristics due to internal quenching. Upon addition of β-CD, the original emission properties of the photosensitizer are restored in the presence of C<sub>8</sub>V<sup>2+</sup> and BV<sup>2+</sup>. These results clearly indicate that the complex is separated in the presence of β-CD. The separation of the complex is attributed to the selective association of C<sub>8</sub>V<sup>2+</sup> or BV<sup>2+</sup> to the hydrophobic cavity of β-CD (8).



Knowing the association constant of the complexes [Zn-TPPS<sup>4-</sup> ... V<sup>2+</sup>], and by assuming that the fluorescence intensity corresponds to free Zn-TPPS<sup>4-</sup> only, the concentration of free sensitizer [Zn-TPPS<sup>4-</sup>]<sub>f</sub> and bound photosensitizer [Zn-TPPS<sup>4-</sup> ... V<sup>2+</sup>] can be estimated at every concentration of β-CD. Also, the concentrations of viologens, associated with Zn-TPPS<sup>4-</sup>, β-CD and in the free forms can be calculated (9). Deriving these parameters enables the calculation of the association constants of C<sub>8</sub>V<sup>2+</sup> and BV<sup>2+</sup> to β-CD (10).

$$[V^{2+} \cdots \beta\text{-CD}] = [V^{2+}]_0 - [\text{Zn-TPPS}^{4-} \cdots V^{2+}] - [V^{2+}]_f \quad (9)$$

where [V<sup>2+</sup>]<sub>0</sub> is the total concentration of C<sub>8</sub>V<sup>2+</sup> or BV<sup>2+</sup>, [Zn-TPPS<sup>4-</sup> ... V<sup>2+</sup>] = [Zn-TTPS<sup>4-</sup>]<sub>0</sub> - [Zn-TTPS<sup>4-</sup>]<sub>f</sub> and [V<sup>2+</sup>]<sub>f</sub> = K<sub>s</sub> · [Zn-TTPS<sup>4-</sup>]<sub>f</sub> / [Zn-TTPS<sup>4-</sup> ... V<sup>2+</sup>]

$$K_{\text{CD}} = [V^{2+} \cdots \beta\text{-CD}] / [\beta\text{-CD}] [V^{2+}] \quad (10)$$

The association constant of C<sub>8</sub>V<sup>2+</sup> and BV<sup>2+</sup> to β-CD are K<sub>CD</sub> (C<sub>8</sub>V<sup>2+</sup>) =  $(5.6 \pm 0.5) \times 10^3$  mol<sup>-1</sup> L and K<sub>CD</sub> (BV<sup>2+</sup>) =  $(1.4 \pm 0.2) \times 10^4$  mol<sup>-1</sup> L.

#### PHOTOREDUCTION OF C<sub>8</sub>V<sup>2+</sup> AND BV<sup>2+</sup>

Photoreduction of 4,4'-bipyridinium salts (viologens) has been extensively explored in the past years since these reduced photoproducts, viologen radicals, mediate H<sub>2</sub>-evolution in presence of metal colloids such as Pt, Pd or Rh<sup>18,19</sup>. Specifically photoreduction of N,N'-bipyridinium salts using Zn(II)-porphyrins as sensitizers has been the subject of various reports<sup>20</sup>. It has been found<sup>20b</sup> that the positively charged Zn(II)-meso-tetramethylpyridinium porphyrin, Zn-TMPyP<sup>4+</sup>, photosensitizes effectively the reduction of N,N'-

dimethyl-4,4'-bipyridinium (methyl viologen), MV<sup>2+</sup>, ( $\phi = 0.75 \pm 0.08$ ), while Zn-TPPS<sup>4-</sup> is a poor photosensitizer for the process ( $\phi < 0.1$ ). As we shall see, the poor activity of Zn-TPPS<sup>4-</sup> as photosensitizer, is due to ground complex formation between the photosensitizer and viologen acceptor.

Continuous illumination of an aqueous solution (pH = 8.5) that includes the photosensitizer, Zn-TPPS<sup>4-</sup>,  $3.2 \times 10^{-6}$  mol L<sup>-1</sup>, one of the electron acceptors, C<sub>8</sub>V<sup>2+</sup> or BV<sup>2+</sup>,  $5 \times 10^{-4}$  mol L<sup>-1</sup>, and the electron donor (NH<sub>4</sub>)<sub>3</sub>EDTA,  $1.0 \times 10^{-1}$  mol L<sup>-1</sup>, does not yield any reduced 4,4'-bipyridinium radical cation, C<sub>8</sub>V<sup>•+</sup> or BV<sup>•+</sup>. Yet, upon introduction of β-CD to the aqueous solution,  $1.0 \times 10^{-2}$  mol L<sup>-1</sup>, effective formation of the radical cations is observed (Fig. 3).  $\phi(\text{C}_8\text{V}^{\bullet+}) = 8 \times 10^{-3}$ ,  $\phi(\text{BV}^{\bullet+}) = 7 \times 10^{-3}$ . Interestingly, when the photosensitizer Zn-TPPS<sup>4-</sup> is substituted by Ru(II)-tris-bipyridine, Ru(bpy)<sub>3</sub><sup>2+</sup>, photoreduction of C<sub>8</sub>V<sup>2+</sup> and BV<sup>2+</sup> occurs in the aqueous medium

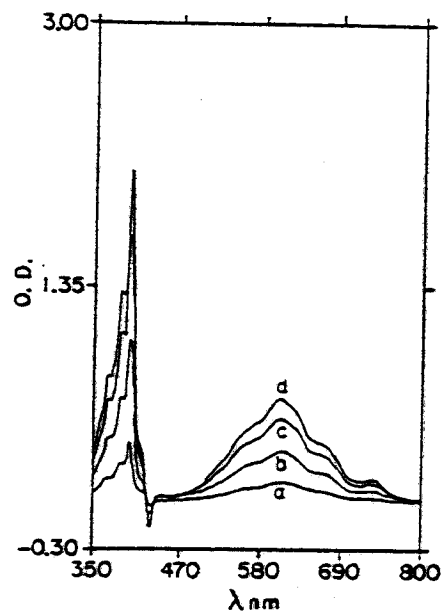


Figure 3. — Absorption spectra of C<sub>8</sub>V<sup>2+</sup> at 1 minute time intervals of illumination: [Zn-TPPS<sup>4-</sup>] =  $3.2 \times 10^{-6}$  mol L<sup>-1</sup>; [C<sub>8</sub>V<sup>2+</sup>] =  $5.0 \times 10^{-4}$  mol L<sup>-1</sup>; [β-CD] =  $1.0 \times 10^{-2}$  mol L<sup>-1</sup>; [(NH<sub>4</sub>)<sub>3</sub>EDTA] =  $1.0 \times 10^{-1}$  mol L<sup>-1</sup>; pH = 8.5.

as well as in the β-CD aqueous media<sup>12</sup>. Nevertheless, in the absence of β-CD the dimer aggregates of ocril viologen radical and benzylviologen radical are formed, (C<sub>8</sub>V<sup>•+</sup>)<sub>2</sub> and (BV<sup>•+</sup>)<sub>2</sub>, (Fig. 4), while in the presence of β-CD the monomer viologen radicals, forms of C<sub>8</sub>V<sup>•+</sup> and BV<sup>•+</sup>, are produced. These results suggest that C<sub>8</sub>V<sup>•+</sup> and BV<sup>•+</sup> aggregate in aqueous solutions (11). This property presumably originates from the hydrophobic nature of the reduced radical cations C<sub>8</sub>V<sup>•+</sup> and BV<sup>•+</sup>. Earlier studies have indeed indicated that amphiphilic bipyridinium radicals tend to aggregate, and with C<sub>14</sub>MeV<sup>•+</sup>, even micellar aggregation in aqueous solutions has been reported. In the presence of β-CD these aggregation processes are eliminated. Selective association of the monomer radical cations C<sub>8</sub>V<sup>•+</sup> or BV<sup>•+</sup> to the hydrophobic cavity of β-CD, that can accommodate the monomer radical only, shifts the monomer-dimer equilibrium and aggregates formation is prevented (12). Thus, we conclude that the β-cyclodextrin molecular receptor prevents the aggregation of C<sub>8</sub>V<sup>•+</sup> and



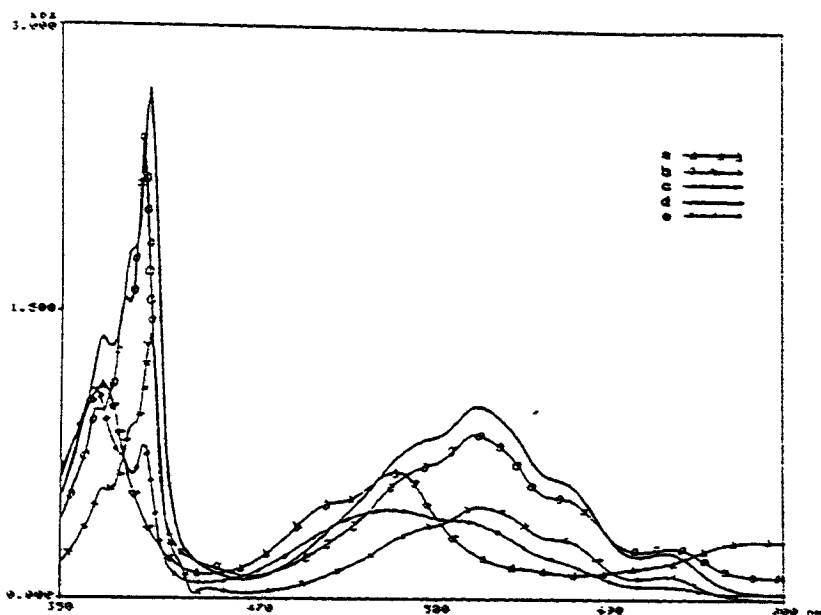


Figure 4. — Absorption spectra of photoreduced products obtained by illumination of the following systems: (a) Photoproduct —  $(C_8V^{\cdot+})_2$ :  $[(C_8V^{2+}) = 5.0 \times 10^{-3} \text{ mol L}^{-1}; [Ru(bpy)_3]^{2+} = 5.5 \times 10^{-5} \text{ mol L}^{-1}; [Na_2EDTA] = 1.0 \times 10^{-1} \text{ mol L}^{-1}; \text{pH} = 5.5$ ; (b) Photoproduct —  $C_8V^{\cdot+}$ : like (a) — in the presence of  $\beta$ -CD ( $1.0 \times 10^{-2} \text{ mol L}^{-1}$ ); (c) Photoproduct —  $(BV^{\cdot+})_2$ :  $[BV^{2+}] = 5.0 \times 10^{-3} \text{ mol L}^{-1}; [Ru(bpy)_3]^{2+} = 5.5 \times 10^{-5} \text{ mol L}^{-1}; [Na_2EDTA] = 1.0 \times 10^{-1} \text{ mol L}^{-1}; \text{pH} = 5.5$ ; (d) Photoproduct —  $BV^{\cdot+}$ : like (c) — in the presence of  $\beta$ -CD ( $1.0 \times 10^{-2} \text{ mol L}^{-1}$ ); (e) Photoproduct —  $BV^{\cdot+}$ :  $[BV^{2+}] = 5 \times 10^{-4} \text{ mol L}^{-1}; [Zn-TPPS^{4-}] = 3.2 \times 10^{-6} \text{ mol L}^{-1}; [(NH_4)_3EDTA] = 1.0 \times 10^{-1} \text{ mol L}^{-1}; [\beta\text{-CD}] = 1.0 \times 10^{-2} \text{ mol L}^{-1}; \text{pH} = 8.5$ .

$BV^{\cdot+}$  in aqueous solutions, due to the specific binding of the reduced photoproduct to the receptor cavity



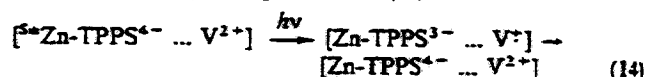
With  $Zn-TPPS^{4-}$  as photosensitizer no photoreduction of  $C_8V^{2+}$  or  $BV^{2+}$  occurs in aqueous media in the absence of  $\beta$ -CD. Control experiments where glucose (the monomer molecule composing  $\beta$ -CD) is added to the aqueous medium to substitute  $\beta$ -CD reveal that no photoreduction of  $C_8V^{2+}$  or  $BV^{2+}$  occurs upon illumination. Also no photoreduction of  $C_8V^{2+}$  or  $BV^{2+}$  is observed in the presence of  $\beta$ -CD when  $(NH_4)_3EDTA$  is excluded from the system. Similarly, no photoreduction of  $C_8V^{2+}$  or  $BV^{2+}$  occurs in the absence of the photosensitizer. These experiments clearly indicate that  $\beta$ -CD does not act as electron donor in the system, and other functions of the molecular receptor in the photosensitized reduction of the bipyridinium salts are operative.

To understand the functions of  $\beta$ -CD in the photosensitized reduction of  $C_8V^{2+}$  and  $BV^{2+}$  by  $Zn-TPPS^{4-}$ , we have examined in detail the photophysical properties of the photosensitizer in the presence of the two electron relays and the effects of added  $\beta$ -CD on the photosensitizer properties by means of laser flash photolysis. Also, the different steps and functions of  $\beta$ -CD involved in the photosensitized transformation were elucidated by this technique. Excitation of  $Zn-TPPS^{4-}$  in an aqueous solution leads to the formation of a short-lived singlet state that decays to the relatively long-lived triplet state ( $\tau = 1.5 \text{ msec}$ )<sup>18</sup> (13).

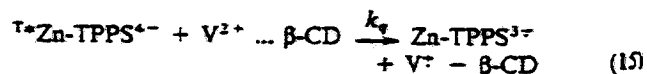


Addition of  $C_8V^{2+}$  or  $BV^{2+}$ ,  $8 \times 10^{-5} \text{ mol L}^{-1}$ , to the aqueous solution of  $Zn-TPPS^{4-}$  prohibits the formation of the triplet excited state and no intermediate charge separation of photoproducts is detected. At these concentrations of the charge relays the photosensitizer is entirely present in the complex structure  $[Zn-TPPS^{4-} \dots V^{2+}]$ . Thus, the elimination of triplet state formation is attributed to static internal quenching of the singlet state by the relay in the complex structure. We believe that the quenching process proceeds via electron transfer yet the stabilization of the intermediate

photoproducts in the complex structure prevents charge separation and rapid recombination of the photoproducts in the encounter cage complex occurs (14).



Addition of  $\beta$ -CD,  $1 \times 10^{-2} \text{ mol L}^{-1}$ , to the aqueous solution separates the photosensitizer-viologen complex, and the bipyridinium relay is associated with the  $\beta$ -CD receptor. Flashing this system results in the restoration of the photophysical properties of the photosensitizer, *i.e.*, the singlet excited state is decaying to the triplet state. At these concentrations of the separated bipyridinium salt, no effect on the  ${}^1Zn-TPPS^{4-}$  lifetime is observed nor are photoproducts detected. Upon increase of the concentration of the viologen relays shortening of the triplet lifetime is observed and the intermediate photoproducts  $C_8V^{\cdot+}$  and  $BV^{\cdot+}$  are detected. Thus, in the presence of  $\beta$ -CD diffusional electron transfer quenching of the triplet  ${}^3Zn-TPPS^{4-}$  by  $\beta$ -CD associated  $C_8V^{2+}$  or  $BV^{2+}$  occurs (15). The quenching rate constants and the charge separation yields are summarized in Table I.



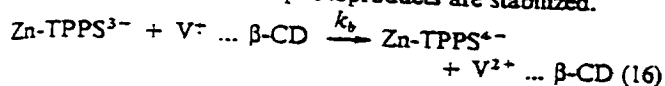
The separated photoproducts recombine via back electron transfer reactions (16). The recombination rate constants are also summarized in Table I.

Table I. — Physical Characteristics of the Photochemical Reduction of  $C_8V^{2+}$  and  $BV^{2+}$  with  $Zn-TPPS^{4-}$  in the Presence of  $\beta$ -CD.

	$\Phi_{2s}^a$	$k_q$ (mol <sup>-1</sup> L sec <sup>-1</sup> )	$\Phi_s^b$	$k_b$ (mol <sup>-1</sup> L sec <sup>-1</sup> )
$C_8V^{2+}$	$8 \times 10^{-3}$	$7.5 \times 10^8$	$2.3 \times 10^{-2}$	$3.5 \times 10^8$
$BV^{2+}$	$17 \times 10^{-3}$	$1.4 \times 10^9$	$2.1 \times 10^{-2}$	$3.8 \times 10^8$

<sup>a</sup> Quantum yield for continuous illumination:  $[Zn-TPPS^{4-}] = 3.2 \times 10^{-6} \text{ mol L}^{-1}$ ;  $[C_8V^{2+}]$  or  $[BV^{2+}] = 5 \times 10^{-4} \text{ mol L}^{-1}$  and  $[(NH_4)_3EDTA] = 0.1 \text{ mol L}^{-1}$ . Photon flux =  $2 \times 10^{22} \text{ einsteins L}^{-1} \text{ min}^{-1}$ . <sup>b</sup> Quantum yield for the separation of the cage structure of electron transfer products in the laser experiments.

The recombination rate constants of the active photoproducts are usually close to a diffusion controlled value. The recombination rate of the photoproduct, Zn-TPPS<sup>3-</sup> and C<sub>6</sub>V<sup>2+</sup> or BV<sup>2+</sup>, are ca. 10-fold retarded as compared to a diffusion controlled process. This stabilization of the photoproducts against back electron transfer is attributed to the association of the reduced photoproducts C<sub>6</sub>V<sup>2+</sup> or BV<sup>2+</sup> to the β-CD cavity. The receptor-relay complex formation protects the reduced acceptor from back reaction and consequently the intermediate photoproducts are stabilized.



We thus conclude that β-CD participates by three complementary functions in the photosensitized reduction of C<sub>6</sub>V<sup>2+</sup> and BV<sup>2+</sup> by Zn-TPPS<sup>4-</sup> (Fig. 5): i) The β-CD molecular receptor separates the ground state sensitizer-acceptor complex. ii) As a result, photoinduced electron transfer followed by charge separation of the photoproducts is affected. The separated photoproducts are then stabilized against back electron transfer reactions by means of the β-CD receptor.

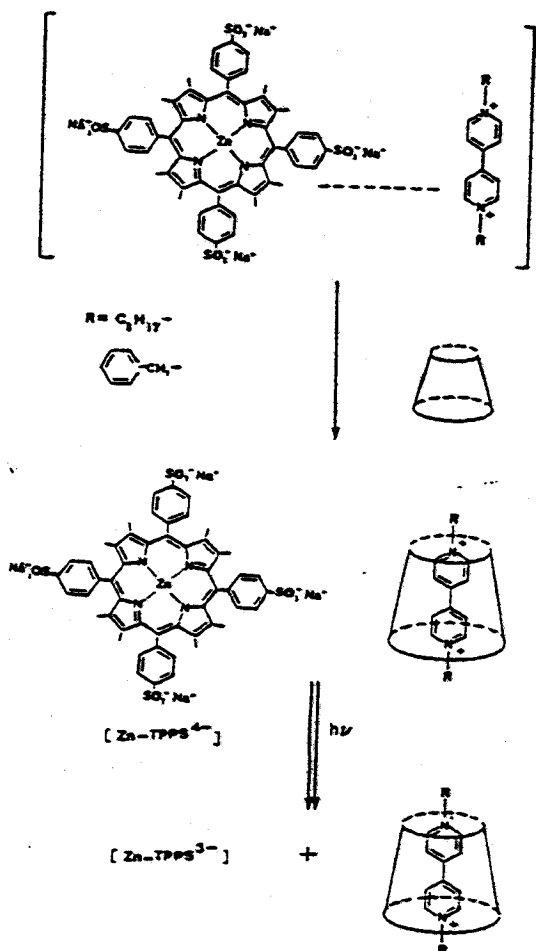


Figure 5. — Scheme of (a) separation of the complex [Zn-TPPS<sup>4-</sup> ... V<sup>2+</sup>] by cyclodextrin. (b) Electron transfer process and the capture of V<sup>2+</sup> in the cyclodextrin.

Once photoproducts are separated, oxidation of the sacrificial electron donor, (NH<sub>4</sub>)<sub>2</sub>EDTA, allows the accumulation of C<sub>6</sub>V<sup>2+</sup> or BV<sup>2+</sup>. iii) The third function of β-CD is the

preservation of the reduced photoproducts in their monomeric forms, a thermodynamically unfavoured state for these photoproducts in aqueous media. All of these β-CD functions are a result of the selective association of C<sub>6</sub>V<sup>2+</sup> and BV<sup>2+</sup> and their reduced products to the hydrophobic cavity of β-CD.

#### Acknowledgement

This research is supported by a grant from the National Council for Research and Development, Israel, and the Kernforschung Anlage, Juelich, Germany.

#### REFERENCES

- 1) a) «Energy Resources Through Photochemistry and Catalysis», Grätzel M., Ed., Academic Press, New York, 1983; b) Bard A. J., *Science*, (Washington D. C.), 1980, 207, 138.
- 2) Grätzel M., *Acc. Chem. Res.*, 1981, 14, 376-384.
- 3) a) Sutin N., Creutz C., *Pure Appl. Chem.*, 1980, 52, 2717-2738; b) Kalyanasundaram K., *Coord. Chem. Rev.*, 1982, 46, 159-244.
- 4) a) Willner I., Laane C., Otvos J. W., Calvin M., in: «Inorganic Reactions in Organized Media», S. L. Holt, Ed., ACS Symposium Series 177, American Chemical Society, Washington, D.C., 1982, pp. 71-95; b) Willner I., in: «Organic Phototransformations in Nonhomogeneous Media», M.A. Fox, Ed., ACS Symposium Series 278, Washington, D.C., 1985, p. 192.
- 5) a) Turro N. J., Grätzel M., Braun A. M., *Angew. Chem., Int., Ed. Engl.*, 1980, 19, 675-696.
- 6) a) Matsuo T., Takuma K., Tsusui Y., Nishigima T., *Coord. Chem. Rev.*, 1980, 10, 195-216; b) Moroi Y., Braun A. M., Grätzel M., *J. Amer. Chem. Soc.*, 1979, 101, 567-572.
- 7) Meisel D., Matheson M., Rabani J., *J. Amer. Chem. Soc.*, 1978, 100, 117.
- 8) a) Willner I., Otvos J. W., Calvin M., *J. Amer. Chem. Soc.*, 1981, 103, 3203-3205; b) Willner I., Yang J. M., Otvos J. W., Calvin M., *J. Phys. Chem.*, 1981, 85, 3277-3282.
- 9) Degani Y., Willner I., *J. Amer. Chem. Soc.*, 1983, 105, 6228-6233.
- 10) Fendler J. H., *J. Phys. Chem.*, 1980, 84, 1485-1491.
- 11) a) Jones C. A., Weaner L. E., Mackay R. A., *J. Phys. Chem.*, 1980, 84, 1495-1500; b) Mandler D., Degani Y., Willner I., *J. Phys. Chem.*, 1984, 88, 4366-4370.
- 12) Adar E., Degani Y., Goren Z., Willner I., *J. Amer. Chem. Soc.*, 1986, 108, 4696-4700.
- 13) a) Saenger A. Q., *Angew. Chem. Int., Ed. Engl.*, 1980, 19, 344; b) Bender M., Kamiyama L., *Cyclodextrin Chemistry*, Springer, 1978.
- 14) Breslow R., *Science*, (Washington D.C.), 1982, 218, 532.
- 15) Tabushi I., *Acc. Chem. Res.*, 1982, 15, 66.
- 16) Wegner E. E., Adamson A. W., *J. Amer. Chem. Soc.*, 1966, 88, 394.
- 17) Benesi H. A., Hildebrand J. H., *J. Amer. Chem. Soc.*, 1949, 71, 2703.
- 18) a) Kiwi J., Grätzel M., *Angew. Chem. Int., Ed. Engl.*, 1979, 18, 624-626; b) Harriman A., Porter G., Richoux M. C., *J. Chem. Soc. Faraday Trans. 2*, 1981, 77, 1939-1948.
- 19) a) Keller P., Moradpour A., Amouyal E., Kagan H. B., *Nouv. J. Chim.*, 1980, 4, 377-384; *J. Amer. Chem. Soc.*, 1980, 102, 7193-7196; b) Okura I., Kim-Thuan N., *J. Chem. Soc. Faraday Trans. 1*, 1981, 77, 1411-1415.
- 20) a) Kalyanasundaram K., Grätzel M., *Helv. Chim. Acta.*, 1980, 63, 478-485; b) Harriman A., Porter G., Richoux M. C., *J. Chem. Soc. Faraday Trans. 2*, 1981, 77, 833-844.

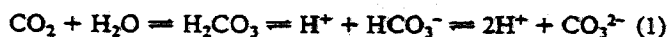
## Characterization of Pd- $\beta$ -Cyclodextrin Colloids as Catalysts in the Photosensitized Reduction of Bicarbonate to Formate<sup>†,1</sup>

Itamar Willner\* and Daniel Mandler

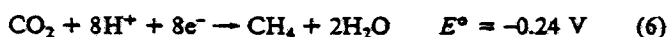
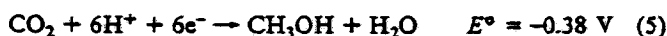
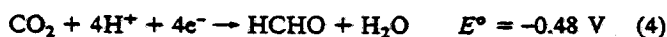
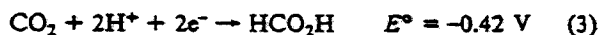
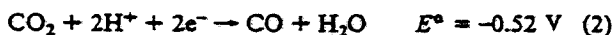
Contribution from the Department of Organic Chemistry, The Hebrew University of Jerusalem, Jerusalem 91904, Israel. Received April 7, 1988

**Abstract:** Photosensitized reduction of bicarbonate,  $\text{HCO}_3^-$ , to formate,  $\text{HCO}_2^-$ , proceeds in an aqueous system composed of deazariboflavin, dRF1 (1), as photosensitizer,  $N,N'$ -dimethyl-4,4'-bipyridinium,  $\text{MV}^{2+}$ , as primary electron acceptor, sodium oxalate as sacrificial electron donor, and in the presence of a Pd colloid stabilized by  $\beta$ -cyclodextrin, Pd- $\beta$ -CD. The process proceeds with a quantum efficiency,  $\phi = 1.1$ . Kinetic characterization of the Pd- $\beta$ -CD catalyst activity reveals the presence of active sites for bicarbonate activation and reduction as well as catalytic sites for  $\text{H}_2$  evolution. The  $\text{HCO}_3^-$  activation sites are specifically inhibited by thiols. The catalytic reduction of  $\text{HCO}_3^-$  to  $\text{HCO}_2^-$  and the respective inhibition processes exhibit enzyme-like kinetic properties. The Pd- $\beta$ -CD colloid shows reversible activities and effects the reduction of  $\text{MV}^{2+}$  by formate. Kinetic characterization of the catalyzed reduction of  $\text{HCO}_3^-$  to  $\text{HCO}_2^-$  and the reverse oxidation of  $\text{HCO}_2^-$  provides a sequential mechanism for the reactions.

Photoreduction of  $\text{CO}_2$ , its hydrated form, carbonic acid, or its dissociated ions, bicarbonate and carbonate (eq 1), using visible



solar light is a challenging subject as a means of mimicking photosynthesis and of solar energy conversion and storage.<sup>2-4</sup> The standard redox potentials<sup>5,6</sup> for the reduction of carbon dioxide (at pH = 7) to  $\text{C}_1$ -carbon fuel products are given in eq 2-7 and



compared to that of  $\text{H}_2$  evolution. It is evident that reduction of  $\text{CO}_2$  in aqueous solutions to several  $\text{C}_1$  products is thermodynamically favored over  $\text{H}_2$  evolution. Nevertheless, reduction of  $\text{CO}_2$  is encountered with severe kinetic difficulties, and extensive efforts are directed toward the activation of  $\text{CO}_2$ , bicarbonate, and carbonate by transition-metal complexes<sup>7,8</sup> or heterogeneous metal surfaces.<sup>9,10</sup>

Reduction of carbon dioxide could basically be accomplished through various pathways. These include hydrogenation,<sup>11</sup> insertion into transition-metal hydride complexes,<sup>12</sup> carbanion nucleophilic attack,<sup>13</sup> or by electron transfer followed by protonation.<sup>14</sup> The methanation process exemplifies an extensively explored hydrogenation of  $\text{CO}_2$  to methane, a process that usually proceeds at elevated temperatures and high pressures.<sup>15</sup> Insertion of  $\text{CO}_2$  into various transition-metal hydrides to form the formate ligand was observed.<sup>16</sup> Electrocatalyzed reduction of  $\text{CO}_2$  was observed in the presence of various transition-metal complexes, i.e.,  $\text{Ni}^{2+}$ - or  $\text{Co}^{2+}$ -cyclams,<sup>17</sup> metal porphyrins or phthalocyanins,<sup>18</sup> and iron-sulfur clusters,<sup>19</sup> or by using Ru or Cu metal catalysts as electrodes.<sup>20</sup> Hydrogenation of bicarbonate using

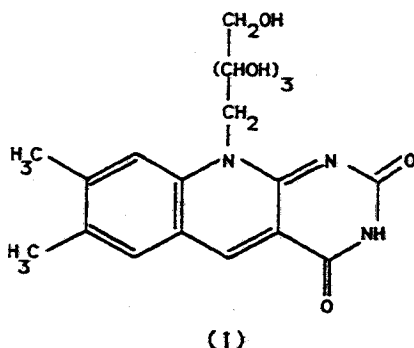
cyanins,<sup>18</sup> and iron-sulfur clusters,<sup>19</sup> or by using Ru or Cu metal catalysts as electrodes.<sup>20</sup> Hydrogenation of bicarbonate using

- (1) Mandler, D.; Willner, I. *J. Am. Chem. Soc.* 1987, 109, 7884.
- (2) Inoue, S. In *Organic and Bioorganic Chemistry of Carbon Dioxide*; Inoue, S.; Yamazaki, N., Eds.; Kodansha Ltd.: Tokyo, Wiley: New York, 1982. p 253.
- (3) Ziesel, R. *Nouv. J. Chim.* 1983, 7, 613.
- (4) Åkermark, B. In *Solar Energy—Photochemical Conversion and Storage*; Claesson, S.; Engstrom, L., Eds.; National Swedish Board for Energy Source Development: Stockholm, Sweden 1977.
- (5) Latimer, W. M. *The Oxidation States of the Elements and their Potentials in Aqueous Solutions*, 2nd ed.; Prentice Hall: New York, 1952.
- (6) Bard, A. J., Ed. *Encyclopedia of Electrochemistry of the Elements*; Dekker, New York, 1976.
- (7) (a) Darenbourg, D. J.; Kudarowski, R. A. *Adv. Organomet. Chem.* 1983, 22, 129. (b) Palmer, D. A.; Eldvik, R. V. *Chem. Rev.* 1983, 83, 651. (c) Eisenberg, R.; Hendriksen, D. E. *Adv. Catal.* 1979, 28, 119.
- (8) (a) Volpin, M. E.; Kolomoitkov, I. S. *Pure Appl. Chem.* 1973, 33, 567. (b) Inoue, S. *Rev. Inorg. Chem.* 1984, 6, 291. (c) Ibers, J. A. *Chem. Soc. Rev.* 1982, 11, 57.
- (9) (a) Solymosi, F.; Erdohelyi, A.; Lancz, M. *J. Catal.* 1985, 95, 567. (b) Solymosi, F.; Erdohelyi, A. *J. Mol. Catal.* 1980, 8, 471.
- (10) Klier, K. *Adv. Catal.* 1982, 31, 243.
- (11) Denise, B.; Sneed, R. P. A. *CHEMTECH* 1982, 108.
- (12) Sneed, R. P. A. *Compr. Organomet. Chem.* 1982, 8, 225.
- (13) Haruki, E. F. in ref 2, pp 5-78.
- (14) (a) Russel, P. G.; Kovac, N.; Srinivasan, S.; Steinberg, M. *J. Electrochem. Soc.* 1977, 124, 1329. (b) Amatore, C.; Saveant, J.-M. *J. Am. Chem. Soc.* 1981, 103, 5021.
- (15) Solymosi, F.; Erdohelyi, A.; Kocsis, M. *J. Chem. Soc., Faraday Trans. 1* 1981, 77, 1003.
- (16) Inoue, Y.; Izumida, H.; Sasaki, Y.; Hashimoto, H. *Chem. Lett.* 1976, 863.
- (17) (a) Fisher, B.; Eisenberg, R. *J. Am. Chem. Soc.* 1980, 102, 7361. (b) Beley, M.; Collin, J.-P.; Ruppert, R.; Sauvage, J. P. *J. Chem. Soc., Chem. Commun.* 1984, 1315. (c) Beley, M.; Collin, J.-P.; Ruppert, R.; Sauvage, J.-P. *J. Am. Chem. Soc.* 1986, 108, 7461. (d) Petit, J.-P.; Chartier, P. *Nouv. J. Chim.* 1987, 11, 751.
- (18) (a) Hiratsuka, K.; Takahashi, K.; Sasaki, H.; Toshima, S. *Chem. Lett.* 1977, 1137; *Ibid.* 1979, 305. (b) Kapusta, S.; Hackerman, N. *J. Electrochem. Soc.* 1984, 1511. (c) Liber, C. M.; Lewis, N. S. *J. Am. Chem. Soc.* 1984, 106, 5033.
- (19) Tezuka, M.; Yajima, T.; Tsuchiya, A. *J. Am. Chem. Soc.* 1982, 104, 6834.
- (20) (a) Frese, K. W., Jr.; Leach, S. *J. Electrochem. Soc.* 1985, 259. (b) Summers, D. P.; Frese, K. W., Jr. *Langmuir* 1988, 4, 51.

<sup>†</sup> Dedicated to the memory of Professor David Ginsburg.

supported Pd catalysts has been the subject of several reports.<sup>21,22</sup> Wrighton et al. have examined the hydrogenation<sup>22</sup> and electroreduction<sup>23</sup> of bicarbonate in the presence of supported Pd catalysts. In these processes effective formate production was accomplished at room temperature and close to the thermodynamic potential. Photoreduction of CO<sub>2</sub> has been reported in photochemical assemblies,<sup>24-26</sup> in the presence of semiconductor powders<sup>27</sup> or electrodes,<sup>28</sup> and in photosystems that include the enzyme formate dehydrogenase as biocatalyst.<sup>29</sup> In general, the reported photosystems of CO<sub>2</sub> reduction proceed with poor or unspecified quantum efficiencies. Photoreduction of CO<sub>2</sub> to carbon monoxide has been accomplished in aqueous media by using Co(II), Co(II)-bipyridine complexes, or Re(I)(bpy)(CO)<sub>3</sub>X as homogeneous catalysts.<sup>24,30</sup> Photoreduction of CO<sub>2</sub> to formate has been reported in assemblies that included Ru(bpy)<sub>3</sub><sup>2+</sup> as photosensitizer and Ru(bpy)<sub>2</sub>L<sub>2</sub><sup>2+</sup> as catalyst.<sup>25,31</sup> Recently, we have shown that heterogeneous Pd colloid stabilized by β-cyclodextrin, β-CD, catalyzes the photoreduction of bicarbonate to formate.<sup>1</sup> Photosensitized reduction of CO<sub>2</sub> to methane has been accomplished in microheterogeneous systems that include Ru or Os as heterogeneous catalysts.<sup>24</sup> Photoelectrochemical reduction of carbon dioxide to mixtures of C<sub>1</sub> products has been reported with semiconductor electrodes,<sup>28</sup> i.e., GaP or GaAs, or powder suspension<sup>27</sup> such as SrTiO<sub>3</sub>. Nevertheless, these processes are inefficient. In the photosystems for CO<sub>2</sub> reduction that include heterogeneous metal colloids or homogeneous catalysts that operate through metal hydride species, H<sub>2</sub> evolution accompanies the CO<sub>2</sub> reduction process in aqueous media and the H<sub>2</sub> formation predominates in its effectiveness.

Here we report on the characterization of the catalytic activity of Pd-β-cyclodextrin colloids, Pd-β-CD, in the reduction of CO<sub>2</sub>/HCO<sub>3</sub><sup>-</sup> using *N,N'*-dimethyl-4,4'-bipyridinium radical, MV<sup>2+</sup>, as electron carrier. The reduced relay is generated through a photochemical system that includes deazariboflavin, dRFI (1), as photosensitizer, *N,N'*-dimethyl-4,4'-bipyridinium, MV<sup>2+</sup>, as electron acceptor, and oxalate as sacrificial electron donor.



## Experimental Section

Absorption spectra were recorded with an Uvikon-860 (Kontron) spectrophotometer equipped with a thermostated cell holder that includes a magnetic stirring motor at the bottom of the unit. NMR spectra were recorded on a 200-MHz instrument (Bruker). A Philips 300 M transmission electron microscope was used to determine the size of colloid particles. X-ray diffraction analyses were performed on a Philips powder diffractometer. Continuous illumination experiments were performed with a 1000-W halogen-quartz lamp, and light was filtered through a 400-nm filter. Incident photon flux was determined by Reinecke salt actinometry<sup>32</sup> to be  $1 \times 10^{17}$  einstein·M<sup>-1</sup>·min<sup>-1</sup>. Laser flash experiments were carried out with a dye laser (DL-12 Moletron) pumped by a nitrogen laser (UV-14 Moletron).

Palladium content in the various colloids was determined by atomic absorption (Perkin-Elmer 403 apparatus). Formate was analyzed by ion chromatography using a Wescan anion-exclusion column,  $2 \times 10^{-3}$  N H<sub>2</sub>SO<sub>4</sub> was eluent, and detection was performed with a conductivity detector (Knauer). Hydrogen was analyzed by gas chromatography (Hewlett-Packard 5890 Instrument) with a 5-Å molecular sieve column and argon as carrier gas. The production of MV<sup>2+</sup> was followed spectroscopically at 602 nm ( $\epsilon = 1.3 \times 10^4$  M<sup>-1</sup>·cm<sup>-1</sup>).<sup>33</sup>

Chemicals were obtained from Aldrich. Deazariboflavin (1) was prepared according to the literature.<sup>34</sup> DCO<sub>2</sub>Na was prepared by hydrolysis of NaCN in D<sub>2</sub>O, and the product was recrystallized from ethanol-water.<sup>15</sup> A solution of sodium hydrogen [<sup>13</sup>C]carbonate was prepared by bubbling <sup>13</sup>CO<sub>2</sub> through a 0.1 M NaOH solution until pH = 7.0.

The active Pd-β-CD colloid for CO<sub>2</sub>/HCO<sub>3</sub><sup>-</sup> photoreduction is prepared by heating while stirring, a  $1.5 \times 10^{-3}$  M Na<sub>2</sub>PdCl<sub>4</sub> solution that includes β-cyclodextrin (1% w/w) at 60 °C for 2 1/2 h. The color of the solution changes from yellow to dark brown. The resulting colloid is deionized with small amounts of Amberlite MB-1 to exclude remains of PdCl<sub>4</sub><sup>2-</sup> (purification of the colloid from PdCl<sub>4</sub><sup>2-</sup> is followed spectroscopically). The resulting colloid is centrifuged (3500 rpm for 10 min) to exclude any precipitated palladium. It should be noted that a decrease in the Pd-β-CD catalyst activity has been observed upon aging. Also, in a series of 10 different batches of the Pd-β-CD colloid we observe up to a 5-fold difference between the most active and least active colloids. The inactive Pd-β-CD catalyst is prepared by a similar procedure, but the temperature of the reaction mixture is maintained at 90 °C. The Pd colloid stabilized by D-glucose was prepared by a method similar to that for Pd-β-CD except that the D-glucose content in the aqueous solution is 0.67% (w/w). Pd colloid stabilized by polyvinylpyrrolidone is prepared by either H<sub>2</sub> bubbling or NaBH<sub>4</sub> addition to an aqueous  $1.5 \times 10^{-3}$  M Na<sub>2</sub>PdCl<sub>4</sub> solution that contains polyvinylpyrrolidone (1% w/w).

Samples of Pd-β-CD for electron microscopy were prepared by the following procedure: A copper colloid-coated grid was placed on a small cork and the cork mounted in a centrifuge test tube. The tube was filled with a 1:1 mixture of Pd-β-CD colloid and 1% gelatin solution and vertically centrifuged (8000 rpm for 20 min). The solution was decanted and the grid was washed with triply distilled water and dried. Samples for X-ray diffraction were prepared by a similar method: A glass plate was mounted on the cork support, and Pd was deposited on the glass plate by centrifugation. The glass plate with deposited Pd was analyzed after drying.

The systems for continuous illumination experiments consisted of a 0.1 M NaHCO<sub>3</sub> aqueous solution that included sodium oxalate ( $5 \times 10^{-2}$  M) as electron donor, deazariboflavin ( $3 \times 10^{-5}$  M) as photosensitizer, *N,N'*-dimethyl-4,4'-bipyridinium, (methyl viologen, MV<sup>2+</sup>;  $1 \times 10^{-3}$  M) as electron acceptor, and Pd-β-CD (40 mg·L<sup>-1</sup>) as catalyst. The solution (3 mL) was placed in a glass cuvette, equipped with a microstirrer and serum stopper. The solution in the cuvette was flushed with oxygen-free carbon dioxide and illuminated,  $\lambda > 400$  nm (resulting pH = 6.8-7.0). Aliquots were taken out at time intervals of illumination and analyzed for HCO<sub>2</sub><sup>-</sup>. The gaseous atmosphere was analyzed for H<sub>2</sub>. The kinetics studies of HCO<sub>2</sub><sup>-</sup> photogeneration as a function of HCO<sub>3</sub><sup>-</sup> concentration were performed in an aqueous system, 3 mL, that consisted of phosphate buffer ( $7 \times 10^{-2}$  M), sodium oxalate ( $5.5 \times 10^{-2}$  M), deazariboflavin ( $3 \times 10^{-5}$  M), MV<sup>2+</sup> ( $1 \times 10^{-3}$  M), and Pd-β-CD (40 mg·L<sup>-1</sup>). The system was flushed with argon, and varying amounts of an aqueous  $4.3 \times 10^{-1}$  M NaHCO<sub>3</sub> stock solution were injected into the system, which was equilibrated for 10 min before illumination. The kinetics of MV<sup>2+</sup> reduction by HCO<sub>2</sub><sup>-</sup> were followed in the following way: 2.9 mL of an aqueous phase that included MV<sup>2+</sup> ( $1 \times 10^{-3}$  M) and Pd-β-CD (45

(32) Wegner, E. E.; Adamson, A. W. *J. Am. Chem. Soc.* 1966, 88, 394.

(33) Thorneley, R. N. F. *Biochim. Biophys. Acta* 1974, 333, 487.

(34) Ashto, T. W.; Brown, R. D.; Tolman, R. L. *J. Heterocycl. Chem.* 1978, 15, 489.

(35) Rapp, G. A.; Melton, C. E. *J. Am. Chem. Soc.* 1958, 80, 3509.

(21) (a) Wiener, H.; Sasson, Y. *J. Mol. Catal.* 1986, 35, 277. (b) Kuda, K.; Sugita, N.; Takezaki, Y. *Nippon Kagaku Kaishi* 1977, 302.

(22) Stalder, C. J.; Chao, S.; Summers, D. P.; Wrighton, M. S. *J. Am. Chem. Soc.* 1983, 105, 6318.

(23) (a) Stalder, C. J.; Chao, S.; Wrighton, M. S. *J. Am. Chem. Soc.* 1984, 106, 3673. (b) Chao, S.; Stalder, C. J.; Summers, D. P.; Wrighton, M. S. *J. Am. Chem. Soc.* 1984, 106, 2723.

(24) (a) Lehn, J.-M.; Ziessel, R. *Proc. Natl. Acad. Sci. U.S.A.* 1982, 79, 701. (b) Hawecker, J.; Lehn, J.-M.; Ziessel, R. *J. Chem. Soc., Chem. Commun.* 1983, 536.

(25) Hawecker, J.; Lehn, J.-M.; Ziessel, R. *J. Chem. Soc., Chem. Commun.* 1985, 56.

(26) (a) Maidan, R.; Willner, I. *J. Am. Chem. Soc.* 1986, 108, 8100. (b) Willner, I.; Maidan, R.; Mandler, D.; Dörr, H.; Dörr, G.; Zengerle, K. *J. Am. Chem. Soc.* 1987, 109, 6080.

(27) (a) Aurian-Blanjani, B.; Halmann, M.; Manassen, J. *Sol. Energy* 1980, 25, 165. (b) Inoue, T.; Fujishima, A.; Konishi, S.; Honda, K. *Nature* 1979, 277, 637.

(28) (a) Bradley, M. G.; Tysak, T.; Gravea, D. J.; Vlachopoulos, N. A. *J. Chem. Soc., Chem. Commun.* 1983, 349. (b) Halmann, M. *Nature* 1978, 275, 115.

(29) (a) Parkinson, B. A.; Weaver, P. F. *Nature* 1984, 148. (b) Mandler, D.; Willner, I. *J. Chem. Soc., Perkin Trans. 2*, in press.

(30) (a) Ziessel, R.; Hawecker, J.; Lehn, J.-M. *Helv. Chim. Acta* 1986, 69, 1065. (b) Hawecker, J.; Lehn, J.-M.; Ziessel, R. *Ibid.* 1986, 69, 1990.

(31) (a) Ishida, H.; Tanaka, K.; Tanaka, T. *Chem. Lett.* 1987, 1035. (b) Kitamura, N.; Tazuke, S. *Chem. Lett.* 1983, 1109.

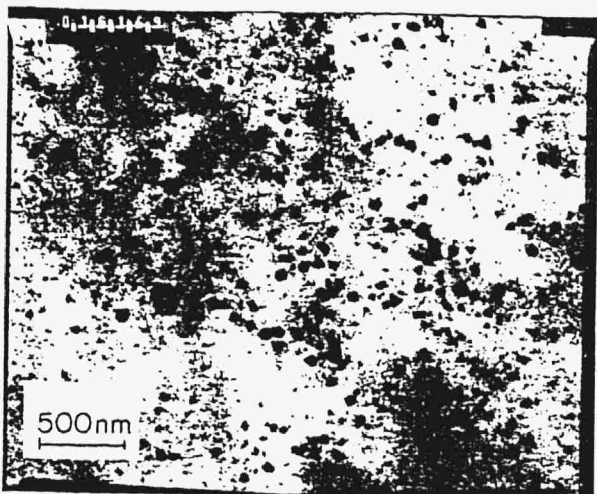


Figure 1. Transmission electron micrograph of active Pd- $\beta$ -CD colloid.

mg-L<sup>-1</sup>) was deaerated with argon and thermostated to the desired temperature. To the resulting solution, mounted in the spectrophotometer, 0.1 mL of sodium formate stock solution was injected (final concentration  $1 \times 10^{-1}$  M). The MV<sup>•+</sup> formation was followed at  $\lambda = 602$  nm. In order to avoid varying activities of the Pd- $\beta$ -CD in D<sub>2</sub>O as a result of the preparation procedures, this colloid was not prepared by direct reduction of PdCl<sub>4</sub><sup>2-</sup> in D<sub>2</sub>O but through an alternative route: The Pd- $\beta$ -CD colloid in H<sub>2</sub>O was lyophilized to dryness, and the resulting Pd- $\beta$ -CD powder was resuspended in D<sub>2</sub>O by vortex stirring. Control experiments revealed that the activity of Pd- $\beta$ -CD colloid was unaffected by the lyophilization/resuspension processes.

#### Properties of Pd Colloids as Catalysts for HCO<sub>3</sub><sup>-</sup> Photoreduction

We find that Pd colloids can be stabilized by cyclodextrins similarly to other metals, i.e., Rh or Pt. We also prepared Pd colloids stabilized by other stabilizing supports such as glucose and polyvinylpyrrolidone. In the present study we mainly characterize the catalytic activities of Pd colloids stabilized by  $\beta$ -cyclodextrins, Pd- $\beta$ -CD, in the reduction of HCO<sub>3</sub><sup>-</sup> to formate and in the reverse process. Some of the catalytic properties of the Pd colloids stabilized by the other supports are also provided. We find that the procedure whereby the Pd- $\beta$ -CD colloid is prepared, dramatically affects its catalytic activity. Preparation of the Pd colloid at 60 °C results in an active catalyst for bicarbonate reduction to formate. In the absence of bicarbonate this catalyst is active in H<sub>2</sub> evolution. This catalyst is also catalytically active in the reverse process that oxidizes formate to bicarbonate. In turn, Pd- $\beta$ -CD colloid prepared at 90 °C is inactive toward HCO<sub>3</sub><sup>-</sup> reduction or the reverse oxidation of formate, but is catalytically active in H<sub>2</sub> evolution. The Pd- $\beta$ -CD colloid is stable for prolonged periods of time, namely, for at least a month. Hydrogen effects aggregation of the colloid, presumably due to interparticle H<sub>2</sub> adsorption. These colloids can be dried through lyophilization. The resulting brown powders can be resuspended in aqueous solution. The regenerated colloids exhibit similar catalytic activities as compared to the original Pd- $\beta$ -CD colloids. This property of the Pd- $\beta$ -CD colloid allows the long-term storage of the catalyst. In the present study we prepared Pd- $\beta$ -CD colloids in D<sub>2</sub>O (vide infra) by resuspension of the Pd- $\beta$ -CD powder in D<sub>2</sub>O.

The electron micrograph of the active Pd- $\beta$ -CD colloid is shown in Figure 1. The metal particles exhibit a broad size distribution in the range of 200–1200 Å. The X-ray diffraction patterns of either the active or inactive Pd- $\beta$ -CD colloids show diffraction bands at angles  $2\theta = 40.0$ , 46.5, and 67.9°. These diffraction angles are characteristic of crystalline Pd metal in cubic crystal structure.

Similarly, Pd colloids that are active toward the reduction of HCO<sub>3</sub><sup>-</sup> and oxidation of formate were prepared by using  $\alpha$ -cyclodextrin, glucose, or polyvinylpyrrolidone as stabilizing supports. With the polyvinylpyrrolidone support, NaBH<sub>4</sub> or hydrogen were used as reducing agents of PdCl<sub>4</sub><sup>2-</sup>. Only the Pd colloids stabilized

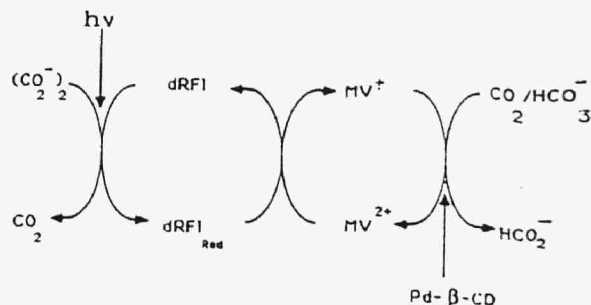


Figure 2. Schematic cycle for the photosensitized reduction of HCO<sub>3</sub><sup>-</sup> to formate.

by cyclodextrins could be lyophilized to powdered catalysts that can be resuspended into aqueous stable colloids.

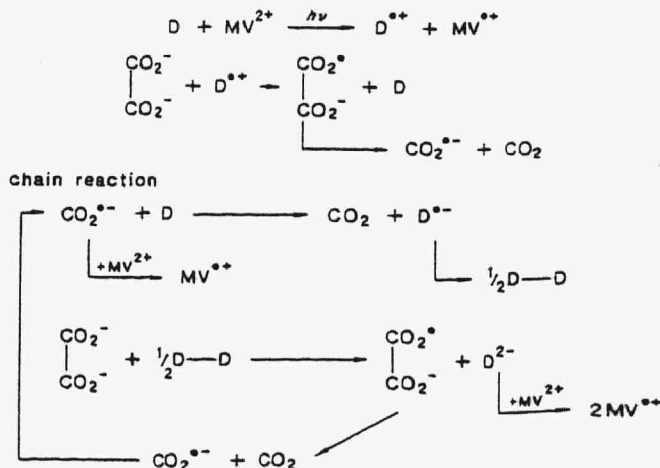
#### Photoreduction of CO<sub>2</sub>/HCO<sub>3</sub><sup>-</sup> to Formate

We have examined the catalyzed reduction of CO<sub>2</sub>/HCO<sub>3</sub><sup>-</sup> using the Pd- $\beta$ -CD colloid and photogenerated *N,N'*-dimethyl-4,4'-bipyridinium radical cation, MV<sup>•+</sup>, as electron carrier for the process. The photosystem for the generation of MV<sup>•+</sup> is composed of deazariboflavin, dRfI (1), as photosensitizer, *N,N'*-dimethyl-4,4'-bipyridinium, methyl viologen, MV<sup>2+</sup>, as electron acceptor, and oxalate as sacrificial electron donor (Figure 2). The reduction of MV<sup>2+</sup> in this specific system has been examined previously by Krasna<sup>36</sup> and proceeds with a quantum efficiency of  $\phi = 3.6$ . The high quantum yield obtained with 1 as photosensitizer is due to complex redox properties of reduced flavin dyes<sup>37</sup> and to several reduction equivalents formed upon oxidative decomposition of the sacrificial electron donor. It should be noted that this unusual photosystem is selected for the production of MV<sup>•+</sup> for two reasons: (i) Common sacrificial electron donors act as inhibitors for the catalyst (vide infra) and eliminate kinetic characterization. (ii) To characterize the kinetic activity of the Pd- $\beta$ -CD colloid, the overall rate of CO<sub>2</sub>/HCO<sub>3</sub><sup>-</sup> reduction should not be controlled by the rate of generation of the primary electron carrier, MV<sup>•+</sup>. The effectiveness of MV<sup>•+</sup> photogeneration with this photosystem provides a means that meets this requirement.

Illumination of an aqueous bicarbonate solution, pH = 6.8, that includes dRfI as sensitizer, MV<sup>2+</sup> as primary charge relay, and oxalate as electron donor results in the formation of methyl viologen radical MV<sup>•+</sup>. In the presence of either of the two Pd- $\beta$ -CD colloids, the reduced methyl viologen mediates different reduction processes: In the presence of the Pd- $\beta$ -CD colloid prepared at 60 °C reduction of CO<sub>2</sub>/HCO<sub>3</sub><sup>-</sup> to formate occurs (Figure 3), and only trace amounts of H<sub>2</sub> are generated. In turn, in the presence of the Pd- $\beta$ -CD colloid prepared at 90 °C only

(36) Krasna, A. I. *Photochem. Photobiol.* 1980, 31, 75.

(37) A chain mechanism outlined in the following set of reactions presumably leads to the high quantum efficiency of MV<sup>•+</sup> (D = dRfI). Cf.: Bliese, M.; Launikonis, A.; Loder, J. W.; Mau, A. W.-H.; Sasse, W. H. F. *Aus. J. Chem.* 1983, 36, 1873.



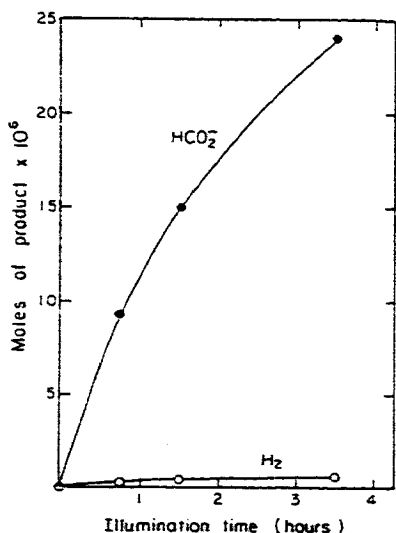


Figure 3. Rates of HCO<sub>2</sub><sup>-</sup> and H<sub>2</sub> formation at the intervals of illumination using the active Pd-β-CD catalyst.

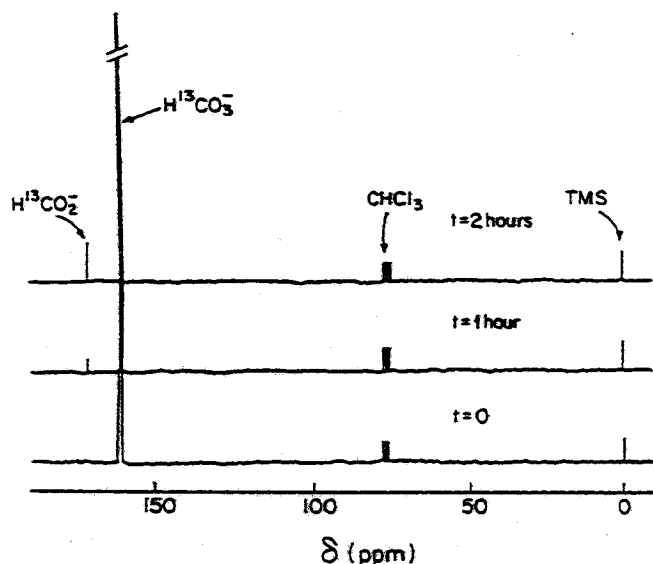


Figure 4. <sup>13</sup>C NMR spectra of samples taken at time intervals of illumination of the photochemical assembly using H<sup>13</sup>CO<sub>3</sub><sup>-</sup> as substrate.

photoinduced H<sub>2</sub> evolution proceeds and no formate could be detected. Figure 3 shows the rates of formate generation and H<sub>2</sub> evolution as a function of illumination time using the active HCO<sub>3</sub><sup>-</sup> reduction colloid. The quantum yield for formate formation corresponds to φ = 1.1. It should be noted that illumination of the system in the absence of CO<sub>2</sub>/HCO<sub>3</sub><sup>-</sup> and in the presence of the active Pd-β-CD bicarbonate reduction colloid results in effective H<sub>2</sub> evolution, φ = 0.12, and no formate is detected. These results clearly indicate that the Pd-β-CD colloid prepared at 60 °C acts as a hydrogen catalyst as well as a CO<sub>2</sub>/HCO<sub>3</sub><sup>-</sup> reduction catalyst. Nevertheless, the latter process is favored in the presence of the substrate CO<sub>2</sub>/HCO<sub>3</sub><sup>-</sup>.

The lack of formate formation in the absence of the substrate indicates that HCO<sub>2</sub><sup>-</sup> originates from CO<sub>2</sub>/HCO<sub>3</sub><sup>-</sup> rather than from an oxidative decomposition route of the oxalate electron donor. This has been firmly confirmed by using [<sup>13</sup>C]bicarbonate as substrate in the photochemical system. Figure 4 shows the <sup>13</sup>C NMR spectra of the system at time intervals of illumination. It is evident that H<sup>13</sup>CO<sub>2</sub><sup>-</sup>, δ = 171.2 ppm, is gradually formed as illumination proceeds.

#### Pd-β-CD Catalyzed Reduction of Bicarbonate

**Kinetics of Bicarbonate Reduction.** The Pd-catalyzed reduction of bicarbonate by hydrogen to form formate has been reported to proceed through hydrogenation of HCO<sub>3</sub><sup>-</sup> by Pd-bound hy-

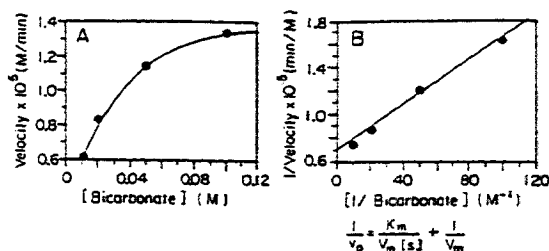
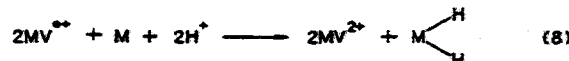
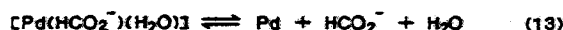
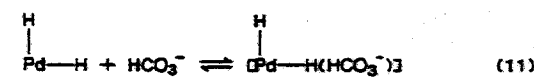
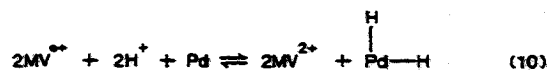


Figure 5. (A) Initial rates of HCO<sub>2</sub><sup>-</sup> photoinduced formation as a function of substrate (HCO<sub>3</sub><sup>-</sup>) concentration. (B) Graphic representation of the reciprocals of the initial rates as a function of the reciprocals of the substrate concentration (1/HCO<sub>3</sub><sup>-</sup>). In all experiments [dRFI] = 3 × 10<sup>-5</sup> M, [MV<sup>2+</sup>] = 1 × 10<sup>-3</sup> M, [(CO<sub>2</sub>Na)<sub>2</sub>] = 5.5 × 10<sup>-2</sup> M, and Pd-β-CD = 40 mg·L<sup>-1</sup>.

drides. These are formed upon dissociation of H<sub>2</sub> on the metal catalyst. Similarly, the photosensitized H<sub>2</sub>-evolution process using *N,N'*-dimethyl-4,4'-bipyridinium, MV<sup>2+</sup>, as charge relay and various metal colloids as catalysts has been extensively studied.<sup>38</sup> It has been shown that metal-bound hydrogen atoms (or hydrides) are formed through a sequential mechanism that involves the charging of the metal colloid by the photoreduced relay MV<sup>•+</sup>, followed by protonation of the charged metal (eq 8, 9). These



observations allow us to suggest the sequence of reactions outlined in eq 10–13 as the mechanistic steps involved in the photoreduction



of HCO<sub>3</sub><sup>-</sup> to formate. In the primary step, photogenerated MV<sup>•+</sup> generates Pd-bound hydrides (eq 10). The Pd catalyst also activates HCO<sub>3</sub><sup>-</sup> through the formation of an activated complex structure, wherein hydrogenation of bicarbonate to formate occurs by discharge of the Pd hydrides.

We have examined the rates of photoinduced formate production as a function of the bicarbonate substrate concentration, and at a constant Pd content of 45 mg·L<sup>-1</sup>. Figure 5A shows the initial rates of HCO<sub>2</sub><sup>-</sup> generation at different bicarbonate concentrations under continuous illumination. It is evident that the rate increases as the substrate concentration is increased and the rate levels off at an approximate substrate concentration of [HCO<sub>3</sub><sup>-</sup>] = 0.1 M. Such behavior could originate if specific sites for bicarbonate activation and reduction are present on the Pd-β-CD catalyst. Namely, the leveling off in the rates of HCO<sub>2</sub><sup>-</sup> formation originates from saturation of these active sites by the HCO<sub>3</sub><sup>-</sup>. In the sequence of reactions that leads to formate, the photogeneration of MV<sup>•+</sup> proceeds with a quantum yield of φ = 3.6. The fact that the quantum yield of formate generation (φ = 1.1) is lower than that of MV<sup>•+</sup> production suggests that the rate of formate production is limited by a dark catalytic process rather than by the photochemical reaction. Indeed, under steady-state illumination MV<sup>•+</sup> is accumulated in the system. It is also well documented<sup>39</sup> that the interaction of a reduced relay

(38) (a) Grätzel, M., Ed. *Energy Resources through Photochemistry and Catalysis*; Academic Press: New York, 1983; and references therein. (b) Harriman, A., West, M. A., Eds. *Photogeneration of Hydrogenation*; Academic Press: London, 1983.

with the metal catalyst to form metal-bound hydrides is a rapid process. Thus, it is conceivable that the formation of the activated complex (eq 11) and subsequent reduction of bicarbonate (eq 12) are rate limiting in  $\text{HCO}_2^-$  photogeneration. This analysis suggests that the activity of Pd- $\beta$ -CD colloid in the photosensitized reduction of bicarbonate is analogous to the active site-substrate model in enzyme activities. Hence the kinetic activity of the Pd- $\beta$ -CD colloid should follow well-established enzyme kinetics relationship.<sup>40</sup>

Consequently, the relation of the initial rates of formate generation as a function of bicarbonate concentration is given by eq 14. Indeed, analysis of the saturation curve (eq 15) through

$$v_0 = \frac{V_{\max}[\text{HCO}_3^-]}{K_m + [\text{HCO}_3^-]} \quad (14)$$

$$\frac{1}{v_0} = \frac{1}{V_{\max}} + \frac{K_m}{V_{\max}} \frac{1}{[\text{HCO}_3^-]} \quad (15)$$

plotting  $1/v_0$  vs  $1/[\text{HCO}_3^-]$  results in a linear relationship (Figure 5B). The derived values of  $K_m$  and  $V_{\max}$  are  $K_m = (1.5 \pm 0.6) \times 10^{-2}$  M and  $V_{\max} = (1.5 \pm 0.3) \times 10^{-5}$  M/min.

A second aspect that has been considered in the activities of the Pd- $\beta$ -CD colloids relates to kinetic isotope effects involved in  $\text{CO}_2/\text{HCO}_3^-$  photoreduction and  $\text{H}_2$ -evolution processes, using the various colloids. The rate of  $\text{CO}_2/\text{DCO}_3^-$  photoreduction in  $\text{D}_2\text{O}$  is not affected as compared to that in  $\text{H}_2\text{O}$ . In turn, a significant isotope effect is observed in the hydrogen-evolution process,  $K_H/K_D \approx 3$ . The observation of an isotope effect in the  $\text{H}_2$ -evolution process using the Pd catalyst is consistent with previous studies that explored the photosensitized  $\text{H}_2$  evolution through interaction of generated radicals with Pt and Au colloids.<sup>41</sup> These studies revealed that charging the metal by the reduced relay and formation of surface-bound hydrogen atoms are rapid reactions, while the discharge of hydrogen atoms through cleavage of metal-hydrogen bonds is rate limiting in  $\text{H}_2$  evolution. Thus, our results imply that the rate-limiting step in  $\text{H}_2$  evolution in the presence of the Pd- $\beta$ -CD catalyst involves the cleavage of a Pd-H bond (eq 16), but the rate of  $\text{HCO}_2^-$  formation is not controlled by cleavage of these bonds.



**Inhibition Effects in the Reduction of Bicarbonate.** The catalytically active Pd- $\beta$ -CD colloid for bicarbonate reduction exhibits high sensitivity toward various additives. We find that aldehydes, amines, and particularly thiols act as inhibitors for the catalyst toward bicarbonate reduction. We have studied in detail the effect of added mercaptoethanol,  $\text{HOCH}_2\text{CH}_2\text{SH}$ , on the kinetics of the photosensitized formate formation. Figure 6A shows the rate of formate formation at different mercaptoethanol concentrations. It is evident that as the concentration of the thiol is increased, the rate of formate formation declines, and at an inhibitor concentration of  $[\text{HOCH}_2\text{CH}_2\text{SH}] = 2 \times 10^{-4}$  M, the photoinduced formation of  $\text{HCO}_2^-$  is completely blocked. Simultaneous to the inhibition in formate generation with added mercaptoethanol,  $\text{H}_2$  evolution from the system occurs. Figure 6C shows the rate of  $\text{H}_2$  evolution upon illumination of the system at different thiol concentrations. We realize that the rate of photosensitized  $\text{H}_2$  evolution increases as the concentration of mercaptoethanol is increased. At a thiol concentration of  $[\text{HOCH}_2\text{CH}_2\text{SH}] = 2 \times 10^{-4}$  M, where formate formation is entirely blocked, the rate of  $\text{H}_2$  evolution is similar to that observed from the system in the absence of the bicarbonate. Thus, in the presence of mercaptoethanol, formate generation is inhibited and the catalyst activity

(39) (a) Meisel, D.; Mulac, M.; Matheson, D. *J. Phys. Chem.* 1981, 85, 179. (b) Meisel, D. *J. Am. Chem. Soc.* 1979, 101, 6133. (c) Henglein, A. *Angew. Chem.* 1979, 91, 449. (d) Henglein, A.; Lillie, J. *J. Am. Chem. Soc.* 1981, 103, 1059.

(40) Segel, I. H., Ed.; *Enzyme Kinetics*; Wiley: New York, 1975.

(41) Koppie, K.; Meyerstein, D.; Meisel, D. *J. Phys. Chem.* 1980, 84, 870, and references therein.

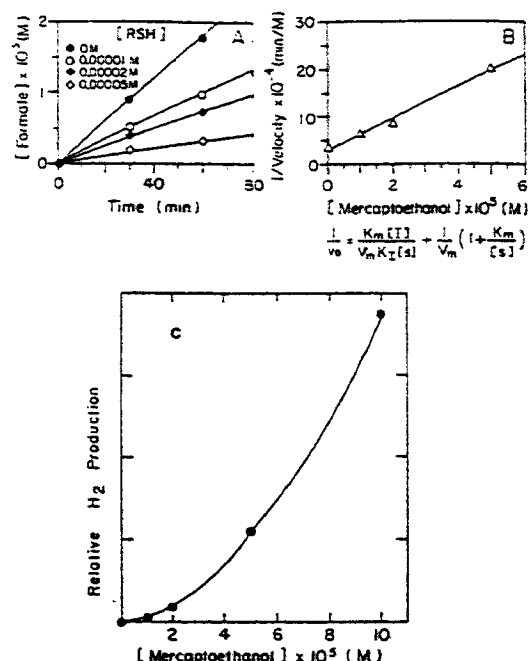
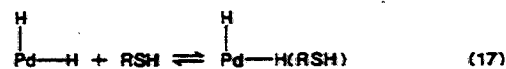


Figure 6. (A) Rates of photoinduced  $\text{HCO}_2^-$  formation of different concentrations of the inhibitor mercaptoethanol. (B) Graphic representation of the reciprocals of rates as a function of inhibitor concentration. (C) Relative rates of  $\text{H}_2$  evolution at different concentrations of mercaptoethanol. In all experiments  $[\text{DRF}] = 3 \times 10^{-5}$  M,  $[\text{MV}2^+] = 1 \times 10^{-3}$  M,  $[(\text{CO}_2\text{Na})_2] = 5.5 \times 10^{-2}$  M,  $[\text{HCO}_3^-] = 0.1$  M, and Pd- $\beta$ -CD = 40  $\text{mg}\cdot\text{L}^{-1}$ .

toward  $\text{H}_2$  evolution (present in the absence of  $\text{CO}_2/\text{HCO}_3^-$ ) is restored. Our results reveal that the active Pd- $\beta$ -CD catalyst toward  $\text{HCO}_3^-$  reduction includes two characteristic types of active sites. One class of sites is catalytically active in the generation of surface-bound H-atoms, sites that subsequently effect  $\text{H}_2$  evolution. The second type of sites is responsible for bicarbonate activation. In the absence of inhibitor, hydrogenation of activated  $\text{HCO}_3^-$  by surface-bound hydrides proceeds, rather than  $\text{H}_2$  evolution, since the former process is faster. Added mercaptoethanol blocks selectively the bicarbonate activation sites, and consequently, only the rather slow  $\text{H}_2$  evolution process occurs.

The inhibition phenomenon observed in the presence of added thiol suggests that the activation of bicarbonate on its active sites (eq 11) is competitively inhibited by binding of mercaptoethanol to the same sites (eq 17). Therefore, the kinetics of the bi-



carbonate reduction process with added mercaptoethanol should follow the rate equations for competitive inhibition of an active site-substrate activated complex. Under such conditions, the relation between the initial rate of formate formation as a function of the inhibitor concentration should be given by eq 18, where  $K_1$  is the dissociation constant of the inhibitor-catalyst complex.

$$v_0 = \frac{V_{\max}}{1 + \frac{K_m}{[\text{HCO}_3^-]} \left( 1 + \frac{[\text{HOCH}_2\text{CH}_2\text{SH}]}{K_1} \right)} \quad (18)$$

$$K_1 = \frac{[\text{H}-\text{Pd}-\text{H}][\text{HOCH}_2\text{CH}_2\text{SH}]}{[\text{H}-\text{Pd}-\text{H}(\text{HOCH}_2\text{CH}_2\text{SH})]}$$

$$\frac{1}{v_0} = \frac{K_m[\text{HOCH}_2\text{CH}_2\text{SH}]}{V_{\max}K_1[\text{HCO}_3^-]} + \frac{1}{V_{\max}} \left( 1 + \frac{K_m}{[\text{HCO}_3^-]} \right) \quad (19)$$

Figure 6B shows that a linear correlation is obtained upon plotting  $1/v_0$  (where  $v_0$  is the initial rate of  $\text{HCO}_2^-$  formation) as a function of mercaptoethanol concentration (eq 19) at a

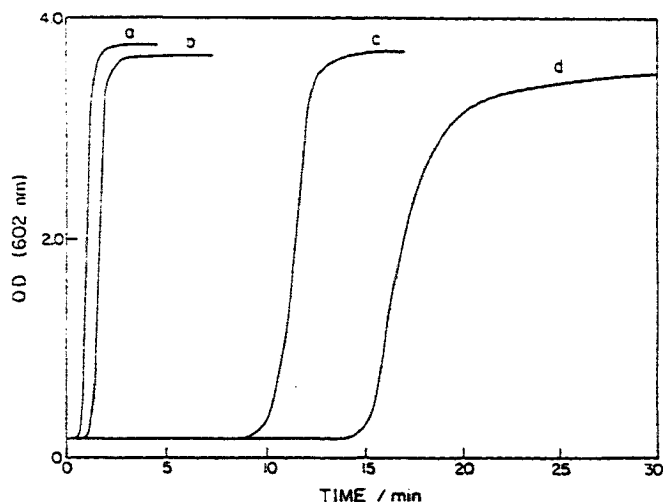


Figure 7. Rate profiles for the dark reduction of MV<sup>2+</sup> by HCO<sub>2</sub><sup>-</sup> at different temperatures followed spectroscopically at λ = 602 nm: (a) 37 °C, (b) 30 °C, (c) 20 °C, (d) 10 °C. In all experiments [MV<sup>2+</sup>] = 1 × 10<sup>-3</sup> M, [HCO<sub>2</sub><sup>-</sup>] = 0.1 M, Pd-β-CD = 45 mg·L<sup>-1</sup>.

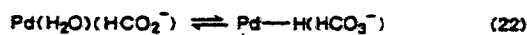
constant concentration of HCO<sub>3</sub><sup>-</sup>. This implies that the bicarbonate activation sites are indeed blocked by the thiol through a competitive inhibition mechanism. From this plot the value K<sub>i</sub> = (2.9 ± 1.5) × 10<sup>-6</sup> M<sup>-1</sup> is derived.

**Pd-β-CD Catalyzed Oxidation of Formate**

**Kinetics of Formate Oxidation.** Similar to enzymes that often exhibit reversible activities, the Pd-β-CD colloids show similar reversible properties. The Pd-β-CD colloid that is active in the photoreduction of HCO<sub>3</sub><sup>-</sup> to formate shows reversible activity, and formate reduces MV<sup>2+</sup> to MV<sup>•+</sup> in the presence of the catalyst (eq 20). In turn, the inactive Pd-β-CD catalyst (prepared at 90



°C) does not exhibit catalytic activity toward this process. Figure 7 shows the rate of MV<sup>2+</sup> reduction to MV<sup>•+</sup> by formate in the presence of the active Pd-β-CD colloid at various temperatures. It can be seen that the formation of MV<sup>•+</sup> is triggered after an induction period. Thereafter, MV<sup>•+</sup> accumulates and levels off to establish a steady-state concentration. As the temperature of the system increases, the induction period for MV<sup>•+</sup> formation is shortened, the accumulation of MV<sup>•+</sup> is enhanced, and a similar steady-state concentration of MV<sup>•+</sup> is formed at the different temperatures. It should be noted that at the time scales of these experiments only trace amounts of H<sub>2</sub> are formed. The reduction of MV<sup>2+</sup> by formate is expected to proceed through the reverse reactions (eq 21-23) that were previously detailed for bicarbonate



reduction to formate, i.e., activation of formate followed by its oxidation to HCO<sub>3</sub><sup>-</sup> and Pd hydride formation, and subsequent reduction of MV<sup>2+</sup> by the Pd hydride. Since the evolution of hydrogen (eq 16) is slow, this process can be disregarded and MV<sup>•+</sup> is formed through the sequential processes, eq 21-23. The induction time required for the generation of MV<sup>•+</sup> is attributed to the buildup of Pd hydrides that is the rate-limiting process. Once the threshold concentration of hydrides is formed, the reduction of MV<sup>2+</sup> is triggered. Subsequently, the rate of MV<sup>•+</sup> accumulation (slope) corresponds to the rate of Pd hydrides formation in the system, which is the rate-limiting process. It is also evident from Figure 7 that as the temperature is increased, the induction period is shortened and the rate of MV<sup>•+</sup> formation (slope) is enhanced, implying that the formation of Pd hydrides

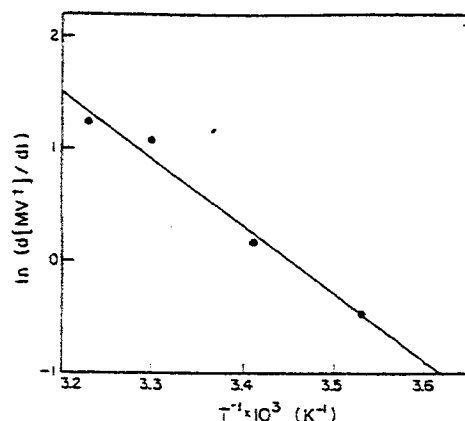


Figure 8. Arrhenius plot for the dark reduction of MV<sup>2+</sup> by HCO<sub>2</sub><sup>-</sup>.

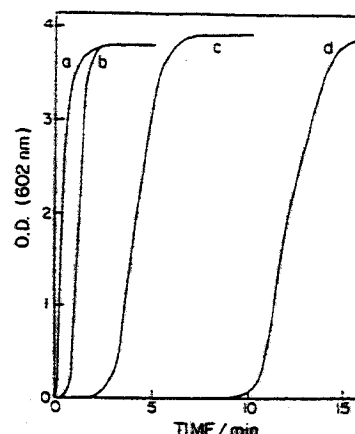


Figure 9. Rate profiles for the dark reduction of MV<sup>2+</sup> by formate in water: (a) by HCO<sub>2</sub><sup>-</sup> in H<sub>2</sub>O; (b) by HCO<sub>2</sub><sup>-</sup> in D<sub>2</sub>O; (c) by DCO<sub>2</sub><sup>-</sup> in H<sub>2</sub>O; (d) by DCO<sub>2</sub><sup>-</sup> in D<sub>2</sub>O. In all experiments [MV<sup>2+</sup>] = 1 × 10<sup>-3</sup> M; [formate] = 0.1 M; 28 °C.

is increased as the temperature rises. From these curves the observed rate constants, k<sub>obsd</sub>, were calculated at various temperatures. The Arrhenius plot (Figure 8) of the observed rate constants for the reduction of MV<sup>2+</sup> by formate gives an activation barrier of E<sub>a</sub> = 13 kcal·mol<sup>-1</sup> for the process. Since the thermodynamic balance for the process outlined in eq 20 is close to ΔG ≈ 0 kcal·mol<sup>-1</sup>, we deduce that the activation barrier for the reduction of bicarbonate to HCO<sub>2</sub><sup>-</sup> exhibits a similar value.

Reduction of MV<sup>2+</sup> by formate is also inhibited by added mercaptoethanol, HOCH<sub>2</sub>CH<sub>2</sub>SH. As the inhibitor concentration increases, the induction period is longer and the rate of MV<sup>•+</sup> formation is retarded. These results suggest that formate is activated toward production of Pd hydrides on the similar sites that lead to activation of bicarbonate and its hydrogenation to formate. Mercaptoethanol acts as a competitive inhibitor to HCO<sub>2</sub><sup>-</sup> for these active sites.

**Isotope Effects in Formate Oxidation.** A second aspect that has been considered in the kinetics of MV<sup>2+</sup> reduction by formate involved the determination of kinetic isotope effects in the reaction. Figure 9 compares the rate of reduction of MV<sup>2+</sup> by HCO<sub>2</sub><sup>-</sup> in H<sub>2</sub>O to the rates of MV<sup>2+</sup> reduction by DCO<sub>2</sub><sup>-</sup> in H<sub>2</sub>O, by HCO<sub>2</sub><sup>-</sup> in D<sub>2</sub>O, and by DCO<sub>2</sub><sup>-</sup> in D<sub>2</sub>O. We realize that using DCO<sub>2</sub><sup>-</sup> in H<sub>2</sub>O or D<sub>2</sub>O results in an isotope effect of k<sub>H</sub>(HCO<sub>2</sub><sup>-</sup>)/k<sub>D</sub>(DCO<sub>2</sub><sup>-</sup>) = 4.8 ± 1.1 in H<sub>2</sub>O and of k<sub>H</sub>(HCO<sub>2</sub><sup>-</sup>)/k<sub>D</sub>(DCO<sub>2</sub><sup>-</sup>) = 4.2 ± 0.7 in D<sub>2</sub>O. Isotope effects are also observed with D<sub>2</sub>O instead of H<sub>2</sub>O; k<sub>H</sub>(H<sub>2</sub>O)/k<sub>D</sub>(D<sub>2</sub>O) = 1.5 ± 0.3 and k<sub>H</sub>(H<sub>2</sub>O)/k<sub>D</sub>(D<sub>2</sub>O) = 1.3 ± 0.2 in HCO<sub>2</sub><sup>-</sup> and DCO<sub>2</sub><sup>-</sup>, respectively. When the composition of DCO<sub>2</sub><sup>-</sup> in D<sub>2</sub>O is used, the multiple of the two isotope effects, k<sub>H</sub>/k<sub>D</sub> = 6.34 ± 1.2 is observed (k<sub>H</sub>/k<sub>D</sub> = 6.4 calculated). Thus, we conclude that the rate-limiting step in the reduction process of MV<sup>2+</sup> by formate involves the cleavage of C-H in formate and H-OH in water. This conclusion is consistent with other reports<sup>21</sup> in which the kinetic isotope effects



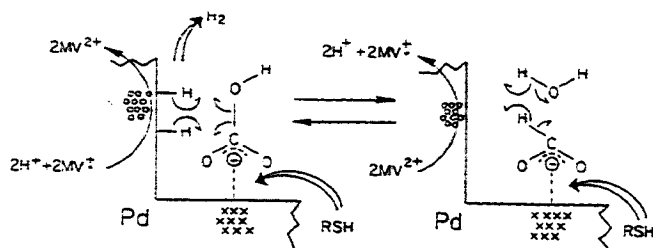


Figure 10. Schematic sequential mechanism for the Pd- $\beta$ -CD catalyzed reduction of  $\text{HCO}_3^-$  to formate and the reverse process.

in the decomposition of formate to hydrogen over a Pd/C catalyst were examined, where cleavage of H-bonds in formate and water participate in the rate-limiting process.

**Mechanistic Aspects Involved in the Photoreduction of  $\text{CO}_2/\text{HCO}_3^-$  to Formate.** The possible participation of the stabilizing support of the Pd colloid,  $\beta$ -cyclodextrin, in the activation of the bicarbonate substrate toward reduction to  $\text{HCO}_2^-$  has been examined. Cyclodextrins are cyclic macromolecular structures of glucose that form cylindrical cavities capable of associating various substrates. We have performed several experiments that exclude the operative participation of the  $\beta$ -CD receptor in the activation of  $\text{HCO}_3^-$ : (i) Addition of *N*-octylpyridinium bromide to the photochemical system that leads to the reduction of  $\text{HCO}_3^-$  to formate does not affect the rate of  $\text{HCO}_2^-$  production. Since *N*-octylpyridinium binds to the  $\beta$ -CD cavity, any activation of  $\text{HCO}_3^-$  through the  $\beta$ -CD cavity should be inhibited. (ii) We find that various other Pd colloids that are stabilized by supports that lack a cavity structure are also active in the photoreduction of  $\text{HCO}_3^-$  to formate. For example, Pd stabilized by glucose or polyvinylpyrrolidone exhibits catalytic activity toward  $\text{CO}_2/\text{HCO}_3^-$  photoreduction to formate. In this context, it is worthwhile to state that a rapid test of Pd colloid activities toward reduction of  $\text{HCO}_3^-$  to formate can be performed by examination of the reverse process, i.e., reduction of  $\text{MV}^{2+}$  by formate. We find that all colloids that were catalytically active in the reverse process were also active in the photoreduction of  $\text{HCO}_3^-$  to formate.

We have examined in the present study various aspects related to the catalytic activity of the Pd- $\beta$ -CD colloid toward the photoreduction of bicarbonate to formate and the reverse oxidation of  $\text{HCO}_2^-$ . The different mechanistic details provide, when united, a comprehensive model that accounts for the catalytic properties of Pd- $\beta$ -CD in these processes. The Pd- $\beta$ -CD catalyst includes two types of active sites (Figure 10): One type generates Pd hydrides, while the other catalytic sites activate bicarbonate toward reduction. The primary step in the photoreduction of  $\text{HCO}_3^-$  involves charging of the metal particles and formation of Pd hydrides (eq 10). Since the  $\text{H}_2$  evolution process is slow, hydrogenation of activated bicarbonate proceeds effectively (eq 12). In the presence of the inhibitor mercaptoethanol, selective in-

hibition of the bicarbonate activation sites occurs. Consequently, the slow  $\text{H}_2$ -evolution process predominates as the only route that utilizes the Pd-H intermediates. The reverse process where formate reduces  $\text{MV}^{2+}$ , involves the similar Pd-H intermediate. The rate-limiting step for  $\text{MV}^{2+}$  production involves the formation of the Pd-H intermediate, as evidenced by the induction period observed in the kinetic profile of  $\text{MV}^{2+}$  formation. We revealed that the rate-limiting step in the reverse reaction involves the cleavage of C-H and H-OH bonds of formate and water, respectively. These results suggest that formation of the Pd-H intermediate proceeds through a concerted mechanism that is displayed in Figure 10. Inhibition of the reverse process by thiols implies that activation of formate toward oxidation occurs on the similar sites that activate  $\text{HCO}_3^-$  for hydrogenation.

### Conclusions

We have highlighted that a Pd- $\beta$ -CD colloid acts as an artificial heterogeneous catalyst for  $\text{CO}_2/\text{HCO}_3^-$  reduction to formate that mimics enzyme activities: (i) It exhibits high specificity and effectiveness toward  $\text{CO}_2/\text{HCO}_3^-$  reduction; (ii) it is competitively inhibited toward the substrate activation and reduction; (iii) it reveals "enzyme-like" kinetics; and (iv) it shows reversible properties. Previously,<sup>29</sup> we have shown that the enzyme formate dehydrogenase acts as biocatalyst for the photoreduction of  $\text{CO}_2/\text{HCO}_3^-$  to formate. The present system is an artificial model that mimics the functions of this biocatalyst.

It should be noted that in the present study a photosystem has been applied to characterize the catalytic activity of the Pd- $\beta$ -CD colloid only as a matter of convenience. The high quantum efficiency of  $\text{MV}^{2+}$  generation in these systems provides a rapid and effective accumulation of the electron carrier,  $\text{MV}^{2+}$ , that does not affect or influence the subsequent kinetics of formate production. In fact, any other route that generates  $\text{MV}^{2+}$  could lead to the catalyzed reduction of  $\text{HCO}_3^-$  to formate. Indeed, electrogenerated  $\text{MV}^{2+}$  similarly mediates the reduction of  $\text{HCO}_3^-$  to formate in the presence of the Pd- $\beta$ -CD catalyst. Our results reveal that the preparation conditions of the Pd- $\beta$ -CD tremendously affect the resulting catalytic activities of the colloids. Although the origin of the different activities of Pd- $\beta$ -CD colloids is not fully understood, we suggest that temperature-controlled morphological differences in the metal colloid clusters are responsible for the different activities. Our results imply that similar Pd catalysts might have potential catalytic activities in hydrogenation or electrochemical reduction of  $\text{CO}_2/\text{HCO}_3^-$ . These aspects, as well as attempts to characterize the activated species of  $\text{HCO}_3^-$  and  $\text{HCO}_2^-$  on the Pd- $\beta$ -Cd catalyst, are now being further examined in our laboratory.

**Acknowledgment.** This research is supported by a grant from the National Council for Research and Development, Israel, and the Kernforschung Anlage, Juelich, Germany, and in part by the Belfer Center for Energy Research, Israel.

# Photochemical Fixation of Carbon Dioxide: Enzymic Photosynthesis of Malic, Aspartic, Isocitric, and Formic Acids in Artificial Media<sup>1</sup>

Daniel Mandler and Itamar Willner\*

Department of Organic Chemistry, The Hebrew University of Jerusalem, Jerusalem 91904, Israel

Photosensitized regeneration of 1,4-dihyronicotinamide adenine dinucleotide phosphate (NADPH) with an artificial photosystem allows the enzymic fixation of CO<sub>2</sub> through carboxylation of α-oxo acids using sacrificial electron donors. Pyruvic acid is carboxylated to malic acid and α-oxoglutaric acid is carboxylated to isocitric acid with the malic enzyme and isocitrate dehydrogenase (ICDH) as biocatalysts, φ = 1.9%. Malic acid formed through the photosensitized process is used as a synthetic building block for subsequent sequestered enzymic transformations, and its conversion into aspartic acid is accomplished with fumarase and aspartase as biocatalysts.

Photoreduction of CO<sub>2</sub> to formate is accomplished in the presence of formate dehydrogenase (FDH) as catalyst. Photosensitized reduction of different bipyridinium relay systems, *i.e.* *N,N'*-dimethyl-4,4'-bipyridinium (MV<sup>2+</sup>) (1), *N,N'*-dimethyl-2,2'-bipyridinium (DM<sup>2+</sup>) (2), *N,N'*-trimethylene-2,2'-bipyridinium (DT<sup>2+</sup>) (3), and *N,N'*-tetramethylene-2,2'-bipyridinium (DQ<sup>2+</sup>) (4), to the corresponding radical cations yields reduced relays that act as cofactors for FDH, which mediates the reduction of CO<sub>2</sub> to formate. The quantum yield for formate formation is in the range φ = 0.5–1.6%

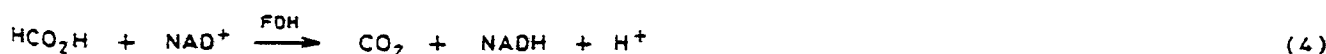
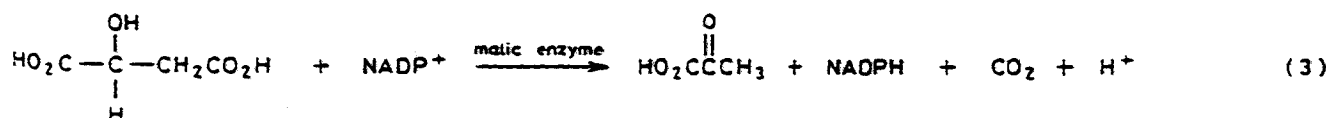
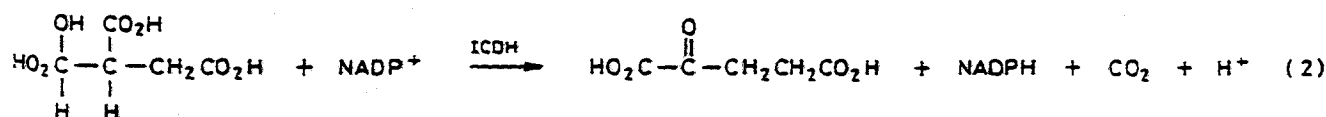
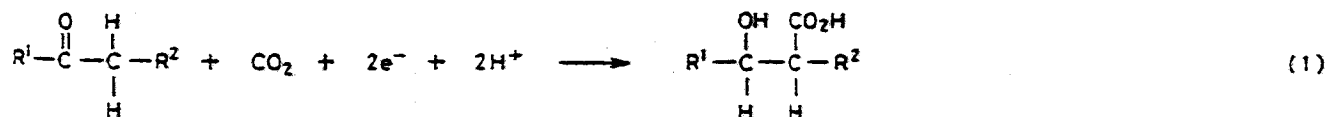
Substantial efforts have been directed in recent years towards the development of solar light conversion and storage systems.<sup>2–4</sup> Specific emphasis has been given to the conversion of abundant materials into fuel products. In this respect, photolysis of water to hydrogen and photoreduction of carbon dioxide to organic fuel products are of special interest.<sup>5</sup> Photosensitized hydrogen evolution from aqueous solutions has been reported in various systems with homogeneous<sup>6</sup> or heterogeneous<sup>7,8</sup> catalysts.

Activation of CO<sub>2</sub> by homogeneous transition metal complexes has been extensively studied in recent years.<sup>9,10</sup> Electrocatalysed reduction of CO<sub>2</sub> to formate, oxalate, methane, *etc.* has been observed in aqueous as well as in non-aqueous media in the presence of specific electrode materials<sup>11</sup> or transition metal complexes,<sup>12,13</sup> though the reduction potentials achieved are usually too negative for application in photochemical reduction processes. A few studies have examined photoreduction of CO<sub>2</sub>. Lehn and his co-workers<sup>14,15</sup> have reported on the photoreduction of CO<sub>2</sub> to CO or formate with Co<sup>II</sup>, Ru<sup>II</sup>, and Re<sup>II</sup> complexes. Photoreduction of CO<sub>2</sub> to organic products has been achieved in low yields by use of

semiconductor powders<sup>16,17</sup> such as strontium titanate (SrTiO<sub>3</sub>), tungsten oxide (WO<sub>3</sub>), and titanium oxide (TiO<sub>2</sub>).

Recently<sup>18</sup> we have demonstrated that carbon dioxide is photoreduced to methane by heterogeneous Ru or Os colloids. The reductive insertion of CO<sub>2</sub> into a carbon–hydrogen bond [equation (1)] might be considered as a simple route for the fixation of CO<sub>2</sub>. In nature many enzymes are active in decarboxylation processes that are anti-CO<sub>2</sub>-fixation routes. For example, in the catabolic cycle, isocitric and malic acids are decarboxylated to α-oxoglutaric acid [equation (2)] and pyruvic acid [equation (3)] in the presence of the cofactor nicotinamide adenine dinucleotide phosphate (NADP<sup>+</sup>) and the appropriate enzyme isocitrate dehydrogenase (ICDH) (E.C. 1.1.1.42) or malic enzyme (E.C. 1.1.1.40). Similarly, formate is decarboxylated in the presence of the cofactor nicotinamide adenine dinucleotide (NAD<sup>+</sup>) and catalysed by formate dehydrogenase (FDH) (E.C. 1.2.1.2) [equation (4)].

Since enzymes are often reversibly active, one might envisage means to reverse the processes occurring in nature and induce carboxylation pathways using biocatalysts, and thereby develop CO<sub>2</sub>-fixation processes. Recently<sup>19,20</sup> we have



developed photoinduced cycles for the regeneration of the NAD(P)H cofactors. We have shown that the photogenerated *N,N'*-dimethyl-4,4'-bipyridinium radical  $MV^{2+}$  mediates the reduction of  $NAD^+$  or  $NADP^+$  to NADH and NADPH in the presence of the enzymes lipoamide dehydrogenase (LipDH) (E.C. 1.6.4.3) and ferredoxin-NADP<sup>+</sup>-reductase (FDR) (E.C. 1.18.1.2), respectively. Furthermore, we were able to couple the photoinduced regeneration cycles to enzyme-catalysed synthesis of amino acids, alcohols, and hydroxy acids. Thus, it seems feasible that  $CO_2$  reduction processes might be driven by the light-induced regeneration of NAD(P)H cofactors, assuming that the enzymes exhibit reversible activity.

In a preliminary note, we have reported<sup>1</sup> on the successful photoinduced carboxylation of pyruvic acid to form malic acid as well as the fixation of  $CO_2$  into  $\alpha$ -oxoglutaric acid to form isocitric acid. Here we present a comprehensive study of several photoinduced enzyme-catalysed  $CO_2$  fixation systems.

These fixation processes were carried out by using either the NAD(P)H photoregeneration cycles coupled to enzymic fixation reactions, or by utilizing an artificially reduced cofactor coupled to an enzyme.

Specifically, we have developed artificial photochemical systems for the reductive carboxylation of pyruvic and  $\alpha$ -oxoglutaric acids to malic and isocitric acids, respectively. Also the reduction of  $CO_2$  to formate has been accomplished by use of various relay systems and formate dehydrogenase as biocatalyst.

Malic acid obtained by the fixation of  $CO_2$  into pyruvic acid could be utilized as a synthetic precursor for sequestered enzyme-catalysed reaction. Specifically, this photoproduct has been coupled to dehydration followed by amination to form the  $C_4$ -aspartic acid product.

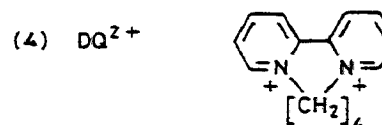
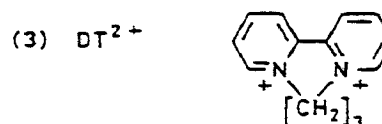
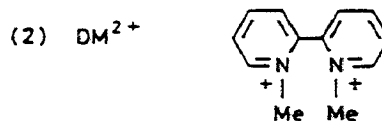
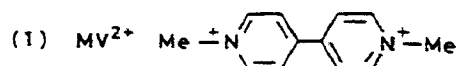
## Experimental

Absorption spectra were recorded with a Uvikon-820 (Kontron) spectrophotometer. Product analyses were performed with an LKB high-pressure liquid chromatograph equipped with Knauer UV and conductivity detectors or with an LKB 4400 amino acid analyser.

Illumination experiments were performed in 5 ml glass cuvettes (1 × 1 cm) equipped with a small stirring bar and a serum stopper. The light source was a 1 000 W halogen quartz lamp, and light was filtered through a 400 nm cut-off filter. Comparison of the different relay systems in formate formation was carried out by placing all the cuvettes on a rotating disc. The disc was immersed in a water-bath, kept at 10 °C, and rotated by an external motor. *N,N'*-Dimethyl-2,2'-bipyridinium ( $DM^{2+}$ ) (2), *N,N'*-trimethylene-2,2'-bipyridinium ( $DT^{2+}$ ) (3), and *N,N'*-tetramethylene-2,2'-bipyridinium ( $DQ^{2+}$ ) (4) were prepared according to the literature methods.<sup>21</sup> All other materials and enzymes were purchased from Sigma or Aldrich.

**Malic acid.** The system was composed of a Tris buffer (4.2 ml; 0.2M; pH 8.0) that included the substrate: pyruvic acid ( $4.7 \times 10^{-2}M$ ),  $MV^{2+}$  ( $1.9 \times 10^{-4}M$ ),  $NADP^+$  ( $1.8 \times 10^{-4}M$ ),  $[Ru(bpy)_3]^{2+}$  ( $2.1 \times 10^{-5}M$ ),  $MnCl_2$  ( $9.5 \times 10^{-5}M$ ),  $NaHCO_3$  (0.2M), and the electron donor 2-mercaptoethanol ( $1.9 \times 10^{-2}M$  initial concentration). To this solution were added FDR (0.2 units) and malic enzyme (1.33 units). The system was illuminated under a gaseous atmosphere of  $CO_2$  and the pH was maintained at 7.9 by gradual addition of KOH. Samples (300  $\mu$ l) of the solution were taken out at intervals, passed through a cation-exchange resin (Dowex 50W × 8), and analysed by h.p.l.c. coupled with a Wescan anion, exclusion column and a conductivity detector (eluant solution  $10^{-3}M-H_2SO_4$ ; flow 0.6 ml  $min^{-1}$ ).

**Aspartic acid.** The system was composed of an aqueous 0.16M-



Tris buffer solution (4 ml; pH 7.9) that included  $[Ru(bpy)_3]^{2+}$  ( $2.3 \times 10^{-5}M$ ),  $NaHCO_3$  (0.16M),  $NH_4^+$  (0.08M), pyruvic acid ( $4 \times 10^{-2}M$ ),  $MV^{2+}$  ( $1.6 \times 10^{-4}M$ ),  $NADP^+$  ( $3.2 \times 10^{-4}M$ ),  $MnCl_2$  ( $8 \times 10^{-5}M$ ), and 2-mercaptoethanol ( $1.6 \times 10^{-2}M$  initial concentration). To the solution were added the enzymes FDR (0.5 units), malic enzyme (0.5 units), fumarase (E.C. 4.2.1.2; 156 units) and L-aspartase (E.C. 4.3.1.1; 3 units). The deaerated solution was illuminated and samples (100  $\mu$ l) were taken out at intervals. Samples were treated with 5-sulphosalicylic<sup>22</sup> acid before analysis. Malic acid and fumaric acid were analysed by ion chromatography using the procedure described for malic acid. Aspartic acid was analysed by an amino acid analyser.

**Isocitric acid.** The system was composed of Tris buffer (4.2 ml; 0.2M; pH 7.2) that included  $[Ru(bpy)_3]^{2+}$  ( $1.4 \times 10^{-5}M$ ),  $MV^{2+}$  ( $1.7 \times 10^{-4}M$ ),  $NADP^+$  ( $1.7 \times 10^{-4}M$ ),  $MnCl_2$  ( $1.7 \times 10^{-3}M$ ),  $NaHCO_3$  (0.17M),  $\alpha$ -oxoglutaric acid ( $4.2 \times 10^{-2}M$ ), and the electron donor DL-dithiothreitol (DTT) ( $8.3 \times 10^{-3}M$  initial concentration). The following enzymes were added: FDR (0.2 units) and isocitrate dehydrogenase (0.47 units) immobilized on poly(acrylamide-co-*N*-acryloyloxysuccinimide) by the procedure developed by Whitesides *et al.*<sup>23</sup> Samples (120  $\mu$ l) of the illuminated solution were passed through a cation-exchange resin (Dowex 50W × 8) and analysed on an RP-18 column (Merck); eluant 0.3M- $H_3PO_4$  (0.8 ml  $min^{-1}$  flow rate). Isocitric and  $\alpha$ -oxoglutaric acids were detected at 210 nm.

**Formic acid.** To a phosphate buffer (3.4 ml; 0.2M; pH 7.0) solution were added  $[Ru(bpy)_3]^{2+}$  ( $3 \times 10^{-5}M$ ), one of the charge relays ( $MV^{2+}$ ,  $DM^{2+}$ ,  $DT^{2+}$  or  $DQ^{2+}$ ;  $1 \times 10^{-3}M$ ), cysteine as an electron donor ( $1 \times 10^{-2}M$ ),  $NaHCO_3$  (0.2M), and formate dehydrogenase (FDH) (0.89 units). Samples (200  $\mu$ l) were taken out at intervals and analysed for formate using an ion chromatograph (Wescan anion-exclusion column; eluant  $10^{-3}M-H_2SO_4$ ; flow rate 0.6 ml  $min^{-1}$ ), as well as by an enzymic assay.<sup>24</sup>

## Results and Discussion

Illumination under  $CO_2$  of the aqueous solution that includes the photosystem  $[Ru(bpy)_3]^{2+}$  as sensitizer, the charge relay  $MV^{2+}$ , and the sacrificial electron donor 2-mercaptoethanol, in the presence of the cofactor  $NADP^+$ , the substrate pyruvic acid, and the enzymes FDR and malic enzyme, results in the formation of malic acid. The rate of product formation is depicted in Figure 1. Control experiments revealed that all the

components are essential for the photoinduced production of malic acid, and exclusion of any of the components of the system prevented the formation of malic acid.

Our previous studies<sup>19</sup> have elucidated the different steps involved in the photoregeneration of NADPH. The excited sensitizer  $[Ru(bpy)_3]^{2+}$  is quenched by  $MV^{2+}$  via an electron-transfer process. The oxidized sensitizer formed by this electron-transfer reaction is reduced and consequently the light-active compound is regenerated. The reduced electron relay  $MV^{•-}$  mediates the reduction of  $NADP^+$  in the presence of the biocatalyst FDR. Indeed, upon illumination of a solution which contains  $[Ru(bpy)_3]^{2+}$ ,  $MV^{2+}$ , 2-mercaptoethanol,  $NADP^+$ , and the enzyme FDR, accumulation of NADPH could be monitored spectroscopically at  $\lambda$  340 nm ( $\phi = 1.9\%$ ). Addition of the malic enzyme in the dark, in the presence of the substrate, pyruvic acid, and  $CO_2$ , resulted in the disappearance of NADPH and the production of malic acid. Thus, we conclude

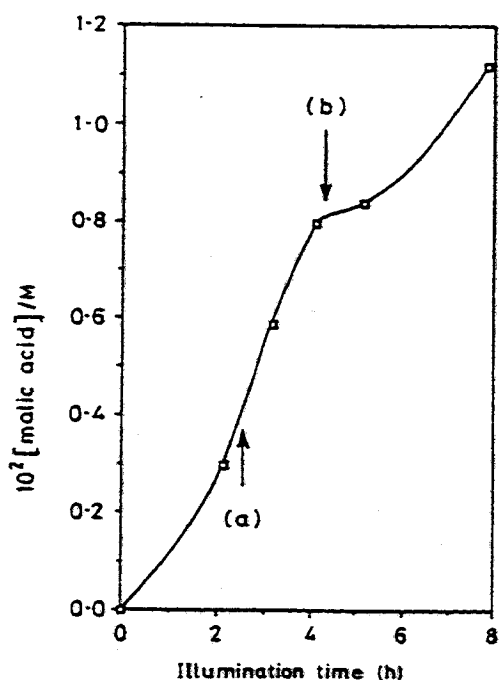


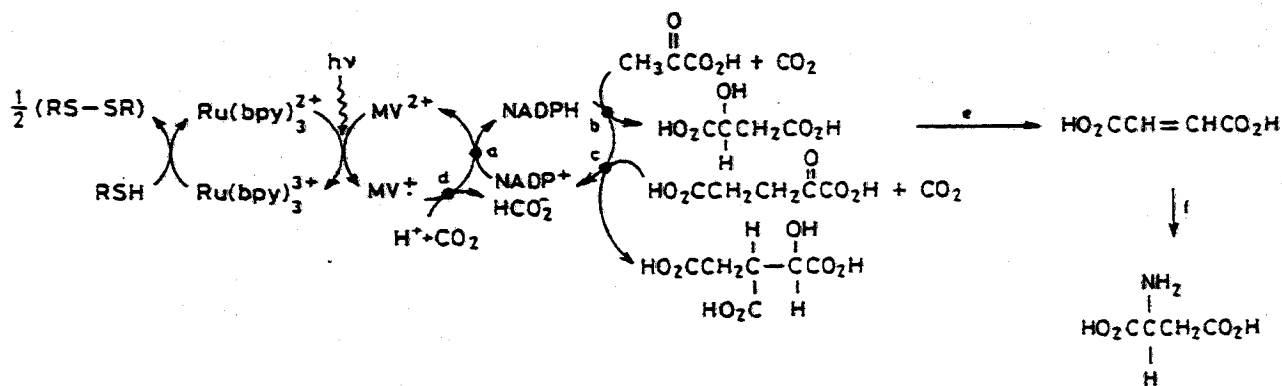
Figure 1. Rate of malic acid formation as a function of illumination time with addition of mercaptoethanol at (a) ( $2.2 \times 10^{-2}M$ ) and (b) ( $2.7 \times 10^{-2}M$ )

that the photoinduced reduction of  $NADP^+$  mediates the reductive carboxylation of pyruvic to malic acid.

Figure 2 summarizes schematically the sequence of catalytic reactions that leads to the fixation of  $CO_2$  into pyruvic acid. Several points should be noted. The nature of the electron donor strongly affects the fixation process. Substitution of 2-mercaptoethanol by other electron donors such as ethylenediaminetetra-acetic acid (EDTA), triethanolamine, or cysteine totally inhibited the formation of malic acid. Since our previous studies have indicated that these electron donors lead to photoinduced regeneration of NADPH, we conclude that the latter donors deactivate the carboxylation catalyst, namely the malic enzyme. In addition, the rate of NADPH formation must be controlled, since accumulation of NADPH in continuous illumination results in degradation of the cofactor. The lability of the cofactor is probably due to partial photochemical activity<sup>25</sup> of the reduced cofactor NADPH that might serve as an electron donor to the oxidized sensitizer. Hence, we had to monitor the rate of NADPH formation, so that a low steady-state concentration of the reduced cofactor was maintained. The experimental conditions described represent a suitable balance for the photochemical generation of NADPH and subsequent chemical consumption of the cofactor. Thus the quantum yield of carboxylated acids is controlled by the quantum yield of NADPH formation,<sup>19</sup>  $\phi = 1.9\%$ . Indeed, it can be shown (Figure 1) that the rate of malic acid formation is maintained constant over a long period of illumination.

Our success in the photocarboxylation of pyruvic acid to form malic acid has encouraged us to try to use photosynthesized malic acid as a 'building block' for the photoinduced synthesis of other  $C_4$ -products by enzymic means. Malic acid can, in principle, be dehydrated enzymically to form fumaric acid, that subsequently, in the presence of another enzyme (aspartase) and ammonium ions, is aminated to aspartic acid.

Illumination of an aqueous system that includes all the components described for the photoinduced production of malic acid, and in addition ammonium ions and the enzymes fumarase and aspartase, yields aspartic acid. Figure 3 displays the rate of aspartic acid formation at intervals of illumination. In the absence of aspartase no aspartic acid is formed and the photoproducts are malic acid and fumaric acid. However in the presence of aspartase only aspartic acid is detected as photoproduct and no accumulation of the intermediate products, *i.e.* malic or fumaric acid, can be detected in the reaction medium. These results are attributed to the equilibrium constant of the last reaction in the sequestered enzymic cycle, *i.e.* the amination process ( $K = 4.3 \times 10^4 \text{ l mol}^{-1}$ ). While the conversion of malic into fumaric acid is unfavourable ( $K =$



a. ferredoxin-NADP<sup>+</sup>-reductase; b. malic enzyme; c. isocitrate dehydrogenase; d. formate dehydrogenase; e. fumarase; f. aspartase

Figure 2. Cyclic scheme for the photoinduced  $CO_2$ -fixation systems

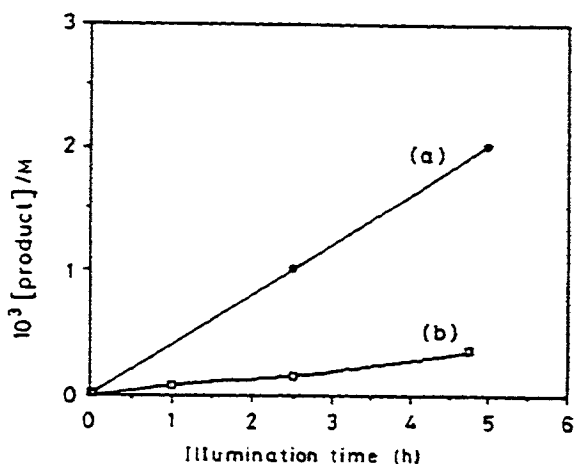


Figure 3. Rate of (a) aspartic and (b) fumaric acid formation as a function of illumination time

0.23), coupling of this reaction to the formation of aspartic acid shifts the equilibrium towards amino acid formation, and consequently, in the presence of aspartase, aspartic acid is the only product.

Figure 2 represents schematically the entire photochemical process leading to the fixation of CO<sub>2</sub> into pyruvic acid to form aspartic acid *via* a multi-enzyme-catalysed process.

A similar approach has been examined for the fixation of CO<sub>2</sub> into  $\alpha$ -oxoglutaric acid to produce isocitric acid. Illumination of an aqueous solution under CO<sub>2</sub> that includes [Ru(bpy)<sub>3</sub>]<sup>2+</sup>, the relay MV<sup>2+</sup>, the electron donor DTT, NADP<sup>+</sup>, the substrate  $\alpha$ -oxoglutaric acid, and the two enzymes FDR and isocitrate dehydrogenase (ICDH) yields only low amounts of isocitric acid (*ca.* 10<sup>-4</sup>M), and the system is deactivated after 1 h illumination. Re-addition of ICDH regenerates the activity of the system towards isocitric acid formation upon illumination, implying that the carboxylating enzyme is deactivated in the artificial environment. We therefore immobilized the ICDH on a water-soluble polyacrylamide derivative containing active ester groups.<sup>23</sup>

Illumination of the previously described system with the immobilized ICDH resulted in the long-term formation of isocitric acid. Figure 4 displays the rate of product formation as a function of illumination time. It is evident that the activity of the system is maintained constant for at least 6 h illumination. Control experiments revealed that all the components included in the system are essential to induce the photosynthesis of isocitric acid, and exclusion of any one component prevents product formation. A stepwise experiment, where ICDH was added in the dark to an aqueous solution that included photogenerated NADPH, was also performed. Addition of the second enzyme (ICDH) resulted in the disappearance of NADPH and formation of isocitric acid. Thus, it is evident that the production of isocitric acid proceeds by a mechanistic cycle similar to that described for malic acid formation (Figure 2). The primary step involves the FDR-catalysed photosensitized regeneration of NADPH; the second step utilizes the reduced cofactor to induce the enzyme-catalysed carboxylation of  $\alpha$ -oxoglutaric to isocitric acid [equation (2)].

The enzymic decarboxylation of formic acid by NAD<sup>+</sup> [equation (4)] in the presence of formate dehydrogenase is well established.<sup>24</sup> This process is thermodynamically favoured towards the oxidation of formic acid ( $\Delta G^\circ = -4.6 \text{ kcal mol}^{-1}$ ).<sup>\*</sup>

Thus, better reducing agents than NADH must be used in order to reverse the naturally occurring process. Previous studies<sup>27</sup> revealed that FDH (from *Pseudomonas oxalaticus*) recognizes various artificial electron relays in addition to NAD<sup>+</sup>,

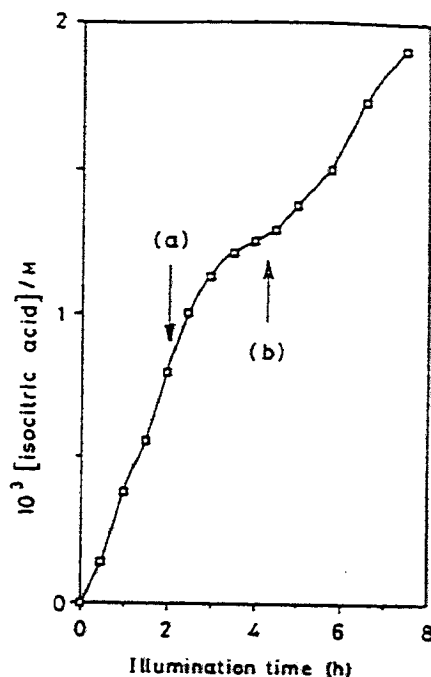


Figure 4. Rate of isocitric acid formation as a function of illumination time with addition of DTT ( $5 \times 10^{-3}$ M) at (a) and (b)

such as methylviologen and benzylviologen radical cation. Therefore, we have examined the ability of a series of reduced relays of bipyridinium structure to act as artificial cofactors for the reduction of CO<sub>2</sub> in the presence of the enzyme FDH.

Interestingly, we have found that several reduced bipyridinium species act as substrates for the enzyme FDH, and the participation of the cofactor, NAD<sup>+</sup>, is not required. Illumination of aqueous solutions under CO<sub>2</sub> (pH = 6.8) that include the sensitizer [Ru(bpy)<sub>3</sub>]<sup>2+</sup>, one of the electron relays *N,N'*-dimethyl-4,4'-bipyridinium (MV<sup>2+</sup>) (1), *N,N'*-dimethyl-2,2'-bipyridinium (DM<sup>2+</sup>) (2), *N,N'*-trimethylene-2,2'-bipyridinium (DT<sup>2+</sup>) (3), and *N,N'*-tetramethylene-2,2'-bipyridinium (DQ<sup>2+</sup>) (4), cysteine as electron donor, and the enzyme formate dehydrogenase, results in the reduction of CO<sub>2</sub> to formate. The rate of formate formation at intervals of illumination is displayed in Figure 5. Control experiments revealed that all the components are essential to induce the reduction of CO<sub>2</sub>, although very small amounts of formate could be detected in the absence of FDH. It should be emphasized that the enzyme FDH is very unstable; upon illumination of these aqueous systems at room temperature (24 °C) complete deactivation of the enzyme is observed within 0.5 h and only limited amounts of formate can be accumulated.

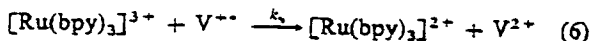
Attempts to stabilize the enzyme through immobilization failed. Nevertheless, by lowering the temperature of the reaction medium the stability of the enzyme is substantially enhanced. Illumination of the aqueous solutions was therefore performed at 10 °C. Under these conditions, the concentrations of formate produced were in the 10<sup>-3</sup>M region (Figure 5). However, even under these conditions deactivation of FDH occurs: the enzyme loses 90% of its initial activity within 6 h illumination. The highest quantum yields for formate formation are observed using the two relays MV<sup>2+</sup> and DT<sup>2+</sup> and correspond to  $\phi = 1.6 \times 10^{-2}$ .

The fact that the various reduced relays mediate directly the reduction of CO<sub>2</sub> to formate in the presence of FDH allows us

\* 1 kcal = 4.184 kJ.

outline the cyclic scheme displayed in Figure 2 as the route for the formation of formate.

It should be noted that the effectiveness of the various relay systems for the reduction of CO<sub>2</sub> to formate does not coincide with their reduction potentials. The quantum yield for the formation of the reduced relay is affected by the quenching rate [equation (5)] and the destructive recombination of the photoproducts by back electron-transfer [equation (6)].



Previous studies<sup>28</sup> have indicated that the effectiveness of electron transfer from excited [Ru(bpy)<sub>3</sub>]<sup>2+</sup> to a series of bipyridinium charge relays depends strongly upon the

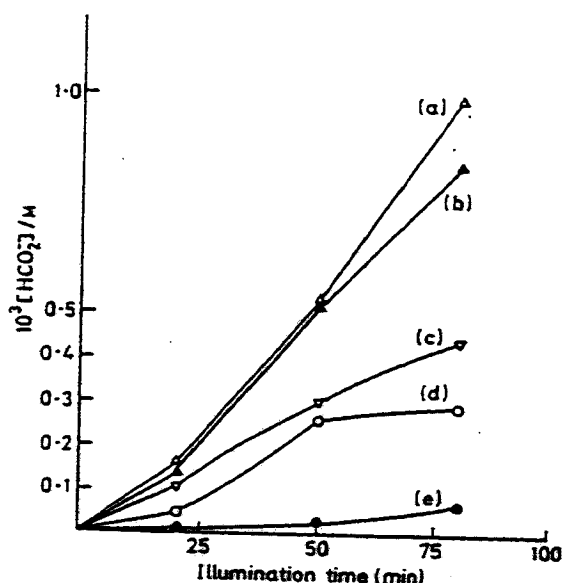


Figure 5. Rate of formate formation as a function of illumination time using various charge relays: (a) MV<sup>2+</sup>, (b) DT<sup>2+</sup>, (c) DQ<sup>2+</sup>, (d) DM<sup>2+</sup>, (e) DT<sup>2+</sup> without FDH

Table 1. Quantum yields, reduction potentials, and quenching constants of the charge relays in the formic acid system

Electron relay	E° (28 °C)/V vs. NHE	10 <sup>-8</sup> k <sub>q</sub> (28 °C)/l mol <sup>-1</sup> s <sup>-1</sup>	φ (%)
MV <sup>2+</sup>	-0.44	10.3	1.6
DT <sup>2+</sup>	-0.55	5.74	1.6
DQ <sup>2+</sup>	-0.65	3.24	1.0
DM <sup>2+</sup>	-0.72	1.8	0.5

reduction potential of the relay. It has been found that the quenching rate constant decreases as the reduction potential of the relay decreases, consistent with electron-transfer theories. In contrast, the back electron-transfer process is only slightly affected by the reduction potential, and with all relay systems used in our studies diffusion-controlled rate constants have been observed. Thus, the effectiveness of the reduced relay production is affected mainly by the electron-transfer quenching process.

Table 1 summarizes the quantum yields for formic acid formation by use of the various relays in comparison with their reduction potentials and electron-transfer quenching rate constants. It is evident that the highest formate yields are obtained with MV<sup>2+</sup>, which exhibits superior quenching properties, while DM<sup>2+</sup> shows the lowest activity as well as a poor electron-transfer quenching rate constant. Thus, it is reasonable to attribute the different quantum yields of formic acid production with the various relay systems to their primary electron-transfer quenching properties. Nevertheless, differences in recognition of the reduced relay by the enzyme FDH and subsequent effects on formic acid production cannot be excluded.

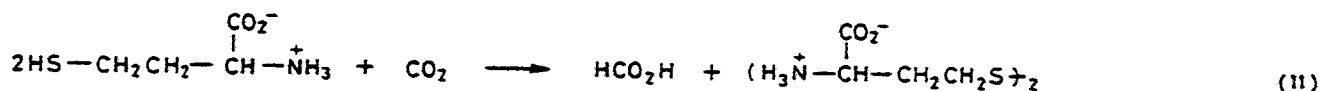
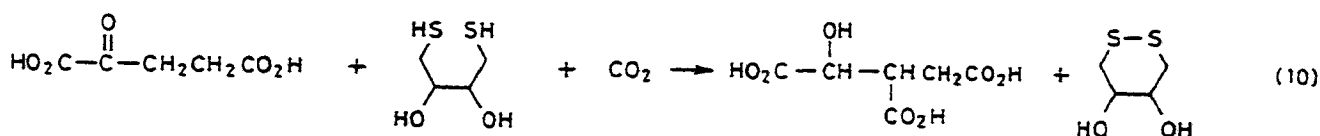
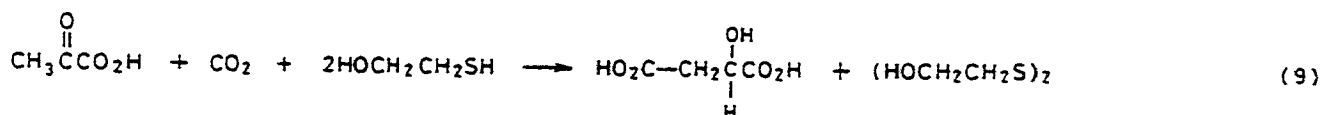
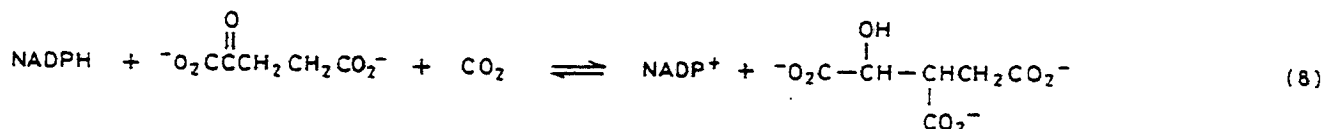
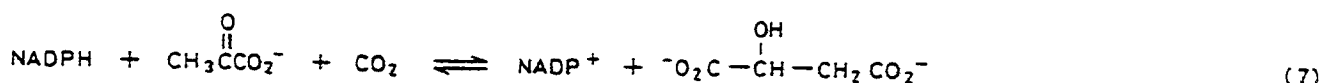
Whenever enzymes are applied as biocatalysts in synthesis, and specifically when they are introduced into artificially tailored systems, their stability must be considered. Table 2 summarizes the turnover numbers (TN) of the enzymes as well as other ingredients included in the various CO<sub>2</sub>-fixation routes. The quoted turnover numbers for the enzymes are lower limits in the sense that enzyme activity is still preserved when these values are determined. It is evident that the enzymes as well as other ingredients are effectively recycled in the various systems. However, we emphasize that different precautions were undertaken to achieve the observed stabilities of the biocatalysts. For malic enzyme, selection of the specific electron donor, i.e. 2-mercaptoethanol, and controlling the rate of NADPH photogeneration are essential to maintain the activity of the system. For ICDH, immobilization on a solid support is required to achieve biocatalyst stabilization. Finally, stabilization of FDH is accomplished by operating the photoinduced CO<sub>2</sub>-fixation process at relatively low temperatures (10 °C).

A further aspect to be considered in these systems relates to the thermodynamic balance of the net photosensitized CO<sub>2</sub>-fixation processes. We have emphasized earlier<sup>29</sup> the synthetic advantages of using the photochemically induced regeneration of cofactors over chemical regeneration routes. The fact that light energy constantly drives the reduction of NAD(P)<sup>+</sup> to NAD(P)H through the photosensitized process eliminates the reverse reduction of NAD(P)<sup>+</sup> by the product as it is accumulated. Consequently, endoergic reactions can be derived and products can be accumulated in amounts that are substantially higher than the estimated dark-equilibrium values. The carboxylation processes of pyruvic acid and α-oxoglutaric acid by NADPH to form malic and isocitric acids, respectively

Table 2. Turnover numbers of the components in the various CO<sub>2</sub>-fixation reactions.

	[Ru(bpy) <sub>3</sub> ] <sup>2+</sup>	MV <sup>2+</sup>	NADP <sup>+</sup>	FDR <sup>a</sup>	FDH <sup>b</sup>	Malic enzyme <sup>c</sup>	ICDH <sup>d</sup>	Fumarase <sup>e</sup>	Aspartase <sup>f</sup>
Malic acid	1 074	117	62.2	2.3 × 10 <sup>4</sup>		7.4 × 10 <sup>5</sup>			
Aspartic acid	174	25	6.3	1.6 × 10 <sup>3</sup>				8.5 × 10 <sup>2</sup>	5.2 × 10 <sup>2</sup>
Isocitric acid	272	23	11.4	2.5 × 10 <sup>3</sup>			5.5 × 10 <sup>4</sup>		
Formic acid	67	2			2 × 10 <sup>3</sup>				

<sup>a</sup> Formula wt. (FW) 40 000 (M. Shin, *Methods Enzymol.*, 1971, 23, 441). <sup>b</sup> FW 300 000 (T. Hopner and A. Trutwein, *Z. Naturforsch., Teil B*, 1972, 27, 1075). <sup>c</sup> FW 280 000 (R. Y. Hsu and H. A. Lardy, *J. Biol. Chem.*, 1967, 242, 520). <sup>d</sup> FW 58 000 (R. F. Colman, *J. Biol. Chem.*, 1968, 243, 2454). <sup>e</sup> FW 48 500 (S. Beekmans and L. Kanarek, *Eur. J. Biochem.*, 1977, 78, 437). <sup>f</sup> FW 48 500 (S. Suzuki, J. Yamaguchi, and M. Tokushige, *Biochim. Biophys. Acta*, 1973, 321, 369).



[equations (7) and (8)] exhibit equilibrium constants of 19.6 and 1.3 l mol<sup>-1</sup>, respectively. Thus, after light-induced generation of NADPH, the two carboxylation reactions are expected to proceed spontaneously.

Nevertheless, the net photosensitized CO<sub>2</sub>-fixation processes that form malic and isocitric acids (Figure 2) correspond to the reductive carboxylation of pyruvic and α-oxoglutaric acids by 2-mercaptoethanol [equation (9)] and D,L-dithiothreitol (DTT) [equation (10)], respectively. The CO<sub>2</sub>-fixation process to form malic acid is endoergic by ca. 11.5 kcal mol<sup>-1</sup> of product formed; in turn, the thermodynamic balance for the process that forms isocitric acid is estimated to be close to ΔG° ≈ 0. Since DTT is a relatively powerful reducing agent (E° ca. -0.3 V vs. hydrogen electrode), the process might exhibit endoergic properties if this electron donor was substituted with donors of weaker reducing properties, i.e. expected to lead to endoergic production of isocitric acid.

Finally, the fixation of CO<sub>2</sub> to formic acid by using FDH corresponds to the light-induced reduction of CO<sub>2</sub> by cysteine [equation (11)]. The thermodynamic balance of this process shows that it is endoergic by ca. 5.5 kcal. mol<sup>-1</sup> of formate formed and demonstrates that in this process light energy is converted and stored in the form of formic acid that might be considered as a fuel.

### Conclusions

The present study has revealed two approaches to the fixation of CO<sub>2</sub> where enzymes and natural cofactors act as catalysts in artificial chemical environments. One approach involves the carboxylation of α-oxo acids by CO<sub>2</sub> and elongation of the organic substrate chain by a single carbon atom. These carboxylation reactions represent the reverse of some processes that occur in the catabolic cycle in nature. For example, the light-induced formation of isocitric acid corresponds to the reverse of one step of the Krebs cycle where decarboxylation occurs. The photoinduced carboxylation reaction allows us to form synthetic building blocks for subsequent sequestered enzymic synthesis. The formation of aspartic acid from pyruvic acid demonstrates a route for the derivatization of organic substrate through the primary fixation of CO<sub>2</sub>. A second

approach for the fixation of CO<sub>2</sub> is exemplified by the formation of formate in the absence of a natural cofactor but with the enzyme FDH as biocatalyst. We have shown that various reduced relay systems act as artificial cofactors for the enzyme. Formate as product is of substantial interest as it acts as a hydrogen storage compound. Subsequent H<sub>2</sub> evolution or utilization of the formate hydride in hydrogenation reactions might be important routes.

The application of biocatalysts in artificial media reveals some complexity in tailoring the systems. Stabilization of the biocatalysts has been accomplished *via* specific and different methods such as immobilization on polymers, inclusion of electron donors that stabilize the enzymes, or lowering the temperature of the reaction medium.

### Acknowledgements

The support of the Belfer Center for Energy Research is gratefully acknowledged.

### References

- For a preliminary report, see I. Willner, D. Mandler, and A. Riklin, *J. Chem. Soc., Chem. Commun.*, 1986, 1022.
- (a) J. Bockris, 'Energy: The Solar Hydrogen Alternative,' Architectural Press, London, 1975; (b) M. Calvin, *Int. J. Energy Res.*, 1977, 1, 299.
- (a) 'Solar Power and Fuels,' ed. J. R. Bolton, Academic Press, New York, 1977; (b) 'Photochemical Conversion and Storage of Solar Energy,' ed. J. S. Connolly, Academic Press, New York, 1981.
- (a) A. J. Bard, *Science*, 1980, 207, 139; (b) N. Sutin and C. Creutz, *Pure Appl. Chem.*, 1980, 52, 2717; (c) M. Gratzel, *Acc. Chem. Res.*, 1981, 14, 376.
- 'Energy Resources Through Photochemistry and Catalysis,' ed. M. Gratzel, Academic Press, New York, 1983.
- (a) G. M. Brown, B. S. Brunschwig, C. Creutz, J. F. Endicott, and N. Sutin, *J. Am. Chem. Soc.*, 1979, 101, 1298; (b) M. Kirch, J.-M. Lehn, and J. P. Sauvage, *Helv. Chim. Acta*, 1979, 62, 1345; (c) A. I. Krasna, *Photochem. Photobiol.*, 1979, 29, 267.
- (a) P. Keller and A. Moradpour, *J. Am. Chem. Soc.*, 1980, 102, 7193; (b) J. Kiwi and M. Gratzel, *Angew. Chem., Int. Ed. Engl.*, 1979, 18, 623.
- (a) A. Henglein and A. Lilie, *J. Am. Chem. Soc.*, 1981, 103, 1059; (b) D. S. Miller and G. McLendon, *ibid.*, p. 6791.

- 9 (a) D. A. Palmer and R. V. Eldik, *Chem. Rev.*, 1983, 83, 651; (b) M. E. Volpin and I. S. Kolomnikow, *Organomet. React.* 1975, 5, 313.
- 10 (a) M. E. Volpin, *Pure Appl. Chem.*, 1972, 30, 607; (b) D. J. Darensbourg and R. A. Kudarowski, *Adv. Organomet. Chem.*, 1983, 22, 129.
- 11 (a) M. Spichiger-Ulmann and J. Augustynski, *J. Chem. Soc., Faraday Trans. 1*, 1985, 81, 713; (b) S. Kapusta and N. Hackerman, *J. Electrochem. Soc.*, 1983, 130, 607; (c) C. J. Stalker, S. Chao, D. P. Summers, and M. S. Wrighton, *J. Am. Chem. Soc.*, 1983, 105, 6318.
- 12 (a) M. Beley, J. P. Collin, R. Ruppert, and J. P. Sauvage, *J. Am. Chem. Soc.*, 1986, 108, 746; (b) C. M. Bolinger, B. P. Sullivan, D. Conrad, J. A. Gilbert, N. Story, and T. J. Meyer, *J. Chem. Soc., Chem. Commun.*, 1985, 796.
- 13 (a) H. Ishida, K. Tanaka, and T. Tanaka, *Chem. Lett.*, 1985, 405; (b) S. Slater and J. H. Wagenknecht, *J. Am. Chem. Soc.*, 1984, 106, 5367.
- 14 (a) J. Hawecker, J.-M. Lehn, and R. Ziessel, *J. Chem. Soc., Chem. Commun.* 1985, 56; (b) J.-M. Lehn and R. Ziessel, *Proc. Natl. Acad. Sci. USA*, 1982, 79, 701; (c) J. Hawecker, J.-M. Lehn, and R. Ziessel, *J. Chem. Soc., Chem. Commun.*, 1985, 536.
- 15 (a) J.-M. Lehn, Proc. 8th Int. Cong. Catalysis, Berlin (West), 1984, vol. 1, p. 73; (b) J. Hawecker, J.-M. Lehn, and R. Ziessel, *Helv. Chim. Acta*, 1986, 69, 1990.
- 16 B. Aurian-Blajeni, M. Halman, and J. Manassen, *Solar Energy*, 1980, 25, 165.
- 17 M. Halman, *Nature (London)*, 1978, 275, 115.
- 18 (a) R. Maidan and I. Willner, *J. Am. Chem. Soc.*, 1986, 108, 8100; (b) I. Willner, R. Maidan, D. Mandler, H. Dürr, G. Dörr, and K. Zengerle, *J. Am. Chem. Soc.*, 1987, 109, 6080.
- 19 D. Mandler and I. Willner, *J. Chem. Soc., Perkin Trans. 2*, 1986, 805.
- 20 D. Mandler and I. Willner, *J. Am. Chem. Soc.*, 1984, 106, 5352.
- 21 R. F. Homer and T. E. Tomlinson, *J. Chem. Soc.*, 1960, 2498.
- 22 E. Mondino, G. Bongiovanni, S. Fumero, and L. Ross, *J. Chromatogr.*, 1972, 74, 255.
- 23 A. Pollack, H. Blumenfeld, M. Wax, R. I. Baugh, and G. M. Whitesides, *J. Am. Chem. Soc.*, 1980, 102, 6324.
- 24 T. Hopner and J. Knappe in 'Methods of Enzymatic Analysis,' ed. H. U. Bergmeyer, Academic Press, New York, 1974.
- 25 R. Maidan and I. Willner, unpublished results.
- 26 R. K. Thauer, G. Fuchs, and K. Jungermann in 'Iron-Sulfur Proteins,' ed. W. Lowenberg, Academic Press, New York, 1977, vol. 3, p. 121.
- 27 A. M. Klivanov, B. N. Alberti, and S. E. Zale, *Biotechnol. Bioeng.*, 1982, 24, 25.
- 28 (a) E. Amouyal and B. Zidler, *Chem. Phys. Lett.*, 1980, 74, 314; (b) *Isr. J. Chem.*, 1982, 22, 117.
- 29 I. Willner, D. Mandler, and R. Maidan, *Nouv. J. Chim.*, 1987, 11, 109.

Received 6th July 1987; Paper 7/1204



## Visible-light-photoinduced Hydrogenation and Hydroformylation by Use of Water-soluble Rhodium Triphenylphosphine Complexes

Itamar Willner\* and Ruben Maidan

Department of Organic Chemistry, The Hebrew University of Jerusalem, Jerusalem 91904, Israel

Chlorotris-(3-diphenylphosphinobenzenesulphonate)rhodium  $[\text{Rh}^{\text{I}}\text{Cl}(\text{dpm})_3]^{3-}$ , acts as a homogeneous catalyst in the photosensitized hydrogenation of ethylene or acetylene and for the hydroformylation of ethylene in the presence of CO.

Considerable efforts are being directed towards the development of light-induced  $\text{H}_2$ -evolution processes using heterogeneous<sup>1,2</sup> and homogeneous<sup>3</sup> catalysts. Hydrogen atoms photogenerated *in situ* and bound to heterogeneous catalysts have been applied in the hydrogenation of unsaturated substrates<sup>4</sup> and of hydrogencarbonate.<sup>5</sup> Photogenerated hydrido transition metal complexes could provide homogeneous catalysts for a variety of hydrogen-transfer reactions.<sup>6</sup>

Recently, photoinduced  $\text{H}_2$ -evolution by use of a water-soluble Rh triphenylphosphine complex has been reported.<sup>7</sup> Here we report the photosensitized hydrogenation and hydroformylation of unsaturated substrates in aqueous media by use of chlorotris-(3-diphenylphosphinobenzenesulphonate)rhodium  $[\text{Rh}^{\text{I}}\text{Cl}(\text{dpm})_3]^{3-}$  (1),<sup>8</sup> as catalyst.

The hydrogenation system was composed of aqueous phthalate buffer (pH 4.5; 3 ml) containing trisbipyridineruthenium(II)  $[\text{Ru}(\text{bpy})_3]^{2+}$  ( $1.4 \times 10^{-4} \text{ M}$ ), as photosensitizer, the rhodium catalyst (1) ( $1.0 \times 10^{-4} \text{ M}$ ), and ascorbate as sacrificial electron donor ( $5 \times 10^{-2} \text{ M}$ ). To the deaerated system was added ethylene or acetylene (0.2 ml), and the solution was illuminated ( $\lambda > 400 \text{ nm}$ ) with a 150 W Xenon arc. In the presence of ethylene, photohydrogenation proceeded to form ethane with concomitant evolution of  $\text{H}_2$ . Photohydrogenation of acetylene yielded ethylene and ethane together with evolved  $\text{H}_2$ . In the absence of the unsaturated substrates only  $\text{H}_2$  evolution was observed. The rates of the photoinduced hydrogenations of ethylene or acetylene and the  $\text{H}_2$ -evolution rates in the presence and absence of the substrates are displayed in Figure 1(A).<sup>†</sup> It is evident that ethylene is hydrogenated to ethane, and that the hydrogenation products of acetylene are ethylene and ethane. It is also evident from Figure 1(A) that the sum of the amounts of hydrogenation products and concomitant hydrogen evolved with ethylene as substrate correspond to the total amount of  $\text{H}_2$  evolved in the absence of the unsaturated substrate. These results imply that a portion of the photogenerated hydrogen is utilized for the hydrogenation of ethylene or acetylene. Control experiments where the amount of photogenerated hydrogen was injected into an aqueous solution (pH 4.5) that included the catalyst (1) and the unsaturated substrate ethylene or acetylene revealed that no hydrogenation of the substrates occurs in the dark within 24 h. Thus, photohydrogenation of ethylene and acetylene involves an *in-situ* photogenerated hydridorhodium intermediate rather than photogenerated molecular hydrogen. It should be noted that hydrogenation of unsaturated substrates proceeds in the dark<sup>8</sup> in the presence of (1) at  $\text{H}_2$  pressure corresponding to 3 atm. However, in the photochemical experiments the partial photogenerated hydrogen pressure corresponds to ca. 0.1 atm.; consequently the dark process is prohibited. The quantum yields ( $\phi$ ) for photohydrogenation of ethylene and acetylene are 1.8 and 0.61%, respectively. The estimated

turnover numbers of the catalyst (1) are 40 and 13 in the corresponding two systems.

Introduction of carbon monoxide (1 ml) and ethylene (0.2 ml) to an aqueous solution (pH 4.5) of  $[\text{Ru}(\text{bpy})_3]^{2+}$ , the catalyst (1), and ascorbate as electron donor, and illumination ( $\lambda > 400 \text{ nm}$ ), results in the hydroformylation of ethylene to form propionaldehyde,<sup>‡</sup> with concomitant evolution of  $\text{H}_2$ . Under these conditions, no hydrogenation of ethylene to ethane occurs. The rate of propionaldehyde formation as a function of illumination time is displayed in Figure 1(B). The quantum yield for propionaldehyde formation ( $\phi$ ) is 0.1% and the turnover number of  $[\text{Rh}^{\text{I}}\text{Cl}(\text{dpm})_3]^{3-}$  (1) is 3.5. A control dark experiment where the photogenerated amount of  $\text{H}_2$  was injected into the aqueous system containing ethylene and CO revealed that no hydroformylation product was formed. Thus, propionaldehyde originates from a hydridorhodium complex rather than from photogenerated molecular hydrogen. It is well established<sup>10</sup> that under hydroformylation conditions,  $[\text{Rh}^{\text{I}}\text{Cl}(\text{PPh}_3)_3]$  is transformed into hydridocarbonyltris(triphenylphosphine)rhodium(I)  $[\text{RhH}(\text{CO})(\text{PPh}_3)_3]$ . Indeed, substitution of (1) by  $[\text{RhH}(\text{CO})(\text{dpm})_3]^{3-}$  (2) in the photochemical system results in the hydroformylation of ethylene at a rate similar to that observed with (1). This suggests that  $[\text{RhH}(\text{CO})(\text{dpm})_3]^{3-}$  is the actual hydroformylation catalyst, with (1) as precursor.

The photosensitized transformation that leads to the reduction of  $[\text{Rh}^{\text{I}}\text{Cl}(\text{dpm})_3]^{3-}$  (1) has been elucidated by laser flash photolysis. The primary step involves the reductive quenching of excited  $[\text{Ru}(\text{bpy})_3]^{2+}$  by ascorbate ( $\text{HA}^-$ ) [equation (1)].<sup>3a</sup> The resulting  $[\text{Ru}(\text{bpy})_3]^+$ ,  $E^0 = -1.28 \text{ V vs. normal hydrogen electrode (n.h.e.)}$ ,<sup>11</sup> reduces  $[\text{Rh}^{\text{I}}\text{Cl}(\text{dpm})_3]^{3-}$  [equation (2)].

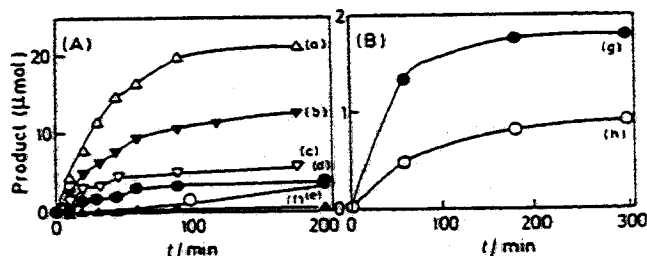
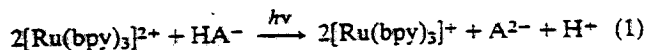


Figure 1. Rates of photoinduced formation of: (A) hydrogenation products and (B) hydroformylation products: (a)  $\text{H}_2$  evolution in the absence of unsaturated substrate; (b) ethane formation from ethylene; (c)  $\text{H}_2$  evolution concomitant with ethylene hydrogenation; (d) ethylene formation from acetylene; (e)  $\text{H}_2$  evolution concomitant with acetylene hydrogenation; (f) ethane formation from acetylene; (g)  $\text{H}_2$  evolution concomitant with ethylene hydroformylation; (h) propionaldehyde formation from ethylene and CO.

<sup>†</sup> The gaseous products were analysed by g.l.c. (MS 5A column for hydrogen; Spherosil XOB 075 column for hydrocarbons).

<sup>‡</sup> Propionaldehyde concentration was determined by h.p.l.c. analysis of the dinitrophenylhydrazone.<sup>12</sup>

# Photochemically Induced Oxidative and Reductive Regeneration of NAD(P)<sup>+</sup>/NAD(P)H Cofactors: Applications in Biotransformations

ITAMAR WILLNER,\* RUBEN MAIDAN AND BILHA WILLNER  
Department of Organic Chemistry and  
The Fritz Haber Research Center for Molecular Dynamics  
The Hebrew University of Jerusalem, Jerusalem 91904, Israel

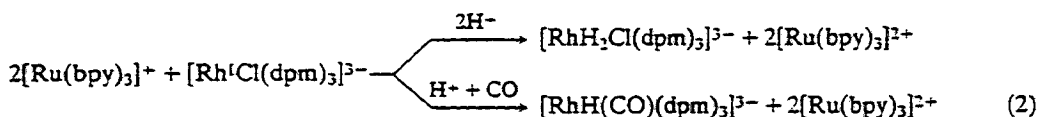
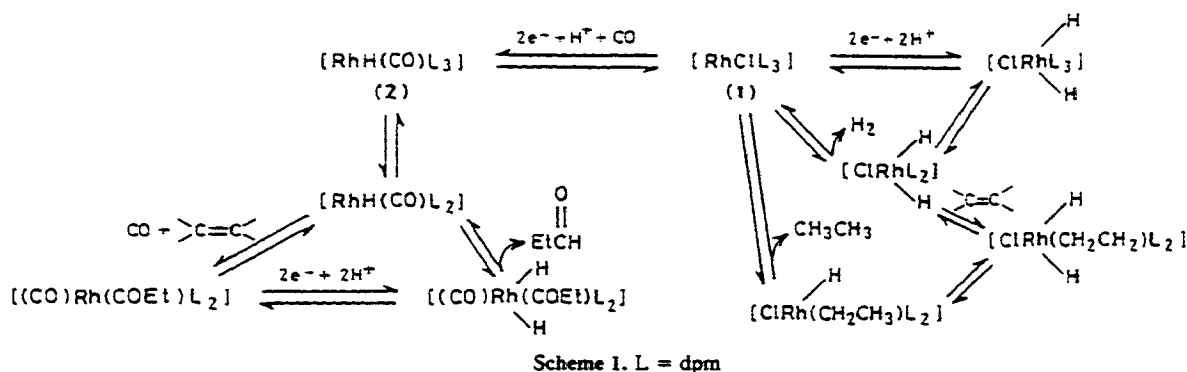
(Received 10 June 1989)

**Abstract.** Photosensitized regeneration of NAD(P)H cofactors is accomplished by biocatalyzed and artificially catalyzed transformations in photochemical assemblies. Photogenerated *N,N'*-dimethyl-4,4'-bipyridinium radical cation, MV<sup>•+</sup>, acts as electron carrier for the reduction of NADPH in the presence of the enzyme ferredoxin reductase and for the reduction of NADH in the presence of lipoamide dehydrogenase. For the photogeneration of MV<sup>•+</sup> and subsequent NADPH formation, three different photosensitizers are applied: Ru(bpz)<sub>3</sub><sup>2+</sup>, Ru(bpy)<sub>3</sub><sup>2+</sup>, and Zn-TMPyP<sup>4+</sup>. The highest quantum yield for NADPH formation is observed with Ru(bpz)<sub>3</sub><sup>2+</sup> and is  $\phi = 1.7 \times 10^{-1}$ . For NADH regeneration only Zn-TMPyP<sup>4+</sup> can be applied. Ru(bpy)<sub>3</sub><sup>2+</sup> and Ru(bpz)<sub>3</sub><sup>2+</sup> interact with NADH in their excited or oxidized forms and therefore cannot be used as light-active compounds in the system. The NADPH regeneration cycle has been coupled to the biocatalyzed synthesis of glutamic acid. Although Ru(bpz)<sub>3</sub><sup>2+</sup> is 42.5-fold more efficient than Ru(bpy)<sub>3</sub><sup>2+</sup> in the regeneration of NADPH, the synthesis of glutamic acid is improved only by a factor of 2 in the presence of Ru(bpz)<sub>3</sub><sup>2+</sup>, implying that the coupled process is rate limiting. Oxidative regeneration of the NAD<sup>+</sup> cofactor is accomplished in a photosystem that includes Ru(bpy)<sub>3</sub><sup>2+</sup> as photosensitizer. The photoprocess is coupled to dehydrogenation of ethanol, propanol, lactic acid, and alanine with concomitant H<sub>2</sub> evolution. A photosystem that includes Ru(bpy)<sub>3</sub><sup>2+</sup> as photosensitizer, ascorbate as electron donor, and chloro-*tris*-(3-diphenylphosphino-benzene sulfonate)Rh(I), RhCl(dpm)<sub>3</sub><sup>-</sup>, is catalytically active in the photoinduced regeneration of NAD(P)H cofactors. Mechanistic investigations show that photogenerated Ru(bpy)<sub>3</sub><sup>2+</sup> mediates the generation of a hydrido-rhodium complex that acts as a charge relay for the production of NAD(P)H.

Application of enzymes as biocatalysts in biotransformations find increasing interest as a selective and effective means for the synthesis of valuable chemicals.<sup>1,2</sup> Substantial progress has been made in recent years in the immobilization of enzymes to various solid matrices and the design of continuous systems of commercial utility.<sup>3</sup> A significant number of natural enzymes require the participation of a cofactor for their activity. Cofactor-dependent enzymes can be classified into sub-classes — enzymes that include the cofactors in the catalytic assembly and that the cofactor does not require a self-regeneration for the biocatalytic process. Cofactors such as pyridoxal phosphate, lipoic acid, biotin, flavin, or porphyrins do not require their regen-

eration. Enzymes such as oxygenases and hydroxylases (that include flavin cofactors) transaminases (including pyridoxal phosphate), carboxylases (that include biotin or lipoic acid as cofactor), and monooxygenases, peroxidase, or mutase (that include porphyrin cofactors) belong to the first subclass of cofactor dependent enzymes. The second subclass involves enzymes that require the participation of cofactors that require their separate regeneration by an enzymatic process. Namely, the cofactor is formed in a biocatalytic process and supplied to the enzymes for the specific biotrans-

\* Author to whom correspondence should be addressed.



The subsequent hydrogenation<sup>12</sup> and hydroformylation<sup>10</sup> reactions by hydridorhodium complexes have been the subject of numerous studies. Scheme 1 represents a possible route that utilizes the photogenerated hydridorhodium product in subsequent H<sub>2</sub> evolution, hydrogenation, and hydroformylation processes.

In conclusion, we have demonstrated that photohydrogenation and photohydroformylation of unsaturated substrates proceed with a water-soluble Rh<sup>I</sup> homogeneous catalyst. The stability of these systems is limited. Spectroscopic studies reveal that the photosensitizer [Ru(bpy)<sub>3</sub>]<sup>2+</sup> is degraded, presumably through photoinduced ligand dissociation to form [Ru(bpy)<sub>2</sub>(dpm)]<sup>+</sup>, and thus a search for other sensitizers and catalysts is desirable. Preliminary studies indicate that ruthenium, rhenium, and palladium dpm complexes are also active H<sub>2</sub>-evolution, hydrogenation, and hydroformylation catalysts.

This research was supported by the Berman Foundation Grant.

Received, 26th November 1987; Com. 1721

## References

- 1 'Energy Resources Through Photochemistry and Catalysis,' ed. M. Grätzel. Academic Press, New York, 1983; 'Photogeneration of Hydrogen,' eds. A. Harriman and M. E. West, Academic Press, London, 1983.
- 2 P. Keller, A. Moradpour, A. Amoyal, and H. B. Kagan, *Nouv. J. Chim.*, 1980, 6, 377; M. Kirch, J.-M. Lehn, and J.-P. Sauvage, *Helv. Chim. Acta*, 1979, 62, 1345.
- 3 (a) C. V. Krishnan and N. Sutin, *J. Am. Chem. Soc.*, 1981, 103, 2141; (b) V. Houlding, T. Geiger, U. Kolle, and M. Grätzel, *Helv. Chim. Acta*, 1978, 61, 2720.
- 4 Y. Degani and I. Willner, *J. Chem. Soc., Perkin Trans. 2*, 1986, 37; D. Mandler and I. Willner, *J. Phys. Chem.*, 1987, 91, 3600.
- 5 D. Mandler and I. Willner, *J. Am. Chem. Soc.*, 1987, 109, 7884.
- 6 'Homogeneous Catalysis with Metal Phosphine Complexes,' ed. L. H. Pignolet, Plenum, New York, 1983.
- 7 S. Oishi, *J. Mol. Catal.*, 1987, 39, 225.
- 8 A. F. Borowski, D. J. Cole-Hamilton, and G. Wilkinson, *Nouv. J. Chim.*, 1978, 2, 137.
- 9 K. Fung and D. Grosjean, *Anal. Chem.*, 1981, 53, 168.
- 10 F. H. Jardine, *Polyhedron*, 1982, 1, 569.
- 11 K. Kalyanasundaram, *Coord. Chem. Rev.*, 1982, 46, 159.
- 12 F. H. Jardine, *Prog. Inorg. Chem.*, 1981, 28, 63.

## On the Structure of Alkali Metal Triphenylstannide Salts in Solution and in the Solid State

Thomas Birchall\* and Joseph A. Vetrone

Department of Chemistry and the Institute for Materials Research, 1280 Main St. West, Hamilton, Ontario L8S 4M1, Canada

Mössbauer data are reported for the Li<sup>+</sup>, Na<sup>+</sup>, and K<sup>+</sup> salts of the triphenylstannide anion; the X-ray crystal structure of Ph<sub>3</sub>SnK(18-crown-6) shows that the triphenylstannide is a naked pyramidal ion (Sn-C 2.224 Å, C-Sn-C, 96.9°): no solvent molecules are incorporated into the structure.

Salts of the triphenylstannide anion have not been well characterized, either in solution or in the solid state, although they are widely used in the syntheses of both organic and inorganic compounds.<sup>1</sup> These anions are easily generated in solution either by treating the parent hydride with alkali metal,<sup>2</sup> or by cleavage of hexaphenylditin, again by alkali metals.<sup>3</sup> The tin-119 Mössbauer spectrum of solid triphenyl-

stannyl-lithium has been reported and shows only a single absorption line.<sup>4</sup> We now report the single crystal X-ray structure of triphenylstannylpotassium-18-crown-6.

For the series of triphenylstannide salts, cation-anion interactions should strongly affect the <sup>119</sup>Sn Mössbauer parameters. We have therefore examined these species as frozen solutions by Mössbauer spectroscopy. Spectra of these

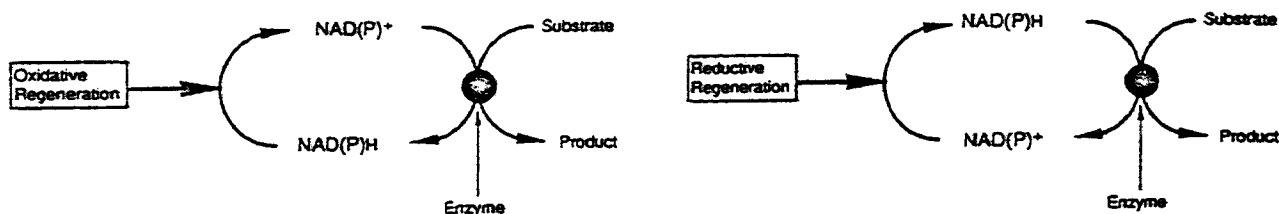
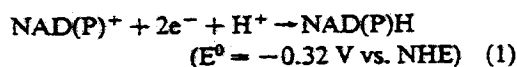


Fig. 1. Biocatalyzed transformations through  $\text{NAD(P)}^+ \rightleftharpoons \text{NAD(P)H}$  regeneration systems.

formation. Cofactors such as adenosine-triphosphate, ATP, nicotinamide dinucleotide,  $\text{NAD}^+$ , nicotinamide dinucleotide phosphate,  $\text{NADP}^+$ , and coenzyme A, CoA, belong to the group of cofactors that require separate regeneration. It is assumed that ca. 70% of the enzymes belong to this class, where the participating cofactor needs separate regeneration.

Nicotinamide cofactors,  $\text{NAD(P)}^+$ , are important cofactors in many oxidative or reductive transformations catalyzed by oxido-reductases. Various transformations require the oxidized form of the cofactor  $\text{NAD(P)}^+$ , while others depend on the reduced form of the cofactor,  $\text{NAD(P)H}$  (eq. 1). Two general schemes



for the oxidative and reductive regeneration of the  $\text{NAD(P)}^+/\text{NAD(P)H}$  cofactors are outlined in Fig. 1. Substantial efforts are directed towards the development of systems for the regeneration of  $\text{NAD(P)}^+/\text{NAD(P)H}^{2,4,5}$  cofactors.

Biocatalyzed chemical regeneration of these cofactors has been extensively studied.<sup>6</sup> Figure 2 summarizes some of the biocatalytic processes for the oxidative

regeneration of  $\text{NAD(P)}^+$  cofactors and Fig. 3 exemplifies enzyme-catalyzed reductive regeneration of  $\text{NAD(P)H}$  cofactors. Electrochemical regeneration of  $\text{NAD(P)H}$  cofactors has also been examined.<sup>7</sup> The direct electroreduction of  $\text{NAD(P)}^+$  leads to the biocatalytically inactive dimerization product of the one-electron reduction product,  $\text{NADP}^\cdot$ . Yet, the electrochemically generated methyl viologen (*N,N'*-dimethyl-4,4'-bipyridinium) radical cation,  $\text{MV}^{\cdot+}$ , that acts as

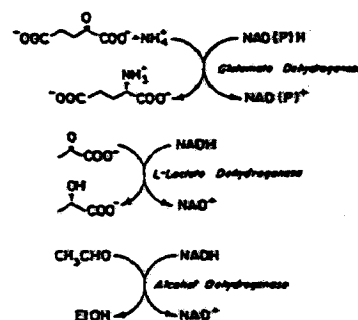


Fig. 2. Biocatalyzed systems for regeneration of  $\text{NAD(P)}^+$  cofactors.

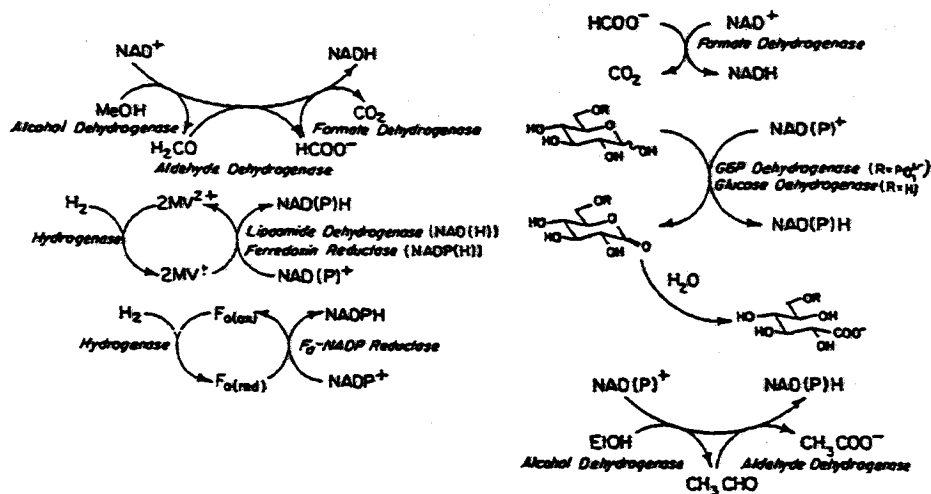
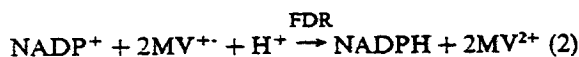


Fig. 3. Biocatalyzed systems for regeneration of  $\text{NAD(P)H}$  cofactors.

electron carrier, mediates the effective reductive regeneration of  $\text{NADP}^+$  to  $\text{NADPH}$  in the presence of ferredoxin-NADP-reductase (FDR, EC1.18.1.2) (eq. 2).<sup>8</sup> The oxidative electrochemical regeneration of  $\text{NAD}^+$  proceeds on Pt electrodes with a 90–99.3% efficiency,<sup>9</sup> and is further improved by immobilization of catechol or enzymes on the electrode.<sup>10</sup>



Photosensitized electron transfer reactions have been examined extensively in recent years as a means of solar energy conversion and storage.<sup>11–13</sup> Electron transfer products can be formed by quenching an excited species (photosensitizer,  $\text{S}^*$ ; Fig. 4). The quenching process can occur through reductive quenching of the excited photosensitizer by an electron donor, D. The resulting reduced photoproduct can then reduce an electron acceptor, resulting in the oxidized and reduced photoproducts,  $\text{D}^+$  and  $\text{A}^-$ . Alternatively, oxidative quenching of the excited species (Fig. 4B) results in the reduced electron acceptor and oxidized photosensitizer. The subsequent oxidation of the electron donor recycles the light-active compounds and yields the photoproducts  $\text{D}^+$  and  $\text{A}^-$ . Reductive regeneration of  $\text{NAD(P)H}$  cofactors could be envisaged by applying  $\text{NAD(P)}^+$  as an electron acceptor in such cycles, or, alternatively, through reduction of  $\text{NAD(P)}^+$  by an intermediary artificial electron carrier,  $\text{A}^-$ , that mediates the reduction of the cofactor. Similarly, oxidative regeneration of  $\text{NADPH}$  could proceed through

direct application of reduced  $\text{NAD(P)H}$  cofactors as electron donors in the photosensitized electron transfer reactions or sequential oxidation of the  $\text{NAD(P)H}$  by the intermediary "hole carrier",  $\text{D}^+$ . Various transition metal complexes such as metal bipyridine complexes<sup>14</sup> or metalloporphyrins<sup>15</sup> or organic dyes, i.e., flavins, exhibit proper photophysical properties for their application as light-active compounds in photosensitized electron transfer reactions. Indeed, photoinduced oxidative regeneration of  $\text{NAD(P)}^+$  cofactors has been accomplished with various organic dyes.<sup>17</sup> For example, photoexcited methylene blue,  $\text{MB}^+$ , or *N*-methylphenazonium methyl sulfate undergoes reductive quenching by  $\text{NAD(P)H}$ . The reductive regeneration of  $\text{NAD(P)H}$  cofactors has been developed recently in our laboratory.<sup>18</sup> We have applied photosensitized electron transfer reactions that generate  $\text{MV}^{2+}$  as primary electron carrier, which mediates the reduction of  $\text{NAD}^+$  to  $\text{NADH}$  in the presence of lipoamide dehydrogenase (LipDH, EC1.6.4.3) and of  $\text{NADP}^+$  to  $\text{NADPH}$  in the presence of FDR. Previous studies<sup>19</sup> reported on the application of the photoinduced regeneration of  $\text{NAD(P)H}$  cofactors in various biotransformations, such as reduction of ketones and keto-acids, reductive amination of keto-acids to amino acids, carboxylation and  $\text{CO}_2$ -fixation processes,<sup>20</sup> and multi-step biocatalytic transformations.<sup>19,20</sup>

In the present study, we describe the further developments in the photosensitized oxidative and reductive regeneration of  $\text{NAD(P)}^+/\text{NAD(P)H}$  cofactors and their application in synthetic routes. We demonstrate that the photophysical properties of the photosensitizers in respect to the reduced cofactor,  $\text{NAD(P)H}$ , control their potential application in oxidative or reductive regeneration cycles. Also, the efficiencies and stabilities of the regeneration systems are affected by the nature of the photosensitizer. Furthermore, we demonstrate an example of light-induced regeneration of  $\text{NAD(P)H}$  cofactors using an artificial homogeneous  $\text{Rh(I)}$  complex that substitutes for the natural biocatalyst.

#### EXPERIMENTAL SECTION

Absorption spectra were recorded with a Uvikon-810 (Kontron) spectrophotometer. Gas chromatographic analyses were performed with Hewlett-Packard 5890 and Tracor-540 gas chromatographs. Liquid chromatography analyses were performed with a Merck-Hitachi 655A-11 HPLC or with an LKB amino acid analyzer. All chemicals and biochemicals were obtained from Sigma or Aldrich. Ruthenium(II)-tris-bipyridine dichloride,<sup>22</sup>  $\text{Ru}(\text{bpy})_3\text{Cl}_2$ , ruthenium(II)-tris-bipyrazine dichloride,<sup>23</sup>  $\text{Ru}(\text{bpz})_3\text{Cl}_2$ , zinc(II)-meso-tetra-

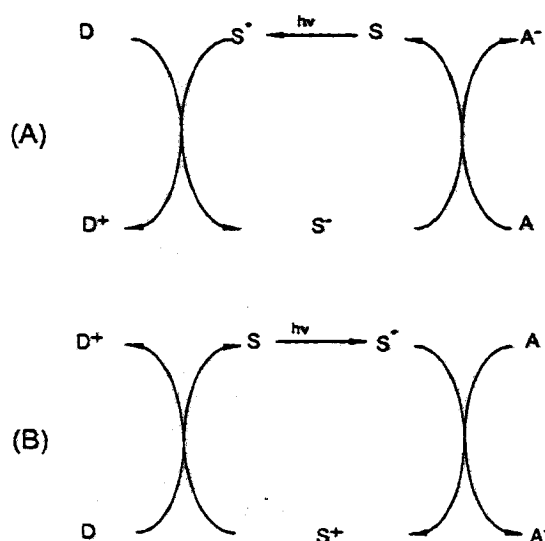


Fig. 4. Photosensitized electron transfer cycles: (A) Through reductive quenching. (B) Through oxidative quenching.

methylpyridinium porphyrin iodide,<sup>24</sup> ZnMPyPI<sub>2</sub>, and chlorotris-(3-diphenylphosphinobenzenesulfonate) rhodium (I),<sup>25</sup> RhCl(dpm)<sub>3</sub><sup>-</sup>, were prepared according to published procedures.

Illumination of samples was performed at room temperature with a 150-W xenon arc lamp in a glass cuvette (4 ml) equipped with a small magnetic stirrer, a valve, and serum stopper. Light was filtered through a 400-nm cutoff filter. The samples (3 ml) were deaerated before illumination by repeated evacuation followed by oxygen-free argon flushings.

#### Photoinduced Biocatalyzed NADPH Regeneration

The systems are composed of 3 ml tris buffer solution, pH = 7.7, that includes *N,N'*-dimethyl-4,4'-bipyridinium, MV<sup>2+</sup>,  $5 \times 10^{-4}$  M, the cofactor NADP<sup>+</sup>,  $1 \times 10^{-3}$  M, the enzyme FDR, 0.2 units, mercaptoethanol,  $2 \times 10^{-2}$  M, and one of the photosensitizers, Ru(bpy)<sub>3</sub><sup>2+</sup>,  $6.2 \times 10^{-5}$  M or Zn-TMPyP<sup>4+</sup>,  $7 \times 10^{-6}$  M. The system that applies Ru(bpz)<sub>3</sub><sup>2+</sup> as photosensitizer includes a similar composition, but the electron donor mercaptoethanol is substituted by triethanolamine, TEOA,  $2 \times 10^{-2}$  M and the photosensitizer Ru(bpz)<sub>3</sub><sup>2+</sup>,  $6.3 \times 10^{-5}$  M is included. The production of NADPH and MV<sup>+</sup> as a function of illumination time was followed spectroscopically at time intervals of illumination at  $\lambda = 340$  nm ( $\epsilon = 6.2 \times 10^3$  M<sup>-1</sup> cm<sup>-1</sup>) and  $\lambda = 602$  nm ( $\epsilon = 1.25 \times 10^4$  M<sup>-1</sup> cm<sup>-1</sup>), respectively.

#### Photoinduced Biocatalyzed NADH Regeneration

The system is composed of 3 ml tris buffer solution, pH = 8.0, that includes Zn-TMPyP<sup>4+</sup>,  $6.5 \times 10^{-6}$  M; MV<sup>2+</sup>,  $4 \times 10^{-3}$  M; NAD<sup>+</sup>,  $1 \times 10^{-3}$  M; mercaptoethanol,  $2 \times 10^{-2}$  M; and the enzyme LipDH, 100 units. Production of NADH was followed spectroscopically at time intervals of illumination,  $\lambda = 340$  nm ( $\epsilon = 6.2 \times 10^3$  M<sup>-1</sup> cm<sup>-1</sup>).

#### Photoinduced NAD(P)H Regeneration with the Homogeneous Catalyst RhCl(dpm)<sub>3</sub><sup>-</sup>

The systems are composed of 2.5 ml phosphate buffer, pH = 6.6, that contains Ru(bpy)<sub>3</sub><sup>2+</sup>,  $1.4 \times 10^{-3}$  M; ascorbate,  $5 \times 10^{-2}$  M; NAD<sup>+</sup> or NADP<sup>+</sup>,  $3 \times 10^{-4}$  M; and RhCl(dpm)<sub>3</sub><sup>-</sup>,  $2.0 \times 10^{-4}$  M. Formation of NAD(P)H was followed spectroscopically at  $\lambda = 340$  nm. The coupled reduction of acetaldehyde was examined in a system composed of 3 ml phosphate buffer, pH = 6.8, that includes Ru(bpy)<sub>3</sub><sup>2+</sup>,  $1.40 \times 10^{-3}$  M; ascorbate,  $5.0 \times 10^{-2}$  M; RhCl(dpm)<sub>3</sub><sup>-</sup>,  $2.0 \times 10^{-4}$  M; NAD<sup>+</sup>,  $3.0 \times 10^{-4}$  M; horse liver alcohol dehydrogenase (AlcDH, EC1.1.1.1), 2 units; and acetaldehyde,  $1.8 \times 10^{-2}$  M. Ethanol formation was followed by gas chromatography with a Porapak T Column.

#### Photosensitized Synthesis of Glutamic Acid

The systems are composed of 3 ml tris buffer solution, pH = 8.0, that includes  $\alpha$ -ketoglutaric acid, 0.1 M; MV<sup>2+</sup>,  $4 \times 10^{-4}$  M; NH<sub>3</sub>, 0.1 M; NADP<sup>+</sup>,  $1 \times 10^{-3}$  M; and the enzymes FDR, 0.2 units, and glutamate dehydrogenase (GluDH, EC1.4.1.3), 42.5 units. The system also included

Ru(bpy)<sub>3</sub><sup>2+</sup>,  $6.2 \times 10^{-5}$  M; and mercaptoethanol,  $2 \times 10^{-2}$  M; or Ru(bpz)<sub>3</sub><sup>2+</sup>,  $6.3 \times 10^{-5}$  M; and TEOA,  $2 \times 10^{-2}$  M, as photosensitizer and electron donor, respectively. The deaerated systems were illuminated and samples (100  $\mu$ l) were taken from the systems at time intervals of illumination. Each sample was treated with 5-sulfosalicylic acid to precipitate enzymes, as described elsewhere.<sup>26</sup> Glutamic acid content was followed with an amino acid analyzer.

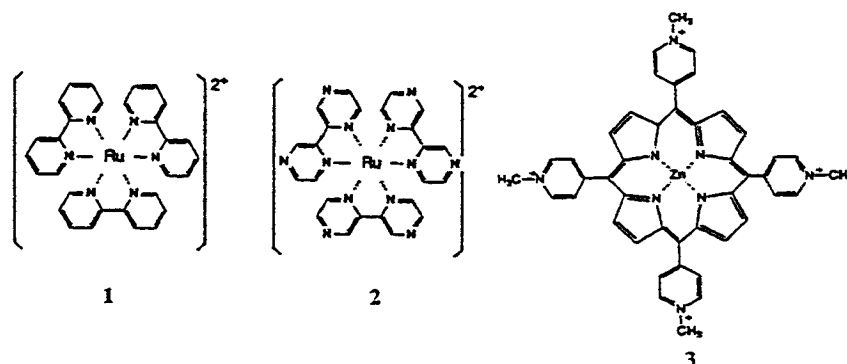
#### Photoinduced NAD<sup>+</sup> Regeneration

The systems are composed of 3 ml aqueous phosphate buffer solution, pH = 6.8, that includes Ru(bpy)<sub>3</sub><sup>2+</sup>,  $1 \times 10^{-4}$  M; MV<sup>2+</sup>,  $1.4 \times 10^{-3}$  M; NAD<sup>+</sup>,  $1.2 \times 10^{-3}$  M; and one of the following substrates and corresponding enzymes: ethanol,  $3.5 \times 10^{-1}$  M, and alcohol dehydrogenase, AlcDH, 0.2 units; propanol,  $2.5 \times 10^{-1}$  M, and AlcDH, 0.2 units; alanine,  $1.8 \times 10^{-1}$  M, and L-alanine dehydrogenase (AlaDH, EC1.4.1.1), 0.4 units. The system that uses lactic acid as substrate is composed of a phosphate buffer, aqueous solution pH = 8.2, that includes Ru(bpy)<sub>3</sub><sup>2+</sup>,  $1 \times 10^{-4}$  M, *N,N'*-dimethylene-2,2'-bipyridinium (DQ<sup>2+</sup>),  $5 \times 10^{-3}$  M; NAD<sup>+</sup>,  $1.2 \times 10^{-3}$  M; the substrate lactic acid,  $1.0 \times 10^{-1}$  M; and lactate dehydrogenase (LacDH, EC1.1.1.27), 8 units. A Pt colloid stabilized by citrate<sup>27</sup> (20 mg liter<sup>-1</sup> Pt) is included in the systems for H<sub>2</sub> evolution. Hydrogen formation at time intervals of illumination was determined by gas chromatography sampling, using a 5 Å molecular sieve column and argon as carrier gas. The dehydrogenation products, acetaldehyde and propionaldehyde, were determined by gas chromatography using a Porapak T column; pyruvic acid was determined by ion chromatography using a Wescan anion exclusion column and  $2 \times 10^{-3}$  M H<sub>2</sub>SO<sub>4</sub> as eluent.

## RESULTS AND DISCUSSION

#### Photoinduced Biocatalyzed Reductive Regeneration of NAD(P)H Cofactors

MV<sup>+</sup> mediates the enzyme-catalyzed reduction of NAD(P)<sup>+</sup> to NAD(P)H. LipDH and FDR catalyze the production of NADH and NADPH, respectively. The photosensitized production of MV<sup>+</sup> has been described in various photosystems that use transition metal complexes such as Ru(bpy)<sub>3</sub><sup>2+</sup> or Zn-porphyrins.<sup>28</sup> We have compared the effectiveness of NAD(P)H regeneration using three different photosensitizers: Ru(bpy)<sub>3</sub><sup>2+</sup> (1), Ru(bpz)<sub>3</sub><sup>2+</sup> (2), and Zn-TMPyP<sup>4+</sup> (3). These photosensitizers differ in their spectral absorption properties in the visible region. Ru(bpy)<sub>3</sub><sup>2+</sup> absorbs at  $\lambda_{\max} = 452$  nm,  $\epsilon = 14,600$  M<sup>-1</sup>·cm<sup>-1</sup>; Ru(bpz)<sub>3</sub><sup>2+</sup> absorbs at  $\lambda_{\max} = 440$  nm,  $\epsilon = 15,000$  M<sup>-1</sup>·cm<sup>-1</sup>; and Zn-TMPyP<sup>4+</sup> exhibits the Soret absorption band at  $\lambda_{\max} = 433$  nm,  $\epsilon = 180,000$  M<sup>-1</sup>·cm<sup>-1</sup> and an extended Soret band of lower intensity at  $\lambda = 560$  nm.



The systems were composed of aqueous buffer solution, pH = 8.0, that included one of the photosensitizers  $\text{Ru}(\text{bpy})_3^{2+}$ ,  $\text{Ru}(\text{bpz})_3^{2+}$ , or  $\text{Zn-TMPyP}^{4+}$ ,  $\text{MV}^{2+}$  as primary relay,  $\text{NADP}^+$  or  $\text{NAD}^+$ , and the enzymes FDR or LipDH, respectively. The electron donor, mercaptoethanol, was used in the systems that applied  $\text{Ru}(\text{bpy})_3^{2+}$  or  $\text{Zn-TMPyP}^{4+}$  as photosensitizers, while TEOA was included as electron donor in the system that included  $\text{Ru}(\text{bpz})_3^{2+}$  as photosensitizer.

Illumination of the photosystems that include the  $\text{NADP}^+$  cofactor and the biocatalyst FDR results in the formation of NADPH. Figure 5, for example, displays the formation of NADPH ( $\lambda = 340 \text{ nm}$ ) at time intervals of illumination in the system that applies

$\text{Ru}(\text{bpz})_3^{2+}$  as photosensitizer. The rate of NADPH formation as a function of the einsteins absorbed by the systems is displayed in Fig. 6. Table 1 summarizes the quantum yields and initial rates of NADPH formation in the various systems. It is evident that the system that includes  $\text{Ru}(\text{bpz})_3^{2+}$  as photosensitizer is the most effective, while the system that applies  $\text{Zn-TMPyP}^{4+}$  is ca. 4.25-fold more effective than that which uses  $\text{Ru}(\text{bpy})_3^{2+}$  as photosensitizer. It should be noted that the system that includes  $\text{Ru}(\text{bpz})_3^{2+}$  as photosensitizer does not operate in the formation of  $\text{MV}^{2+}$  with mercaptoethanol as electron donor. However, in the presence of TEOA as electron donor  $\text{Ru}(\text{bpz})_3^{2+}$  is active in the production of  $\text{MV}^{2+}$ , implying that this photosen-

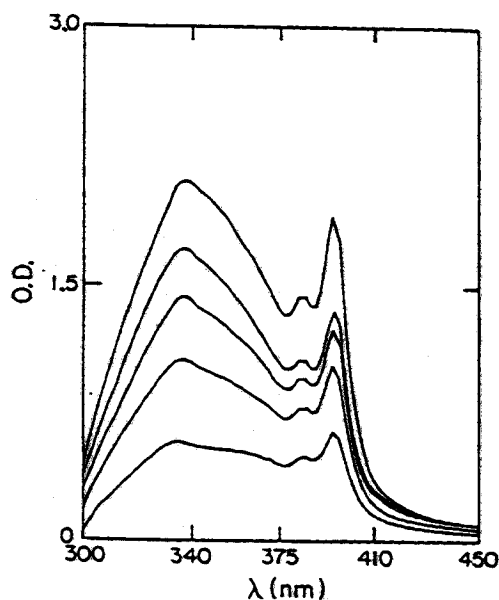


Fig. 5. Spectra of NADPH and  $\text{MV}^{2+}$  at 20-second time intervals of illumination in the system:  $[\text{Ru}(\text{bpz})_3^{2+}] = 6.3 \times 10^{-5} \text{ M}$ ,  $[\text{MV}^{2+}] = 5 \times 10^{-4} \text{ M}$ ,  $[\text{TEOA}] = 2.10^{-2} \text{ M}$ ,  $[\text{NADP}^+] = 1 \times 10^{-3} \text{ M}$ , FDR = 0.2 units.

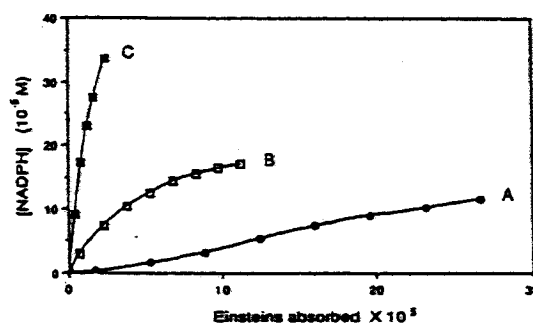


Fig. 6. Rate of NADPH formation as a function of light absorbed by the systems including the photosensitizers: (A)  $\text{Ru}(\text{bpy})_3^{2+}$ ; (B)  $\text{Zn-TMPyP}^{4+}$ ; (C)  $\text{Ru}(\text{bpz})_3^{2+}$ .

Table 1. Efficiency of NADPH Regenerated by the Various Photosensitizers

Photosensitizer	Rate of NADPH regeneration ( $\text{mol} \cdot \text{min}^{-1}$ )	Quantum yield ( $\phi$ ) of NADPH
$\text{Ru}(\text{bpz})_3^{2+}$	$9.2 \times 10^{-2}$	$1.7 \times 10^{-1}$
$\text{Zn-TMPyP}^{4+}$	$1.6 \times 10^{-2}$	$4 \times 10^{-2}$
$\text{Ru}(\text{bpy})_3^{2+}$	$6.8 \times 10^{-3}$	$4 \times 10^{-3}$

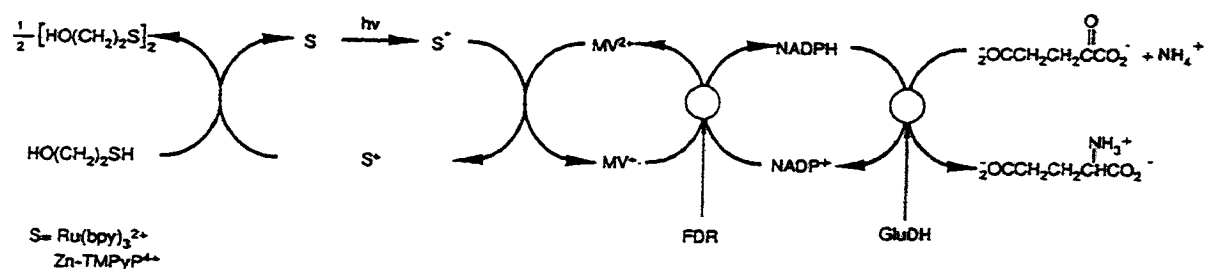
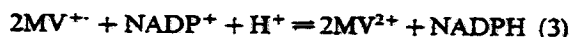
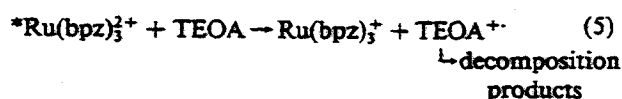
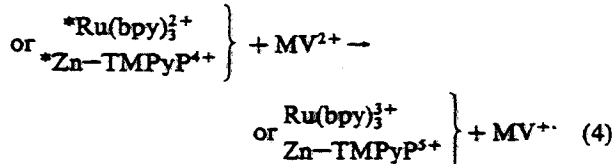


Fig. 7. Scheme for cyclic photosensitized regeneration of the NADPH cofactor, and subsequent biocatalyzed synthesis of glutamic acid.

sensitizer operates by a different mechanism than the other two photosensitizers, Zn-TMPyP<sup>4+</sup> and Ru(bpy)<sub>3</sub><sup>2+</sup> in the generation of the electron transfer product MV<sup>•+</sup>. Elimination of the enzyme FDR from the systems prohibits the formation of NADPH, and MV<sup>•+</sup> is accumulated in the systems upon illumination. Control experiments reveal that without illumination no formation of MV<sup>•+</sup> or NAD(P)H takes place. Furthermore, Fig. 5 shows that MV<sup>•+</sup> is in equilibrium (eq. 3) with NADPH and both of the products are accumulated in the system. The equilibrium constant of this process has been estimated to be  $K = (7.9 \pm 2.8) \times 10^{10} \text{ M}^{-1}$ .



These results indicate that photogenerated MV<sup>•+</sup> acts as an electron carrier that mediates the biocatalyzed reduction of NADP<sup>+</sup> (Fig. 7). The photophysical properties of the various sensitizers are well established, and the formation of MV<sup>•+</sup> in the systems proceeds by different routes. With Ru(bpy)<sub>3</sub><sup>2+</sup> and Zn-TMPyP<sup>4+</sup> oxidative electron-transfer quenching of the excited states results in the formation of MV<sup>•+</sup> (eq. 4). The oxidized photosensitizer subsequently oxidizes mercaptoethanol and the light-active compound is recycled. With Ru(bpz)<sub>3</sub><sup>2+</sup> as photosensitizer, the primary step involves reductive quenching by TEOA (eq. 5). The reduced photoproduct, Ru(bpz)<sub>3</sub><sup>•+</sup> ( $E^0 = -0.86 \text{ V vs. SCE}$ ) subsequently reduces MV<sup>2+</sup> ( $E^0 \text{ MV}^{2+}/\text{MV}^{\bullet+} = -0.42 \text{ V}$ ) (eq. 6).



These results allow us to summarize the photochemical route that leads to the regeneration of the NADPH cofactor by Ru(bpy)<sub>3</sub><sup>2+</sup> or Zn-TMPyP<sup>4+</sup> acting as photosensitizers, as schematically presented in Fig. 7.

In contrast to the application of the three photosensitizers in the regeneration of the NADPH cofactor, only Zn-TMPyP<sup>4+</sup> is active in the regeneration of the NADH cofactor. The other two photosensitizers, Ru(bpz)<sub>3</sub><sup>2+</sup> and Ru(bpy)<sub>3</sub><sup>2+</sup>, fail to regenerate NADH despite the effective formation of MV<sup>•+</sup>. Figure 8 shows the accumulation of NADH in the system at time intervals of illumination, using Zn-TMPyP<sup>4+</sup> as photosensitizer. It can be seen that NADH ( $\lambda_{\text{max}} = 342 \text{ nm}$ ) is accumulated in equilibrium with MV<sup>•+</sup> ( $\lambda_{\text{max}} = 392 \text{ nm}$ ) ( $K = (6 \pm 2) \times 10^{11} \text{ M}^{-1}$ ) and a negative absorption band is observed at  $\lambda = 440 \text{ nm}$ , implying that the photosensitizer Zn-TMPyP<sup>4+</sup> is degraded in the system. Control experiments show that in the absence of the enzyme LipDH no NADH is formed,

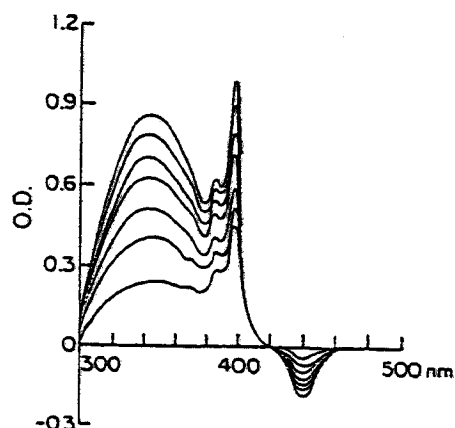
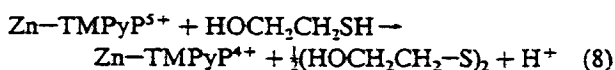
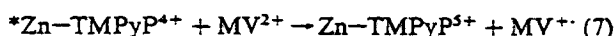


Fig. 8. Spectra of NADH formation at time intervals of 20 seconds of illumination. The system is equilibrated in the dark for 60 seconds before recording each spectrum.



implying that  $MV^{+•}$  mediates the reduction of  $NAD^+$  in the presence of LipDH. The cyclic process that leads to the photochemical regeneration of NADH is displayed in Fig. 9. It involves the primary reductive quenching of excited  $Zn-TMPyP^{4+}$  (eq. 7) followed by the oxidation of the electron donor by the oxidized photosensitizer (eq. 8).



It should be noted that the catalytic properties of LipDH and FDR differ substantially in the photochemical regeneration of NADH and NADPH, respectively. While the photoinduced regeneration of NADPH proceeds with a content of 0.2 units of the enzyme FDR, the regeneration system of NADH requires the addition of 100 units of the enzyme LipDH. Even under these conditions, the illumination of the NADH regeneration system results in the accumulation of  $MV^{+•}$ , and the results shown in Fig. 8 require the dark equilibration of the illuminated system for one minute. These results imply that the photosensitized regeneration of NADPH is kinetically controlled by the photochemical process that generates the electron carrier,  $MV^{+•}$ . In contrast, the photo-induced regeneration of NADH is controlled by the dark-biocatalyzed process, where  $MV^{+•}$  mediates the reduction of  $NAD^+$ . The degradation of the photosensitizer  $Zn-TMPyP^{4+}$  has been discussed previously.<sup>29</sup> It was found that the degradation process depends on the nature of the electron donor and the concentration of  $MV^{2+}$ . We find that the degradation of  $Zn-TMPyP^{4+}$  is less pronounced in the system that includes mercaptoethanol as electron donor compared to systems that include  $(NH_4)EDTA$  or TEOA as sacrificial electron donors.

The net reactions that are accomplished in the photosensitized regeneration systems of NAD(P)H cofactor correspond to the reduction of  $NAD(P)^+$  by mercaptoethanol (eq. 9). The thermodynamic balance of these processes shows that these are endoergic reactions,  $\Delta G \approx 14.5 \text{ kcal} \cdot \text{mol}^{-1}$ . Thus, the photoinduced

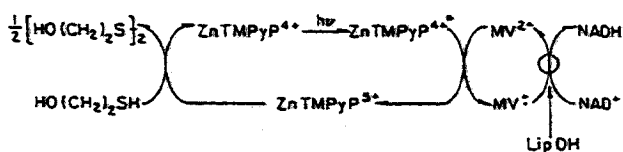
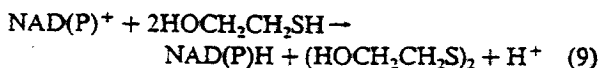


Fig. 9. Scheme for photosensitized regeneration of the NADH cofactor.

reduction of the cofactor represents photosynthetic routes by which light energy is converted into chemical potential that is stored in the reduced cofactors.



The reason for the failure to regenerate photochemically the NADH cofactor with the photosensitizers  $Ru(bpy)_3^{2+}$  and  $Ru(bpz)_3^{2+}$  has been determined by studying the excited state properties of these photosensitizers in the presence of NADH, as well as the interaction of the oxidized photosensitizer with the reduced cofactor. Figure 10 shows the Stern-Volmer fluorescence quenching plot of  $*Ru(bpz)_3^{2+}$  by added NADH. Thus, photoexcited  $Ru(bpz)_3^{2+}$  is reductively quenched by the electron donor (eq. 10) with a quenching rate constant,  $k_q = 4.5 \times 10^9 \text{ s}^{-1}$ , that is close to a diffusion-controlled value. In turn, excited  $Ru(bpy)_3^{2+}$  is not reductively quenched by NADH. Nevertheless, illumination of  $Ru(bpy)_3^{2+}$ , the electron acceptor  $MV^{2+}$ , and NADH results in the effective photosensitized production of  $MV^{+•}$ . This result indicates that NADH acts as electron donor for the oxidized photosensitizer formed by oxidative quenching of the light-active compound by  $MV^{2+}$  (eq. 11).



We thus conclude that the failure in the regeneration of NADH in the presence of  $Ru(bpy)_3^{2+}$  and  $Ru(bpz)_3^{2+}$  originates from internal short circuits in the systems: The photogenerated NADH competes as electron donor for the excited state or oxidized photoproduct and is consumed either in a reductive electron-transfer quenching process or in regeneration of the photosensitizers, rather than being accumulated. This discussion reveals the complexity in the selection of photo-

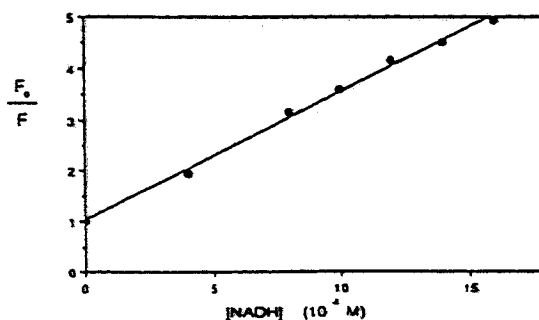


Fig. 10. Stern-Volmer quenching plot of  $Ru(bpz)_3^{2+}$  by NADH.



Table 2. Turnover Numbers, TN,<sup>a</sup> of Various Components in the Photoinduced Synthesis of Glutamic Acid

System	% Conversion <sup>b</sup>	Turnover Numbers, TN			
		MV <sup>2+</sup>	NADP <sup>+</sup>	FDR <sup>c</sup>	GluDH <sup>d</sup>
Ru(bpz) <sub>3</sub> <sup>2+</sup>	68	170	68	8.2 × 10 <sup>4</sup>	6.2 × 10 <sup>5</sup>
Ru(bpy) <sub>3</sub> <sup>2+</sup>	30	75	30	3.6 × 10 <sup>4</sup>	2.7 × 10 <sup>5</sup>

<sup>a</sup> TN = moles of product formed/moles of component.

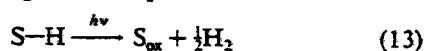
<sup>b</sup> Conversion (%) is estimated after 4 hours of illumination.

<sup>c</sup> F.W. ≈ 40,000 (Shin, M. *Methods Enzymol.*, 1971, 23: 441.)

<sup>d</sup> F.W. ≈ 2,200,000 (Sund, H.; Burchard, W. *Eur. J. Biochem.*, 1968, 6: 202.)

### Photoinduced Biocatalyzed Oxidative Regeneration of NAD<sup>+</sup>

The failure to apply Ru(bpy)<sub>3</sub><sup>2+</sup> as photosensitizer in the reductive regeneration of NADH has been attributed to the short-circuiting reaction of the intermediate oxidized photoproduct with NADH (eq. 11). This result suggests that any oxidative quenching process of Ru(bpy)<sub>3</sub><sup>2+</sup> could be applied for the photoinduced regeneration of NAD<sup>+</sup>. The oxidative quenching of Ru(bpy)<sub>3</sub><sup>2+</sup> by MV<sup>2+</sup> and subsequent H<sub>2</sub> evolution by the reduced photoproduct, MV<sup>•+</sup>, in the presence of various metal catalysts has been studied extensively. We have thus examined a general approach for dehydrogenation of organic substrates (eq. 13) using a photosensitized regeneration process of NAD<sup>+</sup>.



The systems are composed of an aqueous solution that includes Ru(bpy)<sub>3</sub><sup>2+</sup> as photosensitizer, MV<sup>2+</sup> or

DQ<sup>2+</sup> as electron acceptor, and the NADH cofactor. One of the following substrates and respective enzymes has been added to the systems: ethanol or propanol and AlcDH, lactic acid and LacDH, and alanine and AlaDH. With lactic acid as substrate, DQ<sup>2+</sup> is used as electron acceptor, while MV<sup>2+</sup> is introduced as electron relay into the systems of the other substrates. Illumination of these systems results in MV<sup>•+</sup> or DQ<sup>•+</sup>. Exclusion of NAD<sup>+</sup> from the systems prohibits the formation of the reduced photoproduct, MV<sup>•+</sup> or DQ<sup>•+</sup>. Examination of the systems prior to illumination shows that NADH is formed through the biocatalyzed oxidation of the substrates. Table 3 summarizes the steady-state concentrations of NADH (followed at λ = 340 nm) produced in the presence of the various substrates. These results allow us to suggest the cyclic process outlined in Fig. 12 as the mechanism for the reduction of MV<sup>2+</sup> or DQ<sup>2+</sup> through the photosensitized oxidative regeneration of the NAD<sup>+</sup> cofactor. In this cycle NADH is

Table 3. Quantum Yields for H<sub>2</sub> Evolution and Turnover Numbers of Components in the Different Systems

Substrate	φ <sub>H<sub>2</sub></sub> <sup>a</sup>	[NADH], M (steady state)	TN <sub>NAD<sup>+</sup></sub>	TN <sub>enzyme</sub>
Ethanol	2.5 × 10 <sup>-3</sup>	12.5 × 10 <sup>-5</sup>	7.8	12500 <sup>b</sup>
n-Propanol	1.5 × 10 <sup>-3</sup>	8.6 × 10 <sup>-5</sup>	3.2	5100 <sup>b</sup>
Lactic Acid	0.9 × 10 <sup>-3</sup>	7.3 × 10 <sup>-5</sup>	1.3	24500 <sup>c</sup>
L-Alanine	0.4 × 10 <sup>-3</sup>	6.7 × 10 <sup>-5</sup>	1.5	57000 <sup>d</sup>

<sup>a</sup> Light intensity 7.1 × 10<sup>-3</sup> einsteins min<sup>-1</sup>·liter<sup>-1</sup>.

<sup>b</sup> Alcohol dehydrogenase, FW ≈ 83300; Ehrenberg, A.; Dalziel, K. *Acta Chem. Scand.*, 1958, 12: 65.

<sup>c</sup> Lactic dehydrogenase, FW ≈ 140000; Jaenicke, R.; Knof, S. *Eur. J. Biochem.*, 1968, 4: 157.

<sup>d</sup> L-Alanine dehydrogenase, FW ≈ 228000; Yoshida, A.; Freese, E. *Biochim. Biophys. Acta*, 1964, 92: 33.

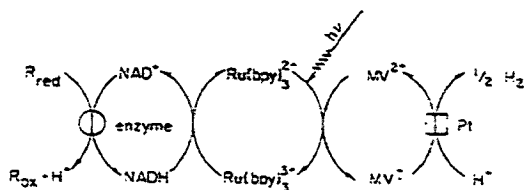


Fig. 12. Cyclic  $H_2$  evolution from substrates, mediated by NADH.

formed by the biocatalyzed oxidation of the substrate. Oxidative quenching of the excited photosensitizer results in  $MV^{2+}$  or  $DQ^{2+}$  and  $Ru(bpy)_3^{3+}$ . The oxidized photosensitizer oxidizes NADH and consequently the oxidized cofactor, and the light-active compounds are regenerated for subsequent cycles.

Introduction of a Pt colloid, stabilized by citrate, results in the evolution of hydrogen. The reduced photoproducts,  $MV^{2+}$  or  $DQ^{2+}$  mediate  $H_2$  evolution in the presence of the noble metal colloid (Fig. 12). The rates of  $H_2$  evolution from the different systems are displayed in Fig. 13. The quantum yields for  $H_2$  evolution and the

turnover numbers of the enzymes and  $NAD^+$  are given in Table 3. It can be seen that the quantum yield for hydrogen formation depends on the steady-state concentration of NADH that is produced by the substrate and the corresponding enzyme. As the amount of NADH increases, the  $H_2$  evolution yield is improved. This result can be explained in terms of a competitive reaction that occurs in the system. The recombination of the primary electron-transfer products (eq. 14) is thermodynamically favored and proceeds with a diffusion-controlled rate constant ( $k_6 = 2 \times 10^9 M^{-1} \cdot s^{-1}$ ). This back electron-transfer process leads to the net destruction of the photoproducts. The electron donor competes with  $MV^{2+}$  for the oxidized photoproduct,  $Ru(bpy)_3^{3+}$  (eq. 15). Therefore, as the steady-state concentration of NADH is higher, the scavenging of the oxidized photoproduct  $Ru(bpy)_3^{3+}$  by the reduced cofactor is improved. Consequently, the effectiveness of  $MV^{2+}$  formation and subsequent  $H_2$  evolution are improved at higher concentrations of NADH.

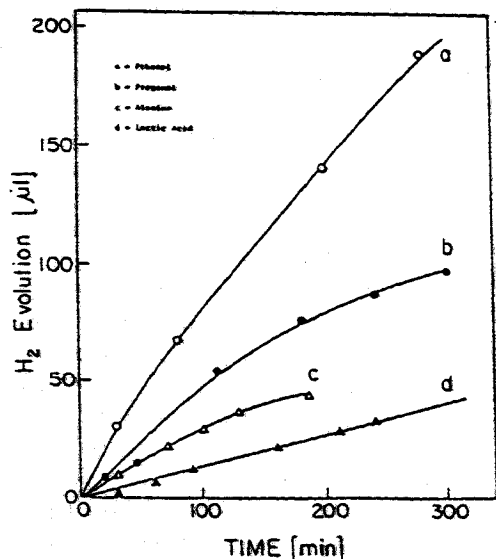
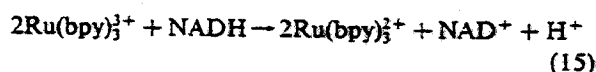
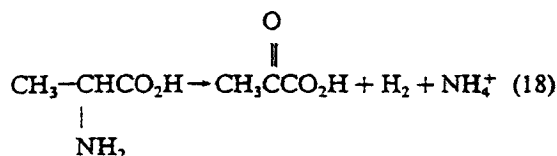
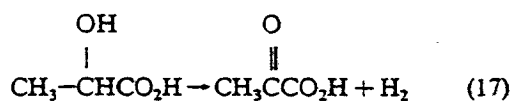
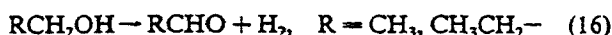


Fig. 13. Yields of  $H_2$  evolution from the various systems as a function of illumination time. (a) Ethanol as substrate,  $3.5 \times 10^{-1} M$ ; (b) Propanol,  $2.5 \times 10^{-1} M$ ; (c) Lactic acid,  $1.0 \times 10^{-1} M$ ; (d) Alanine,  $1.8 \times 10^{-1} M$ . In all systems  $Ru(bpy)_3^{2+}$ ,  $1.0 \times 10^{-4} M$  is used as sensitizer and  $NAD^+$ ,  $1.2 \times 10^{-3} M$ . For systems (a), (b), and (d)  $MV^{2+}$ ,  $1.4 \times 10^{-3} M$  is the electron acceptor. For system (c),  $DQ^{2+}$ ,  $5 \times 10^{-3} M$  is used as electron acceptor.

Table 3 reveals that the enzymes and cofactors are effectively recycled in the various systems that lead to  $H_2$  evolution. The use of  $DQ^{2+}$  as electron acceptor in the system with lactic acid as substrate needs further elaboration. The biocatalyzed oxidation of lactic acid by  $NAD^+$  proceeds at  $pH = 8.5$ . Under these conditions, the thermodynamic potential for  $H_2$  evolution corresponds to  $E^0 = -0.51 V$ . The reduced relay,  $MV^{2+}$ , is thermodynamically not capable of effecting hydrogen production,  $E^0(MV^{2+}/MV^{2+}) = -0.42 V$ . Nevertheless, the reduced electron acceptor,  $DQ^{2+}$ , meets the thermodynamic requirements,  $E^0(DQ^{2+}/DQ^{2+}) = -0.65 V$ , and therefore is used as the electron relay with lactic acid as substrate.

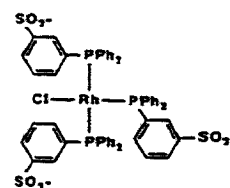
The oxidation products of the various substrates formed concomitantly with  $H_2$  evolution have been identified. Ethanol and propanol are oxidized to acetaldehyde and propionaldehyde, respectively (eq. 16); lactic acid is oxidized to pyruvic acid (eq. 17); and alanine is oxidatively deaminated to pyruvic acid (eq. 18). The thermodynamic balance of these processes reveals that oxidation of ethanol and propanol is endoergic by ca.  $10 \text{ kcal} \cdot \text{mol}^{-1}$ , that of lactic acid by ca.  $10 \text{ kcal} \cdot \text{mol}^{-1}$ , and that of alanine by ca.  $14 \text{ kcal} \cdot \text{mol}^{-1}$ .



#### Photoinduced Reductive Regeneration of NAD(P)H Cofactors Using a Homogeneous Rhodium Phosphine Catalyst

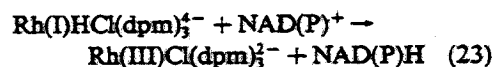
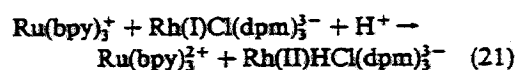
The reductive regeneration of NAD(P)H cofactors has been accomplished by using an artificial charge carrier (MV<sup>+</sup>) that mediates the reduction of NAD<sup>+</sup> and NADP<sup>+</sup> cofactors in the presence of the enzymes LipDH and FDR, respectively. One of our goals was the attempt to substitute for the natural biocatalysts artificial homogeneous catalysts that can simultaneously participate in a photochemical one-electron transfer process and subsequently generate an intermediate species capable of reducing these cofactors. Since the NAD(P)H cofactors are two-electron hydride reductants, it seems reasonable to speculate that the homogeneous catalyst should exhibit a hydride structure capable of transporting an equivalent of two electrons and a proton (a hydride) to the cofactors. Thus, the strategy for the selection of such a homogeneous catalyst involves the search for a transition-metal complex that is reduced by one-electron transfer processes, is capable of acting as a two-electron charge relay (through rapid disproportionation of the single electron-transfer product), and is subsequently capable of generating a hydride intermediate. In addition to these criteria, the catalyst should operate in aqueous media to allow subsequent biocatalyzed transformations with the reduced cofactors. Rhodium complexes exhibit such properties<sup>30</sup> where the Rh(II) oxidation state undergoes rapid disproportionation, and Rh(0) or Rh(I) oxidation states generate hydride species. Recently, we applied RhCl(dpm)<sub>3</sub><sup>2-</sup> (4) as a homogeneous catalyst for the photoinduced hydrogenation and hydroformylation of unsaturated substrates in aqueous media.<sup>31</sup> This process proceeds, presumably, through the intermediate formation of a hydride-rhodium species. Thus, we attempted applying this catalyst for the regeneration of NAD(P)H cofactors.

The NAD(P)H regeneration system is composed of an aqueous solution that includes Ru(bpy)<sub>3</sub><sup>2+</sup> as photo-



4

sensitizer, ascorbate as electron donor, the rhodium catalyst, RhCl(dpm)<sub>3</sub><sup>2-</sup>, and either the oxidized cofactor NAD<sup>+</sup> or NADP<sup>+</sup>. Illumination of either of the two systems results in the formation of the reduced NAD(P)H cofactors (followed at λ = 340 nm). The quantum yields for NADH and NADPH formation are equal, φ = 5 × 10<sup>-3</sup>. Control experiments reveal that the catalyst, RhCl(dpm)<sub>3</sub><sup>2-</sup>, is essential to mediate the reduction of the NAD(P)H cofactors. Also, fluorescence-quenching studies show that the catalyst does not interact with the photoexcited species, \*Ru(bpy)<sub>3</sub><sup>2+</sup>, formed in the system. Since the excited photosensitizer is reductively quenched by ascorbate and, in analogy to the participation of RhCl(dpm)<sub>3</sub><sup>2-</sup> in the photosensitized hydrogen evolution,<sup>32</sup> hydrogenation, and hydroformylation<sup>31</sup> processes, we can formulate the sequence of reactions outlined in eqs. 19–23 as the mechanistic route for the regeneration of the NAD(P)H cofactors.



Attempts to couple the photosensitized regeneration system of NADH with the homogeneous Rh(I)Cl(dpm)<sub>3</sub><sup>2-</sup> catalyst to subsequent NADH-dependent biotransformations have been initiated. Surprisingly, coupling of various substrates and the respective enzymes, e.g., pyruvic acid and lactate dehydrogenase, to the photosensitized NADH regeneration system results in only low conversion yields. A detailed examination of the biocatalysts in the presence of the artificial catalyst reveals that most of the enzymes are strongly inhibited by the free ligand, (dpm). Thus, ligand dissociation of the homogeneous catalyst or its intermediate species presumably deactivates the various enzymes. To over-

come this limitation, low concentrations of the artificial catalyst,  $\text{RhCl}(\text{dpm})_3^-$ , ( $6.5 \times 10^{-5} \text{ M}$ ), have been applied in the photosensitized regeneration of NADH and the system coupled to the reduction of acetaldehyde using alcohol dehydrogenase, as biocatalyst. Under these conditions, ethanol is formed efficiently. Figure 14 shows the rate of ethanol formation in the system as a function of illumination time. The initial rate of ethanol formation corresponds to  $1.5 \text{ mM} \cdot \text{h}^{-1}$ , and after ca. ten hours of illumination, 65% of the original substrate was converted to product. The total turnover numbers were 180 for  $\text{Rh}(\text{dpm})_3^-$ , 39 for NADH, and 1740 for AlcDH. It is evident that the artificial catalyst, cofactor, and coupled enzyme are efficiently recycled in the system.

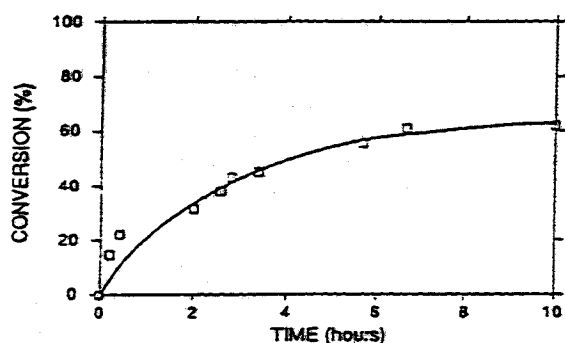


Fig. 14. Rate of photoinduced conversion of acetaldehyde to ethanol, using the NADH cofactor.

We thus see that artificial homogeneous catalysts can be designed for the regeneration of natural NAD(P)H cofactors. Nevertheless, loading the systems with artificial components affects the activity of the coupled biocatalysts. In the present system the free ligand, dpm, deactivates most of the enzymes. The advantages of using artificial catalysts for regeneration of NAD(P)H cofactors are obvious. Further development of other homogeneous catalysts is an encouraging approach to pursue.

#### CONCLUSIONS

We have described different approaches for reductive and oxidative regeneration of NAD(P)<sup>+</sup>/NAD(P)H cofactors. The reductive photoinduced regeneration of NAD(P)H has been accomplished by using enzymes or an artificial homogeneous catalyst as catalyst for the generation of the two-electron hydrido charge relays (NAD(P)H). The primary photochemical electron-transfer reactions that lead to the reduced cofactors can

be designed through an oxidative quenching mechanism or alternatively by a reductive quenching process. It is important to examine the interactions of the reduced cofactor with the excited photosensitizer or any oxidized photoproduct formed in the electron-transfer process. In our systems we have shown that NADH acts as electron donor for excited  $\text{Ru}(\text{bpz})_3^{2+}$  and is reoxidized by  $\text{Ru}(\text{bpy})_3^{3+}$ . These processes eliminate the possibility of their application in the reductive regeneration of NADH. Substitution of biocatalysts by homogeneous artificial catalysts, although attractive, is not free of limitations. Ligand dissociation of transition-metal complexes is likely to introduce inhibition effects on enzymes (as revealed in the present study) and, consequently, introduces difficulties in subsequent coupling of the regenerated cofactor in biotransformations.

The oxidative regeneration of the NAD<sup>+</sup> cofactor and its application in the endoergic dehydrogenation of various substrates is of special interest. Solar-generated hydrogen is considered a fuel of the future. The reverse hydrogenation of various oxidized products, e.g., acetaldehyde, is a feasible exothermic process. In view of the occurrence of various of these substrates, e.g., ethanol, as biomass products, future applications of photosensitized NAD<sup>+</sup>-regeneration cycles in hydrogen fuel production systems can be envisaged.

The use of enzymes in various biotransformations finds broad industrial applicability today. The novel approach of combining solar light energy and enzymes in the regeneration of NAD(P)H cofactors suggests that regeneration of other cofactors, e.g., ATP, could be driven by similar means. The advantage of using light energy in the regeneration of cofactors is obvious as endoergic processes could be driven. Numerous, novel biotechnological applications can be envisaged by coupling solar light energy and biocatalysts. Future developments that involve improved stability and effectiveness of the systems and immobilization of these complex assemblies to solid matrices are essential for further progress.

*Acknowledgments.* The technical assistance of Mr. Shmuel Ravid (Rabinovitz) in part of the experimental work is acknowledged. The research was supported by the Kernforschung Anlage, Jülich, FRG.

#### REFERENCES

- (1) (a) Jones, J.B.; Sih, C.J.; Perlman, D. Eds.; *Applications of Biochemical Systems in Organic Chemistry*; Wiley-Interscience: New York, 1976. (b) Jones, J.B. In *Asymmetric Synthesis*; Morrison, J.D. Ed.; Academic Press: New York, 1983; Vol. 5, p 309–344.

- (2) Whitesides, G.M.; Wong, C.H. *Aldrichimica Acta*, 1983, 16: 27.
- (3) (a) Pollak, A.; Blumenfeld, H.; Wax, M.; Baughn, R.L.; Whitesides, G.M. *J. Am. Chem. Soc.*, 1980, 102: 6324. (b) Zaborsky, O.R. In *Immobilized Enzymes*; CRC Press: Cleveland, Ohio, 1973. (c) Klibanov, A.M. *Anal. Biochem.*, 1979, 93: 1.
- (4) (a) Chenault, H.K.; Whitesides, G.M. *Appl. Biochem. Biotech.*, 1987, 14: 147. (b) Dugas, H.; Penney, C. In *Bioorganic Chemistry*; Springer-Verlag: New York, 1981: p 395.
- (5) Willner, I.; Mandler, D. *Enzyme and Microb. Tech.*, 1989, 11: 467.
- (6) (a) Shaked, Z.; Whitesides, G.M. *J. Am. Chem. Soc.*, 1980, 102: 7104. (b) Wichmann, R.; Wandry, C.; Buckmann, A.F.; Kula, M.-R. *Biotech. Bioeng.*, 1981, 23: 2789. (c) Tischer, W.; Tiemeyer, W.; Simon, H. *Biochimie*, 1980, 62: 331. (d) Wong, C.-H.; Drucehammer, D.G.; Sweers, H.M. *J. Am. Chem. Soc.*, 1985, 107: 4028. (e) Wong, C.-H.; Whitesides, G.M. *J. Am. Chem. Soc.*, 1981, 103: 4890. (f) Hirschbein, B.L.; Whitesides, G.M. *J. Am. Chem. Soc.*, 1982, 104: 4458. (g) Wang, S.S.; King, C.K. *Adv. Biochem. Eng.*, 1979, 12: 119. (h) Klibanov, A.M.; Pugliski, A.V. *Biotech. Lett.*, 1980, 2: 445. (i) Ergorer, P.; Simon, H.; Tanaka, A.; Fukui, S. *Biotech. Lett.*, 1982, 4: 489. (j) Daniclson, B.; Winqvist, B.; Malpote, J.Y.; Mosbach, K. *Biotech. Lett.*, 1982, 4: 673. (k) Payen, B.; Segui, M.; Monsan, P.; Schneider, K.; Friedrich, C.G.; Schlegel, H.G. *Biotech. Lett.*, 1983, 5: 463.
- (7) (a) Jansen, M.A.; Elving, P.J. *Biochim. Biophys. Acta*, 1984, 764: 310. (b) Janik, B.; Elving, P.J. *Chem. Rev.*, 1964, 68: 295. (c) Biellman, J.-F.; Lapinte, C. *Tetrahedron Lett.*, 1978: 683. (d) Burnett, R.W.; Underwood, A.L. *Biochemistry*, 1968, 7: 3328.
- (8) (a) Simon, H.; Bader, J.; Gunther, H.; Newmann, S.; Thanos, J. *Angew. Chem. Int. Ed. Engl.*, 1985, 24: 539. (b) Day, R.J.; Kinsey, S.J.; Seo, E.T.; Weliky, N.; Silvermann, H.P. *Trans. N.Y. Acad. Sci.*, 1972, 34: 588. (c) Shaked, Z.; Barber, J.J.; Whitesides, G.M. *J. Org. Chem.*, 1981, 46: 4100. (d) DiCosimo, R.; Wong, C.-H.; Daniels, L.; Whitesides, G.M. *J. Org. Chem.*, 1981, 46: 4622. (e) Chao, S.; Wrighton, M.S. *J. Am. Chem. Soc.*, 1977, 109: 5886.
- (9) (a) Kelly, R.M.; Kirwain, D.J. *Biotech. Bioeng.*, 1977, 19: 1215. (b) Jaegfeldt, H.; Torstensson, A.; Johansson, G. *Anal. Chim. Acta*, 1978, 97: 221. (c) Aizawa, M.; Coughlin, R.W.; Charles, M. *Biochim. Biophys. Acta*, 1975, 315: 362.
- (10) (a) Jaegfeldt, H.; Torstensson, A.; Gorton, L.G.C.; Johansson, G. *Anal. Chem.*, 1981, 53: 1979. (b) Laval, J.-M.; Bourdillon, C.; Moiroux, J. *J. Am. Chem. Soc.*, 1984, 106: 4701.
- (11) (a) Bard, A.J. *Science*, 1980, 207: 139. (b) Grätzel, M. *Acc. Chem. Res.*, 1981, 14: 376.
- (12) (a) Grätzel, M., Ed.; *Energy Resources through Photochemistry and Catalysis*; Academic Press: New York, 1983. (b) Harriman, A.; West, M.E. Eds.; *Photogeneration of Hydrogen*; Academic Press: London, 1983.
- (13) (a) Heller, A. *Science*, 1984, 223: 1141. (b) Willner, I.; Steinberger-Willner, B. *Int. J. Hydrogen Energy*, 1988, 13: 593.
- (14) (a) Juris, A.; Balzani, V.; Barigelletti, F.; Campagna, S.; Belser, P.; Van Zclewsky, A. *Coord. Chem. Rev.*, 1988, 84: 85. (b) Balzani, V.; Boletta, F.; Scandola, F.; Ballardini, R. *Pure Appl. Chem.*, 1979, 51: 299. (c) Kalyanasundaram, K. *Coord. Chem. Rev.*, 1982, 46: 159.
- (15) Darwent, J.R.; Douglas, P.; Harriman, A.; Porter, G.; Richoux, M.-C. *Coord. Chem. Rev.*, 1982, 44: 83.
- (16) Pileni, M.-P.; Grätzel, M. *J. Phys. Chem.*, 1980, 84: 2402.
- (17) (a) Julliard, M.; LePetit, J. *Photochem. Photobiol.*, 1982, 36: 283. (b) Chambers, R.P.; Ford, J.R.; Allender, J.H.; Baricos, W.H.; Cohen, W. *Enz. Eng.*, 1974, 2: 195.
- (18) (a) Mandler, D.; Willner, I. *J. Chem. Soc., Perkin Trans. II*, 1986: 805. (b) Goren, Z.; Lapidot, N.; Willner, I. *J. Mol. Catal.*, 1988, 47: 21.
- (19) Mandler, D.; Willner, I. *J. Am. Chem. Soc.*, 1984, 106: 5352.
- (20) Willner, I.; Mandler, D.; Riklin, A. *J. Chem. Soc., Chem. Commun.*, 1986: 1022.
- (21) Mandler, D.; Willner, I. *J. Chem. Soc., Chem. Commun.*, 1986: 851.
- (22) Willner, I.; Degani, Y. *Isr. J. Chem.*, 1982, 22: 163.
- (23) Crutchley, R.J.; Lever, A.B.P. *Inorg. Chem.*, 1982, 21: 2276.
- (24) Hambright, P.; Fleischer, E.B. *Inorg. Chem.*, 1970, 9: 1757.
- (25) Borowski, A.F.; Cole-Hamilton, D.J.; Wilkinson, G. *Nouv. J. Chim.*, 1978, 2: 137.
- (26) Mondino, E.; Bongiovanni, G.; Fumero, S.; Ross, L. *J. Chromatogr.*, 1972, 74: 255.
- (27) (a) Kiwi, J.; Grätzel, M. *J. Am. Chem. Soc.*, 1979, 101: 7214. (b) Harriman, A.; Porter, G.; Richoux, M.-C. *J. Chem. Soc., Faraday Trans. II*, 1982, 78: 1955.
- (28) (a) Keller, P.; Moradpour, A.; Amouyal, E.; Kagan, H.B. *Nouv. J. Chim.*, 1980, 4: 377. (b) Keller, P.; Moradpour, A.; Amouyal, E.; Kagan, H.B. *J. Am. Chem. Soc.*, 1980, 102: 7193. (c) Sutin, N.; Creutz, C. *Pure Appl. Chem.*, 1980, 52: 2717. (d) Degani, Y.; Willner, I. *J. Am. Chem. Soc.*, 1983, 105: 6228. (e) Maidan, R.; Goren, Z.; Becker, J.Y.; Willner, I. *J. Am. Chem. Soc.*, 1984, 106: 6217.
- (29) Harriman, A.; Porter, G.; Richoux, M.-C. *J. Chem. Soc., Faraday Trans. II*, 1981, 77: 833.
- (30) Kirsch, M.; Lchn, J.-M.; Sauvage, J.P. *Helv. Chim. Acta*, 1979, 62: 1345.
- (31) Willner, I.; Maidan, R. *J. Chem. Soc., Chem. Commun.*, 1988: 876.
- (32) Oishi, S. *J. Mol. Catal.*, 1987, 39: 225.

Supplementary Material Available: Full listings of fractional atomic coordinates and interatomic bond distances and angles of the 1b-piperidine salt (5 pages). Ordering information is given on any current masthead page.

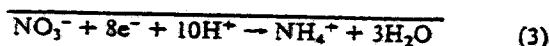
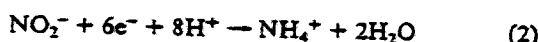
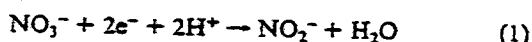
### Photoinduced Enzyme-Catalyzed Reduction of Nitrate ( $\text{NO}_3^-$ ) and Nitrite ( $\text{NO}_2^-$ ) to Ammonia ( $\text{NH}_3$ )

Itamar Willner,\* Noa Lapidot, and Azalia Riklin

Department of Organic Chemistry  
The Hebrew University of Jerusalem  
Jerusalem 91904, Israel

Received September 28, 1988

The reduction of nitrate is of broad interest as a means of mimicking reduction processes of oxido-nitrogen substrates in nature and of developing novel nitrogen fixation systems.<sup>1</sup> Reduction of nitrate to nitrite (eq 1) is catalyzed in nature by the



enzyme nitrate reductase.<sup>2</sup> Reduction of nitrite to ammonia (as ammonium ions) (eq 2) is catalyzed in nature by the enzyme nitrite reductase.<sup>2,3</sup> Substantial efforts are directed toward the reduction of  $\text{NO}_3^-$  by electrochemical and photochemical means. Electrochemical reduction of  $\text{NO}_3^-$  has been accomplished by using catalytic material electrodes,<sup>4</sup> modified electrodes,<sup>5</sup> or in the presence of homogeneous catalysts<sup>6,7</sup> such as Co(III) or Ni(II) cyclams, Ru(II) bipyridine or Fe(III) porphyrin. Photosensitized reduction of  $\text{NO}_3^-$  to  $\text{NO}_2^-$  has been reported by using *N*-methylphenothiazine or *N,N'*-tetramethylbenzidine,<sup>8</sup> and reduction to ammonia was reported to occur at Pd-TiO<sub>2</sub> illuminated suspensions.<sup>9</sup> We have recently applied enzymes as biocatalysts for the photosensitized regeneration of NAD(P)H cofactors<sup>10,11</sup> and performed various biotransformations through photochemical means.<sup>12</sup> Here we wish to report on the photoinduced reduction of  $\text{NO}_3^-$  to ammonia using the two enzymes nitrate reductase and nitrite reductase as catalysts and photogenerated *N,N'*-di-

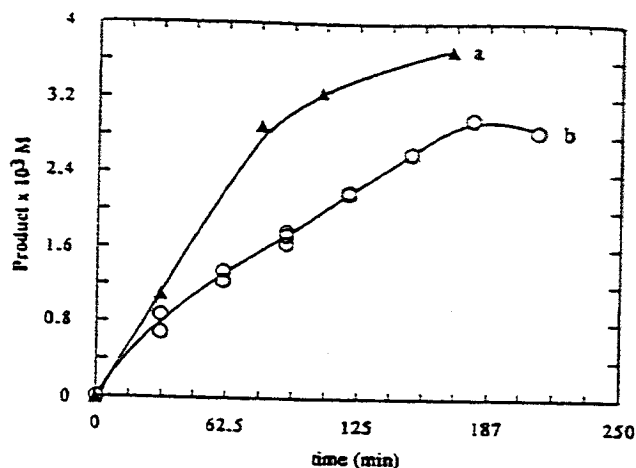


Figure 1. Rates of products formation as a function of illumination time. In all systems  $[\text{Ru}(\text{bpy})_3^{2+}] = 7.4 \times 10^{-5} \text{ M}$ ,  $[\text{Na}_2\text{EDTA}] = 0.02 \text{ M}$ . (a) ( $\Delta$ )  $\text{NO}_2^-$  formation, pH 7.0, Tris buffer 0.1 M,  $[\text{MV}^{2+}] = 3.2 \times 10^{-4} \text{ M}$ ,  $[\text{NO}_3^-] = 9.9 \times 10^{-3} \text{ M}$ , nitrate reductase 0.2 U. (b) ( $\circ$ )  $\text{NH}_4^+$  formation, pH 8.0, Tris buffer 0.1 M,  $[\text{MV}^{2+}] = 4.2 \times 10^{-4} \text{ M}$ ,  $[\text{NO}_2^-] = 0.01 \text{ M}$ , nitrite reductase 0.06 U.

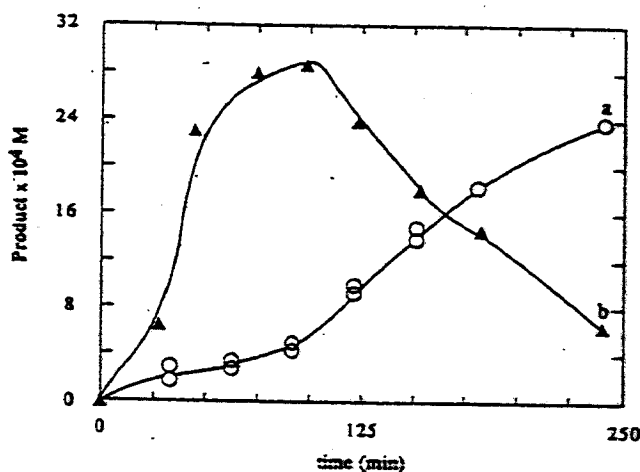


Figure 2.  $\text{NO}_2^-$  and  $\text{NH}_4^+$  concentrations in the combined system, as a function of illumination time. (a) ( $\circ$ )  $\text{NH}_4^+$ . (b) ( $\Delta$ )  $\text{NO}_2^-$ . pH = 8.0, Tris buffer 0.1 M,  $[\text{Ru}(\text{bpy})_3^{2+}] = 7.4 \times 10^{-5} \text{ M}$ ,  $[\text{Na}_2\text{EDTA}] = 0.02 \text{ M}$ ,  $[\text{MV}^{2+}] = 4.2 \times 10^{-4} \text{ M}$ ,  $[\text{NO}_3^-] = 0.01 \text{ M}$ , nitrate reductase 1.0 U, nitrite reductase 0.35 U.

methyl-4,4'-bipyridinium radical cation, viologen radical,  $\text{MV}^{2+}$ , that act as an electron carrier and is recognized by the biocatalysts.<sup>13</sup>

Illumination ( $\lambda > 420 \text{ nm}$ ) of an aqueous 0.05 M phosphate buffer solution, pH = 7.0, that includes Ru(II) tris-bipyridine,  $\text{Ru}(\text{bpy})_3^{2+}$ , as photosensitizer,  $7.4 \times 10^{-5} \text{ M}$ , *N,N'*-dimethyl-4,4'-bipyridinium,  $\text{MV}^{2+}$ ,  $3.2 \times 10^{-4} \text{ M}$ , as electron relay, EDTA, 0.02 M, as sacrificial electron donor,  $\text{NO}_3^-$ ,  $9.9 \times 10^{-3} \text{ M}$ , and the enzyme nitrate reductase (E.C. 1.9.6.1 from *Escherichia coli*), 0.2 units, results in the reduction of  $\text{NO}_3^-$  to nitrite (eq 1). The rate of  $\text{NO}_2^-$  formation<sup>14</sup> at time intervals of illumination is shown in Figure 1a. The quantum yield of  $\text{NO}_2^-$  formation corresponds to  $\phi = 0.08$ . After 310 min of illumination, ca. 60% of the original  $\text{NO}_3^-$  was converted to nitrite. The initial rate of  $\text{NO}_2^-$  formation is  $0.07 \mu\text{mol}\cdot\text{min}^{-1}$ . Illumination ( $\lambda > 420 \text{ nm}$ ) of an aqueous buffer solution, pH = 8.0, that includes  $\text{Ru}(\text{bpy})_3^{2+}$ ,  $7.4 \times 10^{-5} \text{ M}$ ,  $\text{MV}^{2+}$ ,  $4.2 \times 10^{-4} \text{ M}$ , as electron carrier, EDTA, 0.02 M, as

(13) Kiang, H.; Kuan, S. S.; Guilbault, G. G. *Anal. Chem.* 1978, 50, 1319.

(14) Nitrite was analyzed by two complementary methods: ion chromatography (VYDAC 3021C anion exchange column,  $2 \times 10^{-3} \text{ M}$  phthalic acid, pH 5.0 as eluent) and by a spectrometric method, based on diazotization of sulfanilamide and coupling with *N*-(1-*tert*-naphthyl)ethylenediamine hydrochloride. Cf. Snell, F. D.; Snell, C. T. *Colorimetric Method of Analysis*; D. Van Nostrand Company: New York, 1949; p 804.

- (1) Chatt, J.; Dilworth, J. R.; Richards, R. L. *Chem. Rev.* 1978, 78, 555. (2) Holm, R. H. *Chem. Rev.* 1987, 87, 1401. (c) Uegama, N.; Fukase, H.; Hirokizama; Kishida, S.; Nakamura, A. *J. Mol. Catal.* 1987, 43, 141. (2) (a) Payal, W. J. *Bacterial Rev.* 1973, 37, 409. (b) Adams, M. W. W.; Mortenson, L. E. In *Molybdenum Enzymes*; Spiro, T. S., Ed.; John Wiley & Sons: 1985. (3) Losada, M. J. *J. Mol. Catal.* 1975, 1, 245. (4) (a) Horanyi, G.; Rizmayer, E. M. *J. Electroanal. Chem. Interfacial Electrochem.* 1985, 180, 265. (b) Li, H. L.; Robertson, D. H.; Chambers, J. Q.; Hobbs, D. T. *J. Electrochem. Soc.* 1988, 35, 1154. (c) Fletcher, D.; Poorabedi, Z. *Electrochim. Acta* 1979, 24, 1253. (5) Kuwabata, S.; Uezumi, S.; Tanaka, K.; Tanaka, T. *Inorg. Chem.* 1986, 25, 3018. (6) (a) Moyer, B. A.; Meyer, T. J. *J. Am. Chem. Soc.* 1979, 101, 1326. (b) Taniguchi, I.; Nakashima, N.; Yasukouchi, K. *J. Chem. Soc., Chem. Commun.* 1986, 1814. (7) Barley, M. H.; Takeuchi, K. J.; Meyer, T. J. *J. Am. Chem. Soc.* 1986, 108, 5876. (8) Frank, A. J.; Gratzel, M. *Inorg. Chem.* 1982, 21, 3834. (9) (a) Kudo, A.; Domen, K.; Maruya, K.; Onishi, T. *Chem. Lett.* 1987, 1019. (b) Halmann, M.; Tobin, J.; Zuckerman, K. *J. Electroanal. Chem.* 1986, 209, 405. (10) Mandler, D.; Willner, I. *J. Chem. Soc., Perkin Trans. 2* 1986, 805. (11) Mandler, D.; Willner, I. *J. Chem. Soc., Chem. Commun.* 1986, 851. (12) (a) Willner, I.; Mandler, D.; Riklin, A. *J. Chem. Soc., Chem. Commun.* 1986, 1022. (b) Mandler, D.; Willner, I. *J. Chem. Soc., Perkin Trans. 2* 1988, 997.



Table I. Turnover Numbers for Components<sup>a</sup> Involved in the Photosensitized Reduction of NO<sub>3</sub><sup>-</sup> and NO<sub>2</sub><sup>-</sup> to Ammonia

	Ru(bpy) <sub>3</sub> <sup>2+</sup>	MV <sup>2+</sup>	nitrate <sup>c</sup> reductase	nitrite <sup>c</sup> reductase
NO <sub>3</sub> <sup>-</sup> reduction <sup>b</sup>	80	18.5	6.2 × 10 <sup>4</sup>	
NO <sub>2</sub> <sup>-</sup> reduction <sup>c</sup>	38.5	7		2.4 × 10 <sup>4</sup>
combined system <sup>d</sup>	32	6	9 × 10 <sup>4</sup>	2.1 × 10 <sup>4</sup>

<sup>a</sup>Turnover number (TN) is defined as TN = mol of product formed/mol of component. <sup>b</sup>60% conversion of NO<sub>3</sub><sup>-</sup> to NO<sub>2</sub><sup>-</sup>. <sup>c</sup>28.5% conversion of NO<sub>2</sub><sup>-</sup> to NH<sub>4</sub><sup>+</sup>. <sup>d</sup>23.8% conversion of NO<sub>3</sub><sup>-</sup> to NH<sub>4</sub><sup>+</sup>. <sup>e</sup>Molecular weight of nitrate reductase and nitrite reductase was estimated as 200 000 cf. ref 2b.

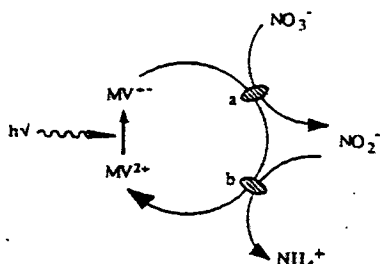


Figure 3. Scheme for biocatalyzed sequential reduction of NO<sub>3</sub><sup>-</sup> to NH<sub>4</sub><sup>+</sup>. a = nitrate reductase, b = nitrite reductase.

sacrificial electron donor, NO<sub>2</sub><sup>-</sup>, 0.01 M, and the enzyme nitrite reductase (E.C. 1.6.6.4), 0.06 units, isolated from spinach leaves,<sup>15</sup> results in the formation of ammonia. The rate of ammonia formation<sup>16</sup> at time intervals of illumination is displayed in Figure 1b. The quantum yield of ammonia formation is  $\phi = 0.06$ . Control experiments reveal that all components in the two systems are required to effect the reduction of NO<sub>3</sub><sup>-</sup> or NO<sub>2</sub><sup>-</sup>, respectively. Also, no reduction of NO<sub>3</sub><sup>-</sup> or NO<sub>2</sub><sup>-</sup> takes place in the two systems in the dark. Exclusion of the enzymes nitrate reductase or nitrite reductase from the respective systems results in the formation of MV<sup>••</sup>. Addition of the enzymes to the respective systems that include NO<sub>3</sub><sup>-</sup> or NO<sub>2</sub><sup>-</sup> and photogenerated MV<sup>••</sup> results in the depletion of MV<sup>••</sup> and reduction of NO<sub>3</sub><sup>-</sup> to nitrite or of NO<sub>2</sub><sup>-</sup> to ammonia, respectively.

Illumination ( $\lambda > 420$  nm) of a photosystem that includes Ru(bpy)<sub>3</sub><sup>2+</sup>, 7.4 × 10<sup>-5</sup> M, as photosensitizer, MV<sup>••</sup>, 4.2 × 10<sup>-4</sup> M, as electron relay, EDTA, 0.02 M, the substrate nitrate, and the two enzymes nitrate reductase, 1.0 units, and nitrite reductase, 0.35 units, results in the reduction of NO<sub>3</sub><sup>-</sup> to ammonia (eq 3) through the intermediate formation of nitrite. The rate of ammonia formation in this system is shown in Figure 2a, and curve 2b shows the amount of NO<sub>2</sub><sup>-</sup> that is present in the system at time intervals of illumination. It is evident that only after a concentration of NO<sub>2</sub><sup>-</sup> that corresponds to 3 × 10<sup>-3</sup> M is formed, ammonia is effectively produced. During the illumination, no MV<sup>••</sup> is accumulated in the system. This suggests that the route of NO<sub>2</sub><sup>-</sup> and ammonia formation is limited by the photochemical process that generates MV<sup>••</sup>. The quantum yield of ammonia formation in the system that includes the two enzymes corresponds to  $\phi = 0.08$ . Table I summarizes the turnover numbers of the various components in the different systems. It is evident that the components are recycled during the reduction of NO<sub>3</sub><sup>-</sup> and NO<sub>2</sub><sup>-</sup> and that the enzymes exhibit stability in the artificial media. Figure 3 represents the schematic sequential cycle that leads to the reduction of NO<sub>3</sub><sup>-</sup> to ammonia through nitrite as an intermediate. The photoinduced electron-transfer process generates MV<sup>••</sup> that acts as electron carrier for the two enzymes.

The primary step involves the reduction of NO<sub>3</sub><sup>-</sup> to nitrite in the presence of nitrate reductase. The latter photoproduct acts as substrate for the enzyme nitrite reductase that mediates the reduction of NO<sub>2</sub><sup>-</sup> to ammonia. The relatively high quantum yields for NO<sub>2</sub><sup>-</sup> or ammonia formation are noteworthy. These

originate from effective charge separation of MV<sup>••</sup> in the photosensitized electron-transfer process and the subsequent complementary dark reduction<sup>17</sup> of MV<sup>••</sup> by the oxidation product of the sacrificial electron donor, EDTA.

We thus describe the light driven reduction of NO<sub>3</sub><sup>-</sup> to ammonia using an artificial photosystem and two biocatalysts. Further experiments to immobilize the enzymes and design of organized assemblies for this process are under way in our laboratory.

**Acknowledgment.** The support of the Belfer Foundation is gratefully acknowledged.

(17) Keller, P.; Moradpour, A.; Amouyal, E.; Kagan, H. B. *Nouv. J. Chim.* 1980, 4, 377.

### Tailored Semiconductor-Receptor Colloids: Improved Photosensitized H<sub>2</sub> Evolution from Water with TiO<sub>2</sub>- $\beta$ -Cyclodextrin Colloids

Itamar Willner<sup>a</sup> and Yoav Eichen

Department of Organic Chemistry  
The Hebrew University of Jerusalem  
Jerusalem 91904, Israel

Arthur J. Frank<sup>b</sup>

Solar Energy Research Institute  
1617 Cole Boulevard, Golden, Colorado 80401

Received October 11, 1988

Redox reactions in microheterogeneous semiconductor systems are of much interest as a means of converting light to chemical energy.<sup>1,2</sup> Either direct excitation of a semiconductor or a photosensitizing dye, adsorbed on the particle surface, can activate electron (or hole) transfer to solution species at the semiconductor-liquid interface. Surface recombination and back electron (or hole) transfer from solution species to either the semiconductor or the adsorbed dye molecule can lower the overall yield of the desired product(s) and thus the conversion efficiency of light to chemical energy. Electrostatic interactions in colloidal semiconductor dispersions have been utilized to control interfacial electron transfer and to improve the quantum yield for H<sub>2</sub> evolution from water.<sup>3</sup> Surface adsorption of  $\beta$ -cyclodextrin ( $\beta$ -CD) to semiconductor colloids has been found<sup>4</sup> to improve the kinetics for charge transfer from the photoexcited semiconductor to electron acceptors retained in the  $\beta$ -CD cavity.  $\beta$ -Cyclodextrin also served to stabilize the colloids against aggregation.

Dye sensitization of a semiconductor affords the possibility of using sub-bandgap light and the electronic transport properties of the semiconductor to effect charge separation. Both organic dyes, such as Rhodamine B, and transition-metal complexes have been utilized as photosensitizers of wide bandgap semiconductor materials.<sup>5,6</sup> Diffusion-limited charge transfer from the pho-

(1) (a) *Energy Resources through Photochemistry and Catalysis*; Grätzel, M., Ed.; Academic Press: New York, 1983. (b) *Homogeneous and Heterogeneous Photocatalysis*; Pelizzetti, E.; Serpone, N., Eds.; D. Reidel Publishing Co.: Dordrecht, 1986. (c) *Photochemical Conversion and Storage of Solar Energy*; Conolly, J. S., Ed.; Academic Press: New York, 1981.

(2) (a) Bard, A. J. *Science* 1980, 207, 139. (b) Grätzel, M. *Acc. Chem. Res.* 1981, 14, 376.

(3) Frank, A. J.; Willner, I.; Goren, Z.; Degani, Y. *J. Am. Chem. Soc.* 1987, 109, 3568.

(4) Willner, I.; Eichen, Y. *J. Am. Chem. Soc.* 1987, 109, 6862.

(15) Ho, C. H.; Tamura, G. *Agric. Biol. Chem.* 1973, 37, 37.

(16) Ammonium was analyzed by ion chromatography (Wescan cation exchange column, 3 × 10<sup>-3</sup> M nitric acid as eluent).

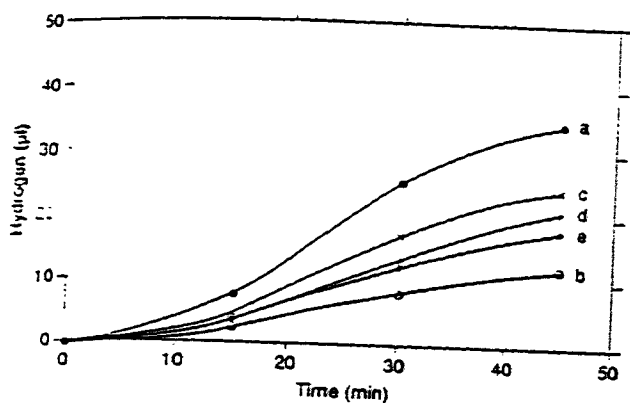


Figure 1. Production of H<sub>2</sub> with irradiation time ( $\lambda_{ex} > 400$  nm) for aqueous solutions (pH 1.8) of Pt-TiO<sub>2</sub> colloids [5% Pt on TiO<sub>2</sub> (w/w)] with  $5.1 \times 10^{-5}$  M proflavin dihydrogen chloride and 0.1 M cysteine. In a 3-mL sample, 2-mL headspace: curves a, Pt-TiO<sub>2</sub>- $\beta$ -CD; b, Pt-TiO<sub>2</sub>-PVA; c-e, Pt-TiO<sub>2</sub>- $\beta$ -CD with *N*-octylpyridinium bromide, C<sub>4</sub>PyBr; c,  $2.2 \times 10^{-4}$  M C<sub>4</sub>PyBr; d,  $4.4 \times 10^{-4}$  M C<sub>4</sub>PyBr; and e,  $8.8 \times 10^{-2}$  M C<sub>4</sub>PyBr.

toexcited dye molecule is generally inefficient, because of the short lifetime of the excited state of the dye and competing reactions. Physical adsorption of dye molecules to the semiconductor surface by means of hydrophobic or electrostatic interactions facilitates charge injection.<sup>7</sup> Molecular interactions in dye aggregates can, however, substantially quench electron transfer.<sup>8</sup> An effective approach to disperse dye aggregates is to use cyclodextrins (CD) to complex the dye monomer in the CD cavity.<sup>9</sup> Formation of inclusion complexes between cyclodextrin and other molecules is mainly based on size selectivity and hydrophobic interactions.<sup>10</sup>

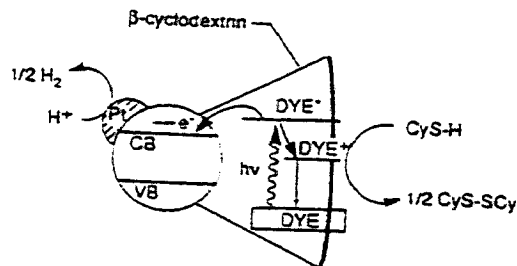


Figure 2. Representation of mechanism: Photoinitiated electron transfer from monomeric dye sensitizer, in cavity of  $\beta$ -cyclodextrin ( $\beta$ -CD), through conduction band of semiconductor (CB) to catalytic Pt surface sites, where H<sub>2</sub> is evolved. The oxidized dye sensitizer is recycled by oxidation of electron donor cysteine, Cys-H.

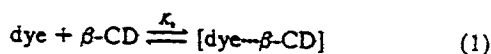
We initiated the research described in this report to determine whether modification of the semiconductor particle surface with  $\beta$ -cyclodextrin ( $\beta$ -CD) would provide an effective microenvironment for both increasing the number of surface sites for dye-semiconductor interaction and promoting photosensitized H<sub>2</sub> evolution from water. The basic semiconductor system consisted of Pt-charged TiO<sub>2</sub>- $\beta$ -CD colloids that were exposed to the photoactive dye proflavin (3,6-diaminoacridine).<sup>11</sup>

Optically transparent TiO<sub>2</sub>- $\beta$ -CD colloids were prepared by slow hydrolysis of TiCl<sub>4</sub> in an aqueous 1% (w/w)  $\beta$ -CD solution at 0 °C. The resulting colloidal solution (2 g L<sup>-1</sup> TiO<sub>2</sub>; pH 1.8) was stable for 9 months, the period of observation. The TiO<sub>2</sub> colloid was loaded with 5% Pt by weight by photoreduction of H<sub>2</sub>PtCl<sub>4</sub>. Hydrogen was analyzed on a gas chromatograph equipped with a thermal conductivity detector, a 5 Å molecular sieve column, and argon carrier gas. Illumination ( $\lambda_{ex} > 400$  nm) of the aqueous colloidal Pt-TiO<sub>2</sub>- $\beta$ -CD solution (pH 1.8) containing proflavin dihydrogen chloride<sup>11</sup> ( $5.1 \times 10^{-5}$  M) and the sacrificial electron donor cysteine (0.1 M) generated H<sub>2</sub> as shown in Figure 1a. The quantum yield for H<sub>2</sub> production in this system was  $1.1 \times 10^{-3}$ . Omission of either the dye or the electron donor eliminated H<sub>2</sub> production. Emission studies revealed that the excited state of the dye was not quenched by either  $\beta$ -CD or cysteine. Absorption and emission spectra indicated no dye aggregation at the concentration of proflavin used. The emission intensity of proflavin showed only a small increase ( $\sim 10\%$ ) in the presence of  $\beta$ -cyclodextrin, implying that the photophysical properties of the dye were not altered appreciably by the  $\beta$ -CD receptor. In the absence of TiO<sub>2</sub>, illumination of  $\beta$ -CD-covered Pt colloids with proflavin and cysteine produced only trace quantities of H<sub>2</sub>. These studies suggest that H<sub>2</sub> evolution involves electron transfer from the photoexcited dye through the conduction band of TiO<sub>2</sub> to catalytic Pt surface sites, as portrayed in Figure 2.

To determine the role of the  $\beta$ -CD molecule on photosensitized H<sub>2</sub> production, a comparative study was made of Pt-TiO<sub>2</sub>- $\beta$ -CD and Pt-TiO<sub>2</sub> colloids; the latter was stabilized against aggregation with poly(vinyl alcohol) PVA (14 000 MW). Figure 1b shows the photoproduction of H<sub>2</sub> in the Pt-TiO<sub>2</sub>-PVA system (5% Pt/TiO<sub>2</sub>, w/w) with proflavin ( $5.1 \times 10^{-5}$  M) and cysteine (0.1 M). The quantum yield for H<sub>2</sub> production in this system was  $4 \times 10^{-4}$ , which is a factor of three less than that of the Pt-TiO<sub>2</sub>- $\beta$ -CD system. The relatively large quantum yield of the Pt-TiO<sub>2</sub>- $\beta$ -CD system for H<sub>2</sub> production correlates, in part, with an enhanced dye concentration on the semiconductor surface. By a flow dialysis technique,<sup>12</sup> 2.5 times more proflavin was found to be associated with TiO<sub>2</sub>- $\beta$ -CD colloids than with TiO<sub>2</sub>-PVA colloids. The photolysis and flow dialysis experiments suggest that the presence of the  $\beta$ -CD receptor effects an increase in the number of dye-semiconductor interactive sites, leading to an im-

(5) (a) Meier, H. *J. Phys. Chem.* 1965, 69, 705. (b) Namba, S.; Hishiki, Y. *J. Phys. Chem.* 1965, 69, 724. (c) Gerischer, H. In *Physical Chemistry: An Advanced Treatise*; Academic Press: New York, 1970; Vol. IXA. (d) Tributsch, H.; Calvin, M. *Photochem. Photobiol.* 1971, 14, 95. (e) Memming, R.; Tributsch, H. *J. Phys. Chem.* 1971, 75, 562. (f) Fujishima, A.; Watanabe, T.; Tsuruta, O.; Honda, K. *Chem. Lett.* 1975, 13. (g) Gerischer, H. *Photochem. Photobiol.* 1975, 16, 243. (h) Gleria, M.; Memming, R. *Z. Phys. Chem. (Munich)* 1975, 98, 303. (i) Hauffe, K. *Photogr. Sci. Eng.* 1976, 20, 12. (j) Tributsch, H. *Z. Naturforsch. A* 1977, 32A, 972. (k) Ghosh, P. K.; Spiro, T. G. *J. Am. Chem. Soc.* 1980, 102, 5543. (l) Memming, R. *Surf. Sci.* 1980, 101, 551. (m) Spittler, M. T. *J. Chem. Educ.* 1983, 60, 330. (n) Krishnan, M.; Zhang, X.; Bard, A. J. *J. Am. Chem. Soc.* 1984, 106, 7371 and references cited therein. (o) Alonso, N.; Beley, V. M.; Charier, P.; Ern, V. *Rev. Phys. Appl.* 1981, 16, 5. (p) Fox, M.-A. In *Topics in Organic Electrochemistry*; Fry, A. J., Britton, W. E., Eds.; Plenum Press: New York, 1986. (6) (a) Spittler, M. T.; Calvin, M. *J. Chem. Phys.* 1977, 66, 4294. (b) Clark, W. D. K.; Sutin, D. *J. Am. Chem. Soc.* 1977, 99, 4676. (c) Fujihira, M.; Oshishi, N.; Osa, T. *Nature (London)* 1977, 268, 226. (d) Fan, F. R. F.; Bard, A. J. *J. Am. Chem. Soc.* 1979, 101, 6139. (e) Andersson, S.; Constable, E. C.; Dare-Edwards, M. P.; Goodenough, J. B.; Hammet, A.; Seddon, K. R.; Wright, R. D. *Nature (London)* 1979, 280, 571. (f) Dare-Edwards, M. P.; Goodenough, J. B.; Hammet, A.; Seddon, K. R.; Wright, R. D. *Faraday Discuss. Chem. Soc.* 1980, 70, 285. (g) Goodenough, J. B.; Hammet, A.; Dare-Edwards, M. P.; Campet, G.; Wright, R. D. *Surf. Sci.* 1980, 101, 531. (h) Hammet, A.; Dare-Edwards, M. P.; Wright, R. D.; Seddon, K. R.; Goodenough, J. B. *J. Phys. Chem.* 1979, 83, 3280. (i) Girardeau, A.; Fan, F. R. F.; Bard, A. J. *J. Am. Chem. Soc.* 1980, 102, 5137. (j) Matsumura, M.; Mitsuda, K.; Yoshizawa, N.; Tsubomura, H. *Bull. Chem. Soc. Jpn.* 1981, 54, 692. (k) Houlding, V. H.; Grätzel, M. *J. Am. Chem. Soc.* 1983, 105, 5695. (l) Gulino, D. A.; Drickamer, H. G. *J. Phys. Chem.* 1984, 88, 1173. (m) Watanabe, T.; Fujishima, A.; Honda, K. In *Energy Resources through Photochemistry and Catalysis*; Grätzel, M., Ed.; Academic Press: New York, 1983; and references cited therein. (n) Shimidzu, T.; Iyoda, T.; Koide, Y. *J. Am. Chem. Soc.* 1985, 107, 35. (o) Duonghong, D.; Serpone, N.; Grätzel, M. *Helv. Chim. Acta* 1984, 67, 1012. (p) Vrachnou, E.; Vlachopoulos, I.; Grätzel, M. *J. Chem. Soc., Chem. Commun.* 1987, 868. (7) Desilvestro, J.; Grätzel, M.; Kavan, L.; Moser, J. *J. Am. Chem. Soc.* 1985, 107, 2988. (8) (a) Fripiat, A.; Kirsch-De Mesmaeker, A. *J. Phys. Chem.* 1985, 89, 1285. (b) Fripiat, A.; Kirsch-De Mesmaeker, A.; Nasielski, J. *J. Electrochem. Soc.* 1983, 130, 237. (9) (a) Dan, P.; Willner, I.; Dixit, N. S.; Mackay, R. A. *J. Chem. Soc., Perkin Trans. 2* 1984, 455. (b) Degani, Y.; Willner, I.; Haas, Y. *Chem. Phys. Lett.* 1984, 104, 496. (10) (a) *Cyclodextrin Chemistry*; Bender, M., Kamiyama, L., Eds.; Springer, 1978. (b) Sanger, A. Q. *Angew. Chem., Int. Ed. Engl.* 1980, 19, 144. (c) Breslow, R. *Science (Washington, D.C.)* 1982, 218, 532. (d) Tabushi, I. *Acc. Chem. Res.* 1982, 15, 66. (11) For photophysical experiments with proflavin, see: (a) Kalyanasundaram, K.; Dung, D. *J. Phys. Chem.* 1980, 84, 2551. (b) Pileni, M. P.; Grätzel, M. *J. Phys. Chem.* 1980, 84, 2402. (12) (a) Ramos, S.; Schuldimer, S.; Kaback, H. R. *Proc. Natl. Acad. Sci. U.S.A.* 1976, 73, 1892. (b) Laane, C.; Willner, I.; Orvos, J. W.; Calvin, M. *Proc. Natl. Acad. Sci. U.S.A.* 1981, 78, 5928.

provement in the quantum conversion efficiency for electron transfer from proflavin to  $\text{TiO}_2$ . The association of the dye with  $\beta$ -CD involves the uptake of the dye monomer into the CD cavity. The association constant  $K_a$  of proflavin with  $\beta$ -CD at pH 1.8 was determined spectrophotometrically to be  $550 \pm 60 \text{ M}^{-1}$ , corresponding to the reaction



Further evidence that the association of proflavin with  $\beta$ -CD improves the efficiency of electron injection from the dye molecule to  $\text{TiO}_2$  came from studies involving *N*-octylpyridinium bromide,  $\text{C}_8\text{PyBr}$ . The *N*-octylpyridinium cation ( $\text{C}_8\text{Py}^+$ ) has a high association constant ( $K_a = 870 \pm 120 \text{ M}^{-1}$ ) for  $\beta$ -CD and is expected to impede the diffusion of proflavin into the CD cavity. Curves c-e of Figure 1 show that as the concentration of  $\text{C}_8\text{Py}^+$  increases, the yield and rate of  $\text{H}_2$  production decrease, indicating a decline in the quantum conversion efficiency for charge transfer from the excited state of proflavin to  $\text{TiO}_2$ . At the highest concentration of  $\text{C}_8\text{Py}^+$  ( $8.8 \times 10^{-2} \text{ M}$ ), the rate of  $\text{H}_2$  production was comparable to that of the Pt- $\text{TiO}_2$ -PVA system. Addition of  $\text{C}_8\text{Py}^+$  to the Pt- $\text{TiO}_2$ -PVA system had no effect on the rate of  $\text{H}_2$  evolution, suggesting that  $\text{C}_8\text{Py}^+$  blocked the inclusion of the dye molecule into the cavity of  $\beta$ -CD. These studies clearly imply that the photosensitization efficiency for charge injection from proflavin to  $\text{TiO}_2$  is improved by the association of the dye monomer with the  $\beta$ -CD receptor on the surface of the semiconductor particles.

In conclusion, the utility of  $\beta$ -cyclodextrin for enhancing dye sensitization of semiconductors has been demonstrated. The  $\beta$ -cyclodextrin molecule offers a unique microenvironment for augmenting the number of surface sites for dye-semiconductor interaction and for promoting charge injection from photoexcited dye molecules to the semiconductor. Further characterization of cyclodextrin complexes with other dye systems is in progress.

**Acknowledgment.** This work was supported by Contract No. 5083-260-0796 from the Gas Research Institute.

## Cyclizations of Ene Radicals. Imidoyl Radicals as Intermediates in the Synthesis of Heterocyclic Compounds

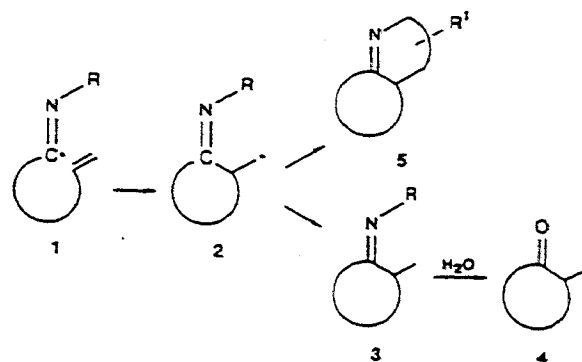
Mario D. Bachi\* and Daniella Denenmark

Department of Organic Chemistry  
The Weizmann Institute of Science  
Rehovot 76100, Israel

Received October 28, 1988

The construction of cyclic systems through the intramolecular addition of carbon centered free radicals to carbon-carbon multiple bonds is well documented.<sup>1</sup> A convenient method for the site-specific generation of carbon-centered free radicals involves the chemospecific homolysis of a C-halogen, C-S, or C-Se bond by trialkyltin radicals generated from the corresponding tin hydrides.<sup>2</sup> The tin hydride induced free radical cyclizations are not restricted to alkyl radical intermediates. Stork has introduced<sup>3</sup> the use of vinyl radicals in synthesis and we have shown<sup>4</sup> that alkoxy-carbonyl

Scheme I



radicals are excellent intermediates in a general synthesis of  $\alpha$ -alkylidene- $\gamma$ -lactones. These results<sup>4</sup> prompted us to investigate the potential that other carbon-centered ene radicals, isoelectronic with vinyl and carbonyl radicals, may have as intermediates in the synthesis of functionalized cyclic compounds. Herein we report on preliminary results that illustrate the employment of imidoyl radicals, as intermediates in the synthesis of cyclic ketones and polyheterocyclic compounds.

This new method for ring formation is based on the tri-*n*-butyltin hydride (TBTH) induced generation of the imidoyl radical, followed by its intramolecular addition to a suitably positioned double bond as outlined in Scheme I.<sup>6</sup> We reasoned that imidoyl radicals of type 1 may cyclize to radicals 2, which carry an exocyclic imine group. Direct hydrogen transfer to 2 would give an imine 3 that could be hydrolyzed to a cyclic ketone 4. In this transformation the imidoyl radical performs as a synthetic equivalent to the carbonyl radical. However, if the R moiety in 2 would bear a radical trapping functionality a second cyclization, to a compound of type 5, may occur. The following preliminary results (Schemes II-IV) prove the validity of these hypotheses. As starting materials we used the selenoimidates 6, 11, and 12 and the thioamides 18 and 20.<sup>7</sup> Under standard conditions standard starting material (1 mmol), TBTH (1.15 mmol), and AIBN (0.15 mmol) were heated (110 °C) in dry degassed toluene for 3-6 h (t.l.c.).

Treatment of selenoimidate 6 with TBTH under standard conditions followed by aqueous workup afforded nitrile 8 (59%) and chromanone 10 (50%) (Scheme II). Although the generation of imidoyl radical 7 is quantitative cyclization to imine 9 is accompanied by fragmentation into nitrile 8 and benzyl radical. When the benzyl group of the starting material was substituted by a lower alkyl group only chromanone 10 was obtained. A different reaction course was observed when *N*-aryl selenoimidates were used. Thus, *N*-tolyl derivative 11 afforded a polycyclic compound 15 (R = Ph).<sup>8</sup> Oxidation by DDQ resulted in the loss of two hydrogen atoms and the formation of chromanoquinoline 16 (84% from 11). Similarly compound 12 was converted into

(5) For additional recent examples see: (a) Marinov, N. N.; Ramanathan, H. *Tetrahedron Lett.* 1983, 24, 1871. (b) Padwa, A.; Nimmeggern, H.; Wong, G. S. K. *J. Org. Chem.* 1985, 50, 5620. (c) Hanessian, S.; Beauvais, P.; Dubé, D. *Tetrahedron Lett.* 1986, 27, 5071. (d) Urabe, H.; Kawazima, I. *Tetrahedron Lett.* 1986, 27, 1355. (e) Beckwith, A. J. L.; O'Shea, D. M. *Tetrahedron Lett.* 1986, 27, 4525. (f) Knight, J.; Parsons, P. J.; Southgate, R. J. *Chem. Soc., Chem. Commun.* 1986, 78. (g) Deiduc, P.; Tailhan, C.; Zard, S. Z. *J. Chem. Soc., Chem. Commun.* 1988, 308. (h) Crich, D.; Forth, S. M. *Tetrahedron Lett.* 1988, 29, 2585. (i) Boger, D. L.; Robarge, K. D. *J. Org. Chem.* 1988, 53, 3377. (j) Coveney, D. J.; Patel, V. F.; Pattenden, E. *Tetrahedron Lett.* 1987, 28, 5949. (k) Bachi, M. D.; Bosch, E. *Heterocycles*, in press. (l) Bachi, M. D.; Denenmark, D. *Heterocycles*, in press.

(6) For different reactions involving imidoyl radical intermediates see: (a) Barton, D. H. R.; Bringmann, G.; Lamotte, G.; Motherwell, B.; Motherwell, R. S. H.; Porter, A. E. A. *J. Chem. Soc., Perkin. Trans. I* 1980, 2657. (b) John, D. I.; Tyrrel, N. D.; Thomas, E. J. *J. Chem. Soc., Chem. Commun.* 1981, 901. (c) Leardini, R.; Nanni, D.; Pedullii, G. F.; Tundo, A.; Zanardi, G. *J. Chem. Soc., Perkin. Trans. I* 1986, 1591. (d) Wirth, T.; Ruchardt, W. *C. Chimia* 1988, 42, 230.

(7) All compounds gave analytical data consistent with the assigned structures.

(8) For completion this reaction required 1.6 equiv of TBTH and 0.8 equiv of AIBN, and heating for 12 h.

(1) Reviews: (a) Surzur, J.-M. In *Reactive Intermediates*; Abramovitch, A. R., Ed.; Plenum Press: New York, 1982; Vol. 2, p 121. (b) Hart, D. J. *Science* 1984, 223, 883. (c) Giese, B. *Radicals in Organic Synthesis: Formation of Carbon-Carbon Bonds*; Pergamon Press: Oxford, 1986. (d) Ramaiah, M. *Tetrahedron* 1987, 43, 3541. (e) Curran, D. P. *Synthesis* 1988, 417, 489.

(2) Neumann, W. P. *Synthesis* 1987, 665.

(3) Stork, G.; Baine, N. H. *J. Am. Chem. Soc.* 1982, 104, 2321. Stork, G.; Mook, R. *J. Am. Chem. Soc.* 1987, 109, 2829 and references cited therein.

(4) Bachi, M. D.; Bosch, E. *Tetrahedron Lett.* 1986, 27, 641.

# Photosensitized Electron-Transfer Reactions in Supramolecular Assemblies

*Itamar Willner and Bilha Willner*

## Scope and Potential Applications of Supramolecular Photochemical Assemblies

Photochemistry at the molecular level is one of the fundamental subjects in modern chemistry. During the past two decades, substantial progress has been made both in the development of theories about photochemical processes and in the analysis of the photophysical properties and photoreactivity of excited species. A new, rapidly developing area involves the characterization of photochemical systems beyond the molecular level, or *supramolecular photochemical assemblies* (SPAs) [1]. A supramolecular photochemical assembly is an organized micro-environment designed to perform a certain function following initiation by light energy. The construction of SPAs involves tailored linkage of several units designed to operate sequentially in performing the desired function. The organized assembly shows performance superior to any random distribution of the components included in the supramolecular structure; in fact, the desired result may be impossible to achieve in the absence of the tailored configuration. A supramolecular structure can be designed on a molecular- or macromolecular-interfacial basis. The several schematic systems in Figure 1-1 illustrate the SPA concept and show the scientific and practical importance of such configurations. The natural photosynthetic apparatus represents a uniquely organized environment in which light energy is transformed into an electrical potential by means of a primary photoinduced electron-transfer process. The microstructure of the photosynthetic membrane induces vectorial electron-transfer via an organized chain of electron acceptors (relays) that tunnel the ejected electron, and it also assures effective physical separation of charges in the resulting photoproducts [2, 3]. Several functions of the photosynthetic apparatus can be duplicated by supramolecular assemblies. Figure 1-1A shows an assembly design composed of a light-harnessing component S linked to a series of electron acceptors A<sub>1</sub>-A<sub>3</sub>. Following photoinduced electron transfer to the primary electron acceptor, the ejected electron is rapidly tunneled along the entire series of acceptors—provided, of course, that the relay components are arranged in a configuration consistent with downhill elec-

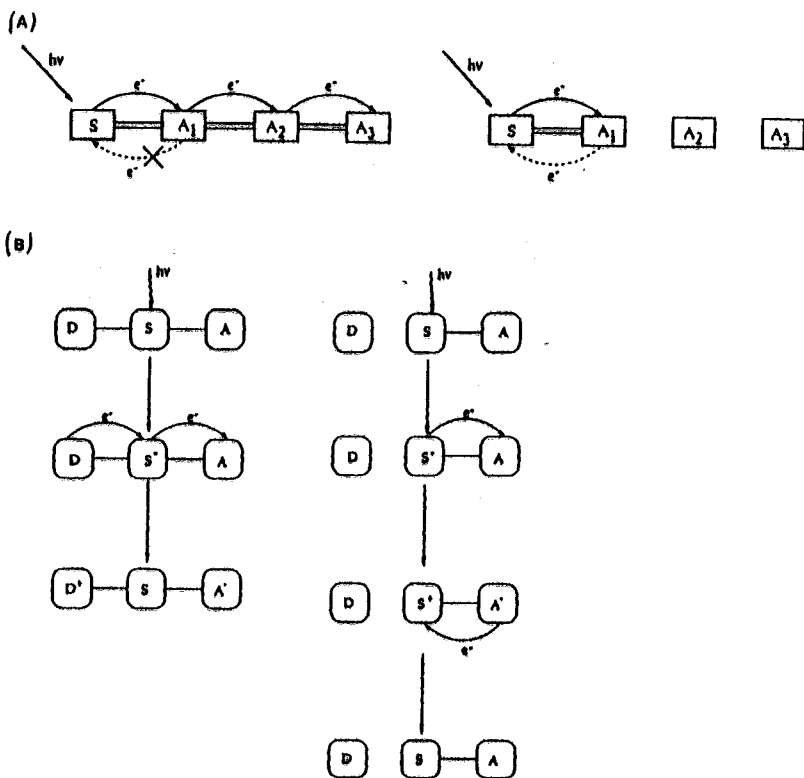
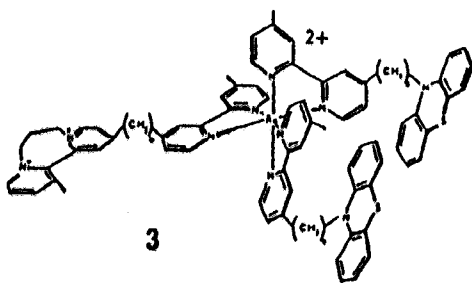
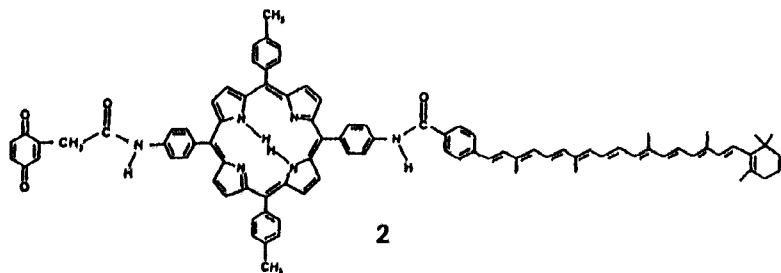
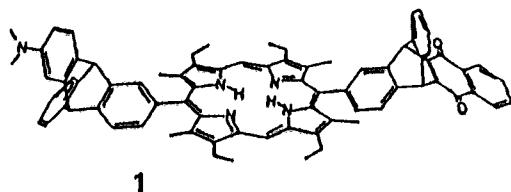


Figure 1-1. (A) Vectorial electron transfer in a photosensitizer-acceptor(1)-acceptor(3) SPA (left); and electron transfer in a random photosensitizer-electron relay photosystem (right). (B) Vectorial electron transfer in a triad donor-photosensitizer-electron acceptor SPA (left), and photoinduced electron transfer in a random donor, photosensitizer, acceptor system (right).

iron transport. This process retards primary degradative back-electron transfer of the primary photoproducts also achieving spatial separation of the photoproducts. For comparison, a random distribution of the assembly components is illustrated at the right of Figure 1-1 A. Here, back-electron transfer of the primary photoproducts predominates, and charge separation is absent. An SPA composed of a photosensitizer and a series of acceptors can be regarded as a molecular photoactivated conducting wire.

Figure 1-1 B depicts an alternative SPA configuration that duplicates functions of the photosynthetic apparatus. The assembly is composed of a triad structure,

with a photosensitizer linked to acceptor (A) and electron donor (D) units. Excitation of the photosensitizer results in electron transfer to the relay component followed by electron transport from the donor unit to the oxidized photosensitizer. The synchronous transport of electrons produces spatially separated photoproducts, and the assembly constitutes a device for pumping electrons by photochemical means (photopump). In a non-organized assembly (Figure 1-1 B, right), back-electron transfer of the primary photoproducts again predominates, and charge separation is eliminated. Various ingenious molecular D-S-A assemblies have already been synthesized [4-6]. The linked triad porphyrin-quinone assemblies 1 and 2 as well as the phenothiazine-Ru(II)-polypyridine-diquat structure ((Ru(Me-bpy-PTZ)<sub>2</sub>(Me-bpy-DQ<sup>2+</sup>))<sup>2+</sup>) 3 are examples of D-S-A assemblies. Excitation of



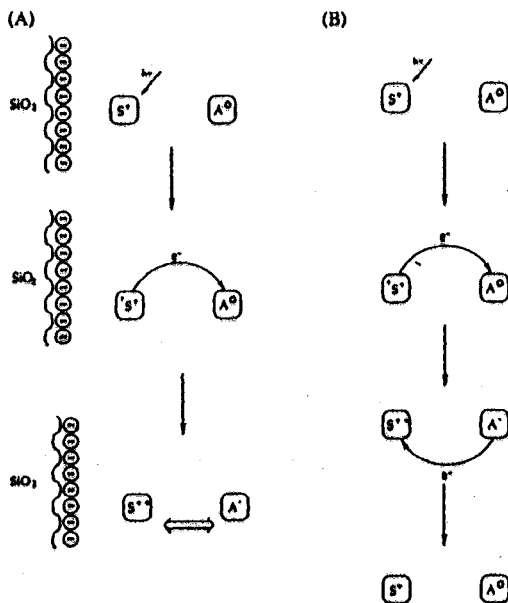


Figure 1-2. (A) Control of vectorial photosensitized electron-transfer reactions in a microheterogeneous system through electrostatic interactions. Repulsive interactions are indicated by  $\leftarrow$ . (B) Competitive reactions operative in a non-organized photosensitized electron-transfer process.

the porphyrin site in 1 results in formation of the porphyrin-quinone ion pair,  $D^{\dagger}\text{-}P^{\ddagger}\text{-}Q^{\ddagger-}$ , which rapidly decays through intramolecular electron transfer to the amine-quinone ion pair  $D^{\dagger}\text{-}S\text{-}Q^{\ddagger-}$  ( $k = 1.4 \times 10^{10} \text{ s}^{-1}$ ). The latter spatially separated ion pair has a lifetime of 2.45  $\mu\text{s}$ . Exclusion of the amine component from the triad structure results only in the primary photoproducts  $P^{\ddagger}\text{-}Q^{\ddagger-}$ , with a lifetime of 180 picoseconds. Thus, the lifetime of the electron transfer products is substantially increased by the spatial separation provided by the macromolecular, multifunctional structure (4).

Control features can be incorporated into the photosensitized electron-transfer processes in utilizing SPAs composed of microheterogeneous interfacial environments (7). Figure 1-2A illustrates the concept of a negatively charged microheterogeneous interface that selectively associates with a positively charged photosensitizer in the presence of a neutral electron acceptor. Photoinduced electron transfer causes selective association of the oxidized photosensitizer to the charged interface, together with electrostatic repulsion of the reduced relay to the interface. Consequently, back-electron transfer of the primary photoproducts is eliminated.

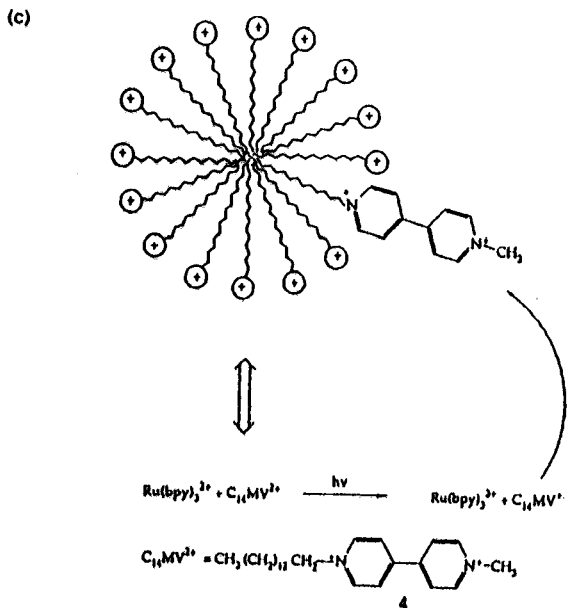


Figure 1-2. (C) Control of the photosensitized reduction of  $\text{C}_{14}\text{MV}^{2+}$  by hydrophobic and electrostatic interactions in a micellar system.

For comparison, Figure 1-2 B shows a random distribution of the photosensitizer-relay components, where back-electron transfer is favored. Further architectural provisions in the supramolecular photochemical assembly might include immobilization of catalysts on the microheterogeneous interface. This would permit sequential use of the reduced and oxidized photoproducts in various reduction or oxidation processes, such as the catalyzed reduction of water to molecular hydrogen [8-10],  $\text{CO}_2$ -reduction [11-14],  $\text{N}_2$ -fixation [15], or oxidation of water to molecular oxygen [16]. In recent years substantial efforts have been made to develop supramolecular photochemical catalytic assemblies (SPCAs) that could serve as artificial photosynthetic systems [17, 18]. Such devices could effect the conversion of solar light energy into electrical (or chemical) energy with subsequent production of fuel products.

The functionalities of the microheterogeneous environments included in SPAs might operate through electrostatic or hydrophilic-hydrophobic interactions. Charged colloids [19, 20], polyelectrolytes [21, 22], or charged micelles [23, 24] represent microheterogeneous environments that induce electrostatic interactions with charged photosensitizer-relay components. Micellar aggregates [23-25], as



well as oil-in-water [26] and water-in-oil microemulsions [27], represent hydrophobic-hydrophilic microenvironments that interact with photosensitizer-relay components by means of hydrophobic-hydrophilic interactions. For example [28], photosensitized reduction of the bipyridinium salt  $C_{14}MV^{2+}$  (4) by  $Ru(bpy)_3^{2+}$  or Zn-porphyrin is controlled in a micellar medium of positively charged CTAB micelles. Upon electron transfer, the reduced electron relay  $C_{14}MV^{\cdot+}$  exhibits hydrophobic character and is extracted into the micellar core, while the positively charged photosensitizer is electrostatically repelled by the micellar interface (Figure 1-2C). As a result, a four-hundred-fold retardation was observed in the back-electron transfer rate of the photoproducts compared to homogeneous solutions. Other examples of microheterogeneous SPAs and SPCAs will also be discussed in this review article.

Additional functionalities that can be triggered by light absorption of supramolecular photochemical assemblies might involve structural or configurational changes of a specific part of the SPA. Figure 1-3A shows an SPA composed of a photochemical site S linked to a light-sensitive receptor site R. Excitation of S causes a structural change in the receptor configuration. Design of the light-acti-

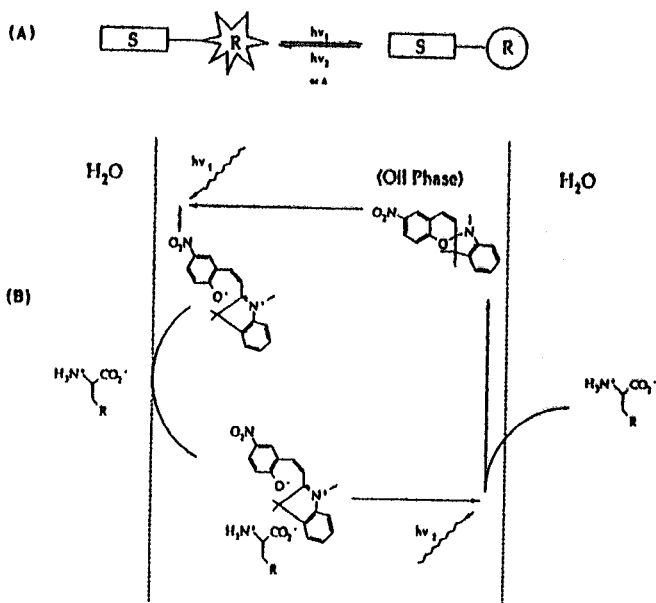


Figure 1-3. (A) Configurational changes in an SPA triggered by a light source. (B) Light-induced active transport of amino acids across an artificial membrane through the light-induced configurational change of a substrate carrier.

vated structure of the receptor for specific and selective association of substrates (i.e., metal ions or organic substrates) could provide the basis for either light-driven active transport of ions or photoregulated catalytic processes.

The possibility of a reversible structural change in the receptor functionality is of special interest, and would have definite practical applications. Photochemical or thermal dark deactivation of the photoactivated configuration to the original passive structure allows for "time- (or light-) controlled" activity of the SPA. Light-activated molecular "ON-OFF" switches can thus be envisaged; applications are anticipated in controlled ion-transport, activation of substrates (catalysis), or electrical conductivity. Introduction of chromophores as a part of crown-ether receptors (i.e., azo-crown ethers) makes possible the control of metal ion affinities at the receptor sites through photoregulation of the structural features of the chromophore component [29, 30]. Similarly, *active transport of amino acids across a membrane* can be *photoregulated* with the aid of a spiropyran photochromic material [31] acting as substrate carrier (Figure 1-3 B). The light-activated zwitterionic structure of the photochromic material is the actual substrate carrier, and vectorial transport is operative across the membrane.

An SPA might also constitute a part of a macroscopic device (i.e., an electrode), and operation of the device could be controlled by the molecular assembly. Figure 1-4 illustrates such a configuration, where the photochemical site and linked functionality are introduced between two electrodes that include immobilized donor (D) and acceptor (A) components. In the passive configuration, the SPA acts as an insulator, and no current is developed in the device. With light activation, however, the structural and photophysical properties of the molecular assembly are altered: electron transfer to the acceptor component occurs, and subsequent reduction of the SPA by the donor-electrode allows current to flow through the external circuit. It should therefore be possible to develop photoresponsive con-

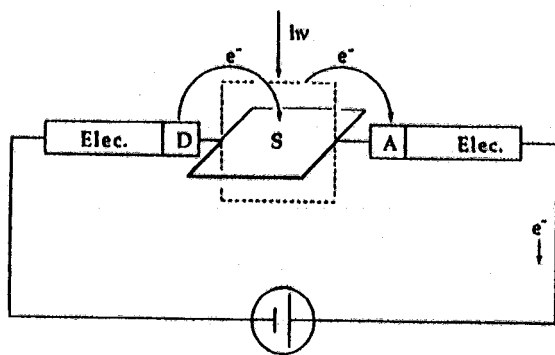


Figure 1-4. Scheme for a photoresponsive electrochemical cell.

ductive materials and to tailor SPA-based electronic devices (i.e., *phototransistors*).

Organic dyes [32] (i.e., acridine or xanthene dyes) or transition metal complexes [33] such as metal-polypyridine complexes or metal porphyrins are frequently applied as light-harnessing components that trigger the functionality of an SPA. *Semiconductor materials* provide alternative *photoactive* components that can be included in *supramolecular assemblies* [34, 35]. Excitation of a semiconductor (S.C.) results in the formation of "electron-hole" pairs. Sequential electron ejection from the semiconductor conduction band to an electrolyte acceptor, followed by electron transfer from a donor component to valence-band holes, provides a means of inducing the photochemical electron-transfer processes (Figure 1-5 A). S.C. materials can also act as charge carriers in photochemical transformations (Figure 1-5 B). The coupling of semiconductors to dye compounds or transition

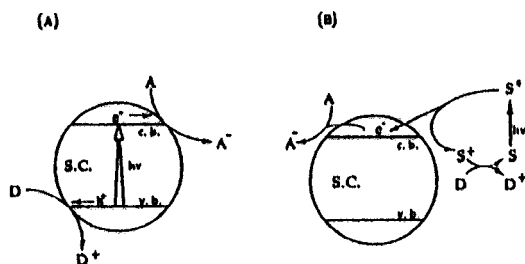


Figure 1-5. Photoinduced electron-transfer processes at a semiconductor-solution interface: (A) Charge ejection through excitation of the semiconductor. (B) Charge injection into the semiconductor through photoexcitation of a dye compound.

metal complexes can lead to excitation of the latter, resulting in electron injection from the excited dye to the S.C. conduction band (photosensitization). Sequential regeneration of the light absorbent by an electron donor along with transport of the injected electrons across the conduction band to a relay or catalyst component, provides an alternative route for the participation of *semiconductors in photoinduced electron-transfer processes*. Substantial progress has been made in the application of S.C.'s as light-active electrode materials in photoelectrochemical cells. The photosensitization process has been used for switching the activity of wide band-gap semiconductors to the visible absorption region in photoelectrochemical devices. Further progress in the application of S.C. materials in photochemical transformations has resulted from the application of S.C. powders or colloids. Excitation of such particles establishes a microcrystalline electrochemical cell by the formation of "electron-hole" pairs. Alternatively, a photosensitiza-

tion mechanism can cause *microheterogeneous S.C. particles* to act as miniature charge carriers in *photochemical assemblies* by a photosensitization mechanism. Thus, organic dyes, metal complexes, or microheterogeneous S.C. materials can be employed as light-active sites that trigger the functions of *supramolecular assemblies*.

## Photosensitized Electron-Transfer Reactions in Colloidal Microenvironments

Ionization of surface groups on colloid particles provides a means of organizing microheterogeneous charged environments that control photosensitized electron-transfer reaction. For example, ionization in basic aqueous medium ( $\text{pH} > 7.5$ ) of silanol groups at the surface of  $\text{SiO}_2$  colloids results in negatively charged particles due to the formation of a diffuse double layer [36]. The surface potential [37] of  $\text{SiO}_2$  colloids, which exhibit a mean diameter of 40 Å, has been estimated to be  $\psi = -170$  mV. Such negatively charged  $\text{SiO}_2$  colloids have been incorporated into photosensitized electron-transfer systems, as have positively charged  $\text{Al}_2\text{O}_3$  and  $\text{ZrO}_2$  colloids [38].

Charged microscopic  $\text{SiO}_2$  particles [19, 37] exert a strong influence on the photosensitized electron-transfer processes in a photosystem that includes Ru(II)-trisbipyridine,  $\text{Ru}(\text{bpy})_3^{2+}$  5, as photosensitizer, *N,N'*-di-(3-sulfonatopropyl)-4,4'-bipyridinium,  $\text{PVS}^0$  6, as electron acceptor, and triethanolamine (TEOA) as sacrificial electron donor. Figure 2-1 a shows the rate of formation of the reduced photoproduct  $\text{PVS}^{\cdot-}$  in the presence of the  $\text{SiO}_2$  colloid. The *quantum yield for PVS<sup>·-</sup> formation* corresponds to  $\phi = 0.04$ . By contrast, illumination of the same photosystem in a homogeneous aqueous phase is considerably less effective in forming the reduced photoproduct  $\text{PVS}^{\cdot-}$ , as shown by Figure 2-1 b ( $\phi = 0.005$ ). The sequence of reactions leading to the photoreduction of  $\text{PVS}^0$  is outlined in equations 2-1 through 2-3. The primary process involves electron-transfer quenching of the photoexcited photosensitizer and formation of the encounter cage complex of photoproducts. The photoproducts can either recombine in the cage structure to ground-state reactants or, alternatively, separate within the medium. Separated photoproducts can interact through the thermodynamically favored back-electron transfer reaction (eq. 2-2). This competes with a process in which the oxidized photoproduct is reduced by the sacrificial electron donor (eq. 2-3), leading to a steady-state accumulation of  $\text{PVS}^{\cdot-}$ . The  $\text{SiO}_2$  colloid provides a microenvironment for controlling these processes (Figure 2-2). Photoreactants are organized in the medium through electrostatic attraction of the photosensitizer,  $\text{Ru}(\text{bpy})_3^{2+}$ , to the  $\text{SiO}_2$  surface. Upon electron transfer, the reduced photoproduct  $\text{PVS}^{\cdot-}$  is re-

ductive materials and to tailor SPA-based electronic devices (i.e., *phototransistors*).

Organic dyes [32] (i.e., acridine or xanthene dyes) or transition metal complexes [33] such as metal-polypyridine complexes or metal porphyrins are frequently applied as light-harnessing components that trigger the functionality of an SPA. *Semiconductor materials* provide alternative *photoactive* components that can be included in *supramolecular assemblies* [34, 35]. Excitation of a semiconductor (S.C.) results in the formation of "electron-hole" pairs. Sequential electron ejection from the semiconductor conduction band to an electrolyte acceptor, followed by electron transfer from a donor component to valence-band holes, provides a means of inducing the photochemical electron-transfer processes (Figure 1-5A). S.C. materials can also act as charge carriers in photochemical transformations (Figure 1-5B). The coupling of semiconductors to dye compounds or transition

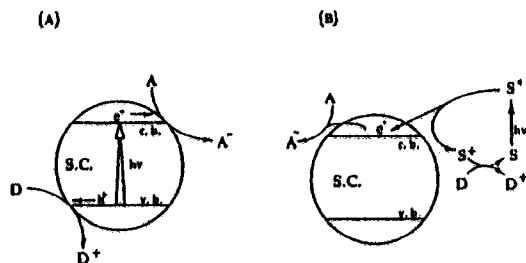


Figure 1-5. Photoinduced electron-transfer processes at a semiconductor-solution interface: (A) Charge ejection through excitation of the semiconductor. (B) Charge injection into the semiconductor through photoexcitation of a dye compound.

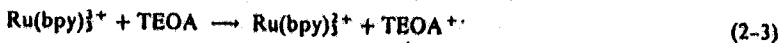
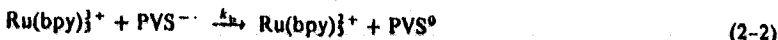
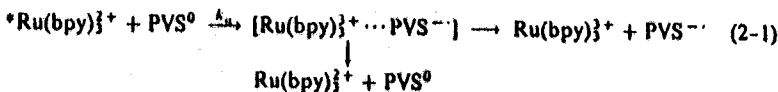
metal complexes can lead to excitation of the latter, resulting in electron injection from the excited dye to the S.C. conduction band (photosensitization). Sequential regeneration of the light absorbent by an electron donor along with transport of the injected electrons across the conduction band to a relay or catalyst component, provides an alternative route for the participation of *semiconductors in photoinduced electron-transfer processes*. Substantial progress has been made in the application of S.C.'s as light-active electrode materials in photoelectrochemical cells. The photosensitization process has been used for switching the activity of wide band-gap semiconductors to the visible absorption region in photoelectrochemical devices. Further progress in the application of S.C. materials in photochemical transformations has resulted from the application of S.C. powders or colloids. Excitation of such particles establishes a microcrystalline electrochemical cell by the formation of "electron-hole" pairs. Alternatively, a photosensitiza-

tion mechanism can cause *microheterogeneous S.C. particles* to act as miniature charge carriers in *photochemical assemblies* by a photosensitization mechanism. Thus, organic dyes, metal complexes, or microheterogeneous S.C. materials can be employed as light-active sites that trigger the functions of *supramolecular assemblies*.

## Photosensitized Electron-Transfer Reactions in Colloidal Microenvironments

Ionization of surface groups on colloid particles provides a means of organizing microheterogeneous charged environments that control photosensitized electron-transfer reaction. For example, ionization in basic aqueous medium ( $\text{pH} > 7.5$ ) of silanol groups at the surface of  $\text{SiO}_2$  colloids results in negatively charged particles due to the formation of a diffuse double layer [36]. The surface potential [37] of  $\text{SiO}_2$  colloids, which exhibit a mean diameter of 40 Å, has been estimated to be  $\psi = -170$  mV. Such negatively charged  $\text{SiO}_2$  colloids have been incorporated into photosensitized electron-transfer systems, as have positively charged  $\text{Al}_2\text{O}_3$  and  $\text{ZrO}_2$  colloids [38].

Charged microscopic  $\text{SiO}_2$  particles [19, 37] exert a strong influence on the photosensitized electron-transfer processes in a photosystem that includes Ru(II)-tris-bipyridine,  $\text{Ru}(\text{bpy})_3^{2+}$  5, as photosensitizer, *N,N'*-di-(3-sulfonatopropyl)-4,4'-bipyridinium,  $\text{PVS}^{\circ}$  6, as electron acceptor, and triethanolamine (TEOA) as sacrificial electron donor. Figure 2-1 a shows the rate of formation of the reduced photoproduct  $\text{PVS}^{\cdot-}$  in the presence of the  $\text{SiO}_2$  colloid. The quantum yield for  $\text{PVS}^{\cdot-}$  formation corresponds to  $\phi = 0.04$ . By contrast, illumination of the same photosystem in a homogeneous aqueous phase is considerably less effective in forming the reduced photoproduct  $\text{PVS}^{\cdot-}$ , as shown by Figure 2-1 b ( $\phi = 0.005$ ). The sequence of reactions leading to the photoreduction of  $\text{PVS}^{\circ}$  is outlined in equations 2-1 through 2-3. The primary process involves electron-transfer quenching of the photoexcited photosensitizer and formation of the encounter cage complex of photoproducts. The photoproducts can either recombine in the cage structure to ground-state reactants or, alternatively, separate within the medium. Separated photoproducts can interact through the thermodynamically favored back-electron transfer reaction (eq. 2-2). This competes with a process in which the oxidized photoproduct is reduced by the sacrificial electron donor (eq. 2-3), leading to a steady-state accumulation of  $\text{PVS}^{\cdot-}$ . The  $\text{SiO}_2$  colloid provides a microenvironment for controlling these processes (Figure 2-2). Photoreactants are organized in the medium through electrostatic attraction of the photosensitizer,  $\text{Ru}(\text{bpy})_3^{2+}$ , to the  $\text{SiO}_2$  surface. Upon electron transfer, the reduced photoproduct  $\text{PVS}^{\cdot-}$  is re-



decomposition products

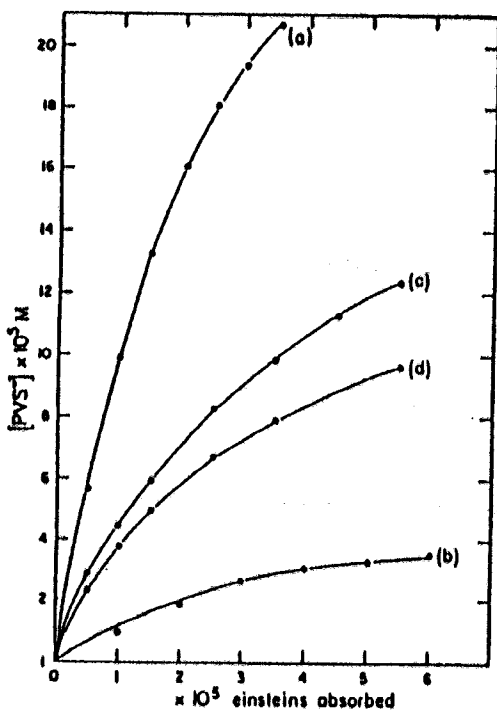


Figure 2-1. Quantum yield of  $PVS^{\cdot-}$  formation using  $Ru(bpy)_3^{2+}$  as photosensitizer. In all systems,  $[Ru(bpy)_3^{2+}] = 6 \times 10^{-5}$  M;  $[PVS^0] = 1 \times 10^{-3}$  M;  $[TEOA] = 1 \times 10^{-3}$  M. (a) In the presence of 0.2%  $SiO_2$  colloid; (b) in a homogeneous aqueous phase; (c) with 0.2%  $SiO_2$  and added  $[NaCl] = 1 \times 10^{-2}$  M; (d) with 0.2%  $SiO_2$  colloid and added  $[NaCl] = 5 \times 10^{-2}$  M.

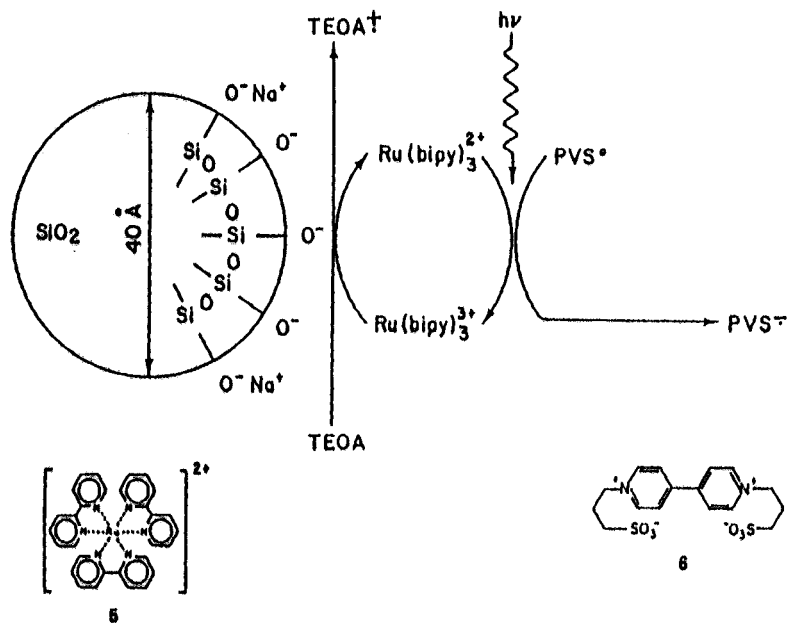


Figure 2-2. Schematic illustration of the role of the SiO<sub>2</sub> colloid in controlling photosensitized reduction of PVS<sup>0</sup>.

pelled by the negatively charged colloid interface, while the oxidized photoproduct associates with it. Consequently, the reactive photoproducts are stabilized against the recombination process, and competitive oxidation of TEOA by Ru(bipy)<sub>3</sub><sup>3+</sup> predominates; retardation of the destructive recombination process leads to an improved quantum yield for PVS<sup>-•</sup> formation under steady-state illumination. Figure 2-3 highlights the effect of the SiO<sub>2</sub> colloid on the recombination process (eq. 2-2), in that the back-electron transfer reaction is examined directly by means of laser flash photolysis. In the homogeneous aqueous phase there is rapid decay of flash-photogenerated PVS<sup>-•</sup> with Ru(bipy)<sub>3</sub><sup>3+</sup> (Figure 2-3 A, eq. 2-2), with a diffusion-controlled back-electron transfer rate constant  $k_b = 7.9 \times 10^9 \text{ M}^{-1} \text{ s}^{-1}$ . In the presence of the SiO<sub>2</sub> colloid, substantially slower decay of PVS<sup>-•</sup> is observed (Figure 2-3 B) ( $k_b = 5.7 \times 10^7 \text{ M}^{-1} \text{ s}^{-1}$ ), implying that the colloid indeed retards the recombination process, and that the photoproducts are stabilized against back-electron transfer.



The effects of the  $\text{SiO}_2$  colloid on back-electron transfer are due to selective electrical repulsion of  $\text{PVS}^{\cdot-}$  from the solid interface. The operation of an electrostatic repulsive mechanism has been confirmed by examining the  $\text{SiO}_2$  colloid photosystem in media of differing ionic strength. The electrical surface potential of the  $\text{SiO}_2$  particles is strongly affected by ionic strength; as the ionic strength increases, the electrical surface potential decreases. This dependence of colloid surface potential on ionic strength is expressed by the Gouy-Chapman theory (with Stern modification), eq. 2-4, where  $\sigma$ , is the particle surface charge density ( $\text{C}\cdot\text{m}^{-2}$ ),  $\psi_s$  is the surface potential,  $C$  is the total molar concentration of electrolyte,  $T$  is the temperature ( $^{\circ}\text{K}$ ), and  $D$ ,  $R$ , and  $F$  represent, respectively, the dielectric constant, gas constant, and Faraday constant.

$$\sigma_s = 2.66 \times 10^{-4} [\text{DRT}]^{1/2} C^{1/2} \sinh \frac{F\psi_s}{2RT} \quad (2-4)$$

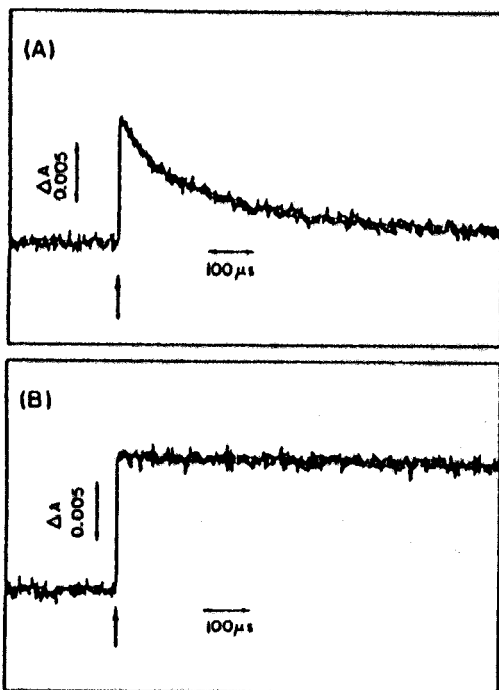
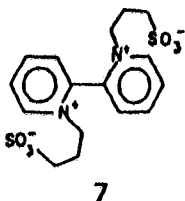


Figure 2-3. Transient absorption changes for  $\text{PVS}^{\cdot-}$ , followed at  $\lambda = 602$  nm. Arrow indicates the later pulse;  $[\text{Ru}(\text{bpy})_3]^{2+} = 3.6 \times 10^{-5}$  M;  $[\text{PVS}^{\cdot-}] = 4 \times 10^{-3}$  M. (A) in a homogeneous aqueous phase; (B) in the presence of 0.2%  $\text{SiO}_2$  colloid.

The rate of  $\text{PVS}^{\cdot-}$  formation in the course of steady-state illumination of a photosystem that includes the  $\text{SiO}_2$  colloid is strongly affected by the ionic strength (Figure 2-1). It is evident that as the ionic strength of the system increases, the rate of  $\text{PVS}^{\cdot-}$  formation declines, and at a concentration of  $[\text{NaCl}] = 0.5 \text{ M}$ , the quantum efficiency for  $\text{PVS}^{\cdot-}$  approaches the value observed for the photosystem in a homogeneous aqueous phase. The specific effect of ionic strength on recombination rates further confirms the notion that the  $\text{SiO}_2$  colloid operates through electrostatic interactions in the *stabilization of the photoproducts against back-electron transfer reactions*. Table 2-1 contrasts the quantum efficiencies of  $\text{PVS}^{\cdot-}$  formation in the  $\text{SiO}_2$  colloid photosystem at different ionic strengths with the corresponding homogeneous photosystem. Details are also provided on the specific electric surface potential of the  $\text{SiO}_2$  colloid and the recombination rate constant. The results clearly reveal that as the surface potential of the  $\text{SiO}_2$  colloid decreases, the recombination rate is enhanced, and the quantum yield under steady-state illumination declines.

The microheterogeneous  $\text{SiO}_2$  colloid also controls the photosensitized reduction of *N,N'*-di-(3-sulfonatopropyl)-2,2'-bipyridine,  $\text{DQS}^0$  (7), where  $\text{Ru}(\text{bpy})\}^+$



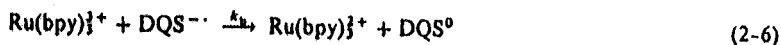
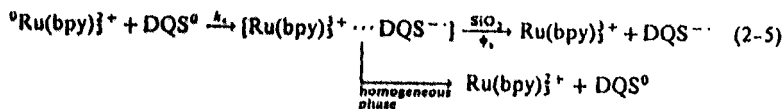
is used as photosensitizer and TEOA as sacrificial electron donor [20]. Upon illumination of this photosystem in a homogeneous aqueous phase, no reduced photoproduct  $\text{DQS}^{\cdot-}$  is formed. However, illumination of the photosystem in the presence of the  $\text{SiO}_2$  colloid yields  $\text{DQS}^{\cdot-}$  with a quantum efficiency  $\phi = 2.4 \times 10^{-2}$ . Detailed analysis of the charge-separation events reveals two important *functions of the  $\text{SiO}_2$  colloid in the photosensitized electron-transfer process*. Primary electron-transfer quenching leads to a primary encounter-cage complex of the photoproducts (eq. 2-5). Under homogeneous phase conditions, the photoproducts recombine within the cage structure, and no free photoproducts are detected. In the presence of the  $\text{SiO}_2$  colloid, however, there is effective separation of the encounter cage complex. The encounter complex of the photoproducts  $[\text{Ru}(\text{bpy})\}^+ \cdots \text{DQS}^{\cdot-}]$  associates with the colloid interface as a result of its net positive charge. Its negative counterpart is repelled by the colloid interface, however, so effective cage escape of the reduced photoproduct is observed ( $\phi = 2.6 \times 10^{-1}$ ). Subsequently, the colloid plays a role in the retardation of diffu-

Table 2-1. Quantum efficiencies and recombination rate constants involved in the photosensitized reduction of PVS<sup>•-</sup> and DQS<sup>•-</sup> in homogeneous and microheterogeneous SiO<sub>2</sub> media.

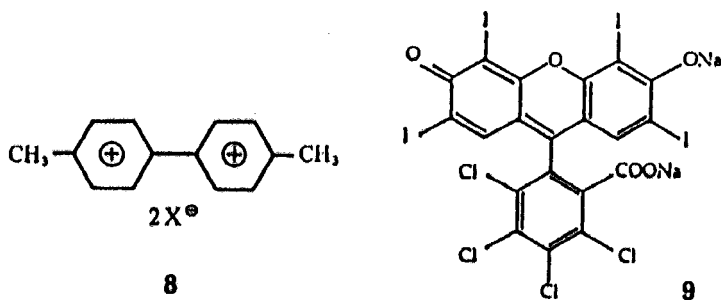
	PVS <sup>•-</sup>							DQS <sup>•-</sup>				
	Homogeneous		With SiO <sub>2</sub>					Homogeneous		With SiO <sub>2</sub>		
	[NaCl] (M)							[NaCl] (M)				
	0	0.01	0.025	0.1	0.2	0.5		0	0.1	0.2	0.4	
$\phi_{\text{sc}}$ (a)	0.005	0.04	0.03	0.022	0.018	0.014	0.009	(d)	0.024	(e)	(e)	(e)
$\phi_c$ (b)	0.38	0.38	0.38	0.38	0.38	0.38	0.38	(d)	0.26	0.26	0.19	0.16
$k_r/M^{-1} \times s^{-1}$	$7.9 \times 10^8$	$5.6 \times 10^7$	$9 \times 10^8$	$2.7 \times 10^8$	$4.3 \times 10^8$	$5.2 \times 10^8$	$3 \times 10^9$	(d)	$1 \times 10^7$	$3 \times 10^8$	$5 \times 10^8$	$8 \times 10^8$
$\psi_s/mV$ (c)	—	-170	-152	-143	-120	-92	-78	(d)	-170	-120	-92	-84

- (a) Quantum efficiencies under steady state illumination.  
 (b) Charge separation quantum yield of the primary encounter cage complex of photoproducts.  
 (c) Surface potential of SiO<sub>2</sub> colloid, calculated by eq. 2-4.  
 (d) No charge separation of DQS<sup>•-</sup> occurs in the homogeneous system.  
 (e) Not determined experimentally.

sional recombination of the intermediate photoproducts (eq. 2-6) through repulsion of  $\text{DQS}^{\cdot\cdot}$  by the colloid-interface, associating the oxidized species. Table 2-1 includes detailed data on quantum yields for the escape of photoproducts ( $\phi$ ), as well as diffusional recombination rate constants for this photosystem at various ionic strengths. The data confirm that the  $\text{SiO}_2$  colloid operates through electrostatic interactions. As the surface potential of the colloid decreases, there is a decline in the effectiveness with which it assists in separation of the encounter complex of photoproducts and the subsequent retardation of the recombination rate is reduced. We therefore conclude that organization of a photosystem by means of electrostatic interactions permits the *control of unidirectional photoinduced electron-transfer reactions*. Directionality is achieved through specific attractive and repulsive interactions between photoproducts and the charged microheterogeneous system.



Supramolecular assemblies might alter the mechanism of photosensitized electron-transfer reactions, thereby affecting the efficiency of such transformations [39]. Xanthene dyes form ground-state complexes with bipyridinium salts such as *N,N'*-dimethyl-4,4'-bipyridinium, methyl viologen,  $\text{MV}^{2+}$  (8). For example, Rose bengal,  $\text{RB}^{2-}$  (9), forms a complex with  $\text{MV}^{2+}$  with



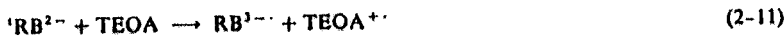
$K_s = (11,000 \pm 1,100) \text{ M}^{-1}$  (eq. 2-7). Electrostatic attractive interactions between the negatively-charged xanthene dye and the positively-charged bipyridinium electron acceptor provide the stabilizing driving forces for these complexes. For-

mation of a photosensitizer-electron relay complex results in static quenching of the excited singlet state of the photosensitizer. The resulting encounter cage complex of photoproducts is non-separable, leading to rapid recombination of the intermediate photoproducts (eq. 2-8). The formation of such ground-state com-



plexes substantially affects the efficiency of the photosensitized reduction of  $MV^{2+}$  under steady-state illumination. Figure 2-4a shows the rate of  $MV^{\cdot+}$  formation upon illumination of a photosystem that includes  $RB^{2-}$  as photosensitizer,  $MV^{2+}$  as electron relay, and triethanolamine, TEOA, as electron donor. The inefficient formation of  $MV^{\cdot+}$  ( $\phi = 8 \times 10^{-4}$ ), is due to rapid recombination of the intermediate photoproducts in the encounter complex (eq. 2-8).

Organization of the photosystem within a microheterogeneous  $SiO_2$  colloid changes the mechanism of this photosensitized electron-transfer process. The  $SiO_2$  colloid separates the ground-state complex  $[RB^{2-} \cdots MV^{2+}]$  through electrostatic association of the electron acceptor to the negatively charged  $SiO_2$  interface, and concomitant repulsion of  $RB^{2-}$  (eq. 2-9).



This separation in turn leads to a new mechanism for photosensitized electron transfer outlined in (eq. 2-10) through (2-12). The separated excited photosensitizer (singlet) decays to the triplet state. Subsequently the triplet-excited photosensitizer is quenched via electron transfer by TEOA. The oppositely-charged photoproducts are selectively subject to either attraction or repulsion by the  $SiO_2$  interface. Consequently, back-electron transfer is retarded, permitting effective reduction of  $MV^{2+}$  by  $RB^{\cdot-}$  (as well as by  $TEOA^{\cdot+}$ ). Figure 2-4b shows the rate of  $MV^{\cdot+}$  formation in this organized microheterogeneous photosystem under condi-

tions of continuous illumination. It can be seen that the quantum efficiency for  $MV^{+\cdot}$  formation ( $\phi = 1 \times 10^{-1}$ ), is 125 times as large as in the homogeneous photosystem.

Further organization of the photosystem is accomplished by immobilization of a Pd metal catalyst on the  $SiO_2$  colloid particles [39], leading to a microheterogeneous catalytic assembly for photosynthetic transformations. The electron acceptor *N,N'*-dibenzyl-(3,3'-dimethyl)-4,4'-bipyridinium,  $BMV^{2+}$  (10), exhibits a reduc-

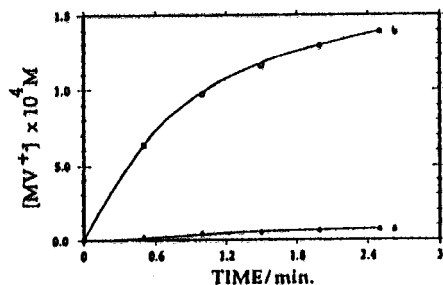
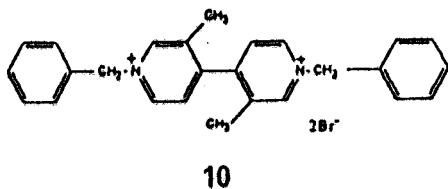
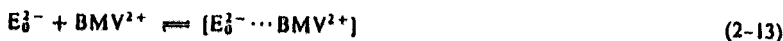
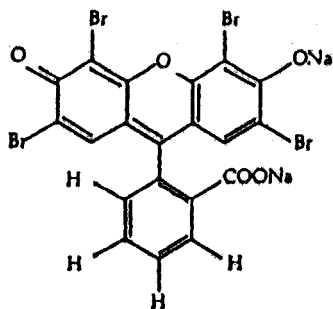


Figure 2-4. Rate of  $MV^{+\cdot}$  formation as a function of illumination time for a system that includes  $[RB^{2-}] = 1 \times 10^{-5}$  M;  $[MV^{2+}] = 1 \times 10^{-3}$  M;  $[TEOA] = 1 \times 10^{-3}$  M, pH = 9.3. (a) In a homogeneous solution; (b) in the presence of 1%  $SiO_2$  colloid.

tion potential ( $E^0 = -0.670$  V vs. NHE) that permits hydrogen evolution in basic aqueous environments, where the controlling effects of the  $SiO_2$  colloid are operative. The electron acceptor  $BMV^{2+}$  forms a ground-state complex with the xanthene dye eosin,  $E_0^{2-}$  (11), as shown in eq. 2-13. Illumination of a photosystem that includes eosin as photosensitizer,  $BMV^{2+}$  as electron acceptor, TEOA as electron donor, and colloidal Pd in a homogeneous aqueous phase does not yield the reduced photoproduct  $BMV^{+\cdot}$ , nor does it cause  $H_2$  evolution. The lack of photoproducts can be rationalized in terms of rapid recombination of the intermediate photoproducts in the encounter cage complex. By contrast, organization of the same photosystem in a catalytic microheterogeneous assembly that includes Pd immobilized on colloidal  $SiO_2$  does result in effective photoinduced  $H_2$ -evolu-



tion ( $\phi = 1.1 \cdot 10^{-3}$ ). The complementary synchronous functions of the Pd-SiO<sub>2</sub> colloid in controlling photosensitized H<sub>2</sub>-evolution are outlined schematically in Figure 2-5. Primary separation of the ground-state eosin-relay complex allows spatial organization of the photosystem components and eliminates internal elec-



11

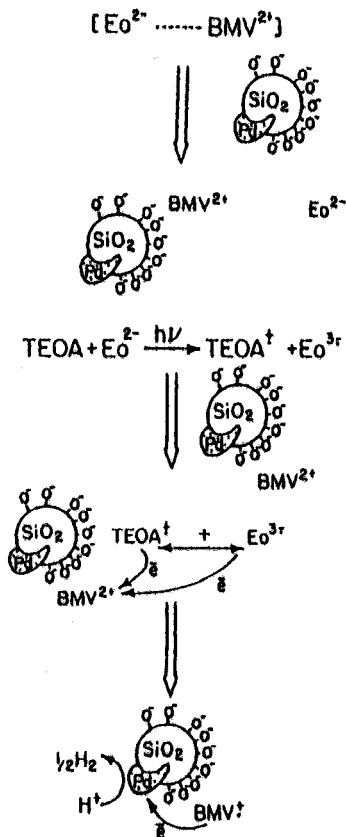


Figure 2-5. Schematic illustration of the role of Pd-SiO<sub>2</sub> colloid in controlling photosensitized reduction of BMV<sup>2+</sup> and subsequent catalytic H<sub>2</sub>-evolution (E<sub>0</sub><sup>2-</sup> used as photosensitizer).

tron-transfer quenching as well as recombination reactions in the encounter complex structure of photoproducts. Subsequent quenching of the excited photosensitizer by triethanolamine yields oppositely charged photoproducts that are oriented in the microheterogeneous system by means of the charged  $\text{SiO}_2$  interface. This orientation eliminates the back-electron transfer from intermediate species, and the final reduced photoproduct,  $\text{BMV}^+$ , formed by reduction of  $\text{BMV}^{2+}$  by  $\text{E}_0^{\text{H}^+}$  and  $\text{TEOA}^+$ , mediates effective  $\text{H}_2$ -evolution at the immobilized Pd catalyst.

These examples demonstrate various functions associated with the charged solid colloid interface in photosensitized electron-transfer reactions:

- i) The interface effects the separation of ground-state photosensitizer-relay complexes that would otherwise have a destructive influence on photoinduced electron-transfer reactions.
- ii) It assists charge separation of the encounter cage complex of photoproducts, and also stabilizes intermediate photoproducts against back-electron transfer reactions.
- iii) It provides a matrix for supporting potential catalytic sites. Orientation of the photoproducts at such catalytic sites by means of the charged  $\text{SiO}_2$  interface facilitates subsequent catalytic transformations (i.e.,  $\text{H}_2$ -evolution).

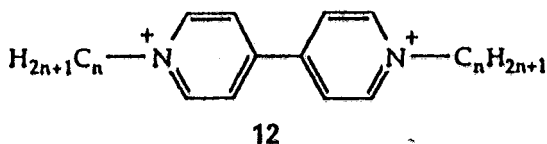
## Photosensitized Electron-Transfer Reactions in Water-Oil Microstructural Systems

*Water-in-oil microemulsions* create microstructural environments for the control of electron-transfer reactions by means of *hydrophilic-hydrophobic interactions*. The role of such interactions in charge separation is illustrated schematically in Figure 3-1A. The reactants tend to exhibit hydrophilic character, and they are localized in the aqueous compartment of a water-oil microstructural system. Photoinduced electron transfer results in the reduced photoproduct, which exhibits hydrophobic character, and this is extracted from the aqueous phase, crossing the interface and passing into the oil phase. Charge separation and stabilization of the photoproducts against back-electron transfer is thus a consequence of compartmentalization of the photoproducts in the two phases. Microstructural hydrophilic-hydrophobic interfacial systems such as micelles and microemulsions provide water-oil boundaries of high surface area, thereby facilitating effective mass-transport (extraction).

Water-in-oil microemulsions with water pools stabilized by dodecylammonium propionate were successfully applied as organized reaction media for photoinduced electron-transfer reactions [27b]. The photosystem itself is composed of  $\text{Ru(II)}$ -tris-bipyridine as photosensitizer,  $(\text{NH}_4)_3\text{EDTA}$  as sacrificial electron do-



nor, and an  $N,N'$ -dialkyl-4,4'-bipyridinium electron acceptor,  $C_nV^{2+}$  (12), in which the alkyl chain length is subject to adjustment ( $n = 1-18$ ). The sequence of



reactions leading to reduction of the electron relay  $C_nV^{2+}$  involves primary electron-transfer quenching of the excited photosensitizer  $Ru(bpy)_3^{2+}$ , separation of

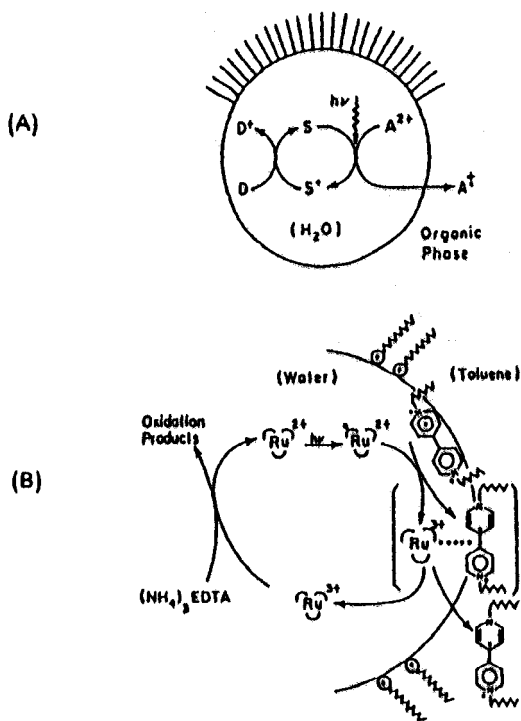
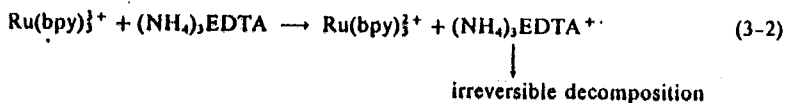
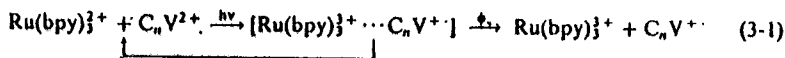


Figure 3-1. (A) Charge separation of photogenerated electron-transfer products through hydrophilic-hydrophobic interactions at water-oil boundaries. (B) Control of the photosensitized reduction of  $C_nV^{2+}$  in a water-in-oil microemulsion with  $Ru(bpy)_3^{2+}$  as photosensitizer.

the encounter cage complex, and irreversible oxidation of  $(\text{NH}_4)_3\text{EDTA}$  by the oxidized photoproduct,  $\text{Ru}(\text{bpy})_3^{3+}$  (eq. 3-1 and 3-2). Quantum yields for the for-



mation of  $\text{C}_n\text{V}^{+ \cdot}$  are controlled by separation of the encounter cage complex and the relative ability of the irreversible process to compete with the back-electron transfer reaction (eq. 3-3). Figure 3-2 shows the rate of  $\text{C}_n\text{V}^{+ \cdot}$  formation in water-in-oil microemulsions containing different electron relays. The electron relay with  $n=1$  is not photoreduced at all in this water-in-oil microemulsion, and  $\text{C}_4\text{V}^{2+}$  forms very inefficiently. A sharp increase in the rate of reduction is apparent with  $\text{C}_6\text{V}^{2+}$ , and  $\text{C}_9\text{V}^{2+}$  represents a further improvement. Longer chain bipyridinium

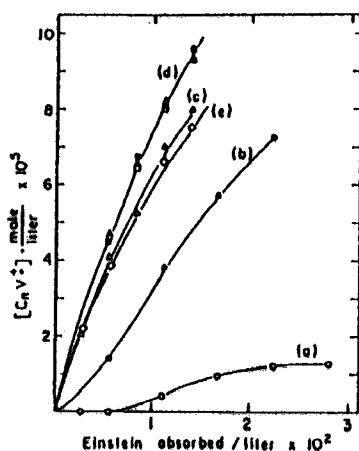


Figure 3-2. Quantum yield for  $\text{C}_n\text{V}^{+ \cdot}$  formation in a water-in-oil microemulsion. (a)  $n=4$ , (b)  $n=6$ , (c)  $n=8$ , (d)  $n=10, 12$ , and  $14$ , (e)  $n=18$ . For all systems,  $[\text{Ru}(\text{bpy})_3^{3+}] = 2 \times 10^{-5}$  M,  $[\text{C}_n\text{V}^{2+}] = 1 \times 10^{-4}$  M, and  $[(\text{NH}_4)_3\text{EDTA}] = 6 \times 10^{-4}$  M.

Table 3-1. Charge separation and steady state quantum yields and recombination rates in the photo-sensitized reduction of  $C_nV^{2+}$ .

$n$	1	4	6	8	14	18
$\phi$ , (a)	0	0.006	0.036	0.040	0.050	0.054
$10^9 \times k_r/M^{-1} \times s^{-1}$ (b)	(d)	26	8	0.7	0.33	1.2
$10^3 \phi_{ss}$ , (c)	$< 10^{-5}$	0.8	2.5	7.5	8.1	7.2

(a) Charge separation quantum efficiency of the encounter cage complex of photoproducts, eq. 3-1.

(b) Recombination rate constants of intermediate photoproducts, eq. 3-3.

(c) Quantum efficiencies of  $C_nV^{2+}$  formation under steady state illumination.

(d) No charge separation of  $C_1V^{2+}$  is observed in the water-in-oil microemulsion.

salts ( $C_{10}V^{2+} - C_{18}V^{2+}$ ) are photoreduced at the same rate as  $C_4V^{2+}$ . Table 3-1 summarizes the corresponding charge separation quantum yields for encounter cage complexes (eq. 3-1), steady-state quantum efficiencies, and recombination rate constants for the intermediate photoproducts (eq. 3-3). A sharp increase in charge-separation efficiencies and the concomitant retardation of back-electron transfer is retarded in photosystems that include  $C_6V^{2+}$  and  $C_8V^{2+}$  as electron acceptors. These electron relays apparently offer the proper hydrophilic-hydrophobic balance for controlling photosensitized transformations in the microstructural water-oil environment (Figure 3-1 B). In its oxidized form the acceptor exhibits hydrophilic properties, so it resides in the water microdroplets. The reduced photoproduct  $C_nV^{2+}$ , on the other hand, exhibits hydrophobic character, and it is extracted into the oil phase. Consequently, the interfacial system assists charge separation of the primary encounter complex of electron transfer products by extraction of the resulting hydrophobic species into the oil phase. Concomitantly, retardation in the back electron transfer rate is achieved by separation of the photoproducts in the two distinct hydrophilic-hydrophobic environments.

## Control of Photosensitized Electron-Transfer Processes with Cyclodextrin Receptor Systems

The various organized photosystems discussed in the previous sections involve microheterogeneous assemblies that control photosensitized electron-transfer reactions. Macromolecular receptor systems that selectively interact with one of the photoreactants or photoproducts could in principle behave similarly in con-

trolling photoinduced electron transfer. One possible scheme for participation of a receptor component in effecting charge separation and stabilization of the photoproducts against back-electron transfer is outlined in Figure 4-1. Through selective association of the electron relay with the receptor site, separation of ground-state photosensitizer-acceptor complexes can be induced, and intramolecular back-reactions can be thereby eliminated. Further association of the reduced photoproduct in the receptor cavity might shield the active intermediate from the external environment and thus stabilize the photoproducts against back-electron transfer reactions.

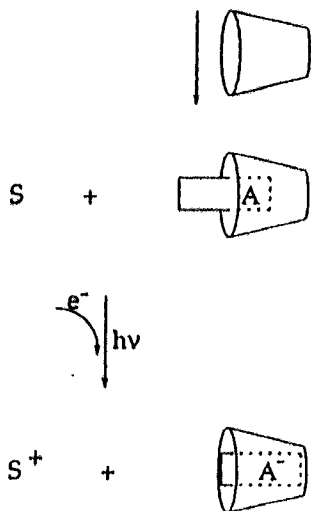
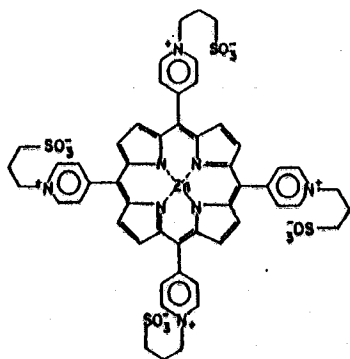
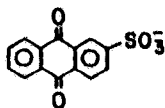


Figure 4-1. Control of photosensitized electron-transfer reactions by means of molecular receptors.

Cyclodextrins (CD) have been used as molecular receptors to control electron-transfer reactions in organized assemblies [40, 41]. Cyclodextrins are cyclic polysugars composed of glucose units linked by  $\alpha$ -glycoside bonds. They are cylindrical in shape, with an internal hydrophobic cavity and hydrophilic peripheries of hydroxyl groups on the two receptor edges. Hydrophobic substrates of proper size and shape associate with the cyclodextrin cavity [42]. Cavity size is controlled by the number of glucose units comprising the macrocycle (6, 7, and 8 glucose units form  $\alpha$ -,  $\beta$ -, and  $\gamma$ -CD, respectively). The association properties of CD receptor



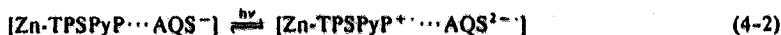
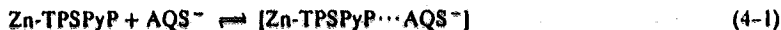
13



14

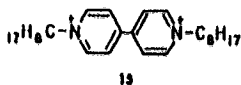
systems have been extensively employed in mimicking enzyme functions by artificial means [43, 44]. Cyclodextrin receptors have also been applied in controlling stereospecific and stereoselective phototransformations.

Cyclodextrins have been examined as reaction media for photosensitized electron-transfer reactions. Zn(II)-*meso*-tetra(*N*-propylsulfonato)pyridinium porphyrin, Zn-TPSPyP (13), forms a ground-state complex with anthraquinone-2-sulfonate, AQS<sup>-</sup> (14), as indicated by eq. 4-1 [40]. Formation of this complex results in quenching of the singlet excited photosensitizer through internal electron transfer followed by rapid recombination of the photoproducts in the complex structure (eq. 4-2). Illumination of a photosystem consisting of Zn-TPSPyP as photosensitizer, AQS<sup>-</sup> as electron acceptor, and cysteine as sacrificial electron donor results in no observable separated, reduced photoproduct due to rapid recombination. In the presence of  $\beta$ -CD, however, the ground-state complex becomes separated

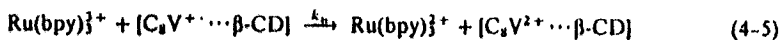
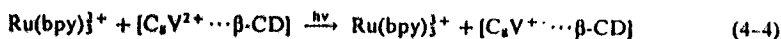


through selective association of AQS<sup>-</sup> with the  $\beta$ -CD receptor cavity. These conditions lead to a change in the mechanism of the photoinduced electron-transfer process: the triplet excited state is now quenched by AQS<sup>-</sup>, which is associated with the  $\beta$ -CD receptor. The resulting reduced photoproduct is protected by the molecular receptor against back-electron transfer; consequently, in a photosystem that includes cysteine as sacrificial electron donor, the protonated semi-anthraquinone radical anion AQHS<sup>-</sup> accumulates during illumination ( $\phi = 1.35 \times 10^{-3}$ ).

The effects of macromolecular  $\beta$ -CD receptors on the photosensitized reduction



of *N,N'*-dioctyl-4,4'-bipyridinium,  $C_8V^{2+}$  (15), by  $Ru(bpy)_3^{3+}$  and  $Zn(II)$ -*meso*-tetraphenylsulfonato porphyrin,  $Zn-TPPS^{4-}$ , have also been examined [40, 41]. With  $Zn-TPPS^{4-}$  as photosensitizer, the ground-state complex  $[Zn-TPPS^{4-} \cdots C_8V^{2+}]$  is formed in aqueous media.  $\beta$ -CD separates this complex and permits effective reduction of  $C_8V^{2+}$  through elimination of the internal back-electron reaction that would otherwise intervene. With  $Ru(bpy)_3^{3+}$  as photosensitizer, photoinduced reduction of  $C_8V^{2+}$  occurs in aqueous solution even in the absence of  $\beta$ -CD, but the photoproduct aggregates to the radical cation dimer,  $(C_8V^+)_2$ . In the presence of  $\beta$ -CD, the electron relay  $C_8V^{2+}$  associates with the receptor cavity (eq. 4-3), and photosensitized electron transfer leads to binding of the reduced photoproduct to the cyclodextrin (eq. 4-4). Since the  $\beta$ -CD cavity can accommodate only the monomeric photoproduct, aggregation of  $C_8V^+$  is eliminated. Association of  $C_8V^+$  with the cyclodextrin also substantially affects back-electron transfer of the photogenerated intermediates. In the absence of CD, the dimer aggregate photoproduct  $(C_8V^+)_2$  efficiently recombines with oxidized photoproduct (recombination rate constant  $k_b = 3.2 \times 10^8 \text{ M}^{-1} \text{ s}^{-1}$ ). Association of  $C_8V^+$  with  $\beta$ -CD protects the reduced photoproduct in the cavity structure against back-electron transfer (eq. 4-5), so the recombination rate is significantly lower ( $k_b = 3.2 \times 10^7 \text{ M}^{-1} \text{ s}^{-1}$ ).



We thus conclude that *cyclodextrin receptors* can participate in photosensitized electron transfer in three complementary ways:

- i) The receptor separates ground-state photosensitizer-relay complexes by selective association of one of the complex components to the CD cavity.
- ii) Association of one of the photoproducts with the CD cavity provides protection against back-electron transfer and lowers the recombination rate.
- iii) The photoproduct is prevented from aggregating due to binding to the CD receptor.

Cyclodextrin receptors also provide a means to control photosensitized electron-transfer reactions at semiconductor (S.C.) solution interfaces. Two different electron transfer processes can occur at an S.C. solution interface: *charge ejection* or *charge injection* (see introduction). Charge ejection of conduction band elec-

trons to a solution relay substrate occurs through photoexcitation of the S.C. (Figure 1-5A). Charge injection to the S.C. occurs through photosensitizer excitation followed by electron transfer to the S.C. conduction band, which acts as a wire for transporting the electrons (Figure 1-5B). The effectiveness of the charge-ejection process (eq. 4-6) is limited by the competitive "electron-hole" recombination process (eq. 4-7). Thus, only relay substrate associated with the S.C. interface is operative in the charge-ejection process. Similarly, charge injection is limited to



photosensitizer species in the vicinity of the S.C. interface, since only for excited entities near the interface is the electron-transfer route competitive with other decay processes. Thus, localization of relay substrates or photosensitizers at S.C. interfaces is expected to enhance both charge ejection and charge injection.

Colloids of semiconductor particles can be stabilized by cyclodextrins [45]. For example, S.C. oxides such as  $TiO_2$  or  $Fe_2O_3$  are stabilized as colloids by either  $\alpha$ - or  $\beta$ -CD. Such an S.C.-receptor assembly would provide an organized microenvironment for controlling electron-transfer reactions at the S.C.-solution interface [45].  $N,N'$ -dioctyl-4,4'-bipyridinium,  $C_8V^{2+}$  (15), associates with  $\beta$ -cyclodextrin,  $K_a = 5.6 \times 10^3 M^{-1}$ , while  $N,N'$ -dimethyl-4,4'-bipyridinium,  $MV^{2+}$ , does not. Examination of the reduction processes of  $C_8V^{2+}$  and  $MV^{2+}$  by photoexcitation of the  $TiO_2$ - $\beta$ -CD colloid and subsequent charge ejection reveals that reduction of the former is 4.2 times more efficient than that of the latter ( $\phi(C_8V^{+ \cdot})/\phi(MV^{+ \cdot}) = 4.2$ ). The reduction of both substrates using a  $TiO_2$  colloid stabilized by poly(vinyl alcohol) ( $TiO_2$ /PVA) proceeds with similar efficiency. The improved quantum yield for the reduction of  $C_8V^{2+}$  in the  $TiO_2$ - $\beta$ -CD receptor assembly can be attributed to the fact that this electron relay is localized at the S.C. interface due to association with the  $\beta$ -CD cavity. Organization of the electron acceptor at the S.C. interface increases the efficiency of charge ejection following excitation of the S.C. (Figure 4-2A). Two complementary experiments illustrate how the receptor sites improve the charge-ejection process. The rate of  $C_8V^{2+}$  photoreduction as a function of the electron relay concentration shows characteristic saturation behavior (Figure 4-2B), and at a concentration  $[C_8V^{2+}] = 1 \times 10^{-4} M$  the reduction efficiency levels off. This implies that saturation of the receptor sites leads to maximum efficiency in the charge ejection process. Inhibition experiments confirm the importance of associating the electron relay in the  $\beta$ -CD cavity in order to improve the electron-transfer process. Thus, addition of phenol lowers the photoreduction efficiency of  $C_8V^{2+}$ . At a phenol concentration of 0.05 M the rate of  $C_8V^{2+}$  photoreduction is similar to that of free  $MV^{2+}$ . Phenol binds to the  $\beta$ -CD cavities, thereby acting as a competitive inhibi-

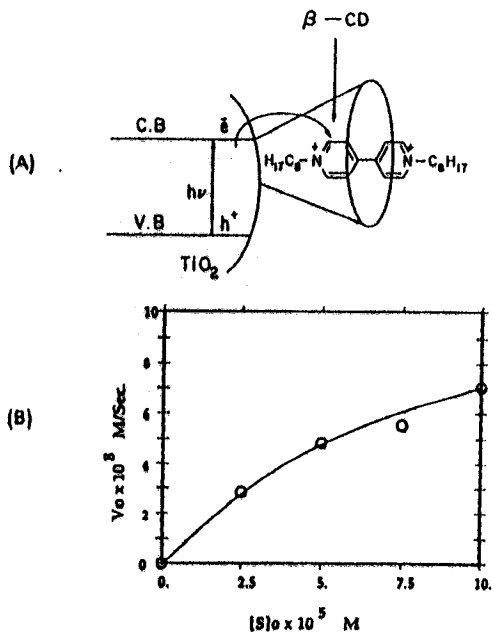
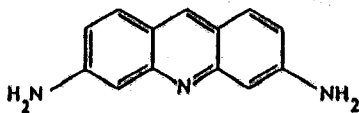


Figure 4-2. (A) Schematic diagram of the role of TiO<sub>2</sub>-β-CD colloid in improving the interfacial electron-transfer process. (B) Rate of C<sub>2</sub>V<sup>2+</sup> photoreduction by the TiO<sub>2</sub>-β-CD assembly as a function of electron-acceptor concentration.

tor with respect to C<sub>2</sub>V<sup>2+</sup>. Consequently, the organization of the electron relay at the S.C. interface is perturbed and the electron-transfer process loses much of its effectiveness.

Photosensitization of S.C. particles can also be improved through association between dyes and tailored S.C.-receptor assemblies [46]. An organized microheterogeneous system composed of Pt immobilized onto TiO<sub>2</sub> and stabilized by β-CD displays photocatalytic H<sub>2</sub>-evolution in the presence of the dye proflavine (16), as shown in Figure 4-3. Proflavine associates with the hydrophobic β-CD cavity ( $K_a = 550 \pm 60 \text{ M}^{-1}$ ), so the dye is bound to the S.C. interface. Illumination of a photosystem containing the Pt-TiO<sub>2</sub>-β-CD assembly in the presence of cysteine as sacrificial electron donor results in hydrogen evolution. This photocatalytic process occurs by primary charge injection of an electron from the excited dye to the S.C. conduction band (Figure 4-3). Cysteine reduces the oxidized dye, thereby recycling the light-harnessing component. Electrons are transported across the conduction band to the catalytic Pt site, which acts as an electron sink and as a catalyst for hydrogen evolution. The tailored catalyst-S.C.-receptor configuration is crucial to achieving a photosensitized transformation. Exclusion of the S.C. that





16

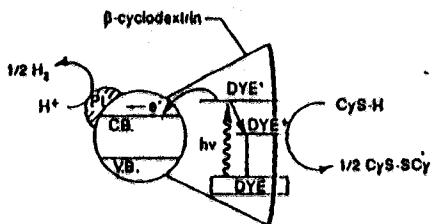


Figure 4-3. Charge injection into a semiconductor through association of dye with the semiconductor- $\beta$ -CD assembly. Charge injection results in charge transport and subsequent  $H_2$ -evolution.

acts as charge carrier also eliminates direct electron transfer from the excited dye to the metal catalyst. Furthermore, association of proflavine with the  $\beta$ -CD receptors has a significant impact on the photocatalytic transformation. Figure 4-4 shows the rate of  $H_2$ -evolution in the organized photosystem alone, together with the effect of added octyl pyridinium,  $C_8Py^+$ . Octylpyridinium,  $C_8Py^+$ , acts as a competitive inhibitor with respect to binding of proflavine to the  $\beta$ -CD receptor sites. It is evident that as the concentration of the inhibitor  $C_8Py^+$  is increased, the efficiency of photosensitized  $H_2$ -evolution decreases. Thus, association of the

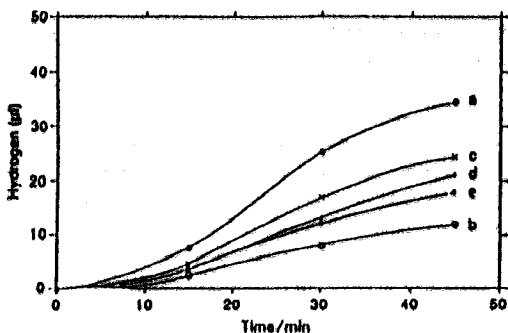


Figure 4-4. Photosensitized  $H_2$ -evolution using  $Pt-TiO_2$  colloids [5% Pt on  $TiO_2$  (w/w)]; [proflavine] =  $5.1 \times 10^{-5}$  M as photosensitizer and [Cys  $\triangleq$  cysteine] =  $1 \times 10^{-1}$  M as electron donor: (a)  $Pt-TiO_2$ - $\beta$ -CD, (b)  $Pt-TiO_2$ -poly(vinyl alcohol), (c)-(e)  $Pt-TiO_2$ - $\beta$ -CD with octyl pyridinium,  $C_8Py^+$ : (c)  $2.2 \times 10^{-4}$  M, (d)  $4.4 \times 10^{-4}$  M, (e)  $8.8 \times 10^{-4}$  M.

dye with the  $\beta$ -CD cavity localizes the excited species at the S.C.-solution interface and provides a means of effectively injecting the charge from the short-lived excited photosensitizer.

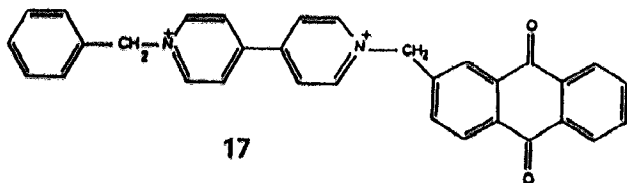
These examples highlight a variety of approaches to control photosensitized electron-transfer reactions with molecular cyclodextrin receptors. There has been considerable progress in the design of artificial receptor systems in recent years. It seems likely that other receptor systems can also serve as ordering media for photosystems. Moreover, chemical modifications of the receptors (i.e., by charged groups) might provide new functionalities for controlling photosensitized electron-transfer reactions.

## Photosensitized Electron-Transfer Reactions in Molecular Photosensitizer-Electron Relay Triad Assemblies

The control of photosensitized electron-transfer reactions in the assemblies so far discussed has been accomplished through tailored interactions of photoreactants and photoproducts with an external interface. This external interface governs the relative locations of the components and subsequently controls the electron-transfer process. However, none of the photoreactants include self-controlling elements with respect to the electron-transfer process.

In nature, the photosynthetic reaction center consists of a microstructural assembly in which a series of organized electron acceptors achieves spatial charge separation through a process of "electron hopping" along a chain of relay components [2, 3]. An appropriate molecular array of electron acceptors, with proper ordering of the reduction potentials and a link to a photosensitizer site (Figure 1-1 A), might be able to mimic the functions of the natural photosynthetic reaction center.

Design of such a molecular assembly, composed of a photosensitizer linked to a series of electron acceptors with proper "downhill" ordering of the reduction potential, S-A<sub>1</sub>-A<sub>2</sub>, could lead to an apparatus that would effect charge separation



at the molecular level [47]. The linked bipyridinium-anthraquinone acceptor *N*-benzyl-*N'*-methylanthraquinone-4,4'-bipyridinium,  $BV^{2+}$ -AQ (17), forms a ground-state complex with Zn(II)-*meso*-tetraphenylsulfonatoporphyrin, Zn-TPPS $^{4-}$ , through association of the bipyridinium component with the porphyrin unit (Zn-TPPS $^{4-}$   $\cdots$   $BV^{2+}$ -AQ). The reduction potentials of the linked electron acceptors at pH = 4.2 [ $E^{\circ}(BV^{2+}$ -AQ/ $BV^{2+}$ -AQ $\cdot^{-}$ ) = -0.19 V;  $E^{\circ}(BV^{2+}$ -AQH $\cdot^{-}$ / $BV^{2+}$ -AQH $\cdot^{-}$ ) = -0.29 V] exhibit the proper ordering to permit construction of a photosensitizer-acceptor(1)-acceptor(2) triad assembly [47].

Photochemical studies indicate that vectorial electron transfer along the electron relay chain does occur when the photosensitizer component is photoexcited. Illumination of the molecular assembly Zn-TPPS $^{4-}$   $\cdots$   $BV^{2+}$ -AQ in the presence of the sacrificial electron donor cysteine results in the formation of  $BV^{2+}$ -AQH $\cdot^{-}$  ( $\phi = 1.1 \times 10^{-3}$ ) through primary electron transfer from the excited photosensitizer to the bipyridinium component and subsequent formation of  $BV^{2+}$ -AQ as a primary intermediate (Figure 5-1). In this photosensitizer-acceptor(1)-acceptor(2)

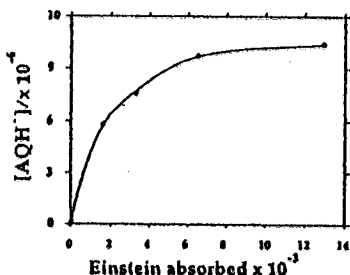


Figure 5-1. Rate of  $BV^{2+}$ -AQH $\cdot^{-}$  formation via illumination of the [Zn-TPPS $^{4-}$   $\cdots$   $BV^{2+}$ -AQ] assembly in the presence of [Cysteine] =  $5 \times 10^{-3}$  M. Illumination at pH = 3.8, [Zn-TPPS $^{4-}$ ] =  $4.65 \times 10^{-6}$  M, [ $BV^{2+}$ -AQ] =  $2.1 \times 10^{-3}$  M.

assembly the photoexcited singlet state of Zn-TPPS $^{4-}$  is statically quenched by the primary bipyridinium associated electron acceptor through an electron transfer process. The primary intermediate photoproducts, [Zn-TPPS $^{3-}$   $\cdots$   $BV^{2+}$ -AQ], are then transferred into the spatial separated photoproducts, Zn-TPPS $^{3-}$   $\cdots$   $BV^{2+}$ -AQH $\cdot^{-}$ , by the downhill reduction of the quinone compound by the intermediary bipyridinium radical cation acting as electron carrier. Thus, the molecular assembly composed of a photosensitizer-acceptor(1)-acceptor(2) array acts as a molecular wire that sequentially tunnels transferred electrons along the chain of relays. This spatial separation of the photoproducts prevents back-electron transfer from the primary intimate photoproducts, and enables effective reduction of the quinone component.

## Concluding Remarks and Prospects for the Future

Supramolecular photochemical assemblies (SPAs) are organized systems that demonstrate unique properties in photochemical transformations as a result of their internal organization and ordering. This contribution has emphasized the effects of organized assemblies on photoinduced electron-transfer reactions. We emphasize that microheterogeneous and microstructural systems as well as tailored molecular assemblies can exert enormous effects in controlling photosensitized electron-transfer reactions. There is widespread interest in utilizing photo-generated electron-transfer products in subsequent syntheses of fuel products (i.e.,  $H_2$  evolution,  $CO_2$  fixation to carbon fuels, and  $N_2$  fixation to ammonia). Organized supramolecular assemblies are likely to be intrinsic components of future artificial photosynthetic devices. Furthermore, the potential importance of supramolecular assemblies in other photochemical transformations should not be overlooked. The application of organized microenvironments for stereoselective photochemical synthesis, photoinduced active transport, and photoactivated chemical switches represent challenging scientific goals [48].

**Acknowledgement:** We gratefully acknowledge financial support from the BMFT Fund (West Germany), the U.S.-Israel Binational Foundation, and the Israel Academy of Humanities and Sciences Fund.

## Symbols and Abbreviations

A	= Electron Acceptor
AQS	= Anthraquinone-2-sulfonate
BMV <sup>2+</sup>	= <i>N,N'</i> -dibenzyl-(3,3'-dimethyl)-4,4'-bipyridinium
BV <sup>2+</sup> -AQ	= <i>N</i> -benzyl- <i>N'</i> -methylanthraquinone-4,4'-bipyridinium
C.B.	= Conduction Band
CD	= Cyclodextrin
C <sub>12</sub> MV <sup>2+</sup>	= <i>N</i> -dodecyl- <i>N'</i> -methyl-4,4'-bipyridinium
C <sub>n</sub> V <sup>2+</sup>	= <i>N,N'</i> -dialkyl-4,4'-bipyridinium
D	= Electron Donor
DQS <sup>o</sup>	= <i>N,N'</i> -di-(3-sulfonatopropyl)-2,2'-bipyridine
E <sup>o</sup>	= Standard Reduction Potential
E <sub>q</sub>	= Eosin
EDTA	= Ethylenediaminetetraacetic acid
K <sub>a</sub>	= Association Constant
k <sub>q</sub>	= Quenching Rate Constant
k <sub>b</sub>	= Back Reaction Rate Constant

MV <sup>2+</sup>	= N,N'-dimethyl-4,4'-bipyridinium
P <sup>+</sup> ·Q <sup>-</sup>	= Porphyrin-quinone ion-pair
PTZ	= Phenothiazine
PVS <sup>n</sup>	= N,N'-di-(3-sulfonatopropyl)-4,4'-bipyridinium
R	= Receptor
RB <sup>2-</sup>	= Rose bengal
S	= Photosensitizer
S.C.	= Semiconductor
SPA	= Supramolecular Photochemical Assembly
SPCA	= Supramolecular Photochemical Catalytic Assembly
TEOA	= Triethanolamine
V.B.	= Valence Band
Zn-TPPS <sup>4-</sup>	= Zn(II)- <i>meso</i> -tetraphenylsulfonato porphyrin
Zn-TPSPyP	= Zn(II)- <i>meso</i> -tetra( <i>N</i> -propylsulfonato)pyridinium
φ	= Quantum Yield
φ <sub>c</sub>	= Charge separation quantum yield
λ	= Wavelength
ψ	= Surface Potential

## References

- [1] Balzani, V., Moggi, L., in "Supramolecular Photochemistry", Balzani, V., Ed., NATO ASI, Series C, D. Reidel Publishing Company, Dordrecht, The Netherlands, 1987, Vol. 214, p. 1.
- [2] a) Deisenhofer J., Epp, O., Miki, K., Huber, R., Michel, H., *J. Mol. Biol.* 1984, 180, 385. b) Deisenhofer, J., Epp, O., Miki, K., Huber, R., Michel, H., *Nature (London)* 1985, 318, 618. c) Chang, C. H., Tiede, D., Tang, J., Smith, V., Norris, J., Schiffer, M., *FEBS Lett.* 1986, 205, 82.
- [3] a) Kaufman, K. J., Dutton, P. L., Netzel, T. L., Leigh, S. J., Rentzepis, P. M., *Science (Washington D.C.)* 1975, 188, 1301. b) Allen, P., Feher, G., Yeates, T. O., Rees, D. C., Deisenhofer, J., Michel, H., Huber, R., *Proc. Natl. Acad. Sci. USA* 1986, 83, 8589.
- [4] Wasielewski, M. R., Niemczyk, M. P., Svec, W. A., Pewitt, E. B., *J. Am. Chem. Soc.* 1985, 107, 5562.
- [5] a) Gust, D., Moore, T. A., Liddell, P. A., Nemeth, G. A., Makings, L. R., Moore, A. L., Barrett, D., Pessiki, P. J., Bensasson, R. V., Rougée, M., Chachaty, C., de Schryver, F. C., Van der Auweraer, M., Holzwarth, A. R., Connolly, J. S., *J. Am. Chem. Soc.* 1987, 109, 846. b) Danielson, E., Elliot, C. M., Merkert, J. W., Meyer, T. J., *J. Am. Chem. Soc.* 1987, 109, 2519.
- [6] a) Moore, T. A., Gust, D., Mathis, P., Minlloq, J. C., Chachaty, C., Bensasson, R. V., Land, E. J., Doizi, D., Liddell, P. A., Lehman, W. R., Nemeth, G. A., Moore, A. L., *Nature* 1984, 307, 630. b) Meyer, T. J., *Acc. Chem. Res.* 1989, 22, 163.
- [7] Willner, I. in "Photosensitized Electron Transfer Reactions in Organized Systems", Fox, M. A. (ed.), ACS Symposium Series 278, American Chemical Society, Washington D.C., 1985, p. 91.
- [8] a) Willner, I., Steinberger-Willner, B., *Int. J. Hydrogen Energy* 1988, 13, 593. b) Sutin, N., Creutz, C., *Pure Appl. Chem.* 1980, 52, 2717.

- [9] a) Keller, P., Mouradpour, A., Amouyal, E., *J. Chem. Soc. Faraday Trans. 1* 1982, 78, 3331. b) "Photogeneration of Hydrogen", Harriman, A., West, M. E. (eds.), Academic Press, London 1983.
- [10] a) Grätzel, M., Kalyanasundaram, K., Kiwi, J., *Struct. Bond.* 1982, 49, 37. b) Kirch, M., Lehn, J.-M., Sauvage, J.-P., *Helv. Chim. Acta* 1979, 62, 1345.
- [11] a) Lehn, J.-M., Ziessel, R., *Proc. Natl. Acad. Sci. USA* 1987, 79, 701. b) Hawecker, J., Lehn, J.-M., Ziessel, R., *J. Chem. Soc., Chem. Commun.* 1983, 536.
- [12] Hawecker, J., Lehn, J.-M., Ziessel, R., *J. Chem. Soc., Chem. Commun.* 1985, 56.
- [13] a) Maidan, R., Willner, I., *J. Am. Chem. Soc.* 1986, 108, 8100. b) Willner, I., Maidan, R., Mandler, D., Dörr, H., Dörr, G., Zengerle, K., *J. Am. Chem. Soc.* 1987, 109, 6080.
- [14] Willner, I., Mandler, D., *J. Am. Chem. Soc.* 1989, 111, 1330.
- [15] Taqui Khan, M. M., Bhardwaj, R. C., Bhardwaj, C., *Angew. Chem. Int. Ed. Engl.* 1988, 27, 923 [*Angew. Chem.* 1988, 100, 1000].
- [16] Khannanov, N. K., Shafirovich, V. Ya., *Kinet. Katal.* 1981, 22, 248. b) Collin, J.-P., Lehn, J.-M., Ziessel, K., *Nouv. J. Chim.* 1982, 6, 405. c) Humphry-Baker, R., Lillie, J., Grätzel, M., *J. Am. Chem. Soc.* 1982, 104, 422. d) Ramaraj, R. A., Kira, A., Kaneko, M., *Chem. Lett.* 1987, 261.
- [17] Lehn, J.-M. in "Supramolecular Photochemistry", Balzani, V. (ed.), NATO ASI, Series C, D. Reidel Publishing Company, Dordrecht, The Netherlands, 1987, Vol. 214, p. 29.
- [18] a) Grätzel, M., *Acc. Chem. Res.* 1981, 14, 376. b) "Energy Resources Through Photochemistry and Catalysis", Grätzel, M. (ed.), Academic Press, New York, 1983.
- [19] Willner, I., Otvos, J. W., Calvin, M., *J. Am. Chem. Soc.* 1981, 103, 3203.
- [20] Degani, Y., Willner, I., *J. Am. Chem. Soc.* 1983, 105, 6228.
- [21] Sasson, R. E., Rabani, J., *J. Phys. Chem.* 1980, 84, 1319.
- [22] Meisel, D., Matheson, M. S., *J. Am. Chem. Soc.* 1977, 99, 6577.
- [23] a) Kalyanasundaram, K., *Chem. Soc. Rev.* 1978, 7, 453. b) Turro, N. J., Grätzel, M., Braun, A. M., *Angew. Chem. Int. Ed. Engl.* 1980, 19, 675 [*Angew. Chem.* 1980, 92, 712].
- [24] a) Grätzel, M., *Isr. J. Chem.* 1979, 18, 264. b) J. K. Thomas, *Chem. Rev.* 1980, 283. c) Matsuo, T., Takuma, K., Tsutsui, Y., Nishigima, T., *J. Coord. Chem.* 1980, 10, 195.
- [25] a) Fendler, J. H., "Membrane Mimetic Chemistry", Wiley and Sons, New York, 1982. b) Matsuo, T., *J. Photochem.* 1985, 29, 41. c) Pileni, M.-P., Braun, A. M., Grätzel, M., *Photochem. Photobiol.* 1980, 31, 423.
- [26] a) Jones, C. A., Weaner, L. E., Mackay, R. A., *J. Phys. Chem.* 1980, 84, 1495. b) Pileni, M.-P., *Chem. Phys. Lett.* 1980, 75, 540.
- [27] a) Atik, S. S., Thomas, J. K., *J. Am. Chem. Soc.* 1981, 103, 7403. b) Mandler, D., Degani, Y., Willner, I., *J. Phys. Chem.* 1984, 88, 4366.
- [28] a) Brugger, P. A., Grätzel, M., *J. Am. Chem. Soc.* 1980, 102, 2461. b) Infelta, P. P., Brugger, P. A., *Chem. Phys. Lett.* 1981, 82, 462. c) Brugger, P. A., Infelta, P. P., Braun, A. M., Grätzel, M., *J. Am. Chem. Soc.* 1981, 103, 320.
- [29] a) Shinkai, S., Nakaji, T., Ogawa, T., Shigematsu, K., Manabe, O., *J. Am. Chem. Soc.* 1981, 103, 111. b) Shinkai, S., Ogawa, T., Kusano, Y., Manabe, O., Kikukawa, K., Goto, T., Matsuda, T., *J. Am. Chem. Soc.* 1982, 104, 1960.
- [30] a) Shinkai, S., Minami, T., Kusano, Y., Manabe, O., *J. Am. Chem. Soc.* 1982, 104, 1967. b) Shimidzu, T., Yoshikawa, M., *J. Membrane Sci.* 1983, 13, 1. c) Shinkai, S., Miyuzaki, K., Manabe, O., *Angew. Chem. Int. Ed. Engl.* 1985, 24, 866 [*Angew. Chem.* 1985, 97, 872].
- [31] Sunamoto, J., Iwamoto, K., Mohri, Y., Kominato, T., *J. Am. Chem. Soc.* 1982, 104, 5502.
- [32] Pileni, M.-P., Grätzel, M., *J. Phys. Chem.* 1980, 84, 2402.
- [33] a) Juris, A., Barigelletti, F., Campagna, S., Balzani, V., Belser, P., von Zelewsky, A., *Coord. Chem. Rev.* 1988, 84, 85. b) Kalyanasundaram, K., *Coord. Chem. Rev.* 1982, 46, 159. c) Darwent, J. K., Douglas, P., Harriman, A., Porter, G., Richoux, M.-C., *Coord. Chem. Rev.* 1982, 44, 83. d) Harriman, A., *J. Photochem.* 1985, 29, 139. e) Gray, H. B., Maverick, A. W., *Science* 1981, 214, 1201.

- [34] a) Heller, A., *Science* 1984, 223, 1141. b) "Homogeneous and Heterogeneous Photocatalysis", Pelizzetti, E., Serpone, N. (eds.), D. Reidel Publishing Company, Dordrecht, 1986.
- [35] a) Fox, M. A. in "Topics in Organic Electrochemistry", Fry, A. J., Britton, W. E. (eds.), Plenum Press, New York, 1986. b) Spitler, M. T., *J. Chem. Educ.* 1983, 60, 330. c) Wrighton, M. S., *Pure Appl. Chem.* 1985, 57, 57. d) Pleskov, Yu. V., *Prog. Surface Science* 1984, 15, 401.
- [36] "The Chemistry of Silica", Iler, R. K. (ed.), Wiley, New York, 1979.
- [37] a) Laane, C., Willner, L., Orvos, J. W., Calvin, M., *Proc. Natl. Acad. Sci. USA* 1981, 78, 5928. b) Willner, L., Yang, J.-M., Laane, C., Orvos, J. W., Calvin, M., *J. Phys. Chem.* 1981, 85, 3277.
- [38] a) Willner, L., Degani, Y., *J. Chem. Soc. Chem. Commun.* 1982, 761. b) Willner, L., Degani, Y., *Isr. J. Chem.* 1982, 22, 163.
- [39] Willner, L., Eichen, Y., Joselevich, E., *J. Phys. Chem.* 1990, 94, 3092.
- [40] Adar, E., Degani, Y., Goren, Z., Willner, L., *J. Am. Chem. Soc.* 1986, 108, 4696.
- [41] Willner, L., Adar, E., Goren, Z., Steinberger, B., *New J. Chem.* 1987, 11, 769.
- [42] a) Saenger, A. Q., *Angew. Chem. Int. Ed. Engl.* 1980, 19, 344 [*Angew. Chem.* 1980, 92, 343]. b) Bender, M. L., Kamiyama, M., "Cyclodextrin Chemistry", Springer, Berlin, 1978.
- [43] a) Tabushi, I., *Acc. Chem. Res.* 1982, 15, 66. b) Breslow, R., *Science (Washington D.C.)* 1982, 218, 532.
- [44] Tabushi, I., Yamamura, K., *Top. Curr. Chem.* 1983, 113, 145.
- [45] Eichen, Y., Willner, L., *J. Am. Chem. Soc.* 1987, 109, 6862.
- [46] Willner, L., Eichen, Y., Frank, A. J., *J. Am. Chem. Soc.* 1989, 111, 1884.
- [47] Willner, L., Rosengaus, J., Eichen, Y., *New J. Chem.* 1990, in press.
- [48] a) Martinek, K., Beretin, L. V., *Photochem. Photobiol.* 1979, 29, 637. b) Willner, L., Rubin, S., unpublished results.

SOLAR-INDUZIERTE REDOXREAKTIONEN IN MIKROHETEROGENEN UND  
HOMOGENEN SYSTEMEN ZUR WASSERSTOFFERZEUGUNG

Projekt-Nr.: 03 E 8686 A

Prof. Dr. H. Dürr

FR 11.2 Organische Chemie

Universität des Saarlandes

D - 6600 Saarbrücken

Kurzfassung

Die artifizielle Photosynthese, die die natürliche Photosynthese in ihrer Funktion nachahmt, wurde studiert.

1) Neue homo- und heteroleptische Ru-polypyridin-Komplexe (Sensibilisatoren) wurden synthetisiert.

2) Ru-Komplexe mit Kryptand- oder Coronand-Struktur wurden hergestellt.

3) Neue Mono- und Bis-Elektronentransferreagentien wurden präpariert.

Die neuen Komplexe zeigten verbesserte photophysikalische Eigenschaften insbesondere im Hinblick auf Absorption, Energie des angeregten Zustandes, verlängerte Lumineszenzlebensdauern, Redoxpotentiale des angeregten Zustandes und effektiven bimolekularen Energietransfer.

Neue Katalysatoren (Pt, Ru, Os, Ir und  $\text{MnO}_2$ ) wurden in sacrificiellen Systemen getestet. Die Wasserstoffherzeugung in vielen Systemen erwies sich dabei als effizient. Sauerstoff konnte - entgegen Literaturberichten - in ausgewählten Beispielen unzweideutig erzeugt werden.

Neue Supramolekulare Sensibilisator-Relais-Anordnungen konnten aufgebaut werden. Diese zeigen wesentlich verbesserte Eigenschaften im Hinblick auf Wasserstoff- und Methan-Produktion. Langfristig können diese Studien einen Beitrag zum Problem des Treibhauseffektes leisten.

Schlusssatz

Artifizielle Photosynthese, Energie-Konversion, Tuning von Sensibilisatoren, Ru-Polypyridin-Komplexe, Relais, Katalysatoren, Wasserstoff-, Sauerstoff- und Methan-Erzeugung



Wesentliche Arbeitsziele dieses Projekts waren im Antrag von 1985 genannt. Sie sind hier noch einmal kurz zusammengestellt:

Die vorgesehenen Arbeiten lassen sich in folgende Hauptbereiche gliedern:

- Sensibilisator und Elektronenüberträger
- Katalysator
- Systemtechnik

Die wissenschaftlichen Arbeitsziele waren:

- Entwicklung und Optimierung von
  - . Sensibilisatoren (Uni Saarbrücken, EPFL, Hebrew University)
  - . Elektronenrelais (Uni Saarbrücken)
- Test und Optimierung von
  - . Reduktionskatalysator
  - . Oxidationskatalysator (Fa. Nukem)

Als technische Arbeitsziele wurden angestrebt:

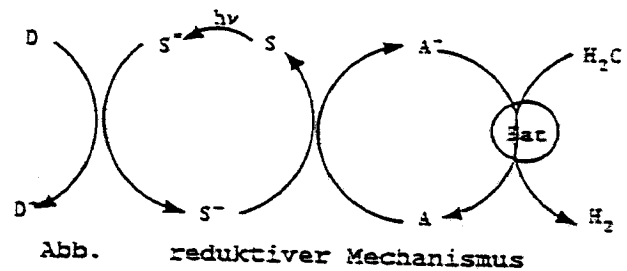
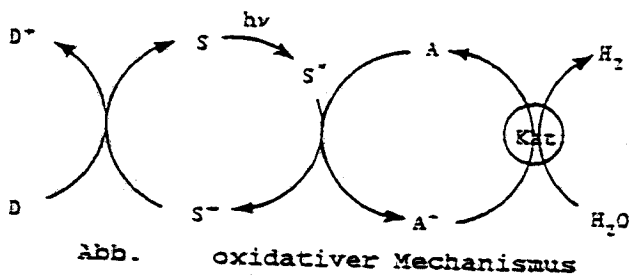
- Reproduzierbarkeit der Herstellung von
    - . Sensibilisatoren (Uni Saarbrücken)
    - . Elektronenüberträger (Uni Saarbrücken)
  - Performancetests und Langzeitverhalten in Kombination mit Industriekatalysatoren (Fa. Nukem)
    - . Stabilität
    - . Wirkungsgrad
- Systemtechnische Entwicklungen (Nukem, Universität Saarbrücken)
- . Erzeugung und Produktion organischer Oxidationsprodukte

Die wissenschaftlichen und technischen Erfolge bzw. Erfahrungen können kurz wie folgt beschrieben werden:

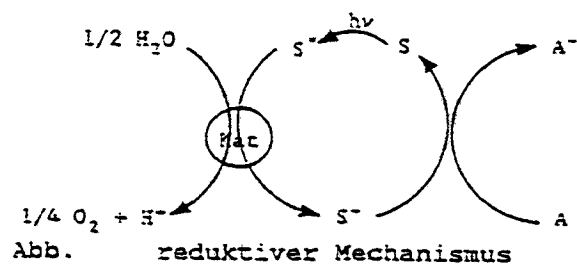
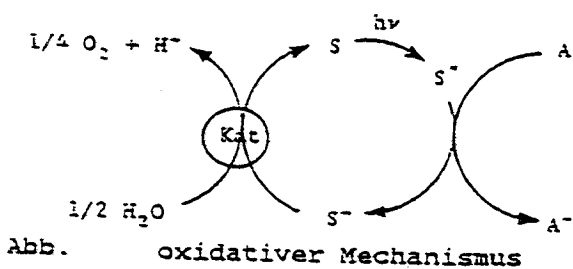
1. Sensibilisatoren: Neue effiziente Ruthenium-Polypyridin-Komplexe als Sensibilisatoren für die photochemische Wasserspaltung konnten hergestellt werden. Diese neuen Komplexe erwiesen sich als besonders effizient. Die Synthese eines neuen Kryptanden als Komplexliganden gelang, der hohe photochemische Stabilität des Ru-Komplexes verspricht.

2. Neue Relais konnten entwickelt werden, die hocheffizient Wasserstoff entwickeln. Besonders hervorzuheben ist die Synthese einer Sensibilisator/Relaisereinheit, in der eine Kombination von Sensibilisator und Elektronenrelais realisiert ist. Die Eigenschaften dieses neuartigen supramolekularen Moleküls zeigen die Überlegenheit mit klassischen Ruthenium-Komplexen. Besonders erwähnenswert ist, daß dabei auch ein System hergestellt werden konnte, bei dem auf das Relais verzichtet werden kann. Mit dieser Sensibilisator/Relaisereinheit ist damit eine Verringerung der Einzelkomponenten des klassischen photochemischen Systems möglich, was für eine Anwendung besonders wesentlich und entwicklungssträchtig ist.

### Wasserreduktion

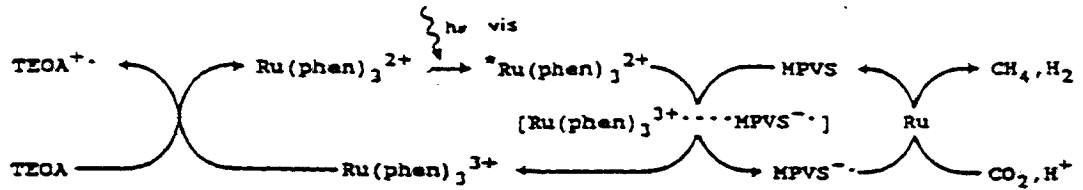


### Wasseroxidation

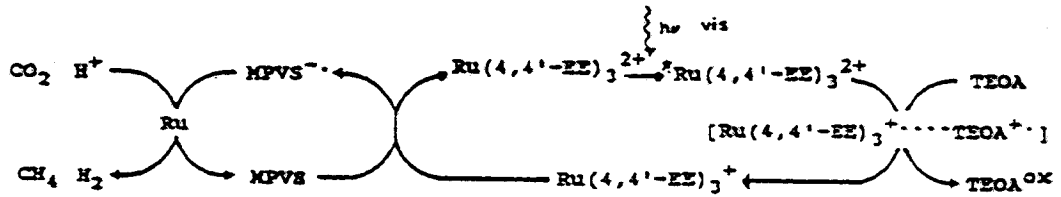


3. Die Studie neuer Katalysatoren in homogener oder mikroheterogener Form zeigte, daß neue Katalysatoren mit hoher Effizienz entwickelt werden konnten. Insbesondere zur  $\text{CO}_2$ -Reduktion müssen spezielle Katalysatoren wie Ruthenium oder Osmium eingesetzt werden. Es konnte gezeigt werden, daß spezielle Katalysatoren für die Sauerstoffentwicklung von Bedeutung sein sollten. Die Langzeitstabilität der Katalysatoren konnte insbesondere durch Platin dotierte Titandioxydpartikel erreicht werden. Der Wirkungsgrad derartiger Katalysatoren ist dabei wesentlich erhöht im Vergleich zu Standard-Katalysatoren.

Schema : Methanentwicklung aus  $\text{CO}_2$  durch oxidative Desaktivierung des Sensibilisators  $\text{Ru}(\text{phen})_3^{2+}$



Schema : Methanentwicklung aus  $\text{CO}_2$  durch reduktive Desaktivierung des  $\text{RuL}_3^{2+}$ -Sensibilisators



4. Zur sakrifiziellen Sauerstoffentwicklung wurde eine neue zuverlässige Sauerstoffbestimmung und Analytik entwickelt. Die entsprechende Meßanordnung erlaubt mit relativ geringem apparativem Aufwand den direkten Nachweis eines Sauerstoff entwickelnden Systems. Weiterhin konnte gezeigt werden, daß insbesondere spezielle Rutheniumdioxidkatalysatoren für die Sauerstoffentwicklung eingesetzt werden können. Als entsprechendes Relais erwies sich jeweils ein Kobaltsalz als geeignet. Ein neuer Sensibilisator/Relaiskomplex erwies sich dem klassischen Rutheniumkomplex als um den Faktor 10 überlegen. Bei der Kohlendioxidreduktion konnte gezeigt werden, daß durch Variation der Sensibilisatoren die Methanentwicklung in gezielter Weise beeinflusst werden kann. Insbesondere erwies sich die Sensibilisator/Relaisereinheit als besonders effizient. Eine Verbesserung um den Faktor 10 im Vergleich mit dem klassischen System bei der Methanentwicklung konnte festgestellt werden. Besonders wichtig ist, daß reduktiv arbeitende Sensibilisatoren zu sehr guten Bildungsraten für die Methanentwicklung führen.

Zusammenfassend läßt sich feststellen: Zum Beginn des Forschungs-  
vorhabens war im Prinzip die photochemische Methode zur Sonnen-  
energiespeicherung an einfachen Sensibilisatoren vom Typ der  
Ruthenium-Komplexe bearbeitet worden. Sakrifizielle Systeme zur  
Wasserstoff- wie auch zur Sauerstoffentwicklung waren vorhanden.  
Eine Verbesserung dieser Systeme war aber wegen der geringen  
Leistungsfähigkeit oder mangelnder Stabilität und einer Weiter-  
entwicklung des photochemischen Verfahrens unbedingt erforder-  
lich. In der Literatur war die photochemische Methode zur cycli-  
schen Wasserspaltung zwar publiziert worden, aber andere Arbeits-  
kreise konnten die ursprüngliche Arbeit (s.u.) in keinem Fall  
reproduzieren. Die Aufgabenstellung dieses Projektes war deshalb  
im wesentlichen, neue Sensibilisatoren und Relais zu entwickeln,  
die sakrifizielle Wasserstoff- und Sauerstoffentwicklung kritisch  
durchzuarbeiten und zu verbessern und erste Untersuchungen für  
die Möglichkeit einer cyclischen Wasserspaltung zu Wasserstoff  
und Sauerstoff zu untersuchen.

Im Laufe des Vorhabens wurde die CO<sub>2</sub>-Reduktion insbesondere zu  
Methan als Zusatzprojekt mit aufgenommen. Dieses Problem steht in  
besonderer Beziehung zur Erwärmung der Erdatmosphäre bedingt  
durch den zunehmenden CO<sub>2</sub>-Gehalt (Greenhouse-Effekt).

## Zusammenarbeit mit anderen Arbeitsgruppen

Zur Durchführung des Forschungsvorhabens war die Zusammenarbeit mit renommierten Wissenschaftlern in In- und Ausland unbedingt erforderlich. Unsere Arbeitsgruppe hat dabei mit folgenden ausländischen Arbeitskreisen zusammengearbeitet: mit Priv.-Dozent Dr. A.M.Braun von Ecole polytechnique federale de Lausanne, Ecublens, Schweiz, wurden im Rahmen dieses Forschungsprojektes vorwiegend zeitaufgelöste dynamische Kinetiken erstellt. Messungen wurden bei Priv.Dozent Dr. Braun in der Schweiz vorgenommen von K.Zangerle, E.Meyer, U.Thiery, Th.Rötsch und A.Beuerlein. Dabei wurden insbesondere Lebensdauermessungen und Fluoreszenz-Quench-Experimente mit zeitaufgelöster Spektroskopie ausgeführt.

Mit der Arbeitsgruppe von Prof. Dr. I.Willner, Dept. of Org. Chemistry, Hebrew University, Jerusalem, besteht ein langer wissenschaftlicher Kontakt. Prof. Willner ist darüber hinaus Unterauftragnehmer in dem genannten Projekt. Im Rahmen eines wissenschaftlichen Aufenthaltes eignete sich H.P.Trierweiler die Technik der  $\text{CO}_2$ -Reduktion zu Methan (Ethan) an und arbeitete sich in die entsprechende Analytik dieser Methode ein. Auch kurzzeitspektroskopische Studien wurden bei Prof. Willner vorgenommen.

Mit Dr. Meißner/Prof. Memming vom Solarinstitut Hannover wurde eine Zusammenarbeit auf dem Gebiet der sakrifiziellen Sauerstoffentwicklung realisiert. G.Heppe konnte in einem mehrwöchigen Forschungsaufenthalt in Hannover sich in die Analytik und Nachweisttechnik der photochemischen  $\text{O}_2$ -Entwicklung einarbeiten und diese Technik für uns zugänglich machen.

Mit Prof. H.D.Breuer von der Universität des Saarlandes werden Lebensdauermessungen von lumineszierenden Ruthenium-Komplexen durchgeführt. Diese Messungen dienen zu ersten Informationen über neue synthetisierte Ruthenium-Komplexe, d.h. Sensibilisatoren.

Weitere Kontakte bestehen mit Prof. Schaffner, Max-Planck-Institut, Mülheim; Prof. M. Hanack, Universität Tübingen.

PHOTOCHEMICAL SYSTEMS FOR THE UTILIZATION  
OF SOLAR LIGHT ENERGY IN THE PREPARATION  
OF FUELS AND CHEMICALS

Submitted by Professor Itamar Willner

Conclusions

We have applied various electron donors in photosensitized  $H_2$ -evolution processes. The unique characteristic of these donors is the fact that they are not destroyed in the photochemical transformation, and there exists a chemical route to regenerate the electron donors from the photoproducts. Thus, the basic principle where photosensitized electron transfer reactions can be used in fuel cells has been demonstrated. It should also be noted that many other substrates can regenerate chemically NADH and therefore various other substrates could be anticipated to act as donors in such photochemical transformations. Of particular interest is the fact that the donors used in this study are biomass products, and thus routes to evolve  $H_2$  from such waste products can be envisaged. It should also be noted that means to regenerate  $NAD^+$  from NADH are of substantial biotechnological interest in the field of cofactors regenerations. Our studies present a novel approach whereby photochemical regeneration is presented.

We thus conclude that molecular mechanics calculations allow us to predict the redox properties of bipyridinium electron relays. This allows us to tailor the structural properties of electron relays and concomitant assessment of their electron transfer quenching properties and subsequent utility in electron-transfer transformation prior to tedious synthesis. Furthermore, our studies allow us to estimate the inductive effects of substituents on redox potentials. Studies that correlate such inductive effects of substituents on the reduction potentials with Hammett parameters are under way in our laboratory.

## Schreibanweisungen:

- Füllen Sie nur die weißen Felder aus.
- Die roten Linien in den weißen Feldern markieren die Angaben oder den Textbeginn.
- Verwenden Sie bitte eine der angegebenen Schrifttypen:  
OCR-B, COURIER 10, PRESTIGE ELITE 12, PICA 10.
- Schreiben Sie mit einer 10er-Schrittschaltung (12er-Schritt bei PRESTIGE ELITE 12) und 1 1/2 zeilig.
- Verwenden Sie bitte nur Einmal-Kohleband. Das Schriftbild muß schwarz sein.
- Für die Angabe „Null“ nicht den Buchstaben „o“ bzw. „O“ verwenden.
- Korrekturen mit Korrekturband ausführen (kein Tipp-Ex verwenden).

## Jahresbericht

BMFT/PBE

**Programm**  
**Energieforschung und Energietechnologien der Bundesrepublik Deutschland**

qqP1qq **Förderschwerpunkt:**

qqP2qq **LPS-Nr.:**

qqP3qq **Tellaktivität:**

qqP4qq **Projekt:**

Solarinduzierte Redoxreaktionen in homogenen Systemen zur Wasserstoffherzeugung

qqP5qq **Laufzeit:**

qqP6qq **Projekt-Nr.:** 03 E - 8686 A

qqP7qq **Durchführung:** Arbeitsgruppe Prof. Dr. H. Dürr:

Dipl.-Chem. U. Thiery, H.P. Trierweiler, T. Röttsch, A. Guldner,  
A. Beuerlein, H. Kraus, G. Heppe

qqP8qq **Verantwortl. Leiter:** Prof. Dr. Heinz Dürr, FB 13 Org. Chemie  
Universität des Saarlandes, 6600 Saarbrücken

qqP9qq **Unterauftragnehmer:**

qqQ1qq

## Projektbeschreibung:

Ziel der photochemischen Wasserspaltung ist es, mit Hilfe des Sonnenlichtes Wasser in Wasserstoff und Sauerstoff zu spalten. Der entstehende Wasserstoff stellt einen speicherbaren chemischen Energieträger dar, der vielfältig eingesetzt werden kann. Da Wasser die auf der Erde auftreffende Sonnenstrahlung nicht absorbieren kann, ist ein Sensibilisator notwendig. Dieser wird durch das Sonnenlicht in einen energiereichen Zustand angeregt und leitet mit Hilfe der aufgenommenen Energie eine Elektronentransferreaktion ein, die zur Spaltung des Wassers führt. Als Sensibilisatoren werden Rutheniumkomplexe sowie zur Elektronenübertragung Elektronenrelais, wie z.B. Methylviologen, eingesetzt. Durch zusätzliche Verwendung von Platin- und Rutheniumoxidkatalysatoren werden kinetische Hemmungen aufgehoben. Zur Optimierung dieses Systems ist die Synthese neuer Verbindungen zu entwickeln, die sich durch größere Stabilität und bessere Red-Ox-Eigenschaften auszeichnen sollen.

Im Jahr 87 wurden weitere heteroleptische Rutheniumkomplexe vom Typ  $Ru(L)_2L'Cl_2$  ( $L, L'$ =Liganden mit Ferroinstruktur) synthetisiert. Diese wurden zusammen mit den im Vorjahr dargestellten Komplexen hinsichtlich ihrer photochemischen Eigenschaften charakterisiert. Neben der Geschwindigkeit des Elektronentransfers wurden die Quantenausbeute der primären Photoredoxreaktion, Photostabilität und Redoxpotentiale untersucht. Die Eignung zur photochemischen Wasserreduktion wurde im sacrificiellen System festgestellt.

Als neues Teilprojekt wurde mit der Untersuchung verschiedener Katalysatoren begonnen. Es wurden quasihomogene und mikroheterogene Systeme vermessen. Als quasihomogene Katalysatoren wurden mit Polyvinylalkohol stabilisierte kolloidale Lösungen von Ruthenium, Osmium und Platin eingesetzt. Die Effektivität der Katalysatoren nahm in oben angegebener Reihenfolge zu. Als mikroheterogene Systeme wurde mit unterschiedlichen Mengen Platin belegtes amorphes Titanoxid studiert.

qqq2qq Gesamtkosten: DM 739.948,-- qqq3qq Förderanteil des Bundes: 100 %qq4qq



## Schreibanweisungen:

- Füllen Sie nur die weißen Felder aus.
- Die roten Linien in den weißen Feldern markieren die Angaben oder den Textbeginn.
- Verwenden Sie bitte eine der angegebenen Schrifttypen:  
OCR-B, COURIER 10, PRESTIGE ELITE 12, PICA 10.
- Schreiben Sie mit einer 10er-Schrittschaltung (12er-Schritt bei PRESTIGE ELITE 12) und 1 1/2 zeilig.
- Verwenden Sie bitte nur Einmal-Kohleband. Das Schriftbild muß schwarz sein.
- Für die Angabe „Null“ nicht den Buchstaben „o“ bzw. „O“ verwenden.
- Korrekturen mit Korrekturband ausführen (kein Tipp-Ex verwenden).

## Jahresbericht

BMFT/PBE

<b>Programm</b> <b>Energieforschung und Energietechnologien der Bundesrepublik Deutschland</b>	
qqP100	Förderschwerpunkt:
qqP200	LPS-Nr.:
qqP300	Tellaktivität:
qqP400	Projekt: Solarinduzierte Redoxreaktionen in homogenen Systemen zur Wasserstoffherzeugung
qqP500	Laufzeit:
qqP600	Projekt-Nr.: 03 E - 8686 A
qqP700	Durchführung: Arbeitsgruppe Prof. Dr. H. Dürr Dipl.-Chem. U. Thiery, H.P. Trierweiler, T. Röttsch, A. Guldner, A. Beuerlein, H. Kraus, G. Heppe
qqP800	Verantwortl. Leiter: Prof. Dr. Heinz Dürr, FB 13 Org. Chemie Universität des Saarlandes, 6600 Saarbrücken
qqP900	Unterauftragnehmer:
qqQ100	

**Projektbeschreibung:**

Ziel der photochemischen Wasserspaltung ist es, mit Hilfe des Sonnenlichtes Wasser in Wasserstoff und Sauerstoff zu spalten. Der entstehende Wasserstoff stellt einen speicherbaren chemischen Energieträger dar, der vielfältig eingesetzt werden kann. Da Wasser die auf der Erde auftreffende Sonnenstrahlung nicht absorbieren kann, ist ein Sensibilisator notwendig. Dieser wird durch das Sonnenlicht ~~in einen energiereichen Zustand~~ angeregt und leitet mit Hilfe der aufgenommenen Energie eine Elektronentransferreaktion ein, die zur Spaltung des Wassers führt. Als Sensibilisatoren werden Rutheniumkomplexe sowie zur Elektronenübertragung Elektronenrelais, wie z.B. Methylviologen, eingesetzt. Durch zusätzliche Verwendung von Platin- und Rutheniumoxiddkatalysatoren werden kinetische Hemmungen aufgehoben. Zur Optimierung dieses Systems ist die Synthese neuer Verbindungen zu entwickeln, die sich durch größere Stabilität und bessere Red-Ox-Eigenschaften auszeichnen sollen.

Im Jahr 87 wurden weitere heteroleptische Rutheniumkomplexe vom Typ  $Ru(L)_2L'Cl_2$  ( $L, L' =$  Liganden mit Ferroinstruktur) synthetisiert. Diese wurden zusammen mit den im Vorjahr dargestellten Komplexen hinsichtlich ihrer photochemischen Eigenschaften charakterisiert. Neben der Geschwindigkeit des Elektronentransfers wurden die Quantenausbeute der primären Photoredoxreaktion, Photostabilität und Redoxpotentiale untersucht. Die Eignung zur photochemischen Wasserreduktion wurde im sacrificiellen System festgestellt.

Als neues Teilprojekt wurde mit der Untersuchung verschiedener Katalysatoren begonnen. Es wurden quasihomogene und mikroheterogene Systeme vermessen. Als quasihomogene Katalysatoren wurden mit Polyvinylalkohol stabilisierte kolloidale Lösungen von Ruthenium, Osmium und Platin eingesetzt. Die Effektivität der Katalysatoren nahm in oben angegebener Reihenfolge zu. Als mikroheterogene Systeme wurde mit unterschiedlichen Mengen Platin belegtes amorphes Titanoxid studiert.

qqq2qq Gesamtkosten: DM 739.948,- qqq3qq Förderanteil des Bundes: 100 % qqq4qq

**OTHER INFORMATION**

For information and declaration of interest please contact the following persons:

**Scientific programme**

Dr W. Paiz  
Commission of the European Communities  
DG XII/E-1  
Rue de la Loi 200  
B 1049 Brussels  
Belgium

**Local organization**

Dr C. Runge  
Ministerium BbA, Saarland  
Postfach 1010  
D 6600 Saarbrücken  
Federal Republic of Germany

**General organization**

H. S. Stephens & Associates  
Conference Organisers  
Agriculture House  
55 Goldington Road  
Bedford MK40 3LS  
England

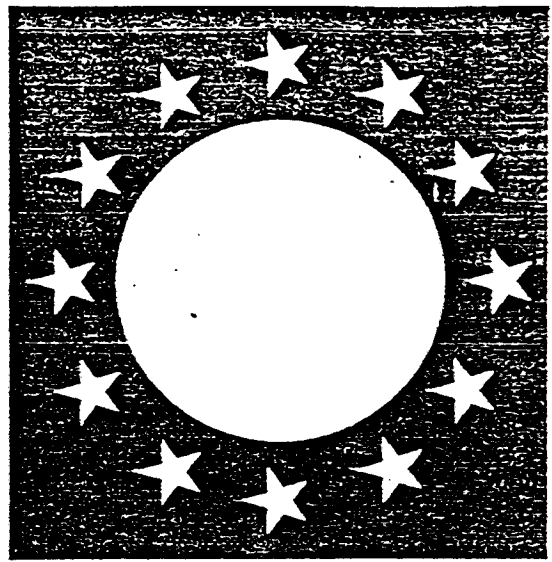
Telephone: National (0234) 49474  
International +4423449474

H. S. Stephens & Associates  
Conference Organisers  
Agriculture House  
55 Goldington Road  
Bedford MK40 3LS  
England

reannouncement

# EUROFORUM NEW ENERGIES Congress and Exhibition

24-28 October 1988  
Kongresshalle, Saarbrücken,  
F.R. Germany



Sponsored by  
Commission of the  
European Communities  
Landesregierung Saarland

# EUROFORUM NEW ENERGIES '88

Thema:

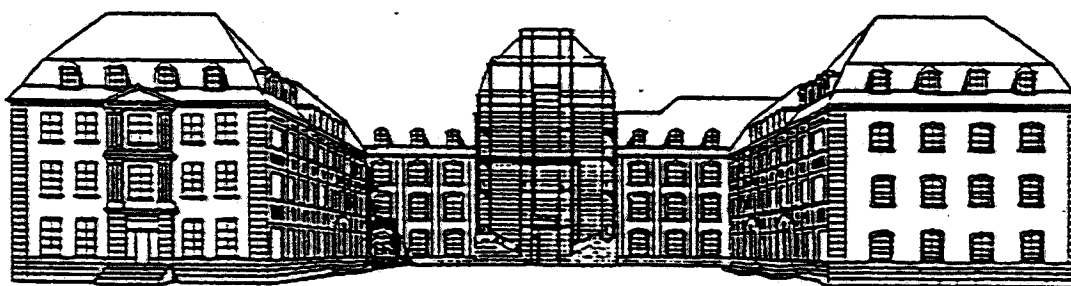
H. Dürr, Photochemical Water cleavage with Ruthenium-complexes

**Workshop on Supramolecular  
Organic Chemistry  
and  
Photochemistry**

**Universität des Saarlandes**

**27. August - 1. September 1989**

**Saarbrücken / FRG**



**Book of Abstracts**

STUDIES OF ELECTRON TRANSFER-REACTIONS IN WATER-REDUCING  
SYSTEMS

H. Dürr\*, A. Beuerlein, St. Boßmann

FB 13.2 Organische Chemie

Universität des Saarlandes, 6600 Saarbrücken, Germany

Electron transfer reactions play an important role in elementary processes of water reducing systems using visible light.

The evolution of hydrogen and oxygen from water with Ru (II) complexes (e.g.  $\text{Ru}(\text{bpy})_3\text{Cl}_2$ ) and electron relays (e.g. methylviologen) are thermodynamically possible, but kinetically hindered; the electron transfer from the reduced relays to water is kinetically sluggish. Using several catalysts it is possible to obtain good yields of hydrogen or oxygen.

Optimized water reducing systems by using several catalysts and by changing the pH of the solution in quasihomogeneous and microheterogeneous systems will be presented.

An investigation of interactions between Ruthenium-sensitizers and  $\text{TiO}_2$ -particles adsorbed on the surface of  $\text{SiO}_2$  colloid will be shown as well.

ROUTES AND FIRST RESULTS TO NEW SUPRAMOLECULAR COMPLEXES  
APPLIED IN PHOTOELECTRON TRANSFER PROCESSES

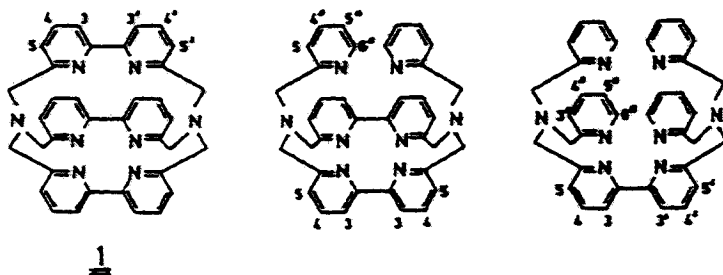
H. Duerr\*, K. Zengerle, H.P. Trierweiler, R. Schwarz

FB 13.2 Organische Chemie

Universität des Saarlandes, 6600 Saarbrücken, Germany

Podands, coronands and cryptands containing 2,2'-bipyridine-units were synthesized.

The aim of these synthetical developments is the prevention of light induced photodissoziation of Ru(II)-polypyridines. These complexes act as sensitizers in artificial photosynthesis.



1

The Ru(II) compound of 1 does not exhibit any luminescence at room temperature. At 77K luminescence can be observed depending on excitation wavelength. Intermolecular quenching does not occur at room temperature, which was shown by Stern-Volmer experiments. The luminescence intensity neither of Ru(bpy)<sub>3</sub><sup>2+</sup> nor Ru(bpz)<sub>3</sub><sup>2+</sup> decrease by addition of 1 to both sensitizers in aqueous solution. That means that 1 does not act as quenching compound.